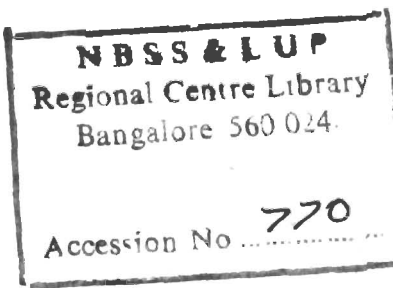


TROPICAL METEOROLOGY

HERBERT RIEHL

*Department of Meteorology
University of Chicago*



McGRAW-HILL BOOK COMPANY, INC.

New York Toronto London

1954

TROPICAL METEOROLOGY

Copyright, 1954, by the McGraw-Hill Book Company, Inc. Printed in the United States of America. All rights reserved. This book, or parts thereof, may not be reproduced in any form without permission of the publishers.

Library of Congress Catalog Card Number 53-12051

IV

52655

551.5(213)

R1E

770

N B S S & : U P
Region : Central Library
Bangkok 1024

Accession No. 770

NBSS & LUP
Regional Centre Library
Bangalore 560 024.

Accession No **770**

TROPICAL METEOROLOGY

PREFACE

In July, 1943, the author first saw the tropics when he arrived in Puerto Rico to join the staff of the Institute of Tropical Meteorology, newly founded through the initiative of Professors C. G. Rossby and H. R. Byers as a cooperative project of the Universities of Chicago and Puerto Rico. On the first evening some of the staff walked along the beach and admired the beauty of the trade cumuli in the moonlight. Well schooled in the ice-crystal theory of formation of rain, they had no suspicions about these clouds with tops near 8,000 feet where the temperature is higher than $+10^{\circ}\text{C}$. Suddenly, however, the landscape ahead of them began to dim; then it disappeared; a roar approached as from rain hitting roof tops. When some minutes later they stood on a porch, drenched and shivering, they had realized that cloud tops with temperatures below freezing were not needed for the production of heavy rain from trade-wind cumulus.

There and then the question arose: How is it with the other theories in so far as they concern the tropics? In the past, weather and circulation in low latitudes had been regarded as steady except for occasional hurricanes. The urgent demand of the U.S. Army Air Corps for research in tropical meteorology, which had provided the impetus for founding the institute, belied the old descriptions. Military forces conducting war in the tropics undeniably found that "weather" on a serious scale did occur in that part of the world. What brought it on, and how could it be predicted?

One thing leads to another. It is well known that the low latitudes furnish a large fraction of the heat needed to balance the radiation deficit elsewhere. If conditions are not steady but variable within the tropics, could one still maintain that the tropics are without influence on variations of the general circulation in middle and high latitudes? The last ten years have shown repeatedly that the investigator of the general circulation cannot proceed like a physicist who turns on a well-controlled flame underneath a tank and then proceeds without further reference to the flame.

The eventual outcome of the many studies that have their roots in the

early 1940's cannot now be foreseen. But the progress since those days, attained by research in many parts of the world, has been as swift and far-reaching as one could possibly expect. The new information is scattered throughout many journals and research papers difficult to secure for student bodies. As time passes, it has become increasingly hard to teach a course in tropical meteorology, especially on the undergraduate level. Plans for this book ripened slowly with the growing need.

Since the text deals with a specialty, knowledge of elementary meteorology as available in several basic texts and many instruction programs is assumed. Every effort, however, has been made to avoid complicated concepts or to discuss their physical significance in a simple way. The use of mathematics has been held to a minimum but, contrary to initial plans, could not be avoided entirely. Meteorology today is engaged in a vigorous effort to emancipate itself from the qualitative stage and become quantitative. This is achieved by the formulation and application of usually simple equations. The reader would be done anything but a service if this growing trend were eliminated from the book by a tour de force, if, for instance, the explanation and subsequent application of the theorem of conservation of potential vorticity were omitted.

Instruction programs, such as those leading to the master's degree, must allocate time for the large number of subjects of modern meteorology in some reasonable proportion. The book therefore attempts to hold the subject matter to what can be covered in one semester containing 45 to 50 lectures. It also tries to give a complete survey of the field, since most meteorologists and workers in allied sciences who may not have an opportunity to return for university training would wish to obtain such general coverage. These two aims limited the amount of material that could be taken up in each chapter. A full treatment of tropical storms alone would require as many pages as are contained in the whole present book. It is hoped that achievement of the dual purpose that has governed the selection of material will outweigh the shortcomings and omissions which in a new subject necessarily must be great.

Wartime experiences and subsequent research have shown spectacularly that there is far more to the subject of formation of clouds and rain than 100 per cent relative humidity. A presentation of the advances in cloud physics, especially the formation of rain from warm clouds, is essential. Since the author has not had experience in this field, it seemed advisable to have the subject handled by a person of authoritative standing. The author was fortunate in securing the collaboration of Dr. Raymond B. Wexler of Harvard University and Massachusetts Institute of Technology.

The influence of many persons and agencies combines to lead to the eventual preparation of a book. Before 1947, the author's work in

tropical meteorology was made possible through support of the U.S. Army Air Forces and the U.S. Weather Bureau. Since 1947, research in the tropical field at the University of Chicago has been sponsored generously and consistently by the Office of Naval Research. Professors C. G. Rossby and H. R. Byers made the arrangements that permitted the author to enter tropical meteorology and continue in the field. Early stimulation in Puerto Rico came from Clarence E. Palmer, first director of the Institute of Tropical Meteorology, and Gordon E. Dunn of the U.S. Weather Bureau. In recent years, the author has enjoyed increasing contact with the program of marine meteorology in the trades conducted by Woods Hole Oceanographic Institution. Just prior to concluding his work on this manuscript he was fortunate in being able to visit a new expedition for the study of cumulus clouds under the leadership of Dr. Joanne S. Malkus. Many discussions at the University of Chicago have served to form and clarify the author's viewpoints. He is especially indebted to his colleagues T. C. Yeh, N. E. LaScur, and Chas. J. Jordan.

Finally, the permission of several publishing houses to reproduce certain figures is acknowledged gratefully, as is also the manuscript assistance of Dr. Ernst Moll.

HERBERT RIEHL

CONTENTS

PREFACE	v
CHAPTER 1. WINDS AND PRESSURE	1
Pressure and wind profiles at the surface—World distribution of winds and pressure—The equatorial trough—Mean winds in the troposphere—Winds in the stratosphere—Steadiness of the upper winds—Basic currents	
CHAPTER 2. TEMPERATURE	34
Seasons in the tropics—World distribution of surface temperature—Seasonal march of temperature—Temperatures of the upper air—Air masses of the continents—Air masses over the oceans—The trade-wind inversion—The trade inversion in the Atlantic Ocean—The northeast trade of the Pacific Ocean	
CHAPTER 3. RAINFALL	72
World rainfall distribution—Seasonal march of rainfall—Rainfall analysis—Effectiveness of rainfall—Variability of rainfall—Daily rainfall amounts and rainstorms	
CHAPTER 4. DIURNAL AND LOCAL EFFECTS	99
Diurnal temperature variation—Diurnal wind variation—Diurnal variation of cloudiness and rainfall—The control of climate by orographic convection cells—Diurnal variation of pressure	
CHAPTER 5. CONVECTION	119
The subcloud layer—Energy exchange near the sea surface—Structure of the subcloud layer—Dry convection cells—The cloud layer—Types of cumulus clouds—The onset of convection—The growth of cumuli—Rates and mechanisms of entrainment—Horizontal wind structure of cumuli—Turbulent exchange in the moist layer	
CHAPTER 6. THE PHYSICS OF TROPICAL RAIN (<i>by Raymond Wexler</i>)	155
Formation of clouds—Precipitation growth in warm clouds—The ice phase—Precipitation growth from ice—The thunderstorm—Artificial precipitation	

X	CONTENTS	
CHAPTER 7. WEATHER OBSERVATIONS AND ANALYSIS	177	
Observations—Surface observations—Upper-air observations—Methods of analysis—The time section—The surface chart—The upper-air charts—Wind computations—Microanalysis		
CHAPTER 8. DIVERGENCE AND VORTICITY	198	
Fields of divergence—Fields of vorticity—Convergence, divergence, and pressure changes—Conservation of potential vorticity—Further applications of the vorticity theorem		
CHAPTER 9. WAVES IN THE EASTERLIES	210	
Model of waves in the easterlies—Dynamic aspects of waves in the easterlies—Forecasting—Formation—Waves in the dry season—Waves in the equatorial easterlies		
CHAPTER 10. SURVEY OF LOW-LATITUDE DISTURBANCES	235	
Disturbances in and near the equatorial trough—The upper troposphere in summer—The Indian-summer monsoon—Disturbances of the cool season—Interaction between high and low latitudes		
CHAPTER 11. TROPICAL STORMS	281	
The life cycle—Surface structure of tropical storms—Surface pressure—Surface temperature—Surface wind—Rainfall—Surface characteristics of the eye—State of the sea—Upper-air structure of tropical storms—Upper-wind structure—Cloud systems of tropical storms—Thermal structure of the rain area—Thermal structure of the eye—Energy aspects—Formation of tropical storms—Average frequencies—Detection of tropical storms—Basic aspects of cyclogenesis—Theories of hurricane formation—The energy input—The starting mechanism—Release of latent heat and circulation in the vertical plane—The mechanical linkage—The cooling system—Dissipation of tropical storms—Motion of tropical storms—Internal forces—External forces—Recurvature—Forecasting methods		
CHAPTER 12. THE GENERAL CIRCULATION	358	
The classical general-circulation model—Collapse of the classical model—Present status of the general-circulation theory—The heat balance—The heat balance as a function of latitude—Heat and moisture transport mechanisms—Momentum balance—Structure of the trades—Moisture and heat balance in the northeast Pacific—Momentum balance in the northeast Pacific—Formation and dissolution of the trade inversion—Further comments on the structure of low and high troposphere		
NAME INDEX	383	
SUBJECT INDEX	385	

CHAPTER 1

WINDS AND PRESSURE

Some people say that the Tropics of Cancer and Capricorn bound the area within which to limit tropical meteorology. Others point to the 30th parallel, which divides the earth's surface between pole and equator in equal halves. Anyone living in the marginal belt will find both definitions arbitrary. The state of Florida certainly experiences tropical weather in summer but rarely in winter. In northern India and Pakistan forecasters reckon with "western disturbances" in the dry season.

If we define the tropics as that part of the world where most of the time the weather sequences differ distinctly from those of middle latitudes, the dividing line between easterlies and westerlies in the middle troposphere serves as a rough guide of the boundaries. Choice of this fluctuating line allows for seasonal variations and for differences between one part of the world and another in the same season. The tropics so outlined will be our major concern. But we are also interested in the connections between tropical and temperate zones. No part of the atmosphere exists alone or can be understood without considering a wider area. Both synoptic and climatic data of this book, therefore, include a portion of the middle latitudes.

Pressure and Wind Profiles at the Surface

Average weather conditions generally change much more with latitude than with longitude. From early times, men have so viewed the climate and coined names such as "doldrums" and "trades." As our first step we shall ascertain the mean conditions in these broad belts.

Sea-level Pressure. In the subtropics, often called "horse latitudes," each hemisphere has a pressure maximum at sea level in both seasons (Fig. 1.1). Between these "subtropical highs" a region of lower pressure is found near the equator—the "equatorial trough" commonly known as the doldrums. The trough is centered near 5°S in January and near 12–15°N in July. It migrates through 20° latitude between seasons; this migration influences the seasonal march of cloudiness and rainfall and the formation of tropical storms. In the annual mean, the trough lies near 5°N rather than on the geographical equator. This latitude has been named the "meteorological equator."

The subtropical high-pressure ridges reflect the asymmetry with respect to the geographical equator. The southern ridge is situated 5° latitude closer to it in the mean than the northern one. Both ridges are an equal distance from the meteorological equator. The width of the belt between

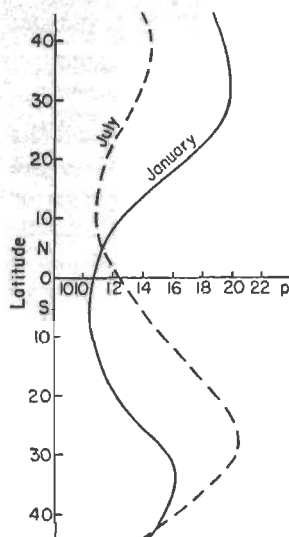


Fig. 1.1. Mean sea-level pressure (mb).

ridges and equatorial trough, largely occupied by the trades, is identical in the yearly mean in both hemispheres (30°). But this width undergoes a distinct seasonal variation; although the subtropical ridges shift in phase with the equatorial trough, their displacement amounts to little more than 5° latitude, while that of the trough is 20° . In consequence the intervening belt is much broader in the winter (35°) than in the summer hemisphere (25°).

At the subtropical-ridge lines, pressure is practically equal in both hemispheres, varying from 1015 mb¹ in summer to 1020 mb in winter. We observe that the whole tropical belt changes accordingly. In each hemisphere, the mass in the tropics decreases from winter to summer. Because this mass does not escape completely to the polar regions (34),² a net export takes place from summer to winter hemisphere across the equator.

Resultant Winds. If we wish to make statements about the wind field that are as quantitative as those just made about the pressure, we must confine our attention to the oceans. The *Atlas of Climatological Charts of the Oceans* (40) contains extensive statistics on wind and other weather elements in "squares" bounded by 5° latitude and longitude intervals. Similar statistics over land do not exist and would be very hard to compute. Oddly enough, less is known about the circulation over wide continental stretches than over remote ocean areas crossed by shipping lanes. Local topography exercises a strong influence on the wind at any land station; the difference in ground friction alone renders a combination of ocean and land winds impossible. So we shall restrict the analysis to the oceans. A glance at world streamline charts (Fig. 1.7), however, reveals that the wind belts over land are quite similar to those over the oceans.

¹ NOTE ON UNITS. In meteorology, there exists a grotesque confusion in respect to units. We have temperature in $^{\circ}\text{C}$, $^{\circ}\text{A}$, $^{\circ}\text{F}$; pressure in mb, mm, and inches of mercury; length in cm, inches, feet, km, land miles, nautical miles, etc.; these units and others occur in any number of combinations. Nothing is more annoying than the time constantly lost by everyone through unnecessary conversions; adoption of one world-wide system of units should be achieved by the profession.

² Figures in parentheses refer to the references listed at ends of chapters.

A plot of the direction of the resultant wind vector against latitude (Fig. 1.2) looks quite unconventional for meteorology. It features straight lines with abrupt breaks rather than smooth curves as in Fig. 1.1. Separation between the wind belts is very sharp. At the edges of the diagram, we see the beginnings of the polar westerlies. These lie about 5° closer to the equator in winter than in summer. Next comes a break in wind direction across the subtropical ridges. It is significant

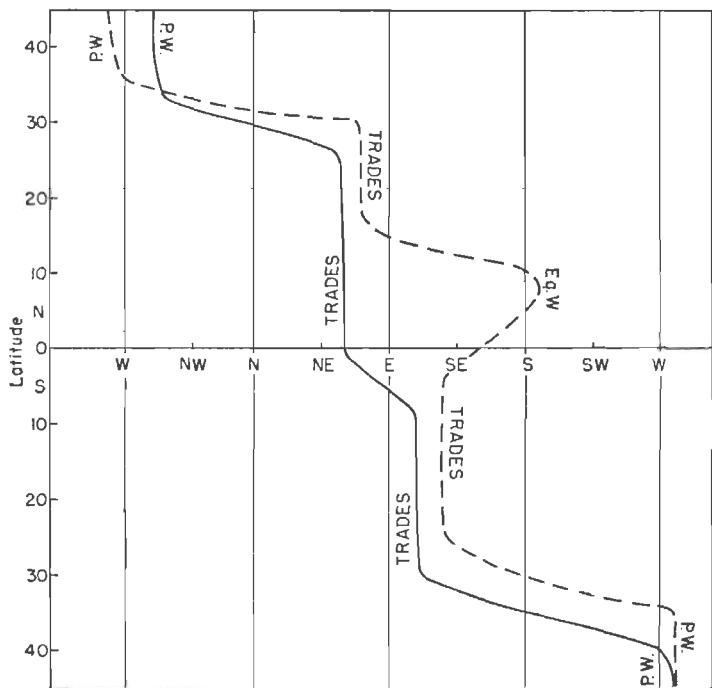


Fig. 1.2. Resultant surface-wind direction for January (solid) and July (dashed).

that winds turn from west to east through north in the northern hemisphere and through south in the southern hemisphere. This implies a net flow of air through the subtropical high-pressure belt, a flow directed toward the equator in both hemispheres.

The trades occupy the bulk of the tropics. Broadly speaking, they blow from ENE in the northern hemisphere and from ESE in the southern hemisphere. But the flow points a little more toward the equator in winter than in summer. The average wind direction in the northern hemisphere is $50\text{--}60^{\circ}$ in winter and 70° in summer;¹ in the southern hemisphere it is $120\text{--}130^{\circ}$ in winter and 110° in summer. Thus, northern

¹ Measured clockwise from north on the 360° compass.

and southern trades blow across the latitude circles in the mean with equal angles: $30\text{--}40^\circ$ in winter, 20° in summer.

Up to this point the symmetry in the pressure fields of both hemispheres relative to the meteorological equator has held true in the wind field. A marked difference appears at the equatorial margin of the trades. In January, the break in wind direction between the trades occurs quite properly near 5°S . In July, however, southerly flow occupies the belt $0\text{--}15^\circ\text{N}$, and the resultant direction even is west of south between 5 and 10°N . Here the method of averaging around latitude circles is not satisfactory. The westerly component arises as the southern trade makes wide incursions into the northern hemisphere on a clockwise curving path (Fig. 1.7). These incursions take place only in limited belts of longitude, mainly in the Indian Ocean. If this ocean were

excluded from the computation, the July curve would be very different between the equator and 15°N .

Turning next to the resultant wind speed (Fig. 1.3), we observe four belts of high speed in each season—the trades and polar westerlies. Regions of low speed are interspersed in the subtropics and near the equatorial trough. Both trades and westerlies increase in strength from summer to winter; the intensity of the trades nearly doubles. In the northern hemisphere the highest speed is 2.4 mps in summer and 4.3 mps in winter; in the southern hemisphere 3.3 mps in summer and 5.3 mps in winter. The increase in both cases is 2 mps. We find that the speed of the southern trade exceeds that of the

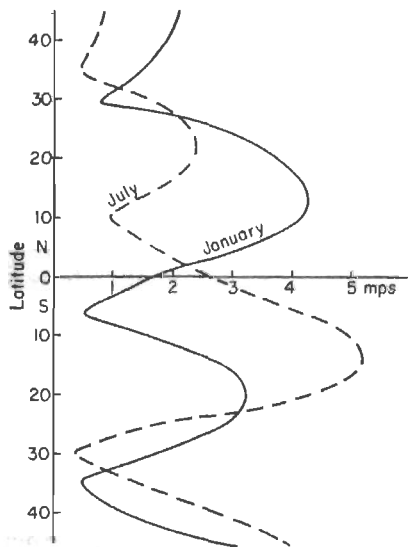


Fig. 1.3. Resultant surface-wind speed (mps).

northern by 1 mps in both seasons trade in both hemispheres shifts about 10° equatorward from summer to winter.

The foregoing applies to the *resultant speed*. This, however, may not tell us much about the *average speed* of the winds, i.e., the mean of all wind speeds regardless of direction. We know that the subtropical ridge oscillates northward and southward many times in the course of one winter. It is possible that in consequence the subtropical latitudes experience alternating east and west winds of considerable strength but

that these winds cancel when the resultant is taken. We should call such a regime unsteady. In contrast, a region with relatively constant wind direction has a steady regime.

Climatology offers several methods to determine steadiness of the winds. One measure is the correlation between average and resultant wind speed. This correlation has been computed for July by dividing the tropics into three portions with the help of Fig. 1.7: the belt within 5° of the equatorial trough, the belt from the equatorward margins of the subtropical ridges to the poleward limits of the map, and the intervening trade-wind belt. The linear correlation coefficients are 0.70, 0, and 0.94, respectively. It follows that winds in the subtropics are highly variable. Near the equatorial trough the variability is less; in the trade-wind zone winds are steady.

We have set down numerically the experience of the old seafarers, who often spent anxious days in the horse latitudes and doldrums but sailed the trades with little concern. Profiles of wind constancy against latitude (Fig. 1.4) further confirm this. Constancy here is defined as the per cent frequency of all observations with wind direction within 45° of the most frequent direction, or mode. For instance, if the wind at some station blows most often from NE and it blows anywhere between N and E 75 per cent of the time, the constancy is 75 per cent. The profiles of Figs. 1.3 and 1.4 are very similar. High resultant speeds coincide with high constancy and low resultant winds with low constancy. This relation holds for the regional distribution so that the isotachs of Fig. 1.7 might, with some approximation, have been labeled lines of equal constancy.

In the trades the constancy attains 80 per cent; in no other regime on earth do the winds blow so steadily. Life has adjusted to this uniform wind stream in numerous ways. On many islands the towns lie on the leeward side, which affords better protection to shipping from wind and ocean. Many busy airports have only one runway along the direction of the resultant wind, though this at times has proved a mistake.

The steadiness also introduces a certain monotony in trade-wind weather. The author recalls from his days in Puerto Rico that there

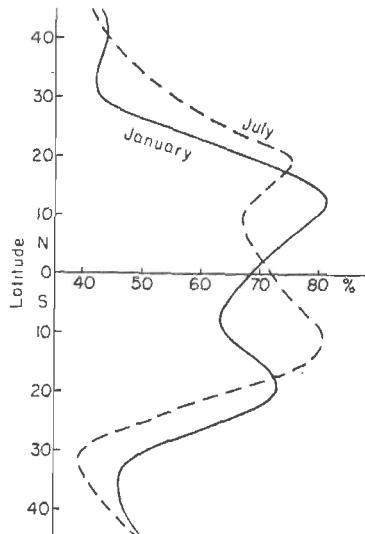


Fig. 1.4. Constancy of surface wind (per cent).

always was a great deal of excitement in the office during one of the rare "interruptions of the trade."

Resultant Wind Components. Latitudinal profiles of the resultant wind components play a role in a variety of problems such as the general circulation and the distribution of cloudiness and rainfall. The mean meridional circulation (Fig. 1.5) has formed a cornerstone of many theories since the days of Hadley. It is quite surprising that no one has computed its actual strength before 1950 (22, 26, 27). Before accepting

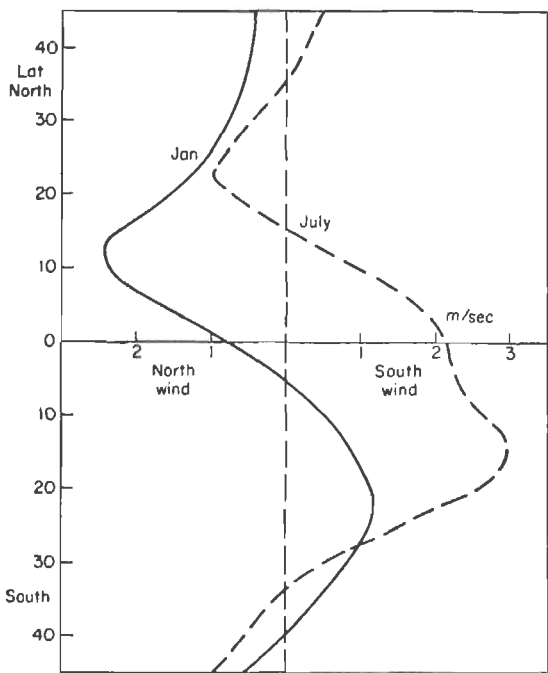


Fig. 1.5. Mean meridional wind (27).

the curves of Fig. 1.5, some checking is necessary. North and south components could alternate around the globe on any latitude circle so that the resultant could be a statistically insignificant difference between large numbers. We can make a test by counting on each latitude circle the number of 5° latitude-longitude squares with north and south components (Table 1.1).

Equatorward components dominate so strongly that the validity of Fig. 1.5 in the trades during winter is assured. Farther poleward the mean meridional circulation becomes very small; in the summer hemisphere north and south components alternate much more. Here the statistics are less impressive. We conclude that the tropics contain only

TABLE 1.1. NUMBER OF 5° LATITUDE-LONGITUDE SQUARES WITH (A) MEAN POLEWARD AND (B) EQUATORWARD WIND COMPONENT IN THE TRADES, IN WINTER

	<i>A</i>	<i>B</i>
<i>July:</i>		
5-10S	4	54
10-15S	2	58
15-20S	1	54
20-25S	7	50
<i>January:</i>		
5-10N	3	53
10-15N	0	59
15-20N	0	54
20-25N	0	52

one large circulation cell—in the winter hemisphere. There, a broad sweep of air around the globe flows toward and beyond the equator at considerable speed (2-3 mps). In the subtropics air crosses the sub-

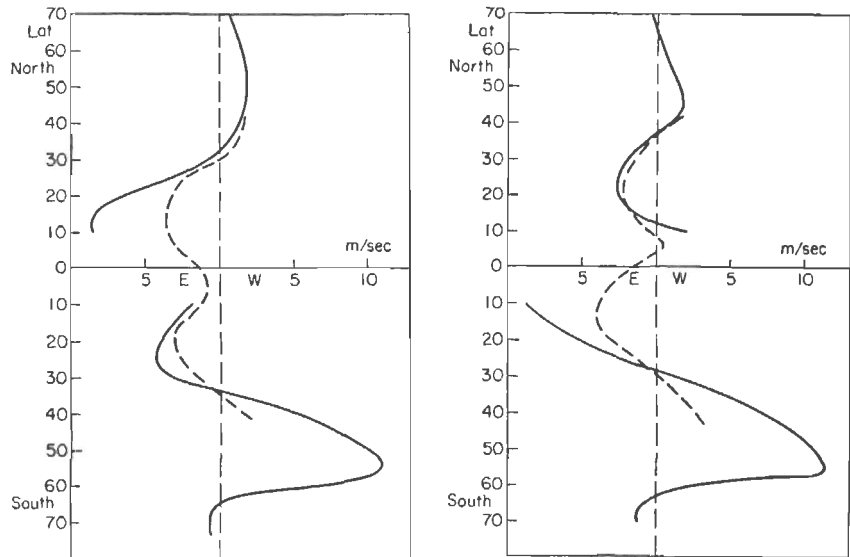


Fig. 1.6. Mean zonal wind (mps, broken) and geostrophic wind (solid) (17). *Left:* January. *Right:* July.

tropical ridge from the westerlies to the trades; the latitude separating equatorward and poleward wind components lies 5° or more poleward from the high-pressure ridge. In the equatorial zone the crossover latitude from north to south components is 5°S in January and 15°N in July, in good agreement with the equatorial-trough positions.

Turning to the zonal component (Fig. 1.6), an east wind of 1.5–2 mps blows on the equator in both seasons (17). Such an east component is not found on all stellar bodies of which we have knowledge. In the observable layers of the sun's atmosphere the equatorial drift is westerly; a westerly circulation also has been produced in rotating dishpan experiments. Scanty data for the planet Mars, however, suggest equatorial easterlies (13); the general circulation resembles that of the earth to a remarkable extent, for there are not only equatorial easterlies but also cellular subtropical ridges.

Figure 1.6 includes geostrophic wind profiles to latitudes 10° . Agreement between observed and computed winds is good at the subtropical ridge. Equatorward from the subtropics the gap between geostrophic and actual winds widens. Below latitudes 20° , the geostrophic computation is quite useless as an indicator of true resultant winds in winter. Comparison of instantaneous geostrophic and observed winds yields similar results (Chap. 7).

World Distribution of Winds and Pressure

Anyone who sets out to prepare a set of charts such as Figs. 1.7–1.8 will soon realize that this is not a small or wholly satisfactory task. Although every atlas or textbook carries some picture of the mean wind field, there are important differences, not easy to reconcile. This book draws mainly on the *Climatological Atlas* (40) for the oceans and several special publications (3, 9, 18, 32, 33, 37–39, 43) for the land areas.

Analysis of Fig. 1.7 was carried out with the streamline technique developed by V. Bjerknes (1) and extensively applied to tropical work by Palmer (21). Chapter 7 contains a description of the technique. In view of our computations of wind constancy, the streamlines in the trades represent mean air trajectories; those of the subtropics merely indicate net mass displacements. Nevertheless, the anticyclonic singular points in the eastern parts of the subtropical oceans are one of the most striking features of the maps. Such singular points occur in all oceans in both seasons except the south Indian Ocean in July. There the data suggest an anticyclonic line source of streamlines. All subtropical cells execute the seasonal shift deduced before.

The streamlines which emanate from the subtropics diverge widely as they pass through the trades, especially in the southern hemisphere in summer. Approaching the equator, they curve clockwise over the eastern parts of the oceans. Eventually the SE trades move from SW, W, and even NW in some areas. This turning is often ascribed to monsoonal effects; a portion of the trades, called "deflected trades," is thought to be drawn toward the heated continents. Freeman (11) has suggested

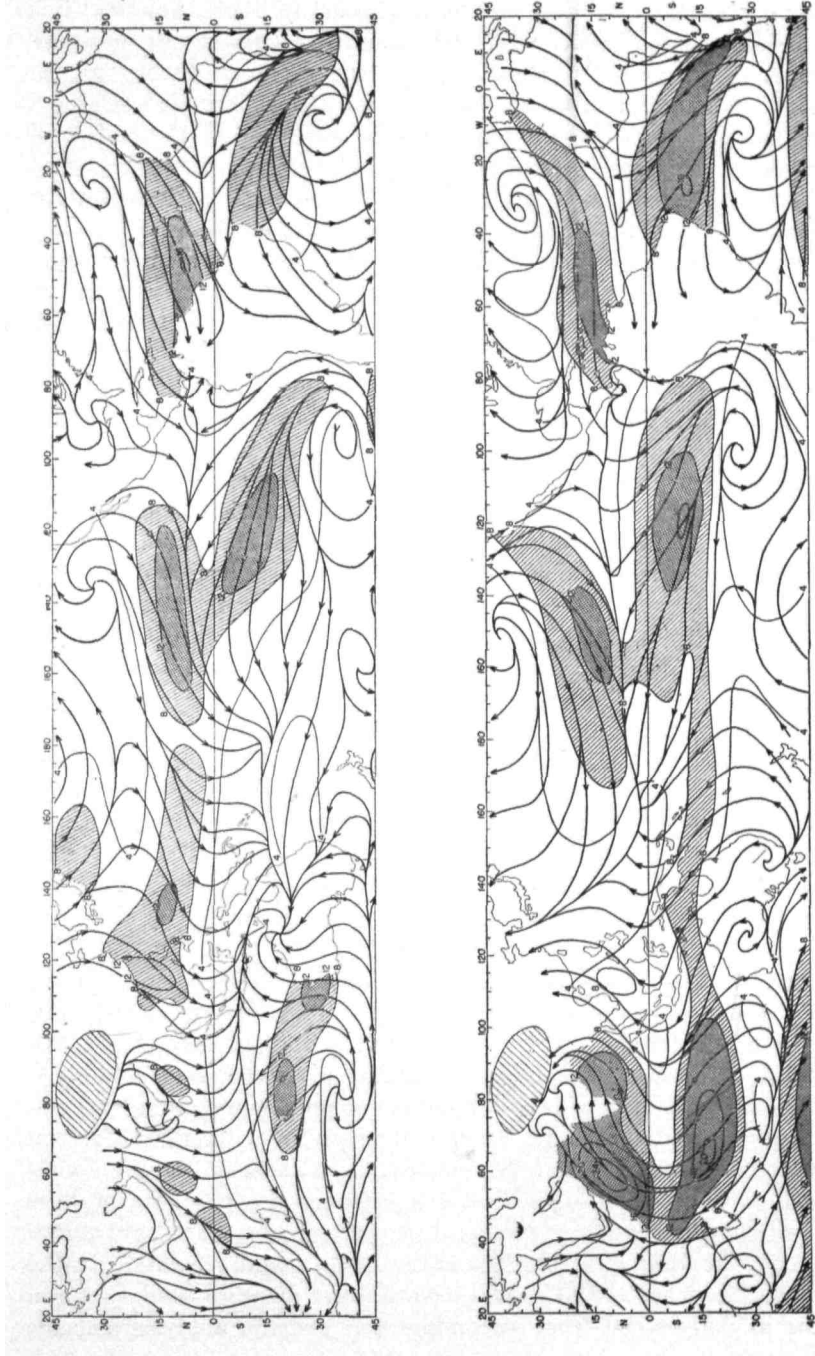


Fig. 1.7. Resultant streamlines and isotachs. *Top:* January. *Bottom:* July. Light shading denotes areas with wind speed greater than 8 knots; heavy shading, greater than 12 knots.

another explanation, at least for the west coast of South America; this explanation is based on the idea of hydraulic-pressure jumps under an inversion. Various facts cast doubt on the monsoon theory of the deflected trades. For instance, the northern-hemisphere air executes a corresponding turning—counterclockwise in this case—in the middle of the Indian and Pacific Oceans in January. There can, however, be no doubt that the charts prove the existence of monsoons; air flows toward the continents in summer and from the continents in winter.

In general, the equatorial trough is situated where the streamlines from both hemispheres converge. Its position is clear-cut in January, apart from the central south Pacific, where a convergence line oriented SE-NW emanates from the subtropics and becomes part of the equatorial trough between 160°W and 180° . The trough slopes from ENE to WNW over all three oceans. This implies a northward shift from east to west across the continents, evident over Africa (20° latitude) and Australia (10°).

In July the trough can be located with ease only over Africa, the Atlantic, and the Pacific to about 150°E . In the eastern hemisphere it lies over the mainland of Asia and appears in the streamlines only over India and Pakistan, where detailed data exist. Analysis is most difficult in the western Pacific. The zone of streamline convergence that extends southeastward from Korea does not represent the mean position of the equatorial shear lines found on daily charts. These lines extend, on the average, across the Philippines and the South China Sea. Winds are highly variable in the western tropical Pacific; large typhoons are frequent, and the mean streamlines probably reflect the influence of these storms.

Low resultant speeds prevail in the subtropics and in the equatorial trough, high resultant speeds in the trades just as in Fig. 1.3. Each trade region contains definite centers of high speed (and high wind constancy) that reach 12–16 knots. Speeds are highest over the Indian Ocean in July—more than 24 knots in the Persian Gulf.

Figure 1.8 shows the relations between world streamlines and isobars. This set of charts was difficult to draw, especially in the equatorial zone, where pressure gradients are weak. Many published maps leave this area blank. The oceanic isobars are based on analyses in several publications (30, 31) and on additional pressures recorded largely at island stations and collected in "World Weather Records" (7). After completion of preliminary isobars the author superimposed them on the previously finished streamlines; definite relations between the two sets of lines appeared which resemble those found on daily charts. The subtropical ridges coincide fairly well with the anticyclonic singular points. In the trades, air blows across the isobars toward lower pressure; the equatorial troughs as determined from streamline and isobaric analysis coincide

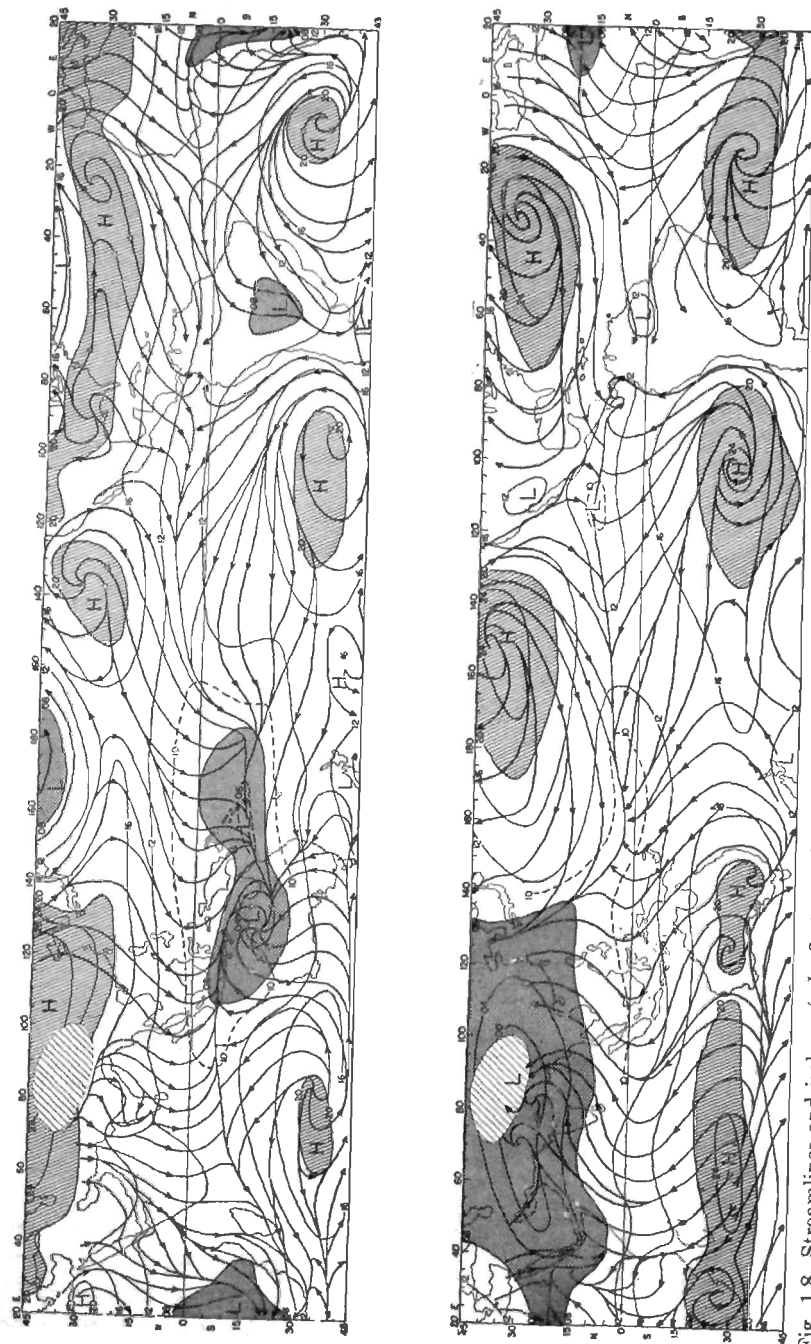


Fig. 1.8. Streamlines and isobars (mb, first two digits omitted). Top: January. Bottom: July. Areas with pressure above 1,020 mb, hatched; below 1,008 mb, shaded.

fairly well. Further, the streamlines cut equatorward across the subtropical high-pressure belt, especially in winter. This occurs in all parts of the globe, indicating that most longitudes take part in the equatorward flow of air across the subtropics.

Correspondence between streamlines and isobars was deficient in some areas. This may not be objectionable; it is not obvious what relations between isobars and streamlines we should find on mean maps, especially in regions of unsteady flow. The areas of disagreement, however, were also those with sparse data. Agreement was excellent where data was plentiful as in the north Atlantic. For this reason the pressure distribution was adjusted to the wind field wherever the discrepancies were not too great and where isobaric gradients were so weak that the lines could have been drawn one way as well as another. No reconciliation was attempted over the continents, especially South America. An unsatisfactory area also remains in mid-Pacific between 180° and 140°W south of 30°S .

Figure 1.8 permits us to compare the average angle of cross-isobar flow in the western parts of the oceans (*W*), where isobars trend poleward, with that of the eastern portions (*E*), where they trend equatorward. The result follows:

	NE trades		SE trades	
	<i>W</i>	<i>E</i>	<i>W</i>	<i>E</i>
Winter.....	52°	42°	46°	43°
Summer.....	20°	29°	32°	33°

In winter, the angle between streamlines and isobars is very large and considerably greater than in summer. Particularly in the northern hemisphere, it is actually greater over the western than over the eastern parts of the oceans in winter.

The Equatorial Trough

In Figs. 1.1-1.6 we have attempted to establish some of the most cogent features of the tropical circulation as a function of latitude alone. Figures 1.7-1.8 show that the longitudinal variations are for the most part small enough so that the general results of Figs. 1.1-1.6 cannot be challenged. We see, however, that the equatorial trough meanders northward and southward in each season. This meandering (Fig. 1.9) amounts to about 25° latitude. In January the mean position ranges from 17°S to 8°N , in July from 2°N to 27°N . In agreement with prior estimates,

the mean latitude computed from Fig. 1.9 is 4°S in January and 13°N in July.

The seasonal trough displacement varies sharply around the globe. Over most of the western hemisphere the trough shifts little more than 5° latitude; it oscillates more than 30° over large parts of the eastern hemisphere. It would be hard to deny that this difference is related to

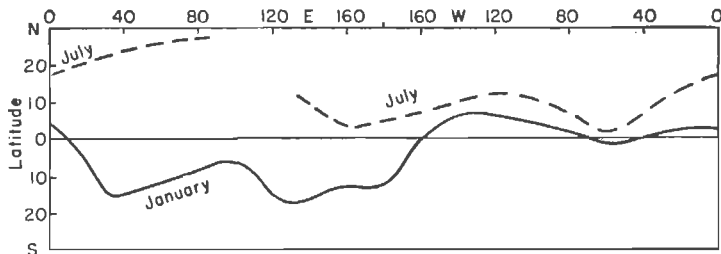


Fig. 1.9. Mean positions of equatorial trough.

the distribution of the land and water masses. Because the seasonal extremes fall in February and August, Fig. 1.9 somewhat underestimates the oscillation. Even over the continent of Africa (Fig. 1.10) the trough does not reach its highest latitude until late July and early August, and this is true in many parts of the northern hemisphere. An equatorial-trough type of circulation frequently overlies Barbados and Trinidad in

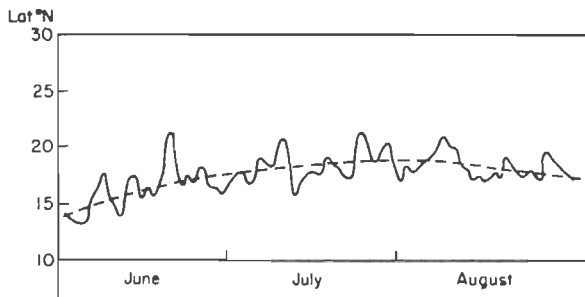


Fig. 1.10. Latitude of equatorial trough at longitude 32°E in 1942 (35).

the Lesser Antilles in September. The author has observed such systems in the northeastern Caribbean as late as early October (Chap. 10).

Because of the meandering, Fig. 1.11 has been prepared; this shows pressure, meridional wind component, and wind constancy relative to the equatorial trough. Such computations are made as follows: At intervals of 10 to 20° longitude, values of pressure and other variables are tabulated on the trough line and on lines parallel to the trough situated 5, 10°, etc., northward and southward from it. Then all pressures tabulated on

the trough line are averaged, and the same is done on each of the parallel lines. In this way we obtain profiles *relative* to the trough.

Pressure on the trough line is lower than in Fig. 1.1, which should be expected in view of the method of averaging. It is 1,008 mb in July and 1,009 mb in January. The profiles are quite symmetrical about the trough in both seasons, and their slopes are nearly identical.

In the relative measure the meridional wind component assumes the meaning of flow toward or away from the trough. We find that the flow everywhere is directed inward. It attains a maximum 10–15° from the trough line with a speed of 2 mps, slightly higher in winter than in summer; profiles for both seasons and hemispheres are symmetrical. Of particular interest again is the wind constancy. It is only in the immediate surroundings of the trough—5° or less—that winds are unsteady.

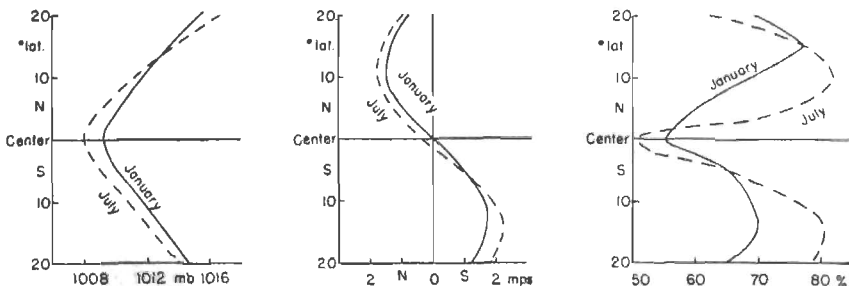


Fig. 1.11. Profiles relative to equatorial trough. Left: Pressure. Center: Meridional wind (mps). Right: wind constancy (per cent).

A narrow meandering belt exists in the heart of the tropics, where winds vary a great deal; this belt is surrounded by broad regions of very steady flow.

Mean Winds in the Troposphere

A treatment of the upper winds over the tropics must fall far short of the surface-wind summary because data are much scarcer. Information mainly comes from balloon ascents made at scattered continental and island stations and from observation of upper-cloud drift. Over the oceans and over the large, sparsely settled land areas huge gaps remain. Such data as exist must be treated with much caution for the purpose of determining the average wind field. The frequency of pilot-balloon observations at any station decreases with increasing altitude, and this decrease is not distributed at random with wind direction and speed. Low-level winds from the equatorial zone, especially those which retain their westward component, usually are associated with ascent; winds from the higher latitudes, with descent (23). Disturbed weather gen-

erally accompanies the former; good weather, the latter. Particularly during periods of southeasterly flow in the northern hemisphere and northeasterly flow in the southern hemisphere, pilot balloons are quickly lost in the clouds. Consequently the published summaries of pilot-balloon ascents yield a highly selective picture.

Qualitative inclusion of upper-cloud observations produces a much fairer picture. For instance, the mid-tropospheric winds observed by balloon at the Alfred Observatory on Mauritius (20°S , 57°E) in the year 1927–1928 were mostly westerly. When the middle-cloud direction was taken into account, northeast winds appeared with at least equal frequency.

Streamlines at 700 and 300 Mb. Well aware of these obstacles, the British Meteorological Office nevertheless has attempted to draw mean streamline and isotach maps for the tropics at several levels (4). These charts undoubtedly represent the closest approach to the upper-air circulation over the tropics now possible.

In some ways, the upper streamlines (Figs. 1.12 and 1.13) are similar to those at the surface; in others they are very different. We note belts of westerlies and easterlies and interspersed anticyclonic cells in the subtropics. These cells are elongated east–west compared with those at the surface. The strong equatorward component of the surface flow is missing, as is also the streamline convergence in the equatorial trough. Equatorial westerlies overlie the Indian Ocean at 700 mb in July, but not at 300 mb.

All these features are backed by sufficient data to warrant acceptance *in principle*. Details remain doubtful, such as the location of the centers of the subtropical cells. An eastern cell end, for instance, lies over India in winter; if streamlines are drawn on the basis of mean upper-cloud directions, the peninsula is underneath a western cell end.¹ While the slope of the cells with longitude thus remains uncertain in many areas, the slope with latitude is fairly reliable. The subtropical ridge, also known as the *base of the polar westerlies*, shifts closer to the equator with increasing altitude. In the annual average the base of the westerlies is situated a little closer to the equator in the southern than in the northern hemisphere (Table 1.2). Statistically the difference is hardly significant, but the close approach of the southern westerlies to the equator is striking in many synoptic situations (Chap. 10). The mean slope of the base of the westerlies is $\frac{1}{3}00$ from the surface to 700 mb and $\frac{1}{4}00$ from 700 to 300 mb.

The annual march of subtropical-ridge line and upper westerlies considerably lags behind the solstices. Throughout the troposphere the

¹ Y. Mintz and G. Dean, Dept. of Meteorology, University of California, Los Angeles. Multigraphed.

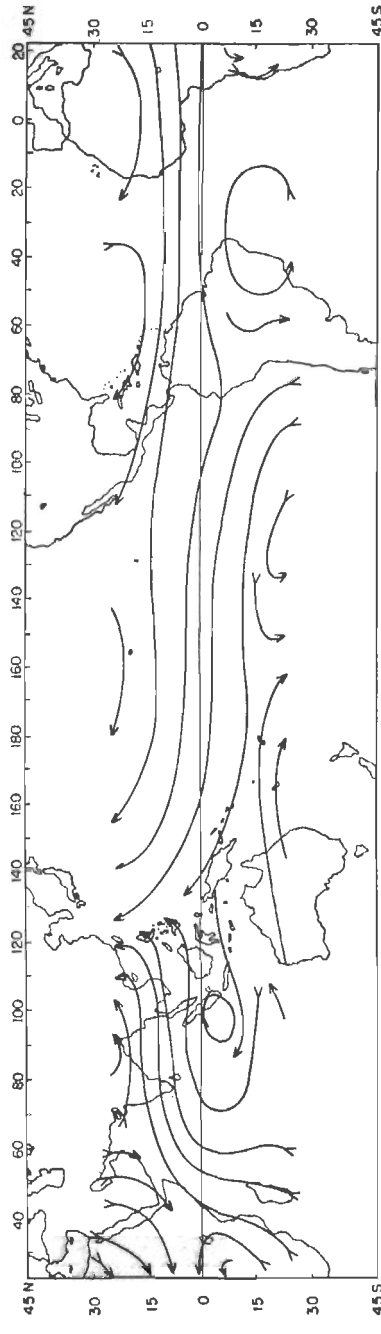
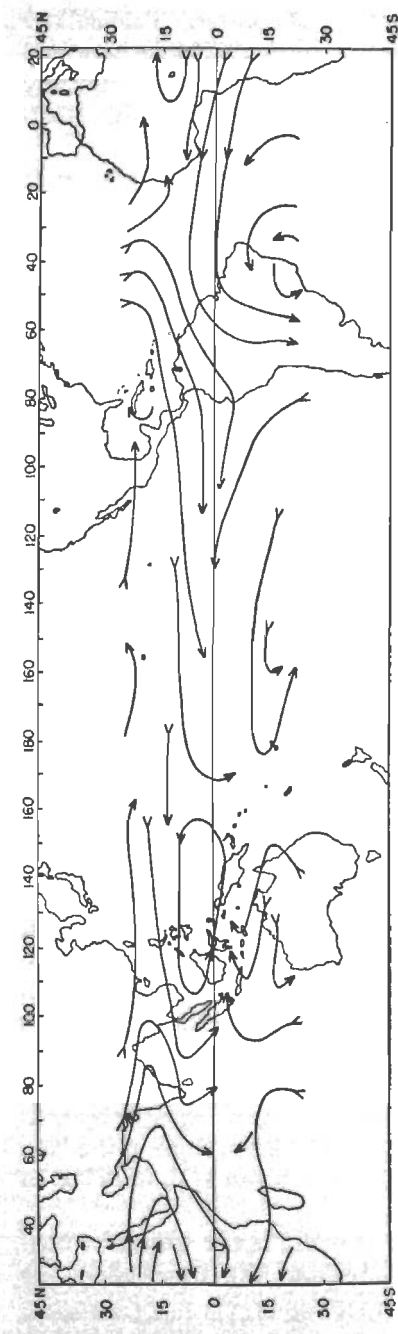


Fig. 1.12. Mean streamlines at 700 mb. Top: December–February. Bottom: June–August (4).

45 N
30
0
15
30
45 S

45 N
30
0
15
30
45 S

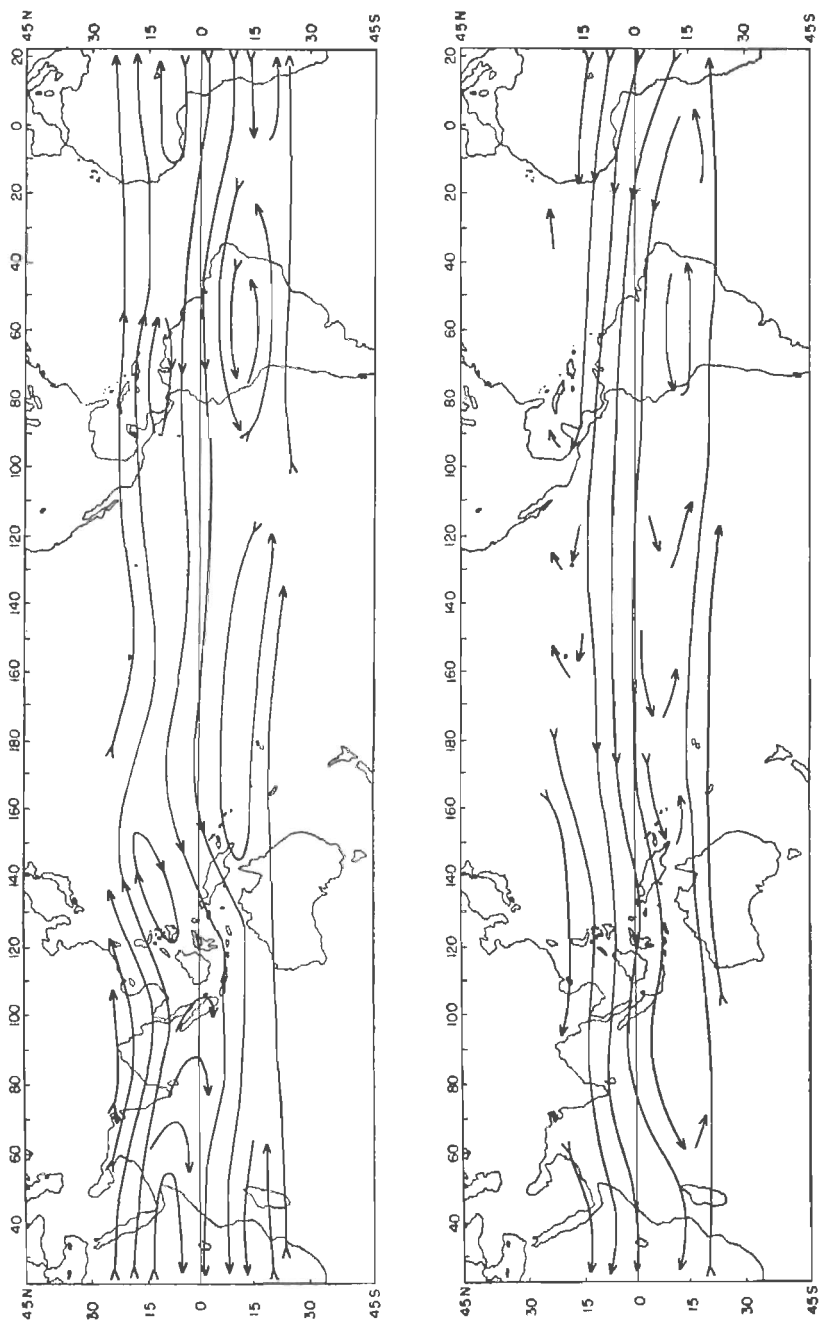


Fig. 1.13. Mean streamlines at 300 mb. Top: December–February. Bottom: June–August (4).

TABLE 1.2. MEAN LATITUDE OF THE BASE OF THE POLAR WESTERLIES

	Winter		Summer		Year	
	N	S	N	S	N	S
Surface.....	32	28	38	32	35	30
700 mb.....	17	18	29	25	23	21
300 mb.....	9	12	21	15	15	13

northern-hemisphere ridge attains its highest latitude in August–September, its lowest latitude in February–March. Such a lag is not unreasonable, as heat accumulation and depletion do not end at the time of the solstices and since the heating and cooling originate at the surface and propagate upward only slowly.

Vertical Sections and Wind Profiles. Cross sections prepared along several meridians (6, 12, 15, 20, 45) show the vertical structure of the upper winds over the tropics in different parts of the world. The sections at 80°W (Fig. 1.14) in the northern hemisphere and 170°E (Fig. 1.15) in the southern hemisphere are based mainly on geostrophic computations made by means of radiosonde ascents of aerological stations located roughly on these meridians. Upper-wind reports from the Panama Canal Zone supplement Fig. 1.14; the author has added rawin¹ data from Phoenix Island (4°S, 172°W), Tarawa (1°N, 172°E), and Kwajalein (9°N, 168°E) in Fig. 1.15.

In winter, the slope of the base of the westerlies is similar in northern and southern sections. It is smallest near the ground and becomes very steep near 300 mb. Over the bulk of the trade-wind belt the easterlies decrease with height. This decrease is strongest near the poleward boundary of the tropics, and it becomes very small close to the equator. There the sections suggest, as does also Fig. 1.13, that easterlies prevail even in the high troposphere in the mean; this is in contrast to the equatorial Atlantic, where the *Meteor* expedition observed westerly winds in a layer several kilometers thick under the tropopause. Mean conditions do not, of course, reveal much about the daily wind field in unsteady regions, but periods with strong westerlies (30–50 mph) certainly occur on the equator at high levels in the central Pacific (14).

Above 2 km, conditions at 170°E in the lower latitudes are similar in summer and winter, with a small poleward shift of all features in summer. At 80°W, however, we observe large differences. The zero line separating east and west winds is vertical at 28°N in summer. To the south of the line the easterlies, at least as given by the geostrophic computation,

¹ Wind measured with radar equipment.

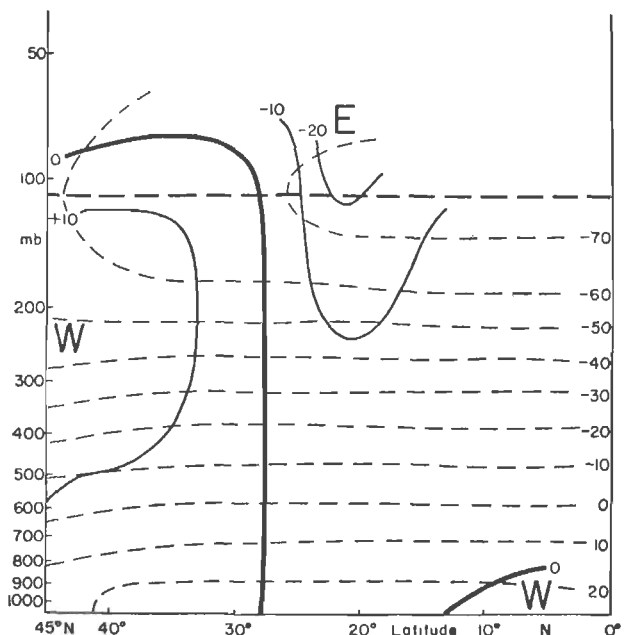
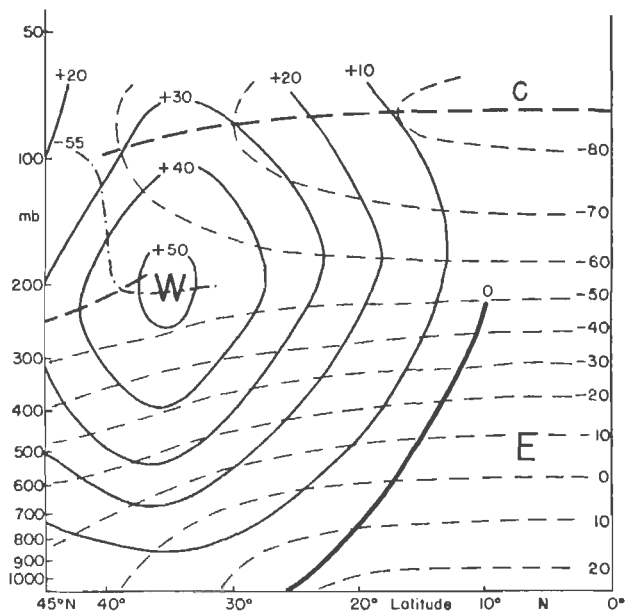


Fig. 1.14. Vertical section of zonal wind speed (mps) and temperature ($^{\circ}\text{C}$, dashed) at 80°W (Northern Hemisphere). *Top:* Winter. *Bottom:* Summer (12).

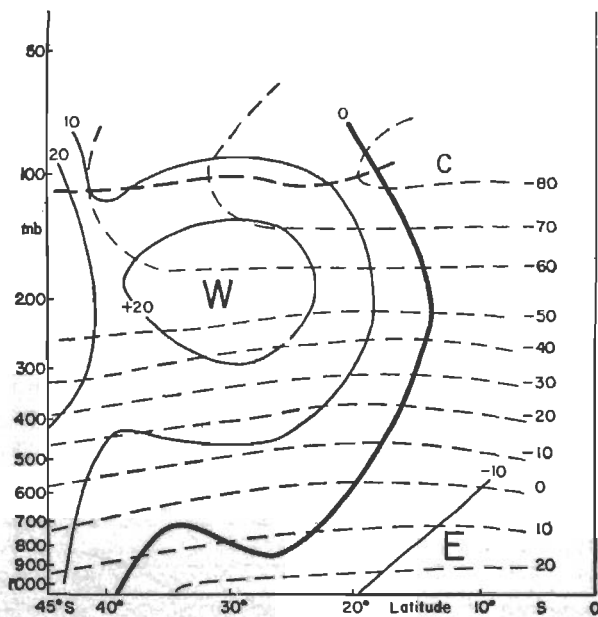
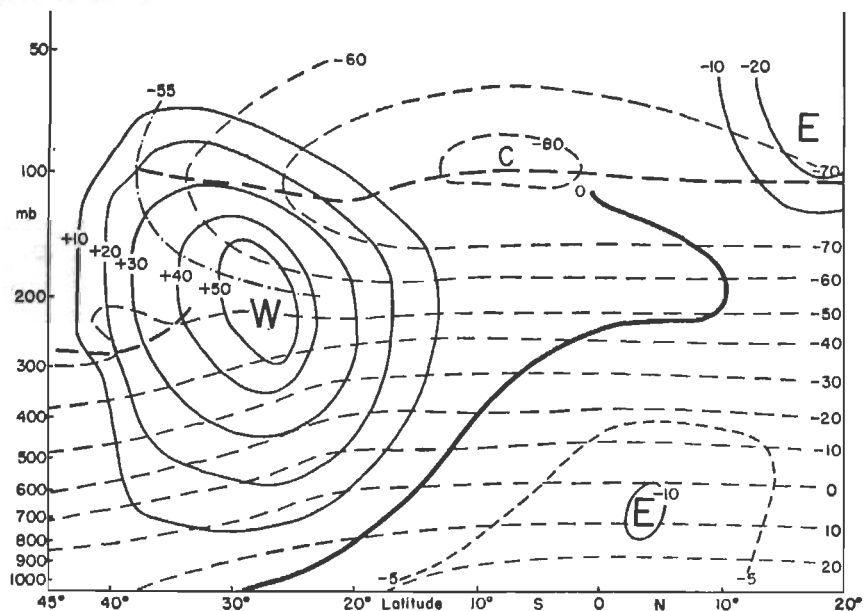


Fig. 1.15. Vertical section of zonal wind speed and temperature at 170°E (Southern Hemisphere). *Top:* Winter. *Bottom:* Summer (15).

increase upward. This is a peculiarity of the western Caribbean that is not matched at Puerto Rico in the eastern Caribbean (10, 36). There the easterlies weaken with height even in the middle of summer and disappear at 10–12 km. Over the western Pacific the vertical wind structure of summer (Fig. 1.16) corresponds to that of Puerto Rico. At Djakarta, however, the east component increases with height throughout the year in the troposphere (41) (Fig. 1.17). The Djakarta profile for December-

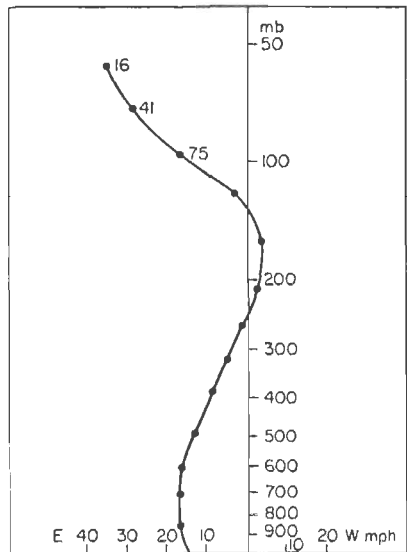


Fig. 1.16. Vertical profile of zonal flow in Pacific during September, 1945 (25).

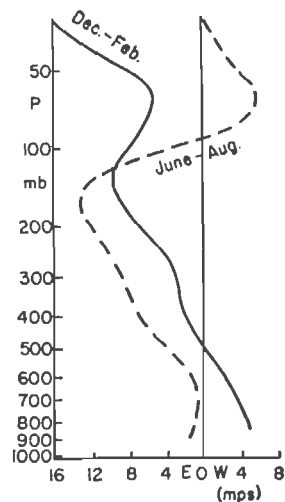


Fig. 1.17. Vertical profiles of zonal flow at Djakarta (mps) (41).

February is matched by the winds over India in summer, but not in winter.

Mean Charts for August, 1945. This mass of conflicting evidence shows clearly how dangerous it is to draw sweeping conclusions about the tropics as a whole from observations taken at a few stations and over short periods only. It is necessary to gain a view on the tropical belt as a whole. Because of the scarcity of aerological material south of the equator we must rely on evidence from the northern hemisphere. For several months toward the end of the Second World War simultaneous upper-air observations were taken throughout the tropical belt. Daily charts for the period were analyzed at the University of Chicago (28) both at low and high levels as far as latitude 10°N. These charts were then combined into monthly mean charts.

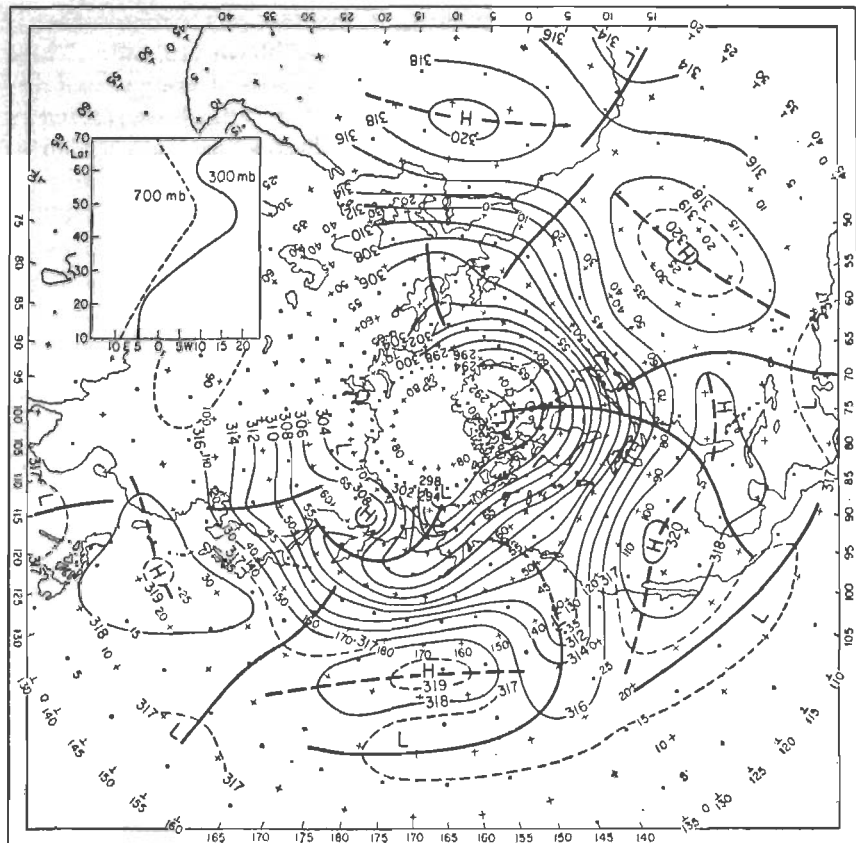


Fig. 1.18. Contours of 300-mb surface (100's, feet) for August, 1945 (26). Insert: Meridional profile of zonal wind at 700 and 300 mb (mps).

One of these analyses, that for August, 1945, has been chosen for illustration (Fig. 1.18). In August the equatorward extent of the polar westerlies attains its seasonal minimum. Any tendency toward an increase of east wind with height in low latitudes should be displayed most prominently. We note from Fig. 1.18 that, even though we are dealing with a monthly mean chart, marked contour patterns are nevertheless evident.¹ In higher latitudes a well-defined westerly current (jet

¹ Any interpretation of these contour patterns in terms of wind requires some assumption about pressure-wind relations. The assumption made here is as follows: The major component of the wind vector is oriented along the contours, but its magnitude may differ from that demanded by geostrophic computations. The turning of wind with height is in the same sense as given by the mean-temperature field. Again the magnitude may differ.

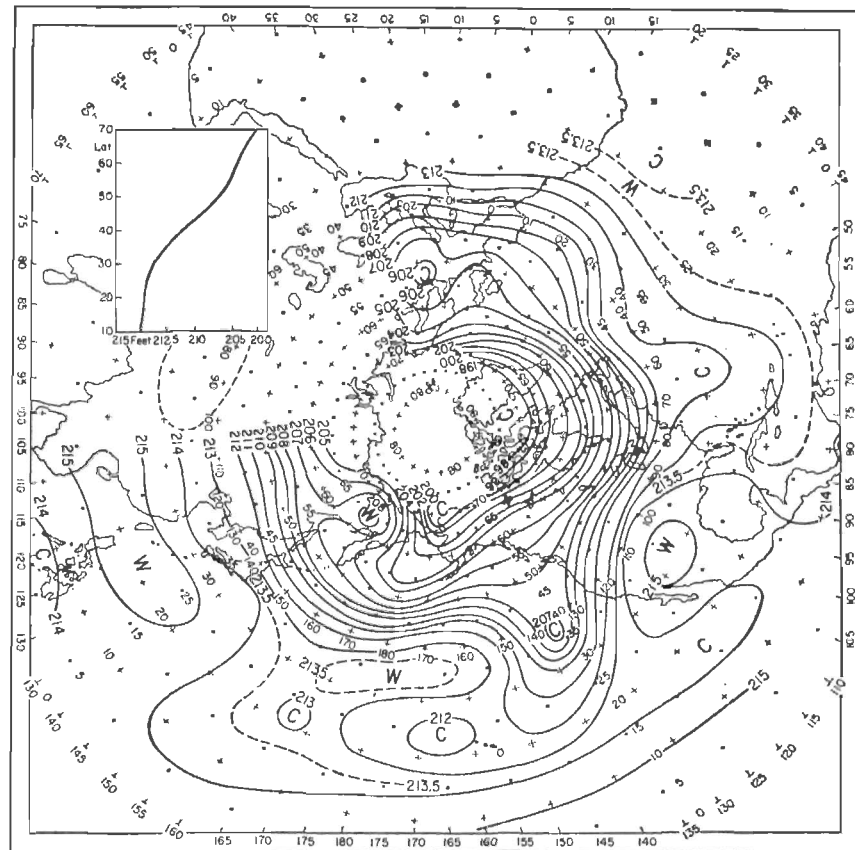


Fig. 1.19. Relative topography of the 300- above the 700-mb surface (100's feet) for August, 1945 (26). *W* stands for warm and *C* for cold. *Insert*: Meridional profile of relative topography (100's feet).

stream) meanders through a pronounced trough-ridge pattern consisting of four or five waves. The outstanding feature of lower latitudes is the array of cellular subtropical highs with intermittent troughs.

Figure 1.18 strikingly demonstrates that there is no zonal symmetry in the sense that all meridians show the same features. Regions of north and south components alternate. A general antitrade, demanded in classical general-circulation theories as a complement to the low-level trade, is not present. All major troughs of high latitudes have counterparts in the tropics; even on the monthly chart the great extended troughs are a very impressive feature. The number of troughs in low latitudes exceeds that in high latitudes, in part corresponding to the much greater circumference of the earth. If in addition to the positions in Fig. 1.18 we avail-

ourselves of the knowledge that a very persistent upper-air trough lies near longitudes 75–80°E during summer (42), we obtain a hemispheric wave number of 7 or 8 for the low latitudes. Perhaps the most remarkable asymmetry between high and low latitudes occurs in the eastern Pacific Ocean.

Figure 1.19 shows the associated thickness (mean-temperature) field for the layer 700–300 mb. Around the globe there are broad areas where the temperature gradient is directed northward at all latitudes. Interspersed are regions with reversed temperature gradient. If the mean-temperature field indicates the sense of the vertical wind shear down to latitude 10°, all conflicting evidence regarding the variation of the strength of the easterlies with height can be put in an orderly pattern. Over several broad areas the east component decreases upward. Over others, notably the central Pacific and Mexico, it increases with height between 20 and 30°N. The same is true for the western Pacific south of 20°N, as further confirmed by rawins over the Philippines and Palau. Figure 1.19 perhaps brings out most clearly that there is *no single meridian that will yield a representative picture of the hemisphere*. Agreement is good between the cross section of Hess (Fig. 1.14) and Fig. 1.19 since the warmest air lies near 25°N at 80°W. A little to the east, over the Antilles, the east wind decreases upward.

If the contours of Fig. 1.19 are summarized for all latitudes, the resulting profile shows a northward-directed temperature gradient everywhere. This gradient is so small south of 30°—the mean subtropical ridge line in August—that it is best to count it as zero. Certainly that would be true if all of Africa and Asia could have been included. As just seen, this does not mean that barotropy exists in any particular region. Areas of northward- and southward-directed temperature gradient alternate aloft. The temperature gradient is directed northward in the mean troughs; there the east wind decreases with height. Equatorward of the subtropical cells at 300 mb the temperature gradient is reversed, and the east wind increases with height. This increase may be strongest over the Asiatic continent, where the low-level westerlies give way to easterlies above 10,000–20,000 feet. Certainly, however, such increases are not an exclusive continental feature as proved by the central Pacific cell.

Winds in the Stratosphere

Whatever their differences in the troposphere, all records agree that winds are easterly in the stratosphere of the summer hemisphere and that these easterlies increase to great heights. Observed spectacularly after the great eruption of Krakatao (6°S, 105°E) in 1883, these easterlies acquired the name “Krakatao winds.” As described by Wexler (44),

the main body of the volcanic cloud moved from east to west in the stratosphere with a mean speed of 73 mph and completed at least two circuits of the earth in low latitudes. It became drawn out to a length of 5,000–7,000 miles by the vertical shear. Within 1 month the cloud spread laterally through the tropical belt but then took nearly 2 months to penetrate poleward across the northern-hemisphere subtropics. Wexler suggests that lack of north-south exchange of air across the subtropical ridge of the stratosphere acted as a barrier until, with the change of season, the ridge dropped southward and the volcanic cloud was drawn into the eddying circulations of the polar westerlies.

This description highlights the structure of the stratospheric winds over the tropics in the summer hemisphere. Quite regularly balloons reaching the 100-mb level turn westward and increase in speed (10, 14, 19, 25, 36). Colón (8) found that the direction of the stratospheric winds is almost due east up to 23 km in summer at Puerto Rico and that their speed increases from 3 to 16 mps between 16 and 23 km.

The situation in the winter hemisphere is less clear. Over the poles, the stratospheric air is extremely cold to great heights in winter and extremely warm in summer (29). The isobaric surfaces of the stratosphere, say 50 mb, therefore drop more or less continuously from one pole to the other. If winds are approximately geostrophic, the summer hemisphere should have easterlies and the winter hemisphere westerlies. A transition zone, possibly with unsteady winds, should be found near the equator. However, even in the winter hemisphere, reports of east winds are common, though their speed is less and their direction more variable than in summer. Colón (8) noted that the mean wind direction over Puerto Rico in winter is 100–120° between 20 and 24 km, with a resultant speed of about 5 mps.

Palmer¹ has analyzed the largest continuous sample of stratospheric winds existing in the tropics, collected largely during atomic-bomb tests conducted during March–May, 1951. He found persistent westerlies between the equator and 7°N. These westerlies were most steady at 70,000 feet, while winds from all directions occurred at 60,000 and 90,000 feet. As nearly as can be determined, such westerlies also prevailed in other years.

Working in the transition season, Palmer was able to trace the equatorward progression of the separation zone between easterlies to the north and westerlies to the south at 65,000–70,000 feet. Early in April, 1951, the steady easterlies extended to about 20°N, while winds fluctuated in the belt 10–20°. At the end of this month the easterlies had reached 15°N; at the end of May, 10°N. Scanty data from other years indicate that the time of the transition may vary considerably from year to year.

¹ Institute of Geophysics, University of California, Los Angeles. Mimeographed.

Steadiness of the Upper Winds

The steadiness of the average flow patterns aloft, like those at the surface, is of great meteorological interest. Quantitative treatment, however, is difficult. Mintz¹ has published 500-mb northern-hemisphere charts of wind constancy as defined earlier. These charts show that in the middle troposphere the constancy nowhere attains values equaling those of the surface layer in the tropics. A pronounced minimum of about 30 per cent lies near latitudes 10–15° in January and a lesser one (40 per cent) near 25° in July. Roughly, these are the latitudes at which the base of the westerlies crosses the 500-mb surface and where the vectorial resultant speeds are lowest in the respective seasons.

Another measure of wind steadiness (S), widely used in climatology, is $S (\%) = V/V \times 100$, where V is the vector resultant speed and V the average speed regardless of direction. Figure 2.30, computed with this formula, shows an upward decrease of steadiness in the northeast trade of the Pacific Ocean. The same is apparent from Stone's (36) study of the upper winds over Puerto Rico. Steadiness there is lowest near 10–11 km in summer and 4–5 km in winter. The minima coincide closely with the level at which, in the mean, the lower easterlies reverse to westerlies with height.

As carefully noted by Stone, his diagram mainly demonstrates the seasonal change of depth of the trades. Caution is necessary if further inferences are desired from computations of wind constancy or steadiness. The steadiness is always zero when V is zero. It is always 100 per cent when the wind keeps blowing from the same direction irrespective of fluctuations in wind speed. Steadiness computations can yield misleading results when applied to a variety of problems. For instance, meteorologists like to divide the wind field into a basic current—that part of the motion which is steady or which varies only slowly in time and space—and the disturbances which are superimposed on this basic motion. Such a division if correctly made can be a powerful analytical tool. Suppose now that the basic current is given by the wind profile of Fig. 1.16 and that the disturbances consist of alternating north and south winds of uniform strength throughout the troposphere. The intensity of the disturbances then is independent of height. But a steadiness computation would indicate that winds fluctuate very little near the ground and very much high up. Evidently the formula is not capable of measuring one of the important quantities of meteorology: the vertical variation of the intensity of the disturbances.

Recognizing such pitfalls Brooks *et al.* (4) have devised the "standard vector deviation." The vectorial difference is taken between the vector

¹ Mintz and Dean, *op. cit.*

resultant wind and each of the individual wind vectors which make up the resultant. Then the standard deviation of the lengths of the difference vectors is computed, irrespective of direction. This measure represents a great improvement over the steadiness formula. Still stricter measures of the variability of the wind can be computed by calculating the standard deviations of the zonal and meridional wind components (u, v) and the correlation between these components.¹

Without describing these criteria in detail we may note that the standard deviations (σ) of the wind components alone yield important information. Let the individual wind report be composed of a basic current (\bar{u}, \bar{v}) and a perturbation (u', v'). If n is the number of reports in a sample, $\sigma_u^2 = \Sigma u'^2/n$ and $\sigma_v^2 = \Sigma v'^2/n$. The standard deviations furnish a measure of the kinetic energy of the disturbances since the kinetic energy is proportional to the square of the wind speed. They may therefore be compared to the total kinetic energy and to that of the basic current. Figures 1.20–1.23 illustrate such computations for the period July–September, 1945, at Tarawa (1°N, 173°E) and Palau (7°N, 135°E). During these months the total kinetic energy at Tarawa, basic current plus perturbations, was about 10 per cent less than at Palau. Weaker perturbations account for this difference. Comparing perturbation and basic-current kinetic energies for the layer 1000–100 mb, the perturbation strength amounts to 60 per cent of that of the basic current at Tarawa and to 85 per cent at Palau. Along the vertical the perturbations are strongest at both stations in the high troposphere, just under the tropopause (Fig. 1.20); both curves run quite parallel. The basic-current structure, in contrast, differs radically. At Tarawa (Figs. 1.21 and 1.24) nearly all kinetic energy is concentrated below 400 mb, and the profile accords with Fig. 1.16. At Palau the basic current is nearly zero below 500 mb, and all energy is found in high-tropospheric easterlies. At both stations the speed of the easterlies increases strongly above the tropopause just as in Fig. 1.16.

Figure 1.22 shows the perturbation kinetic energy in per cent of the total kinetic energy at each isobaric surface. A two-layer structure of the troposphere is brought out clearly, in particular at Tarawa. There the perturbations contribute only a small fraction to the total energy below 500 mb. In the upper troposphere they control the wind field completely. We observe the opposite at Palau. The disturbances govern the field of motion near the surface but lose in importance with increasing altitude. As seen from Figs. 1.20 and 1.21 this inverse behavior of the field of motion results from differences in basic-current structure. Above the tropopause the disturbances nearly vanish at both stations.

¹ Derived by E. Hovmoeller, Stockholm.

We can gain further insight by comparing zonal and meridional kinetic energy or, as is more significant for some purposes, the kinetic energy along and normal to the direction of the basic current. In our case these computations become identical since the basic current is almost due east. At both stations σ_v^2 is an irregular fraction of σ_u^2 , varying roughly from

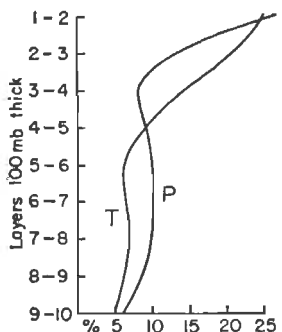


Fig. 1.20. Perturbation kinetic energy at Tarawa (T) and Palau (P), July-September, 1945. Expressed in per cent of total perturbation kinetic energy for the layer 1,000-100 mb.

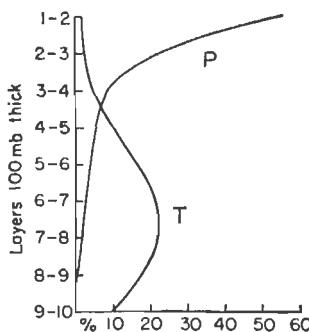


Fig. 1.21. Kinetic energy of basic current. Expressed in per cent of total kinetic energy of basic current for the layer 1,000-100 mb.

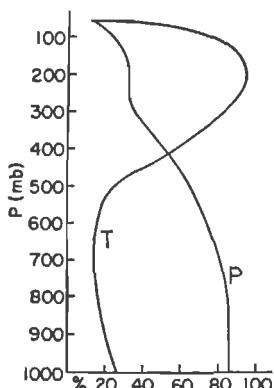


Fig. 1.22. Per cent contribution of perturbation to total kinetic energy at each level.

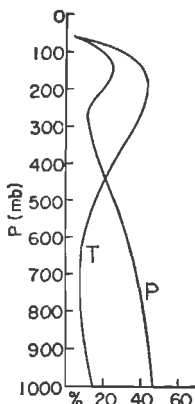


Fig. 1.23. Per cent contribution of meridional to total kinetic energy at each level.

25 to 100 per cent. A plot of total meridional energy in per cent of total energy (Fig. 1.23), however, reveals a structure similar to that of Fig. 1.22. The north-south motion accounts for nearly 50 per cent of the total kinetic energy at Palau in the low levels and at Tarawa in the high troposphere. In the other layers the contribution of the north-south flow is small.

Representative time sections from the period covered by these computations qualitatively reveal the structure just brought out. At Tarawa (Fig. 1.24) winds are almost uniformly easterly in the lower atmosphere up to about 600 mb. Higher up the fluctuations increase. Extreme restlessness rules in the upper troposphere, to subside only as we cross the tropopause into the stratosphere. At Palau (Fig. 1.25) winds are most variable near the surface and become more steady with increasing altitude. Even so, as shown by Fig. 1.20, the vertical variation of eddy energy is nearly identical at both stations.

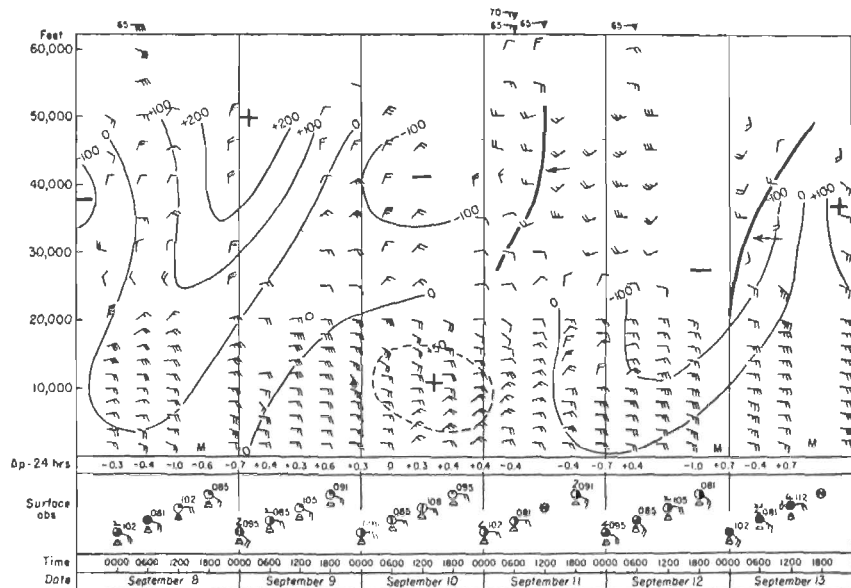


Fig. 1.24. Vertical time section at Tarawa, Sept. 8–13, 1945 (25). Light solid lines give 24-hour height changes (feet) of constant-pressure surfaces.

Chapter 10 shows typical maps for the same period. They provide a horizontal view of the disturbances seen so far in individual station records. Above the broad, quasi-uniform trade stream of the surface layer a series of large clockwise and counterclockwise vortices exist in the high troposphere; these are not stationary but moving. Thus the classical viewpoint of the steady antitrade, not present in the monthly 300-mb chart for August, 1945 (Fig. 1.18), is contradicted even more strongly by the daily charts. We must put a more realistic picture in its place. In the tropics as in higher latitudes, disturbances exist everywhere in the atmosphere. In the trades, their energy is weak at the surface compared with that of the basic current; they merely appear as minor deformations of the streamlines. At high levels they control the wind field.

Conditions as shown by Fig. 1.25 are representative along large portions of the equatorial trough, though not its whole length. Relative to the basic current, eddy motion is strongest near the ground and weak above 30,000-40,000 feet. The vertical gradient of disturbed activity is opposite to that of the trades. Such a reversal is usually present. Pronounced eddies in the streamline field are found either above or below

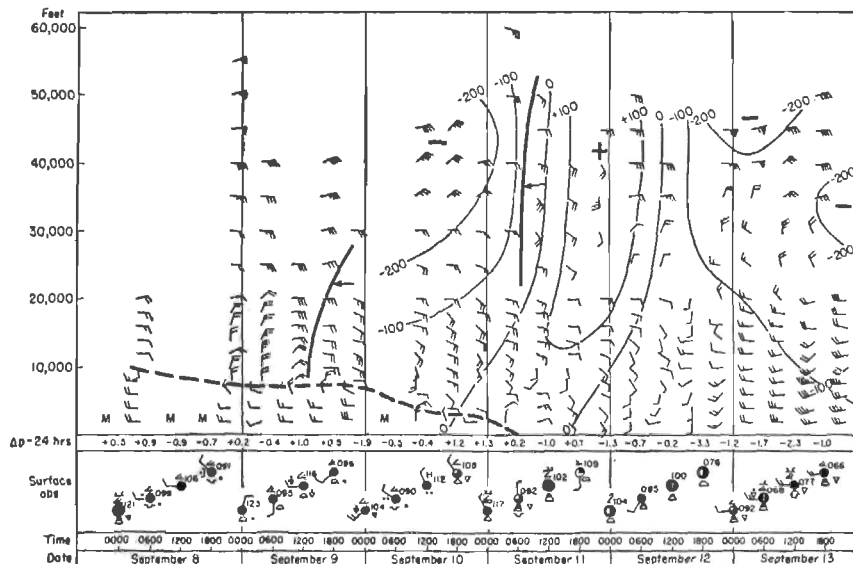


Fig. 1.25. Vertical time section at Palau, Sept. 8-13, 1945 (25). Heavy dashed line denotes equatorial trough.

the middle troposphere (500 mb). They rarely extend through the entire troposphere, in distinction to troughs and ridges of higher latitudes.

Basic Currents

The structure of disturbances in a variable broad-scale flow pattern depends in part on the structure of the basic currents, their direction, and vertical shear. In higher latitudes the westerly current almost always increases with elevation; a single type of basic current predominates. In contrast the easterlies sometimes increase and sometimes decrease upward. Moreover the tropics are subject to much larger changes of basic-current structure than the higher latitudes. As a result, the variety of disturbances is greater, and their occurrence has a definite seasonal course.

One can distinguish the most important zonal currents according to the following classification:

As in the case of the air-mass classification of higher latitudes it is of advantage to introduce a shorthand notation. The basic letters will be *E* and *W*, which denote the wind direction in the lower levels. The subscript *i* or *d* indicates whether the current strength increases or decreases upward. Sometimes the vertical shear is so great that the wind direction reverses above the low troposphere and the upper current carries the disturbances that determine the weather. In such cases the direction of the upper current is also added. *E_dW*, for instance, identifies a shallow trade with upper westerlies of sufficient strength and depth to govern the course of cloudiness and weather. *E_d*, however, denotes a gradual decrease of the easterlies. Any westerlies that may exist have little influence on the weather.

This classification, as all others, is necessarily incomplete and will be found wanting in some areas and situations. Experience has shown that it pays to classify only the main features. Excessive classification is cumbersome and often defeats its own end. This has been seen in the many attempts to refine the basic Norwegian air-mass scheme and the extreme breakdown to which the original Koeppen classification of climates has been subjected.

A brief description of the main currents of the tropics, using the notation just introduced, follows:

1. The deep trades *E_d* (Fig. 1.16) extend to 8–10 km and frequently to higher levels. They attain their broadest extent in summer and are located mainly in regions of mean troughs aloft. In winter they are restricted to a narrow belt along the equator.

2. The deep trades *E_i* (Fig. 1.17, June–August) also are mainly a summer current. They occur just equatorward from the mean subtropical high cells aloft and in portions of the equatorial zone.

3. The equatorial westerlies *W_d*, *W_{dE}* lie equatorward from the equatorial trough in a fairly narrow belt (Figs. 1.17, December–February, and 1.25). They are a feature of the summer hemisphere and are best developed in the northern summer. They also have been called "Indian westerlies" and "southwest monsoon" (9). Since these westerlies do not always act as would be expected from a purely monsoonal current, it is best to avoid terminology that carries a causal connotation. The term "equatorial westerlies" simply refers to the geographic fact that a broad intervening wedge of easterlies separates these westerlies from the polar westerlies.

Although the equatorial westerlies are usually confined to a portion of the troposphere, they may at times reach to the tropopause. Such situations have been noted by Bouscaren (2) on the East African coast.

4. The subtropical easterlies *E_d* occupy the poleward margin of the tropics in summer; ~~Regional Central Library~~ they tropical belt in winter.

Bangalore 560 024.

We also find this current equatorward of high-level shear lines in persistent situations with meridional highs (Chap. 10).

5. The polar westerlies W_i appear only intermittently near the poleward boundary of the tropics in winter.

The basic-current structure over any region cannot be deduced from single balloon ascents but only from cross sections or time sections. In view of the discussion of wind variability the instantaneous wind represents a combination of basic current and disturbance. For synoptic purposes running graphs of the wind averaged over a period from 3 to 5 days will isolate the basic current and its slow variations at one station.

REFERENCES

- (1) Bjerknes, V. F. K., *et al.*, *Dynamic Meteorology*, Vol. II. Washington, D.C.: Carnegie Institution of Washington, 1911.
- (2) Bossolasco, M., *Tellus*, **2**: 134 (1950).
- (3) Brooks, C. E. P., *Bull. Am. Meteor. Soc.*, **18**: 313 (1937).
- (4) Brooks, C. E. P., *et al.*, *Meteor. Off. Gr. Britain Geophys. Mem.* 85, 1950.
- (5) Brooks, C. E. P., and T. A. Mirrlees, *Meteor. Off. Gr. Britain Geophys. Mem.* 55, 1932.
- (6) Chaudhury, A. M., *Tellus*, **2**: 56 (1950).
- (7) Clayton, H. H., "World Weather Records," *Smithsonian Misc. Collections*, Vols. 79, 90, 105.
- (8) Colón, J. A., *Bull. Am. Meteor. Soc.*, **32**: 52 (1951).
- (9) Deppermann, C. E., *The Mean Transport of Air in the Indian and South Pacific Oceans*. Manila: Bureau of Printing, 1935.
- (10) Fassig, O. L., *Trans. Am. Geophys. Union*, **14**: 69 (1933).
- (11) Freeman, J. C., *Bull. Am. Meteor. Soc.*, **31**: 324 (1950).
- (12) Hess, S. L., *J. Meteor.*, **5**: 293 (1948).
- (13) Hess, S. L., *ibid.*, **7**: 1 (1950).
- (14) Hubert, L. F., *J. Meteor.*, **6**: 216 (1949).
- (15) Hutchings, J. W., *J. Meteor.*, **7**: 94 (1950).
- (16) Jordan, C. L., *Bull. Am. Meteor. Soc.*, **32**: 375 (1951).
- (17) Jordan, C. L., *Quart. J. Roy. Meteor. Soc.*, **76**: 343 (1950).
- (18) Knoch, K., in *Handbuch der Klimatologie*, Vol. II, Part G, W. Köppen and R. Geiger, eds. Berlin: Verlagsbuchhandlung Gebrüder Borntraeger, 1930 *et seq.*
- (19) Kuhlbrot, E., *Z. Geophys.*, **4**: 385 (1928). For other references on *Meteor* see Meinardus, W., *Ann. Hydr.*, **69**: 37 (1941).
- (20) Loewe, F., and U. Radok, *J. Meteor.*, **7**: 58 (1950).
- (21) Palmer, C. E., in *Compendium of Meteorology*. Boston: American Meteorological Society, 1951.
- (22) Priestley, C. H. B., *Australian J. Sci. Research*, **3**: 1 (1950).
- (23) Riehl, H., *Dept. Meteor., Univ. Chicago, Misc. Rept.* 17, 1945.
- (24) Riehl, H., *Dept. Meteor., Univ. Chicago, Misc. Rept.* 24, Part I, 1948.
- (25) Riehl, H., *J. Meteor.*, **5**: 247 (1948).
- (26) Riehl, H., *Tellus*, **2**: 1 (1950).
- (27) Riehl, H., and T. C. Yeh, *Quart. J. Roy. Meteor. Soc.*, **76**: 182 (1950).
- (28) Riehl, H., T. C. Yeh, and N. E. La Seur, *J. Meteor.*, **7**: 181 (1950).
- (29) Scherhag, R., *Neue Methoden der Wetteranalyse und Wetterprognose*, Berlin: Verlag Julius Springer, 1948.

- (30) Schott, G., *Geographie des Atlantischen Ozeans*. Hamburg: C. Boysen, 1944.
- (31) Schott, G., *Geographie des Indischen und Stillen Ozeans*. Hamburg: C. Boysen, 1935.
- (32) Serra, A., *La circulation générale de l'Amérique de Sud*. Rio de Janeiro: Serviço de Meteor., Brazil, 1939.
- (33) Serra, A., and L. Ratisbonna, *As massas de ar da America do Sul*. Rio de Janeiro: Serviço de Meteor., Brazil, 1942.
- (34) Shaw, Sir Napier, *Manual of Meteorology*, Vol. II. Cambridge: Cambridge University Press, 1936.
- (35) Solot, S. B., *Bull. Amer. Meteor. Soc.*, **31**: 85 (1950).
- (36) Stone, R. G., *Bull. Amer. Meteor. Soc.*, **23**: 4 (1942).
- (37) Taylor, G., *Australian Meteorology*. New York: Oxford University Press, 1920.
- (38) Taylor, G., in *Handbuch der Klimatologie*, Vol. IV, Part S, W. Köppen and R. Geiger, eds. Berlin: Verlagsbuchhandlung Gebrüder Borntraeger, 1930 et seq.
- (39) U.S. Department of Commerce, Weather Bureau, *Airways Meteorological Atlas for the United States*. Washington, D.C., 1941.
- (40) U.S. Department of Agriculture, Weather Bureau, *Atlas of Climatological Charts of the Oceans*. Washington, D.C., 1938.
- (41) Van Bemmelen, W., *Meteor. Z.*, **41**: 133 (1924).
- (42) Wagner, A., in *Handbuch der Klimatologie*, Vol. I, Part F, W. Köppen and R. Geiger, eds. Berlin: Verlagsbuchhandlung Gebrüder Borntraeger, 1930 et seq.
- (43) Werenskiold, W., *Geof. Publikasjoner*, Vol. 2, No. 9, 1923.
- (44) Wexler, H., *Bull. Am. Meteor. Soc.*, **32**: 52 (1951).
- (45) Yeh, T. C., *Tellus*, **2**: 173 (1950).

CHAPTER 2

TEMPERATURE

The middle latitudes go through a cycle of seasons which, seen climatically, is both definite and regular. As the sun rises toward the zenith, spring and summer follow winter; as it sinks, fall and winter succeed summer. Closer to the equator this seasonal rhythm, which so strongly patterns middle-latitude life, becomes less and less clear-cut. The growing season, at least seen thermally, lasts through the whole year; the need for heated homes and seasonal clothing disappears. Overhead, the sun reaches the zenith, not only once, but over most of the tropics twice (Fig. 2.1). The middle-latitude traveler needs a long time to

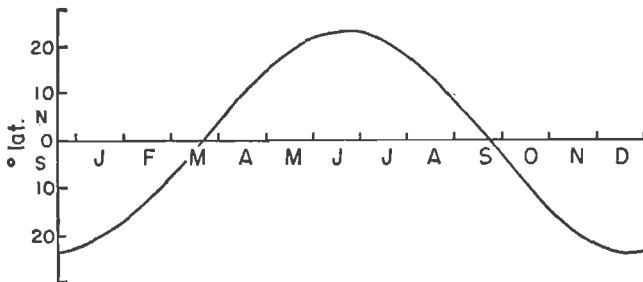


FIG. 2.1. Annual march of sun's zenithal latitude.

accustom himself to the fact that his shadow points the "wrong" way in the noon hours.

In mountainous countries the slopes offer relief from the heat of the lowlands. Many cities and summer residences lie at an altitude of several thousand feet, where living is pleasant and refreshing. The climatic changes with height are well known to the inhabitants; in Central and South America one speaks of the "torrid," "temperate," and "frigid" zones.

Seasons in the Tropics

As the sun's position changes only gradually at the solstices (Fig. 2.1), the time spent by the sun poleward of a given latitude increases very rapidly just equatorward from the Tropics of Cancer and Capricorn. Already at latitudes 20° (Fig. 2.2) this time amounts to 2 months, and

these are months of nearly constant overhead sun. At latitudes 15° the sun passes the zenith at the end of April and in August in the northern hemisphere, at the end of October and in February in the southern hemisphere. A simple rise and fall of temperature as the sun advances and recedes in the sky is not to be expected in the heart of the tropics.

In place of the temperature cycle moisture comes into the foreground. Life in the tropics is completely dependent on abundant rain. Annual rainfall, however, varies much more widely from place to place than mean annual temperatures; the concept of "dry" and "rainy" seasons replaces the four-season temperature cycle of middle latitudes. The forecaster seldom is asked what the temperature will be; but everyone wants to know about the expected rainfall, especially the seasonal rainfall that spells success or failure for the crops.

On any latitude circle the dry and rainy seasons do not occur simultaneously at all longitudes. The regular shifts of the major wind systems are not accompanied by equally regular shifts of the precipitation belts. Thus, in Chap. 1, the terms "winter" and "summer" were used as extensions of the middle-latitude climates. This was not unreasonable, since the circulation does change substantially in accordance with the large fluctuations outside the tropics. To the extent that we compute averages in the treatment of temperature and rainfall, we shall continue to apply this procedure.

World Distribution of Surface Temperature

Figure 2.3 gives the mean annual temperature range, defined as the temperature difference between warmest and coldest month. This range approaches the vanishing point everywhere near the equator. We should not infer from this that the minute changes pass unnoticed by the residents—natives and high-latitude-born alike. As the fluctuations of temperature decrease, our sensitivity to small variations multiplies. We may feel a drop of 1°C in the tropics as acutely as the change from October to November in northern climates.

From the climatological standpoint the annual temperature range becomes so insignificant in the equatorial zone that it is impossible to guarantee the shape and extent of the 1°C line in Fig. 2.3; even the course of the 2.5°C line is dubious in places. As might be anticipated, the temperature range not only decreases equatorward from middle latitudes;

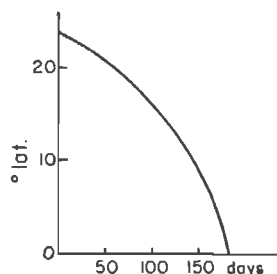


Fig. 2.2. Number of days spent by sun poleward of a given latitude.

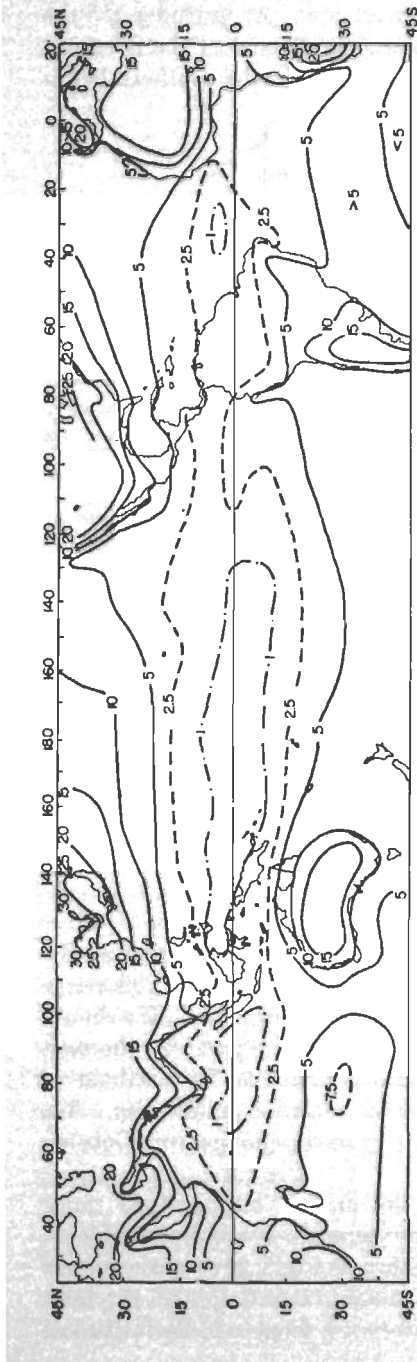


Fig. 2.3. Mean annual temperature range ($^{\circ}\text{C}$) at sea level.

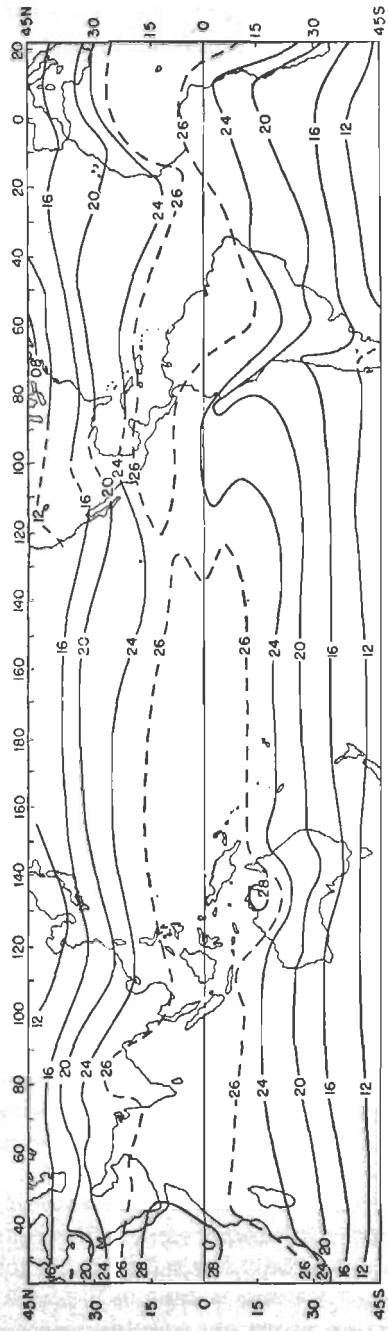


Fig. 2.4. Mean annual isotherms ($^{\circ}\text{C}$) at sea level.

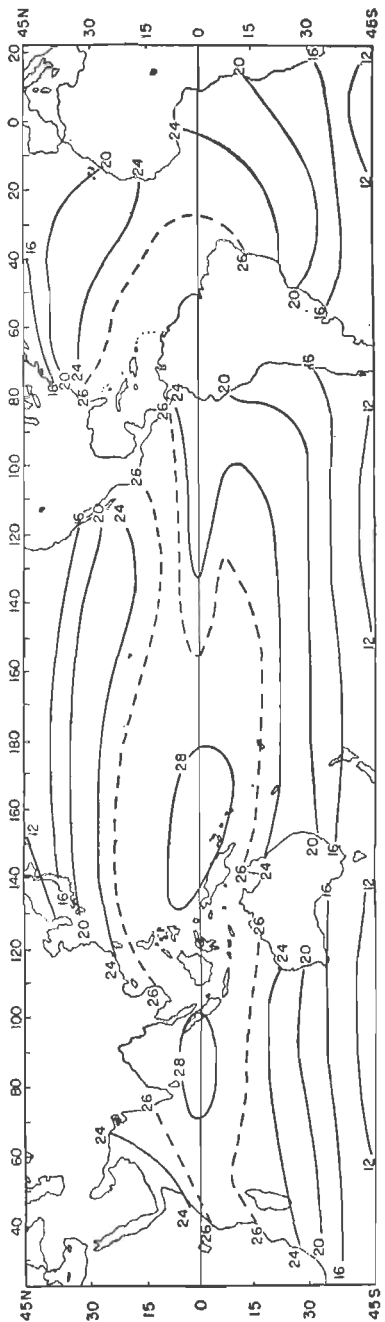


Fig. 2.5. Mean annual temperatures ($^{\circ}\text{C}$) of the sea surface.

on any latitude circle, except quite close to the equator, it remains much greater over the continents than over the oceans. Over the continents the range may be 5–10° or more on latitudes where the oceanic range is 2–3°.

Because of the smallness of the temperature range a cursory comparison of the temperature field in different seasons cannot reveal changes as striking as in the wind field. We therefore need only glance at a map of the mean annual temperature distribution (Fig. 2.4). The isotherms so nearly follow the latitude circles that the predominant solar control of the temperature climate is placed beyond dispute. Various anomalies exist, however. Over the continents the isotherms bulge poleward, and this cannot be attributed entirely to reduction of temperature to sea level. Continental mean temperatures exceed those over the oceans; stronger insolation during the warmer seasons overcompensates for any negative anomalies in the cooler seasons. Over the oceans the outstanding fact is the equatorward trend of the isotherms from west to east. The western parts of the oceans are warmer than the eastern portions. In broad terms we can readily relate this fact to the wind circulation (Fig. 1.7). The strongest equatorward transport of air by the trades takes place in the eastern parts of the oceans; this air coming from middle latitudes is relatively cold.

The pattern of Fig. 2.4 bears a striking resemblance to the oceanic surface-temperature field (Fig. 2.5). This coincidence between the two sets of lines is so close that differences between ocean and air temperature greater than 1°C are rare; it is impossible to draw reliable lines of this temperature difference. The largest part of the tropical oceans appears to be slightly warmer—near 0.5°C on the average—than the air, both in the annual mean and the seasonal breakdowns.

Seasonal March of Temperature

Since the isotherms by and large run so nearly parallel to the latitude circles, we can average temperatures around the globe as we did for pressure in Fig. 1.1. This yields a graph of the mean temperature of latitude circles in different seasons (Fig. 2.6). The latitude with highest temperature migrates with the equatorial trough. In January, the air is warmest near 5°S, exactly the latitude of the trough; in July, it is warmest at 20°N, slightly to its north. This displacement results from the very high temperatures over the northern subtropical deserts.

The cross-over point between the January and July curves is near 5°N, the mean annual latitude of the trough. From there the seasonal temperature range increases, but at a more rapid rate in the northern than in the southern hemisphere. The range amounts to 13°C at 30°N and

7°C at 30°S . This is reasonable because of the large land masses in the north.

Mean annual temperatures are distributed symmetrically not with respect to the geographical equator but with respect to the "heat equator"— 5°N . Throughout the tropics the southern hemisphere is slightly cooler than the northern hemisphere— 1.4°C at latitude 10° , 2.3°C at 20° , and 1.9°C at 30° .

A revealing picture of longitudinal variations in mean temperature and its seasonal course is furnished by Fig. 2.7, where temperature is plotted against longitude at 15°S . Outstanding are the tremendous depressions of temperature just west of the American and African continents, which are accentuated in winter. These depressions result not only from the equatorward transport of polar maritime air over the eastern parts of the oceans; the familiar upwelling of cold water along west coasts is also responsible. Since both South America and South Africa protrude westward with decreasing latitude, in contrast to North America and North Africa, and since the strength of the mean winds at the coasts does not decrease from summer to winter as in the northern hemisphere, the effect of the upwelling is

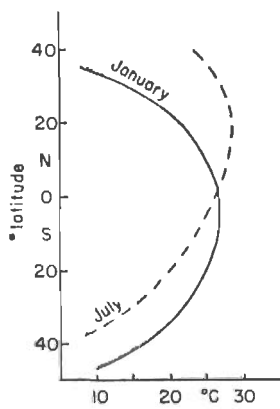


Fig. 2.6. Mean sea-level temperature profiles ($^{\circ}\text{C}$).

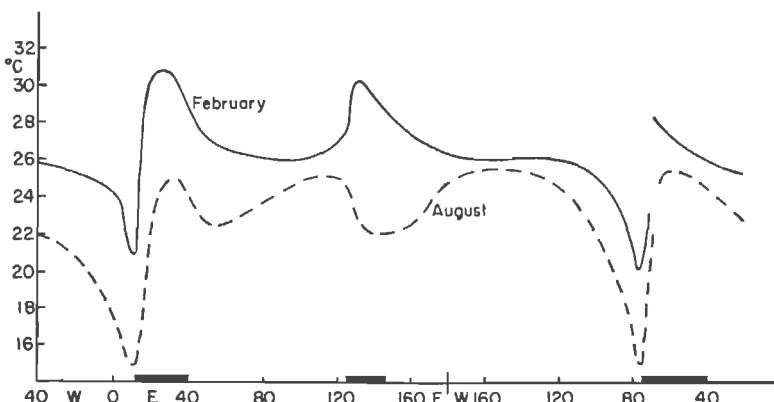


Fig. 2.7. Longitudinal profile of mean sea-level temperature ($^{\circ}\text{C}$) at 15°S .

greatest in the southern hemisphere. It extends to much lower latitudes, and it does not disappear in winter.

Elsewhere Fig. 2.7 confirms the features of the temperature distribution just discussed: the small temperature range over the oceans compared

with the continents—especially Africa and Australia—the peak temperatures over land, and the gradual lowering of temperature from west to east across the oceans, evident everywhere except in the Indian Ocean in August.

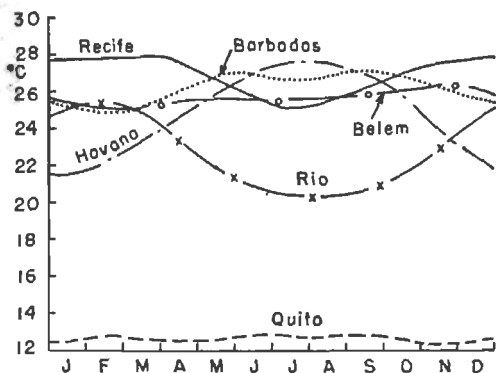


Fig. 2.8. Seasonal course of mean monthly temperature ($^{\circ}\text{C}$) along the eastern shore of the Americas: Havana (24°N , 82°W), Barbados (13°N , 59°W), Belem (1°S , 48°W), Recife (8°S , 35°W), Rio de Janeiro (23°S , 43°W). Also Quito, Ecuador (0° , 78°W ; elevation 9,200 feet).

Next we shall glance at the annual course of temperature at individual places. Our interest lies in discovering something about the typical behavior of the temperature cycle; detailed climatography is not our objective. So we shall restrict the analysis to three cross sections—one running along the east coast of South America to the Antilles, another

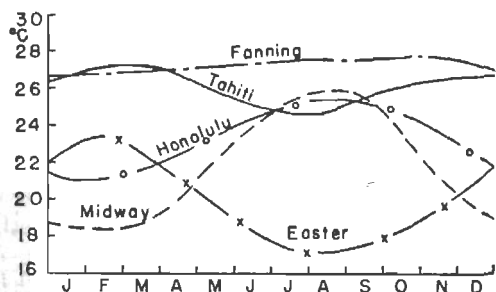


Fig. 2.9. Seasonal course of mean monthly temperature ($^{\circ}\text{C}$) in the east central Pacific Ocean: Easter Island (29°S , 109°W), Tahiti (18°S , 148°W), Fanning Island (4°N , 159°W), Honolulu, Hawaii (21°N , 158°W), Midway Island (28°N , 177°W).

north-south in the middle of the Pacific Ocean, and a third through the interior of Africa.

Both in the Pacific and on the South American coast, exposed to the easterly trades of the Atlantic (Figs. 2.8 and 2.9), we should look for "oceanic"-type temperature curves in the subtropics with late summer

maxima and late winter minima. We observe such curves at Rio de Janeiro in South America and at Havana, its Caribbean counterpart; at Tahiti and Honolulu, in the south and north Pacific. In accentuated form similar curves appear at Midway and Easter Islands, located near the equatorial margin of the belts of polar westerlies in the Pacific.

Closer to the equator we look for a flattening of the subtropical summer maxima. This we observe both at Recife and Barbados. Near the equator itself, at Fanning Island and Belem, the curves are quite indifferent. This also holds for Quito, Ecuador, which has been added for comparison in Fig. 2.8. Here the mean annual temperature is low since the city lies near 3,000 m altitude in the Altiplano of the Andes. The temperature curve, one of the steadiest in the world, oscillates irregularly over a range of about 1°C. Combination of the agreeable mean temperature with so small an annual range, but a strong diurnal variation, gives Quito one of the most desirable climates in the tropics, in the opinion of many.

If the mean monthly temperature on the equator varied strictly with the sun, we should find two minima at the solstices and two maxima at the equinoxes. Cloudiness and rainfall, however, enter as factors of at least equal importance. In the rainy season, frequent daytime showers hold the maximum temperatures down; an equal increase of minimum temperatures due to reduced nocturnal radiation is seldom found. Changes in the maximum temperature largely determine the course of the mean temperature, which then has a tendency to drop during the rainy season. Actually the curves of all three equatorial stations in Figs. 2.8 and 2.9 tend to run inversely to their rainfall curves, especially Belem and Fanning (Chap. 3).

The third section, taken from south to north through the mountainous interior of Africa near 30°E (Fig. 2.10), departs strikingly from the oceanic regimes. Khartoum in the Sudan and Bulawayo in Southern Rhodesia have strong seasonal temperature changes; the minima quite properly fall in the center of the respective winters. In these dry locations all cloudiness and rainfall are concentrated in a brief summer period. Temperatures rise sharply through the spring months, but this increase ends abruptly with the advent of the rainy season. Khartoum experiences its greatest heat in May–June, Bulawayo in October–November. Then temperatures drop under the influence of the increased cloud cover, even though the precipitation may be quite small.

Khartoum also has a secondary temperature maximum in September–October, a feature not in evidence at Bulawayo. This secondary maximum, typical for large parts of the monsoon countries, develops as the rainy season ends while the sun is still high in the sky. From many accounts, especially from India, we hear that the recurrence of great heat in September and October is very trying for persons who have just lived

through the spring heat and the humid summer and who are anxious for the start of the cooler and more pleasant winter period. Not everywhere, however, does the cool season bring unmixed blessing. In the Sudan, for instance, it is the time of prolonged sandstorms.

The Bulawayo and Khartoum curves can serve as limits for the type of temperature trace typical in monsoon countries. Khartoum has a double maximum of temperature with a secondary August minimum; Bulawayo just shows a gradual drop of temperature after the late spring maximum. Anyone glancing over the vast number of temperature records accumulated in monsoon countries, especially India, will find all kinds of temperature curves that lie intermediate between those reproduced here.

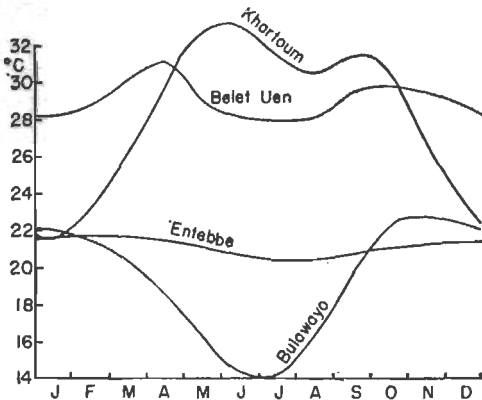


Fig. 2.10. Seasonal course of mean monthly temperature ($^{\circ}\text{C}$) in Africa: Bulawayo (20°S , 29°E ; elevation 4,400 feet), Entebbe (0° , 32°E ; elevation 3,800 feet), Khartoum (15°N , 32°E ; elevation 1,200 feet). Also Belet Uen (5°N , 45°E ; elevation 600 feet).

Entebbe, situated on the northern shore of Lake Victoria, lacks a marked temperature cycle, as is typical for the other equatorial stations. On the equator the difference between continental and oceanic regimes vanishes, as also apparent from Fig. 2.3 and the curve of Quito (Fig. 2.8). Entebbe differs from the other stations in that the rainy season coincides with the highest temperatures, while the cooler season is the dry season. Thus we cannot lay down any rule on the relation between temperature and rainfall cycles that is valid throughout the equatorial belt. Many local factors come into the foreground, as the presence of Lake Victoria in the case of Entebbe.

Finally we have the temperature trace from Belet Uen, located on the barren desert shore of East Africa near 5°N . Superficially this trace looks fairly similar to that of Khartoum. Yet the explanation of the summer minimum of temperature must be different since Belet Uen is completely dry in summer. In this season the station lies in a regime of very strong southerly winds with some onshore component. Other

places, such as Zanzibar (6°S , 39°E) and the Seychelles Islands (5°S , 55°E), also report lower temperatures from June to August. We can reason that the southern-hemisphere air is advected so rapidly across the equator that it lacks time for complete transformation from its original polar characteristics. In addition, the wind stress on the ocean produces an upwelling of cold water along the coast north of the equator just as along the West African coast; this intensifies the temperature anomalies. Indeed, farther north toward Cape Guardafui (12°N , 51°E) there exists a fog regime which in origin is fully comparable with those of the subtropical west coasts.

Belet Uen shows that a temperature curve with two maxima and a secondary minimum cannot simply be adjudged as indicative of a monsoon regime. This case is not unique. As we go around the equatorial belt, we find a manifold variety of temperature curves conditioned by the combination of a host of general and local factors. Of these, we have been able to present only a few basic types. But Belet Uen should emphasize that only a careful study of local conditions can lead to an interpretation of the details of the temperature climate at any station near the equator.

Temperatures of the Upper Air

One fact about the thermal structure of the atmosphere over the tropical oceans overshadows everything else in importance. Over the eastern portions we encounter a temperature inversion in the lower atmosphere, the *trade-wind inversion*; generally situated below 3 km (Fig. 2.11). Below the inversion the atmosphere is filled with many cumulus clouds, and the temperature lapse rate is very steep. Above it the air is exceedingly dry, and the lapse rate becomes steeper with increasing altitude to reach values of $0.8\text{--}0.9^{\circ}\text{C}/100\text{ m}$, not far from the dry-adiabatic lapse rate, in the layer under the tropopause.

In the equatorial-trough zone and over the western parts of the trade-wind belt an inversion does not exist as a mean condition, though stable layers appear in specific weather patterns. The lapse rate is nearly moist-adiabatic through the bulk of the troposphere, and the moisture content of the air is higher than in the regions with inversion. But there is often a level above which the relative humidity drops to low values in spite of thermal instability; this is shown by the sharp decrease of relative humidity above 800 mb in the solid curve of Fig. 2.11. We shall study this curious phenomenon in Chap. 5. Here we merely wish to establish the fact that, except for the active portions of disturbances, the tropical troposphere generally can be divided into a *lower moist* and an *upper dry layer*.

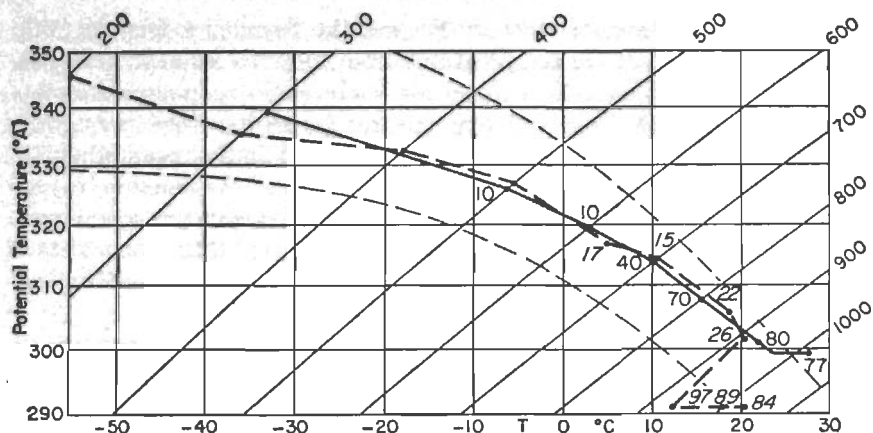


Fig. 2.11. Tephigram of the radiosonde ascents at 30°N, 140°W, July 10, 1949, 0300Z (dashed), and at San Juan, Puerto Rico, Aug. 14, 1943, 0300Z (solid). Numbers on curves indicate relative humidity (per cent).

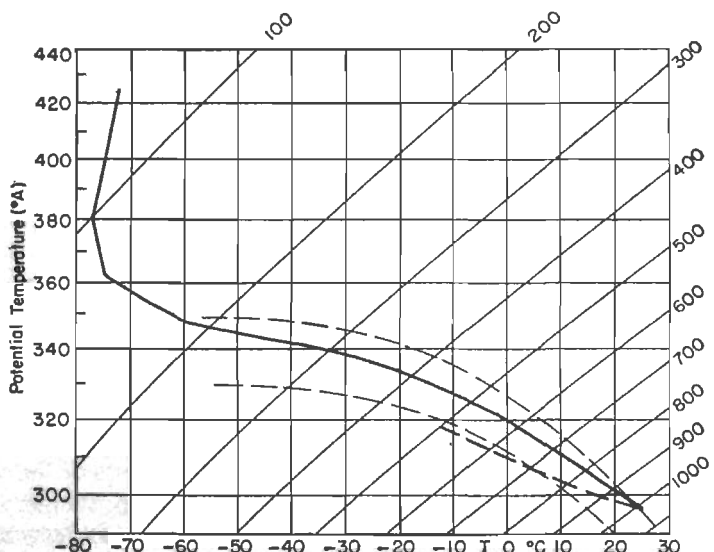


Fig. 2.12. Tephigram of the mean atmosphere for the Caribbean during the hurricane season (19). Temperature (solid); wet-bulb potential temperature (dashed).

Mean Tropical Atmosphere. The structure of the trade inversion is quite complex. Over the western parts of the oceans, in contrast, the temperature of the tropical atmosphere is nearly homogeneous in the horizontal, especially during the rainy season. We can show its average properties by mean soundings. Schacht (19) has prepared such a sounding for the Caribbean area from radiosonde data of the rainy season at

San Juan, Puerto Rico; Swan Island (17°N , 84°W); and Miami, Florida. Table 2.1 gives the pertinent numerical data, and Fig. 2.12 shows the lapse rates of temperature and wet-bulb potential temperature. The temperature lapse rate exceeds the moist-adiabatic rate below 600 mb, then equals it to 300 mb. This temperature distribution alone shows

TABLE 2.1. MEAN TROPICAL ATMOSPHERE AT MIDNIGHT FOR THE CARIBBEAN AREA DURING THE RAINY SEASON

Level, mb	Height		Temperature, °C	Specific humidity, g/kg	Relative humidity, per cent	Wet-bulb potential temperature, °A
	10's, ft	10's, m				
1,013.6	0	0	25.3	18.1	85	
1,000	39	12	24.7	17.4	85	297
900	341	104	19.5	13.5	83	295
800	672	205	14.2	9.5	73	293
700	1,039	317	8.4	6.2	60	292
600	1,452	443	1.5	3.7	52	291
500	1,927	587	-6.8	2.2	48	291
400	2,487	758	-17.3			
300	3,173	967	-32.6			
200	4,067	1,240	-54.8			
175	4,342	1,323	-61.2			
150	4,652	1,418	-68.0			
125	5,006	1,526	-74.3			
100	5,428	1,654	-77.0			
75	5,974	1,821	-72.0			

the dominant role of convection in shaping the tropical atmosphere. The tropopause lies at 100 mb with a temperature of -77°C ; the sounding already begins to stabilize at 180 mb, a reflection of secondary tropopauses in disturbances (6).

As seen from Table 2.1 the moisture decreases steadily with height. No division between moist and dry layers appears. This should be expected since the depth of the moist layer fluctuates strongly from day to day—in contrast to temperature—and the averaging process washes out any pronounced boundaries. The lapse rate of wet-bulb potential temperature, a function of temperature and moisture lapse rates, exceeds the moist-adiabatic rate to 500 mb. Formerly considered very significant, the wet-bulb potential temperature has declined in importance in modern meteorology since it is not as conservative an air-mass property as it was once thought to be. It remains true, however, that this temperature must decrease upward for large-scale convection to occur.

Mean soundings can be prepared for other tropical regions. Colón (3) has computed such a sounding from nighttime ascents during the typhoon

season at Guam (13°N , 144°E). This sounding departs surprisingly little from that for the Caribbean. Guam is only slightly warmer and more moist in the low levels, slightly cooler in the high troposphere.

Seasonal Temperature Changes. Corresponding to the small surface-temperature changes, the seasonal range of upper temperatures below 300 mb generally lies within $1\text{--}2^{\circ}\text{C}$. Swan Island (Fig. 2.13) is typical. The cool and dry seasons coincide. Nearly all the cooling takes place below 700 mb, and here the air becomes a little more stable, as is common throughout the tropics in the dry season. Figures 2.14 and 2.15 give

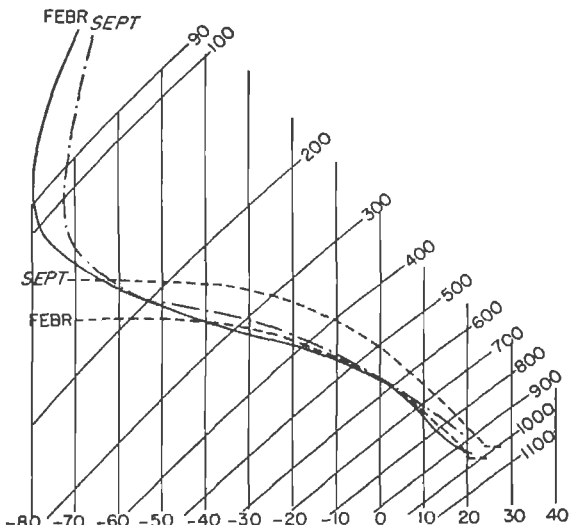


Fig. 2.13. Mean tephigram for February and September at Swan Island (17°N , 84°W) (13).

the seasonal temperature changes at 80°W and 170°E , computed from Figs. 1.14 and 1.15. They illustrate how negligible are these changes in the low and middle troposphere.

Over the western Pacific the northeast monsoon regime prevails in winter. There we might look for greater seasonal temperature changes than in the Caribbean, especially greater stability of the low troposphere in winter. The changes, however, are small even here. Typical ascents for typhoon and winter monsoon seasons at Guam are shown in Figs. 2.16 and 2.17. Above 700 mb the soundings are nearly identical. Lower down the monsoon sounding actually is warmer than the summer sounding, but it has a deep isothermal stratum between 900 and 800 mb with relatively dry air in the stable layer. As is evident also from Figs. 2.14 and 2.15 the seasonal temperature changes through a deep layer of the

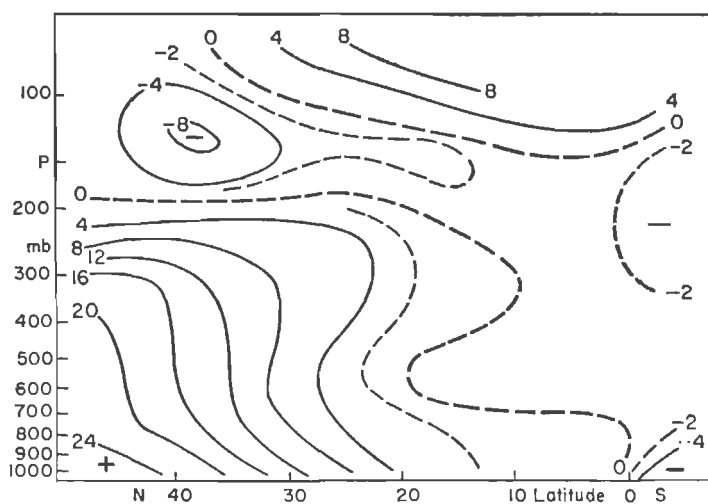


Fig. 2.14. Seasonal temperature changes from winter to summer ($^{\circ}\text{C}$) at 80°W (from Fig. 1.14).

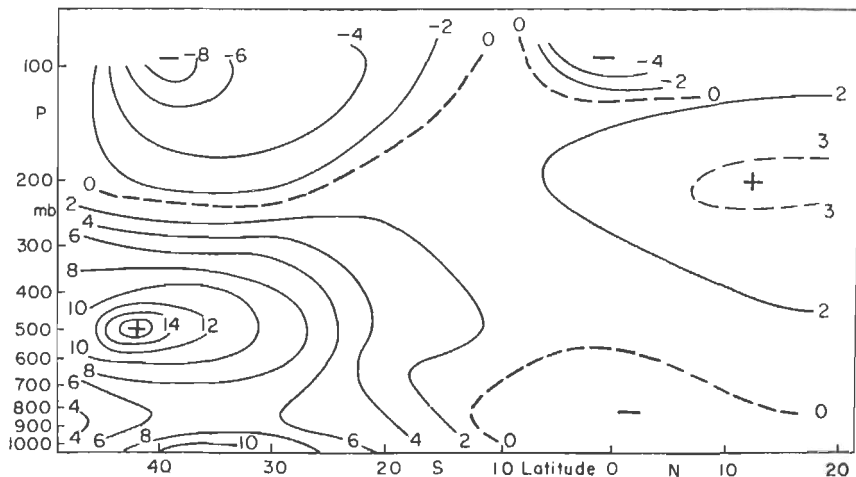


Fig. 2.15. Seasonal temperature changes from winter to summer ($^{\circ}\text{C}$) at 170°E (from Fig. 1.15).

troposphere are very small. They can even run opposite to the sun's march, as in Fig. 2.15 north of the equator.

Above 200 mb, the picture of Fig. 2.13 is quite different. The winter atmosphere is decidedly colder— 8°C at 90 mb—and the mean tropopause height is about 30 mb higher. Figure 2.14, which incorporates the data of Fig. 2.13, shows the same seasonal trend, and this is further confirmed by a time section of seasonal temperature anomalies above 10 km at

Puerto Rico (Fig. 2.18), based on data for 1942–1943 (6). The seasonal trends over Puerto Rico and nearby Swan Island are not identical. At Puerto Rico, the layer from 10 to 16 km actually is warmest in the middle of winter; temperatures drop only above 16 km. Puerto Rico, like Swan Island, experiences a rise of the tropopause from summer to winter, which

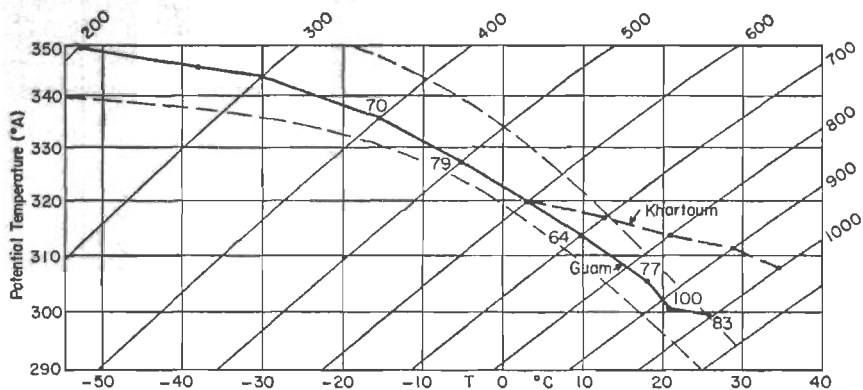


Fig. 2.16. Tephigram for Guam, Aug. 7, 1951, 1500Z (solid), and for maritime tropical air at Khartoum [dashed (22)].

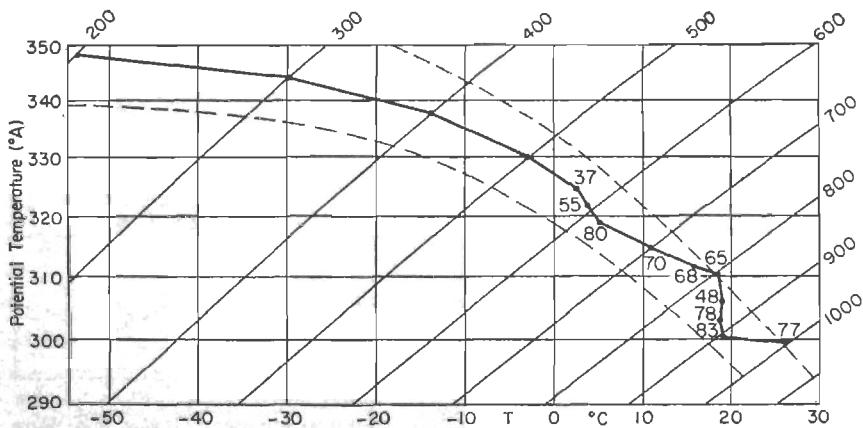


Fig. 2.17. Tephigram for Guam, Dec. 6, 1951, 1500Z.

leads to a very large seasonal temperature range at 18 km, no less than 13°C . Such strong fluctuations of temperature near the tropopause do not occur everywhere in the tropics (Fig. 2.15). Thus the course of high-level temperatures observed over the Caribbean and other regions with similar temperature changes cannot be explained entirely by radiation or convection theories of tropopause formation. In fact, the tropopause changes over the Caribbean run counter to the convectional hypothesis, which

demands highest tropopauses in the season of strongest convective activity.

Over the tropical continents temperature changes far exceed those over the oceans. Much has been published about this subject in India, Australia, and South America (21). Here we present data on Khartoum in the Sudan (22) (Table 2.2), which may be compared with the annual

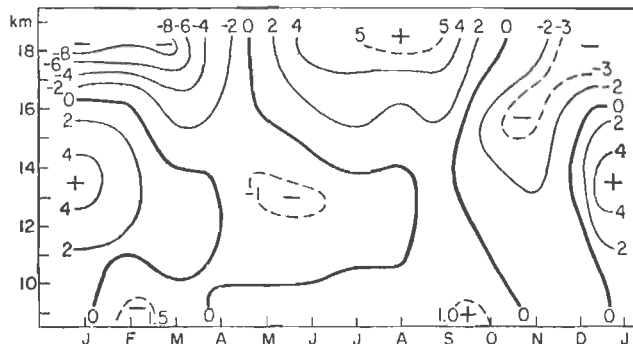


Fig. 2.18. Seasonal temperature anomalies ($^{\circ}\text{C}$) from the annual means above 10 km at Puerto Rico (6).

march of surface temperature (Fig. 2.10). The surface layer experiences two maxima and minima. This double cycle is noticeable up to 800 mb; above 700 mb the whole seasonal temperature variation approaches zero. All changes are confined to the lowest 3 km, just as in the oceanic regime of Swan Island. By analogy, a second layer of large temperature

TABLE 2.2. MEAN SEASONAL SOUNDINGS AT KHARTOUM (22)

	Sur- face	900 mb	800 mb	700 mb	600 mb	500 mb	450 mb
Virtual temperature, °C:							
November–April.....	31	25	19	12	3	-7	-11
May–June.....	39	32	23	14	4	-6	-9
July–August.....	33	26	20	12	3	-6	-10
September–October.....	36	29	21	12	3	-7	-11
Mixing ratio:							
November–April.....	7.5	6.3	4.0	3.5	3.0		
May–June.....	10.7	9.5	7.0	5.3	4.5		
July–August.....	17.5	15.0	11.0	7.6	5.8		
September–October.....	11.8	10.0	7.8	6.0	4.4		
Relative humidity:							
November–April.....	26	29	23	29	38		
May–June.....	25	30	34	40	57		
July–August.....	60	66	66	65	82		
September–October.....	33	37	42	50	59		

changes may be found in the tropopause region. Table 2.2 also shows that, at variance with the march of temperature, the moisture content of the atmosphere and the relative humidity go through a simple annual cycle, with maximum in July-August and minimum in November-April.

Air Masses of the Continents

It is reasonable to suppose that large seasonal temperature changes reflect the predominance of different air masses in the classical sense at different times of the year, especially when the amplitude of the changes weakens with height. At Khartoum, air-mass characteristics range from

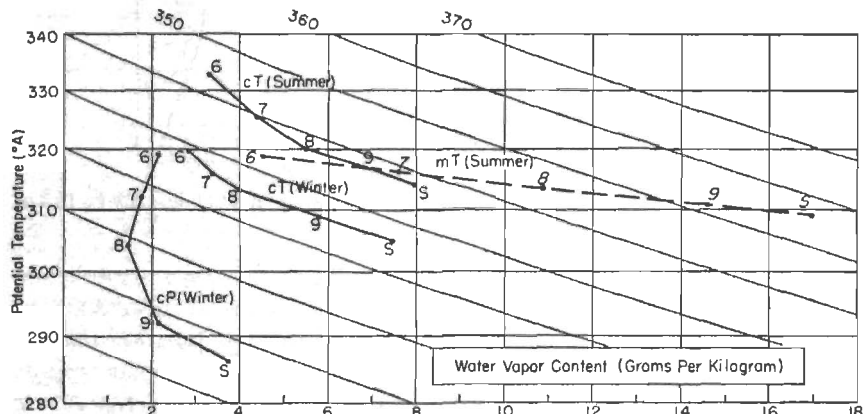


Fig. 2.19. Rossby diagram of the principal air-mass curves at Khartoum (22). Numbers along curves indicate pressure (100's mb).

modified continental polar air (cP) of winter to continental tropical air (cT) of summer, for which, of course, North Africa is the home ground. Figure 2.19 and Table 2.3 show the characteristic properties of the principal air masses.

Outstanding is the great heat of the cT and its rather stable lapse rate above 800 mb, which suggests that subsidence is partly responsible for the very high temperatures. On some days, one can even find inversions above 600 mb. The moisture content of cT is not nearly so small as one might suspect from the extremely low relative humidities. These are brought about by the high temperatures with large saturation specific humidities. During summer the moisture content of cT is comparable with that of cP and mP over Europe and North America in that season (cf. 2).

In maritime tropical air (mT), the distribution of specific humidity parallels that of the mean atmosphere over the oceans. The wide devia-

tion of the temperature curve (Fig. 2.16) is certainly a consequence of land heating, because the temperature difference between mT over sea and land is largest at the ground and vanishes at 600 mb. As over the oceans, one cannot distinguish a moist and a dry layer in the mean. For Khartoum this is reasonable, since mT reaches this part of the Sudan in depth only in disturbed situations when a depression in the equatorial trough passes through the Sudan and when, in consequence, the mT has undergone much convergence.

The structure of the cP air is typical for polar air that has, with subsidence, moved far equatorward from its source. A temperature inversion is situated between 900 and 800 mb; a minimum of specific humidity marks the inversion top; this structure is typical for currents that subside with divergence. Very often, the subsidence inversion is characterized not only by a sharp moisture decrease through the inversion but also by some increase of moisture content at higher levels.

TABLE 2.3. TYPICAL AIR-MASS PROPERTIES AT KHARTOUM (22)

	Sur- face	900 mb	800 mb	700 mb	600 mb
Virtual temperature, °C:					
cT (summer).....	41	35	27	21	15
cT (winter).....	32	27	20	12	3
mT (summer).....	35	29	21	13	3
cP (winter).....	13	10	12	9	3
Mixing ratio:					
cT (summer).....	8.0	6.8	5.5	4.4	3.3
cT (winter).....	7.5	5.8	4.0	3.4	2.8
mT (summer).....	17.0	14.7	10.9	7.5	4.5
cP (winter).....	3.8	2.2	1.5	1.8	2.2
Relative humidity:					
cT (summer).....	16	16	19	19	18
cT (winter).....	24	23	22	26	35
mT (summer).....	46	51	55	53	56
cP (winter).....	42	26	14	17	28

Air Masses over the Oceans

The literature carries a large number of air-mass definitions for the oceans. Among these are "maritime equatorial," "maritime tropical," and "trade-wind" air. Such definitions imply that certain areas act as source regions for these varying air-mass structures; that soundings which correspond to these structures are observed at individual stations in succession as disturbances pass over them; and that the observed changes of thermal and moisture properties may be explained mainly by horizontal

advection. This picture is drawn in analogy to the Norwegian method of describing changes of temperature and moisture in high latitudes.

It is true that modified polar air sometimes reaches the tropical oceans in winter (Chap. 10). It is also true that radiosonde observations on tropical islands report changes of temperature, temperature lapse rate, and moisture content from day to day. But it is far from certain that we can interpret these changes as given above. The amplitude of the changes increases upward over the oceans, in contrast to Khartoum and other continental locations, where they decrease upward in conformity with air-mass concepts. Near the surface, temperature variations seldom exceed 1°C . They are therewith entirely in the range of error of the measuring instruments and local modifications of the air due to cloudiness and evaporation from falling rain. As also stressed by Palmer (14), it is tenuous to deduce the existence of important air-mass changes from such minute, often accidental fluctuations.

When looking at the distribution of upper temperatures and moisture values around disturbances, we can offer an interpretation of these distributions alternate to the air-mass hypothesis. In many quasi-stationary or slowly moving wave troughs in the easterlies, cloudiness, rainfall, and lack of stable layers predominate in the eastern half of the system; relatively clear skies associated with stable layers or temperature inversions, in the western half. This weather pattern and associated thermal structure do not vary with time relative to the system. The air itself, moving with the winds, passes from one side of the disturbance to the other within 1–2 days. *It is then, in the same air, that the soundings record a deep moist layer and absence of inversions on one day and a shallow moist layer with inversions on the next.* Changes must take place within the moving air to permit the soundings to record what they do record. If advection of air masses from different source regions governed the temperature and moisture field, it would never be possible for these fields to remain stationary while the air moves through them.

We herewith must abandon the advective hypothesis as the only valid explanation of temperature and moisture changes. *Dynamic features of the wind field often govern the observed gradients of temperature and moisture aloft.* Basically, the tropical current is nearly homogeneous in its horizontal properties. We may interpret increases in the depth of the moist layer as being due to low-level convergence on account of mass-continuity considerations and decreases plus the appearance of stable layers as being due to low-level divergence (16).

A thermodynamic classification of air masses over the tropical oceans is not only largely without point but quite likely to lead to an erroneous view of temperature and moisture changes. In particular we must modify the classical concept of formation and maintenance of mT air as a

tropical air mass with high moisture content extending to great heights. The tropical current encountered over the vast oceanic regions does not possess such a deep moist layer. On the average, the top of the convective clouds is found near 8,000 feet, variable mainly with the season. Only convergence associated with specific disturbances produces large increases in the depth of the moist layer. Maritime tropical air with a deep moist layer does not have a persistent source region. It is generated locally east of wave troughs in the easterlies and other disturbances of the trade-wind belt; it also arises in portions of the equatorial-trough zone (Chaps. 9 and 10). Air masses with considerable moisture content have arrived at the Gulf coast of the United States during periods of southerly flow without any previous sign of their existence on the Swan Island radiosonde observation. The mT found to the rear of wave troughs in the easterlies cannot be traced back to the equatorial Atlantic. As the severe convection zones reach the Lesser Antilles, the northern coast of Brazil and the western part of the equatorial Atlantic retain the low moist layer so typical of that region during the northern-hemisphere summer.

The characteristic potential and wet-bulb potential temperatures of the mT air depend to a certain extent, of course, on the temperature of the underlying ocean surface and on the length of the oceanic trajectory. Unless convergence is present, however, mT air will not form at all. And whenever sufficient convergence is observed, it will always be produced to a greater or lesser degree. The occasional appearance of mT air over the eastern parts of an ocean in winter can usually be traced to convergence at the approach of a strong trough. It is not necessary to search for a long trajectory from the equatorial latitudes of the western part of the ocean.

THE TRADE-WIND INVERSION

The trade-wind inversion, perhaps the most important regulating valve of the general circulation, has attracted the interest of meteorologist and geographer since its discovery about the middle of the last century. It acts as a strong lid to oppose vertical cloud development; aridity prevails throughout the inversion regime. The desertlike cold-water coasts on the western shores of America and Africa lie at the source of the trade current. Islands with high mountain peaks that stand in the way of the trade often have heavy rainfall at low altitudes. As we ascend the mountain slopes, the forests and fertile fields vanish abruptly and we enter a region that is treeless and barren.

During the summer of 1856 an expedition under the direction of C. Piazzi-Smyth visited the island of Teneriffa in the Canary Islands with the purpose of making astronomical measurements for several months near the top of the Peak of Teneriffa. On two of the trips up and down

the mountain slope, Piazzi-Smyth (15) carefully measured the temperature, moisture, and wind at numerous intervals during the journey and obtained the first detailed observations of the inversion. Figure 2.20 is the plot of temperature and relative humidity during the first of these trips in August, 1856.

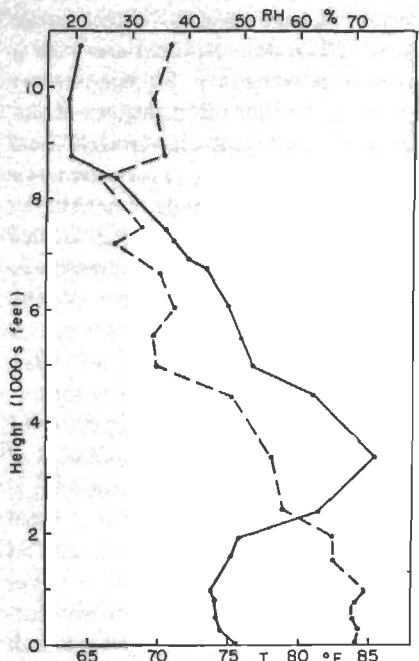


Fig. 2.20. Variation of temperature (solid line, °F) and relative humidity (dashed line, per cent) as observed during descent from the Peak of Teneriffa (28°N , 16°W) by Piazzi-Smyth (15).

Figure 2.20 is the plot of temperature and relative humidity during the first of these trips in August, 1856. We note the same features, though not the extreme character, of the vertical temperature and moisture distribution at 30°N , 140°W in the middle of the east Pacific Ocean in July, 1951 (Fig. 2.11).

Piazzi-Smyth believed that the explanation for the inversion was implicit in his observations. The inversion was not located at the top of the northeasterly trade regime which he found near 9,000 feet altitude in the vicinity of the peak. On the contrary, it was situated in the very middle of the current, and thus it could not be explained as a boundary between two streams of air from different directions. This observation of Piazzi-Smyth has been confirmed in the century since his expedition. Neither wind speed nor wind direction varies discontinuously with height at lower or upper inversion boundary.

Piazzi-Smyth clearly saw from his high vantage point that the top of the cloud layer correlated with the inversion height. He suggested that strong reflection of incident radiation from the cloud tops or evaporation of water from the upper cloud surface accounted for the inversion. This implied that the inversion was produced by cooling of the stratum below the base. We know today that this viewpoint is not correct. The temperature at the inversion base is in approximate equilibrium with the temperature of the underlying sea surface, *i.e.*, air parcels ascending from the ground will reach the inversion base with a temperature that is not very different from that prevailing there. It is the heat and dryness of the air in and above the inversion that is the anomalous feature of the inversion regime.

A combination of heat and dryness always suggests subsidence. We believe today that the inversion is formed by broad-scale descent of air from high altitudes in the eastern ends of the subtropical high-pressure cells. While descending, the current meets the opposition of the low-level maritime air flowing equatorward. This lower stream is turbulent and maintains a nearly constant wet-bulb potential temperature throughout its depth. The inversion forms at the meeting point of these two strata, which flow in the same direction. The height of the inversion base is a measure of the depth to which the upper current has been able to penetrate downward; the inversion layer is the mixing zone between the two

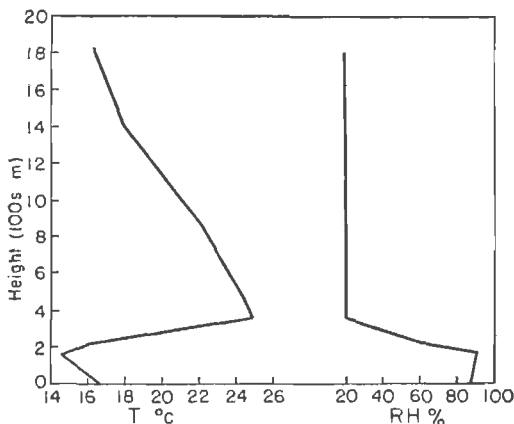


Fig. 2.21. Vertical profiles of temperature and relative humidity, July 28, 1926, at 22°S, 8°E (from *Meteor* data).

masses. Its thickness sometimes is very shallow (Fig. 2.11) and sometimes fairly broad (Fig. 2.20). The height of cloud tops and inversion base are correlated, not because the cloud tops act to produce the inversion, but because the inversion is a formidable lid which the lower cumuli enter but can penetrate only rarely.

A partial exception to this explanation occurs only in the immediate vicinity of the American and African coasts. Here the surface air is cooled from below as it moves over the narrow strip of cold water produced by upwelling along these coasts (25). Turbulence distributes this cooling throughout the layer below the inversion, which is thus strengthened, not only by subsidence higher up, but also by cooling from below. The combined action leads to extreme situations, two of which are shown in Figs. 2.21 and 2.22. These soundings were taken with kites by the *Meteor* expedition (7) in the cold-water strip near the African west coast at latitude 22°S. Of special interest is Fig. 2.22b, which indicates that

the inversion base has descended to less than 50 m above the sea—in fact, to the ship's mast.

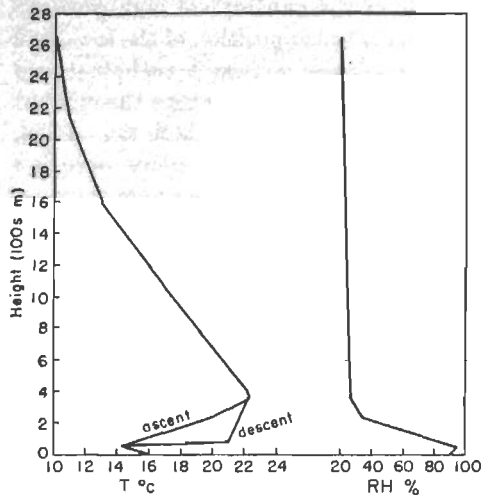


Fig. 2.22a. Vertical profiles of temperature and relative humidity, July 29, 1926, at 22°S, 11°E (from *Meteor* data).

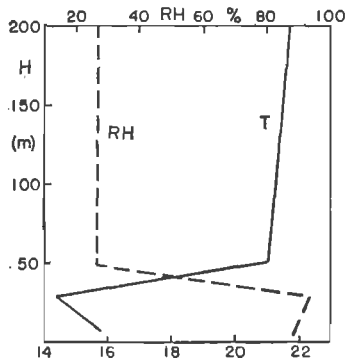


Fig. 2.22b. Same as Fig. 2.22a on expanded scale for the lowest 200 m, using descent data.

The Trade Inversion in the Atlantic Ocean

Interest in the trade inversion has been particularly active in Germany. Subsequent to an extensive treatise by the Norwegian oceanographer and meteorologist Sverdrup, when associated with the Geophysical Institute at Leipzig (24), German meteorological circles organized the *Meteor* expedition. Its observational program, its projected route, and the scope of its objectives remain unparalleled. To this day its data furnish the principal information on wind, temperature, and humidity of the low levels over the tropical Atlantic.

Evaluation of the meteorological part of the expedition data was undertaken mainly by H. v. Ficker and his students (4, 5, 9). A survey of their papers leads one to note quickly that, in spite of the great wealth of data collected, these data proved disappointing in some respects. Apparently the expedition plans were built on the hypothesis that conditions were nearly steady in the tropical Atlantic from day to day but that they varied slowly with the season. Accordingly several cross sections of the trade structure in each season, constructed from a few traverses of the ocean oriented E-W to NE-SW (in the northern hemisphere), should give the complete space distribution of the properties of the atmosphere and its seasonal changes. Actually the expedition encountered what

we have come to accept as routine: strong synoptic variations, especially of the inversion layer. In order to be able to prepare any chart material, it proved necessary to smooth the observations strongly.

Ficker's first diagram (Fig. 2.23) shows the average height of the inversion base; both hemispheres are as symmetrical as can be expected. Along the northern and southern coasts of Africa the inversion height has a distinct minimum near the shore and rises westward from there. In the northern hemisphere this minimum centers near 15° , but in the southern

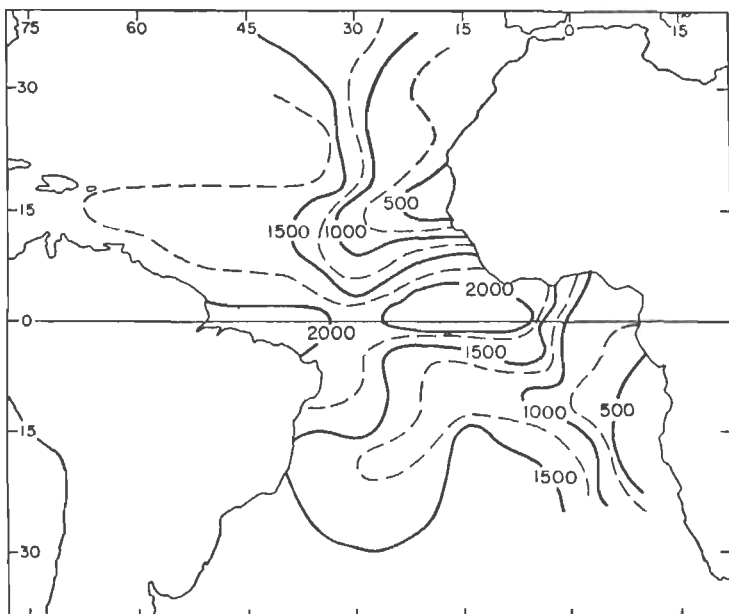


Fig. 2.23. Height of the base of the trade-wind inversion (m) (4).

hemisphere the data do not give the limit of the low-inversion regime. Poleward termini of the inversion are not found. In both hemispheres the contours run nearly north-south at the boundaries of the chart; we are led to suspect that the "roots" of the inversion extend into middle latitudes. Certainly this is true in the Pacific Ocean, where the beginnings of the inversion lie in the fogbound regions of the northern California and central Chile coasts in summer.

Equatorward from latitudes 15° the inversion base rises both westward and equatorward. It lies above 2000 m in the equatorial-trough zone. Here as well as elsewhere over the western tropical Atlantic, the *Meteor* found many situations without inversion, especially in the northern hemisphere. This is only reasonable in view of Fig. 1.9. Glancing

back at the streamlines of Fig. 1.7,¹ we see that the inversion rises downstream along the streamlines, not only where these lines converge into the equatorial trough, but also where they curve clockwise through the whole trade belt to the western ends of the ocean without reaching the trough.

The amounts of temperature increase and relative-humidity decrease from bottom to top of the inversion are shown in Figs. 2.24 and 2.25. These two figures are strongly correlated. A large temperature increase

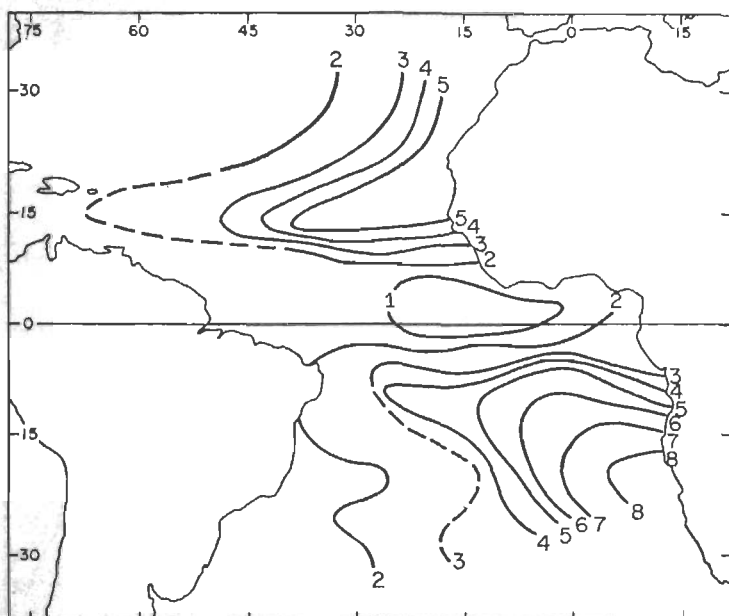


Fig. 2.24. Amount of temperature increase ($^{\circ}\text{C}$) from bottom to top of inversion (4).

corresponds to a large humidity decrease, while the areas of small temperature increase coincide with the areas of small humidity decrease. The pattern of Figs. 2.24 and 2.25 is very similar to that of Fig. 2.23. *The inversion base is strongest where the height of its base is lowest, and its intensity weakens as the base ascends.* This also holds in other parts of the world; we find that it applies even to daily situations. Ficker notes that the thickness of the inversion layer can vary from a knife-edge discontinuity of only a few meters' width to more than 1000 m. On the average the thickness is near 400 m.

¹ Except for a slight clockwise turning with height the surface streamline pattern remains largely unchanged in the layer below the inversion.

Ficker also shows charts of highest temperature at the inversion and of difference between ocean temperature and highest temperature at the inversion. The pattern of both charts resembles that of the inversion base. In view of Fig. 2.24 and the prevalence of steep lapse rates below the inversion, the inversion temperature must decrease as the inversion height rises. The difference between temperature at sea surface and inversion top must correspondingly increase. We obtain a much more significant result if we eliminate the inversion slope by plotting the potential temperature distribution at the inversion top (Fig. 2.26). A

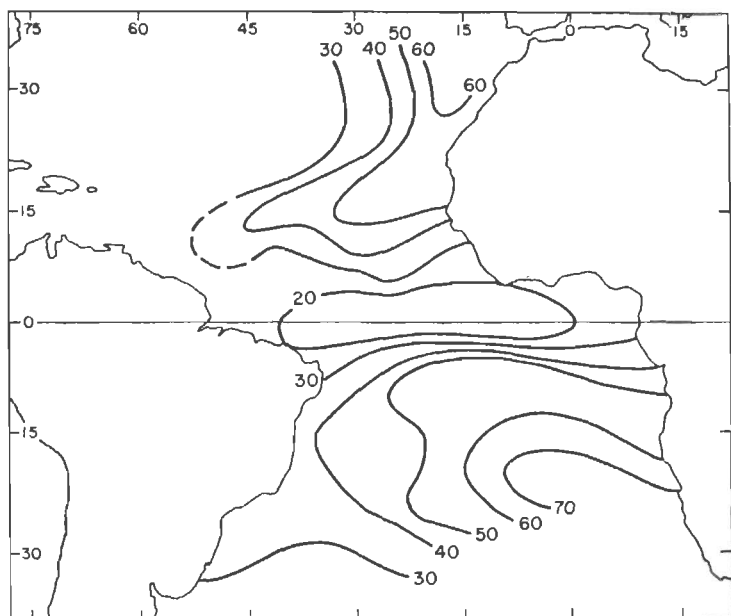


Fig. 2.25. Decrease of relative humidity (per cent) from bottom to top of inversion (4).

pattern results which is still similar to Fig. 2.23. The potential temperature increases downstream along the trade currents, therefore also the sensible heat content of any air parcel moving downstream along the inversion top. We shall explore the significance of this chart in Chap. 12.

Schnappauff (20) has studied the structure of the atmosphere in the tropical Atlantic, as given by the *Meteor* data, with mean charts at selected levels rather than following the inversion as Ficker did. Near sea level (Fig. 2.27) the temperature is highest in the equatorial trough and decreases from there poleward in both directions. The same pattern holds at 500 m, a level generally situated below the inversion. At 3 km, however, the temperature gradient has reversed; the normal temperature

decrease with height continues in the equatorial-trough zone while we pass through the inversion layer in the trade-wind belts. This leads to the conclusion that we cannot regard the equatorial trough as the warmest zone on earth at all heights. As found earlier (Fig. 1.19), the temperature field above 3 km (700 mb) is complicated, with a variable gradient. In some regions the sense of the surface-temperature gradient reappears in the high troposphere. In others the inverted gradient continues

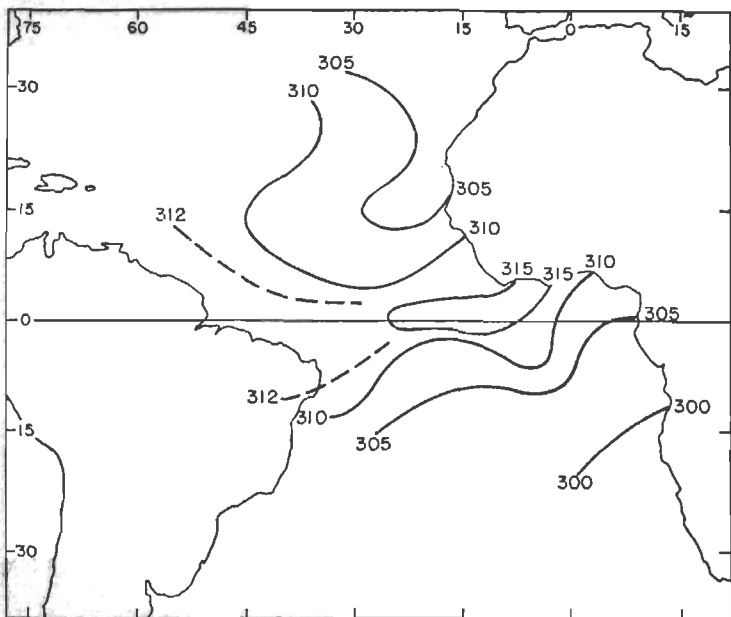


Fig. 2.26. Potential temperature at top of trade inversion (computed from the *Meteor* data).

through the troposphere, at least in summer. A resolution into a very simple general-circulation model is impossible.

Figure 2.28 shows the lapse-rate structure in the equatorial zone that leads to the vertical variation of the temperature field. Below 200 m, the lapse rate is nearly everywhere superadiabatic, suggesting transport of air toward warmer water. In the layer 200–500 m the lapse rate becomes less steep, and in the areas of lowest inversion we even find some negative lapse rates in the mean picture. In the layer 500–1,000 m very stable lapse rates appear in many squares. But the pattern is so irregular that Schnapauff preferred to give the computed numbers rather than draw isolines.

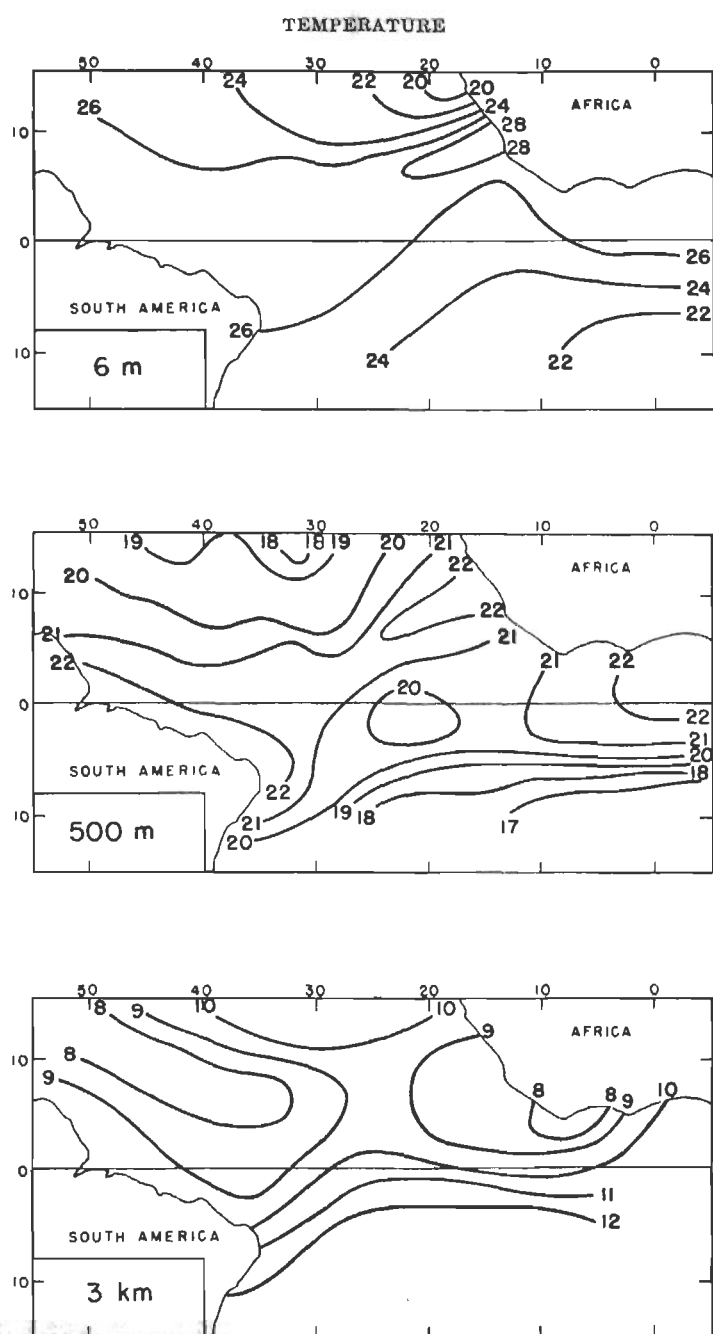
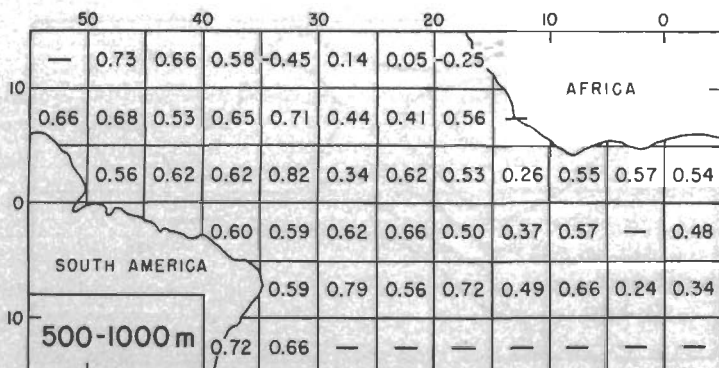
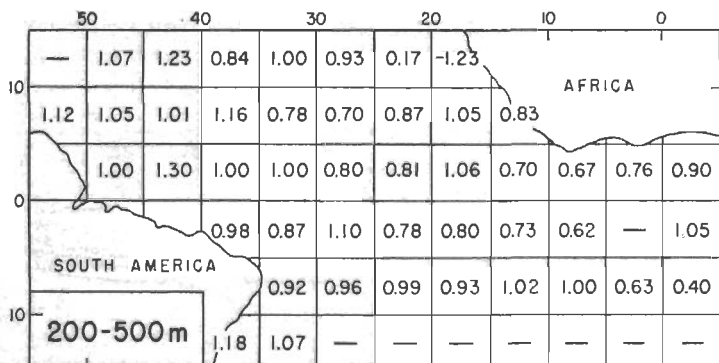
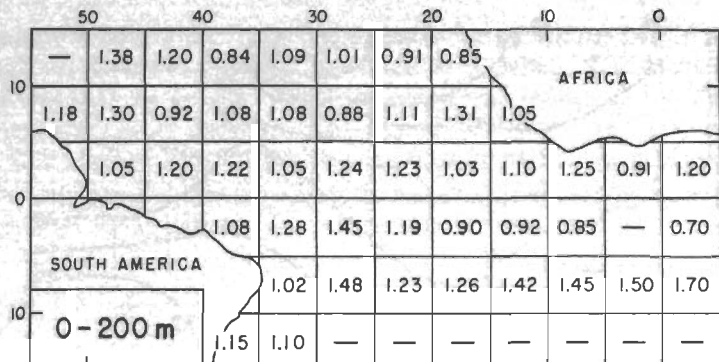


Fig. 2.27. Mean temperature ($^{\circ}\text{C}$) in the equatorial Atlantic for the indicated heights (20).

TROPICAL METEOROLOGY

Fig. 2.28. Mean lapse rates ($^{\circ}\text{C}$ per 100 m) for the indicated layers (20).

The Northeast Trade of the Pacific Ocean

Following the *Meteor* expedition no comparable special observations were made in the Atlantic. The pilot-balloon and radiosonde records that have accumulated since then at many stations throughout the tropics, too extensive to be treated in detail, essentially confirm the *Meteor* findings.

During 1944 and 1945, the United States Navy maintained stationary air-sea rescue vessels in the trade-wind region of the northeastern Pacific Ocean. The meteorological observations of these vessels for the period July–October, 1945, were utilized by the author and his collaborators (17)

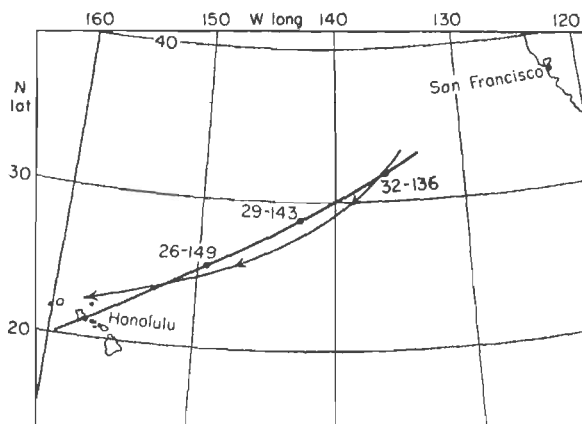


Fig. 2.29. Location of weather ships July–October, 1945, and mean surface-air trajectory for period (17). The average clockwise turning of wind direction with height amounted to only 6° up to 3 km.

to compute the wind, temperature, and humidity structure of the Pacific trade regime up to 3 km along the mean trajectory shown in Fig. 2.29.¹

Wind Structure. Figures 2.30–2.33 show the wind structure of the region. First we inspect the distribution of wind steadiness (Fig. 2.30), defined in Chap. 1. This figure also depicts the presence of four layers (*cf.* also Figs. 2.34–2.35): the *subcloud layer* extending from the surface to the bases of the cumuli, the *cloud layer* which ends at the inversion base, the *inversion layer*, and the *air above the inversion top*. The sub-cloud and cloud layers together form the *moist layer*.

The distribution of wind steadiness is striking. Values are high everywhere and approach the maximum possible in the southwestern portion. A general increase takes place as the air moves away from the influence of the aperiodic disturbances of middle latitudes. Along the vertical,

¹ Further extensive observations, made by research vessels of Scripps Institute of Oceanography, La Jolla, Calif., have been analyzed by Neiburger (12).

steadiness is uniform everywhere in the subcloud layer, and decreases are small in the cloud layer. Above the inversion base the steadiness decreases rapidly with height. The change in gradient is so pronounced that the lines have been drawn with a first-order discontinuity which may be an exaggeration. There can be no doubt, however, that the character of the field of motion changes radically as we pass upward beyond the moist layer in which vertical circulations predominate. Synoptic disturbances are held to a minimum below the inversion base, but their intensity increases upward rapidly within the inversion layer.

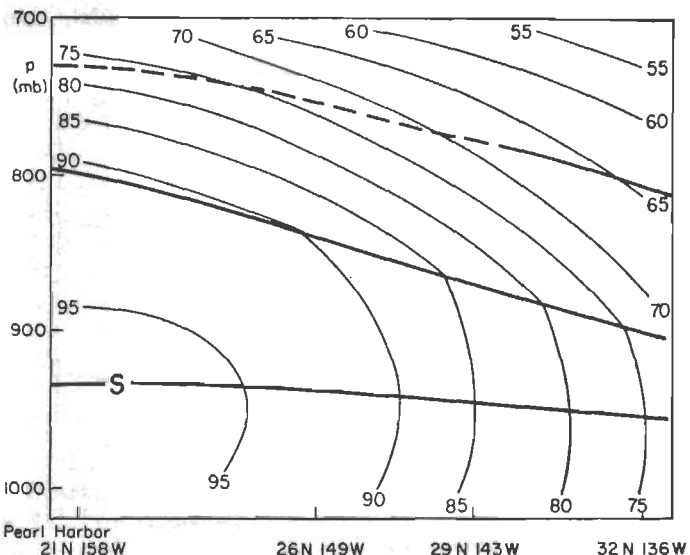


Fig. 2.30. Vertical cross section of wind steadiness (per cent.). Heavy lines mark the boundary of cloud layer and base and top of trade inversion (17).

Figure 2.31 is a vertical cross section of wind speed. Winds are highest throughout the lower portion of the cloud layer, near the cloud bases. This agrees with Stone's (23) observation that the trade is strongest between 750 and 1000 m at San Juan, Puerto Rico. Wind speeds decrease downward and upward from the cloud bases. The easterlies over the area disappear near 500 mb during July–October (cf. Chap. 1).

It is possible to compute one component of the field of horizontal velocity and mass divergence from Fig. 2.31, the component given by variation in wind speed along the streamlines. This component, averaged over the whole section, is positive throughout the entire layer, *i.e.*, there is divergence (Fig. 2.32). A level of nondivergence is situated at the very top near 700 mb. Evaluation of the total divergence field would require knowledge of the other component, given by the coming together or

going apart of the streamlines (for further discussion of divergence see Chap. 8). This component is not available since all ships were placed along the mean air trajectory and none normal to it. We note, however,

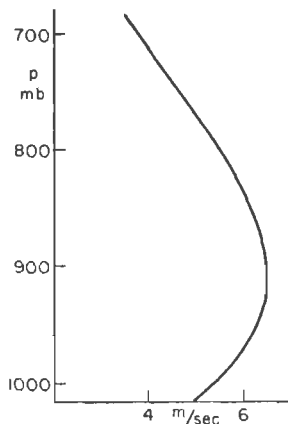


Fig. 2.31. Vertical cross section of wind speed (m/sec) (17).

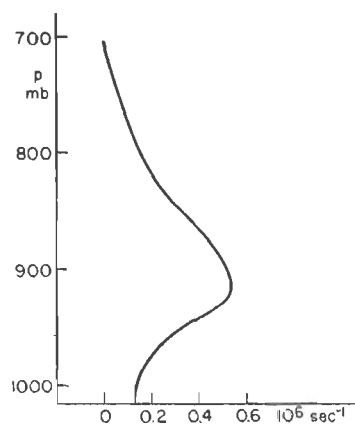


Fig. 2.32. Vertical distribution of divergence (10^6 sec^{-1}) (17).

that the surface streamlines go apart in the area (Fig. 1.7) and that strong mass divergence prevails at the ground (Chap. 3). Unless the fanning out of the streamlines disappears very quickly above the ground, the divergence computed from Fig. 2.31 has the correct sign but its magnitude is too small.

We are interested in the divergence because we can compute from it the field of vertical motion by using the continuity equation (Chap. 8). It follows from Fig. 2.32 that the motion is downward at all heights (Fig. 2.33). The rate of sinking is quite appreciable in the upper parts of the layer. As the air needs 6 days to traverse the region, the net downward displacement between 32°N , 136°W and Honolulu amounts to 400 m. This is also likely to be an underestimate.

Whereas the inversion ascends downstream, individual columns descend, shrink vertically, and spread horizontally (Fig. 2.34). The trade-wind inversion is not a material surface separating an upper current, dry and potentially warm, from a lower current, moist and potentially cold. Trajectories cross both inversion top and base. Large masses of air,

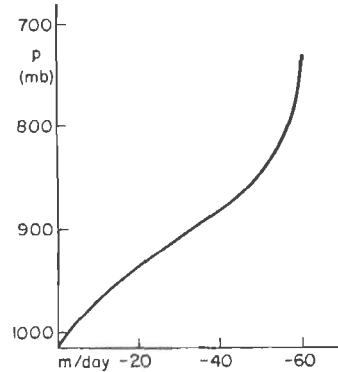


Fig. 2.33. Vertical distribution of vertical motion (m/day) (17).

located above the inversion at 32°N , 136°W , become a part of the cloud layer before they reach Honolulu.

If we consider the previous history of the air passing the Hawaiian Islands, we can make the following divisions (Fig. 2.35):

1. The air that has been below the inversion throughout the journey from 32°N , 136°W .

2. The air that has been incorporated into the cloud layer.

3. The air that has been incorporated into the inversion layer.

Chapter 12 will describe a mechanism for the rise of the inversion against the mean downward motion.

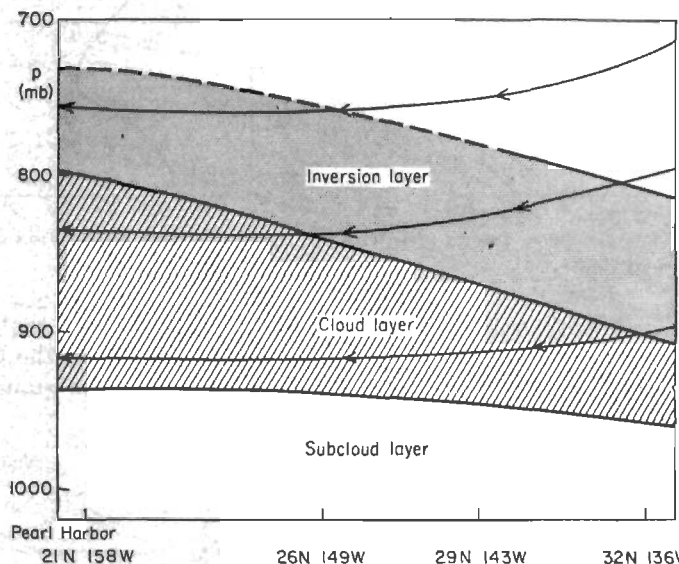


Fig. 2.34. Illustrating the four layers of the trade-wind zone in relation to sample air trajectories (17).

Field of Temperature. Although two soundings were taken daily at the stations shown in Fig. 2.29, only the nighttime ascents were used to determine the temperature distribution. This restriction avoided the difficulties which arise because of diurnal variations in temperature and inversion height, the latter amounting at least to 500 feet (10). Perhaps the most striking feature of the temperature field (Fig. 2.36) is that the isotherms run nearly parallel to the inversion. The 12°C isotherm follows the base and the 10°C isotherm the top, as far as it is possible to identify it. A layer with an upward increase of temperature does not appear, but merely a deep isothermal stratum. Day-to-day variations in the height of the inversion are responsible for this spreading. As in the Atlantic, individual soundings (Fig. 2.11) record strong inversions up to 10°C ,

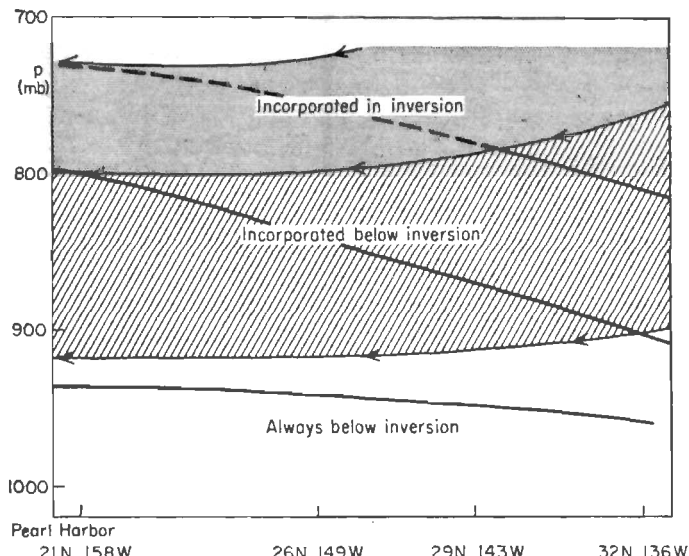


Fig. 2.35. The flow of mass through the trade inversion (17).

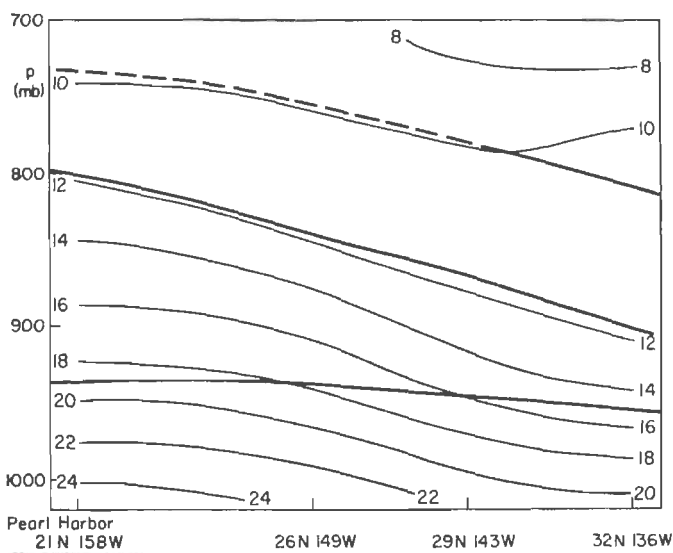


Fig. 2.36. Vertical cross section of temperature ($^{\circ}\text{C}$) (17).

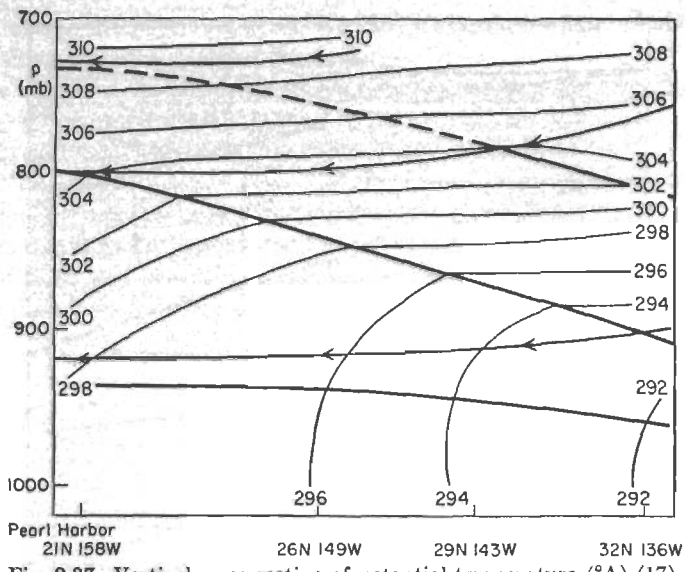


Fig. 2.37. Vertical cross section of potential temperature ($^{\circ}\text{A}$) (17).

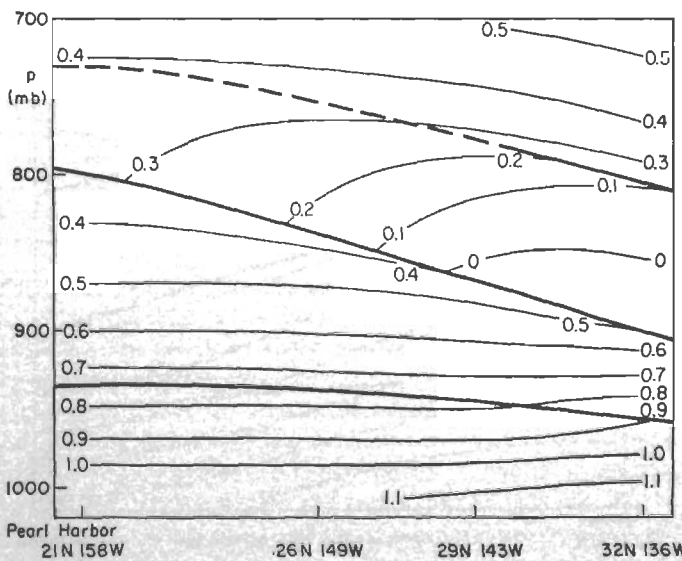


Fig. 2.38. Vertical cross section of temperature lapse rate ($^{\circ}\text{C}$ per 100 m) (17).

often contained in a shallow layer of as little as 20 mb. This happens especially at the northeastern end of the section. In agreement with Fig. 2.24 the intensity of the inversion diminishes with increasing height.

The potential-temperature field (Fig. 2.37) agrees with that to be expected (1, 20). Near the ground the potential temperature at first decreases, then is constant with height. It increases slowly through the upper part of the subcloud layer and somewhat more rapidly through the cloud layer. A first-order discontinuity marks the inversion base. Within the inversion layer the potential-temperature gradient is large, but it decreases slowly from the northeastern to the southwestern end of

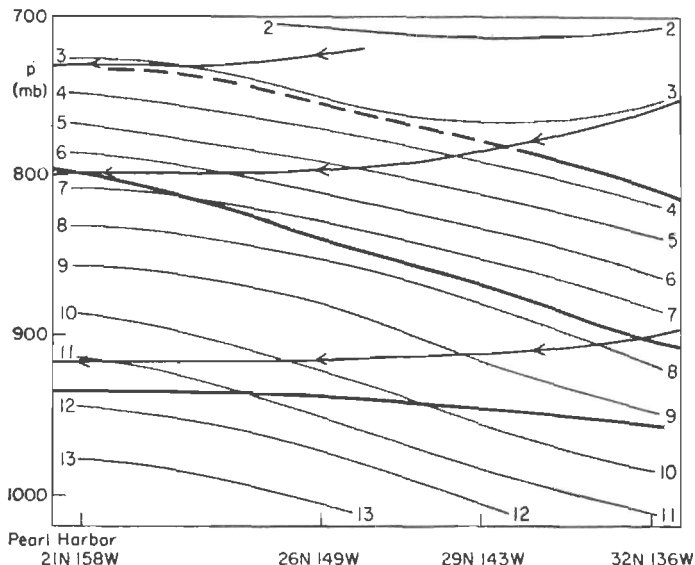


Fig. 2.39. Vertical cross section of specific humidity (g/kg) (17).

the section. As in Fig. 2.26, the potential temperature increases downstream along the top of the inversion.

Many of the pertinent features of Figs. 2.36 and 2.37 become clearer from the field of temperature lapse rate (Fig. 2.38). In the lowest levels the lapse rate is dry-adiabatic or greater, especially in the northeast (*cf.* Fig. 2.28). Near the cloud bases the stability increases quite rapidly, then more gradually in the cloud layer. The lapse rate is discontinuous at inversion base and top, but it has been drawn as a continuous line in those portions of the section where, in the mean, the upper boundary is marked merely by a gradual steepening of the lapse rate. A downstream weakening of the inversion is apparent.

Moisture. As in the case of temperature, the lines of equal specific humidity (Fig. 2.39) run parallel to the inversion. The air motion is

toward higher moisture content. A section of relative humidity (Fig. 2.40) shows a very satisfactory picture. Relative humidity is almost constant throughout the moist layer, with a slight maximum located near the cloud bases and in the lower part of the cloud layer. Almost the

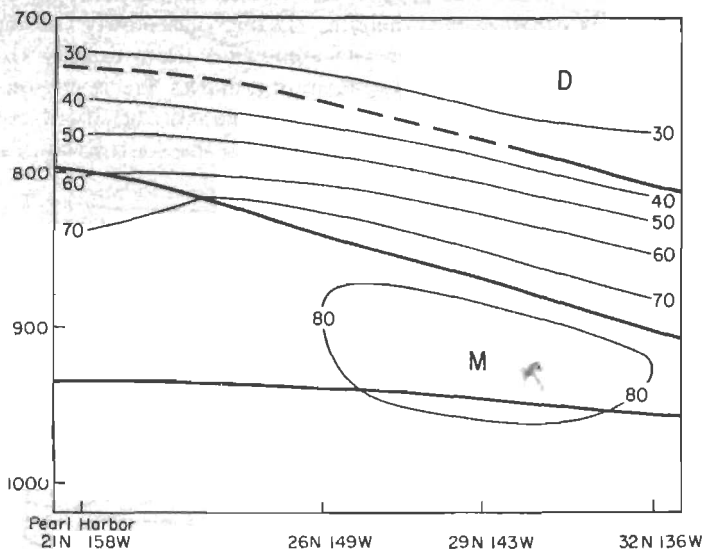


Fig. 2.40. Vertical cross section of relative humidity (per cent) (17).

entire gradient of relative humidity is contained within the inversion layer (*cf.* Fig. 2.25). Above the inversion the atmosphere is very dry.

REFERENCES

- (1) Bunker, A. F., *et al.*, *Mass. Inst. Technol. and Woods Hole Oceanog. Inst.*, Vol. 11, No. 1, 1949.
- (2) Byers, H. R., *General Meteorology*. New York: McGraw-Hill Book Company, Inc., 1944.
- (3) Colón, J. A., *Bull. Am. Meteor. Soc.*, **34**: 333 (1953).
- (4) Ficker, H., *Veröff. Meteor. Inst., Berlin*, Vol. 1, No. 4, 1936.
- (5) Ficker, H., *Veröff. Preuss. Akad. Wiss., Phys. Math. Kl., Berlin*, No. 11, 1936.
- (6) Graves, M., *Bull. Am. Meteor. Soc.*, **32**: 54 (1951).
- (7) Kuhlbrodt, E., *Z. Geophys.*, **4**: 385 (1928).
- (8) Landsberg, H., *Physical Climatology*. State College, Pa.: Pennsylvania State College Press, 1941.
- (9) Laskowski, H., *Veröff. Meteor. Inst., Berlin*, Vol. 2, No. 1, 1937.
- (10) Leopold, L. B., *Pacific Sci.*, **2**: 81 (1948).
- (11) Loewe, F., and U. Radok, *J. Meteor.*, **7**: 58 (1950).
- (12) Neiburger, M., and D. S. Johnson, *Bull. Am. Meteor. Soc.*, **33**: 400 (1952) (abstract).
- (13) Palmén, E., *Geophysica*, **3**: 26 (1948).

- (14) Palmer, C. E., *Quart. J. Roy. Meteor. Soc.*, **78**: 126 (1952).
- (15) Piazzi-Smyth, C., *Trans. Roy. Soc. London*, **148**: 465 (1858).
- (16) Riehl, H., *Dept. Meteor., Univ. Chicago, Misc. Rept.* 17, 1945.
- (17) Riehl, H., et al., *Quart. J. Roy. Meteor. Soc.*, **77**: 598 (1951).
- (18) Riehl, H., and T. C. Yeh, *Quart. J. Roy. Meteor. Soc.*, **76**: 182 (1950).
- (19) Schacht, E. J., *Bull. Am. Meteor. Soc.*, **27**: 324 (1946).
- (20) Schnapauff, W., *Veröff. Meteor. Inst., Berlin*, Vol. 2, No. 4, 1937.
- (21) Serra, A., and L. Ratisbonna, *As Massas de ar da America do Sul*. Rio de Janeiro: Serviço de Meteor., Brazil, 1942.
- (22) Solot, S. B., *Bull. Am. Meteor. Soc.*, **31**: 85 (1950).
- (23) Stone, R. G., *Bull. Am. Meteor. Soc.*, **23**: 4 (1942).
- (24) Sverdrup, H. U., *Veröff. Geophys. Inst., Berlin*, Vol. 2, No. 1, 1917.
- (25) Sverdrup, H. U., et al., *The Oceans*. New York: Prentice-Hall, Inc., 1942.

CHAPTER 3

RAINFALL

Classical descriptions tell us that the subtropics have deserts which on their equatorward side give way to "savannah" and "tropical rain forests." This simple scheme, though correct in its gross features, is subject to tremendous exceptions. It is particularly difficult for a teacher of meteorology in Florida to convince his students that the subtropics are arid and for one in Brazil to insist that all of the equatorial belt has abundant rain. Around the equator regions with hundreds of inches of rain per year alternate with dry zones. In the trades, a curious spectacle awaits us when we arrive at the beautiful island of St. Thomas in the West Indies (18°N , 64°W), located at the western cell end of the subtropical high in the Atlantic and therefore supposedly receiving ample rain. Large portions of the hills around the capital, Charlotte Amalie, are cemented, and cisterns at the bottom catch the runoff rain water. This is a major source of water since underground springs and running brooks are almost entirely lacking. The vegetation of the island consists mainly of brush, and in years with subnormal rainfall water must be imported by ship. This situation is by no means uncommon.

World Rainfall Distribution

Of all the data so far considered, those on rainfall are by far the least satisfactory. Over none of the oceans are there stations that record rainfall. Over land, especially in mountainous areas, the record at any station is notorious for representing only the immediate environment. This situation is accentuated in the tropics compared with higher latitudes, since most of the tropical rainfall data come from continental and island stations subject to strong orographic effects.

In spite of all difficulties mean rainfall charts have been prepared for the continents. Supan (26) first attacked the problem of mean annual precipitation over the oceans. He thought that ship reports gave a rather good rainfall frequency distribution. If, in addition, he could obtain some idea as to the average amount of rain per rainy day, he could by multiplication construct isolines of mean annual rainfall. A few ships had attempted rain measurements. From their data Supan drew profiles of the average amount of rain per rainy day. His published rainfall chart covers the Atlantic and parts of the Indian Ocean.

Subsequently Supan's approach was extended to cover all oceans with the aid of measurements from oceanographic expeditions and commercial and other vessels. When Wuest (33) showed that salinity and the difference between evaporation and precipitation are related linearly, another approach to rainfall estimates over the oceans was open, provided that the evaporation could be determined. In Chap. 5 we shall describe the evaporation process and discuss a way of measuring it exactly. Lacking such measurements, the following techniques have been used in the past:

1. Measurement by evaporation pans. This method has always been regarded as doubtful since conditions differ with regard to a pan and the free water surface.
2. Estimate through computation of an oceanic heat balance (4, 5, 28).
3. Estimate through application of the turbulence theory (4, 5, 27, 28; cf. also Chap. 5).

The latter two techniques have yielded values ranging from good agreement to differences greater than 50 per cent when both were applied to the same data. This, then, is also the order of accuracy of oceanic-rainfall calculations. Two important and independent checks, however, corroborate that the computed rainfall probably is correct within a factor less than 2. These are (*a*) the heat balance of the atmosphere, (*b*) the water balance over oceans and continents.

According to heat-balance computations the radiation deficit of the atmosphere is offset by the heat released during condensation and rainfall. We shall see in Chap. 12 that the estimated rainfall agrees well with that needed for balance.

Since the height of the ocean surfaces remains essentially unchanged from year to year, evaporation from the oceans must equal the rainfall into the oceans plus runoff from the rivers. Following Wuest (33), the evaporation per unit area averages 20 inches per year over land and 33 inches over the oceans; the precipitation, 29 inches over land and ocean alike. The land therefore has a water surplus of 9 inches and the oceans a deficit of 4 inches. Since the territory of the oceans is roughly $2\frac{1}{2}$ times larger than that of the continents, the surplus over land equals the deficit over the oceans. Balance must be provided by water return through the rivers. Actual, though crude, measurements of river discharge have the order of magnitude required by the preceding computations and confirm their validity in principle.

The probability is small that these balances are all accidental. Nevertheless in all studies of rainfall over large areas we move in a network of rough estimates and theoretical computations. Wuest's work implies an average annual rainfall depth for the world of 70 cm; the data of Meinardus (8, 9), to be shown presently, a depth of 100 cm. This difference lies entirely within the range of error of the data and calculations. The

author prefers the Meinardus chart on the grounds that Wuest's rainfall values in the equatorial-trough zone of the north Pacific cannot be reconciled with the much higher amounts recorded on many of the small atolls which have a maximum elevation of only a few feet. But our graphs of seasonal rainfall will be based on Wuest since Jacobs, whose work (4, 5) is the source, has reduced the Meinardus totals to those of Wuest. This inconsistency should be kept in mind by the reader.

Supan, evaluating his computations, said, "The method which I have proposed is of course almost exactly as defective as the computation of the population of uncivilized countries from estimates of population density in small areas. In both cases we must pull ourselves up by our bootstraps, unless we wish to forgo an approximate solution of the respective problems entirely. And it is very difficult to resign ourselves to that." The author agrees with Supan here and now offers his data.

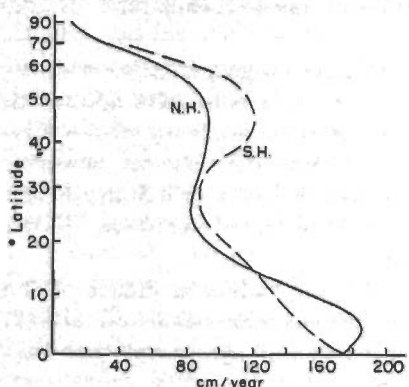


Fig. 3.1. Latitudinal profiles of average annual rainfall.

Farther poleward the precipitation reaches secondary maxima along the cyclone tracks in the belts of polar westerlies. On account of these maxima the world rainfall—amounting to about 5×10^{14} tons per year as computed from Fig. 3.1—is not concentrated in quite such overwhelming measure in the tropics as one might have thought. The northern hemisphere receives only two-thirds of its rainfall equatorward of latitude 30°; the southern hemisphere, even less.

Glancing at the world distribution of annual rainfall (Fig. 3.2), we observe a marked crowding of isohyets (lines of equal rainfall) near the equator. The belt of heaviest rain closely coincides with the average position of the equatorial trough. Farther north and south general dryness prevails in the trade-wind belts except at the western ends of the oceans, where, in the northern hemisphere, a clockwise curving tongue of heavier rainfall extends poleward east of Asia and North America. Similar tongues are found over the southern oceans, though less distinctly.

The crowding of isohyets at the boundary of the equatorial-trough zone

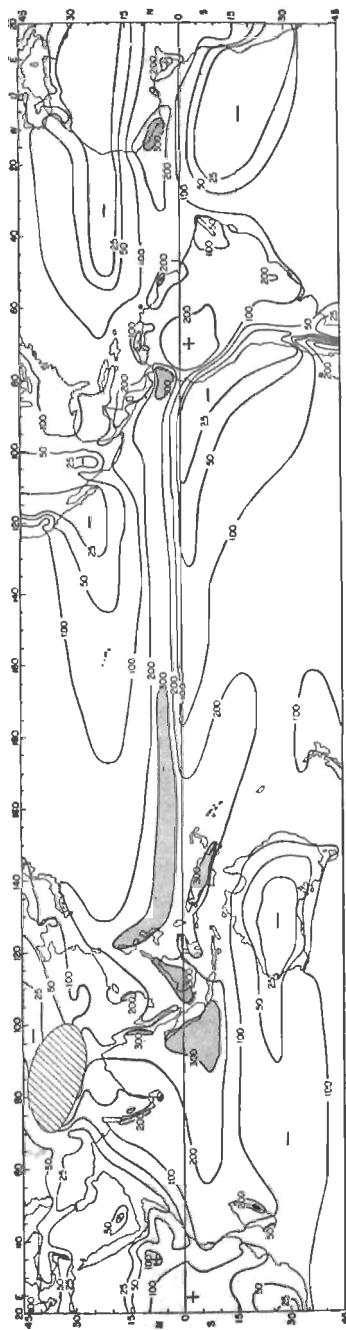


Fig. 3.2. Mean annual rainfall (cm) (8). Regions with precipitation over 300 cm/year shaded.

in many parts of the world indicates strong climatic gradients. Trough shifts of as little as 2–3° latitude from one year to the next can produce extreme rainfall differences in the marginal zone. Glancing along the trough line, we find one dry regime over the East African shore, especially north of the equator, and over the Arabian Sea. Another overlies the south Atlantic and a large part of northeastern Brazil. The marginal rainfall in this area, the "hump" of Brazil, has received much attention since it is one of the few remaining territories on earth where large-scale population settlement is still possible.

The most famous dry zone is situated a little south of the equator in the central part of the equatorial Pacific. Especially during the northern-hemisphere summer, heavy rainfall along the trough gives way on its south side to almost complete aridity (23). The width of this dry zone is only a few degrees latitude. Still farther south a moister belt extends along the island chain of the south Pacific. Heavier rainfall here can be connected with a large trough and convergence line emanating from the polar zone and extending northwest toward the equatorial trough (Figs. 1.7 and 1.8).

The arid belt coincides with a tongue of cold water protruding far across the Pacific from the South American coast (Fig. 2.5). At one time the explanation offered for the dryness was simply that the cold water stabilized air passing over it and so prevented convection. This hypothesis became difficult to maintain when oceanographic expeditions discovered that ocean temperatures often are lower in the middle of the Pacific than upstream toward South America and that a dry inversion overlies the area. Like the trade inversion, this stable layer cannot be accounted for by cooling from below, but only by considerable descent with adiabatic compression. Such descent implies horizontal divergence in the low levels. Actually the surface winds diverge in the mean (19); rainfall and divergence patterns are remarkably well correlated.

Seasonal Rainfall. Jacobs, in the studies quoted above (4, 5), has ventured to draw seasonal-rainfall charts for the oceans. For this purpose he made the following assumptions:

1. The average amount of rain per rainy day does not change with the seasons.
2. Charts of average seasonal rain frequency at noon, Greenwich mean time, contained in the *Atlas of Climatological Charts of the Oceans* (31), can be used to apportion the mean annual rainfall. If, for instance, the annual rainfall in a certain region is 100 cm, if the annual rain frequency is 150 days, and if the frequency is 50 days for the period June–August, then, following Jacobs, the mean rainfall for June–August is 33 cm.

These assumptions are superimposed on those entering into the computation of the mean annual rainfall. But we must remember that

Jacobs has done the best that probably can be attained for many years to come.

The seasonal profiles¹ (Fig. 3.3) show that rainfall in the warm season exceeds that in the cool season away from the equator. Precipitation is nearly zero over the continents between latitudes 10° and 25° in the respective winters—a true desert condition. In the southern rainy season the precipitation peak over land occurs much farther south than the oceanic peak. We may relate this difference to the fact that the equatorial trough makes wide incursions into the southern-hemisphere continents at

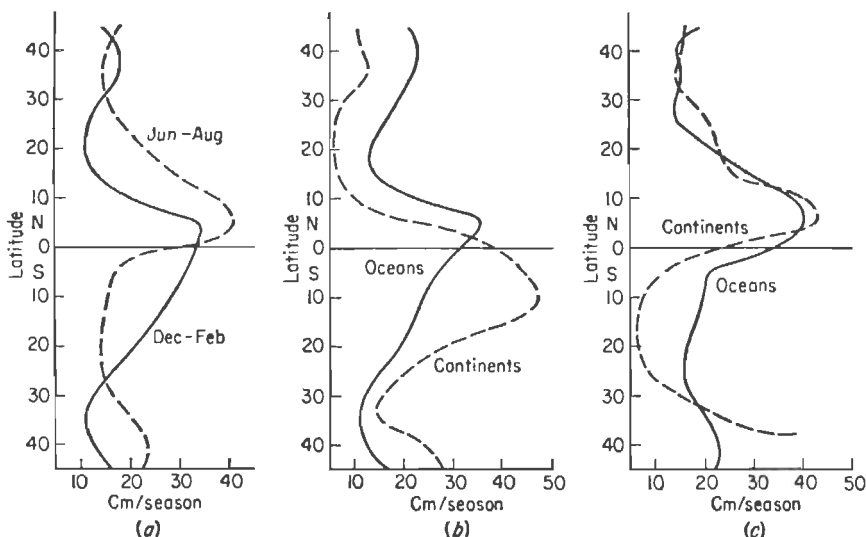


Fig. 3.3. Latitudinal profiles of rainfall. *Left:* December–February and June–August. *Center:* December–February, oceans and continents separate. *Right:* June–August, oceans and continents separate.

that time of year. Thus the continental rainfall reflects the trough migration much better than the oceanic rainfall.

The mean seasonal-rainfall distribution is a general-circulation feature which may be correlated with the average ascent and descent near the surface. We can compute the direction of the vertical motion in the low levels from Fig. 1.5. In the vicinity of the ground, air must escape upward in zones of convergence; it must descend in zones of divergence. Figure 3.4 shows the latitudinal profiles of convergence and divergence; these agree closely with Fig. 3.3. The precipitation and convergence peaks coincide. Rainfall is lowest in the belts with strongest divergence.

¹ The reader should be reminded that the oceanic rainfall in the following is based on Wuest's estimates.

There is also a good correlation between the regional distribution of seasonal divergence and convergence (19) and charts of rain frequency and cloudiness. This correlation extends to such features as the dry zone of the Pacific.

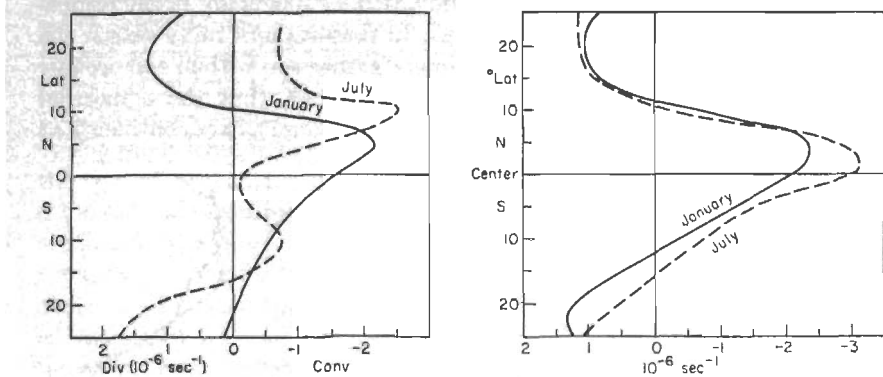


Fig. 3.4. Profiles of surface convergence and divergence against latitude (19) (left) and relative to equatorial trough (right).

Equatorial trough and heavy rainfall coincide seasonally as well as in the annual mean over the oceans. The rainfall maxima over land lie equatorward of the trough wherever it deviates markedly from the equator. Especially over Africa in July and Australia in January the

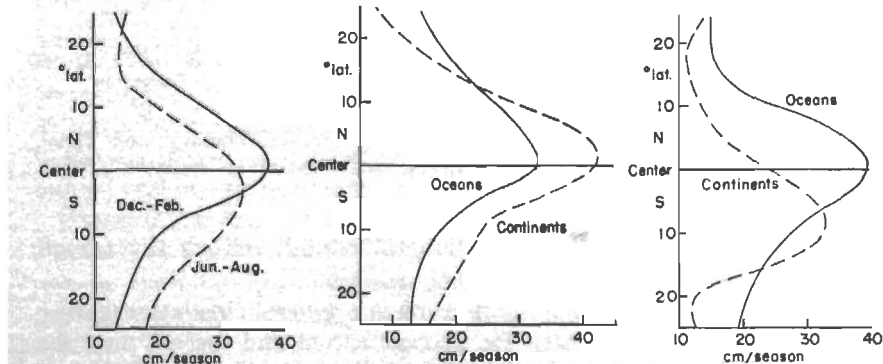


Fig. 3.5. Latitudinal profiles of rainfall relative to equatorial trough. Left: December–February and June–August. Center: December–February, oceans and continents separate. Right: June–August, oceans and continents separate.

trough line marks the poleward margin of the rainy belt, in agreement with synoptic experience. Along the convergence line itself cT air, as described in Chap. 2, begins to flow over mT air at the ground. Because the cT is relatively dry, the skies are entirely clear at the trough even with occasionally extreme convergence. The precipitation belt remains

well to the south, where the mT air is present in depth and where the temperature difference between the ascending cT and the mT has disappeared.

When we average the rainfall relative to the equatorial trough (Fig. 3.5), we obtain symmetrical profiles over the oceans. During the southern summer the continental peak lies about 2° latitude north of the trough; in the northern summer it departs much farther. Correlation is perfect between the oceanic-rainfall profiles and profiles of surface convergence and divergence taken relative to the trough (Fig. 3.4). The regression equation computed from a scatter diagram (Fig. 3.6) is

$$RR = 22 + 6 \text{ convergence},$$

where the units are those of Fig. 3.6; the linear correlation coefficient is 0.98. As already mentioned, the rainfall values upon which the seasonal diagrams are based appear to be low. In particular it is difficult to accept a seasonal total of only 35–40 cm in the heart of the equatorial-trough zone. Improved rainfall data are likely to show that both the intercept of the regression line at zero convergence and its slope are numerically too small but that the linear correlation is valid.

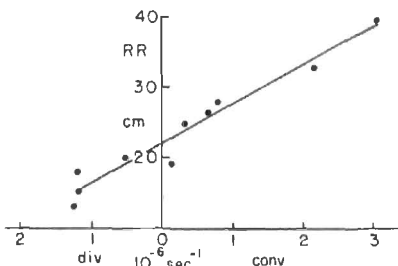


Fig. 3.6. Correlation diagram between convergence and rainfall relative to equatorial trough, from Figs. 3.4 and 3.5.

Seasonal March of Rainfall

Ideally, seasonal-rainfall maxima should migrate with the equatorial trough, not only in the averages around the globe but also at individual stations. As the trough reaches its extreme latitudes in February and August, the equatorial margins of the trade-wind belt should experience a single rainfall peak. Farther equatorward the trough passes any latitude circle twice; here we should look for double rainfall maxima. If the trough oscillates symmetrically about the equator, rainfall should be heaviest on the equator in May and November, allowing for a lag of trough movement with respect to the sun.

As is evident from Fig. 1.9, this simple scheme cannot hold everywhere because of great differences in the behavior of the trough at different longitudes. In addition, the controls of rainfall are not of a simple thermal kind. Dynamic effects in the upper troposphere, including a close linkage with events outside the tropics, exercise an important influence. Therefore we must expect considerable variations of the seasonal march of rainfall from one part of the tropics to another, quite apart from the extreme local influences to be discussed in the next chapter.

As in the treatment of temperature, only a few basic rainfall types can be presented as a guide in this book. For more details, the reader may consult an excellent monograph by Crowe (2).

West African Shore (Fig. 3.7). Simultaneously with the exploration and colonization of Africa, the early climatologists evolved the picture of tropical rain that has come to be recognized as standard. Small wonder, therefore, that we are able to find the classic model with greatest perfection on this continent.

Our first profile extends along the West African shore from 15°N to 9°S . At Dakar, 7 months of the year are completely dry. The brief

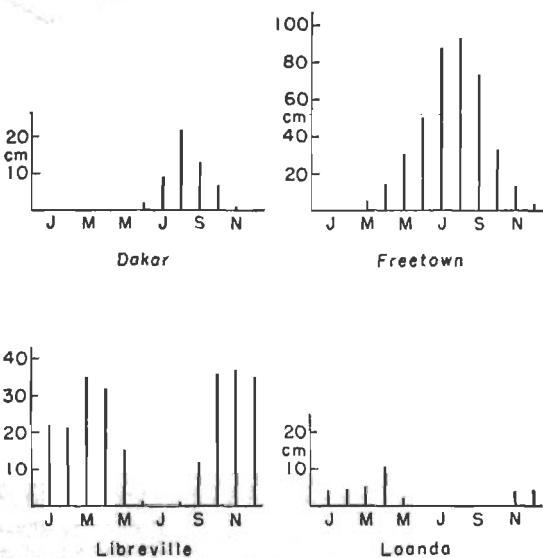


Fig. 3.7. Monthly rainfall at the coast of West Africa: Dakar (15°N , 17°W), Freetown (8°N , 13°W), Libreville (1°N , 10°E), Loanda (9°S , 13°E).

rainy season correlates well with the excursion of the equatorial trough into North Africa. But we must not suppose the rain to be steady, produced only by the presence of the trough. A few disturbances—partly waves in the easterlies—are responsible for most of the precipitation. Occasionally small but intense cyclones accompany passage of the wave troughs.

At Freetown the rainy season is longer, but here we see the overpowering effect of a mountain range down wind, the Sierra Leone. South of Freetown the rainfall regime changes rapidly. At Libreville we encounter a typical double rainfall structure, very "regular," with two peaks of equal intensity. Since the equatorial trough oscillates about a mean position well to the north of the geographical equator, the dry season is

severe in the northern-hemisphere summer; the trough never passes far enough south to permit complete cessation of rain during the southern summer.

Loanda is the southern-hemisphere counterpart to Dakar, even though the latitude is only 9°S —further evidence of the difference between geographical and meteorological equator. In the mean the trough does not reach this latitude. According to the best available descriptions, the scanty rainfall comes during situations when the equatorial-trough zone takes on a double structure, with the southern branch reaching from Ascension Island (8°S , 14°W) to the African shore.

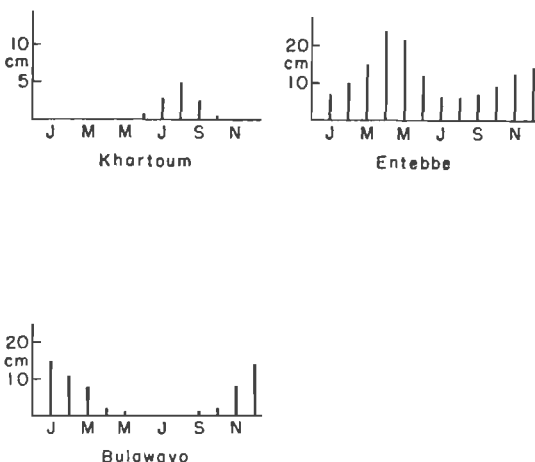


Fig. 3.8. Monthly rainfall in Central Africa: Khartoum (16°N , 32°E), Entebbe (0° , 32°E), Bulawayo (20°S , 29°E).

Central Africa (Fig. 3.8; cf. also Fig. 2.10). The rainfall at Khartoum corresponds to that at Dakar, so that here continental and shore regimes do not differ. At Entebbe the two peaks coincide well with the two passages of the equatorial trough. Over East Africa the southward migration of the trough is very large. Thus Bulawayo, even though located at 20°S , has considerable rain from summertime disturbances. The curve is out of phase with Khartoum, but the precipitation is much larger and corresponds to a northern-hemisphere location a little south of Khartoum.

South American East Coast and Caribbean (Fig. 3.9). The regime of Rio de Janeiro is considered typical for the western ends of the subtropical high-pressure cells: some rain falls in all months, but summer has the most. We note that the summer maximum is very flat, and in individual years the highest rainfall may be recorded any time between November and April.

At Recife, on the "bulge" of Brazil, we find a simple and very symmetrical curve. The average annual rain (165 cm) is more than at Rio (110) and much more than on the semiarid highlands west of Recife. Stations on the bulge generally report highest rainfall between March and

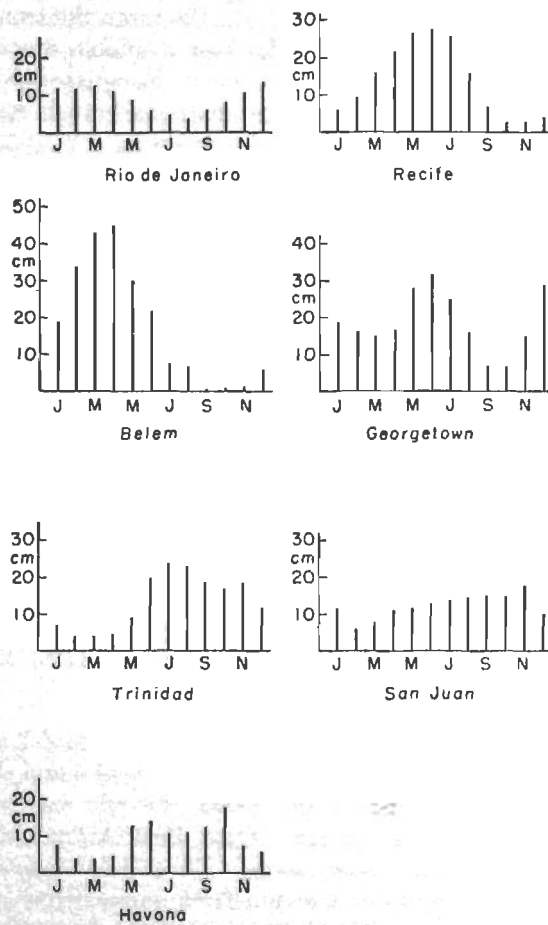


Fig. 3.9. Monthly rainfall along the South American east coast and Caribbean: Rio de Janeiro (23°S , 43°W), Recife (8°S , 35°W), Belem (1°S , 48°W), Georgetown (7°N , 58°W), Trinidad (10°N , 61°W), San Juan (18°N , 66°W), Havana (23°N , 82°W).

June. No satisfactory explanation for this regime or for the remarkable aridity of the inland area has so far been offered.

An equatorial-trough type of rainfall first appears at Belem. Since the trough, in the mean, hardly penetrates south of the equator in South America, rainfall is heavy from February to May and negligible from

August to November at the mouth of the Amazon River. The lag of the rainfall with respect to the sun's migration is very large—fully 3 months.

We can easily trace the trough movement from Belem to Georgetown, where the annual rainfall (223 cm) is heaviest along the whole section from Rio to Havana. The Belem maximum occurs in March-April and shifts to June at Georgetown, indicative of the trough's northward progression at that time of year. A second peak occurs in December during the return of the trough.

At first glance, the Trinidad curve appears to be a logical continuation of the Georgetown rainfall. But synoptic experience as well as climatic data contradicts an explanation in terms of the equatorial trough. The trough sometimes reaches the Lesser Antilles between August and October, but we do not observe a regular double passage with the seasons. Although definite information is lacking, it is probable that the most intense portions of waves in the easterlies (Chap. 9), as well as tropical lows, pass over the southern part of the Antilles early and late in the season and that this accounts for the double maximum.

Over Puerto Rico waves in the easterlies and other disturbances produce the broad summer peak. The hurricane influence is much weaker than often assumed, because hurricane frequency and rainfall are not correlated. Indeed, more rain has fallen on days with a rather weak circulation than during some hurricane passages. San Juan is considered typical for the lower latitudes at the western end of the Atlantic high. In view of the flatness of the curve, however, the reader will not be surprised to learn that over Puerto Rico and adjacent islands he can discover stations with maximum rainfall occurring any time between May and November, and also stations with double peaks.

Havana should correspond to Rio, but the similarity at best is weak. No less than two major peaks and a minor one appear. The minor peak may be ascribed to extratropical disturbances in midwinter. The two summer peaks cannot have any connection with an equatorial-trough movement. They are correlated with the position of a mean upper-air trough extending southward from the middle latitudes (17), which lies over Cuba and Florida in early summer. The low-latitude portion of this trough migrates into the Gulf of Mexico by the middle of summer. In September and October it returns to the Florida-Cuba area. We can conclude that Havana has high rainfall when the trough is nearby and that the midsummer minimum results from its westward displacement.

This analysis shows that any attempt to derive the annual course of precipitation as a simple function of latitude must be very conservative. Only a few gross features can be gleaned in this way; conditions vary widely and cannot be explained from surface climatic data alone.

Pacific Ocean (Fig. 3.10). Both the Marianas Islands of the north Pacific and the Fiji Islands of the south Pacific lie along the western cell ends of the respective subtropical highs at the equatorial margin of the trade-wind belt. Both are touched by the equatorial trough with attendant tropical disturbances, which accounts for the heavy rainfall in late summer. Waves in the easterlies produce much of the early-season rainfall, at least at Guam, and here they are observed intermittently throughout the year. In all major features the curves of Guam and Suva are nearly identical, with great late summer maxima and relatively dry winters. They differ markedly from Havana, San Juan, and Trinidad in the Atlantic, a fact which must be ascribed to the stronger fluctuation of the equatorial trough and associated disturbances in the western

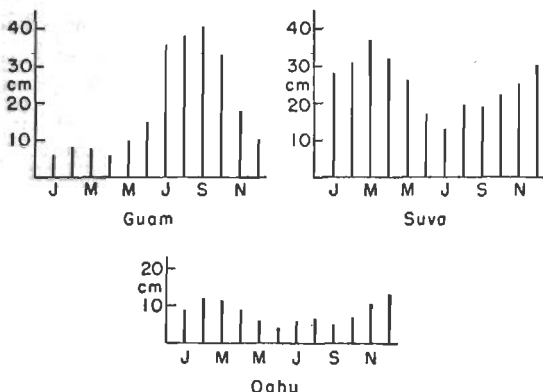


Fig. 3.10. Monthly rainfall in the Pacific: Suva (18°S , 178°E); Guam (13°N , 144°E); 21 stations on Oahu, Hawaii (21°N , 158°W).

Pacific. It should be emphasized that here also actual typhoon passages contribute little to the shape of the curves.

The rainfall regime of the eastern Pacific is completely opposite to that of the western Pacific. Guam has summer rain and winter dryness; Hawaii has winter rain and summer dryness. The trade-wind rain over the eastern parts of the oceans is in phase with the Mediterranean-type rainfall of the west coasts, where the trades originate. The rain-producing circumstances of course differ.

At first sight one is tempted to smooth out the very complicated Oahu curve. But the large amount of work done on Hawaiian rainfall since 1945 (32) has established the validity of all features. Rainfall is lowest in June and September when the high-level subtropical ridge crosses the latitude of the islands (18); disturbances are then held to a minimum. In July and August some wave troughs in the easterlies and an occasional cold low aloft pass the islands and yield rain.

The secondary decrease of precipitation in winter is also real. Namias and Mordy (11) have related it to a large fluctuation in strength and position of the upper westerlies noted by Namias (10) in late winter. Quite generally, fluctuations of winter rain over Hawaii are related to events in the westerlies (35). Further, the rainy season over eastern and western Pacific alike is linked to the variability of the high-tropospheric winds (34). In summer, the upper winds are relatively steady over Hawaii and fluctuate greatly over the western Pacific. Summer, then, is the rainy season for the Marianas and the trade region of the western Pacific. In winter, the variability of the upper winds is largest over the eastern Pacific; winter is the rainy season at Hawaii.

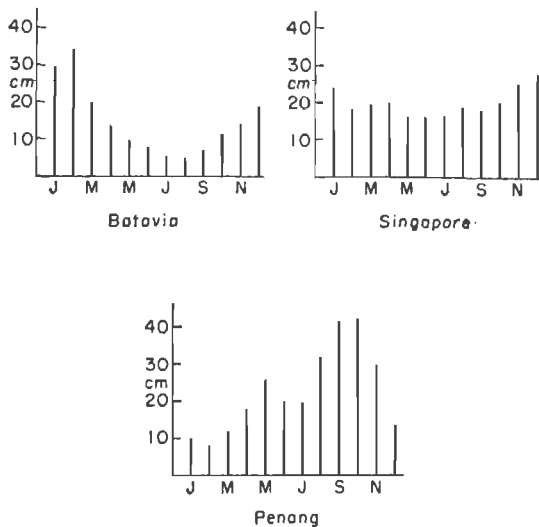


Fig. 3.11. Monthly rainfall in the Far East: Djakarta, formerly Batavia, (6° S, 107° E), Singapore (1° N, 104° E), Penang (5° N, 100° E).

Far East (Fig. 3.11). The stations chosen lie in the monsoon regime of the Malay peninsula and the East Indies. At Djakarta, a single rainfall peak coincides with the season of prevailing north to northwest winds and the proximity of the equatorial trough (Figs. 1.7 and 1.8). The season of southeasterly winds, in contrast, brings marked aridity. On the whole, Djakarta's total rain for the year is small considering that Buitenzorg in the nearby hills reports over 300 thunderstorm days per year, the highest recorded frequency on earth.

The transition from southern to northern hemisphere differs greatly from that seen on both sides of the Atlantic. There, as well as in the interior of Africa, dry and rainy season alternate near the equator. At Singapore, however, rainfall is heavy and nearly uniform in each month.

This is baffling, especially as just a little to the north, at Penang, a clear double peak appears. This double peak gives way to the single large peak of monsoon climates as we go farther north toward Burma, Thailand, and Indochina.

Indian Ocean (Fig. 3.12). The last section across the equator also contains features that distinguish it from all other regions. At Mauritius the rainfall distribution is similar in general outline to that of Rio de Janeiro, perhaps even more to that of Havana. This is suggested by the slight maximum in winter, which is quite definite, and by the weak indication of a double peak in summer.

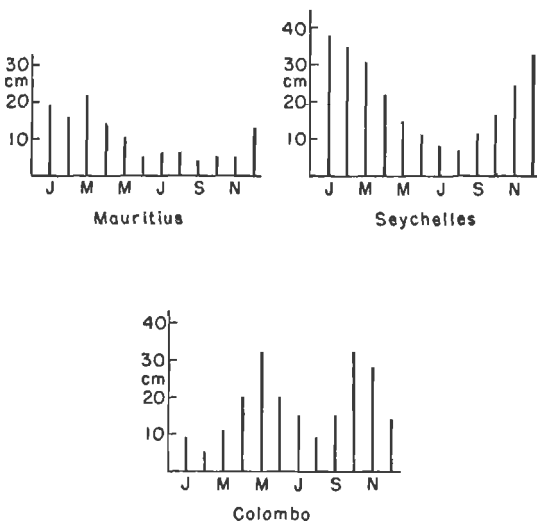


Fig. 3.12. Monthly rainfall in the Indian Ocean: Mauritius (20°S , 58°E), Seychelles (5°S , 55°E), Colombo (7°N , 80°E).

The Seychelles Islands trace is surprising. Even though located in an area where we should expect double peaks, we do not find them. This is even more surprising since the rainfall curve at Colombo, Ceylon, shows one of the most regular double peaks found anywhere.

In summary, tropical-rainfall regimes are far more complicated and less amenable to simple classification than we might wish. Only within the trades and near their equatorial margin are the gross features of the rainfall regimes fairly similar in all parts of the world. Winter is the rainy season over the eastern parts of the oceans, where the trade inversion dominates; the western parts have their rainy season in summer. Closer to the equator, the observed number of rainfall types becomes large. We have found places with two maxima, one maximum, or no marked maximum. The seasons with high and low rainfall differ from

region to region. We can, besides, trace a regular progression of the equatorial trough in some areas and some seasons but none at all in others. It follows that we cannot explain equatorial rainfall in terms of a simple scheme of trough movement; the understanding of equatorial rainfall is still deficient. Someday a common denominator may be discovered to link all the varied regimes and permit their classification. This, however, must await a great improvement in the understanding of the dynamics of the tropical atmosphere.

RAINFALL ANALYSIS

For purposes of applied and synoptic climatology it is necessary to examine the composition of the average monthly-rainfall curves. We shall consider (a) the effectiveness of rainfall, (b) the variability of rainfall, (c) daily rainfall amounts and rainstorms.

Effectiveness of Rainfall

This is a loose, utilitarian term; its definition depends entirely on use of the rainfall. In the tropics, as elsewhere, interest centers on the conservation of water for agriculture and on the production of hydroelectric power. In some areas even the problem of water for human consumption is acute, as mentioned earlier.

In the tropics much more rain is needed to keep the fields moist than in middle latitudes. Even in the temperate zones the "efficiency" of summer and winter rain differs greatly. Most readers will be able to confirm from their own experience that the drought season over mid-latitude continents with summer-rainfall peaks does not occur in January and February, when precipitation is small. The soil dries out gradually during summer, and the cumulative effect is such as to create the lowest water levels and drought danger in late summer and early autumn.

This inverse course of rainfall and water levels illustrates the problem of the tropics. A much smaller percentage of the precipitation is retained in the soil in the tropics and in middle latitudes during summer than in middle latitudes during winter, given equal conditions of slope, soil, and vegetation. Tropical rainfall largely stems from cumulus clouds. The rate of rainfall is as much as an order of magnitude greater from these clouds than from the stratus and altostratus decks that yield most of the cold-season precipitation over middle-latitude land areas. At Batavia, for instance, the annual rainfall comes down in only 360 hours (6). Run-off from cumulus-type precipitation far exceeds that from stratus. This will benefit the hydroelectric engineer if he can store the water. But a good fraction of the rainfall is lost to the farmer. We always hear that

what is needed after a drought is a spell of gentle, but lasting, rain, not a cloudburst.

Some rainfall also is evaporated back into the air right away without having a chance to penetrate into the soil. Evaporation increases rapidly with temperature and wind speed. Especially in the trade-wind zones, where high wind speeds combine with high temperature and therefore with low relative humidities, in daytime, large areas are destitute of water in spite of superficially abundant rain. The author has seen stretches on Puerto Rico where the soil was not capable of supporting natural tree growth in spite of annual rainfall well in excess of 60 inches. On the other hand, it is just this high evaporation rate that renders human life agreeable in the trades.

Of particularly little value for water content of the ground are brief afternoon showers. Not only are temperature and wind, and therefore evaporation, highest at this time of day; the cloudiness is intermittent, and the sun frequently shines within a few minutes after a shower ends. The steam rising from roads and fields is often a pretty sight, but one rarely calculated to benefit farm operations. In studies of tropical rainfall it is advisable to exclude these small showers. The question, of course, is where to draw the line, and this remains fairly arbitrary. Plant ecologists have recommended values ranging from 0.10 to 0.25 inches per day as the lower limit of effective precipitation. These small showers fortunately do not contribute much more than 10 per cent to the total rainfall in most regions. But the number of days with only small showers can be very high. In the central part of Oahu, Hawaii, for instance, 40 to 60 per cent of all days with rain fall into this class.

We could continue this discussion of rainfall effectiveness at great length. Certainly it is clear that for many purposes of applied climatology we should replace mean-rainfall amounts with some other quantity which more nearly measures effective precipitation. Thornthwaite (29) has proposed the nearest known approach to a modification of rainfall maps through introduction of an index based on the ratio of evaporation to precipitation. Applications of this index to various parts of the world including India (24) and Venezuela (30) have improved understanding of the climates for agricultural purposes. We should be led too far afield if we presented Thornthwaite's work in detail; but enough has been said to warn the reader against unqualified acceptance of average tropical-rainfall data for applied purposes.

Variability of Rainfall

When we inspect a curve of mean monthly precipitation, it is of paramount interest to know the extent to which we can expect a certain

monthly rainfall to occur and to what extent there will be deviations. If the probability is, let us say, 80 per cent, then we can count on the rainfall with relatively little risk. But rainfall distributions nearly everywhere are notorious for their wide spread, and this spread is not normally distributed about the mean but highly skewed. A few periods with heavy to excessive rainfall combine with many periods of subaverage rainfall to form the mean. Thus the latter is not representative for many applied purposes and for these should be replaced by the median, as emphasized by Landsberg (7) and many others.

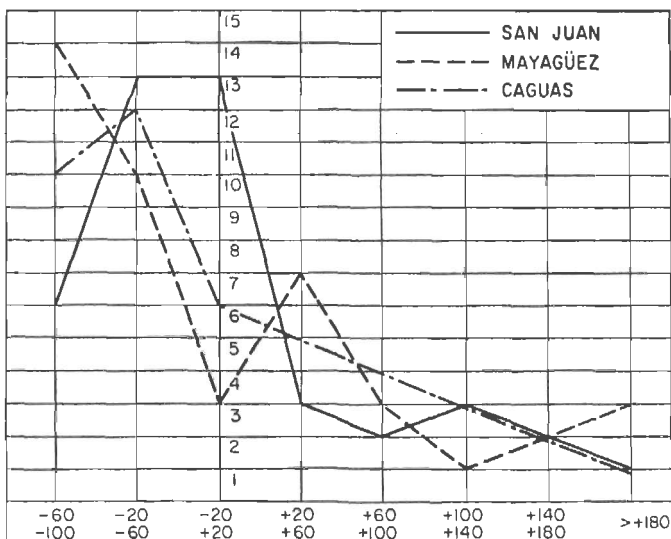


Fig. 3.13. Frequency distribution of the deviations of February rain from the mean at San Juan, Mayagüez, and Caguas, Puerto Rico (21), for 44 years.

The foregoing remains true irrespective of the time interval over which calculations are made. For instance, such severe droughts may occur during the dry season of Puerto Rico (Fig. 3.13) that water and electric-power consumption in the cities must be curtailed and livestock in the mountains must be driven for many miles to the few springs and brooks that have not dried out completely. The dry-season rainfall from one year to the next varies greatly. In February the average rainfall at San Juan is 2.69 inches. The mean difference in precipitation for that month from one year to the next is 2.15 inches, or 80 per cent of the mean rainfall. In some portions of the island this variability exceeds 100 per cent of the mean. As commonly noted in the tropics, the per cent aperiodic change is greatest in months with smallest average precipitation and decreases as the rainfall increases.

Figure 3.13 contains three frequency distributions¹ of the rainfall deviations from the mean for February, expressed in per cent of the average. It is striking how infrequently is rainfall near the mean recorded in individual years; large deviations are the rule rather than the exception. The frequency of negative deviations greatly exceeds the positive ones, which shows the effect on the mean of a few years with excessive rain. Indeed, the frequency of Februaries with rainfall less than 60 per cent of average is very high; about one-quarter falls in this extreme class.

If we combine the Puerto Rican records with information such as that at Honolulu, where February rainfall has varied from 0.50 to 23.50 inches since 1874 (7), it becomes evident that the mean-rainfall curves shown earlier will seldom be realized in individual years. It also follows that long-period records are needed to compute "stabilized" means and medians. For a sample of 22 stations on Oahu, Landsberg (7) required a record of 40 years to stabilize the median in the rainy season and 20 years in the dry season. This suggests that station records should cover at least 40 years to qualify for serious rainfall analysis.

The skewness of the rainfall frequency distribution persists even if we analyze annual means. Landsberg (7) has plotted the differences between medians and means of the annual rainfall for 22 Oahu stations against mean annual rainfall (Fig. 3.14). These differences, expressed in per cent of the mean, are extreme at low annual rainfall and become much smaller in regions with heavy orographic rains. On a monthly basis the skewness is similar. Landsberg also gives the limits of the scatter band. Although the skewness decreases with increasing rainfall, the absolute range over which the rainfall varies increases. The latter amounts to 1.5 inches for a mean rainfall of 2 inches and rises to 4.5 inches for a mean rainfall of 6.5 inches.

The impact of annual-rainfall variations on climate perhaps is shown most strikingly by a world chart of relative variability of annual rainfall (Fig. 3.15) prepared by Biel (1). Relative variability is defined as the ratio of the sums of all deviations from the mean, averaged without respect to sign, to the mean. The isolines on the chart closely follow the lines of equal precipitation so that the two sets of lines are inversely correlated. In accord with Figs. 3.13 and 3.14, *the relative variability is low where rainfall is high, and the variability is high where the rainfall is low*, an unfavorable outcome for all dry areas. Regions with variability less than 15 per cent are restricted in the main to the Congo Basin, the Amazon Basin, and parts of the East Indies. From there, the variability increases toward the subtropical deserts and also toward the bulge of Brazil in South America, where variability is extreme.

¹ For location of the stations see Fig. 4.1.

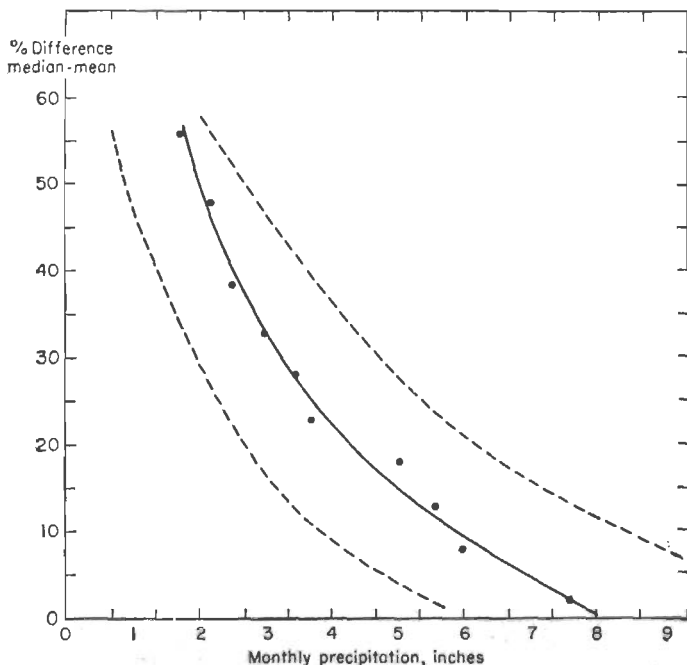
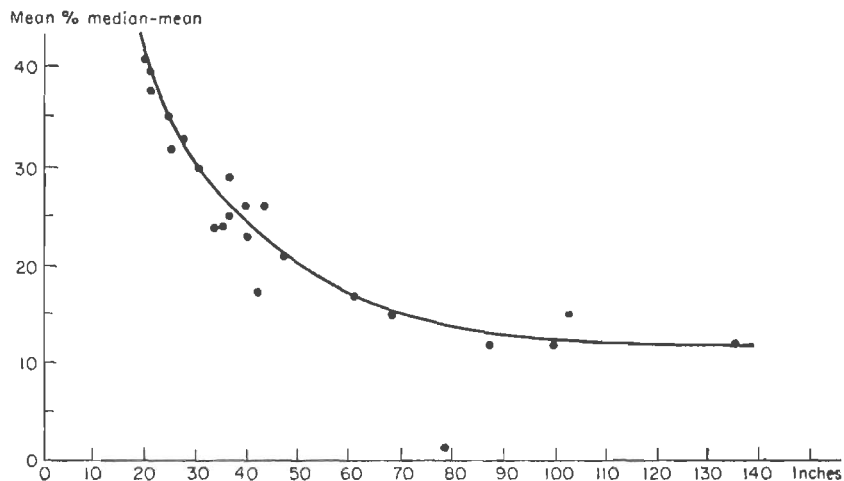


Fig. 3.14. Skewness (ordinate) of annual rainfall for 22 stations on Oahu as a function of rainfall (7) (top); skewness (ordinate) and limits of scatter band of monthly rainfall (bottom).

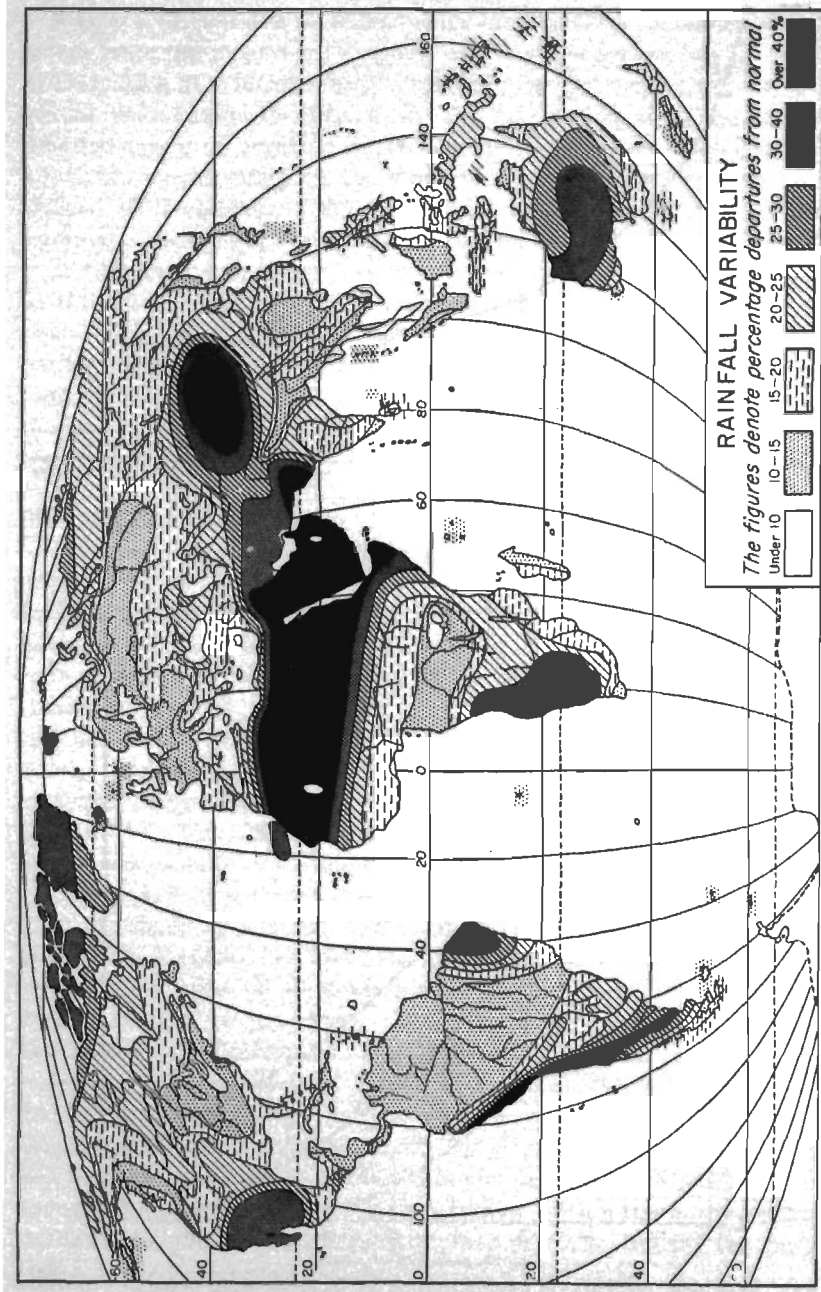


Fig. 3.15. Annual rainfall variability of the globe (per cent) (1).

Biel's chart affords an interesting comparison between the tropics and high latitudes. There, in spite of much lower annual-rainfall totals, wide territories enjoy reliable precipitation, notably Europe, parts of Russia, and the eastern United States. Certainly the rainfall of low latitudes is not more reliable on a per cent basis than that outside the tropics. Rainfall variability is highest in the subtropics, especially at the eastern ends of the subtropical high-pressure cells. At all latitudes there are regions with high and low variability.

Daily-rainfall Amounts and Rainstorms

Investigation of the composition of tropical rainfall can be carried further by considering the daily amounts. As we take up this time scale, we leave the broad climatological aspects and become more concerned with suggestions inherent in the data as to the mechanisms that produce rain.

The bulk of low-latitude precipitation falls in the form of showers. It has been the custom to portray convection as occurring predominantly with a random spatial distribution, limited only by climatic boundaries. This picture follows from the conception of a steady tropical circulation. Slight rainfall variability should accompany the minute fluctuations of surface temperature and wind. As we have just seen, this does not hold true from the seasonal viewpoint. In any given area, excess rainfall may flood the fields in one year, and drought may strike in the same season or the next. If we determine the manner in which individual days contribute to the rainfall totals, the discrepancy between the classical description and reality becomes still more striking, even though we hear that in many localities showers begin every day at a certain hour with clocklike regularity, and even though the Hawaiian tongue contains no word for "weather."

In any area, clear and rainy spells alternate, and this alternation occurs in definite relation to changes in the upper wind field (16, 17). Bad weather concentrates in narrow zones near trough lines. Here we observe high relative humidity to great heights, a characteristic of the air mass usually labeled "maritime tropical." Elsewhere the atmosphere has a lower moist and upper dry layer, with a boundary between 5,000 and 10,000 feet depending on location and season. Thus there are good qualitative indications that the bulk of the rainfall is derived in large measure from disturbances.

This statement can be studied quantitatively by determining the extent to which an excess or deficit of disturbances accounts for rainfall variations. Such an analysis was carried out for the drought season January-March on Puerto Rico (21). Experience in analysis over 4 years had

led to the conclusion that precipitation will fall in excess of 0.25 inch per 24 hours during the dry season only with a marked disturbance except near the higher mountain ranges. Local showers and weak or dissipating disturbances account for the lesser amounts. Rainfall above 0.25 inch therefore was taken as an indication of a pronounced disturbance. This is, of course, a subjective procedure useful only as a first approximation. Because of the showery character of the rainfall, precipitation problems should whenever possible be treated with area integrals of rain rather than with individual station data.

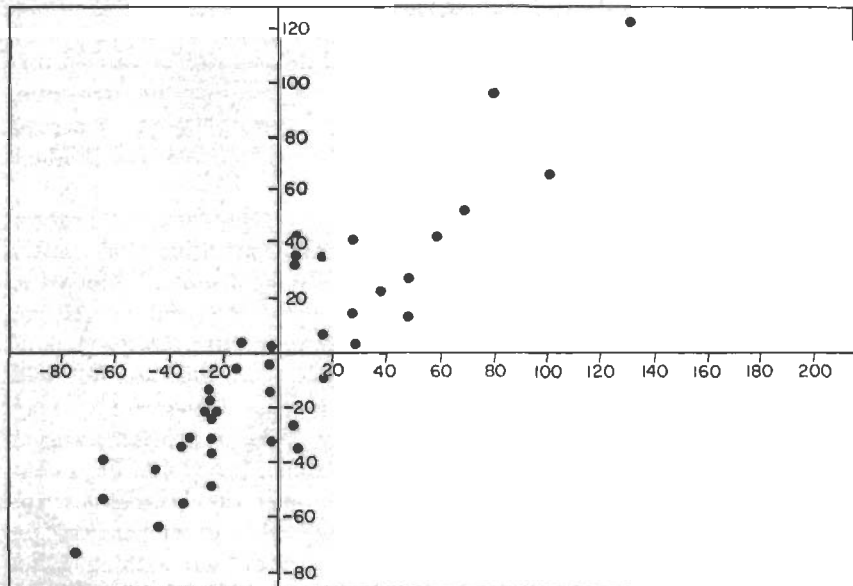


Fig. 3.16. Per cent deviations of rainfall from average January-March (ordinate), against deviations (per cent) of number of days with rain more than 0.25 inch (abscissa) at Mayagüez, Puerto Rico (21).

We obtain a striking result by correlating the departure of drought-season rainfall from the mean with departure of rain frequency greater than 0.25 inch. At Mayagüez, the correlation coefficient is 0.91; the scatter diagram (Fig. 3.16) proves that this coefficient is composed of contributions from all years in the sample and is not dependent on a few extreme values. It follows that variations in frequency and intensity of disturbances govern the rainfall variations.

One weakness of the foregoing is the 24-hour interval used. Climatological records summarize rainfall for periods of 24 hours; this unit, however, is arbitrary and without necessary relation to the conditions that produce rain. A more suitable measure is the total rainfall from begin-

ning to end of a rainy period. This unit, employed in numerous hydrologic studies, may be termed a *rainstorm*. The author used this concept in studying rainfall at 21 stations distributed over the pineapple and sugar districts of Oahu (18), reaching the general conclusion that rainstorms account for 90 per cent of the winter precipitation and slightly less of the summer precipitation. Figure 3.17 shows the monthly-rainstorm frequency for a 10-year period. The average per month is very low, ranging from 1 in June to 3 in February and March. The annual mean is 24.

Rainfall produced by the storms varies greatly from one case to the next. If we subdivide the storms according to the rain they yield, we find that only 40 per cent, or 10 storms, produce more than 0.75 inch. These 10 storms account for over two-thirds of the annual precipitation,

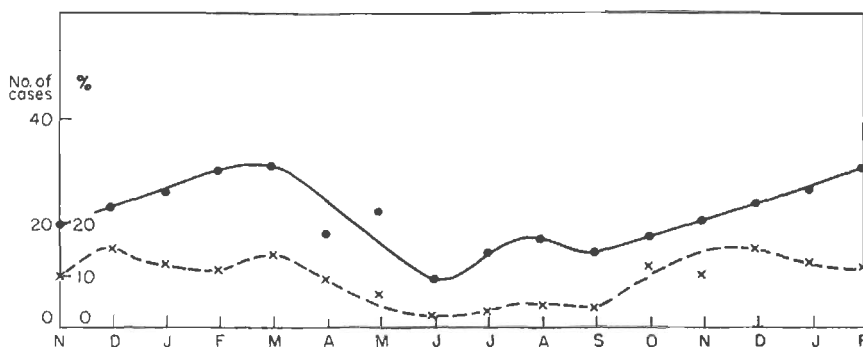


Fig. 3.17. Rainstorm frequency on Oahu, Hawaii, per 10 years (solid curve, 30-day months); contribution (per cent) of precipitation due to rainstorms in each month to annual precipitation (broken) (18).

a curious result. We see now why rainfall in individual months tends to depart so radically from the average. If even one disturbance fails to materialize, the monthly rainfall may be 50 per cent or more below average. Conversely, one extra disturbance may raise the total above 200 per cent of the mean.

In an extensive study, Solot (25) noted certain correlations between Hawaiian rainfall and monthly sea-level pressure anomalies over the northern hemisphere. On the basis of the foregoing these denote a basic state of the general circulation favorable or unfavorable for generating a few potent disturbances. They do not indicate deviations of the properties of the broad-scale flow from average that would tend to raise or suppress rainfall throughout the month.

As far as one can judge, all tropical regions have a rainfall composition similar to Hawaii. Even in the monsoon season over India this appears to be largely true (14). Thus the mean monthly-rainfall curves we have discussed indicate a tendency of the atmosphere to produce two or three

major storms on the average in some months and suppress them in others. When we speak of "equatorial-trough rainfall," we do not mean rainfall on all days when the trough is present, but heavy rain on a few days with passage of some wind-field anomaly.

We must now reexamine the excellent correlations found earlier between the mean seasonal fields of divergence at the surface and rainfall. Evidently we cannot relate rainfall to the mean vertical motion in a simple way if most rainfall is concentrated in a few days. We must infer a complex interpretation of the mean-divergence charts. An average convergence in a certain area implies that a few disturbances with intense convergence will select similar paths. The cumulative effect of these

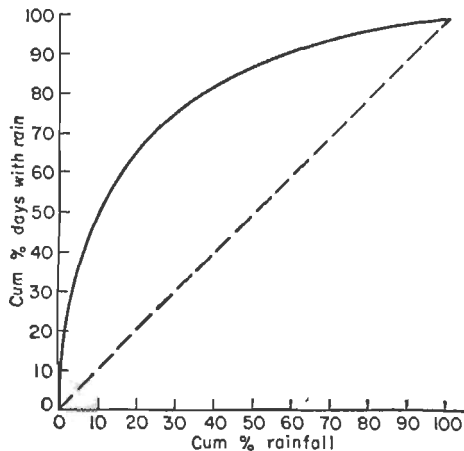


Fig. 3.18. Cumulative number of days with rain (per cent) (ordinate) against cumulative rainfall (per cent) in Argentina (12).

disturbances, and not persistent convergence throughout the month, produces the mean-convergence belts. Palmer (13) has established the validity of this reasoning for a limited period during June, 1946, in the central equatorial Pacific Ocean. If we view the composition of the mean-convergence zones in this light, we must postulate unsteady flow conditions. Comparison of Figs. 1.4 and 1.11 with Figs. 3.3 and 3.5 indeed reveals a negative correlation between wind constancy and convergence.

We can solidify the foregoing further by asking: What percentage of the number of days with rain accounts for what percentage of the total rainfall? Olascoaga (12) has treated this question in an analysis of rainfall over Argentina. This country extends from the subtropics to the subarctic; it has high mountains and large plains; annual rainfall varies from 8 to 125 cm. In spite of these differences all areas except the southern tip of Patagonia gave a uniform result. It was possible to combine

the data for all of Argentina and all seasons to arrive at a general distribution curve of the relation of number of days with rainfall to total rain. Figure 3.18 shows the result, plotted on an accumulative per cent basis. Essentially, 10–15 per cent of the days with rain account for 50 per cent of the rainfall; 25–30 per cent of the days account for 75 per cent of the rainfall. Conversely, the rainfall derived from the 50 per cent of days with smallest rain amounts to only 10 per cent of the total. Since Fig. 3.18 represents such widely divergent regimes in latitude, orography, and mean rainfall, its pattern is likely to hold for most areas. This contention cannot be proved, but it is supported by such data as have been analyzed in the manner described. In addition to Hawaii, the plot for Puerto Rico (19) closely resembles Fig. 3.18. For Hongkong (15), at least parts of the Philippines (19), and Germany (3) the same relation obtains. Exceptions are found in the higher parts of mountains ranges with almost daily showers.

All the foregoing proves that the classical picture of random convection in the tropics must be discarded. Most rainfall occurs in consequence of organized, not unorganized, convection. *Within relatively few and narrow zones of disturbed weather the tropical atmosphere obtains the largest share of that portion of its heat which is derived from condensation and precipitation.* These zones, the "secondary" disturbances of low latitudes, act as the tropical counterpart of the cyclones of higher latitudes.

REFERENCES

- (1) Biel, E. R., Fig. 137, in *Introduction to Weather and Climate*, 2d ed., by G. T. Trewartha. New York: McGraw-Hill Book Company, Inc., 1943.
- (2) Crowe, P. R., *Trans. Inst. Brit. Geogr.*, No. 17, 1951.
- (3) Flohn, H., and J. Huttary, *Z. Meteor.*, **6**: 304 (1952).
- (4) Jacobs, W. C., *J. Marine Research*, **5**: 37 (1942).
- (5) Jacobs, W. C., *Bull. Scripps Inst. Oceanog. Univ. Calif.*, **6**: 27 (1951).
- (6) Kendrew, W. C., *Climates of the Continents*. New York: Oxford University Press, 1942.
- (7) Landsberg, H., in *Am. Meteor. Soc. Mon.* 3, p. 7, 1951.
- (8) Meinardus, W., *Met. Z.*, **51**: 345 (1934).
- (9) Meinardus, W., *Peterm. Geogr. Mitt.*, **80**: 1 (1934).
- (10) Namias, J., *J. Meteor.*, **7**: 130 (1950).
- (11) Namias, J., and W. Mordy, *J. Meteor.*, **9**: 180 (1952).
- (12) Olascoaga, M. J., *Tellus*, **2**: 312 (1950).
- (13) Palmer, C. E., *Quart. J. Roy. Meteor. Soc.*, **78**: 126 (1952).
- (14) Rahmatullah, M., *J. Meteor.*, **9**: 176 (1952).
- (15) Ramage, C. S., *J. Meteor.*, **8**: 289 (1951).
- (16) Riehl, H., *Dept. Meteor., Univ. Chicago, Misc. Rept.* 17, 1945.
- (17) Riehl, H., *Dept. Meteor., Univ. Chicago, Misc. Rept.* 22, 1947.
- (18) Riehl, H., *Bull. Am. Meteor. Soc.*, **30**: 176 (1949).
- (19) Riehl, H., *Tellus*, **2**: 1 (1950).
- (20) Riehl, H., et al., *Quart. J. Roy. Meteor. Soc.*, **77**: 598 (1951).

- (21) Riehl, H., and E. J. Schacht, *Trans. Am. Geophys. Union*, **28**: 401 (1947).
- (22) Schott, G., *Ann. Hydr.*, **61**: 1 (1933).
- (23) Seelye, C. J., *New Zealand J. Sci. Technol.*, (B) **32**: 11 (1950).
- (24) Siddiqi, K. U., master's thesis Department of Meteorology, University of Chicago, 1949.
- (25) Solot, S. B., *U.S. Weather Bureau Research Papers* 28 and 32, 1948 and 1950.
- (26) Supan, A., *Peterm. Geogr. Mitt.*, **44**: 179 (1898).
- (27) Sutton, O. G., *Quart. J. Roy. Meteor. Soc.*, **75**: 335 (1949).
- (28) Sverdrup, H. U., *Oceanography for Meteorologists*. New York: Prentice-Hall, Inc., 1942.
- (29) Thorntwaite, C. W., *Geogr. Rev.*, **21**: 633 (1931).
- (30) Thorntwaite, C. W., *Bull. Am. Meteor. Soc.*, **32**: 166 (1951).
- (31) U.S. Weather Bureau, *Atlas of Climatological Charts of the Oceans*. Washington, D.C., 1938.
- (32) Various contributors, "On the Rainfall of Hawaii," *Am. Meteor. Soc. Mon.* 3, 1951.
- (33) Wuest, B., "Landerkundliche Forschung," *Festschr. Norbert Krebs*, p. 347, 1936.
- (34) Yeh, T. C., *Tellus*, **2**: 173 (1950).
- (35) Yeh, T. C., *et al.*, in *Am. Meteor. Soc. Mon.* 3, p. 47, 1951.

CHAPTER 4

DIURNAL AND LOCAL EFFECTS

The broad-scale aspects of wind, temperature, and rainfall discussed so far furnish the traveler to the tropics with a rough indication of what he is likely to encounter. Arriving at his destination—for instance, Honolulu—he will find that a major choice is still to be made as to the climate where he wishes to live. He may settle in the fashionable beach district around Diamond Head, where sunshine is profuse, rain is rare, and the days often are hot in summer. Only a few miles away on the hill slopes, temperature will be much lower during day and night, the days mostly overcast, and the relative humidity high so that care is necessary that clothing and other equipment do not mold.

In touring the island of Oahu, the traveler can drive in one hour from dense tropical jungle across fertile pineapple fields and irrigated sugar plantations to country so dry that only thorny cactus can survive. He can also ride up a gently sloping valley toward the mountains in the northeast until, arriving at the pass, he is surprised and chilled by the trade wind blowing with violent gusts up to 50 mph through the gap. Beyond the pass, the mountains drop vertically 1,000 feet. After descent over the highway, here of alpine construction, the visitor can see in the sheer walls perfect vertical semicylinders, hundreds of feet high and a few feet wide, carved by rainwater flowing down from the upper jungle with annual rainfall of more than 200 inches. If all this does not provide enough variety, he can go to the island of Hawaii, ride up from the city of Hilo through the plantations, forests, and barren, lava-covered territory above the trade inversion to the observatory on the volcano Mauna Loa (13,680 feet), and, if visiting in late winter, try a bit of skiing.

Such extreme variety within short distances illustrates the important place local climate occupies in tropical meteorology.

Diurnal Temperature Variation

Over the tropical oceans the diurnal temperature range remains within about 1°C at all longitudes and latitudes. Over land it far exceeds the seasonal range. In the equatorial belt it is the diurnal temperature cycle that governs the habits of life throughout the year.

Puerto Rico, located within the trade regime of the Atlantic, furnishes

a good illustration. Wind direction on the average varies only slightly through the year; the large seasonal changes of the diurnal regime which characterize the monsoon regions with their complete wind reversal between seasons are missing.

Besides the prevailing wind direction and speed, the local factors that shape the diurnal course of temperature are topography, altitude, nature of the underlying surface, and cloudiness. An island like Puerto Rico provides several combinations of these factors. Its geographical structure is simple (Fig. 4.1). The coasts form a rectangle, with the longer side oriented east-west. Its length is about 100 miles, and its width 40 miles. A mountain range averaging 2,500 feet in height, but with highest elevations near 4,400 feet, extends from east to west across the whole length of the island.

We shall compare three Puerto Rican stations. San Juan, situated on the windward northern coast, has good sea breezes during the daytime.

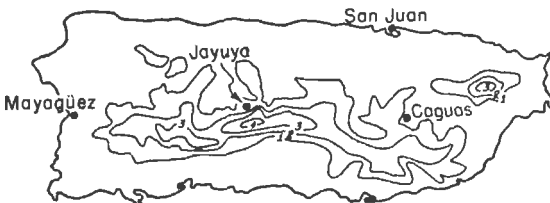


Fig. 4.1. Outline of the island of Puerto Rico, with contour lines at 1,000-foot intervals.

At night a weak land breeze reaches the city only in periods of weak trade. Jayuya lies at an altitude of 1,700 feet in a valley of the gently sloping northern foothills. Here we can expect cold-air drainage at night; indeed the whole valley is often covered with dense radiation fog in the morning. This situation is by no means unusual. Pockets of radiation fog, even fog blankets over jungles, are far more common than once was believed. Mayagüez, finally, is situated on the leeward western shore, where at night drainage from the mountains reinforces the trade so that the wind is often high and gusty in the night. The sea breeze tends to move inland from the west during the day, but to do so, it must overcome the trade. Therefore the time of arrival of the sea breeze is quite variable; it is often delayed till 2 or 3 p.m., which permits the temperature to reach a high maximum.

This description suggests that we should expect an "oceanic" climate at San Juan and more "continental" climates at Jayuya and Mayagüez, though the latter is located on the coast, as is San Juan. All lee areas have relatively continental conditions, and the present case is no exception. The average diurnal temperature range is 23°F at Mayagüez, 24°F at Jayuya, and only 10°F at San Juan. Remarkably enough, the range

is almost invariant at all three stations throughout the year. As the weather changes from the dry season January–March to the wet season in summer, with a large increase in the total moisture content of the air, a reduction of the diurnal temperature range may be expected. But this is not observed. Nor is the range less than over middle-latitude continents, where the moisture content is appreciably lower than over Puerto Rico.

Figure 4.2 shows the annual course of mean daily maximum and minimum temperatures. Perhaps most striking is the parallel course of all

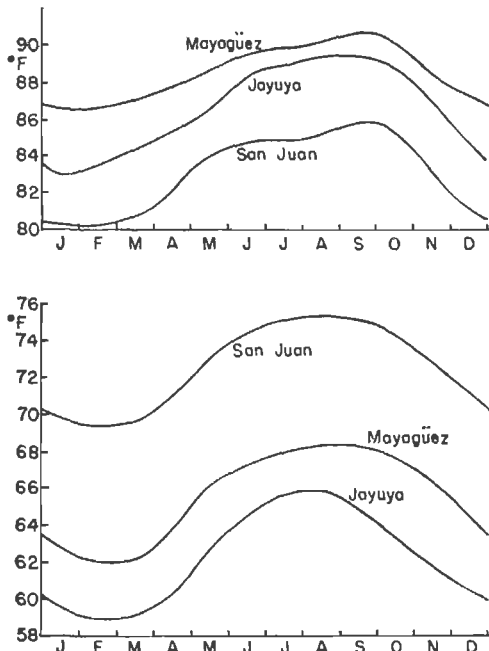


Fig. 4.2. Seasonal variation of mean daily maximum and minimum temperature ($^{\circ}\text{F}$) at three Puerto Rico stations shown in Fig. 4.1.

lines. Throughout the year, Mayagüez has the highest maximum temperature, with a peak in September–October at the height of the rainy season. Jayuya temperatures are a close second, especially in summer, when daytime showers occur almost daily and when we might look for relatively low maximum temperatures. San Juan is considerably cooler, and this is easily explained by the sea breeze. The slight hump in July–August results from particularly strong trade winds in these months.

At night the inverse picture holds. San Juan is warmest, in accord with the local wind circulation. The small diurnal range at San Juan compared with the other stations comes both from lower daytime and

higher nighttime temperatures—an illustration of the predominant marine influence. From the viewpoint of human comfort, Jayuya and Mayagüez are to be preferred. The nighttime temperatures, 6–10°F lower than at San Juan, permit better sleeping, and one needs a light blanket toward morning. The daytime temperatures, though higher, are coupled with strong wind and low relative humidity, so that the cooling power is much higher than at San Juan.

Table 4.1 gives the temperature extremes on record. Considering the heat waves which the city dweller in the United States must endure, one might go in summer to Puerto Rico to keep cool. The chance is almost nil that the temperature will reach 100°F. Even though the mountains are only of moderate height, rather cool temperatures can be found,

TABLE 4.1. TEMPERATURE EXTREMES AT THREE PUERTO RICAN STATIONS

	Maximum	Minimum
San Juan:		
Winter.....	87	62
Summer.....	94	70
Jayuya:		
Winter.....	92	46
Summer.....	98	58
Mayagüez:		
Winter.....	91	51
Summer.....	99	60

including 51°F on the shore. Similar temperature records can be found at thousands of stations in the tropics.

Diurnal Wind Variation

Although the diurnal temperature variation over the sea is negligible, observations confirm the existence of diurnal wind variations (8). Over the Pacific upstream from Hawaii, the wind increases 1–2 mps in the whole subcloud and cloud layers from noon to midnight (14). At the same time the trade inversion lowers several hundred meters (5). Since the nocturnal increase affects the whole layer of strongest trade, the diurnal wind cycle cannot be explained on the basis of turbulent exchange with higher layers. Some attempts have been made to connect the diurnal wind and pressure oscillations (8), but no definite relation has been found.

Over land the diurnal wind variation takes a course like that in the temperate zone in summer. At night the wind speed approaches zero as the vertical momentum exchange is curtailed by increased thermal

stability. When the stable ground layer is wiped out by insolation during the morning, the wind speed increases and becomes gusty as air with higher wind speed is mixed downward. In rarer situations when the air aloft is nearly calm, or when the wind decreases upward, irregular local wind systems develop during the daytime, depending on topography.

Land and Sea Breeze. Most important for the diurnal wind variation in coastal areas and over islands are the land and sea breezes. These circulations are set up by differential heating and cooling over land and water. Suppose there is no pressure gradient in the early morning. As daytime heating begins, the air warms more rapidly over land than over sea. Upward expansion of the air columns over land produces a pressure gradient aloft directed from land to sea; seaward acceleration of the upper air results. Over land the surface pressure now begins to fall so that a low-level pressure gradient from sea to land is established. In this way the sea breeze is produced. The vertical circulation is in the sense that warm air ascends and cooler air descends; it therefore can generate kinetic energy. The sea breeze continues to accelerate until ground friction offers enough resistance and until the land-sea temperature gradient is reduced by the movement of cooler air inland and by subsidence over the sea. Then the breeze becomes steady for a few hours or goes through several cycles of increase and decrease. When insolation lessens in the afternoon as the sun goes down or as the clouds, stimulated by the sea breeze, shield the ground from the sun's rays, the sea breeze weakens and dies. At night, all the foregoing applies in reverse and leads to the formation of land breezes. These are rarely as strong as the sea breeze, at least over land, usually amounting to 2–5 mph compared with 10–20 mph.

Upon this basic scheme of a "simple heat engine" a host of factors is superimposed. A *dynamic influence*, dependent only on latitude, is the *Coriolis force*. In equatorial regions this force is small; the sea breeze moves inland on a straight path and may have time to penetrate 50 miles (4). In middle latitudes the winds are gradually deflected, clockwise in the northern hemisphere, so that after some time the breeze blows parallel to the coast. This limits the sea-breeze regime to a coastal strip roughly 20 miles wide.

A second factor, noted in connection with the diurnal temperature cycle, is the *prevailing wind*. At San Juan and vicinity, the sea breeze normally reinforces the trade; one merely notes a gradual strengthening of wind speed during the morning. At Mayagüez, however, the sea breeze arrives from the west and so must overcome the trade. This requires a stronger surface-pressure gradient. As the morning progresses, the land heating is not interrupted and the cooler air over the sea, trying to enter, piles up in depth, held offshore by the trade. In the end the

landward-directed surface-pressure gradient becomes sufficiently strong so that the sea air begins to accelerate and comes inland as a miniature cold front, with gusty winds and a shower or squall line at its forward edge. The temperature drops rapidly—in extreme cases on the African coast from 35 to 20°C—while the relative humidity jumps as much as from 20 to 90 per cent. When the wind opposing the sea breeze exceeds 15 mph, development of a sea breeze is unlikely.

Third, since land and sea breezes are better developed with clear than with cloudy skies, they are strongest in the dry seasons.

Finally, topography and vertical stratification of the air produce a multitude of sea-breeze structures. The size of the heat source is important. Sea breezes are weak, often nonexistent, on small islands when the wind is strong. During light wind, however, when the air is exposed to land heating for periods upward of 20–30 minutes, even tiny islands disturb the general current and give rise to large cloud streets. On a big peninsula such as Florida the sea breeze may enter from both sides (1)—a double sea breeze. Proximity of other heat sources within 50 miles of a coast line produces a variety of conflicting and complicated regimes, such as are encountered in the East Indies (4).

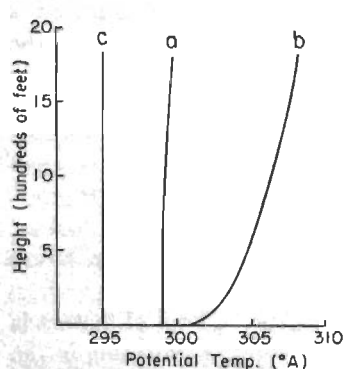


Fig. 4.3. Vertical gradient of potential temperature in summer: (a) over sea; (b) on north slope of Puerto Rico at time of highest temperature; and (c) at time of lowest temperature.

Since the potential temperature in the adiabatic layer over the sea remains constant with height, the potential-temperature gradient between land and sea, only 1–2°C at sea level, will amount to 8°C at 1,700 feet altitude (Fig. 4.3). The rise of the land is of major importance in stimulating and maintaining the sea breeze; this is illustrated schematically in Fig. 4.4.

Much depends on height and configuration of the mountains, the angle of incidence of the prevailing wind, and the stratification of the air above

If the land is not flat like an atoll but rises and has hills and mountains, the sea breeze is always reinforced. Because the heat source is raised, the temperature difference between the air over land and the mixed subcloud layer over the sea (Chap. 5) can increase upward. According to Fig. 4.2 the mean maximum temperature at Jayuya is 4–6°F or 2–3°C higher than at San Juan; considering the elevation of both places the potential-temperature difference is 7–8°C. This difference represents the heating of the air as it moves from the coast to the mountains in roughly 1 to 2 hours.

the subcloud layer. From a large number of choices to illustrate combinations of these factors we select Leopold's work on the sea breeze of Hawaii (6). There the trade current with a marked inversion flows against obstacles of various shapes and sizes (Fig. 4.5). If the inversion lies between 6,000 and 8,000 feet, the air tends to go around larger obstacles whenever possible since energy must be expended in climbing over them. Leopold at first investigated the sea breeze over smaller islands with sides of 10–50 miles in length and highest elevation near 3,000 feet where the stable upper layer meets no obstacle (Lanai and Molokai in Fig. 4.8). On the northern shores the sea breeze reinforces the trade as at San Juan. On the leeward sides southerly onshore winds develop in a shallow layer. During the middle of the day these opposing wind systems can meet in surprisingly narrow zones. On one island the airstrip,

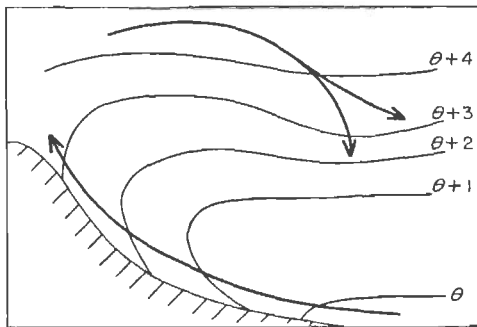


Fig. 4.4. Model of fully developed sea breeze along mountain side. Solid lines are isentropes.

located inland and 3,800 feet long, often has northeast trade at one end of the field and a southerly breeze at the other end.

The surface pressure acts in the required sense. At night the barometer may register 0.5 mb higher inland than on the coasts, which are only 10 miles distant. In the daytime the gradients are reversed. Air entering from the south is caught in the trade and doubles back on its track after rising in the convergence zone between the opposing winds. A quasi-stationary cloud line is maintained over the convergence area. Individual clouds drift away from this line with the trade and dissolve over the sea while new clouds form in the previous position. Neither the small size of the islands nor the proximity of other heat sources appears to prevent this circulation.

Next we consider a larger island where a volcano of 10,000 feet altitude occupies one corner (Maui, Fig. 4.8). That the trade tends to flow around this mountain is seen in the fact that on the windward side the highest annual rainfall (400 inches) is recorded at an elevation of 3,000

feet and then decreases to 20 inches at the top. In contrast, another cone of 5,000 feet elevation, located at the other end of the island, has its highest rainfall on the summit. Figure 4.5 shows the deflection of the trade around the large volcano. The sea breeze, entering from the south and southwest in the trade-protected lee, is flanked on both sides by the strong, channeled trade. Thus a clockwise-shear zone develops to the right of the sea breeze and a counterclockwise-shear zone to the left, which in this case is better developed for topographic reasons. The rising air reinforces the two channels, and two cloud streets extend down wind along the trade.

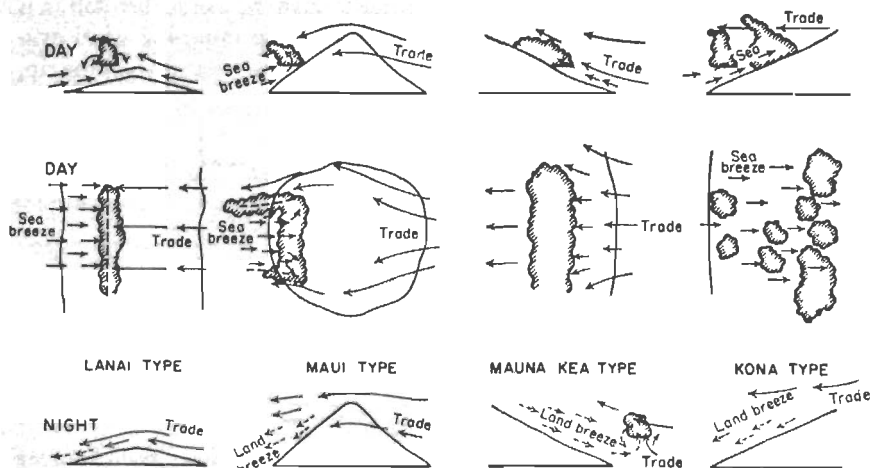


Fig. 4.5. Schematic representation of four types of interaction of sea breeze and trade wind over Hawaii (6). Daytime conditions (*top and middle*) shown in vertical and horizontal sections, nocturnal conditions (*bottom*) in vertical section only.

On the main island of Hawaii (Fig. 4.8) two volcanoes rise almost to 14,000 feet, and the mountainous area is too large to be entirely circumvented by the wind. A strong current blows through a saddle of about 6,000 feet height between the two cones. Since the clouds in the saddle are very shallow, there is a suggestion that the inversion is actually lower there than over the sea. The breeze on the lee side again is caught by the trade and doubles back. In this case, however, the elevation of flow reversal is sufficiently high for shower-producing clouds to form in the sea-breeze air alone.

Although a reasonable qualitative description of orographic sea-breeze regimes is possible, an exact solution of the dynamics is a very difficult task. Evidence is abundant that dynamic aspects play a principal role in shaping the observed sea-breeze structures. When an inversion is present, there is always a tendency to excite stable or unstable waves in

the inversion surface. Internal waves develop in stratified flow without inversion. A treatment of the very difficult problem of the details of flow over the mountains is beyond the scope of this book. Suffice it to say that in the immediate lee the upper air often does not subside but rises steeply (9). The most violent vertical currents, up and down, are encountered here, as are turbulence, severe convection, and hail. Such violence is not to be expected where the trade inversion is strong and the upper air dry as over Hawaii. Even there, however, it is of interest that parts of the lee side at the Kona coast pictured in Leopold's last diagram have their rainfall maximum in summer when the northeast trade is strongest, in complete opposition to the predominant course of rainfall over the islands (Chap. 3). This suggests a strong dynamic pumping effect in addition to land and slope heating.

Further Comments on Land and Sea Breezes. In most areas the strength of the sea breeze greatly exceeds that of the land breeze. At first sight this is rather strange considering that we are analyzing a thermally induced circulation. Usually the surface-temperature difference between land and sea is much greater at night than during the day (4). Figure 4.2 confirms this. The daytime maxima average from 2 to 8°F higher than the sea surface temperature; the nighttime minima average from 7 to 18°F lower. According to one explanation the strongest land breeze should be observed over sea just as the strongest sea breeze is observed over land. Therefore observations made at fixed stations during day and night should not be compared.

Although some evidence supports this hypothesis, it certainly cannot be regarded as more than a partial explanation. Strong land breezes over land and sea usually blow where steep mountain slopes reinforce the thermal effect so that the downward-flowing air acquires a fall velocity due to its weight. Under such conditions strong and gusty land breezes indeed occur.

Following Wexler (17) one sees that the nocturnal circulation is not as intense as that of daytime either in velocity or in depth because cooling is not mixed through a deep layer, like heating, and because, therefore, the land breeze is restricted to a shallower layer near the ground. This solution is probably more nearly correct, as further demonstrated by Fig. 4.3 for mountainous regions with gentle slope. The area between curves (a) and (c) is less than 50 per cent of the area between (a) and (b). At night the temperature on the higher slopes does not decrease much below the free-air temperature at the same altitude. A steady-temperature field is reached since the potential temperature is roughly constant along the ground and downslope winds will not appreciably affect the coastal temperature in either sense.

The vertical depth and structure of the sea breeze have been the subject

of many studies. In addition to topography much depends on the stratification of the air. Sometimes an inversion is present below the convective-condensation level. Then the whole circulation takes place in the adiabatic layer underneath the inversion. Air parcels can complete closed paths; the same parcels may move in from the sea more than once. This requires rapid descent over the sea. Pilot balloons in the East Indies have been seen driven out over the water in the upper outflow, only to be blown back to the coast at sea level by the sea breeze (4)—persuasive evidence of a closed path. The downdraft over the sea must have exceeded the free lift of the balloons.

Odd things can happen. Along some coasts factories lie a little distance back from the shore so that the onset of the sea breeze usually brings clearer air and better visibility to the beaches. Imagine the amazement of a shore observer when suddenly the industrial pollution begins to arrive from the sea! Yet this can occur. In the convergence zone over land the smoke is carried aloft, and from there out to sea, then downward and inland again to the chimneys from which it came.

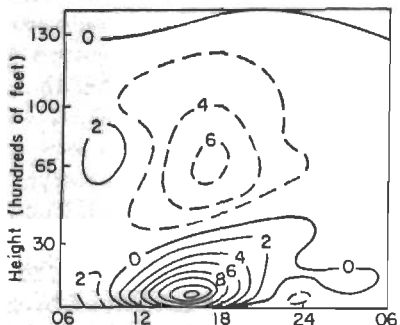


Fig. 4.6. Diurnal variation of wind speed and direction at Djakarta (16).

These stable layers sharpen during the day but do not descend to sea level. New air constantly enters the circulation near the ground and is evicted aloft. When clouds form in the current rising along mountain slopes, the total depth of the sea breeze may reach to several times the height of the mountains.

Van Bemmelen's (16) frequently published diagram on the sea-breeze structure of Djakarta shows the depth of the circulation and its diurnal course (Fig. 4.6). The sea breeze reaches its greatest strength during the middle of the afternoon at a height below 1,000 feet. The return current centers at 6,500 feet, and it is clear that it cannot descend from that height to sea level within a few hours. Correspondingly Fig. 4.3 proves that the air rising over the mountains of Puerto Rico must be carried downstream with the trade if the sea breeze is to be maintained. Continuity is provided by the arrival of fresh air from the ocean.

When the sea breeze extends above an inversion or when there is no inversion, closed paths are unlikely. The descent over the sea brings air columns down in which the potential temperature increases upward. Stable layers develop (3, 11) on the shore and over the water above the subcloud layer, coupled with a decrease of the specific humidity.

Diurnal Variation of Cloudiness and Rainfall

According to results of oceanographic expeditions (8) the low cloudiness over sea increases at night and decreases during the day. Total cloudiness is highest near sunrise. This is verified also by longer weather-ship records (10). Because cloud observations are made visually, all records, however, are open to justifiable doubt, especially since the apparent diurnal variation is only one-tenth of sky cover. At night it is difficult to estimate the cloudiness accurately. This difficulty becomes quite obvious when the diurnal course of middle and high cloudiness is calculated separately for days centered about full moon and all other days. During the latter days the middle and high cloud cover decreases after sunset and increases at sunrise, while such a variation fails to materialize during nights with a full moon (10). It is safest to say that the diurnal variation of cloudiness over the oceans is small.

Reports of nocturnal-rainfall maxima also must be received with caution. We have seen that at least in some areas the low-level wind speed increases at night and that the trade inversion lowers appreciably. Such lowering implies a decreased vertical thickness of trade cumuli at night, a trend not easy to reconcile with an increase of precipitation.

In coastal areas the land- and sea-breeze regime governs the diurnal course of cloudiness and rainfall. At Puerto Rico the trade blows parallel to the mountain range on many days with undisturbed trade. Under such circumstances the orographic-convection cell pattern induced by the sea breeze attains its most regular development. During the morning, the clouds on the coast and offshore to a distance of 20 miles dissipate as cumuli congesti build up over the mountains. All day long one can sit safely on the shore and watch the shower activity, often heavy, only a few miles away. A change sets in about 4 P.M., when the big clouds begin to break away from the mountains and move over the coastal plains. For an hour or two the sky appears "chaotic" with many cloud layers and cumuli of all shapes and sizes present. Gradually the clouds inland disappear at sunset as rows of clouds, often in single file, develop on the coast or slightly offshore.

In principle, this description holds nearly everywhere in the tropics. Inland, cloudiness and rainfall reach their peak during the day, and the nights are clear. Walls of clouds containing showers are banked on the shore or over the sea at night. Forenoon is usually the time of day with least precipitation.

Again a vast variety of local influences produces deviations from the basic rhythm. Along the western Gulf coast of the United States, the sea breeze often begins around 9 A.M., producing an unusual morning maximum of rainfall and thunderstorms. Figure 4.7 shows how compli-

cated the diurnal rainfall curve is even at San Juan, where the terrain and other features are relatively simple. This curve, of course, is composed of the rainfall of all days, not just days with undisturbed trade. Nevertheless, the four-peak structure is surprising until one has learned to appreciate the local situation. The nocturnal-shower activity increases and decreases rhythmically several times during the night; this is faithfully reflected in Fig. 4.7. The afternoon peak results from rain in disturbed situations when the general wind has a south component. This precipitation is produced in no small measure by the most remarkable cloud within the author's experience.

Referring again to Fig. 4.1, an isolated mountain stands near the eastern end of Puerto Rico. This is a major convection point. On days with

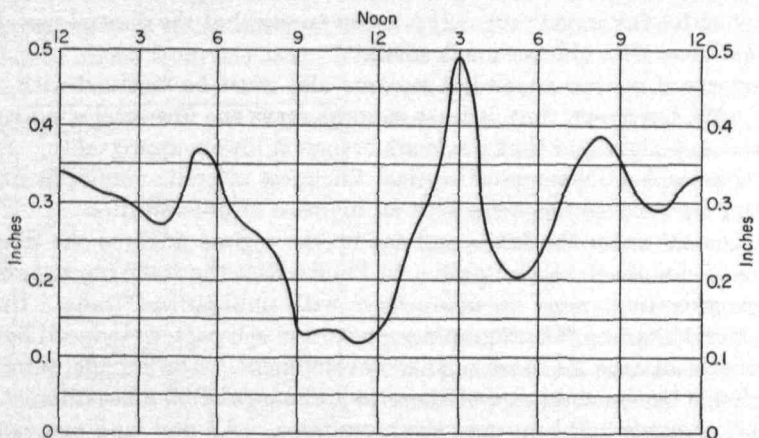


Fig. 4.7. Mean hourly precipitation at San Juan, Puerto Rico, for November (11, after R. G. Stone).

east-southeast to southeast winds a cloud street extends downstream from this mountain which reaches the sea near San Juan. When this cloud street is fully developed, it consolidates into a single imposing roll cloud. The length of the cloud is 20 to 40 miles, its lateral width hardly 1 mile. It extends from 2,000 to 8,000–10,000 feet altitude. Ragged cloud matter can be seen rotating rapidly, and the whole formation is tube-shaped. The cloud organizes shortly before noon and dissipates 3–4 hours later, shifting its position very little. In that time more than 4–5 inches of rain may fall in the narrow underlying zone. The size of the raindrops is huge—larger than any the author has seen fall from cumulonimbus. The top of the roll cloud is not uniform. Peaks and valleys alternate, with amplitude of 1,000–2,000 feet and spacing of a few miles, indicating superposition on the roll of a wave motion. The precipitation rate rises to an extreme at the arrival of the peaks where convergence is strongest.

Similar roll clouds and many other types of orographic-convection cells are abundant on all mountainous tropical islands. Even atolls have a definite effect on the local cloud structure and its diurnal course. We cannot pursue the description of these manifold patterns. Instead we turn to their cumulative climatic effect.

The Control of Climate by Orographic-convection Cells

Orography influences both the total annual rainfall and its seasonal course. Mean-rainfall maps published for many tropical regions attest

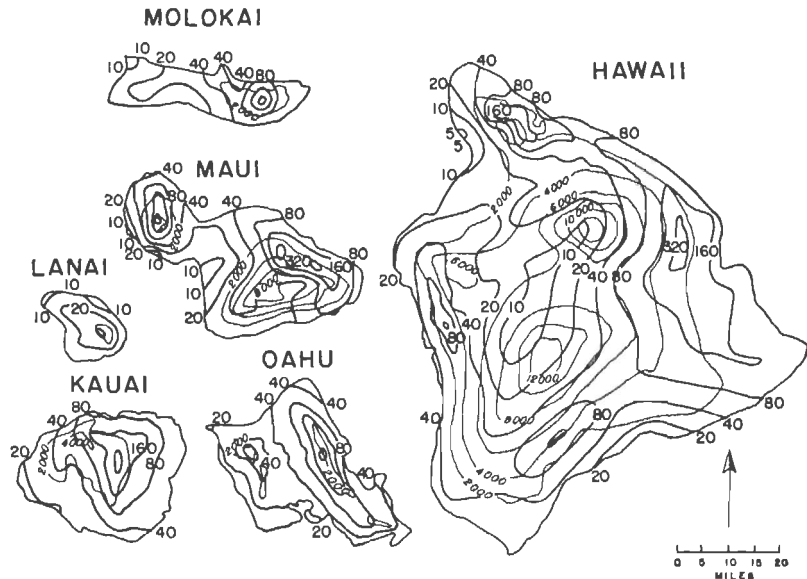


Fig. 4.8. Mean annual rainfall (inches) on the islands of Hawaii (7). The interval between isohyets is logarithmic.

the profound importance of the semipermanent areas of ascent and descent created by the mountains. Chosen from a very large number of published charts, Fig. 4.8 illustrates the annual rainfall over the Hawaiian Islands (7), with which we have already become familiar. Of particular interest is the manner in which rainfall amounts increase inland from the coast. If the isohyets are spaced in geometric progression, the distance between them becomes nearly uniform. This is a rainfall characteristic which does not hold equally well in all tropical mountain areas.

On the islands of Molokai, Kauai, Oahu, and Lanai the height of the mountain ranges is below 5,000 feet. The trade wind blows over these ranges and deposits the maximum amounts just beyond the crests. Excepting Lanai a central isohyet of 320 inches appears on all islands.

Such extreme amounts occur only in limited mountain regimes, such as northeast India and the Sierra Leone and Cameroon mountains of West Africa. In the lowlands annual rainfall may be as little as 1 per cent of the maximum in the mountains.

A debate of long standing concerns the variation of precipitation with height along mountain slopes. At one time the opinion prevailed that precipitation is heaviest near 3,000 feet and diminishes upward from that level since the saturation specific humidity, and therewith the maximum water content in a column above the surface, decreases. Undoubtedly the precipitation diminishes for this reason near the summit of very high ranges. But rainfall is a function not only of water content of the air but also of its rate of ascent. Depending on local conditions this rate may increase to unknown heights. It is not surprising that in the course of the years measurements of runoff have proved that in many high mountain ranges the precipitation far exceeds early estimates. Even explorers climbing the high Himalayas have encountered severe snowstorms, and many expeditions have perished because of them.

In Hawaii the situation is clear-cut in that the three high summits on Maui and the main island which penetrate the inversion are arid on the top, while the 320-inch isohyet is centered near 3,000 feet altitude. Lesser peaks up to 7,000 feet receive their highest precipitation on the summit. Many details of Fig. 4.8 also point to mean horizontal eddy patterns. Going south, for instance, along the 3,000-foot contour line from the zone of heaviest precipitation in the eastern part of the island of Hawaii, rainfall decreases to a mere 40 inches 20 miles away, then rises rapidly to 160 inches, and again drops to 40 inches at the southern tip of the island.

Analyzing the seasonal precipitation, Stidd and Leopold (15) found that the mean monthly rainfall as well as rainfall in individual months for all stations on any of the islands can be represented by a straight line on a diagram of monthly against annual rainfall (Fig. 4.9). This straight line has the form $y = a(x - R) + b$, where y is the monthly rainfall, x the annual rainfall, a a constant determining the slope of the line, and b its intercept with some selected annual-rainfall value (R). This attack in terms of slope and intercept has been fruitful. Success of the straight-line approximation has made it possible to treat the great variety of climatic regimes on one island in a very simple manner. Even the differences between islands are sufficiently small so that for practical purposes the Territory of Hawaii can be treated as one unit in the relation of monthly to annual rainfall. In view of Fig. 4.8 this result is astonishing indeed.

Stidd and Leopold interpret the constant b as "a geographically constant quantity derived from a rainfall blanket of uniform thickness over the whole island and adjacent open sea." Therefore b represents essen-

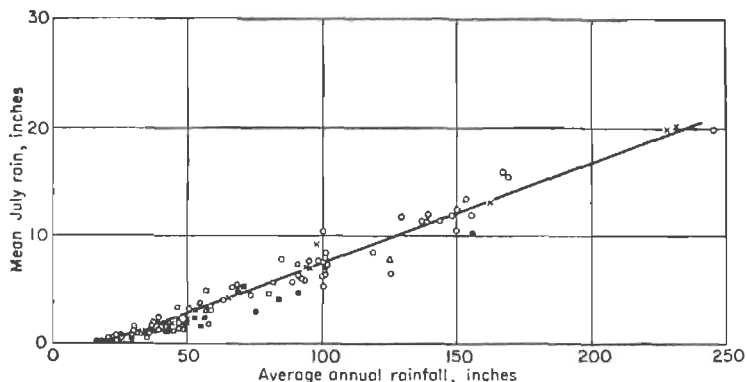


Fig. 4.9. Mean July rainfall vs. mean annual rainfall on Oahu, Hawaii (15).

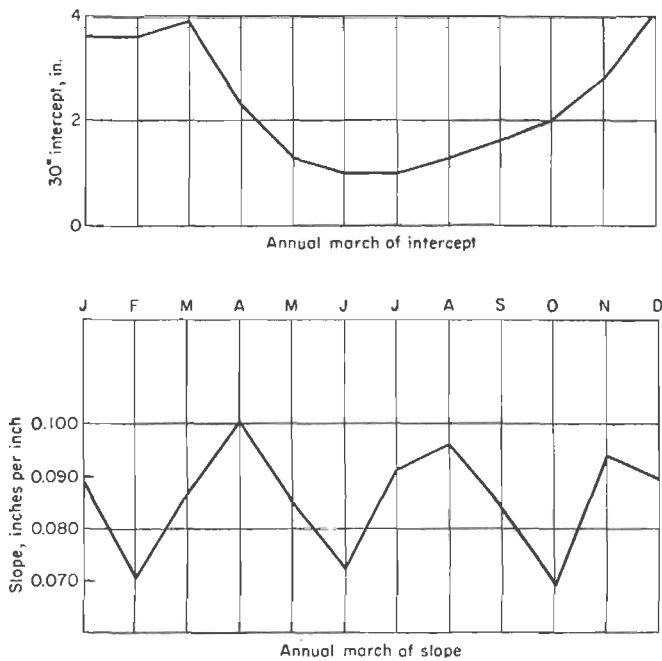


Fig. 4.10. Seasonal march of 30-inch intercept (cyclonic component) of Hawaiian rainfall (top) and of slope (orographic component) (bottom) (15).

tially the precipitation derived from rainstorms. When determined for all months, the twelve values of b should add up to the mean annual rainfall over the open sea in the vicinity of the islands. This mean annual rainfall is then the quantity R of the above formula since $y = b$, when $x = R$. Its amount cannot be determined conclusively but, judging from world-rainfall maps (Fig. 3.2), 30 inches is plausible. The annual march

of the 30-inch intercept (Fig. 4.10) then should express the annual march of rainfall due to general storms computed in Fig. 3.17. The two curves closely resemble each other, in support of Leopold's physical interpretation of the constant.

We may now divide the annual rainfall at any Hawaiian station into two parts, that due to the march of the 30-inch intercept with constant slope, and that due to variations of the slope. The annual march of the

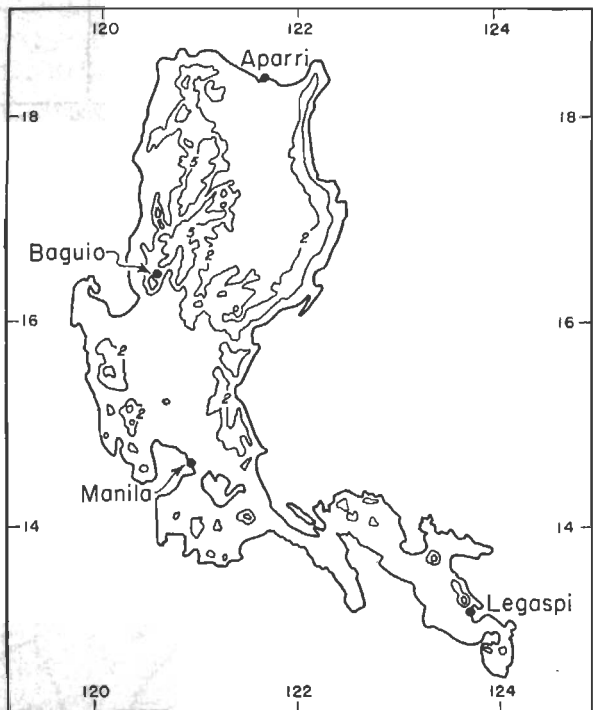


Fig. 4.11. Topographic outline of the island of Luzon in the Philippines (2,000- and 5,000-foot contours).

slope (Fig. 4.10) is given by a peculiar curve with three peaks for which no ready explanation has been found. Variations in the slope assume an increasing importance in shaping the observed rainfall curve with increasing annual rainfall. Therefore the annual march of rainfall at stations with small annual totals resembles the march of the intercept and gradually changes to curves resembling the march of the slope at high annual precipitation, with peaks in April, July-August, and November-December. With this, the rainfall of Hawaii has been put in a neat package.

Seasonal Rainfall on Luzon. Statistical techniques as described for Hawaii should prove useful in many tropical mountain areas. But it is

doubtful to what extent the particular parameters used can be applied generally. For comparison, Fig. 4.11 shows the topographic outline of Luzon, the main island of the northern Philippines; Fig. 4.12 gives the rainfall curves for the stations shown in Fig. 4.11. Baguio lies in the mountains, the other stations near the coast. The annual march of rainfall at Manila is usually considered standard for the Philippines. In winter the dry and stable northeast monsoon prevails. At that time of year Manila is a lee station, and rainfall is near zero. In summer the equatorial trough lies a little north of Manila in the mean, oriented east-west. Many typhoons and weaker depressions pass near the city, which

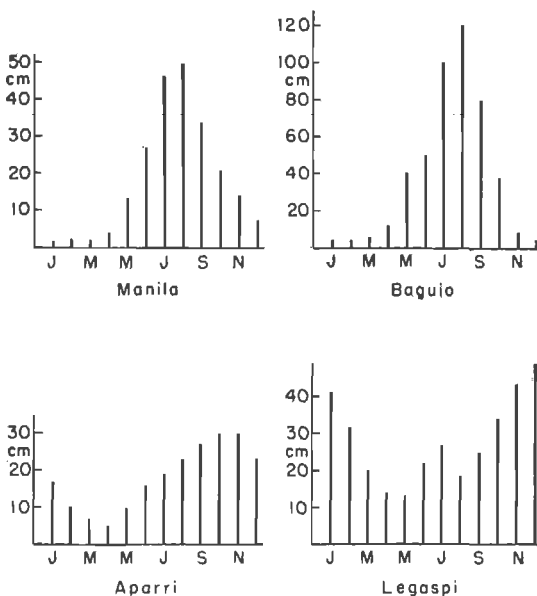


Fig. 4.12. Seasonal variation of rainfall for the stations shown in Fig. 4.11.

now assumes a windward location with a mean west wind. These factors combine to produce heavy summer rain.

At Baguio the broad-scale influences are similar to those at Manila. But the town lies in the mountains, and in addition it is situated almost exactly on the mean equatorial-trough position in August. The effect on the summer rain is vast, even compared with Manila, where rainfall is quite appreciable. Baguio receives more precipitation in an average August than most middle-latitude stations during the whole year. Nevertheless, the city serves as summer capital for the Philippines, cool as it is because of the elevation and daytime showers and cloudiness.

The two remaining stations have rainfall regimes almost inverse to those of Manila and Baguio. They are situated to windward during the

northeast-monsoon season; Legaspi also lies to leeward in summer. Onshore lifting of the monsoon contributes heavily to the winter rain, especially at Aparri, but the small summer precipitation on the north shore is not easily explained.

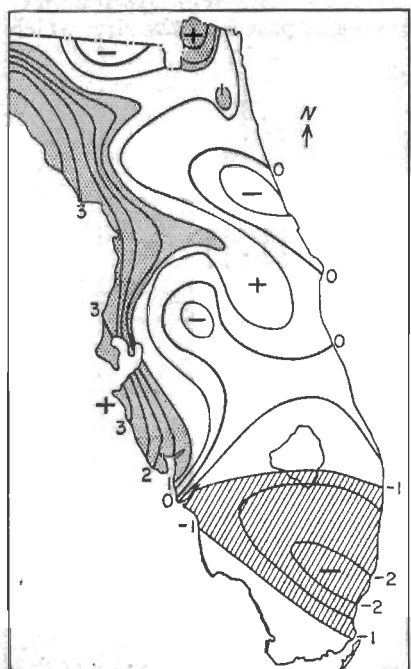
Combined Local and Broad-scale Influences. Large and seemingly irregular rainfall variations over short distances are not confined to mountainous territory. The Florida peninsula is shaped as regularly and is topographically as simple as one can hope to find. In May-June the

rainy season begins; thunderstorms are frequent throughout the summer. The width of Florida is ideal for development of a "double sea breeze" (1) and therefore high thunderstorm incidence. Even so the peninsula does not act as one unit in its average variations through the summer.

In Chap. 3 we noted that at Havana, Cuba, two rainfall maxima occur during summer, one early and the other late. In July and August the precipitation is considerably reduced, a feature explained on the basis of migration of the mean trough aloft in the area (13). The Cuban regime extends into southern and eastern Florida but rapidly terminates over the western shore of the peninsula. Figure 4.13 shows that rainfall decreases from June to July by over 2 inches in the south but increases by 3 inches and more less than 100 miles to the northwest. An irregular pattern of increases and decreases marks the whole center of the peninsula. In spite of the unusual homogeneity of the area it is impossible to define a single general rainfall type.

Fig. 4.13. Difference in average rainfall (inches), July minus June, for the Florida peninsula.

The increase of rainfall in the west and northwest which continues around the whole Gulf coast may be partly related to the westward shift of the mean trough across the peninsula when coupled with the decrease in the south and east. Rainfall is usually much heavier in the southerly winds east of a trough than in the northerly winds on the west side. Thus the variation in summer rain on the peninsula has to be explained



on the combined basis of mean trough migration, double sea breeze, and such minute topographic variations as must be responsible for the four alternations between increase and decrease from northern to southern end of the peninsula.

Diurnal Variation of Pressure

A few words should be said about the semidiurnal pressure oscillation, which is a regular and monotonous feature of barograph traces in low latitudes throughout the year. Figure 4.14 shows a typical trace. The maxima come at 10 A.M. and 10 P.M., the minima at 4 A.M. and 4 P.M. The amplitude is 1-1.5 mb. Because the amplitude is relatively large, it must be subtracted from pressure tendencies before it can be used in forecasting. The diurnal variation, however, is not constant from day to day but changes with cloudiness and other factors. Many analysts therefore prefer to use the 24-hour tendency exclusively.

The change of the diurnal pressure oscillation with height is not known with certainty. Based on observations from mountain stations, early workers concluded that the amplitude of the semidiurnal wave decreases upward as the pressure itself. This conclusion has not yet been confirmed from data for the free atmosphere. But radiosonde ascents are open to suspicion. During the daytime the sun shines on the instrument so that the latter may not report the true air temperature, leading to erroneous pressure-height computations.

During October and November, 1944, special soundings were released daily at two stations in the eastern Caribbean at 3-hour intervals, the only such series known (12). After elimination of the solar-insolation factor, based on careful laboratory measurements by the U.S. Weather Bureau, the ranges of the diurnal pressure and temperature variation at different heights were calculated. These are shown in Table 4.2. For practical purposes the diurnal pressure variation is independent of height. This is brought about by the large diurnal temperature variation, with highest temperature recorded when the sun is at the zenith.

Although doubt remains that the radiation effect has been wholly subtracted, later observations, less complete but made with instruments supposedly free of radiation errors, have not shown appreciably different results. While this does not prove the validity of Table 4.2, the results are at least worth while presenting.

Owing to the diurnal temperature variation the pressure curve becomes

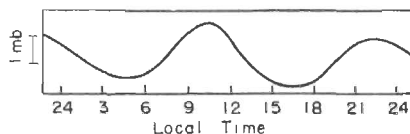


Fig. 4.14. Surface-diurnal-pressure variation at San Juan, Puerto Rico, October-November.

a single wave with increasing height. Haurwitz (2) has undertaken a harmonic analysis of the oscillation. The amplitudes of the 24- and 12-hour wave components (A_1 and A_2) are given in Table 4.2. As the importance of the 24-hour wave increases upward, that of the 12-hour wave declines. Even so, this decrease is much less rapid than that of the pressure; at 16 km the amplitude is over three times larger than assumed in the early theory.

TABLE 4.2. RANGE OF DIURNAL PRESSURE AND TEMPERATURE VARIATIONS

Height	P , mb	T , °C	A_1 , mb	A_2 , mb
Surface	2.3	4.1	0.20	0.97
1,525 m	2.9	1.1	0.60	0.95
3,050 m	2.9	1.8	0.77	0.86
4,575 m	3.0	2.0	1.01	0.79
6,100 m	3.1	2.0	1.17	0.76
10,000 m	3.0	2.3	1.38	0.61
13,000 m	2.8	3.0	1.37	0.46
16,000 m	2.2	2.4	1.10	0.36

REFERENCES

- (1) Byers, H. R., and H. R. Rodebush, *J. Meteor.*, **5**: 275 (1948).
- (2) Haurwitz, B., *Bull. Am. Meteor. Soc.*, **28**: 319 (1947).
- (3) Hatchern, R. W., and J. S. Sawyer, *Quart. J. Roy. Meteor. Soc.*, **73**: 391 (1947).
- (4) Kimble, G. H. T., et al., *Bull. Am. Meteor. Soc.*, **27**: 99 (1946).
- (5) Leopold, L. B., *Pacific Sci.*, **2**: 81 (1948).
- (6) Leopold, L. B., *J. Meteor.*, **6**: 312 (1949).
- (7) Leopold, L. B., in *Am. Meteor. Soc. Mon.* 3, p. 1, 1951.
- (8) Meinardus, W., *Ann. Hydr. Marine Meteor.*, **69**: 37 (1941).
- (9) Queney, P., *Bull. Am. Meteor. Soc.*, **29**: 16 (1948).
- (10) Riehl, H., *Bull. Am. Meteor. Soc.*, **28**: 37 (1947).
- (11) Riehl, H., *ibid.*, 137, 1947.
- (12) Riehl, H., *ibid.*, 311, 1947.
- (13) Riehl, H., *Dept. Meteor., Univ. Chicago, Misc. Rept.* 22, 1947.
- (14) Riehl, H., et al., *Quart. J. Roy. Meteor. Soc.*, **77**: 598 (1951).
- (15) Stidd, C. K., and L. B. Leopold, in *Am. Meteor. Soc. Mon.* 3, p. 24, 1951.
- (16) van Bemmelen, W., *Beitr. Phys. fr. Atm.*, **10**: 169 (1922).
- (17) Wexler, R., *Bull. Am. Meteor. Soc.*, **27**: 272 (1946).

CHAPTER 5

CONVECTION

For the visitor to the tropics, the outstanding element of the scenery is the cumulus cloud, set off against the blue sky by day or reflecting the moonlight by night. Its graceful appearance on a travel poster may have helped lure the visitor to the tropics. The cumulus cloud is the queen of beauty in the realm of the atmosphere. It is one of the amusements reserved for the meteorologist to stroll through a picture gallery and deduce the weather situation from the clouds appearing in the landscapes, especially the cumuli. Since good painters are accurate observers, their clouds contain an excellent feeling for the kind of motion in them.

Cumuli are not all serenity; they sometimes act to produce turbulence and rain. Their growth, movement, and decay reveal secrets of the air circulation. In height, thickness, and slope they portray the synoptic situation. The structure and maintenance of great vortices, even hurricanes, are governed in part by cumulus development. Convection is the most important mechanism for funneling heat upward in the atmosphere, and it provides a basic link in maintaining the general circulation.

As he watches the tropical sky, the meteorologist soon realizes that the cloud sequence is not the same day after day. The average height, thickness, and distribution of cumuli change from one day to the next. Sometimes they are erect, and sometimes they slant with height. Often they are arranged in neat rows parallel or normal to the wind. And often no such pattern can be discerned. Besides our observation that the main features of the current sky differ from the pattern of preceding days, we find a great variety of cloud forms and sizes within it at any moment. This variety is a result of the fact that cumuli go through a *life cycle* which is not of uniform length and accomplishment. We can observe the life cycle and its variations most easily by time-lapse motion pictures projected at normal speed, so that the events of 1 minute or more may pass in 1 second before our eyes. If the clouds are trade cumuli of average thickness, roughly 5,000–7,000 feet at peak development, their life has a length of $\frac{1}{2}$ hour or more. The growing stage is brief, 10–15 minutes; the decay lasts longer, 20 minutes and more. Therefore we see more clouds that have reached maturity or are dying than clouds that are growing. Clouds rarely persist for more than a few minutes in "steady state," *i.e.*, without changing their shape and structure. This is

rather awkward, for it is much more difficult to measure and understand transient conditions than steady-state.

When we look at skies with larger clouds, perhaps including cumulonimbus, we can expect to find a longer life span. The period of growth may consume $\frac{1}{2}$ hour; while the average life of a cumulonimbus is 60–90 minutes, it may be protracted over many hours. But again there is no completely steady state. While the naked eye sees the continuing existence of one great cloud mass, there are contained within it several active cells. Many such cells can grow and decay during the life of the whole cloud as the activity keeps shifting to new cells.

These sketchy observations are only a beginning of all the interesting things we can see in a cumulus sky. This is a wide field for investigation, a field in which many data have been collected and in which theory has advanced rapidly. In this chapter we shall take up (a) the energy sources for cumulus formation; (b) the layer below the clouds; (c) "onset" criteria that determine whether cumuli will or will not form; and (d) the structure and life cycle of trade cumuli.

THE SUBCLOUD LAYER

Release of latent heat of condensation is the major energy source for the building and driving of cumuli. To initiate convection, however, an independent energy source and a dynamic mechanism are required. Best known is the heating of land in the daytime by the sun, which produces an unstable vertical stratification near the ground. Soon overturning sets in, and some air "parcels," accelerated upward in "thermals," reach their "convective condensation level." If the ground is quite level and its radiation properties are uniform, the first formation of cumuli may take place anywhere. Over most land areas the ground is at least slightly hilly, and vegetation and soil types vary, so that the absorption of the sun's rays is not uniform. Clouds will tend to form where the heating is strongest, where the general air stream is forced upward in hilly or mountainous country, and where differences in surface friction between adjacent areas produce convergence. When of limited size, we refer to such areas as "convection points." Not infrequently do we see here a stationary cloud persisting for hours even though the wind may be blowing at a high rate. Trains of quasi-stationary clouds may extend downstream from such convection points, spaced in a wave-like manner (23).

Over the oceans, where the diurnal temperature changes and sea-air temperature differences are very small, cumuli are started by processes quite different from the thermals observed over land in the afternoon. The first problem is the introduction of energy into the trade air at the surface; the second is the upward transport of the energy absorbed.

Energy Exchange near the Sea Surface

Energy is transferred from ocean to atmosphere when small masses of air descend to the ocean surface, have their temperature and moisture content slightly raised, and again leave the surface. The descent of the smoke at point *B* of Fig. 5.7 and the ascent at point *A* illustrate such eddying motion. For the energy transfer to take place, the sea surface temperature must be higher than the air temperature coming in contact with the water, and the vapor pressure over the water must exceed that of the air. Since the vapor pressure over the ocean surface usually is assumed to be equal to that over a flat water surface at saturation, the water temperature determines the vapor pressure over the surface (36). The relative humidity of the air almost always is less than 100 per cent in the tropics. Therefore both latent and sensible heat will be absorbed by the air when the sea surface temperature exceeds the air temperature. The ocean does the work required for the evaporation process.

The heat exchange per parcel of air in unit time will increase with the temperature and vapor-pressure gradient. The heat exchange in a given area per unit time also depends on the rate at which air particles are brought to and removed from the surface, since this determines the maintenance of temperature and vapor-pressure differences. A strong wind will serve this purpose best. But in touching the ocean, the air particles also change their wind speed because of the frictional braking action of the water. In the trades, this means that the east wind is reduced or, as it is frequently stated, that the air has received westerly momentum from the earth. Ascending particles should therefore have moisture and temperature above average and wind speed below average. For steady state the mean wind speed must be maintained by importation of stronger wind from above, or upstream, or by generation through pressure forces. The heat and moisture acquired from the ocean must be removed to higher levels, or downstream.

This is the physical picture of the energy exchange between ocean and atmosphere. Now it is not possible to follow each air eddy to determine whether the foregoing is true or not. We can, however, note whether recorder traces of instruments placed aboard a ship reveal fluctuations of temperature, moisture, and wind as the air passes the ship and how these fluctuations are correlated. Figure 5.1 shows a sample of such traces obtained by J. Wyman and A. H. Woodcock on an expedition to Puerto Rico and Panama.¹ It is the first outstanding proof that marked fluctuations of temperature and humidity do take place when the sea surface temperature exceeds the air temperature. Such fluctuations nearly

¹ Woods Hole Oceanographic Institution, Woods Hole, Mass. Mimeographed, 1946.

vanish south of Panama, where the air moves over a colder sea surface. Second we can detect a positive correlation between the variations of temperature and moisture in Fig. 5.1 as long as attention is confined to the smaller eddies with dimensions of a few hundred yards. The figure also reveals larger eddies. The temperature increases and the vapor pressure decreases from the left to the right edge of the diagram, indicating a negative correlation between temperature and moisture. If this is characteristic for larger eddies, the smaller ones must provide for the upward flow of latent and sensible heat. The wind correlation is much

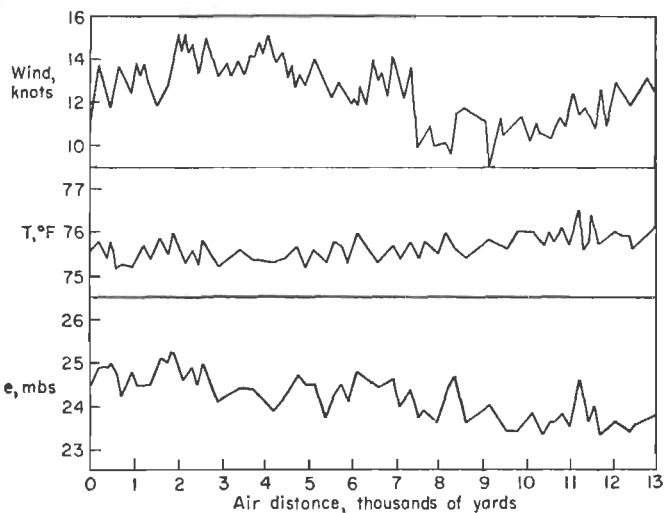


Fig. 5.1. Fluctuations of surface wind, temperature, and vapor pressure on April 23, 1946, recorded on ship near Puerto Rico (9, 27).

poorer, but we observe some weakening of wind speed with increasing temperature.

A precise calculation of the energy transfer from ocean to air from data as shown in Fig. 5.1 cannot be made since there is a missing observational link, the measurement of vertical motion. The flow of heat or momentum past some level—the ship's deck level, for instance—is proportional to the difference in heat content between the ascending and descending masses. A measurement of vertical motion would enable us to calculate the net upward heat flow. Such computations would show, through analysis of the turbulence spectrum, which eddy size or sizes are effective in producing the net flow. The difficulty has been lack of a suitable instrument to measure vertical motion. Swinbank (38) and others have perfected instrumentation suitable over land. Over the open sea measurements must be made from moving and rolling ships;

the perfecting of a vertical-motion meter here is still in the future.¹ Therefore the qualitative indication of Fig. 5.1 must suffice for the present.

Lacking direct flux calculations, oceanographers and meteorologists have attempted for many years to calculate the heat exchange by the approaches described in Chap. 3. A treatment of these techniques is outside the scope of this book, but the reader will find a concise presentation in Sverdrup's text on oceanography (36). Only one further concept may be mentioned, the "smooth" and the "rough" ocean surface where whitecaps appear. Following Sverdrup (37), the coefficient measuring intensity of evaporation changes discontinuously as the ocean surface passes from the smooth to the rough state; it increases by no less than 100 per cent. Unfortunately the theory is not fully settled, since extensive evaporation calculations in the United States² support the evaporation formulas of Sverdrup (35) and Sutton (34) rather than the 1946 formula of Sverdrup (37). But it is of more than casual interest that according to the latter work the break between smooth and rough sea occurs at 6-7 mps, almost precisely the average (not resultant) wind speed over the largest part of the trade-wind belt. Because the speed of the trades oscillates considerably about the mean in a semicyclic fashion (Chap. 10), the total evaporation over broad ocean areas may vary by high percentages from one week to the next, thus affecting the general circulation. This suggests that the energy exchange at the sea surface not only is important for the production of cumuli but is a factor in large-scale and longer period circulation changes.

Structure of the Subcloud Layer

Information on the structure of the subcloud and cloud layers has been furnished by numerous airplane traverses, vertical and horizontal, made by the above-mentioned Wyman-Woodcock Caribbean expedition and subsequent expeditions by the Woods Hole Oceanographic Institution. Figure 5.2 is typical of their findings. Throughout the subcloud layer the temperature lapse rate is almost dry-adiabatic, and the moisture content is constant. Thus the layer turns out to be almost completely "mixed" and can be so regarded for all large-scale problems. Figure 5.2 may be compared with Figs. 2.28, 2.37, and 2.38. The data for the eastern Atlantic and eastern Pacific reveal a similar structure, but the lapse rates are somewhat steeper near the ground and the vertical moisture gradient is larger.

¹ It should be noted that the Woods Hole Oceanographic Institution has been developing means to measure vertical motions from aircraft.

² J. J. Marciano and A. E. Harbeck, *U.S. Geol. Survey Circ.* 229, 1952.

In spite of the general homogeneity of the subcloud layer near Puerto Rico, we can observe small but significant differences in temperature and moisture lapse rates in upper and lower portions of the layer. The dry potential temperature is quite constant only in the lower half (about 300 m thick) and then increases very slowly upward at a rate of about 0.2°C per 100 m. Conversely, the mixing ratio decreases. As these gradients have inverse effects on the stability, the virtual potential temperature was also calculated from the expedition data. This quantity varies as the dry potential temperature. Thus the upper half of the subcloud layer has very slight thermal stability with respect to dry-adiabatic vertical displacements. This has been regarded as evidence

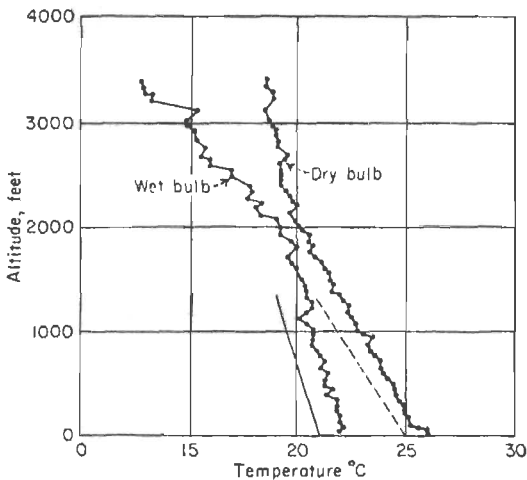


Fig. 5.2. Vertical structure of subcloud layer near Puerto Rico, Apr. 2, 1946 (9, 27).

(9) that any convection cells present near the surface must be damped out in the upper portion of the subcloud layer and that they cannot furnish the roots of the cumuli. As corollary evidence, the accelerometer record of the Wyman expedition (Fig. 5.3) has shown that the strongest vertical accelerations in the subcloud layer ($0.2g$) occur near the 300-m level. This evidence, however, is rather weak; according to Fig. 5.3 the turbulence is fairly uniform through the subcloud layer, and the principal weakening takes place near the base of the clouds, where the temperature lapse rate decreases markedly.

More formidable is the observation that horizontal turbulence gradients as revealed by the airplane traverses were very small and that not even underneath the clouds themselves was there an increase of turbulence. Finally, throughout most of the subcloud layer, the fluctuations of temperature and moisture are not only very small but also tend to be out of

phase, whereas at ship's deck level they are in phase. In a convective atmosphere positive correlation should prevail generally. These observations would seem to rule out dry thermals as the roots of the trade-wind cumuli over sea. They further suggest that the structure of the subcloud layer and its essentially steady state result from small-scale diffusion rather than convection.

Certain other evidence, however, should not be overlooked. Figure 5.1, as noted, indicates the existence of large eddies with dimension of thousands of yards. The possibility remains, if not the likelihood, that vertical-motion gradients exist even in the absence of turbulence gradients (27). If we postulate the presence of patterns of horizontal convergence and divergence of the scale suggested by Fig. 5.2, we can still seek the roots of the cumuli in the subcloud layer as a whole. Malkus (23) points to gradual variations in the depth of the mixed layer as the most plausible origin of the cumuli. Such gradual changes, amounting up to hundreds of meters, are observed.

On some occasions the top [of the mixed layer] reached or exceeded the condensation level, and it was, in the mean, noticeably higher in cloudy than in clear areas. One or more mechanisms, then, causing spatial oscillations in the thickness of the mixed layer are needed. These are probably of the dimension of the cloud clusters, random eddying in these regions accounting for the outbreak of individual clouds. It is readily shown that fluctuations in the thickness of the mixed layer are only very weakly coupled with variations in the height of the trade inversion and the depth of the moist layer as a whole. Attention must therefore be directed to independent, weakly convergent flows set up within the subcloud layer itself. Langwell¹ has proposed unstable gravitational waves at the interface between the nearly adiabatic ground layer and the isothermal stratum on its top. One should also inquire about more random causes such as slight inhomogeneities in the sea surface roughness, radiative properties, or temperatures on a 10-30 km scale.

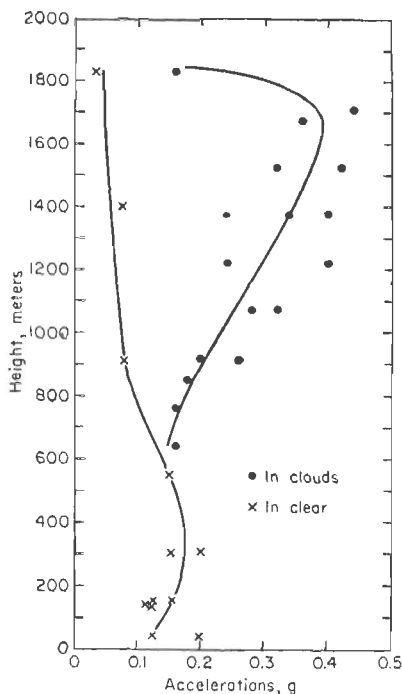


Fig. 5.3. Maximum accelerations in clear and in clouds near Puerto Rico (9).

¹ P. A. Langwell, Department of Meteorology, New York University, 1951.

Dry Convection Cells

Whatever the uncertainties about the precise mechanism of cumulus initiation, the existence of convection cells in the lower part of the subcloud layer has been proved, as well as their disappearance in the upper part of the layer. In several classical experiments, performed about the turn of the twentieth century, Bénard (5) observed that a pattern of convection cells tends to develop in a thin sheet of liquid uniformly heated at the lower surface. In response to this heating the liquid starts to overturn, at first in an irregular manner. After some time ranging from seconds to many minutes, depending on the viscosity of the liquid, a steady state develops in which the vertical motion is ordered into regular hexagons. The ratio of the length of the sides of these hexagons to the cell height, *i.e.*, the thickness of the layer, is about 2 to 1. Fluid ascends in the center of the hexagons, diverges at the surface, and descends along the edges, with maximum downward motion concentrated at the cell edges. When the liquid is subjected to shear, the cells are replaced by horizontal strips, or rolls, with axes parallel to the direction of shear.

Bénard's experiments have been repeated many times, and everyone can produce convection cells with ordinary kitchen equipment. Meteorologists associated with G. C. T. Walker of Great Britain also have generated such cells in air confined between two glass plates, making the motions visible by the introduction of smoke (Fig. 5.4). The relative dimensions of these cells are the same as those of cells in liquids, but the air descends in the cell centers and ascends along the edges.

It would lead us too far afield to cover the difficult theoretical researches and all experiments concerning convection cells. A general review of work done on convective motion is given in the literature (39). We may note here that a principal result has been "onset criteria"; these state how large the thermal gradient produced by heating must become before overturning sets in that leads to cell formation. Williams (41) and Baum (4) have demonstrated that overturning in air near the ground need by no means develop when the lapse rate exceeds the adiabatic or autoconvective rates. Owing mainly to viscous forces, a quiescent atmosphere can be observed even when the density increases upward. On warm and sunny days the lapse rate near the ground may exceed the dry-adiabatic rate by a hundred or even thousand times (17). Over the sea there is frequently a temperature difference of 1°C between the sea surface and ship's deck level. The thermal gradients necessary for cell formation are therefore probably present over both land and ocean. A generally verified onset criterion, however, is still lacking for the atmosphere. Baum (4) presents the closest theoretical approach. Modifying Lord Rayleigh's classical derivation (26), he finds that the limiting lapse rate

for cell formation is given by the autoconvective rate plus a term that is inversely proportional to the fourth power of the thickness of the layer. This term, important for shallow layers, rapidly becomes insignificant as the depth of the layer with steep lapse rate is increased.

Looking for evidence of convection cells in the atmosphere, Brunt (8), Walker (40), Mal (21), and many others have pointed out the similarity of various cloud forms and their dimensions to the forms and dimensions

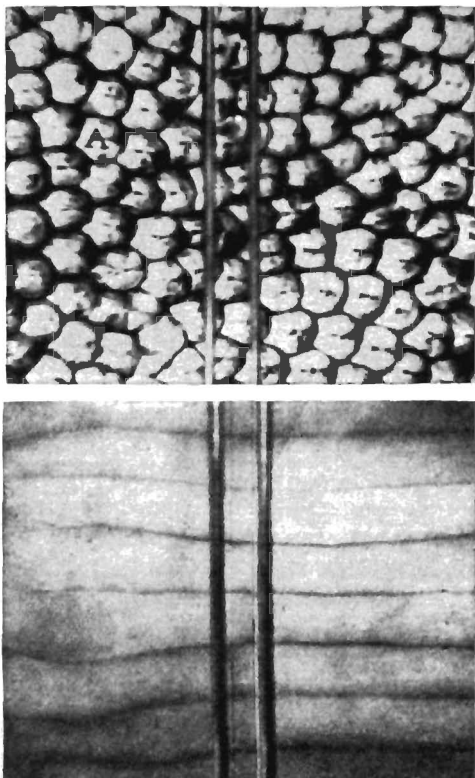


Fig. 5.4. Polygonal convection cells indicated by smoke. *Top:* Small shear. *Bottom:* Large shear (42).

of the cells produced in the laboratory. Durst (16), in a study of wind gusts, found convection patterns in the lower air over open country. Woodcock (42) has adduced some of the principal evidence for the sub-cloud layer over the sea. In one of the ingenious papers of meteorology, he related the flight of herring gulls off the New England coast of the United States to the sea-air temperature difference and the wind speed:

From October until spring the air over the ocean off the coast of the United States is on the average colder than the water. The heating of this air by the

water produces ascending convective motions which are columns in form during light winds, and which change with higher winds to vertical sheets extending indefinitely up and down parallel with the wind These convective motions of air over the sea are revealed by the soaring routines of herring gulls living in this air. The first suggestive feature of their movement lies in the fact that they are not seen far (100 miles and more) at sea until the fall, when cool air from the continent flows out over the warmer sea. The probable reason for this correlation is that the birds are unable to maintain a proper balance between their food supply and the energy requirements for flight until the development of the strong thermals of the fall and winter months makes moving about over the sea physically easy.

From the patterns in which the birds arranged themselves Woodcock deduced the shape of the convection cells. When the birds were soaring, either they circled in columnar thermals, usually with some tilt, or they soared straight to windward, gaining altitude rapidly (Fig. 5.5). Soaring did not occur when the air was warmer than the water, clearly demonstrating the energy source for the low-level convection. Woodcock found that the birds soar in columns when the wind speed is below 7 mps and that linear soaring predominates at speeds between 7 and 13 mps. At still higher speeds the convection cells apparently break down; Woodcock no longer could detect any ordered patterns of bird flight.

Subsequently Woodcock turned his attention to the trades when a Wood's Hole group (see p. 121) tried to make the low-level convection cells visible through the release of chemical smoke from ships and airplanes (43). This proved possible when the water temperature exceeded the air temperature, even though the air-sea temperature difference rarely was more than 2°C. Figure 5.6 furnishes spectacular proof of a convection-cell pattern. This pattern drifts downstream with the wind. Whereas the direction of the axis changes more than 45° from one portion of the smoke plume to another, the surface wind fluctuated by no more than 5° in the hour prior to the smoke release. Woodcock and Wyman show that if such angular departures of the wind direction from the mean occur in an ordered pattern of the Bénard cell type, the measured lateral displacement of the smoke and the changes in orientation of the plume can be explained. If several adjacent plumes are laid down, separated by as little as 60 m, the distortions of the axes are by no means parallel but vary widely, again in accord with the concept of convection cells. The length of the sides of these cells has the order of 500 m.

In addition to the general meandering of the plume in Fig. 5.6 we observe that its thickness widens downstream. This suggests that turbulence of a smaller scale, diffusion, is superimposed on the convection-cell pattern.

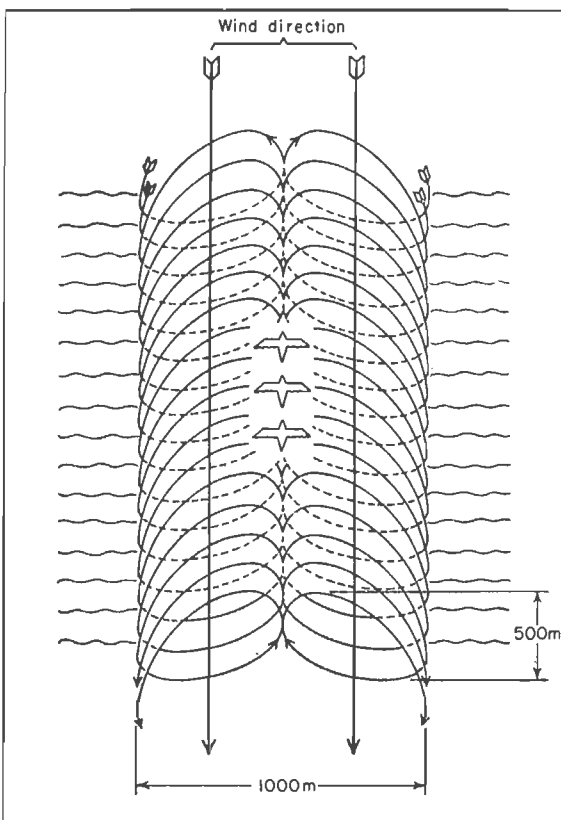
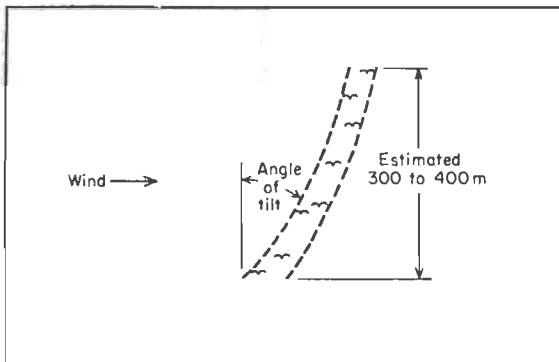


Fig. 5.5. Columnar soaring (top); soaring in longitudinal rolls (bottom) (42).

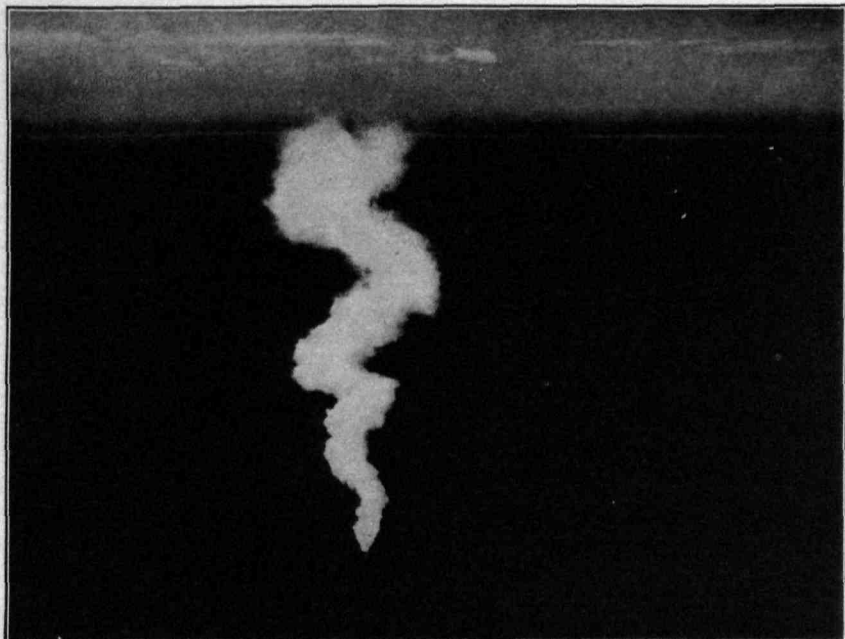


Fig. 5.6. Smoke from stationary source near Panama, seen from above (43). (Courtesy of New York Academy of Sciences.)

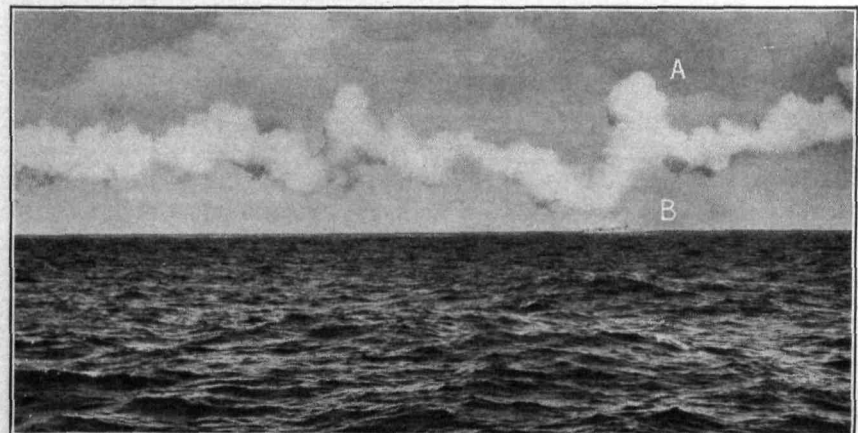


Fig. 5.7. Vertical distortion of smoke laid parallel to wind by airplane flying horizontally at 100 m altitude (43). (Courtesy of New York Academy of Sciences.)

The lateral smoke displacements should be accompanied by vertical oscillations. Figure 5.7 shows that these exist. In this case the plume has been laid parallel to the wind by aircraft flying near 100 m altitude. Thus the plume could descend as well as ascend, and this occurred. The vertical motion of the plume attained 1 mps.

It is difficult to relate the vertical smoke displacement to the shape of the convection cells, as this requires knowledge of the orientation of the plume relative to the cells. Such knowledge is not available. We merely note that the average height of the cells appears to be about 300 m, about half the length of the cell sides, in agreement with Bénard's experiments. The top of the cells coincides with the altitude at which the stratification of the subcloud layer becomes slightly stable.

THE CLOUD LAYER

Types of Cumulus Cloud

The factors that control the development of cumuliform clouds in the tropics are (a) horizontal convergence in the wind field, (b) the mean depth of the moist layer, (c) orography, and (d) the vertical stability (31). Depending on relative importance and distribution of these parameters, various cloud types develop. These range from cumulus humilis to cumulonimbus as in the temperate zone. But the classification in the international code—cumulus humilis, cumulus congestus, cumulonimbus—is entirely inadequate for the tropics, where we find many significant cloud types intermediate between cumulus humilis and cumulus congestus. Figure 5.8 shows some of the types. The subsequent description follows that of the *Handbook of Meteorology* (31).

Cumulus humilis is far more frequent in the tropics than was once supposed. It often has a rough, tattered appearance caused by turbulence; then it is frequently called *fractocumulus* or *stratocumulus*. The cloud thickness is limited to about 3,000 feet or less, indicating an unusually shallow moist layer and a weather situation with much subsidence.

Trade cumulus in general has a “blocklike” appearance since it ends abruptly in the lower stratum of the trade inversion. A group of fully grown clouds shows considerable symmetry because their bases are located at about the same level, and they do not differ greatly in maximum penetration into the inversion layer. They occur mostly under average undisturbed conditions.

Chimney clouds have much greater vertical than horizontal extent. Frequently they take the form of long “necks” protruding from the tops of the lower cloud mass above a weak inversion or stable layer. Chimney clouds occur in a moist layer of moderate height, though it may be higher

than average for the area and season. The necks may lean with height, indicating the vertical wind shear.

Showers will fall from trade cumuli and chimney clouds, especially when they form clusters with the tallest clouds in the center of convection-cell-type arrays. Rain from cumulus humilis is rare, but the author has observed heavy precipitation trails even from such shallow clouds in the outskirts of some tropical storms.

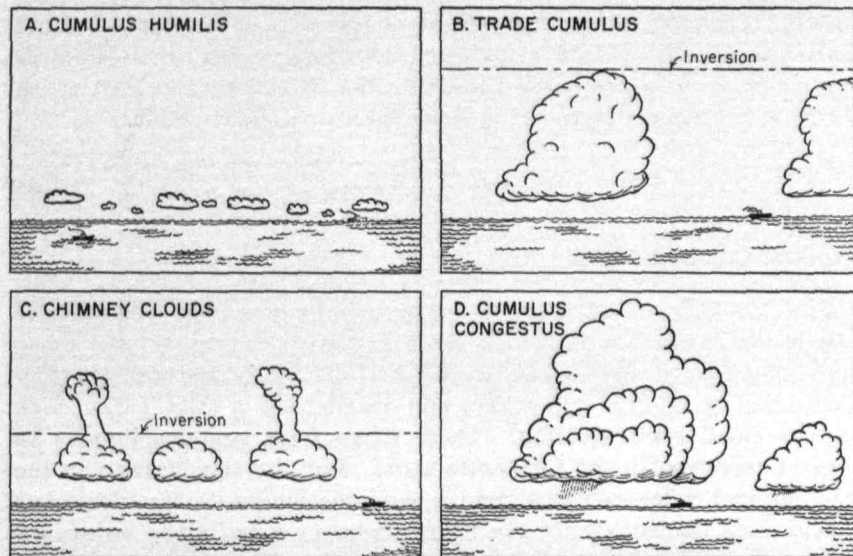


Fig. 5.8. Types of cumuli in the trades (31).

Cumulus congestus forms when cumuli build to considerable height—roughly above 12,000 feet—and take on a massive, mountainous appearance. At the edges of the main body of these clouds are smaller developments, called *outriders*, which give the cloud a very broad base. Showers from *cumulus congestus* often are heavy.

Cumulonimbus forms when a *cumulus congestus* builds far into the freezing layer. The height of individual *cumulonimbi* varies from 25,000 to 55,000 feet, the mean height of the tropopause. This cloud has many outriders; sheets of altostratus and cirrostratus are formed by lateral spreading. After the parent cloud disintegrates, some of these sheets may remain for a long time. Precipitation is heavy; thunderstorms may develop; but hail hardly ever reaches the ocean surface.

This variety of cumulus clouds presents a host of questions. When will cumuli form? Where will their tops and bases be located? What governs their size, shape, and the total cloud cover? Will the axes of



Fig. 5.9. Trade cumuli. (*Courtesy of Dr. J. S. Malkus, Woods Hole Oceanographic Institution.*)

the clouds lean with height, and if so, in what direction? How fast do the clouds move? When will they grow to become thunderstorms?

We begin by asking when cumuli will form and where their bases will be.

The Onset of Convection

Suppose we give an upward push to a small mass of air located in a large environment at rest and specify that it shall not mix with the surroundings. Then this mass will be further accelerated upward—it is buoyant—if the upward acceleration due to the pressure-gradient force exceeds the downward acceleration of gravity. Given the net vertical acceleration dw/dt , the pressure-gradient acceleration $-1/\rho' \partial p'/\partial z$, and the gravitational acceleration g ,

$$\frac{dw}{dt} = -\frac{1}{\rho'} \frac{\partial p'}{\partial z} - g. \quad (5.1)$$

Here ρ' is the density and $\partial p'/\partial z$ the pressure gradient along the vertical across the particle. In the surroundings the air is accelerated neither upward nor downward, so that $0 = -1/\rho \partial p/\partial z - g$; the balance is hydrostatic. It is now a premise in nearly all convection work, though its validity is open to question, that the rising particles immediately adjust to the pressure of their surroundings, so that $\partial p/\partial z = \partial p'/\partial z$. With this assumption we can eliminate the pressure gradient from (5.1), and $dw/dt = g[(\rho - \rho')/\rho']$. With the aid of the equation of state for air,

$$\frac{dw}{dt} = g \frac{T' - T}{T}, \quad (5.2)$$

where T is the temperature. This is the well-known buoyancy formula. Parcels which are warmer than their surroundings will accelerate upward. Parcels which are colder will accelerate downward and return to and beyond their starting place. If rising parcels can ascend until their relative humidity becomes 100 per cent, cumuli will begin to form, subject to the considerations of Chap. 6.

Given a radiosonde observation, we can locate on a thermodynamic diagram the level at which clouds should first appear, the convective-condensation level. The procedure, described in nearly all basic textbooks (*cf.* 10), requires no repetition. Over land one usually computes the temperature to which the surface air must be heated in order to reach the convective-condensation level. Clouds should begin to form about the time when the surface temperature rises to the requisite value. Unless this value is reached, the sky will remain clear. As long as the parcel method is used in this way as an "onset criterion," observations decisively support its validity. It permits prediction of the time of first

cumulus formation over land and the approximate height of the cloud bases. It is remarkable to see how uniform these bases are when thousands of cumuli are in the sky.

Over the sea such an onset criterion is meaningless in regions with a mixed subcloud layer. Even here, however, we can estimate the approximate height of the cloud bases from surface temperature and dew point since moisture and potential temperature are nearly constant through the layer.

The Growth of Cumuli

Parcel Method. The technique just described has been applied not only to find the time of formation and the height of the bases of cumuli over land but also to predict the height of cloud tops and the probability of thunderstorm formation. After an air parcel passes the condensation level, it receives added heat energy through the condensation process. On a thermodynamic chart its upward path should be given by the moist-adiabatic lapse rate. This path may intersect the sounding again after penetration of only a shallow layer, especially when a marked stable layer or inversion is present. When this happens, the parcel method gives a correct prediction of the cloud tops. The cumuli will be shallow; their bases will be broad, and the sky may assume the character of strato-cumulus. Over the oceans, this occurs generally where the trade-wind inversion is situated only 1,000-3,000 feet above the convective-condensation level.

On many summer days over land, and quite generally over the oceans away from subsidence inversion, the temperature lapse rate lies between the dry- and moist-adiabatic rates to great heights, often to 300 mb and more. The atmosphere then is called "conditionally unstable." Air ascending moist-adiabatically should continue to gain buoyancy and upward speed to high levels. Tall clouds and thunderstorms should form. But predictions made on this basis very frequently fail, proving that the simple buoyancy theory does not suffice to explain the cumuli except for their beginnings.

Equation (5.2) describes a very powerful acceleration. Say, for example, that $T = 300^{\circ}\text{A}$ and that $T' - T = 2^{\circ}\text{C}$, a very small value in parcel-method calculations. Air starting from rest near the ground will reach the 3-km level after 5 minutes under such conditions and the tropopause after 10 minutes. For larger temperature differences, the time increments are correspondingly smaller. The cloud growth predicted by this calculation exceeds by a large factor that usually observed. We must conclude that resistive forces not considered by the parcel method operate normally against the buoyancy force. In particular we

have neglected (a) the continuity of mass and (b) the interaction between the rising air and its environment.

The Slice Method. J. Bjerknes (6) was among the first to recognize the shortcomings of the parcel method, which at one time was held by

many to be a complete and satisfactory convection theory. He allowed for mass continuity by considering both upward and downward motion within a limited area. Later, Cressman (15) extended Bjerknes's development by permitting net convergence or divergence to take place inside this area and so including synoptic effects.

Bjerknes discusses the motion of air from below and above past a reference surface in the cloud layer (Fig. 5.10), in order to find a criterion indicating whether or not convection is likely to grow. The criterion, as in the case of the parcel method, is the temperature difference between ascending and descending currents. As long as the rising air is warmer, the convection will intensify, following the buoyancy principle.

Fig. 5.10. Illustrating the slice method.

Since Bjerknes stipulates no net convergence or divergence in the area under discussion, the upward and downward mass transports across the reference surface must be equal. If A_a and A_d are the areas covered by updrafts and downdrafts, respectively, and w_a and w_d are the corresponding vertical motions, the continuity requirement is $A_a w_a = -A_d w_d$, neglecting the small density difference between the opposing currents. For a given amount of upward mass flow the area covered by clouds must be small if the updrafts in the cumuli are large; a slow settling motion takes place in the broad clear spaces. Conversely, the area covered by clouds will be large if the updrafts are weak. Since, in general, strong updrafts are found in tall clouds and weak updrafts in shallow clouds, cumulonimbus and cumulus congestus should be widely spaced with large intervening clear spaces, and in a region of shallow cumuli under an inversion the total cloud cover should be large. These deductions agree very well with observations.

Bjerknes assumes that the ascending current follows the moist-adiabatic and the descending the dry-adiabatic path. Without going into the complete mathematical details, the temperature difference between the rising and sinking air ($T_a - T_d$) at the reference surface is given by $T_a - T_d = [w_a(\gamma - \gamma_m) - w_d(\gamma - \gamma_d)] \Delta t$, where γ_d , γ_m , and γ are the dry-adiabatic, moist-adiabatic, and observed lapse rates and Δt is

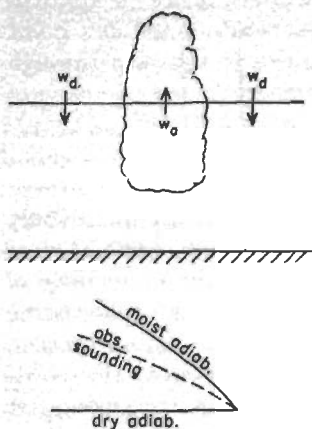


Fig. 5.10. Illustrating the slice method.

the time interval during which the convection has been occurring. The criterion for cloud growth is $T_a - T_d > 0$; thus $w_a(\gamma - \gamma_m) > w_d(\gamma - \gamma_d)$ or, in view of the continuity requirement, $A_d > (\gamma_d - \gamma)/(\gamma - \gamma_m)A_a$. Since $A_a + A_d = A$, the whole area,

$$\frac{A_d}{A} > \frac{\gamma_d - \gamma}{\gamma_d - \gamma_m} \quad (5.3)$$

for cloud growth. The ratio A_d/A is the percentage of clear sky.

The criterion remains somewhat inconclusive since of the two variables, A_d and γ , only the lapse rate can be measured from radiosonde data before convection sets in. It is necessary to wait until convection is well under way before determining the per cent sky cover and clear areas. Prior to the onset of convection, (5.3) says only that convection is more likely the closer the lapse rate is to the dry-adiabatic.

Cressman (15) introduces net convergence and divergence by permitting a net transport of mass across the reference surface, either upward or downward. He finds that the modification is most important when the observed lapse rate is near the moist-adiabatic. Even weak convergence in the low levels will then produce an intense growth of convection. Divergence acts as a strong damping factor. Thus, it is important to predict map features on the synoptic scale in order to arrive at an estimate of convective activity.

Since the slice method involves the difference between T_a and T_d , Bjerknes (6) and Petterssen (25) have considered qualitatively the solenoid field in relation to cloud growth. As long as T_a exceeds T_d , the circulation around the solenoids is accelerated. The clouds will then grow in proportion to the strength of the solenoid field. Since both ascending and descending air arrives at the reference surface with a temperature higher than initially present if the lapse rate is conditionally unstable, the whole slice becomes warmer; this helps to maintain the general heat balance of the atmosphere. As the mean temperature of the area increases with time, the rising current will lose buoyancy. Eventually the air funneled upward through the reference surface will return in the descending branch. If the condensed moisture has rained out completely or in part, the descending current will finally become warmer than the rising air. Then the circulation is decelerated, and the clouds begin to die. We are herewith led to the concept of a cumulus *life cycle* of limited duration, as observed.

In spite of the advances achieved by the slice method, unsolved problems remained. The cloud tops tend to evaporate in a dry environment as stated, and the lapse rate inside of cumuli is steeper than the moist-adiabatic lapse rate. These facts suggest direct interaction between the clouds and their surroundings. Although this hypothesis has been voiced

intermittently in the past, it was not until the Wyman-Woodcock expedition of 1946 that it began to be explored systematically. Then a spectacular advance in cumulus theory ensued.

Before we discuss this advance, it will be well to relate briefly what is known about the vertical temperature structure of cumuli and about temperature differences between these clouds and their environment.

Cumulus Temperatures. Since detailed measurements of in-cloud temperatures must be made by airplane, the quality of the data is proportional to the reliability of the aircraft instruments. Dynamic corrections must be applied to observations taken with most types of temperature-measuring devices. The amount of the correction is uncertain inside clouds. Most reliable, therefore, are in-cloud lapse rates because any correction errors vary little with height and therefore do not affect the vertical temperature gradients. All measurements (*cf.* 3, 7, 9, 12) show lapse rates considerably in excess of the moist-adiabatic rate and very nearly equal to those prevailing outside the clouds. This is the strongest evidence that points to mixing between the air rising in clouds and their environment.

The data gathered by the Wyman-Woodcock expedition indicate that temperatures may be somewhat higher inside cumuli than outside in the lower parts of the cloud, while the opposite applies near the tops. On account of a wide scatter of values this evidence is rather weak; this scatter may be due to the fact that growing and decaying clouds could not be treated separately in the statistic. In several flights made with specially instrumented aircraft from Guam (3), the author noted that on horizontal traverses in the cloud-top region the temperature rose slightly when an actively growing top was entered. Other data indicate a similar relation. It appears safe to conclude that young cumuli are slightly less dense than their surroundings; in the trades the dry temperature difference may average 1°C , that of virtual temperature 2°C . As shown by our earlier computation from Eq. (5.2), such temperature differences suffice to produce very large buoyancy accelerations.

Further information comes from the Thunderstorm Project conducted by the University of Chicago under the auspices of the U.S. Weather Bureau (13). From numerous aircraft traverses through thunderstorms Braham (7) found that temperatures vary widely within a given thunderstorm cell but that vertical-draft speed and temperature are correlated in the mean picture. The strongest updrafts coincide with the highest temperatures; the strongest downdrafts, with the lowest temperatures. This confirms that buoyancy is the mechanism acting to accelerate air along the vertical; we shall now inquire further as to why we do not observe, in most instances, temperature lapse rates and vertical-draft speeds of the amount predicted by the buoyancy formula.

Entrainment. In 1947, Stommel (32) put forward the idea that the observed cumulus structure could be explained if one assumed that environment air was being entrained and mixed with the ascending cloud air. Stommel did not have any direct evidence of entrainment. Such evidence was furnished by Byers and Hull (14), who showed that swarms of pilot balloons released around towering cumuli and thunderstorms converged strongly in the low and middle troposphere. Figure 5.11

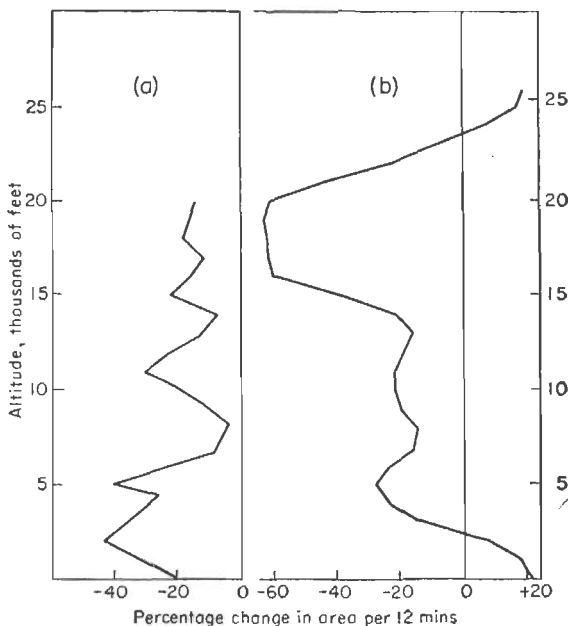


Fig. 5.11. Distribution of divergence with height in the vicinity of (a) bulging cumulus and (b) mature thunderstorms (12, 14).

shows two generalized distributions of divergence with height. In bulging cumulus the level at which the lower convergence goes over into upper divergence is not reached in the diagram. In mature thunderstorms it lies at the rather high elevation of 24,000 feet (400 mb). Evidently, the level of nondivergence is much lower in trade cumuli.

Stommel asks this question: Given the observed temperature and moisture distribution along the vertical inside and outside of cumuli, what entrainment of outside air into the cloud must have taken place to produce the observed inside temperature and moisture structure? The physical principles he uses are the laws of conservation of energy and mass (both dry air and water in vapor or liquid form). To these Malkus (22) later added the law of conservation of horizontal momen-

tum. Although all processes take place simultaneously, we may apply the conservation laws successively for purposes of the following analysis:

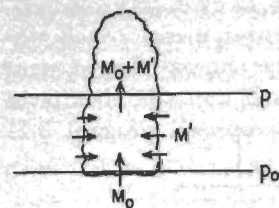


Fig. 5.12. Illustrating entrainment.

Then we add the effects

The sensible heat h of the mass $M = M_0 + M'$ at p , omitting moisture, is

$$h = c_p T^*(M_0 + M'), \quad (5.4)$$

where c_p is the specific heat of air at constant pressure and T^* the temperature of the mixture. Because of the principle of conservation of energy, $h = h_0 + h'$. Now $h_0 = c_p(T_0 - \Delta T)M_0$, and $h' = c_p T' M'$, where ΔT is obtained by raising the mass M_0 dry-adiabatically from p_0 to p . Then .

$$T^* = \frac{(T_0 - \Delta T)M_0 + T'M'}{M_0 + M'}. \quad (5.5)$$

The total moisture content, assuming that all moisture is carried along, is computed by similar reasoning. Thus

$$q^* = \frac{q_0 M_0 + q' M'}{M_0 + M'}, \quad (5.6)$$

where q^* , q_0 , and q' are the specific humidities of M , M_0 , and M' , respectively. If there is to be a cloud, q^* must exceed the saturation specific humidity q_s at T^* and the excess water vapor must have condensed. The amount of heat released by the condensation can be computed from the first law of thermodynamics. Since the condensation is assumed to take place at constant pressure, the final cloud temperature

$$T = T^* + L/c_p \times (q^* - q_s). \quad (5.7)$$

In this integrated form of the first law L is the heat released by condensation of 1 g of water.

Combining (5.4)–(5.7), Stommel solves for the entrainment rate, defined by $1/M dM/dp$ or, for a finite pressure interval, more simply by

M'/M_0 , the ratio of air entrained to that entering through the base. Evaluation is carried out most conveniently on a diagram with T and q as coordinates. Figure 5.13 is an example. The curves AB and $A'B'$ represent inside and outside soundings. Points A and A' are situated at 940 mb, the cloud base; points B and B' , at 840 mb. The air at A is a

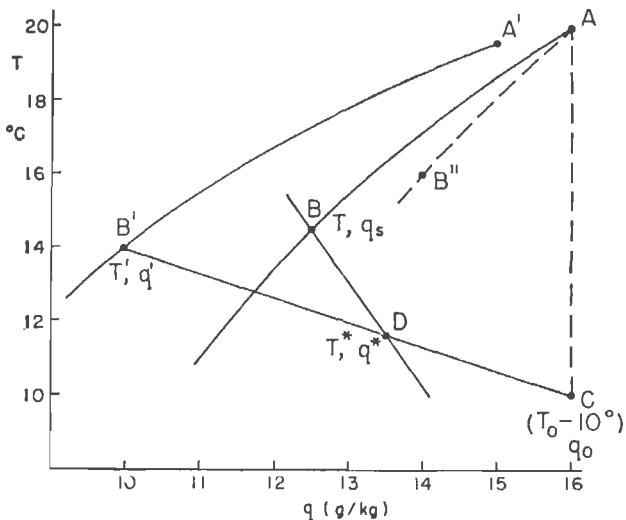


Fig. 5.13. Illustrating entrainment calculation.

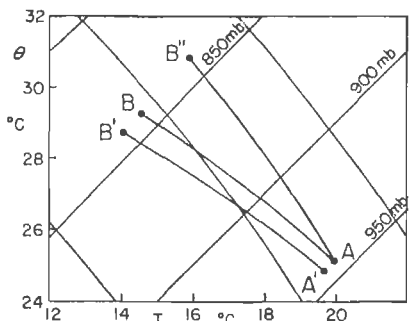


Fig. 5.14. Tephigram showing reduction of "positive area" due to entrainment for the case of Fig. 5.13.

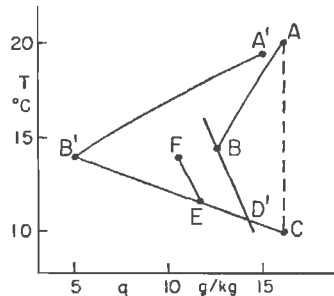


Fig. 5.15. Illustrating the effectiveness of a dry environment in stopping cumulus growth.

little warmer and moister than that at A' , which suggests an initial buoyancy impulse. Both temperature lapse rates are nearly identical as we see from the small temperature difference at 840 mb. For comparison the moist-adiabatic ascent AB'' is also shown. If the air had risen without entrainment, it would have arrived at 840 mb with the properties of point B'' —with temperature 1.5°C warmer and specific

humidity 1.5 g/kg higher than at B' . The accompanying tephigram (Fig. 5.14) shows the large reduction of positive area through entrainment. Following is the entrainment computation:

1. We raise the air at A dry-adiabatically for 100 mb. Since q remains constant, the process occurs along the vertical line AC ($\Delta T = 10^\circ\text{C}$).

2. We draw the line $B'C$. The point D , representing T^* , q^* , must lie on this "mixing line."

3. Equation (5.7) is linear and therefore represented by a straight line on a diagram with coordinates T , q . Condensation of 1 g/kg of water vapor will raise the temperature of 1 g of air by 2.47°C . We draw a line with this slope through B and find point D at the intersection between this line and $B'C$.

The following is to be noted:

1. The ratio of the segments DC and DB' gives the entrainment rate M'/M_0 , which in this case is 2 to 3. For each 3 kg of air flowing through the cloud base, 5 kg flows through the 840-mb level.

2. The difference in moisture content between B and D gives the amount of liquid water available for precipitation. This difference is 1 g/kg in our case. Each kilogram of air moving through the 840-mb level carries with it 1 g of liquid water in droplets. These droplets form the cloud.

The foregoing has demonstrated how it is possible to produce lapse rates inside cumuli steeper than the moist-adiabatic rate.

Figure 5.15 illustrates the profound effect on cumulus growth by the moisture content of the environment. In this figure nothing is changed from Fig. 5.13 except that the specific humidity at B' is 5 g/kg, which still gives a relative humidity of 43 per cent at this point. The segment $D'C$ is now a much smaller fraction of $D'B'$, in fact only $\frac{1}{5}$ compared with $\frac{2}{3}$. If a cloud is to exist at 840 mb with properties of point B , the entrainment rate must be reduced from 2:3 to 1:5. If entrainment took place at the higher rate, the cloud properties would be found on the line EF which intersects $B'C$ at E . The temperature at F is the same as that of the outside sounding; cloud growth could still barely proceed at this temperature because on account of the water-vapor difference the inside air remains slightly less dense than the outside air. But the specific humidity at F is only 10.5 g/kg, which is 1.7 g/kg less than the saturation specific humidity. Therefore a cloud can no longer exist.

It had been Stommel's objective to determine whether or not the observed lapse rates of temperature and moisture inside cumuli could be explained with the entrainment mechanism. He has succeeded in showing that they can, but, as frequently happens, his study has opened many new problems:

1. Stommel assumes the cloud to be in a steady state. Actually we have found that the clouds go through a rather rapid cycle of growth and decay. This aspect must be faced eventually.

2. Temperature and moisture within the cloud are considered uniform at any level. Actually, wide fluctuations occur. This question has been discussed mainly in connection with thunderstorm structure where the fluctuations are most spectacular (12, 13).

3. If continual entrainment takes place throughout the depth of cumuli, the upward mass flux must be greatest near the tops.

4. The wind structure of the cumuli and their drift relative to the surroundings must be affected by entrainment.

5. We have computed the entrainment rates which must have prevailed in order to account for the structure of certain cumuli. If we wish to understand their variable structure, life span, and size, we must ask how entrainment is produced and what determines the rates of entrainment. This raises the problem of the dynamics of the cumuli.

Rates and Mechanisms of Entrainment

Although Stommel does not prescribe a mechanism for entrainment, he suggests that the buoyant air rising from the cloud base may be likened to an aerodynamic jet stream moving through an environment nearly at rest. Turbulent mixing at the edges imparts some of the momentum of the jet to the environment, which is thus set in motion along the direction of the jet. Another mechanism, called "dynamic entrainment," has been proposed by Austin (1) and Austin and Fleisher (2).

Suppose that a buoyant stream moves upward from the cloud base. Since this stream is accelerated, the upper portions ascend more rapidly than the lower ones. Austin (1) comments:

If the outer boundaries of the column of rising air form a cylinder it follows that more mass is leaving the top portion of any section of the cylinder than is entering the base. This state is impossible as it violates the condition of continuity. The continuity of mass requires that air be brought in through the sides of the cylinder, but this is not possible in view of the assumption [in the buoyancy formula (5.2)] that the pressure inside the cylinder is equal to the pressure outside. Alternatively, continuity may be satisfied by allowing the horizontal dimensions of the rising stream to decrease with height. This case does not appear physically real as a model for a cumulus cloud as it leads to a very narrow current moving with a large velocity.

Byers and Braham summarize the distinction between the two mechanisms in a very clear way (12):

In the case of a jet stream or a mechanically driven jet, the environment is entrained frictionally and distributed through the jet by eddy diffusion and

turbulent mixing. In addition . . . there are accelerating vertical currents of air that pull in air from the environment by pressure readjustments. Therefore in considering entraining rates, it appears necessary to consider two terms: one dealing with the geometry of the system and the kinematic viscosity, and the other concerning the density difference between the updraft region and the environment.

Until now three resistive effects have been found that reduce the huge buoyant energy computed by means of the parcel method. These are:

1. Compensatory sinking of the whole environment.
2. Entrainment of outside air through lateral mixing.
3. Dynamic entrainment of outside air through development of an inward-directed pressure gradient. The two entrainment mechanisms may reduce the parcel energy to zero.

To these should be added:

4. Drag forces, analogous to those of aerodynamics (29). These consist partly of a "form" or "profile drag" due to the pushing aside of the surrounding air as the jet grows and accelerates this air back as a counter-current (23). In addition there is skin friction arising from viscous forces at the boundary of the rising jet.

Malkus (23) suggests that the last-named forces may prove negligible compared with the others since the problem is not one of a solid body moving through a fluid as in the case of airplane design. She has attempted, however, to define the drag forces for the cumulus problem (24). The question is not settled, and the foregoing summary shows the extent to which the complexity of the cumulus problem has grown since the days of the simple parcel method.

Further progress has been confined to the entrainment approach. Austin (1, 2) assumed a cylindrical shape of the cumulus. Given such shape and steady state, he computed the lapse rate inside the cloud with suitable assumptions about the entrainment rate. This problem is the inverse to that solved by Stommel and leads to comparable results.

Houghton and Cramer (19) next made explicit application of Austin's suggestion that outside air is entrained only in such amount as to meet the requirements of mass continuity. This leads to a substantial advance, for the entrainment rate needs no longer be assumed or computed; it becomes one of the dependent variables of the problem. Houghton and Cramer write continuity equations for the vertical flow of mass and sensible and latent heat as above; to these they add the continuity requirement for vertical momentum, as is also done by Stommel (33). Considering two pressure surfaces as in Fig. 5.12, the vertical momentum flow through the upper surface is equal to the lower inflow plus the momentum generated in the layer, since the entrained

air is initially at rest and does not bring in vertical momentum. Both Houghton and Stommel assume that the source term can be calculated with Eq. (5.2), Stommel with more justification since he is not dependent on horizontal pressure gradients for the inward acceleration. As we have seen, (5.2) assumes that pressures inside and outside of the cloud are equal, a difficulty felt by Austin in the quotation given above. If there is no horizontal pressure gradient, there is no mechanism for "dynamic entrainment." Nevertheless Houghton and Cramer arrive at a reasonable result, at least for dry-air convection. One must suppose that for computational purposes the horizontal pressure force makes only a second-order contribution even though it furnishes the whole dynamic basis for the motion. This situation is not unusual and is frequently encountered in meteorology and in physics in general.

Stommel (33) computes the entrainment rate by the methods shown in Fig. 5.13 and obtains the vertical velocity profile with the continuity equation for vertical momentum. He points out that these speeds are large for trade cumuli, up to 10 mps. The entrainment is far greater than that needed for mass continuity in a vertical cylinder. It follows that in this model the cloud diameter must increase upward, which is occasionally observed, but not regularly. This discrepancy would be considerably reduced if we could assume that not all entrained air is carried along indefinitely in the rising current. Let us suppose that the mixing between rising jet and environment is not complete, or that a part of the condensed water sinks relative to the rising current, *i.e.*, moves upward less rapidly or falls out as rain. Then a large fraction of the entrained air might not be able to remain saturated and might cease ascending soon after evaporation of the remaining water droplets. The vertical mass flow and the width of the cloud would be reduced in this way. Malkus, calling Stommel's calculation "gross entrainment," has proposed another mechanism, the vertical shear of the horizontal wind (22, 24) that can eject a part of the air drawn into cumuli.

In spite of many difficulties yet to be overcome there can be little doubt that the concept of direct interaction between rising columns and their environment has set the research on cumuli in the right direction. Entrainment enables us to answer the question raised in Chap. 2, why the tops of the trade cumuli often are situated precisely in that portion of the low troposphere where the "positive area" on thermodynamic charts, as calculated with the parcel method, increases rapidly upward. This is the region of the top of the moist layer; as cumuli try to penetrate to greater heights, they are dissipated by mixing with the upper dry air. The vertical moisture gradient turns out to be a primary factor controlling cumulus growth in a conditionally unstable atmosphere.

One more point may be mentioned. The entrainment rate is defined

as the per cent mass increase. Byers and Braham (12) have measured entrainment rates for bulging cumulus of about 100 per cent in 500 mb. These rates are about five times smaller than those computed by Stommel for trade cumuli. Suppose that lateral mixing acts on the boundaries of bulging and trade cumulus and that the intensity of the mixing per unit surface of the circumference is equal in both cases. If this is true, the entrainment rate should depend on the ratio of the length of the boundary to the mass (roughly the area) of the cloud. Given r_1 and r_2 as the radii of bulging and trade cumulus and a fivefold difference in entrainment rates, then $2\pi r_1/\pi r_1^2 = \frac{1}{5} \times 2\pi r_2/\pi r_2^2$, or $r_1 = 5r_2$. This result is reasonable and supports the lateral-mixing hypothesis. It further suggests that the effectiveness of entrainment in reducing the buoyant energy inside ascending jets will depend on the width of these jets. As the width increases, the core of the rising air becomes more protected from the influences of the environment. A narrow central portion may then have higher temperatures and larger updraft speeds than the bulk of the cloud, in agreement with observations (7).

Horizontal Wind Structure of Cumuli

If a cumulus builds in an atmosphere with uniform wind along the vertical, entrainment does not affect the horizontal wind inside the cloud except as a result of the pressure-gradient accelerations discussed by Austin and by Houghton and Cramer. Essentially the wind inside remains the same as that outside. The cloud moves with the speed of the wind, and its axis is vertical. More often the wind speed either increases or decreases with height. The clouds then no longer move with the mean speed of the surrounding wind, and their axes lean vertically in the direction of the shear (Fig. 5.9). In the shallow layer through which trade cumuli usually extend, the wind direction seldom changes appreciably. But cumulus congestus and cumulonimbus commonly reach into strata with a wind structure differing radically from the low levels. The cloud axis is still oriented along the wind shear, which will differ in direction from the low-tropospheric wind. We then observe the twisted structure characteristic of the upper portion of many tall clouds.

The effect of the vertical wind shear on cumulus has been the subject of quantitative study (13, 22, 24). These analyses have mainly treated two-dimensional problems, *i.e.*, changes of wind speed but not of direction with height. Such models usually satisfy conditions in the layer of trade cumuli. Using the law of conservation of momentum, a continuity equation is set up for horizontal momentum similar to those above for sensible heat and moisture. Referring to Fig. 5.12, the momentum flow through the upper pressure surface must equal the sum of the momentum

fluxes through the bottom and the sides. Given suitable assumptions regarding the vertical shear in the environment and the entrainment rate, we can compute the horizontal wind speed and the slope of the cloud axis as a function of altitude (22, 24). The direction of the slope is that of the external shear, as mentioned before; the wind inside the cloud is less than that outside when the outside wind increases with height; it is more when the outside wind decreases with height.

The foregoing permits us to deduce the vertical shear of the wind from cloud observations alone. This is a main reason why shear observations should be included in synoptic codes (Chap. 7). Malkus (24) also suggests that the vertical wind structure has a major bearing on the life cycle of cumuli. During the Thunderstorm Project (7, 11, 13) it has been noted that cumulonimbi grow by putting up successive towers at or near their tops. Trade cumuli act similarly. "If the wind shear is weak, the cloud turrets will remain nearly vertical even as their upward velocities decay and they dissipate. New turrets can then grow into and entrain air moistened by their predecessors. When, on the other hand, the external shear is strong, the dissipating towers become very strongly slanting and the new vigorous towers, which grow much more nearly vertically, are penetrating dry air" (23). We may add that rainfall also becomes progressively inhibited as the slope increases. Raindrops grow mainly from collision with other drops (Chap. 6). A minimum vertical cloud thickness is needed, given general characteristics of the air mass, for drops to grow sufficiently to fall out as rain. Any slant of the axis of a cumulus reduces the vertical cloud thickness and diminishes the chance of precipitation. Such raindrops as do form evaporate before reaching the ground. Not infrequently do we see the spectacle of shearing trade cumuli completely "raining out" aloft (30).

Malkus (22) also has related the vertical slope of cumuli to the turbulence pattern. The reasoning follows that just offered. New towers building upward from the lower cloud parts tend to be more vertical than the older ones since entrainment has not yet had an opportunity to adjust completely the freshly rising air to environmental conditions. Because the heaviest turbulence is associated with new towers, we should expect turbulence to be strongest on the upwind side when the external wind increases and on the down-wind side when the external wind decreases with height.

Several important deductions follow from this:

1. It is possible to estimate the turbulence pattern from the slope of the cloud axis alone.
2. The clouds should build into the wind, *i.e.*, move slower than the surrounding air when the wind shear is positive; they should move faster when it is negative. Direct measurement has proved the reality of such

relative motion (13); it is substantiated further by lapse-time motion pictures of cumuli which show that cloud matter commonly streams out on one side alone—the side toward which the cloud leans with height (22).

Since not all rising air is visible cloud matter, an airplane should encounter turbulence outside the cloud when approaching it on the building side. The turbulence should decrease before the aircraft has left the cloud on the opposite side. Malkus has been able to substantiate this contention from the records of the Wyman-Woodcock expedition. Figure 5.16 illustrates the mean turbulence pattern for eight traverses when the wind increased upward, as shown by the shear vector. The

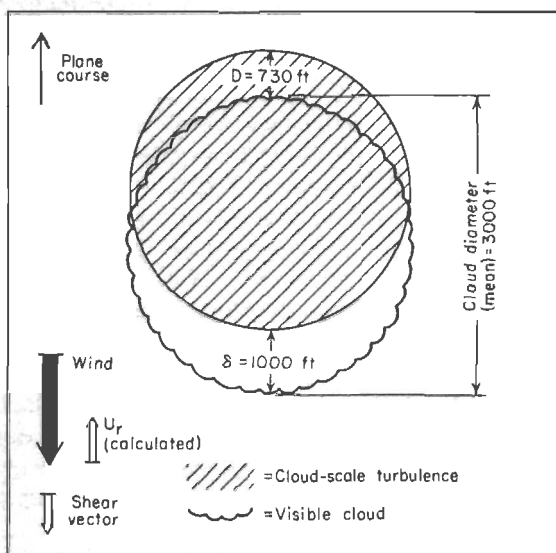


Fig. 5.16. Distribution of turbulence relative to clouds. Average of eight horizontal-plane traverses (22).

arrow U_r is the cloud motion that is seen by an observer moving with the outside wind. In consequence the cloud slopes with height from the upper to the lower end of the diagram. The airplane, entering from the down-wind side, at first encounters nonturbulent cloud matter. Upon leaving the cloud, cloud-scale turbulence (cf. Fig. 5.3) persists for the distance D of 730 feet. In a single case of weak opposite shear the turbulence pattern differed in the requisite sense.

The foregoing shows that the advance in knowledge of the wind structure of cumuli has indeed been spectacular. With time a comprehensive dynamical theory undoubtedly will be evolved. Such a theory may well be based on a vorticity theorem formulated similar to Eq. (8.10). Lapse-time motion pictures reveal that the cumuli revolve about the horizontal

axis normal to the wind when a vertical shear, and therefore vorticity about the horizontal axis, is present. If u and w are the horizontal- and vertical-velocity components along the x and z axes of Fig. 5.17, the vorticity about the y axis, which points normal to the plane of the diagram, is given by $\eta = \partial u / \partial z - \partial w / \partial x$. Analogous to Eq. (8.10),

$$\frac{d\eta}{dt} + \eta \left(\frac{\partial u}{\partial x} + \frac{\partial w}{\partial z} \right) = 0. \quad (5.8)$$

This two-dimensional formulation cannot yield a complete theory since the density variations and friction, which lead to cumulus growth and decay, are neglected. But it may serve for orientation for the state that the atmosphere tries to attain, just as Houghton and Cramer (19) could

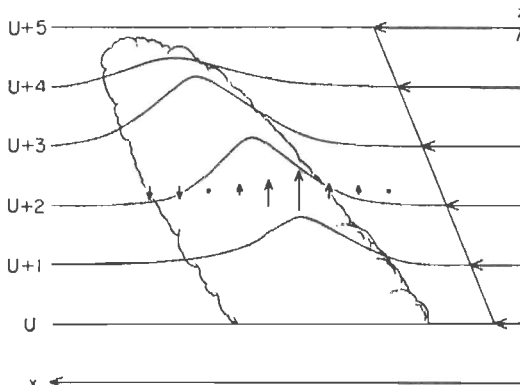


Fig. 5.17. Model of horizontal-wind distribution in trade-wind cloud when external wind increases with height. Vertical-motion gradient sketched.

calculate dynamic entrainment in spite of the assumption that the pressure inside and outside of cumuli is the same. If motion along the y axis is neglected, mass continuity demands that $\partial u / \partial x + \partial w / \partial z = 0$ and $\eta = \text{constant}$ for each moving parcel or column of air. This also is not quite realistic, but it permits us to ascertain the extent to which the data contain an indication of conservation of vorticity.

Figure 5.17 is a model for the case of positive shear. The undisturbed external wind (U) increases linearly with height. The cloud leans downwind, and inside it the wind increases upward at a much slower rate than outside. The vertical-motion arrows are patterned on the lapse-time motion pictures.

The vorticity to be conserved is that of the environment, $\partial U / \partial z$. Thus, $\eta = \partial u / \partial z - \partial w / \partial x = \partial U / \partial z$, or $\partial / \partial z(u - U) - \partial w / \partial x = 0$. Consider first some trajectory entering the cloud on the upwind

side. During the approach $\partial u / \partial z$, and therefore also $\partial / \partial z(u - U)$, increases. Thus $\partial w / \partial x$ must be positive and also must increase if the above relation is to hold. This we observe. On the down-wind side $\partial w / \partial x$ is negative. Therefore $\partial / \partial z(u - U)$ should also be negative, again in agreement with the observations. It follows that a tendency toward conservation of vorticity exists that may be capable of furnishing a dynamic model for mature trade cumuli in a current with a shear in wind speed but with uniform direction along the vertical.

Turbulent Exchange in the Moist Layer

We return to the problem with which the chapter started, the energy cycle. We have examined the facts that are known about the energy transfer from ocean to atmosphere and in the subcloud layer. Since all turbulence dies out rapidly in the clear areas above the top of the subcloud layer (Fig. 5.3), all further transport must be accomplished by the cumuli and synoptic disturbances.

Figure 5.18 shows the structure of the whole layer below the trade inversion as interpreted by Bunker (9). Above the top of the subcloud layer a shallow stable layer is encountered in the clear areas between the clouds; the moisture decreases substantially in this layer. This boundary suggests a transition from the diffusion regime below to a convection regime higher up. Organized sinking in the clear, which compensates for the ascent in the clouds, would lead to the formation of such a boundary, since above the subcloud layer the potential temperature increases upward and the specific humidity decreases. We may regard the stable layer as the manifestation of the compensatory sinking discussed by J. Bjerknes (6).

In the following we shall try to estimate whether or not convection is capable of effecting the upward transport of water vapor required for continuity. For this purpose we shall utilize the data for the northeast-trade regime in the Pacific Ocean (28). The structure of the trade in this region has been described in Chap. 2; we shall present the heat and moisture balance in Chap. 12. This balance computation shows the amount of moisture which the cumuli must transport through the cloud layer.

Within the cloud layer there will be cloud areas with active ascent and clear spaces with sinking motion. But not all of the cloud matter rises. Since the growing stage of cumuli consumes only one-third or less of the total life span of the clouds, most water particles we see in the sky are either inactive or descending. Our specific question then will be: What fraction of the cloud area must consist of actively ascending towers in order to accomplish the total moisture flow?

We consider a reference surface in the middle of the cloud layer (Fig. 5.19). The whole area $A = A_a + A_c + A_d$, where the subscript a refers to the actively ascending cloud portions, c to the stationary or descending cloud portions, and d to the descending clear air. Climatological atlases give the mean low cloudiness of the region as five-tenths of sky cover so

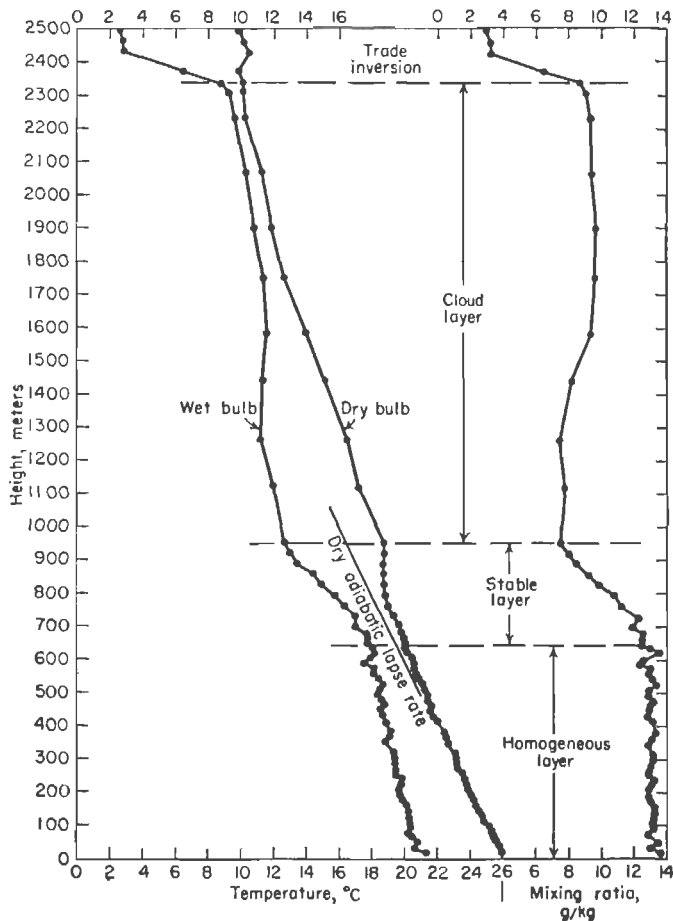


Fig. 5.18. Vertical airplane sounding near Puerto Rico, Apr. 27, 1946 (9).

that $A_a + A_c = A_d$. This value may be somewhat too high, but the effect of an error of one-tenth or even two-tenths of sky cover on what follows is relatively small.

The vertical velocities in the three areas will be w_a , w_c , and w_d . In the clear, the vertical temperature and moisture distributions are taken as the means of Figs. 2.36 and 2.39. In the clouds, the temperatures will

be considered as equal to those in the clear and the moisture as given by the saturation specific humidity.

The net moisture flux F is the residual of all upward and downward transports of water vapor through the reference surface. Thus

$$F = \rho(w_a q_s A_a - w_c q_s A_c - w_d q A_d). \quad (5.9)$$

Here q_s and q are the specific humidities in cloudy and clear areas, respectively, and ρ is the density, considered uniform (a very slight approximation). All quantities are mean values at the reference surface and the

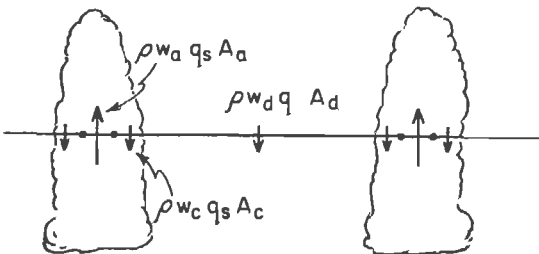


Fig. 5.19. Illustrating vertical moisture transport in cloud layer.

vertical velocities are treated as positive numbers. Mass continuity demands that

$$w_a A_a - w_c A_c = w_d A_d. \quad (5.10)$$

Combining (5.9) and (5.10),

$$w_d = \frac{F}{\rho(q_s - q) A_d}. \quad (5.11)$$

All quantities necessary for evaluation of this equation are known from the data or from calculations. Figure 12.10 shows the moisture flux F . Inserting the numbers, $w_d = 2.3$ cm/sec, which is a reasonable value.

If we now say that the growing stage of cumuli averages 10 minutes and that the mean cloud thickness is 5,000 feet, $w_a = 2.5$ m/sec. Solving (5.10) for A_a ,

$$A_a = \frac{w_c + w_d}{w_a + w_c} A_d. \quad (5.12)$$

There are still two unknown quantities, and a solution requires either more factual knowledge or some assumption about w_c . Suppose that the inactive cloud matter, when averaged for all cloud particles, descends. This mean descent is not likely to exceed that of the clear spaces, or the clouds would disappear rapidly. If we assume, for a maximum case, that $w_c = w_d$, (5.12) can be solved. A_a turns out to be nearly 1 per cent of

the whole area or 2 per cent of the cloud area. Further, A_c amounts to 49 per cent of the whole area, or 98 per cent of the cloud area.

This rather extreme result shows clearly that cumulus convection is an effective transport mechanism, capable of moving upward through the cloud layer the latent heat energy added to the trade air. For the moisture flux beyond the mean height of the cumuli we must look to the synoptic disturbances.

REFERENCES

- (1) Austin, J., *J. Meteor.*, **5**: 103 (1948).
- (2) Austin, J., and A. Fleisher, *J. Meteor.*, **5**: 240 (1948).
- (3) Barrett, E. W., and H. Riehl, *J. Meteor.*, **5**: 304 (1948).
- (4) Baum, W. A., *J. Meteor.*, **8**: 196 (1951).
- (5) Bénard, H., *Rev. Gén. Sci.*, **2**: 1261, 1309 (1900).
- (6) Bjerknes, J., *Quart. J. Roy. Meteor. Soc.*, **64**: 325 (1938).
- (7) Braham, R. R., *J. Meteor.*, **9**: 227 (1952).
- (8) Brunt, David, in *Compendium of Meteorology*. Boston, Mass.: American Meteorological Society, 1951.
- (9) Bunker, A. F., et al., *Papers Phys. Oceanog. Meteor.*, Mass. Inst. Technol. and Woods Hole Oceanog. Inst., Vol. 11, No. 1, 1949.
- (10) Byers, H. R., *General Meteorology*. New York: McGraw-Hill Book Company, Inc., 1944.
- (11) Byers, H. R., and L. J. Battan, *Bull. Am. Meteor. Soc.*, **30**: 168 (1949).
- (12) Byers, H. R., and R. R. Braham, *J. Meteor.*, **5**: 71 (1948).
- (13) Byers, H. R., and R. R. Braham, *The Thunderstorm*. Washington, D.C.: Government Printing Office, 1949.
- (14) Byers, H. R., and E. C. Hull, *Bull. Am. Meteor. Soc.*, **30**: 90 (1949).
- (15) Cressman, G. P., *J. Meteor.*, **3**: 85 (1946).
- (16) Durst, C. S., *Quart. J. Roy. Meteor. Soc.*, **59**: 361 (1933).
- (17) Geiger, R., *The Climate near the Ground*. Cambridge, Mass.: Harvard University Press, 1950.
- (18) Holmboe, J., et al., *Dynamic Meteorology*. New York: John Wiley & Sons, Inc., 1945.
- (19) Houghton, H. G., and H. E. Cramer, *J. Meteor.*, **8**: 95 (1951).
- (20) Langwell, P. A., *J. Meteor.*, **5**: 243 (1948).
- (21) Mal, S., *Beitr. Phys. fr. Atm.*, **17**: 40 (1930).
- (22) Malkus, J., *Trans. Am. Geophys. Union*, **30**: 19 (1949).
- (23) Malkus, J., *Tellus*, **4**: 71 (1952).
- (24) Malkus, J., *Quart. J. Roy. Meteor. Soc.*, **78**: 530 (1952).
- (25) Petterssen, S., *Weather Analysis and Forecasting*. New York: McGraw-Hill Book Company, Inc., 1940.
- (26) Rayleigh, J. W. S., *Phil. Mag.*, **32**: 529 (1916) (and other papers).
- (27) Riehl, H., *Tellus*, **2**: 1 (1950).
- (28) Riehl, H., et al., *Quart. J. Roy. Meteor. Soc.*, **77**: 598 (1951).
- (29) Schmidt, F. H., *Mededel. en Verhandelingen*, Ser. B, The Hague, No. 1, 1947.
- (30) Sherman, L., *Tellus*, **3**: 203 (1951).
- (31) Staff, Institute of Tropical Meteorology, in *Handbook of Meteorology*, pp. 763ff., F. A. Berry et al., eds. New York: McGraw-Hill Book Company, Inc., 1945.
- (32) Stommel, H., *J. Meteor.*, **4**: 91 (1946).
- (33) Stommel, H., *ibid.*, **8**: 127 (1951).

- (34) Sutton, O. G., *Quart. J. Roy. Meteor. Soc.*, **75**: 335 (1949).
- (35) Sverdrup, H. U., *J. Marine Research*, **1**: 3 (1937).
- (36) Sverdrup, H. U., *Oceanography for Meteorologists*. New York: Prentice-Hall, Inc., 1942.
- (37) Sverdrup, H. U., *J. Meteor.*, **3**: 1 (1946).
- (38) Swinbank, W. C., *J. Meteor.*, **8**: 135 (1951).
- (39) Various contributors, "Convection Patterns in the Atmosphere and Ocean," *Ann. N.Y. Acad. Sci.*, **48**: 705 (1947).
- (40) Walker, G. T., *Quart. J. Roy. Meteor. Soc.*, **58**: 23 (1932).
- (41) Williams, N. R., *Bull. Am. Meteor. Soc.*, **29**: 106 (1948).
- (42) Woodecock, A. H., *J. Marine Research*, **3**: 248 (1940).
- (43) Woodecock, A. H., and J. Wyman, *Ann. N.Y. Acad. Sci.*, **48**: 749 (1947).

CHAPTER 6

THE PHYSICS OF TROPICAL RAIN

By Raymond Wexler

Two features distinguishing the formation of clouds in the tropics from that in temperate latitudes are high temperature and high humidity. Therefore, when condensation occurs, the clouds have a relatively high liquid-water content that is important in initiating precipitation as well as in promoting heavier rainfall. The frequency with which rain occurs, even from clouds only a few hundred feet thick, is often remarkable to the visitor to the tropics. Likewise, the torrential rains of thunderstorms, which occur with maximum frequency in the East Indies, Central America, and South Central Africa, exceed the experience of many visitors from temperate zones.

This chapter will deal with the formation of cloud and the initiation and growth of precipitation, both natural and artificial. Before the Second World War many meteorologists believed that only the ice phase could initiate precipitation; many recent observations, however, both from temperate and tropical regions, show conclusively that rain can form in clouds considerably above freezing. There are indications that a high percentage of clouds in the tropics produce rain without the aid of the ice phase.

Formation of Clouds

Clouds are formed by the ascent and adiabatic cooling of air. As air is cooled, the amount of water vapor it can hold decreases, so that rising air becomes saturated and condensation occurs. In pure water vapor, condensation takes place only with supersaturation of about 400 per cent varying with temperature, but in the atmosphere it is greatly facilitated by the presence of impurities, called *condensation nuclei*. Nuclei may be hygroscopic, *i.e.*, with an affinity for water, such as sea salt, which holds water even at low relative humidities; or they may be solid insoluble particles on which the water condenses at high relative humidities. The size of these nuclei ranges from about 10^{-6} to 10^{-4} cm. With these particles present, the atmosphere attains less than 1 supersaturation during condensation.

Small expansion chambers, like the Aitken dust counter, have been used to measure the number of condensation nuclei in the atmosphere. These instruments, however, give little indication of the nuclei count in natural cloud formation since, because of the high supersaturations produced, they measure nuclei extending to smaller sizes, which are much more numerous than those involved in atmospheric condensation. It is interesting, nevertheless, to note that the number, as measured by such instruments, averages about $150,000 \text{ cm}^{-3}$ over cities, $50,000 \text{ cm}^{-3}$ over open country, and $1,000 \text{ cm}^{-3}$ over oceans or mountaintops. However, there are wide variations from these averages, with an absolute minimum of 2 cm^{-3} over the oceans (13).

It was believed by Aitken and others that only hygroscopic particles could act as condensation nuclei. Boylan's (6) findings that the insertion of a cloud of carpet dust into the Aitken counter did not increase the nuclei count appeared to corroborate this idea. However, Junge (16) showed experimentally that nonhygroscopic particles can act as condensation nuclei and explained Boylan's results by showing that the added number of dust particles was insignificant compared with the number of particles involved in condensation in the Aitken counter.

From an analysis of visibilities and humidities in the British Isles, Wright (41) in 1939 concluded that the dominant condensation nuclei are derived from sea salt. Simpson (30) objected to this conclusion, pointing out that spray from the oceans did not produce salt nuclei to account for the global rainfall. Simpson, however, took for granted that all rain is derived from a coalescence of cloud drops, each of which requires a separate nucleus—an assumption which may not be correct.

To determine the number of nuclei which grow to cloud-drop size, it would be desirable to know the concentration of nuclei of different sizes, but information exists only on the largest. Woodcock (39) has found droplets containing 10^{-13} g NaCl in concentrations of about 10 cm^{-3} at elevations up to 10,000 feet over the oceans; he also found a few giant sea salt nuclei of mass 10^{-9} g in concentrations of $1,000 \text{ m}^{-3}$. Woodcock's findings indicate that the largest nuclei consist of sea salt. Recent electron-microscope investigations of evaporated cloud or fog droplets indicate, however, that the majority of smaller nuclei are combustion products, both hygroscopic and nonhygroscopic.

The important properties that determine growth of these nuclei to cloud-drop size are their curvature and the molecular concentration of the solute. The smaller the size of the drop, the greater is its tendency to evaporate. Solution causes the drops to grow in saturated air. At a given relative humidity, a drop is in equilibrium if the growth tendency (due to a hygroscopic nucleus) is balanced by the evaporation tendency (due to curvature). The equation of equilibrium, first derived by Kohler,

may be written

$$100 - \text{RH} = \frac{A}{d} - \frac{B}{d^2} \quad (6.1)$$

where RH is the relative humidity in per cent and d is the drop diameter in cm. The constants A and B depend, respectively, on the surface tension of the condensing fluid and on the molecular concentration and electrolytic dissociation of the solute (23). Figure 6.1 shows equilibrium curves for droplets containing various amounts of NaCl in solution; it also includes the curve for pure water droplets, or droplets containing insoluble particles. Examining the curve for droplets containing 10^{-15} g NaCl, we see that the equilibrium diameter increases rather slowly as the relative humidity approaches 100 per cent. When the air becomes supersaturated, the equilibrium size increases at a somewhat faster rate. Beyond a critical supersaturation of 0.11 per cent, the droplet is no longer capable of remaining in equilibrium and begins to grow rapidly. When this critical supersaturation is exceeded, the nucleus is said to be activated toward cloud-drop growth. The smaller the amount of dissolved substance in the droplet, the greater is the critical supersaturation required for activation. Thus, a nucleus containing 10^{-14} g NaCl requires a supersaturation of only 0.035 per cent for activation, while one containing 10^{-16} g NaCl requires 0.35 per cent.

Insoluble particles may act as condensation nuclei, provided they are wetted by water at or below the peak supersaturation attained in the rising air. All substances become wet at sufficiently high supersaturations. It may be seen from Fig. 6.1 that if the peak supersaturation is 0.35 per cent, all droplets containing nonhygroscopic particles with diameters greater than 0.6μ are activated, as well as all droplets containing salt with equilibrium diameter greater than 0.4μ . The number of insoluble particles that act as condensation nuclei are probably relatively few compared with the number of hygroscopic particles, but they may, nevertheless, be of considerable importance as freezing nuclei.

The number of nuclei activated toward cloud-drop growth depends on the mass distribution of nuclei and the rate of cooling of the air during initial condensation. In rising saturated air containing a distribution of sizes, the largest and most hygroscopic nuclei are first activated. The supersaturation increases to a peak value within about a minute after cloud formation and then decreases. After this peak value has been attained, no further nuclei may be activated and the condensing water is deposited on the growing cloud droplets. In cumulus clouds with updraft velocities greater than 1 mps at their base, the number of cloud drops may reach $1,000 \text{ cm}^{-3}$. Stratiform clouds with smaller cooling rates have an average droplet concentration of about 300 cm^{-3} .

A constant updraft velocity near the cloud base, with a continuous distribution of nuclei sizes, produces a rather narrow range in drop size at every level of the cloud. Such a range is often observed, but broad distributions are frequently found. A broad distribution in drop size might result if the vertical velocities near the cloud base varied over a considerable range and if the resultant cloud drops were mixed by turbulence within the cloud. A discontinuous size distribution of nuclei, such

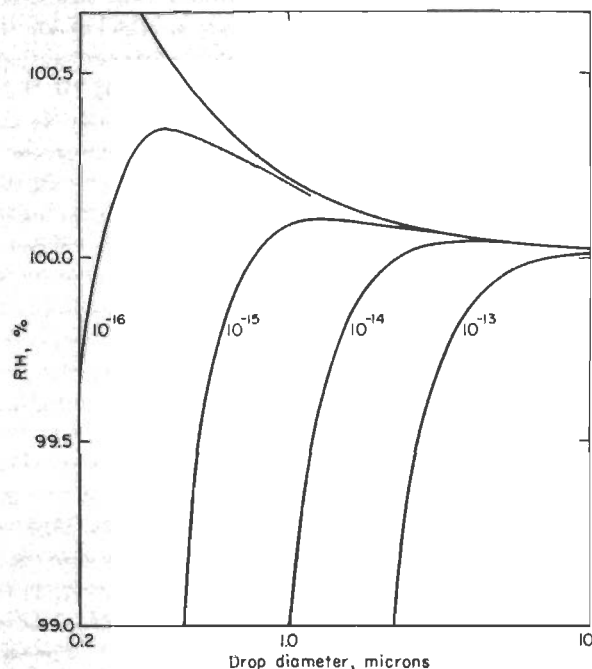


Fig. 6.1. Equilibrium curves for water droplets containing in solution different masses (g) of NaCl. The top curve applies to pure water droplets or droplets containing insoluble particles.

as a combination of a few giant ones with a much larger number of smaller nuclei, could result in a broad range of cloud-drop size. This is of considerable importance in initiating the growth of cloud drops to rain.

Aircraft investigations reveal that the drop-size range in small cumulus clouds is narrow, with a most frequent drop diameter of 15μ . With increasing cloud thickness, *i.e.*, with increasing liquid-water content, the drop-size spectrum increases; in thick cumuli, drop diameters ranging from 4 to 200μ have been observed (2). In stratiform clouds the most frequent drop diameter is between 11 and 14μ (11); the range of drop size is broader than in small cumuli but narrower than in dense cumuli.

Over the United States, the liquid-water content in cumuli has been found to range from 0.02 to more than 2.0 g/m^3 , with an average of about 0.5 g/m^3 . Values in stratiform clouds range from 0.01 to 0.7 g/m^3 , with an average of 0.13 g/m^3 (19). Some liquid-water measurements in small cumulus clouds of about 4,000 feet thickness show an increase from the cloud base to a maximum of $0.3\text{--}0.4 \text{ g/m}^3$ just below the tops (35). These values are only 20 per cent of those attained by the adiabatic expansion of saturated air from the base of the cloud. Hence, they show that considerable mixing with the environment and evaporation of the cloud takes place along the top and side boundaries. In the central portions of larger precipitating cumulus clouds, the liquid-water content has been found to be over 50 per cent of the amount obtained by adiabatic expansion (32). The percentages were probably considerably higher prior to the onset of rain. Some evidence from aircraft measurements indicate that the liquid-water content in the central portion of cumulonimbus may approach that obtained by adiabatic expansion although considerable mixing with the environment may take place along the sides (9, 20).

In the trade-wind regions, cumulus clouds transport moisture aloft from the top of the subcloud layer and by mixing and evaporation increase the humidity of the environment (Chaps. 5 and 12). As a result, succeeding cumuli are able to penetrate the inversion layer, and the height of the inversion thereby increases downstream. The depth of the cloud layer also increases, an important factor in raising the probability of rain downstream. A portion of the precipitation of the trades does not involve the ice phase since the inversion remains well below the 0°C level in height.

Precipitation Growth in Warm Clouds

Precipitation from clouds entirely above freezing (hereafter called warm rain) has so far been observed over or near the oceans and generally in tropical regions. Warm rain falls frequently in the Bahamas during the winter from a combination of stratocumulus and cumulus clouds. During the summer there are indications that a high percentage of warm rain occurs from cumulus (33). In the trades near Guam, moderate rain showers have fallen from stratiform decks 4,000 feet thick with temperature above 0°C . Warm rain has been observed in East Africa from cumulus over the hills 20 miles inland from the ocean (10). Light rain was encountered near Washington, D.C., on the outer perimeter of a hurricane from low broken clouds only about 500 feet thick and with a temperature of 70°F (36).

The factors that are important in cloud-drop growth do not govern the

growth of drops to precipitation size. Even if the supersaturation were extraordinarily high, the time required for cloud droplets to grow to small raindrops by condensation is about a day, whereas rain can fall less than an hour after cloud formation. Hence, another physical process must be responsible for precipitation growth.

Schumann (29) showed that, for clouds containing 1 g/m^3 of liquid water, the most important growth process of cloud drops greater than 10μ is the collision and coalescence of different drop sizes due to differences in fall velocity. He assumed that a large drop coalesces with all smaller ones in its path. The first calculation of the growth of cloud drops to rain by coalescence was made by Langmuir (17). He showed that growth by accretion proceeds slowly at first but increases rapidly when the drop acquires higher fall velocity and a larger cross section. As the drop falls, it sweeps through an approximately conical volume, catching a certain fraction E of the liquid water in its path. E is defined as the collection efficiency and depends on the relative sizes of the large and small drops. On the assumption that the smaller drops have negligible dimensions compared with the larger drops, a theory was developed for computing E , later verified experimentally (13). Langmuir calculated the time required for drops of various sizes to grow to a diameter of 6 mm, approximately the size at which falling raindrops break into smaller ones. These smaller drops would also grow by accretion to break up in turn; thus, a chain reaction of rain production would result.

Bowen (4) has extended Langmuir's theory. Using a hypothetical cloud of drops of 20μ diameter and a liquid-water content of 1 g/m^3 , he postulated that two drops, perhaps of slightly different size, coalesced. He then computed the subsequent growth of the large drop by coalescence, using Langmuir's collection efficiencies, and determined a time-height trajectory of the large drop for various updraft velocities. He showed that the final raindrop size at the base of the cloud depends primarily on the updraft velocity and is almost independent of the assumed collection efficiency or liquid-water content. His results are shown in Figs. 6.2-6.3. Given an updraft of 1 mps, a drop is carried to a height of 6,950 feet above the cloud base in about 35 minutes, where it has a diameter of 0.2 mm; after descent to the cloud base in another 17 minutes, the diameter attains 1.5 mm. Hence, during the descent through the cloud, which takes about one-half the time for the ascent, the mass increases by a factor of more than 400.

The basic difficulty in the theory of growth by coalescence in cumulus clouds is the slow initial rate of growth. If we assume that a cloud contains 1 g/m^3 of liquid water and a relatively high collection efficiency of 75 per cent, a $20\text{-}\mu$ drop requires about an hour to grow to 40μ by coalescence. During this time the drop would be carried to the cloud top,

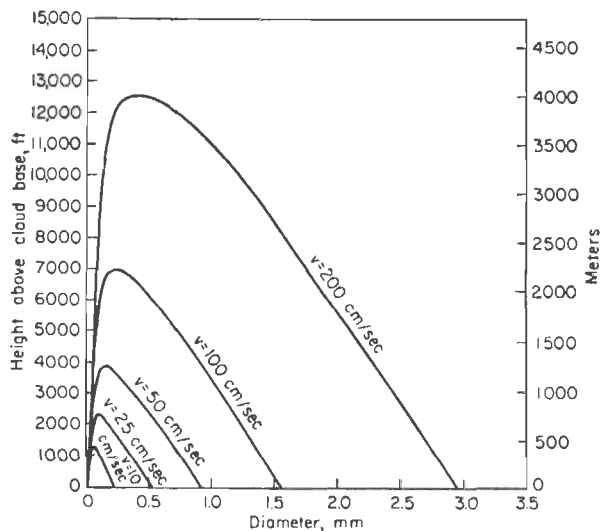


Fig. 6.2. Change of drop diameter with height for different updraft velocities (4).

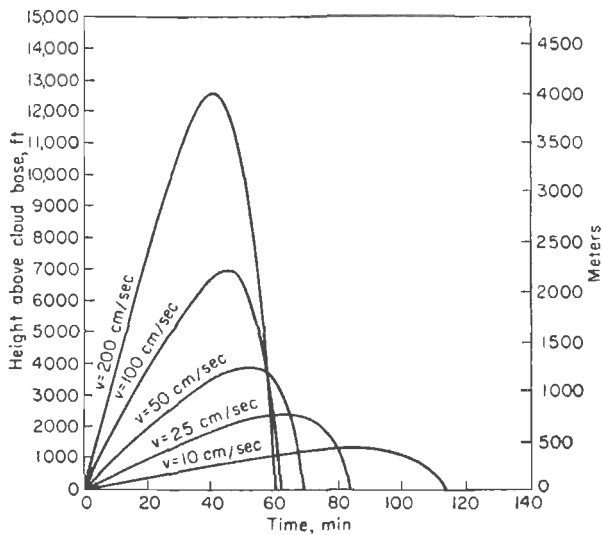


Fig. 6.3. Trajectories of drops which grow by coalescence (4).

where it would not be of sufficient size to resist evaporation and to be able to descend through the updraft. Ludlam (21) solved this difficulty by postulating that large drops 40–80 μ in diameter are present near the base of cumulus clouds; he attributed their origin to the giant salt nuclei found by Woodcock. These nuclei have equilibrium diameters up to 20 μ at 70 per cent relative humidity and if carried into the cloud can easily

grow by direct condensation to diameters of 40 to 80 μ within a few hundred meters above the cloud base. Ludlam computed the subsequent growth of such drops, using corrected values of Langmuir's collection efficiencies for drops smaller than 0.1 mm, and determined time-height trajectories for clouds with different updraft velocities. His computations show that if precipitation is to be initiated in a cumulus cloud, the large drops must have reached diameters of 0.3 mm by the time they are carried to the top of the cloud. This size would be sufficient to survive a fall of several hundred meters from evaporating summits without much change and could therefore settle back into the cloud bulk and resume

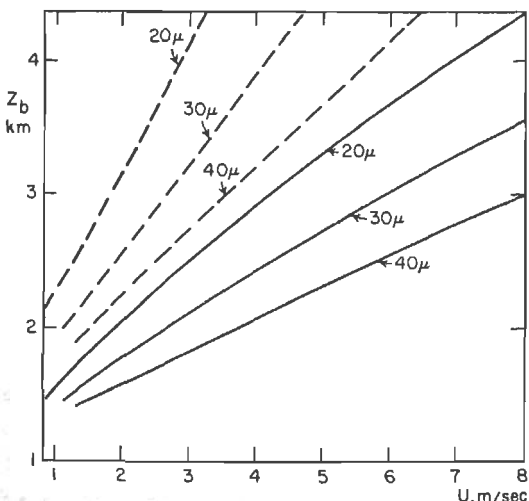


Fig. 6.4. The variation in the minimum cloud depth Z_b for shower development as a function of the updraft U , for initial droplet radii of 20 to 40 μ in clouds with base temperatures of -5°C (dashed lines) and 20°C (21).

rapid growth; smaller drops would completely evaporate. Using an 0.3-mm drop as a critical value, he then computed for adiabatic conditions the minimum cloud depth required for shower development by coalescence as a function of the updraft velocity, the base temperature of the cloud, and the initial size of the large drop. His results (Fig. 6.4) reveal that the minimum cloud depth is 1.5–2 km for a cloud with base temperature of 20°C and an updraft of 2 mps.

An analysis from stratiform-cloud data from northern Ireland by Mason and Howorth (25) shows that drizzle falls predominantly from clouds warmer than -5°C and thicker than 600 m, which suggests growth by coalescence. Rain occasionally falls from such clouds, but mainly from clouds with tops colder than -12°C . This suggests growth from ice crystals. In a subsequent article (24), Mason analyzed the

growth of drizzle in stratiform clouds with updraft velocities in the order of 10 cm/sec. He considered that turbulent diffusion limits the life of an individual drop in such clouds and showed from probability theory that a few drops are likely to remain within the cloud for periods of a few hours. He assumed that the drops grow to 40 μ diameter solely by condensation and then mainly by coalescence. Calculations show that 3-4 hours must elapse before a drizzle drop of diameter 0.2-0.3 mm can fall out of a cloud base through a uniform updraft of 10 cm/sec; about 2 hours of this time is required for the drops to grow to 40 μ by condensation. It is likely that growth by coalescence of cloud drops smaller than 40 μ also occurs and may be more important than growth by condensation since a supersaturation of 0.05 per cent is relatively high except near the cloud base. However, more accurate collection-efficiency values for small cloud drops are necessary to make a better quantitative analysis of the growth of drizzle in a thin stratiform deck.

In conclusion, there are two ways by which precipitation may be initiated in warm clouds, depending on the type of cloud. Time is of the utmost importance in broadening drop-size distribution in stratiform clouds with relatively low updraft velocities. This is important so that a few drops, under the influence of turbulent diffusion, may remain within the cloud for a few hours and grow to rain by coalescence with smaller drops. In cumuliform clouds with relatively high updraft velocity large drops about 40 μ in diameter appear to be necessary near the base; smaller drops would not have sufficient time to grow large enough to resist evaporation when carried to the cloud top. The source of these large drops may be giant sea salt nuclei near ocean areas or possibly large dust particles over continental interiors.

The Ice Phase

Supercooled water clouds have been observed in the atmosphere at temperatures as low as -35°C . In the absence of impurities, clouds produced experimentally in Wilson-type expansion chambers consist of water at temperatures as low as -41°C . Below this temperature water droplets may appear initially in cloud formation, but they very quickly become ice. X-ray diffraction studies reveal that the internal structure of supercooled water becomes more icelike as the temperature is lowered.

Experiments using uncleaned surface air in Wilson cloud chambers show that the concentration of ice particles increases exponentially with linear decrease of temperature. According to the results of different investigators (Fig. 6.5) an average concentration of about 10 ice particles per m^3 may be expected to appear at -10°C , increasing to about 10^6 m^{-3} at -30°C . There is considerable discrepancy in the results, which may

be due in part to different experimental methods and localities. Even in the same locality the concentration of ice particles appearing at the same temperature varies from day to day. At Mt. Washington in the United States, ice-particle counts made over a 4-year period in an outside cold chamber with a temperature of -18°C varied from less than 10 m^{-3} to about 10^7 m^{-3} (28).

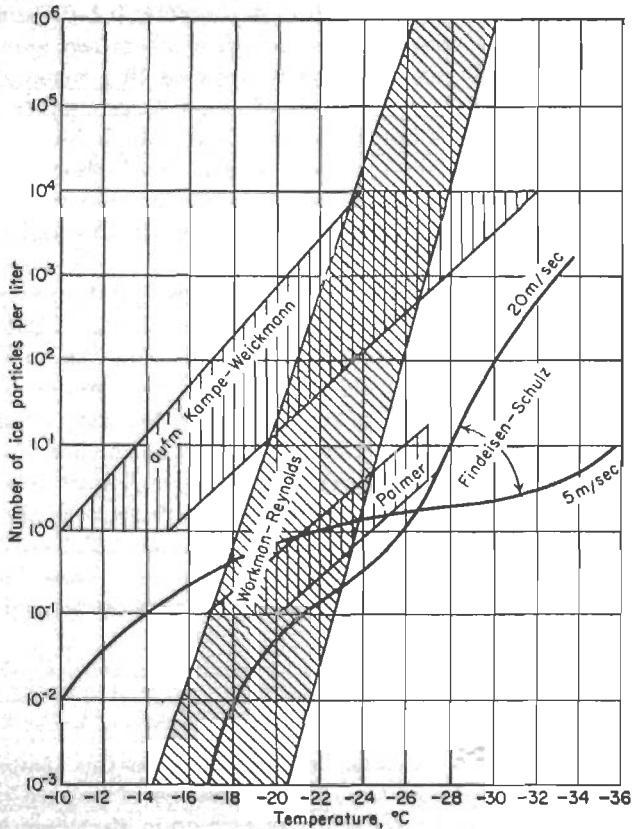


Fig. 6.5. Effectiveness of natural aerosols as freezing nuclei observed by different investigators (1).

Supercooled water may be frozen in three ways: (a) by homogeneous nucleation, or introduction of ice which causes water to freeze at any temperature below 0°C ; (b) by heterogeneous nucleation, the introduction of a foreign particle to act as a freezing nucleus; (c) spontaneously without the aid of nuclei, which for small drops occurs at -41°C . Experiments indicate that the only substance on which water vapor sublimes directly (sublimation nucleus) is ice itself. The temperature at which a freezing nucleus becomes active depends on its physical properties, the

most important of which appear to be wettability and surface effects. The process of heterogeneous nucleation is not yet completely understood. Freshly ground sand begins to be active as a freezing nucleus at -3°C , wind-blown sand at -9°C . Various soil particles are active at temperatures between -9 and -25°C . Electron-microscope investigations of the nuclei of natural ice crystals indicate that the majority of them are derived from the soil (26). Silver iodide, used in rain-making experiments, begins to be active at -4°C .

Experiments with distilled water show that larger drops freeze at higher temperatures than smaller ones. Dorsch and Hacker (12) cooled distilled waterdrops on a platinum foil at rates of $0.2\text{--}0.5^{\circ}\text{F/sec}$. They

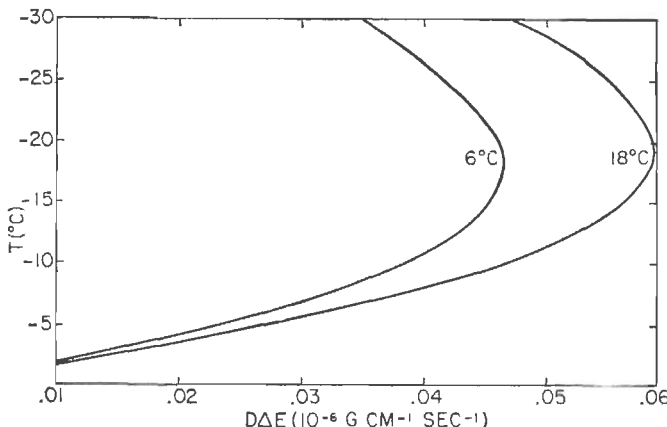


Fig. 6.6. Variation of $D \Delta E$ in a water-saturated cloud for wet-bulb potential temperatures of 6 and 18°C . The growth rate of ice crystals at water saturation is proportional to $D \Delta E$.

found an exponential relationship between the drop diameter and the temperature at which it froze, such that $10\text{-}\mu$ drops froze at -32°C and 1-mm drops froze at -17.5°C . A similar relationship has been obtained by Mason, who cooled distilled waterdrops between two layers of oil at a slower cooling rate (0.5°C/min); his results show that 0.1-mm drops freeze at -31°C and 1-mm drops at -24°C . A statistical theory based on the probability that aggregates of small nuclei exist within the drops was proposed as the reason for the dependence on temperature of different sized drops.

If supercooled water and ice particles are present in a cloud, the ice grows at the expense of the water. At temperatures below 0°C the equilibrium vapor density for ice is less than that for water, so that water vapor tends to evaporate from the drops and diffuse toward the ice. The temperature of a growing ice particle is higher than that of its surroundings because of the latent heat of fusion released at its surface. By

equating the heat of fusion added to the particle with the heat lost by conduction to the air, it is possible to compute the temperature of the ice and the vapor-density difference between the ice and the surrounding air. The results of such computations are shown in Fig. 6.6; the maximum growth rate of ice crystals at water saturation occurs at air temperatures between -15 and -20°C . The growth rate decreases to zero at 0°C .

Precipitation Growth from Ice

The methods of growth from ice to precipitation are sublimation, coalescence of ice crystals with other ice crystals to form snow flakes, and coalescence of ice crystals with supercooled cloud drops to form graupel (soft hail) or hail. Sublimation is the most important growth process in the early stages of the crystal. After a mass of about 0.01 mg has been attained, subsequent growth depends on the distribution of liquid water in the cloud.

In a given volume of air that contains precipitating ice particles and supercooled cloud drops, the updraft makes available a new supply of vapor which would preferentially sublime on the ice, with any remainder condensing on the cloud drops. In stratiform clouds with low updraft velocity the demands of the ice crystals may exceed production by the updraft so that the liquid-water content diminishes and sublimation may become the most important growth process in the major portion of the cloud. In cumuliform clouds the high updraft velocity initially creates more moisture than the available ice crystals can consume. The liquid-water content then reaches high values, and coalescence with cloud drops becomes the most important growth process of the crystals.

Widespread precipitation from stratiform clouds, with updraft velocity of the order of 10 cm/sec, represents the nearest approach to a steady-state condition in which as much water is consumed by the precipitating particles as is produced by the updraft. Aircraft investigations in warm-front rain show that icing is confined to a shallow region of the cloud just above the 0°C level, an indication that little supercooled water exists above that region. In addition, radar measurements of the echo intensities returned from the precipitation between the -5°C level and the top portion of the cloud suggest that the precipitation consists of ice crystals growing by sublimation and that all the water produced by the updraft is deposited directly on the ice crystals (37). From about -5 to the 0°C level, the ice crystals grow somewhat slowly by sublimation and by coalescence with cloud drops. The main growth in this region is by coalescence of ice crystals with others to form snowflakes. This coalescence is probably aided by the wetness of the crystals as they approach the 0°C level. Individual ice crystals before coalescence have a mass of about

0.1 mg, while the average snowflake has a mass of 1 mg. Below the 0°C level, coalescence continues, and the snowflakes melt to form rain. This type of precipitation characterizes much of the cyclonic precipitation in temperate latitudes and occasionally occurs in the tropics.

In cumuliform clouds the ice crystals grow initially by sublimation and are carried aloft by the updraft. Because of their fall velocity they lag behind, and cloud droplets from below overtake them and freeze on contact. In the early stages of growth the collection efficiency is relatively small, but as drops are caught, the fall velocity increases rapidly and the collection efficiency becomes relatively large. In a cloud containing 1 g/m³ of liquid water, growth by coalescence with cloud drops exceeds growth by sublimation at a crystal diameter of about 0.15 mm. Soon thereafter growth by sublimation becomes negligible. The crystals are then transformed into graupel, or soft hail of spherical shape, which consists of rime ice with a low density due to the numerous air spaces between the frozen drops. The soft hail acquires a fall velocity greater than the updraft and so descends through the cloud, growing at an increasing rate. In cumulonimbus clouds the soft hail may then develop into hail consisting of several layers of rime ice and clear ice. The formation of clear ice occurs because the soft hail is unable to freeze all the water droplets with which it comes into contact during a given time interval. If it is to freeze all the water, it must dispose of the heat of fusion by conduction to the air or by evaporation. As the hail descends toward the 0°C level, only a portion of the water caught will be frozen. Some will evaporate, some will remain as a thin film on the hailstone, and the remainder will flow from the lee side as small raindrops. The portion of the water frozen during the "wet" stage will be clear ice. In a cumulonimbus cloud hail may descend through several layers of relatively high and low liquid-water content and form alternate layers of clear ice and rime ice. Twenty to 25 concentric layers have occasionally been observed (31). A large hailstone may first become wet at temperatures as low as -30°C (20).

There is a continuous transition between the two extremes of ice-crystal growth in stratiform clouds and hail growth in cumulonimbus. At intermediate updraft velocities and liquid-water content in clouds, rimed ice crystals and soft hail may develop. If the cloud liquid-water content exceeds 0.4 g/m³ over a distance of a few hundred meters, it is likely that soft hail will develop. With smaller liquid-water contents the ice particles are likely to maintain their crystalline shape despite some riming. At some mountain stations in the tropics (*i.e.*, Chacaltaya, Bolivia), soft hail is the most frequent form of precipitation.

A frequently observed cloud system consists of a stratiform deck, penetrated at intervals by cumulus towers, created by surges of high updraft, and associated with relatively high liquid-water content. Because of

wind shear, this region of high liquid-water content often slopes considerably with height and may be considered a layer. The ice particles, with their greater fall velocity, have a different slope and may spend only a portion of their trajectory in the layer. Depending on the liquid-water content and the trajectories of the particles, they may emerge from the layer as rimed crystals or soft hail. The layer of high liquid-water content may be considered a transitory phenomenon, occasionally produced by a surge of updraft but used up through riming. The rain which arrives at the ground is derived from the melting of a mixture of snowflakes, rimed crystals, and soft hail.

The character of the precipitation in a cumuliform cloud invariably changes during the life history of the cloud. In later stages numerous precipitation particles may consume more water than the updraft supplies; in addition they may be instrumental in partially suppressing the updraft through the drag of precipitation on the air. As a result, the liquid-water content decreases to a value where snow crystals and snowflakes are the dominant precipitation particles and the cloud becomes stratiform.

Showers observed by radar initially have the appearance of a group of cells, each a few miles in diameter. These cells are often aligned in parallel bands of precipitation. The individual cells retain their identity for 20–40 minutes before they either dissipate or, as they do frequently, enlarge and merge with other cells, becoming more stratified in character. Sometimes we observe a transformation of the precipitation pattern from a cellular structure in parallel bands to a fusion of cells and, then, to a continuous rain pattern.

The Thunderstorm

The thunderstorm consists of a group of convective cells, each of which may be in a different stage of development. The life cycle of one of these cells may be divided into three stages: the cumulus, the mature, and the dissipating (Figs. 6.7–6.9). In the cumulus stage an updraft is in evidence throughout the entire cloud. Velocities may range from 1–2 mps near the cloud base to more than 10 mps below the cloud top. The top of a growing cumulus may be observed as a series of towers, each of which rises and then subsides, to be succeeded by another tower, which may penetrate to a higher level before subsiding. The liquid-water content increases from the base to a maximum below the cloud top, in extreme cases more than 5 g/m^3 . Along the side boundaries of the cloud, entrainment from the surroundings may decrease the liquid-water content and increase the lapse rate within the cloud.

In the mature stage, which, according to Byers (9), begins when pre-

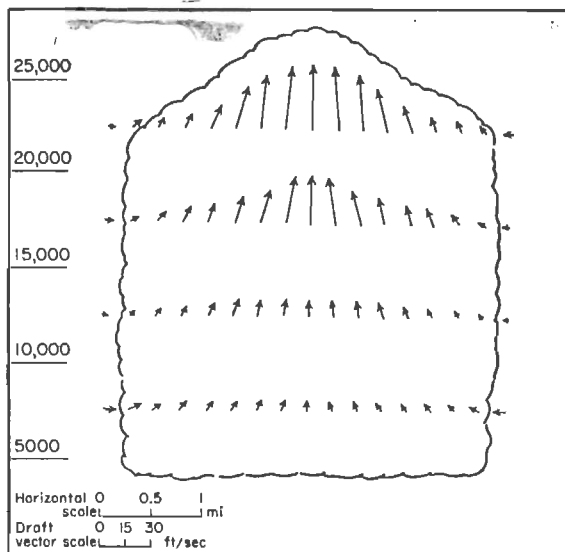


Fig. 6.7. The early stages of a thunderstorm (9).

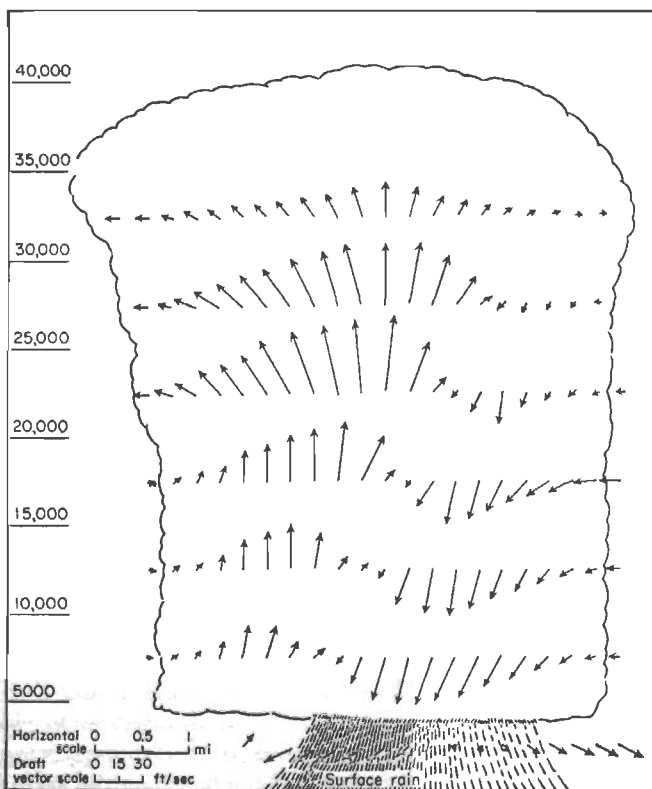


Fig. 6.8. The mature stage of a thunderstorm (9).

cipitation reaches the ground, the cloud contains concentrated regions of updrafts and downdrafts. The high concentration of precipitating particles in certain regions of the cloud probably aids the development of the downdraft by their drag on the air. Precipitation within the cloud may consist of rain, hail, and snow. In German experiments (38) in which glider planes ascended into thunderstorms, hail was always encountered.

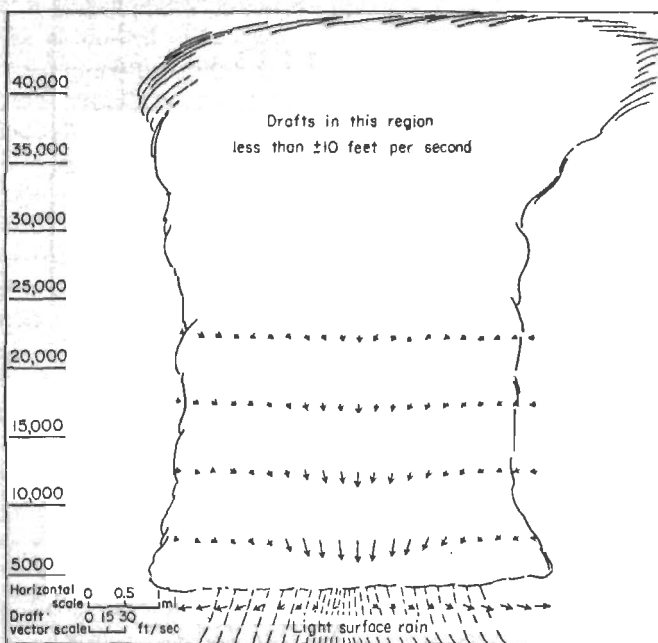


Fig. 6.9. The dissipating stage of a thunderstorm (9).

The Thunderstorm Project (9), however, observed hail on only a small percentage of occasions, possibly because soft hail observed from aircraft may be mistaken for snow. The larger, denser hail would most probably be encountered in relatively small concentration at elevations below -10°C .

In the dissipating stage the entire cloud degenerates in weak down currents from which the liquid water has been almost entirely depleted by riming and evaporation and in which the precipitation above the freezing level consists entirely of snow.

As we have seen previously, precipitation in cumuliform clouds may be initiated by ice crystals or by large water droplets near the base of the cloud. Observations and experiments on thunderstorm electricity indicate that the ice phase must be involved in thunderstorms. It is possible, however, that ice might form in clouds where the precipitation

has been initiated by large water droplets. On the assumption that $40\text{-}\mu$ drops are present at the base of a cloud and that ice crystals are present at -10°C , Ludlam (22) has found that initiation by large water droplets is favored in a cloud with a 5-mps updraft for a base temperature higher than 5°C .

In clouds where precipitation is initiated by the ice phase, the ice nuclei active at relatively high temperatures (above -20°C) and present in relatively low concentration are likely to develop into hail. The more numerous ice crystals at lower temperatures consume the available water and transform the upper levels of the cloud into an ice anvil, a striking characteristic of cumulonimbus viewed from a distance.

When hail has developed in a thunderstorm cloud and the wet stage has been reached, the surplus water, incapable of being frozen by the hail, will be shed in the form of small raindrops. These drops may also grow by coalescence into larger raindrops. Some, because of their size, may freeze to form hail with cores of clear ice. Examination of the interior of 25 hailstones during one thunderstorm revealed that 20 had opaque cores (rime ice), indicating growth by riming of ice crystals. The remaining 5 had clear ice cores, indicating freezing of raindrops (31). If precipitation were initiated by large water droplets, all the hail in such clouds would have clear ice cores.

The shedding of droplets by wet hail may be responsible for the initiation of thunderstorm electricity. There is, however, much controversy on this subject (40).

Calculations from results of the Thunderstorm Project indicate that, of the total liquid water produced in a cumulonimbus, 45 per cent evaporates in the downdraft, 36 per cent evaporates from the cloud sides or remains within the cloud after the storm, and only 19 per cent descends to the ground as precipitation (7).

Appreciable wind shear hinders the development of thunderstorms because the top portion of the cloud may be physically separated from the lower portion and because the growing precipitation particles may descend outside the cloud, where they undergo evaporation (Chap. 5).

Artificial Precipitation

Natural precipitation may be initiated by two methods: the action of freezing nuclei in a supercooled water cloud, and the growth of large droplets originating near the base of a cumulus cloud. These at once suggest possible methods of inducing artificial precipitation. The concentration of freezing nuclei below 0°C varies over a wide range, and there may be occasions when none are present in a supercooled water cloud otherwise suitable for precipitation growth. Likewise Woodcock

has occasionally found no giant sea salt nuclei in trade-wind air over Hawaii, so that large droplets may not always be present near the base of cumulus clouds. We might therefore expect that the introduction of ice particles into appropriate supercooled clouds or of droplets of about 50μ diameter into the base of suitable cumulus clouds would lead to precipitation growth.

There is considerable evidence that precipitation often occurs naturally from the ice phase when the temperature at the cloud top is as high as -12°C . On the other hand, not all clouds with temperatures below -12°C give precipitation. During 19 days of observation in New Mexico, it was found that, of clouds with minimum temperatures between -12 and -24°C , only 20 per cent gave radar echoes to indicate the presence of precipitating particles. There were no echoes from clouds with temperatures higher than -12°C , but 72 per cent of clouds colder than -24°C gave echoes. The release of silver iodide from the ground during 5 of these days did not increase the percentage of precipitating clouds (8).

An experimental clue to cloud seeding was observed in 1946 by Schaefer (28), who, by dropping a pellet of dry ice into a simple cold chamber containing a supercooled water cloud, was able to transform the cloud into ice. A similar effect was later observed by Vonnegut when silver iodide smoke was introduced into the chamber.

During November, 1946, Schaefer dropped dry ice from aircraft into a supercooled cloud layer over New England and soon afterward observed snow streamers falling from the cloud. Continued experiments showed that no appreciable precipitation could be obtained by seeding stratiform clouds but that a clearing path in the cloud could occasionally be produced. Similarly, seeding of small supercooled cumulus clouds also produced snow streamers, which usually evaporated before reaching the ground and often caused dissipation of the cloud.

On Oct. 14, 1948, a well-developed cumulus cloud in New Mexico, approximately 18,000 feet thick, was seeded with dry ice. The subsequent thunderstorm, which produced heavy rain over 4,000 square miles, was ascribed to the seeding. On July 21, 1949, the release of silver iodide from a ground generator was thought to have caused the development of heavy rain from a cumulus cloud down wind from the generator.

Experiments in seeding were conducted by the U.S. Weather Bureau, U.S. Air Force, and the National Advisory Committee for Aeronautics during 1948 and 1949. Of 67 cumulus clouds seeded with dry ice, 18 produced precipitation. In 16 cases rain reached the ground, but within 30 miles natural showers were already occurring. Twelve clouds were seeded with water, but no favorable results were observed. It was concluded from the experiments that partial dissipation was the usual result

from seeding. In most of the cases where development occurred, natural growth of the cloud was in progress before seeding.

Experiments in cloud seeding with dry ice were made over Hawaii during 1948 and 1949 in cumulus congestus formed by the interaction of trade wind and sea breeze (18). Results of numerous experiments and observations showed that when the clouds were capped by a temperature inversion of 1°C and more, as is normal in Hawaii, seeding with dry ice produces either a partial dissipation or no noticeable effect. It was also observed that a large wind shear through the levels between base and top of the cloud tends to blow off the top of the cloud so that no rain results. Experience indicated that after an initial depression of the cloud, which immediately followed the seeding, the cloud would recover and grow higher than its pre-seeding condition if it had been actively growing before seeding. The experiments were conducted on days with high probability of natural rain, when rain usually did occur in the area near or at the time of seeding. Rainfall amounts, however, were generally higher over the seeded areas than over the nonseeded. Of 19 clouds in which the temperature was higher than 0°C , rain or virga fell from 10 clouds following seeding, but amounts were measurable only in 2 cases. In one of these 1.25 inches of rain fell from the cloud which penetrated the 0°C level after seeding and during the rain. Of 8 cases with cloud temperatures between 0 and -5°C there were 6 with heavy rain, 1 with a trace of rain, and 1 in which the cloud dissipated. The warm temperatures of the clouds suggest rain production without the ice phase, although icing was occasionally experienced by the airplane in the super-cooled clouds. It appears possible that the dry ice or the airplane increased the supply of large droplets in the cloud, thus initiating the coalescence process and producing rain.

The best-organized series of experiments with aircraft seeding were made by the Australian Division of Radiophysics (5) from 1948 to 1950. Eighty-eight flights were made, and only clouds which appeared to have completed their vertical development were chosen for seeding. Precipitation was verified through the use of radar. The experiments were considered successful when the seeded clouds precipitated while adjacent clouds remained unchanged and unsuccessful when no precipitation fell after seeding. The data were not used if adjacent clouds produced rain during the experiment. The results from the series follow:

1. The chance of producing rain by dry ice seeding depends primarily on the temperature at the top of the cloud. At temperatures of -7°C or colder there is 100 per cent probability of producing rainfall. As the temperature increases from -7 to 0°C , the chances of success decrease progressively to zero.
2. The time at which precipitation appears at the base of the seeded

cloud depends primarily on the cloud thickness. A gestation period of about 10 minutes is evidently required for the ice crystals to grow, followed by an additional minute for every 800 feet of cloud thickness.

3. Rain just reaches the ground if the height of the cloud base is not more than twice the cloud thickness. The intensity of precipitation is directly proportional to the cloud thickness. From 0 to 0.25 inches of rain falls within 40 to 60 minutes after seeding, after which the cloud almost invariably dissipates.

4. When atmospheric conditions are just right, clouds may turn into cumulonimbus and produce rain up to 0.5 inch over a longer period than 60 minutes. This behavior is very uncommon and has occurred only on 3 per cent of the seeded occasions.

A few experiments were made by seeding the tops of clouds with silver iodide from aircraft. No success was obtained with cloud tops at -6 to -8°C . The only successful experiment was with the cloud-top temperature at -13°C —the temperature region where rain might occur naturally.

Several experiments were made in which a spray, consisting of drops of about $50\ \mu$ diameter, was introduced into the base of a cumulus cloud at the rate of 100 pounds of water per mile. Of seven cases in which the cloud was less than 5,000 feet thick, virga fell on six occasions, after which the cloud dissipated. Of four cases where the cloud thickness exceeded 5,000 feet, light rain developed in one and heavy rain mixed with hail in the others.

The annual rain-making opportunities in the region of Sidney, Australia, have been estimated at varying from 5 to 10 per cent of the days.

Commercial rain makers usually employ ground generators of silver iodide smoke (AgI) at several sites in an effort to induce rain over a target area in the down-wind sector. It is thought that the AgI is carried aloft into the cloud, where it acts as freezing nucleus, thereby initiating precipitation. It is not known how many particles may be expected to reach a cloud under different atmospheric conditions. No particles would be likely to arrive in clouds located above inversion layers, but for daytime cumulus it is reasonable to expect that some of the AgI particles would travel upward into a cloud with the ascending convective currents.

As noted previously, AgI begins to act as a freezing nucleus at temperatures between -4 and -7°C ; hence, its chances of producing rain should be less than with dry ice. Dry ice, which produces ice crystals just below 0°C , has the advantage of about 3,000 feet of extra cloud depth in which the ice particles may grow to adequate size. The results from Australia appear to corroborate this conclusion.

In addition, several experiments indicate that AgI loses its property

as a freezing nucleus when exposed to ultraviolet light in amounts present in ordinary sunlight. This photolytic effect, in which AgI is converted to metallic silver, was first reported by Reynolds *et al.* (27) in 1951. They found that nucleating activities decreased 2 orders of magnitude per hour in bright noon sun. The experiment was corroborated by Inn (15), who reported complete inactivation of AgI in a cloud chamber at -20°C 20 minutes after exposure to such light. Different results, however, were found by Vonnegut and Neubauer (34) in an experiment which indicated that the concentration of ice-forming nuclei was more than 40 per cent in a -15°C supercooled cloud after 1 hour of exposure to ultraviolet light. Birstein (3) showed that photolysis of AgI depends on the relative humidity; at 100 per cent in a -20°C cloud complete inhibition as a nucleus occurred after $2\frac{1}{2}$ hours of exposure, while at 60 per cent it occurred after 1 hour. The Australian group has measured the decay rate of AgI in the atmosphere under various weather and wind conditions by means of a cloud chamber in aircraft. During the release of AgI by a ground generator, the particles could not be detected at elevations higher than 2,000 feet nor farther downwind than 10 to 12 miles from the generator. It was found that the particles lose their activity as freezing nuclei by a factor of 10^4 in 30 minutes.

In conclusion, experiments indicate that it is possible to produce rain, in rare occasions heavy rain, by dry ice seeding. Whether it is economical to employ aircraft for that purpose is open to question. Certainly AgI seeding from aircraft is much less successful than dry ice seeding. Because of the photolytic effect and the dependence on uncertain upward currents, the effective use of AgI from the ground is even more doubtful. In tropical regions, seeding at the base of cumulus clouds with a spray of waterdrops of 0.05 to 0.1 mm diameter holds considerable promise, but more experiments are needed.

REFERENCES

- (1) aufm Kampe, H. J., and H. K. Weickmann, *J. Meteor.*, **8**: 283 (1951).
- (2) aufm Kampe, H. J., and H. K. Weickmann, *ibid.*, **9**: 167 (1952).
- (3) Birstein, S. J., *Bull. Am. Meteor. Soc.*, **33**: 431 (1952).
- (4) Bowen, E. G., *Australian J. Sci. Research*, (A) **3**: 193 (1950).
- (5) Bowen, E. G., *Weather*, **7**: 204 (1952).
- (6) Boylan, R. K., *Proc. Roy. Irish Acad.*, (A) **37**: 58 (1926).
- (7) Braham, R. R., *J. Meteor.*, **9**: 227 (1952).
- (8) Braham, R. R., *et al.*, *J. Meteor.*, **8**: 416 (1951).
- (9) Byers, H. R., and R. R. Braham, *The Thunderstorm*. Washington, D.C.: Government Printing Office, 1949.
- (10) Davies, D. A., *Meteor. Mag.*, **79**: 354 (1950).
- (11) Diem, M., *Meteor. Rundschau*, **1**: 261 (1948).
- (12) Dorsch, R. G., and P. T. Hacker, *Natl. Advisory Comm. Aeronaut. Tech. Notes* 2142, 1950.

- (13) Gunn, K., and W. Hitschfeld, *J. Meteor.*, **8**: 7 (1951).
- (14) Houghton, H. G., in *Compendium of Meteorology*. Boston, Mass.: 1951.
- (15) Inn, E. C. Y., *Bull. Am. Meteor. Soc.*, **32**: 132 (1951).
- (16) Junge, C., *Meteor. Z.*, **53**: 186 (1936).
- (17) Langmuir, I., *J. Meteor.*, **5**: 175 (1948).
- (18) Leopold, L. B., and W. A. Mordy, *Tellus*, **3**: 44 (1951).
- (19) Lewis, W., and W. H. Hoecker, *Natl. Advisory Comm. Aeronaut. Tech. Notes* 1904, 1949.
- (20) Ludlam, F. H., *Quart. J. Roy. Meteor. Soc.*, **76**: 52 (1950).
- (21) Ludlam, F. H., *ibid.*, **77**: 402 (1951).
- (22) Ludlam, F. H., *Weather*, **7**: 199 (1952).
- (23) McDonald, J. E., *J. Meteor.*, **10**: 68 (1953).
- (24) Mason, B. J., *Quart. J. Roy. Meteor. Soc.*, **78**: 377 (1952).
- (25) Mason, B. J., and B. P. Howorth, *Quart. J. Roy. Meteor. Soc.*, **78**: 226 (1952).
- (26) Okita, T., *Science Repts. Tōhoku Imp. Univ.*, (5) **4**: 78 (1952).
- (27) Reynolds, S. E., et al., *Bull. Am. Meteor. Soc.*, **32**: 47 (1951).
- (28) Schaefer, V. J., in *Compendium of Meteorology*. Boston, Mass.: 1951.
- (29) Schumann, T. E. W., *Quart. J. Roy. Meteor. Soc.*, **66**: 195 (1940).
- (30) Simpson, G. C., *Quart. J. Roy. Meteor. Soc.*, **67**: 99 (1941).
- (31) Souter, R. K., and J. B. Emerson, *Natl. Advisory Comm. Aeronaut. Tech. Notes* 2734, 1952.
- (32) Squires, P., and C. A. Gillespie, *Quart. J. Roy. Meteor. Soc.*, **78**: 387 (1952).
- (33) Virgo, S. E., *Meteor. Mag.*, **79**: 327 (1950).
- (34) Vonnegut, B., and R. Neubauer, *Bull. Am. Meteor. Soc.*, **32**: 356 (1951).
- (35) Warner, J., and T. D. Newnham, *Quart. J. Roy. Meteor. Soc.*, **78**: 46 (1952).
- (36) Wexler, H., *Bull. Am. Meteor. Soc.*, **86**: 156 (1945).
- (37) Wexler, R., *Quart. J. Roy. Meteor. Soc.*, **78**: 363 (1952).
- (38) Wichmann, H., *Arch. Meteor. Geophys. u. Bioklimatol.*, (A) **5**: 187 (1952).
- (39) Woodcock, A. H., *J. Meteor.*, **9**: 200 (1952).
- (40) Wormell, T. W., *Quart. J. Roy. Meteor. Soc.*, **79**: 3 (1953).
- (41) Wright, H. L., *Quart. J. Roy. Meteor. Soc.*, **66**: 66 (1940).

CHAPTER 7

WEATHER OBSERVATIONS AND ANALYSIS

The operations of any weather service are geared to the demands it has to meet. In former days the forecaster was required only to give hurricane warnings and in some countries, notably India, to make seasonal-rainfall predictions. Many forecast offices were closed entirely during the dry season.

All this has changed with the advent of air routes across the equator, war in the tropics, development of hydroelectric power, advances in agronomy, offshore oil drilling, and many other aspects of modern technology. General weather prediction, as of rain, wind, and ocean waves, is in demand. Forecasts are wanted ranging from a few hours ahead to seasons and even longer periods. Forecasting schedules of weather bureaus and other advisory services extend over the entire year; their key offices maintain large staffs. Observations of the upper air have multiplied; synoptic charts are drawn to high levels. Moreover, middle-latitude forecasters are gradually coming to the realization that tropical analysis can aid prediction outside the tropics, especially when the prediction is to cover several days or more.

OBSERVATIONS

In the tropics, the diurnal-cycle and small-scale weather gradients tend to overshadow changes brought about by synoptic disturbances, except the strongest ones. The wind direction, for instance, may change drastically from night to day (Chap. 4); gross errors result if such changes are accepted as synoptic. The city of Port-au-Prince on the island of Haiti in the Greater Antilles lies in a valley flanked by mountain chains oriented east-west (Fig. 7.1). The ocean is to the west, and during the day the sea breeze comes in from the west, producing a wind shift of 180° . Some forecasters, new to the area, thought at first a cold front had passed. Soon they also noticed that such a front passed Port-au-Prince every day and that this front could never be followed to Puerto Rico, the next island to the east.

This example highlights the need to emphasize departures from average weather rather than the weather itself. In the case of Port-au-Prince the correct question would be: Has the sea breeze arrived earlier or later

than average? The answer furnishes a direct clue as to whether the strength of the trades in the area is above or below average. Similar reasoning applies to all surface and low-level weather reports. Cumulus clouds should be reported in terms of departure from the mean. Perhaps it is impractical to do this with all elements. But much could be done to improve observation routines and codes of transmission to make the data more meaningful. At present, the analyst must be fully acquainted with the peculiarities of all stations on his map. He must know how to translate the reported state of weather into *deviations from the average* if the reports are to be of value to him.

Surface Observations¹

Temperature. In higher latitudes temperatures plotted on synoptic charts serve to distinguish air masses of different origin. In the tropics this function is fulfilled only rarely. Over the oceans, temperature differences between "air masses" are usually so slight that they are without synoptic significance; besides, small-scale fluctuations and local effects mask any minute synoptic gradients (Chaps. 2 and 4). Such masking is quite evident over islands, especially when the country is hilly or mountainous. Here, the diurnal temperature variation is about an order of magnitude greater than the synoptic variation; it can differ by a factor of 2 or more between closely adjacent stations.

Over continents and oceans alike, a strong negative correlation also exists between temperature and cloudiness and rainfall in the daytime. Above-average cloudiness lowers the maximum temperature. Rainfall, even small orographic showers, quickly cools the air to the wet-bulb temperature through evaporation, a means of lowering the temperature so potent that it is a standard method for air conditioning in hot desert countries. Downdrafts in large convective clouds can produce such strong cooling that the arrival of a heavy shower or thunderstorm resembles the passage of a mid-latitude cold front. The regular association of rainfall and temperature drop has led to many faulty frontal analyses.

Dew Point. On account of the evaporation from falling rain the dew point, as the dry-bulb temperature, undergoes many small-scale variations. It mainly serves to detect air that is drier than normal. Dew points tend to be lower on the lee side than the windward side of islands because drier air is mixed down in large lee eddies from aloft. During periods of pronounced subsidence, vertical mixing may depress the dew point over the ocean surface. In some areas of semipermanent subsidence, especially the central equatorial Pacific, isolated regions of low dew point appear on climatic charts.

¹ This section largely follows the treatment in reference 3.

Although temperature and dew point, as they are now measured, seldom reward the effort put into synoptic reporting, plotting, and analyzing, it is not to be inferred that useful information could not be obtained from these quantities, especially when reported from atolls and ships at sea. They are important, for instance, in the prediction of formation of hurricanes and the weakening or dissipation of such storms over the open sea (Chap. 11). Together with wind and sea surface temperature, they provide a measure of evaporation from the oceans (Chap. 5); longer-period variations in evaporation probably influence changes in the general circulation. The techniques of measuring temperature and dew point, however, would need to be refined, and also those for the ocean temperature, if these elements are to become useful for such purposes. In particular average values over, say, an hour will have to be measured, rather than instantaneous values.

Pressure. When the station height is accurately known, the sea-level pressure of coastal and plains stations is representative except in and near heavy showers. The reduction of pressure to sea level in mountainous areas is a dubious practice in all latitudes. In addition to the errors introduced by the assumption of a mean temperature between the height of the barometer and sea level, there are important dynamic effects in mountainous country. The dynamic-pressure drop across a mountainous island can amount to 3 mb. In channels between islands a persistent pressure reduction of 1 mb or more can exist. The analyst must reckon with these dynamic effects and their variability with wind direction and wind speed.

The diurnal pressure variation is largest in the tropics and far outweighs most synoptic fluctuations (Chap. 4). Hence, plotting and analysis of 3-hour tendencies is useless. At times the suggestion has been made that subtracting the diurnal from the observed tendency would give the synoptic tendency as residual. This proposal encounters the objection that the diurnal variation itself is not constant from day to day; that the synoptic 3-hour tendency is usually so small as to fall within the range of error in reading barometers; and that the influence of local cloud systems on pressure introduces unrepresentative changes.

Many analysts have found that 24-hour tendencies yield the most reliable, though not ideal, representation of the pressure-change field. Twenty-four-hour tendencies form the cornerstone of Dunn's work (4); they are used exclusively in this book.

Wind. Observations over ocean areas well removed from land are representative except in heavy showers. In coastal areas and over land, surface-wind observations are notoriously unrepresentative as Fig. 7.1 shows; a multitude of factors affect the wind. In the trades one should mainly attempt to determine, following Dunn (4), whether the strength

of the current is above or below average and whether abnormal wind directions are reported, such as a west wind on the windward side of islands in the daytime.

Clouds. In Chap. 5, we have seen how important it is to distinguish clearly between the several types of cumulus cloud. Further detailed information on these clouds would perhaps be the largest contribution that surface reports can make to analysis and forecasting. Such information is not contained in the international code; yet good cloud observations would be much more valuable than some of the data which are transmitted, such as 3-hour pressure tendencies. We wish to know in particular (a) whether and how the cumuli are leaning with height; (b) whether they occur at random or form lines or groups; (c) whether they tend to break through an inversion, *i.e.*, have "necks" or a "chimney"

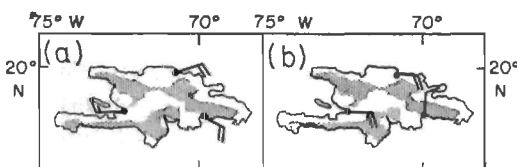


Fig. 7.1. Typical wind circulation at 2,000 feet on the island of Hispaniola during (a) afternoon and (b) night. Port-au-Prince is the westernmost station.

appearance; (d) the shear near the cloud tops, especially in the case of cumuli congesti and cumulonimbi; and (e) the direction and speed of middle and high clouds.

In the *International Cloud Atlas*, characteristics of this kind are called "varieties." They can, of course, occur in various combinations. The combined features thought to recur most frequently and to be most important for analysis are listed below in code form:

- (0) Vertical, without arrangement.
- (1) Leaning upwind, without arrangement.
- (2) Leaning down wind, without arrangement.
- (3) In groups or lines, vertical.
- (4) In groups or lines, leaning upwind.
- (5) In groups or lines, leaning down wind.
- (6) Chimney appearance.
- (7) Frequent chimney clouds with evidence of lateral shear.
- (8) Marked top shear present.
- (9) Marked upwind or lateral shear above 10,000–15,000 feet.

Accurate reporting of direction of cloud motion is of paramount importance. One of the greatest obstacles to successful analysis is that the high standard in the measurement of cloud direction attained in the early part of the twentieth century has declined since the advent of upper-wind measurements. Stations sending up balloons are few compared with surface-reporting stations. Except for weather ships there are none

over the oceans. Moreover pilot balloons are lost quickly in the low clouds in bad-weather areas, just when information is most needed. Thus the analyst is deprived of what might be his largest data source for tropical upper-air analysis. Over some ocean areas, notably the central Atlantic Ocean, drawing of upper-air charts is virtually impossible at the time of this writing, in spite of the importance of this area in hurricane forecasting. Most information about this part of the world dates from the turn of the twentieth century, when deductions were made which cannot be matched in the 1950's.

Hydrometeors. As in higher latitudes, it is essential to distinguish between steady and showery precipitation. In former days nearly all tropical rainfall was thought to fall in showers, but we now know (7) that extensive sheets or precipitating altostratus occur. Such sheets are indicative of high-level disturbances, and they also develop in areas of incipient tropical storms. The forecaster therefore has every interest in knowing which type of precipitation is falling.

Showers are notorious for their diurnal course (Chap. 4) and also their spottiness. Even the precipitation in an intense zone of convection may miss individual stations completely, leaving the analyst at great disadvantage. It is also of little help to be informed about the current shower intensity which is subject to drastic change within 5 minutes. A provision for detailed description of the weather over the preceding 6 hours in the codes would be very profitable. For instance, "stability indices" have often been proposed but never adopted. After averaging over 6 hours and inclusion of all weather within range of an observer's vision, such indices can provide a potent analysis tool. One visual stability classification which has been put forward (3) follows:

1. *Extreme stability throughout atmosphere.* Poor visibility, haze layers, stratiform clouds only or none at all.
2. *Extreme stability in one layer.* Flat-topped cumulus, haze layer, perhaps altostratus and altocumulus high above inversion.
3. *Slight stability.* Haze layers, trade cumulus over the ocean, limited tops to the cumulus and often stratocumulus.
4. *Slight instability.* Good visibility, no haze layer, chimney cumulus, some cumulus congestus, occasional light showers. High build-ups over mountain chains of islands.
5. *Extreme instability.* Organized cumulus congestus and cumulonimbus with associated cirrus, altostratus, and stratocumulus decks; frequent moderate to heavy showers, often with light steady rain between showers.

Upper-air Observations

Surface measurements include clouds and hydrometeors; they therefore contain considerable information about upper-air conditions. Measure-

ments made aloft should always be analyzed in conjunction with cloud data.

Upper-air measurements are taken (*a*) with balloons released from the ground or from aircraft; (*b*) from aircraft in flight; and (*c*) with radar or range-finding equipment from the ground.

Balloon ascents measure (*a*) the upper wind and (*b*) pressure, temperature, and humidity aloft. The two functions are profitably combined when radiosonde balloons are tracked with theodolite or radar.

Wind Measurements. The instruments designed for upper-wind measurements have undergone a broad development, beginning with single theodolites trained on pilot balloons and advancing to complex electronic radar equipment. These installations, expensive to acquire and maintain, require attendance by well-trained technicians. But they have great advantages compared with the inexpensive pilot balloons, such as: (*a*) an ascent rate of the balloon is not assumed; (*b*) overcasts no longer prevent upper-wind readings; (*c*) balloons can on the average be tracked to much greater heights.

Both pilot-balloon and rawin data are apt to provide more accurate high-altitude observations in low than in high latitudes, since in the tropics the wind direction frequently reverses somewhere in the troposphere (Chap. 1). The balloons, after drifting away from a station, often approach it again at high levels. The angle of elevation of the balloon above the horizon, therefore, does not become so small that minor errors in reading introduce large errors in the computed wind.

The upper winds are perhaps the most representative element of tropical observations; good analyses lean heavily on the information gained from them. However, the analyst must take certain precautions. Wind observations which report less than 5 mph cannot be used for any purpose other than to note that winds are light. Orographic influences affect the wind well above the mountain peaks and often distort the wind pattern far more than synoptic disturbances. A semipermanent cyclonic shear often marks the passage between two islands, such as the Windward Passage between Hispaniola and Cuba in the Greater Antilles. This cyclonic shear coincides with the trough in the pressure field mentioned earlier. Unless caution is exercised, especially concerning continuity, fictitious wave troughs will appear in these passages on nearly every map.

Radiosonde Observations. As in the case of the wind data, the techniques for measuring pressure, temperature, and humidity aloft have gradually but substantially improved. The lag in the temperature and humidity elements of the instruments has been reduced so that soundings taken since the Second World War show the abrupt moisture and lapse-rate discontinuities that frequently occur.

Unfortunately, the analyst still has to overcome several severe handicaps before tropical radiosonde data will completely serve his purpose:

1. Local effects detract from the synoptic validity of the ascents, especially in the low levels, as they do for all other weather elements.

2. Daytime soundings are affected by the sun shining directly on the instruments. Although much effort has been expended to overcome this drawback, analysis of the nighttime observations is generally more satisfactory.

3. In analyzing a large area, the diurnal pressure variation aloft should be considered just as it must be on the ground.

4. Upper pressures and temperatures computed from different types of instruments often are not identical. Standardization is urgently needed.

5. The upper pressures and temperatures are correct only within limits, and these limits have the magnitude of the synoptic variations.

This last point is the most damaging. The reader may wonder why we should examine radiosonde data at all apart from noting the trade inversion, tropopause, and dry layers. There is, in fact, little evidence that upper-level analysis based on radiosonde data has contributed materially to the success of forecasts in the tropics. Nevertheless, when radiosonde observations at reliable stations are plotted in time-section form, rather regular variations are observed; these are in accordance with wind changes and weather. At one time, meteorologists considered it unlikely that such agreement could be attained. It was expected that balloons would report low or high temperatures and humidities depending on whether they ascended in clouds or in clear spaces. Of course, balloons should not be released into large clouds. But it has been shown that local variations of temperature over short periods are much less than anticipated, since entrainment reduces the temperature difference between clouds and clear spaces (Chap. 5). Occasionally a sounding made in a thunderstorm downdraft will report very cold temperatures. Such an ascent, however, is spotted without difficulty.

Pilot Reports. Except for weather-reconnaissance flights, weather reporting is generally a secondary objective of aircraft missions. The analyst must keep this in mind when he tries to interpret in-flight reports.

Messages transmitted from aircraft contain as standard elements (a) the time of report, usually in Greenwich civil time; (b) the position of the aircraft in degrees and tenths of latitude and longitude; and (c) the flight altitude in thousands of feet. The positions of successive observations should be not more than 200 miles apart; special reports should be sent for all significant changes of wind or weather.

Instantaneous winds at flight level are obtained with the drift meter. The double drift method is recommended, although other methods using the drift meter are reasonably accurate. Winds estimated should never

be reported, because they are often wrong and will be misleading. The mean wind over an appreciable distance obtained from radio aids to navigation such as Loran and Shoran are helpful when the pilots watch for rapid wind shifts and report them in special messages.

Types and layers of clouds should be reported separately, each with amount in tenths and heights of tops and bases. Since several types of clouds are often present at the same time, it is desirable to allow for three or four in the codes.

Aircraft codes generally provide for in-flight weather, past weather, visibility, icing, and turbulence.

METHODS OF ANALYSIS

Tropical meteorology has not produced any innovations in synoptic representation of data. Surface and upper-level or constant-pressure charts are plotted and analyzed as in the temperate zone. Since the station density over most parts of the tropics, especially the oceans, is very low, the use of time sections at key stations has consistently been advocated and sometimes been practiced. Special tools have also been developed as aids to forecasting for very short periods.

The Time Section

An analyst's success may largely depend on keeping good time sections. Such sections show the complete picture of the state of the weather at one location, information not furnished by any other means of representation. They provide a means for observing time of passage, structure, and intensity of disturbances, for aiding the analysis over a radius up to 500 miles depending on the situation, and for predicting the weather downstream. In correlating the different elements of a time section the analyst can fully employ all his synoptic and theoretical knowledge. He is also enabled to detect errors and unrepresentative observations with greatest certainty.

The vertical coordinate of time sections can be height, pressure, or pressure altitude. Time is plotted from left to right on the section when the station is located in the trades, where systems predominantly move from the east. It is plotted from right to left for the westerlies. If disturbances move at a fairly steady rate, the time section then becomes equivalent to a space cross section.

The following elements are suggested for plotting: (a) all upper winds; (b) 24-hour surface-pressure changes as often as available; (c) 3- or 6-hour surface reports; (d) 24-hour changes of the height of upper isobaric surfaces; (e) pressures, temperatures, and humidities of upper air. The

analysis consists in entering (a) trough lines and shear lines (orange); (b) height of the 5 g/kg moisture surface in the rainy season and 3 g/kg in the dry season (green); (c) base and top of trade inversion (purple); (d) tropopause (purple); (e) base and top of equatorial or polar westerlies; and (f) isolines of 24-hour height changes of upper isobaric surfaces. If shape and rate of motion of the disturbances change only slowly, the analyst can plot 24-hour surface-pressure and upper height changes in the center of the 24-hour interval. The pattern, not the amount, then indicates the instantaneous pressure-change field. Greatly improved insight

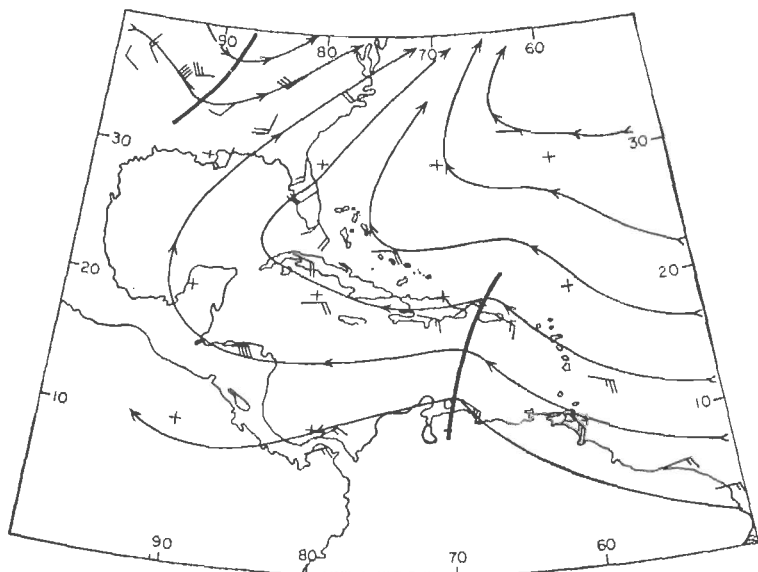


Fig. 7.2. Streamlines at 5,000 feet for the western Atlantic, Aug. 15, 1944, 1500Z (6).

into correlations between pressure changes and weather and wind shifts is provided by this technique. Figure 7.3 presents an example of such height-change analysis for the map situation shown in Fig. 7.2.

Bellamy (1) has advocated time section or cross-section analysis in terms of altimeter corrections as an alternate to the height-change method. The height of each standard isobaric surface is subtracted from a standard atmosphere; the difference, the altimeter correction, is plotted, and lines of equal altimeter correction are drawn, usually at 100- or 200-foot intervals. This is an excellent method for locating troughs and ridges at all altitudes and for determining their vertical slope. Further, the vertical thickness between two isobaric surfaces can be expressed in terms of departure from the thickness in a standard atmosphere.

Bellamy calls this the *specific temperature anomaly*. Analysis of this anomaly field reveals the warm and cold areas.

It is the advantage of Bellamy's method that it eliminates the average gradients of pressure and temperature along the vertical, which are always large compared with the horizontal and time variations. Difficulties arise in the choice of a standard atmosphere. Usually departures from the International or U.S. Standard Atmosphere are computed. This is not satisfactory for the tropics since the altimeter corrections will always be positive, increasing upward strongly through the troposphere. The aim of the technique is hereby largely defeated. As alternate solution a tropical standard atmosphere (Chap. 2) can be employed. Although this

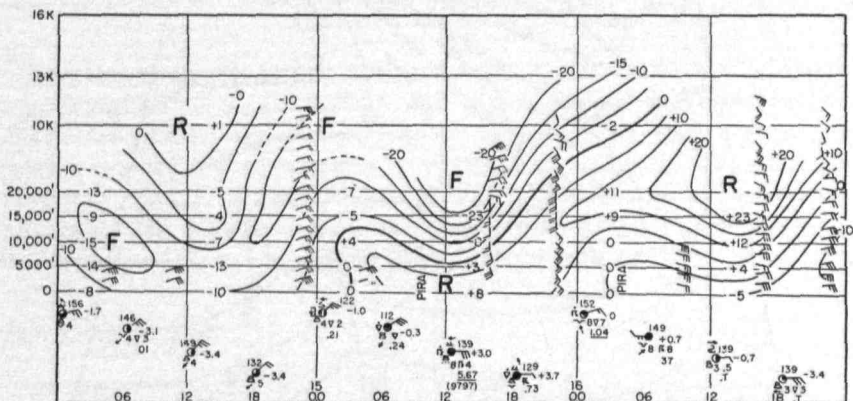


Fig. 7.3. Time cross section for San Juan, Puerto Rico, Aug. 14-17, 1944. Solid lines are isolines of equal 24-hour height change (10's feet) and displaced forward in time 12 hours (6).

introduces an undesirable feature, the abandonment of a universal standard atmosphere, it would seem to be the only way to utilize Bellamy's system profitably within the tropics.

Another drawback stems from the fact that due to the diurnal variation of pressure and temperature aloft, apparent or real, only soundings taken at the same time of day can be used. In this respect the 24-hour-change method is superior, provided that soundings are taken with strict regularity.

The Surface Chart

Analysis of conventional surface charts at 6-hour intervals has remained the standard practice of forecast services. Isobars are drawn at 3-mb intervals; 2-mb, even 1-mb intervals are more appropriate equatorward of latitudes 20° .

Often the reward of much effort spent on the surface map has been poor. We have mentioned the host of local influences and errors that render meaningful analysis of surface charts in the tropics one of the hardest analytic tasks in meteorology. In addition, the configuration of sea-level isobars drawn over a considerable range of longitude will have a marked diurnal variation. Superposition of the semidiurnal pressure wave on the synoptic pressure pattern produces appreciable deformations. These deformations change with each 6-hour map.

Finally, the pressure field reflects the weather pattern only weakly in many areas. In the Caribbean, for instance, most disturbances increase upward in intensity. The lower troposphere compensates for the pressure and temperature gradients existing aloft so that the upper troughs and ridges are damped toward the surface. The author, in trying to overcome the difficulties posed by surface analysis, has suggested that representative elements of the surface observations be plotted on a low-tropospheric wind chart (9). He emphasized, however, that surface charts are useful when tropical storms are present and on the rare occasions when a pronounced cold front penetrates well into the tropics. These systems are most pronounced at the ground. Surface charts are further useful for determining the 24-hour pressure change field and for differential (thickness) analysis between the ground (1000-mb surface) and some standard isobaric surface aloft.

The Upper-air Charts

As found in Chap. 1, the tropical troposphere is usually divided into a lower and an upper portion with different flow configurations. Waves of small amplitude moving in a broad basic current often characterize one layer, while vortices of large dimension predominate in the other. The low-latitude forecaster will obtain maximum benefits if he chooses levels for analysis which are representative of these layers. A suitable level for low-altitude analysis is 5,000 feet (850 mb); for high-altitude analysis, 40,000 feet or 200 mb. Choice of the lower level depends somewhat on region and season. In the western Pacific during the typhoon season 2,000-foot streamlines prove very helpful.

Near the boundary between the two tropospheric layers the wind often shifts rapidly (*cf.* Fig. 1.24); the height of the boundary fluctuates in space and time. The analyst who works with charts located in the layer of strong vertical shear is at a serious disadvantage. Winds are weak; the flow pattern is complicated and changes in the most irregular way. Worst of all, even a good prognosis at that level has little if any meaning in terms of the weather to be expected. This holds especially for the 500-mb surface, in spite of the high reputation this surface enjoys in

higher latitudes. The 300-mb level may be part of the transition zone in the rainy season in the hurricane areas, while 700-mb is often poor in the dry season in the trades because the strength of the easterlies weakens upward rapidly through this surface at that time of year.

Plotting Model (Fig. 7.4). Wind direction and speed are entered following international usage, but it is recommended that direction and speed be written alongside the wind vector or below the station circle. For instance, 0725 denotes a wind from 70° with speed of 25 knots. Small changes of wind are significant from the viewpoint of weather in many parts of the tropics. Every effort must be made to obtain an accurate picture of these small changes. In plotting winds, it is very difficult to distinguish accurately between winds from 80° and 100° ; yet this is important. The analysts benefits if the wind report in code form is added to the vector.

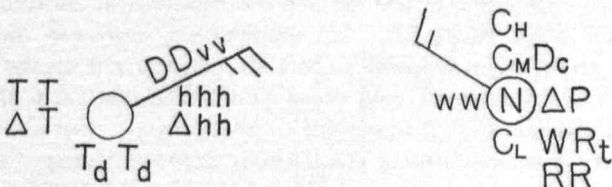


Fig. 7.4. Left: Plotting model recommended for upper-air observations. Right: Plotting model recommended for combination of representative surface data and low-level wind reports (9).

At radiosonde stations, the height of the appropriate pressure surface (10's of feet, first digit omitted) and the temperature (nearest $^{\circ}\text{C}$) are plotted according to established custom. The 24-hour height and temperature changes are entered below the current values. Moisture data (specific or relative humidity, or dew point) are plotted below the station circle.

Figure 7.4 also shows a plotting model devised for forecast offices that wish to eliminate the surface chart and plot representative surface data on the low-level wind chart as suggested above. All symbols are the same as those of the international code except Δp , which stands for the 24-hour surface-pressure change (tenths mb).

A model suitable for plotting aircraft in-flight reports may be found in the literature (3).

Streamline Analysis. Since the slopes of isobaric surfaces in the tropics are very small, it is never possible to make a reliable analysis from pressure-height data alone. The soundings are subject to the many errors listed above, and the spacing between two stations is often so great that a large disturbance can exist between them without affecting either. Contour analysis should never be attempted without close reference to

the time sections, continuity, and the winds. This is no simple task because wind and contour directions can deviate appreciably. Further, upper contour charts must be prepared with aid of the differential analysis (thickness) technique in order to avoid gross errors in drawing contours in open networks; otherwise computations made from such charts are likely to fail. Several basic textbooks give a description of this method.

Streamline analysis is often more satisfactory. Its object is to represent the fields of wind direction and wind speed, and therefore the fields of vorticity and divergence, which are so important in all synoptic work.

The degree to which these objectives are attainable depends entirely on quantity and quality of the observations. When stations are widely spaced and located mainly along a line, usually an air route, and when confidence in any existing pilot reports is low, many analysts extrapolate trough lines, shear lines, and centers from the time sections and past maps and then sketch streamlines that approximately outline the field of wind direction. It is the property of streamlines to parallel the wind direction everywhere. Figure 7.2 illustrates this type of analysis. Beyond depicting wind directions, very little is attempted. This is entirely proper considering the data situation. The author must warn against attempting too much with poor and sparse data. A reasonable balance should always exist between the observations that make up a chart and what the analyst tries to deduce from these observations. Otherwise, serious errors in the form of fantastic map constructions inevitably result.

A qualitative picture of the field of wind direction, though very useful, leaves much to be desired. When a dense network (not a line) of carefully taken wind reports is available, the analyst can resort to more sophisticated methods.¹ Streamlines can be drawn with spacing inversely proportional to the wind speed. This, however, is a cumbersome task requiring much time. More practicable methods have been developed by V. Bjerknes (2) and Sandström (10); Palmer² has applied these extensively to the tropics.

The fields of wind direction and wind speed are drawn separately. As before, the field of wind direction is represented by streamlines fitted so that the lines everywhere are tangent to the wind. Very often it is difficult to arrive at an accurate streamline analysis by freehand drawing. For this reason it has been recommended that isogons, lines connecting points with equal wind direction, be drawn prior to the streamlines. Construction of an isogon field is quite difficult and requires much practice.

¹ For such networks the need for analysis may be entirely eliminated by fitting polynomial expressions to the data.

² C. E. Palmer, The Equatorial Front. Appendix to fifth quarterly report of the Tropical Project at the University of California, Los Angeles, 1949.

Isogons need not be continuous lines like isobars. For instance, at the center of a vortex the wind is zero; all wind directions are found a short distance away. Isogons for all directions therefore emanate from a vortex center (Fig. 7.5). The isogon technique requires concentrated attention to detail; therefore it should be carried out in limited areas only and on large-scale Mercator base maps. Often, qualitative streamlines must be drawn prior to the isogons in order to locate singular points such as vortex centers. This proved necessary for the situation of Figs. 7.5-7.6.

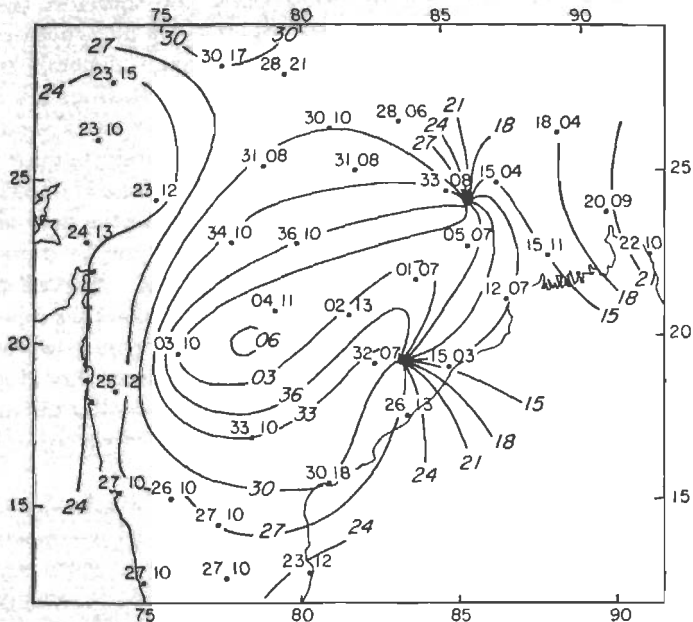


Fig. 7.5. Isogon field over India-Pakistan, Sept. 19, 1952. Data give wind direction measured clockwise from north on 360° compass and wind speeds (mph).

After completion of the isogons, the field of wind direction is defined uniquely everywhere. We can now draw a number of short lines on each isogon parallel to the wind direction. In practice, this is quickly done with an "isogon board." Many new "winds" are created by this technique to aid in the drawing of streamlines. Analysis carried through in this way (Fig. 7.6) probably is more accurate than freehand construction of streamlines. It should not be overlooked, however, that we have employed a scheme which mainly inflates the data; its application is warranted only if the isogons are reliable. In an open network the routine can produce a pretty but entirely imaginary flow pattern, just as a series of beautiful polar-front waves can be put into an ocean map devoid of actual data.

Figure 7.6 contains several special streamline configurations found in wind fields. These result from the operation of deformation, divergence, and rotation. The special characteristics may be of higher or of lower order. Following are several low-order characteristics:

1. Points of convergence or divergence, as drawn in the central part of the Indian west coast in Fig. 7.6. At these points the wind speed is zero and therefore the direction indeterminate. They are called "singular" points. In a field of pure divergence, the streamlines emanate from a

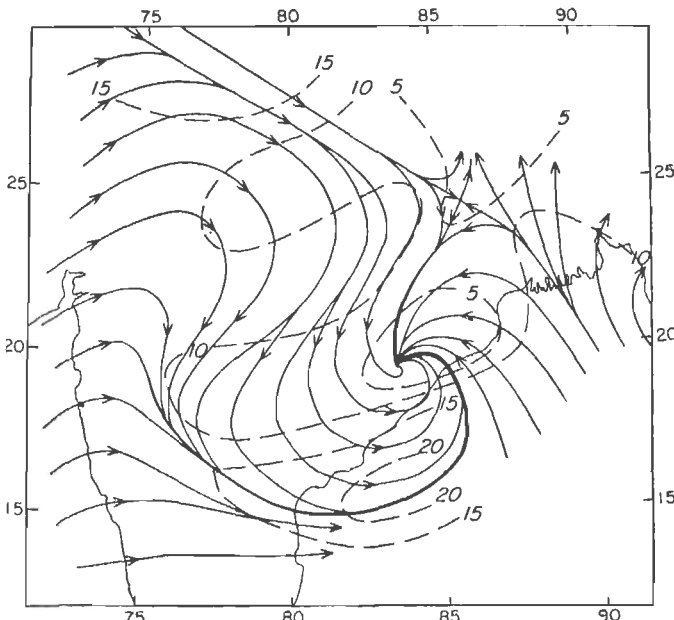


Fig. 7.6. Streamlines and isotachs (mph) over India-Pakistan, Sept. 19, 1952. Streamlines prepared from Fig. 7.5. Heavy lines denote principal lines of streamline convergence.

center as already mentioned or converge toward it as straight lines (*cf.* also 8). If rotation is added, the streamlines spiral inward or outward, either clockwise or counterclockwise.

2. Neutral points, also called *cols* or *saddle points* (northwest of Calcutta in Fig. 7.6). At a neutral point the air is calm so that neutral points are also singular points.

3. Lines or curves of streamline convergence and divergence (in the south-central part of Fig. 7.6). Palmer calls these lines *asymptotes*.

4. Line discontinuities of the wind as found along middle-latitude and tropical shear lines.

Some well-known higher-order characteristics are points of maximum curvature, often used to identify troughs and ridges, and inflection points.

To the extent to which he can, the analyst should locate the special features at the outset of the analysis and mark them. The sketching of streamlines should then start in the simplest portions of the map and proceed from there to the more complicated areas. Enough lines should be drawn to depict the whole field, but not too many. At the end, it is convenient to mark troughs, ridges, streamline convergence and divergence lines, and wind discontinuities with an orange pencil. In the northern hemisphere singular points with clockwise rotation are labeled *A* (anticyclonic), points with counterclockwise rotation *C* (cyclonic). Past positions of all special features and tracks of centers are entered in ink.

Lines connecting points with equal wind speed are called *isotachs* or sometimes *isovels*. They are usually drawn after the streamlines. The gradient of wind speed in the area must dictate the isotach interval to be used. For the low levels of the tropics isolines of 5-knot intervals are recommended. In the high troposphere, especially when jet streams with wind speed exceeding 100 knots are present, 10- or even 20-knot intervals may be most suitable. In jet-stream zones the isotachs tend to be parallel to the streamlines, and the centers of high wind speed are ellipses with a long major and short minor axis (Figs. 10.9-10.10). Isotachs are drawn with the same rules that apply to isobars.

The reader will note that the isotach analysis of Fig. 7.6 is not unique. Over a large part of the map the wind speed is nearly uniform. Here, the drawing of lines has little meaning. In the southeast, the highest speeds have been placed on the principal "asymptote" to minimize the amount of divergence.

Wind Computations

We have stressed how difficult it is to make reliable isobaric or contour analyses in low latitudes. Even when given a perfect chart, we encounter further difficulties if we wish to utilize it for a computation of the wind field.

The stoutest defenders of the geostrophic wind become cautious when the tropics are mentioned. At the equator geostrophic balance is impossible since the Coriolis parameter is zero. Much debate has concerned the subject at which latitude, as it is put, the geostrophic relations break down. No plausible theoretical argument has been offered; so we must have recourse to the observations. Jordan (5), in a statistical study, has given an answer for the low troposphere (Fig. 7.7). He finds that at 2,000-3,000 feet altitude—levels supposedly situated near the top of the friction layer—departures from the geostrophic wind are small north of

20°N but increase rapidly equatorward from there. At latitude 10° the mean difference between observed and geostrophic wind is no less than 9 mps, larger than the wind itself. Equatorward of latitude 20° over 75 per cent of all observations in Jordan's study had subgeostrophic wind. It follows that the geostrophic formula is not valid for wind computations in most situations in the low levels of the tropics. This, as noted in Chap. 1, holds even for long-term means (Fig. 1.6).

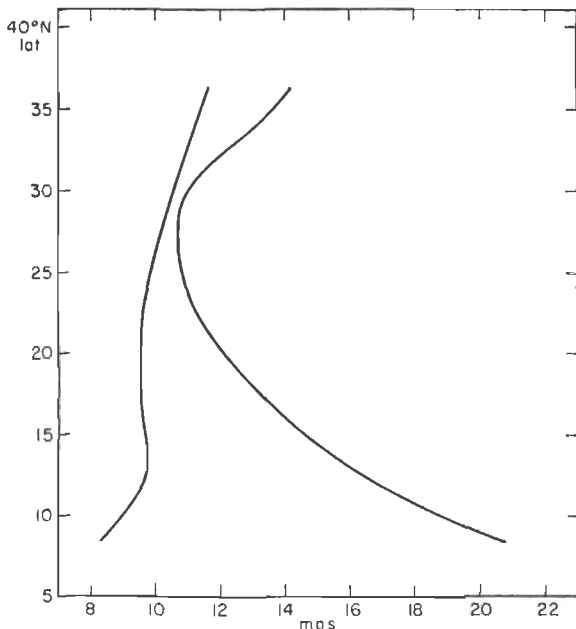


Fig. 7.7. Latitudinal profiles of mean geostrophic wind at 2,000-3,000 feet (right) and observed wind (left) (5).

In the higher troposphere no clear observational result for the pressure-wind relations yet exists. There is evidence (Chap. 12) that the winds may on the average be frictionally retarded in the high troposphere, at least in some areas, while the retardation is small near 700-600 mb, in the vicinity of the mean level of nondivergence.

As shown by Schove (11) for the Guinea coast of Africa, the correct sign of the vertical wind shear, though not its magnitude, is generally given by the geostrophic shear. The upward decrease of the easterlies in the trade-wind belt and the stronger decrease in winter compared with summer may be related with confidence to the observed poleward drop of temperature (*cf.* Chap. 1). This by no means implies, as is sometimes heard, that the temperature gradients "cause" the observed winds.

Temperature gradients, after all, are not ordained; the winds are a large factor in shaping them. We can only say that if an analyst can draw a mean-temperature or thickness pattern between two isobaric surfaces, he usually obtains the correct sense of the wind shear between these surfaces, even in the trades.

Gradient-wind computations have sometimes been proposed as superior to the geostrophic wind. Statistical tests have been conducted only in middle latitudes, and here the gradient wind has given little if any improvement in the mean. This surprising outcome is not necessarily applicable to the tropics. The radii of trajectory curvature are much smaller, for instance, in most hurricane centers than in middle-latitude cyclones. Here it is the Coriolis force that may be sufficiently small to be neglected. If so, the balance is between pressure-gradient and centrifugal forces. One then speaks of the "cyclostrophic" wind, certainly a far better approximation in tropical storms than the geostrophic wind. Commonly the geostrophic wind is 400–500 knots and the cyclostrophic perhaps 150 knots when the observed hurricane winds are near 100 knots.

Cyclostrophic balance can exist only in cyclonically curving air since in the anticyclonic case centrifugal and pressure-gradient forces act in the same direction. This has led to the hypothesis that cyclones but not anticyclones can persist on the equator, a conclusion not upheld by observations. A quasi-stationary high-pressure area, for instance, overlies the

equator in the western Pacific Ocean with considerable frequency in some seasons. Still another type of balance must exist in such cases.

Steady Motion near the Equator. The factor complicating wind calculations in the tropics is not the question of superiority of any of the foregoing three choices, either in general or in particular situations. These all demand flow along the isobars; in reality the tropical current flows across isobars at an appreciable angle at the top of the "friction layer" or well above it (5, 12). This should lead to accelerations; Fig. 7.7 implies changes of wind speed of 10 mps per day. Such changes seldom happen.

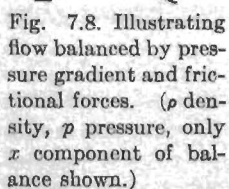


Fig. 7.8. Illustrating flow balanced by pressure gradient and frictional forces. (ρ density, p pressure, only x component of balance shown.)

The air may flow toward lower or higher pressure for long periods without appreciable changes in wind speed. We must conclude that frictional forces do not vanish at 2,000–3,000 feet and that vertical turbulence balances the pressure-gradient acceleration.

Consider Fig. 7.8, which may represent an equatorial flow pattern. The air moves westward toward lower pressure. If its speed does not change, a frictional force F , equal and opposite to the pressure-gradient force, must retard the wind speed. Such a force will exist at level H in

Fig. 7.9 If vertical turbulence acts on the wind profile shown in this diagram. Air particles moving through H both from below and above are likely to arrive at H with lower easterly momentum than present there. As long as the air flows toward lower pressure, the wind profile may be maintained. Conversely, turbulence will tend to speed up the wind at H in Fig. 7.10. For steady motion the air must cross isobars toward higher pressure in this case. It follows that the wind field cannot be

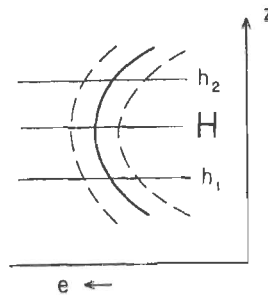


FIG. 7.9.

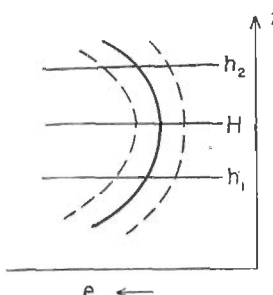


FIG. 7.10.

Figs. 7.9 and 7.10. Two types of wind profiles. Axes are altitude (Z) and east-wind speed (e). Dashed lines show assumed scatter of wind speeds around mean.

computed from the pressure field in the equatorial zone; here a substitute for actual wind data does not exist.

Microanalysis

For many civilian and military purposes, such as air operations, football games, and outdoor political meetings, forecasts of a general nature indicating roughly the cloudiness and rain over a large area do not suffice. Very specific information is needed, easy to request and hard to furnish. The forecaster will be asked whether rain will fall on a stadium within a certain 2-hour interval and just what cloud and wind conditions will prevail near an aircraft carrier at the time its airplanes are expected to return.

When such information is requested days in advance, as it will be, little can be done except to make an estimate of the general weather situation and assay the chances of disturbed conditions. It is always advisable to inform the person requesting the forecast of the tenuous nature of the prediction. Even when the event is close at hand, prediction can be unnerving. In Puerto Rico, the author was asked one noon for the outlook for a parade later in the day when a wave trough in the easterlies had just passed and large clouds were building over both land and sea. He immediately inquired about time and location of the parade. It was to be held in the northern plains near San Juan (cf. Fig.

4.1) and was expected to terminate about 4 P.M. Because of the strength of the orographic control and the fact that showers rarely move into the coastal area from the mountains before late afternoon, no rain was predicted in the specified location until 4 P.M. Later, strains of martial music could be heard thinly between loud claps of thunder; but it did not rain at the site of the parade.

For a more scientific procedure in such a tight corner, the forecaster can employ weather-distribution charts and station-circle observations (3), together with thorough knowledge of the forecast area. Probability calculations, based on the approach of "synoptic climatology," are also of much value.

The distance scale of a weather-distribution chart must be large enough so that large individual clouds can be located on it. A scale of

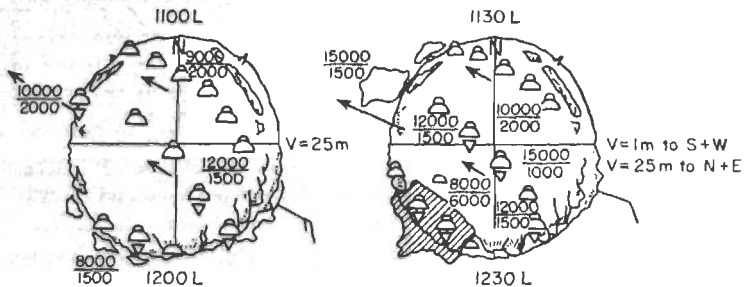


Fig. 7.11. Model of station-circle analysis (3).

1° latitude per inch will satisfy most needs. Each cumulonimbus cloud is drawn on the map in its exact position at the time of observation. Cumuli congesti are entered individually if prominent enough. Where many cumuliform clouds are present over a considerable area, scattered symbols suffice. The density of these symbols should be proportional to the cloud cover and their size proportional to that of the clouds. Heights of tops and bases are entered beside the cloud symbols. In general, the distribution of rain is determined most accurately from radar. Data from the screens can be plotted on the weather-distribution chart in green. It is always worth while to follow development and decay of individual convection cells as well as displacements of rain bands as a whole.

Wind direction and speed for a particular level may be plotted on the weather-distribution chart, but it is preferable to use separate wind and divergence analyses whenever possible.

The observer who has no data apart from what he can see from his vantage point can help himself by plotting the local weather distribution on maps with the observation point in the center. Topography and horizon are permanent features of this map (Fig. 7.11). The outline of clouds in the distance is drawn around the periphery of the circle. Clouds

within the circle are located as accurately as possible and plotted with the symbols used for the weather-distribution chart. Wind arrows with barbs show the direction and force of the surface wind.

Beside the station circle, the observer should note the amount of each cloud type, heights of tops and bases, visibility, and other phenomena. Since the cloud direction is of major significance, it must be determined with great accuracy. Radar observations extend the observer's knowledge of weather conditions far beyond his visual range; they furnish perhaps the most important data.

Station-circle observations must be frequent to be of value. Successive plots permit tracing the path and life cycle of each prominent cloud or shower. For short-period prediction, observations should be made every 15 minutes, certainly at intervals no longer than 30 minutes. The forecaster who regularly employs the station-circle technique will find that he is supplied with far more definitive information and guidance than he can obtain by looking out of the window from time to time.

REFERENCES

- (1) Bellamy, J. C., *J. Meteor.*, **2**: 1 (1945).
- (2) Bjerknes, V., et al., *Dynamic Meteorology and Hydrography*, Part II, Kinematics. Washington, D.C.: Carnegie Institution of Washington, 1911.
- (3) Civilian Staff, Institute of Tropical Meteorology, "Tropical Synoptic Meteorology," in *Handbook of Meteorology*. New York: McGraw-Hill Book Company, Inc., 1945.
- (4) Dunn, G. E., *Bull. Am. Meteor. Soc.*, **21**: 215 (1940).
- (5) Jordan, C. L., *Quart. J. Roy. Meteor. Soc.*, **79**: 153 (1953).
- (6) López, G., *Bull. Am. Meteor. Soc.*, **29**: 227 (1948).
- (7) Palmer, C. E., in *Compendium of Meteorology*. Boston, Mass.: 1951.
- (8) Petterssen, S., *Weather Analysis and Forecasting*. New York: McGraw-Hill Book Company, Inc., 1940.
- (9) Riehl, H., and E. Schacht, *Bull. Am. Meteor. Soc.*, **27**: 569 (1946).
- (10) Sandström, J. W., *Ann. Hydro. Maritime Meteor.*, **37**: 242 (1909).
- (11) Schove, D. J., *Quart. J. Roy. Meteor. Soc.*, **72**: 105 (1946).
- (12) Sheppard, P. A., and M. H. Omar, *Quart. J. Roy. Meteor. Soc.*, **78**: 583 (1952).

CHAPTER 8

DIVERGENCE AND VORTICITY

Analysis of weather charts is aimed at enabling us to say something about the current weather and the weather to come. The chances of good prediction will improve greatly if we can account rationally for the weather at map time. Meteorology has been able to come to grips with this task with tools of "direct aerology" only since the advent of the radiosonde and rawin networks; this work is still in its infancy. Since, however, the most prominent advances of the future are likely to come from a combination of theory and empirical work, we shall discuss the dynamics of the air and its energy sources and sinks wherever possible. The knowledge of *energy transformations* is very limited; a fairly concrete statement can be made only with regard to the formation of tropical storms. This chapter summarizes some concepts about the *fields of motion* utilized in Chaps. 9-12. A thorough account of the theoretical background may be found in standard textbooks (5, 7).

Fields of Divergence

A wind analysis as shown in Fig. 7.6 permits complete evaluation of the field of velocity divergence. This field is produced by (a) variations of wind speed along the streamlines and (b) coming together or going apart of the streamlines.

When the wind speed increases downstream in a field of parallel streamlines, we have divergence; when it decreases, convergence (Fig. 8.1).

When the streamlines go apart in an area with uniform wind speed along the streamlines, we have divergence; when they come together, convergence (Fig. 8.1b).

Usually, both components of the divergence are combined. Streamline fanning alone need by no means denote divergence. It is a serious mistake to assume such an identity—a mistake that has sometimes crept into the literature.

When the wind speed increases downstream and the streamlines fan out, we have divergence (Fig. 8.1c).

When the wind speed decreases downstream and the streamlines approach each other, we have convergence (Fig. 8.1d).

The situation is complicated when the wind speed decreases downstream and the streamlines spread out (Fig. 8.1e) and when the wind speed increases downstream and the streamlines come together (Fig. 8.1f). In such cases the two components tend to nullify each other. When they are exactly equal, the flow is nondivergent.

In middle and high latitudes, the patterns of Fig. 8.1e, f are most frequent, *i.e.*, the geostrophic wind is a fair approximation. The divergence is a small residual of two large opposing terms. In general it cannot be measured, since only a minor error in evaluating either component, or both, can alter the sign of the small residual. Even so, we shall see that divergence of the magnitude associated with weather-bearing disturbances cannot exist uniformly through the atmosphere but that the sign of the divergence must change with height.

In the tropics, the geostrophic control is much weaker, and direct evaluation of the divergence field has a better chance of success. For instance, in Fig. 7.6 convergence takes place around the cyclonic center, where streamlines come together and the wind speed decreases inward. Convergence is also indicated in the lee of the western Ghats, where the streamlines crowd together rapidly in a field of almost uniform wind speed. It is a good rule for the analyst to locate the areas where both components of the divergence act in the same sense. These are the active regions. Elsewhere little development is likely, as the flow tends to be "balanced."

Fields of Vorticity

In Chaps. 9–11 we shall frequently use vorticity as an analytic and prognostic tool. The vorticity about the vertical axis relative to the earth can be evaluated from analyses as shown in Fig. 7.6.

Instructions for computation and construction of vorticity fields from streamline-isotach analyses are contained in numerous manuals and books. Qualitatively, inspection of the wind field usually reveals the

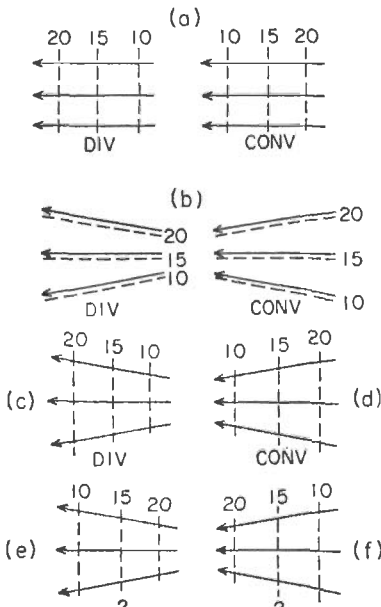


Fig. 8.1. Models of flow patterns with divergence and convergence.

vorticity field in at least a portion of the map. The relative vorticity, also called *curl* or *rotation*, is composed of (a) the flow curvature and (b) the shear. The curvature term is given by V/r_s , where V is the wind speed and r_s the radius of streamline curvature. The expression for the shear term is $-\Delta V/\Delta n$, where ΔV is the difference in wind speed over a distance Δn and the n axis is placed normal to the streamlines and taken positive to the left of the current looking downstream. In general, one defines cyclonic vorticity as positive, in the same sense as the earth's own rotation, and anticyclonic vorticity as negative. According to this

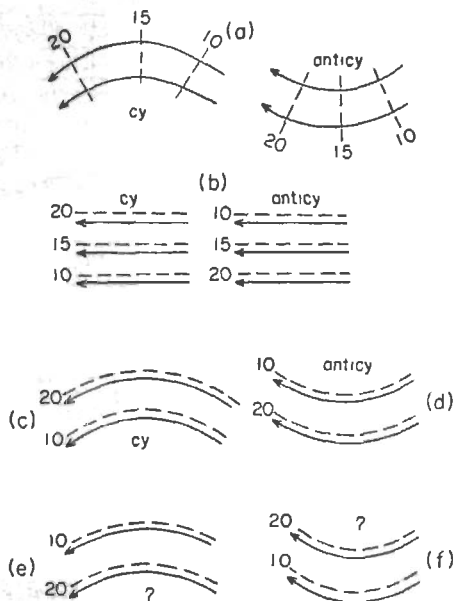


Fig. 8.2. Models of flow patterns with cyclonic and anticyclonic vorticity.

convention, the vorticity of a current crossing the equator with uniform curvature changes sign at the equator. The convention is not a necessary one and has its origin in high-latitude meteorology. Although useful in most situations to latitude 5° , it has at times proved an active hindrance in understanding equatorial-flow patterns.

There are six possible combinations of the two components of vorticity, illustrated in Fig. 8.2 and discussed for the northern hemisphere case.

(a) In a current of uniform speed, or with isotachs normal to the streamlines, the curvature alone determines the sign of the vorticity, positive or negative.

(b) In a straight current, the vorticity is cyclonic if the wind speed decreases to the left of the current looking downstream and anticyclonic if it increases.

(c) If the curvature is cyclonic and the speed decreases to the left of the current, the vorticity is cyclonic.

(d) If the curvature is anticyclonic and the speed increases to the left of the current, the vorticity is anticyclonic.

Whenever the flow has any of the foregoing characteristics, the sign of the vorticity can be determined at once by inspection of a wind analysis.

(e, f) When the curvature is cyclonic and the speed increases to the left of the current, the two terms oppose each other and the sign of the relative vorticity is not obvious. The same holds when the curvature is anticyclonic and the speed decreases to the left of the current.

Often, especially in jet-stream zones, a velocity maximum is present within a current. Inspection then reveals the sign of the vorticity in some parts of the map only. Figure 8.3 illustrates two principal models. The velocity maximum is centered in the trough in Fig. 8.3a. South of the axis of strongest wind the vorticity is cyclonic; on the north side it is indeterminate since the curvature is cyclonic and the shear anticyclonic. In Fig. 8.3b the vorticity is anticyclonic north of the center of the current but indeterminate to its south.

In Fig. 7.6 the vorticity is given mainly by the curvature, as most of the isotachs cross the streamlines at large angles and as the wind speed varies only slowly. Thus, the vorticity in the ridge is anticyclonic; at the convergence point it is cyclonic. Pronounced gradients of wind speed have been drawn only in the south. The vorticity is cyclonic to the left of the main convergence line because curvature and shear are cyclonic. To the right the shear is anticyclonic, so that curvature and shear terms have opposite signs.

Convergence, Divergence, and Pressure Changes

A barometric change measures the change in mass above the barometer. In view of the static law,

$$\frac{\partial p_0}{\partial t} = g \int_0^{\infty} \frac{\partial \rho}{\partial t} dz, \quad (8.1)$$

where p_0 is the surface pressure, ρ the density, g the acceleration of gravity, and z the vertical coordinate. The integration is extended from

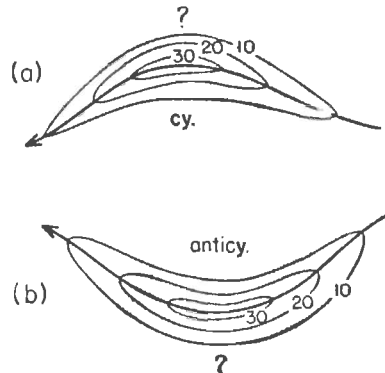


Fig. 8.3. Vorticity distribution in wavelike easterly current with narrow wind maximum. Velocity units arbitrary.

bottom to top of the atmosphere, since all layers may contribute to the surface-pressure change. Mass is removed from the volume above the barometer when the pressure falls; mass is added to this volume when the pressure rises. Since, now, the mass of the atmosphere is conserved, the amount of mass inside a given volume, *i.e.*, the density, changes as mass diverges from or converges into this volume. For a unit volume

$$\frac{\partial \rho}{\partial t} = - \operatorname{div} (\rho \mathbf{V}). \quad (8.2)$$

Here, $-\operatorname{div} (\rho \mathbf{V})$ is the mass divergence (units: mass/volume/time) and \mathbf{V} the three-dimensional velocity vector. We now introduce the rectangular coordinate system x, y, z pointing eastward, northward and upward. If u, v, w are the velocity components along x, y, z ,

$$\frac{\partial \rho}{\partial t} = - \left[\frac{\partial}{\partial x} (\rho u) + \frac{\partial}{\partial y} (\rho v) + \frac{\partial}{\partial z} (\rho w) \right]. \quad (8.3)$$

Since, for instance, $\partial/\partial x(\rho u) = u \partial \rho / \partial x + \rho \partial u / \partial x$, (8.3) states that the density at any point can be changed by bringing in air with different density ($u \partial \rho / \partial x$) or by velocity convergence or divergence ($\rho \partial u / \partial x$). In the tropics, the horizontal density gradients are so small that we may neglect density advection compared with velocity divergence with little loss of accuracy. Then

$$\frac{\partial}{\partial x} (\rho u) + \frac{\partial}{\partial y} (\rho v) = \rho \left(\frac{\partial u}{\partial x} + \frac{\partial v}{\partial y} \right) = \rho \operatorname{div}_2 V, \quad (8.4)$$

where V is the horizontal velocity vector. Combining (8.1) and (8.3) with this modification,

$$\frac{\partial p_0}{\partial t} = -g \int_0^{\infty} \rho \operatorname{div}_2 V dz, \quad (8.5)$$

since the vertical mass flow cannot affect the surface pressure.

Now, it is well known that the surface pressure changes little in a day. In the tropics, a drop of only 3 mb per 24 hr is viewed by the forecaster as an ominous sign although it amounts only to one-third of 1 per cent of the surface pressure. Hurricanes are an exception; there the pressure may fall by as much as 10 per cent in one day, but this is the extreme. The net divergence from top to bottom of the atmosphere is nearly always extremely small.

Equation (8.5) is subject to criticism. If pressure changes are small, it may not be permissible to neglect small amounts of density advection in the "tendency equation" (8.1). This objection is valid; nevertheless, by evaluating (8.5), we can deduce one of the most important facts of

synoptic meteorology. For the purpose of this computation we choose $\rho = 10^{-3}$ g/cm³ and $dz = 10$ km. After multiplying, $\rho dz = 1$ kg/cm², or 1,000 mb in pressure units, the normal pressure near sea level. Measurements of horizontal divergence¹ have shown that values of 10^{-5} sec⁻¹ are typical in disturbances. In straight flow this is equivalent to saying that the wind increases or decreases by 1 mps in 100 km, a small amount. Inserting these values in (8.5) we find that $\partial p_0/\partial t \approx 1,000$ mb/day, or a whole atmosphere. This result is wrong by no less than 3 orders of magnitude. It follows that divergence with values of 10^{-5} sec⁻¹ cannot exist through a whole vertical column but only in a limited layer and that layers of convergence and divergence must alternate along the vertical. These almost nullify each other in their effect on the total mass, a form of compensation. Between these alternating layers we find one or more surfaces of nondivergence. Although the altitude is quite variable, the average pressure of the principal surface of nondivergence in the troposphere is 700–500 mb, with mean pressure near 600 mb, nearly the middle of the troposphere by weight.

These computations prove that, except those atmospheric motions resulting from barotropic, *i.e.*, nearly nondivergent, processes, *any synoptic discussion must consider at least a two-layer structure of all disturbances*. Otherwise it is not possible to secure a reasonable understanding and prediction of weather. Mainly for this reason, *analysis and forecasting with the use of one level alone, be it surface or upper air, makes no sense. The whole troposphere forms the weather.*

We can also approach the subject by considering the formation of clouds and rain. Any computation of vertical moisture flow demonstrates that we require a rate of ascent of several cm/sec in order to transport upward enough water vapor to realize the amounts of precipitation recorded in disturbances. The magnitude of the divergence needed to produce such vertical motion can be computed from (8.3). Since $\partial\rho/\partial t$ is a very small quantity, it may be neglected. Introducing (8.4) into (8.3),

$$\frac{\partial}{\partial z} (\rho w) + \rho \operatorname{div}_2 V = 0. \quad (8.6)$$

This form of the continuity equation is applied frequently and can be used to solve the present problem. For order-of-magnitude computations in layers of limited thickness we can also neglect the vertical density gradient without much loss of accuracy. This is merely a laborsaving step. Then

$$\operatorname{div}_2 V + \frac{\partial w}{\partial z} = 0, \quad (8.7)$$

¹ From here on, the terms "divergence" and "convergence" will refer to horizontal velocity divergence and convergence.

strictly valid for a homogeneous incompressible fluid. If $\operatorname{div}_2 V$ represents the average divergence in a layer of thickness dz between the levels H_1 and H_2 ,

$$w_{H_2} - w_{H_1} = -\overline{\operatorname{div}_2 V}(H_2 - H_1). \quad (8.8)$$

In the particular case when H_1 is located at the surface,

$$w_H = -\overline{\operatorname{div}_2 V}H, \quad (8.9)$$

where H now stands for the distance above the ground. This is the simplest possible form of the continuity law. Given $H = 4$ km, about the mean height of the 600-mb surface, and a convergence of 10^{-6} sec^{-1} ,

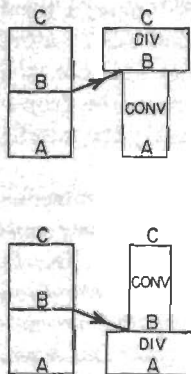


Fig. 8.4. Models of two-layer atmosphere.

$w_H = 4 \text{ cm/sec}$. Ascent at this rate will produce much bad weather when lasting several hours. It follows that *convergence with a magnitude of 10^{-6} sec^{-1} must exist if we are to have large rainstorms; a two-layer arrangement of the troposphere must exist if in disturbances the surface-pressure change is to remain a very small fraction of the total pressure*. This is one of the most important conclusions of synoptic meteorology.

Figure 8.4 illustrates two models of a two-layer troposphere. At the ground (A) and at the tropopause (C) the vertical motion is considered as zero. In the upper diagram lower convergence gives way to upper divergence. Therefore the mid-tropospheric air identified as (B) moves upward. The lower convergent part of the troposphere expands vertically through the level of nondivergence and shrinks horizontally; we find lateral spreading and vertical shrinking in the upper divergent column. All air is ascending.

The lower diagram sketches the inverse case, lower divergence and upper convergence. Downward motion takes place at all heights, both in the layers of convergence and divergence. A general correlation between the signs of vertical motion and divergence thus does not exist, though this error occasionally has entered the literature. In the vicinity of the ground, of course, air can only escape upward in areas of convergence. There Eq. (8.9) holds. Conversely, the sense of the vertical motion in a layer of upper convergence is indeterminate, and (8.8) must be applied.

Conservation of Potential Vorticity

So far the divergence has entered our considerations only through the mass-continuity requirement. The theorem of relative vorticity derived

by Rossby (9) is a form of the laws of motion which contains the divergence explicitly; it therefore permits us to relate the preceding remarks to the dynamics.

Previously we have defined the relative vorticity in the "natural" coordinate system (s, n) . Figure 8.5 shows the relation between the natural and rectangular (cartesian) coordinate systems. Thus

$$\xi = \frac{V}{r_s} - \frac{\partial V}{\partial n} = \frac{\partial v}{\partial x} - \frac{\partial u}{\partial y}.$$

Given the Coriolis parameter f and the absolute vorticity $\zeta_a = f + \xi$, the vorticity equation is

$$\frac{d}{dt}(f + \xi) = -(f + \xi) \operatorname{div}_2 V. \quad (8.10)$$

In this formulation terms arising from vertical motion gradients and horizontal density gradients have been neglected. This is proper for large-scale motion in the tropics.

The operator d/dt in (8.10) is called the "individual" or "substantial" derivative; it is the differentiation following a given mass. So far in this chapter we have considered the divergence within a fixed area;

$$\operatorname{div}_2 V = \frac{\partial u}{\partial x} + \frac{\partial v}{\partial y}.$$

In order to solve (8.10), it is of advantage to define the divergence with respect to a given mass. This definition is given by the per cent change of the horizontal area A occupied by the mass. For a thin layer

$$\operatorname{div}_2 V = \frac{1}{A} \frac{dA}{dt}.$$

With some restrictions, the continuity equation, when defined for an individual column, is $A \Delta p = \text{constant}$, where Δp is the pressure difference between top and bottom of the column. Then

$$\operatorname{div}_2 V = \frac{1}{A} \frac{dA}{dt} = -\frac{1}{\Delta p} \frac{d\Delta p}{dt}. \quad (8.11)$$

Eliminating the divergence from (8.10) through introduction of (8.11),

$$\frac{f + \xi}{\Delta p} = \text{const.} \quad (8.12)$$

This theorem, whose importance can hardly be overestimated, is known as the *theorem of conservation of potential vorticity* (9). The individual

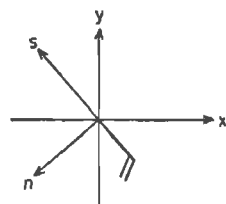


Fig. 8.5. Cartesian (x, y) and natural (s, n) coordinate systems.

components of (8.12) may change, but the whole expression remains constant. Analogous to the definition of potential temperature, this constant may be viewed as the value which ξ would have to assume when referred to some standard latitude and Δp .

It is the outstanding achievement in the derivation of (8.12) that a dynamic property has been found which is *conserved by individual air columns*. A large part of physics research has been given to the discovery of conservative properties. The existence of any such property is a powerful means for prediction since it may be "extrapolated" with complete confidence. In the atmosphere, potential vorticity is the only dynamic property so far discovered that can claim to be nearly if not wholly conserved by individual masses. This claim is most valid in the tropics.

If we replace the relative vorticity in (8.12) by the shear and curvature terms of the natural coordinate system,

$$\frac{f + V/r_s - \partial V/\partial n}{\Delta p} = \text{const.} \quad (8.13)$$

This equation shows that for a wind and weather forecast further manipulation of the conservation law is necessary. There are still four variables within its framework, and the law gives no certain clue how these will act in relation to each other. Consider, for instance, a southerly current. As this current moves toward higher latitudes, therefore increasing f , it may compensate by decreasing cyclonic curvature or shear, increasing Δp , or by various combinations. It is essential to know which of these possibilities will occur in order to predict wind and weather.

Numerical Prediction. As a first step, research workers have tried to find circumstances under which neglect of one or more variables may be justified. In the mean the sign of divergence changes near 600 mb. In investigating the motion near this level, it may be reasonable to omit the divergence and hold Δp constant. Then

$$f + \frac{V}{r_s} - \frac{\partial V}{\partial n} = \text{const.} \quad (8.14)$$

If we consider a broad current with constant speed and little lateral shear,

$$f + \frac{V}{r_s} = \text{const.} \quad (8.15)$$

The only variables then left are f and r_s . When a cyclonic current moves toward higher latitudes, therefore increasing f , r_s must also increase and eventually change from cyclonic to anticyclonic. The reverse holds true for southward motion. A wave motion results for which Rossby (10) has been able to give a formal solution, the so-called *constant absolute*

vorticity trajectories (CAVT). Although (8.15) is a very restricted form of the vorticity theorem, CAV trajectories¹ have often proved to be a major forecasting aid. Cressman (3) has demonstrated that they may give a good approximation to the wind field of the equatorial zone during flow across the equator. He computed several sample trajectories starting with different initial characteristics in the southern hemisphere (Fig. 8.6); these provided an explanation for clockwise eddies in the equatorial-trough zone of the Atlantic (Fig. 10.26).

Development of high-speed electronic computing equipment since the 1940's has presented an opportunity to dispense with formal integrations of (8.10); prediction can instead be carried out on a stepwise basis over short time intervals. It would lead too far to describe these calculations

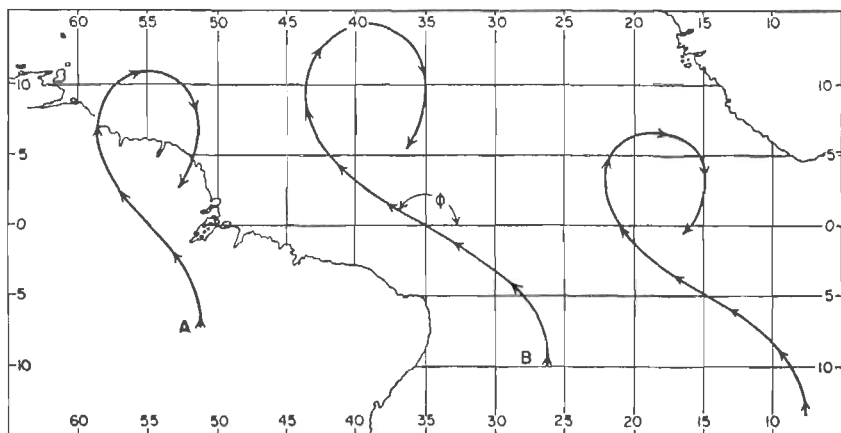


Fig. 8.6. CAV trajectories across the equator (3).

in detail. Attempts at numerical forecasting in the tropics have not yet been made. But these will come, and so it is worth while to say something about the method in principle.

Returning to (8.10), if we assume nondivergence,

$$\frac{d}{dt} (f + \xi) = 0.$$

Since in this equation $d/dt = \partial/\partial t + u \partial/\partial x + v \partial/\partial y$ in rectangular coordinates,

$$\frac{\partial \xi}{\partial t} = - \left(u \frac{\partial \xi}{\partial x} + v \frac{\partial \xi}{\partial y} + v \frac{\partial f}{\partial y} \right). \quad (8.16)$$

Given an initial wind field, the tendency $\partial \xi / \partial t$ at the starting time can be computed with this relation since the right side contains only space deriv-

¹ Fultz (4) and Hess (6) have described techniques of calculating CAV trajectories.

atives. This tendency is held constant for a suitable time interval; 1-3 hours has been found practical. Then the new vorticity and wind distributions are calculated, and also a new vorticity tendency, which is extrapolated over the next 1-3 hours. Results of some 24-hour forecasts so computed (1) have been sufficiently encouraging to stimulate attempts to improve on the "barotropic" model (8.16) and to allow for the baroclinity of the atmosphere.

The essential difference between barotropic and baroclinic models is inclusion of the divergence. As demonstrated earlier, "weather" is produced when layers of convergence and divergence alternate along the vertical. In forecasting clouds and rain, changes of Δp in (8.12) or (8.13) cannot be ignored. If air moves northward with increasing relative vorticity, it must be undergoing convergence and vertical stretching. If it moves southward with increasing anticyclonic relative vorticity, it must be undergoing divergence and vertical shrinking. The freedom of operation within the vorticity theorem is probably responsible for the variety of synoptic patterns to be described.

Numerical prediction may provide a means of anticipating which of the numerous alternatives will materialize in any situation. Initial attempts to include the divergence look very promising (2). Some of the assumptions used, however, are perhaps inapplicable to low latitudes, especially the quasi-geostrophic approximation. The computing techniques are also dependent on fairly reliable and dense observations, a reasonable requirement. Difficulties therefore lie ahead before the tropical forecaster can fully utilize the numerical methods.

Further Applications of the Vorticity Theorem

Since the divergence reverses with height in weather-producing disturbances, the change of absolute vorticity also must reverse sign. The vertical distribution of vorticity change must be such as to prescribe the proper sign for vertical motion—upward in bad-weather areas and downward in zones of fair weather. At some distance from the equator $f + \zeta$ is usually positive for the respective hemisphere; here *the lower air must gain and the upper air lose cyclonic vorticity in rain areas. The opposite is true for good-weather areas.* Qualitatively we may use (8.12) as an aid in analysis. In the lower troposphere successive streamline charts must be drawn so that air is guided into an area of disturbed weather with increasing absolute vorticity. The curvature term frequently determines the relative vorticity. Then the objective is achieved if the curvature remains constant or becomes more cyclonic during poleward travel of air; equatorward motion requires a sharp increase in cyclonic curvature to compensate for the decrease in latitude. For dynamic consistency, the

high-level charts must provide for divergence over a precipitation area. An equatorward-moving current may travel in a field in which the stream-lines remain straight or become more anticyclonic. If the wind direction is away from the equator, the chart must provide for a rapid increase of anticyclonic or decrease of cyclonic flow curvature on the moving columns.

Close to the equator, in each hemisphere, $f + \xi$ may be small, zero, or even negative. If $f + \xi = 0$, divergence cannot produce vorticity changes. Then (8.14) holds strictly except for the processes not considered in its derivation. Air with zero absolute vorticity is likely to conserve this vorticity closely for short periods.

Interesting situations arise during marked cross-equator flow when, for instance, air with southern-hemisphere vorticity crosses into the northern hemisphere as in Fig. 8.6. Suppose that the change in relative vorticity is determined by the change in flow curvature alone, as demanded for Rossby's CAV trajectories. Suppose further that the air initially located at 5°S, 15°W, in Fig. 8.6 makes sharper anticyclonic bends after crossing the equator than CAV flow prescribes. Then the absolute vorticity is no longer conserved but, from the northern-hemisphere viewpoint, becomes more anticyclonic (negative). Since $f + \xi$ is negative at the start (again as seen from the northern hemisphere), this negative value increases (*cf.* also 8) and the air converges. If the current moves along a trajectory with less anticyclonic curvature than the CAV trajectories demand, it diverges. If the flow occurs in the low troposphere, the current with sharp anticyclonic bend should contain bad weather and that with weak anticyclonic bend good weather. These deductions have not yet been properly tested by observations.

REFERENCES

- (1) Charney, J. G., *et al.*, *Tellus*, **2**: 237 (1950).
- (2) Charney, J. G., and N. A. Phillips, *J. Meteor.*, **10**: 71 (1953).
- (3) Cressman, G. P., *Dept. Meteor., Univ. Chicago, Misc. Rept.* 24, Part II, 1948.
- (4) Fultz, D., *Dept. Meteor., Univ. Chicago, Misc. Rept.* 19, 1945.
- (5) Haurwitz, B., *Dynamic Meteorology*. New York: McGraw-Hill Book Company, Inc., 1941.
- (6) Hess, S. I., and S. M. Fomenko, *J. Meteor.*, **2**: 238 (1945).
- (7) Holmboe, J., *et al.*, *Dynamic Meteorology*. New York: John Wiley & Sons, Inc., 1945.
- (8) Palmer, C. E., *Quart. J. Roy. Meteor. Soc.*, **78**: 126 (1952).
- (9) Rossby, C.-G., *et al.*, *J. Marine Research*, **2**: 38 (1939).
- (10) Rossby, C.-G., *Suppl. Quart. J. Roy. Meteor. Soc.*, **66**: 68 (1940).

CHAPTER 9

WAVES IN THE EASTERLIES

The unsteadiness of the atmosphere described in Chaps. 1 and 3 may be classified under the summary title of "turbulence." But this turbulence can be subjected to techniques of analysis other than those usually employed in physics in turbulence problems. There one visualizes a vast number of random motions and eddies within a certain medium. Individual motions cannot be discussed. Instead, physical and statistical laws are developed concerning the net effect of the turbulence on the medium as a whole. The concept of "temperature" is an illustration.

To the extent that the sum of all atmospheric disturbances produces the general circulation, we can speak of turbulence. But not all the turbulent elements need be viewed as random fluctuations, accessible to study only by recording their aggregate. It is true that their magnitude in space and time covers a wide range; this "spectrum," however, shows concentrations of frequency and energy of the disturbances in a few "spectral lines." We speak of "centers of action," "secondary disturbances," "convection cells," etc. Each of these scales of turbulence is investigated separately for the laws governing its particular, discrete appearance and behavior in time and space.

Weather prediction makes sense only when this procedure is feasible and physically sound. Though the number of flow configurations observed on any map with a scale of, say, 1 to 10,000,000 is infinite, this is not due to the appearance of an infinite variety of turbulence elements. Again and again we find that these elements have common characteristics of structure and behavior, though they vary in detail from one occasion to another. It therefore becomes one principal function of the meteorologist to discover and set down in the form of models the basic similarities of the turbulence elements. Next, he tried to find the parameters that determine their variations.

In attempting to do just this, the science of meteorology has confronted itself with a problem of a high order of difficulty. Its concern with this problem, of course, stems from the demands for forecasts. In asking what the weather will be tomorrow or whether the winter will be cold, people testify to their own experience of discrete scales of turbulence within the atmosphere. They are also demanding a great deal. While

meteorology has traveled far toward an understanding of its medium, much time will pass before all the demands of the public can be satisfied.

The following chapters discuss turbulence elements with scales of 1,000–2,000 miles and a duration of days. These are the so-called "synoptic disturbances." According to experience from all parts of the world they take the form of (a) transverse waves within broad currents; (b) shear zones, such as wind discontinuities and jet streams; and (c) vortices.

We begin with the class of transverse waves.

Model of Waves in the Easterlies

We usually speak of waves in a current when it executes fairly sinusoidal oscillations. The most permanent currents of the atmosphere are the polar westerlies and the tropical easterlies, both of which at times oscillate in a wavelike manner. Thus, we speak of waves in the westerlies and of waves in the easterlies. The former have been the subject of much research, the latter of very little.

Although waves occur in the easterlies over many parts of the tropics, observations in the Caribbean area have led to the formulation of wave models. Dunn (3) found that a chain of isallobaric centers at sea level moved across the islands from east to west in the hurricane season. These centers were useful in forecasting the formation of tropical storms. Definite changes in the depth of the moist layer were connected with them.

As upper-wind data began to increase, it became evident that definite wind shifts accompanied the isallobaric centers. These wind changes suggested that the isallobaric centers that Dunn had noted were manifestations of wave propagation (11).

Figure 9.1 illustrates the kind of observation which led to the wave model. A strong oscillation in the wind field takes place during the period given. The direction of the basic current in the low levels is ESE, the mean flow direction over the Antilles during the rainy season. Winds at first point at an increasing angle to the left of this direction. After a sharp wind shift on July 12, they point to the right. By the end of the period they begin to return to their initial direction. Thus, Puerto Rico experiences two ridges and one trough in a period of 4 days. This is not far from the statistical average.

Figure 9.2 shows the synoptic situation at the time of trough passage over Puerto Rico. Measuring from ridge to ridge, the wave length is about 20° longitude (the average is closer to 15°). Assuming that the shape of the wave does not change during the period, its rate of propagation toward WNW is 13 knots.

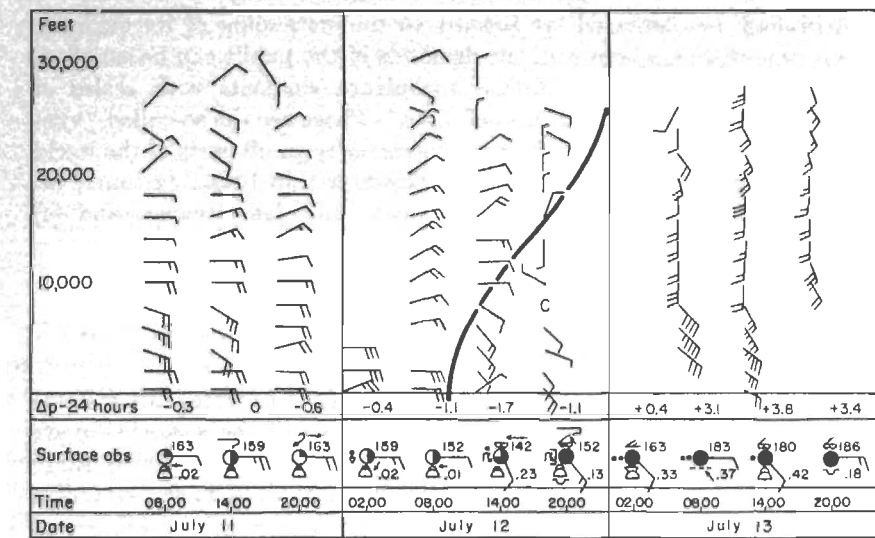


Fig. 9.1. Vertical time section at San Juan, Puerto Rico, July 11-13, 1944 (15).

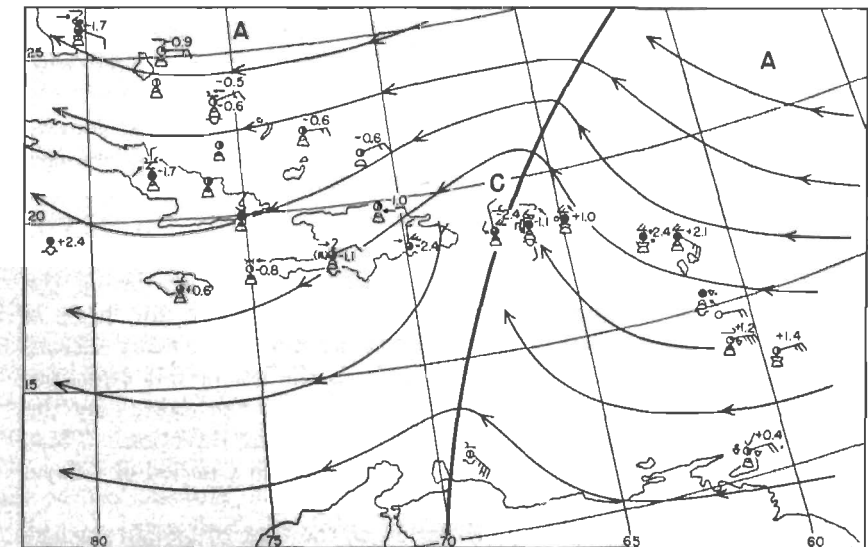


Fig. 9.2. 5,000-foot winds, surface 24-hour pressure changes and weather reports for the Caribbean area, July 12, 1944 (15). (For plotting technique, see Chap. 7.)

Surface-pressure Field. In Fig. 9.1 the 24-hour surface-pressure changes are plotted below the winds. We may follow the suggestion made in Chap. 7 and mentally move these changes back 12 hours. The sign of the 24-hour changes should then indicate the instantaneous synoptic tendency. Ahead of the wind-shift line, pressure falls at first increase, then decrease. The zero isallobar almost coincides with this line (*cf.* also Fig. 7.3), and to its rear the pressure rises. This establishes the fact that a pressure wave accompanies the wave in the wind field. The ridges in the wind field are ridges in the pressure field; the trough in the wind field is a trough in the pressure field.

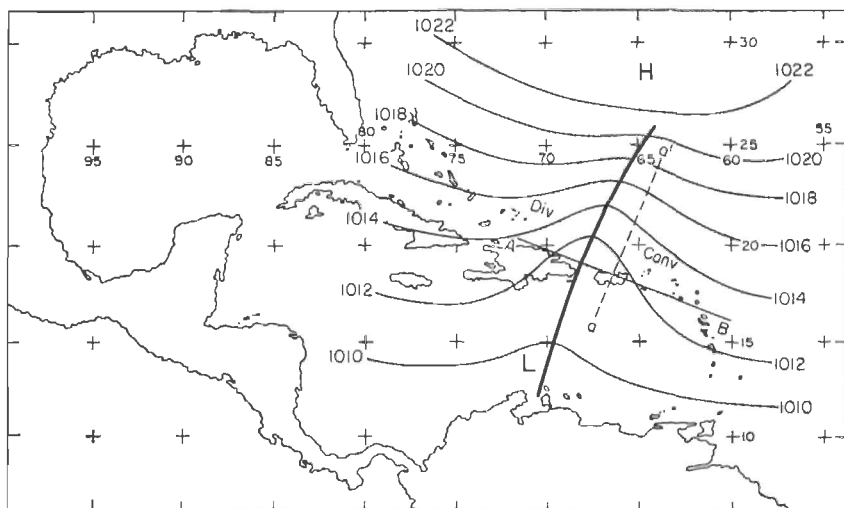


Fig. 9.3. Model of waves in the easterlies: surface chart (14).

Figure 9.3 illustrates the typical surface isobaric pattern in model form. The trough, marked by a heavy line, lies normal to the mean orientation of the isobars. This line should not be thought of as a boundary comparable with high latitude fronts. It represents a transition zone 50–100 miles wide in which the weather changes gradually.

Toward the north, the wave amplitude decreases toward the central, thermally stable portions of the Azores-Bermuda high, but it can often be traced to its inner isobars. To the south the waves may extend to the equator and beyond. Waves centered on the equator will be discussed later in this chapter.

Pressures and Temperatures Aloft. Waves of weak or moderate strength attain their greatest intensity in the middle troposphere, from 700 to 500 mb; they then decrease upward. Above 300 mb, disturbances with a wind field entirely different from that in the low levels may pre-

vail (Chap. 10). Strong waves are associated with pressure and temperature variations up to the tropopause. This is shown statistically, at least up to 10 km, in Fig. 9.4, which depicts the mean fluctuations of 15 intense disturbances in 1944 and 1945 (5). Each wave was divided into five parts: E_f , undisturbed current in front of surface trough; T_f , front part of trough; T_c , central part of trough; T_r , rear part of trough; E_r , undisturbed current in rear of trough. The averaging was done with respect to the wave portions so defined.

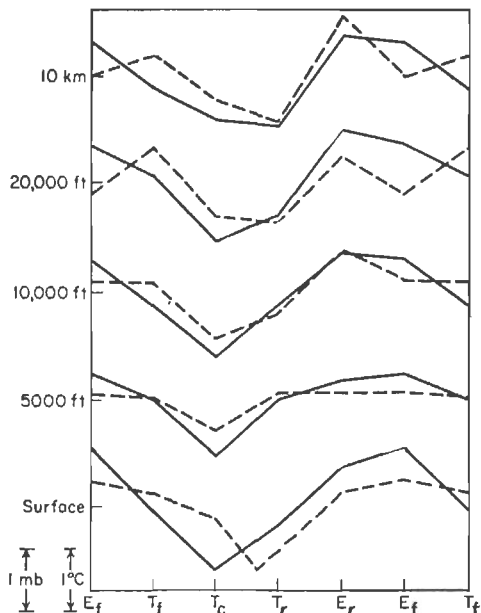


Fig. 9.4. Average variation of pressure (solid) and temperature (dashed) during passage of wave troughs in the easterlies at San Juan (5).

At the surface, pressure and temperatures are nearly in phase. The temperature minimum closely follows the pressure minimum. This is usually the zone of most active weather. Cooling results from decreases in insolation due to cloud cover, evaporation from falling rain and from downdrafts in large convective clouds.

Throughout the troposphere the lowest temperatures are located to the rear of the surface trough. For hydrostatic reasons this introduces an eastward slant of the trough line with height, opposite to the direction in which the waves are traveling. In the westerlies, the lowest temperatures also occur to the rear of the surface trough, and the waves have a vertical tilt opposite to their direction of motion, in this case to the west. Thus, the vertical structure of waves in easterlies and westerlies is quite similar.

This analogy holds good up to the tropopause. In the westerlies the tropopause is generally lower in troughs than in ridges. In the easterlies most radiosonde ascents do not reach the primary tropopause (100 mb). It has therefore not yet been possible to study its variations. But secondary lower tropopauses appear at pressures ranging from 130 mb to as low as 250 mb (5). They seldom are so intense that an isothermal layer can be located on a radiosonde flight; but the lapse rate distinctly decreases. The potential temperature at the top of the stable layers is much lower than that of the primary tropopause, indicating a formative process rather than descent of the main tropopause.

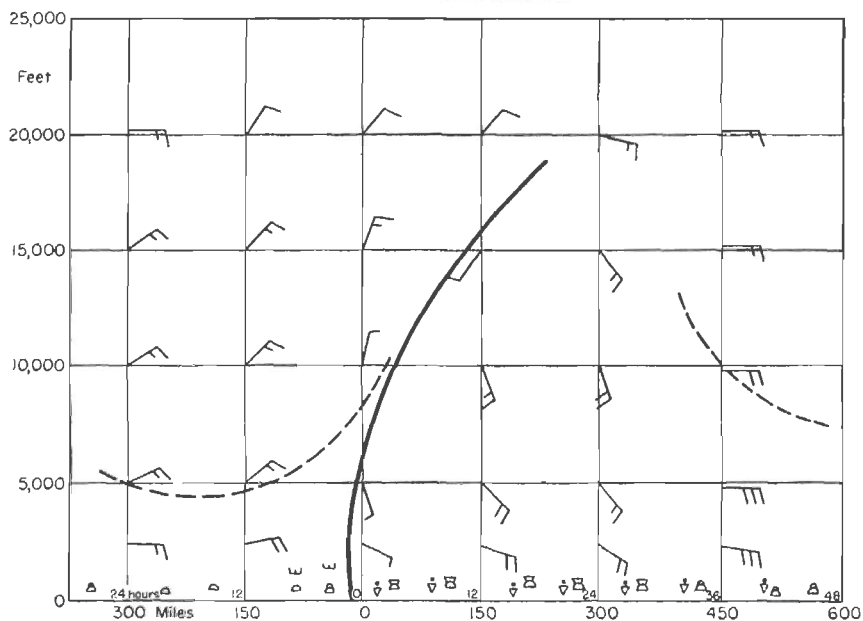


Fig. 9.5. Model of waves in the easterlies: wind, weather, and depth of moist layer (dashed) in vertical section (14).

The upper cooling and the secondary tropopause cannot be explained on the basis of advection of air masses with different initial properties. The temperature structure moves with the waves while the air passes through them, usually from east to west at low levels and in the opposite direction higher up. Just as in middle latitudes, the secondary tropopause and its changes in height compensate for the temperature changes underneath. Above 200–150 mb, the disturbances decrease in intensity. They seldom extend above 100 mb; instead they give way to steady stratospheric easterlies.

Wind Field and Weather. A model of the typical wind field accompanying waves in the easterlies is shown in Figs. 9.5–9.7. As in the case of the

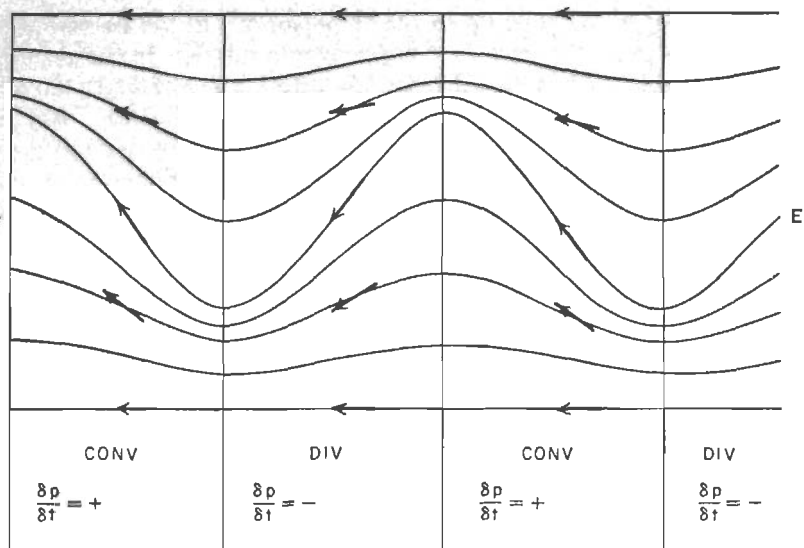


Fig. 9.6. System of converging and diverging easterly isobars (after J. Bjerknes, 1).

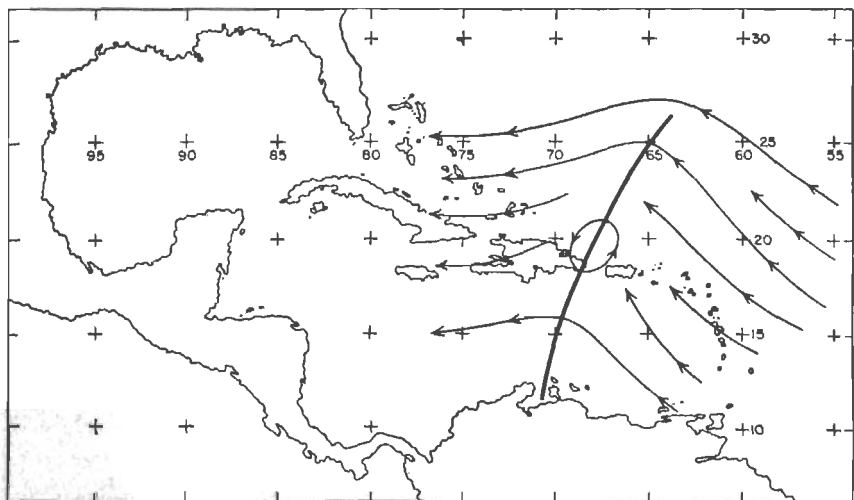


Fig. 9.7. Model of waves in the easterlies: 15,000-foot streamlines around strong wave trough (14).

pressure field, the trough line in the wind field slopes eastward above the lowest levels. Near the ground, the east component of the wind is strong in the ridges but weakens progressively toward the line aa' of Fig. 9.3; the meridional component vanishes toward the subtropical high. As a result a zone of low-level divergence, therefore also of descent, is found

ahead of the wave trough, and a zone of low-level convergence and ascent to its rear. Since the surface pressure falls ahead of the trough and rises behind it, the field of low-tropospheric divergence and convergence governs the sign of the pressure change. Regions of low-level divergence correspond to the areas of pressure fall and regions of low-level convergence to the areas of pressure rise.

In front of the trough line, the east component diminishes with elevation to at least 15,000–20,000 feet. To its rear it also decreases upward when the trough line slants toward the east, as in Fig. 9.5. If a closed upper low is present (Fig. 9.7), westerlies are encountered in a limited area above 15,000–20,000 feet. Above 400 mb (25,000 feet) the vertical wind structure is variable, depending on the interaction with independent disturbances of the high troposphere. But for the waves to exist, the depth of the easterly current must be at least 20,000–25,000 feet.

Ahead of the trough line the north component increases upward, while to its rear the south component is most marked between 5,000 and 15,000 feet. Along the trough line, the meridional wind components generally vanish. But, depending on the orientation of the axis, passage of a wave trough may be marked merely by an increase of the south component or by disappearance of the north component.

The foregoing model is typical but not unique. Later we shall discuss some situations that depart from the model. This also applies to the weather distribution, which is described below for the typical case.

The field of motion controls the depth of the moist layer. About 200 miles ahead of the wave trough, the top of the layer reaches a minimum, often as low as 5,000 feet, and exceptionally fine weather prevails. It rises rapidly near the trough line and attains a maximum well above 20,000 feet in the zone of most intense convergence. Here, large squall lines and rows of cumulonimbi are found. According to Regula (13), the severe tornadoes of West Africa occur mainly about 12 hours to the rear of such westward-moving trough lines. One should not imagine, however, that this region east of the trough line, even in the case of very strong waves, is entirely covered with cumulonimbi and cumuli congesti. Wide zones of subsidence occur between individual clouds; areas of updrafts 5–20 miles wide are situated within the larger field of convergence with a net upward component of motion. In addition, as suggested by Palmer (10), the convective activity tends to be concentrated along one or more convergence lines so that conditions will not be uniform for an observer traveling parallel to the wave trough. Such a concentration is suggested by Fig. 9.6, which is a model developed by J. Bjerknes (1) turned upside down for the easterly case. It is also indicated in Fig. 9.3, where an area with maximum pressure gradient has been drawn north of the 1,012-mb isobar, and a wide space with little gradient farther south.

This area corresponds to the closed low aloft (Fig. 9.7), which should be pictured centered south of the 1,012-mb isobar. Such closed circulations are likely to be accompanied, in addition to the convective clouds, by an altostratus sheet not derived from cumulonimbus. Steady moderate rain may be falling, especially in the northeastern part of the circulation. It is possible that the excessive amounts of rainfall at times recorded during wave passages—as much as 12 inches per 24 hours—indicate this central zone, but proof cannot be offered.

In the eastern outskirts of the trough, the moist layer again descends, and regular trade-wind weather is resumed.

A cloud and weather sequence follows that may be experienced over the sea during passage of a typical wave:

In ridge: Trade cumulus of average height, no precipitation.

Ahead of trough: Cumulus humilis, few build-ups, strong haze, no precipitation.

Close to trough line: Cumulus of above-average development, some cirrus and altocumulus, improving visibility, scattered showers.

At trough line: Large cumulus and cumulus congestus, broken to overcast cirrus, altocumulus. Frequent showers or rain.

To rear of trough line: Cumulus congestus and cumulonimbus, with layers of stratocumulus, altostratus and altocumulus, and cirrus. Frequent moderate to heavy showers, with light rain between showers. Thunderstorms.

In eastern outskirts: Large cumulus and cumulus congestus, occasionally still cumulonimbus. Some stratocumulus, altocumulus, cirrus. Moderate showers, decreasing.

Over island chains weak waves are often difficult to locate accurately. The convergence accompanying them may merely result in an intensification of the diurnal cloudiness over islands. On account of the magnitude of local effects, island observers will note great deviations from the outlined weather sequence. At San Juan, Puerto Rico (see Fig. 4.1), the increased north component in the forward portion of the waves tends to augment the nocturnal convection on the shore (Chap. 4) and carry these clouds farther inland than usual. The downslope motion to the rear of the trough lines, associated with southerly winds north of the mountain range, tends to diminish the cloudiness along the north coast, while huge cumulonimbi remain banked against the southern slope of the mountains.

López (9) has attempted to correlate the isallobaric patterns aloft with the intensity of the subsequent weather. Four principal types of isallobaric patterns exist (Figs. 7.3 and 9.4):

1. Falls decreasing with height and changing to rises. This pattern correlates well with subsequent worsening weather. Of 49 cases analyzed by López, he verified 39.

2. Falls increasing with height. This pattern is also followed by worsening weather (30 cases out of 42).

3. Rises decreasing with height and changing into falls. This pattern does not show any definite correlation with subsequent weather. Of 42 cases studied, 22 were followed by worsening weather and 20 by improving weather. This is reasonable since the pattern is representative of the period after surface-trough passage. All depends on whether the sounding studied is taken just to the rear of the trough or farther away.

4. Rises increasing with height. This type correlates with improving weather (37 out of 44 cases).

López's results corroborate the preceding description of the waves. When careful radiosonde and rawin observations are taken at isolated stations, they may be used even as a means for short-term prediction of the weather on a single-station basis.

Dynamic Aspects of Waves in the Easterlies¹

No complete treatment of the dynamics of waves in the easterlies has yet been offered. Certain theories, however, that have been found applicable for waves in the polar westerlies can be applied with modification to waves in deep easterly currents. We shall assume that the waves travel in steady state, that the theorem of conservation of potential vorticity $(f + \xi)/\Delta p = \text{constant}$ [Eq. (8.12)] is the leading dynamical principle, and that we can proceed without treating the energy cycle. For justification of the last assumption we refer to Rossby's (18) observation that in rotating fluids similar types of flow configurations tend to develop irrespective of the dimensions of the fluid and the specific mode of energy infusion.

Consider a system of sinusoidal easterly streamlines as in Fig. 9.2. Air particles moving northward in the eastern portion of the map are going toward higher latitudes and therefore increasing f . If Δp remained constant, ξ would have to decrease and eventually become anticyclonic. If, now, the low-level particles are moving westward more rapidly than the wave itself, they will catch up with the trough line. They are therefore moving into a region where the cyclonic curvature is greater than where they were situated initially. If the curvature term makes the largest contribution to the relative vorticity and its changes, the relative vorticity of the particles increases. Since both f and ξ increase, Δp must also increase to satisfy Eq. (8.12). *A nondivergent wave in the easterlies is impossible under these circumstances.* Convergence must exist east of the

¹ Symbols are defined as in Chap. 8: ξ , relative vorticity; f , Coriolis parameter; Δp , depth of column considered; V , wind speed, r_s , radius of streamline curvature; n , axis normal to flow.

trough line. Conversely, air particles acquire anticyclonic curvature (ξ decreasing from positive to negative values) west of the trough, where f also becomes smaller. Therefore Δp must decrease; in other words, there must be divergence.

We can evaluate the constant in (8.12) by considering the properties of the air approaching the trough at some initial time, say when it was passing the ridge to the east. If we denote initial conditions by the subscript zero and consider the relative vorticity as given by the curvature alone,

$$\frac{\Delta p}{\Delta p_0} = \frac{f + V/r_s}{(f + V/r_s)_0}. \quad (9.1)$$

Assuming Δp to denote the depth of the moist layer, we can evaluate the changes of this depth from (9.1). The wind speed V may be 10 mps at

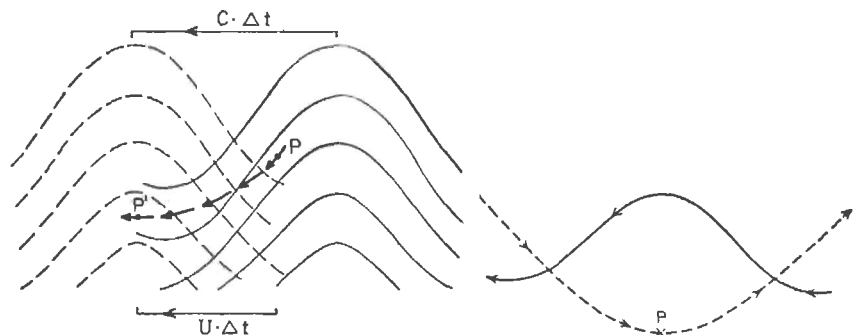


Fig. 9.8. Left: Model showing air east of trough being overtaken by trough line. Right: Streamline (solid) and trajectory relative to waves (dashed) for wave moving westward faster than air (14).

both trough and ridge lines for the purpose of this computation; the radius of streamline curvature will be taken as 1,000 km, anticyclonic at the ridge and cyclonic at the trough; and the air will be assumed to have moved from latitude 15 to 20° while going from ridge to trough. Inserting these values in (9.1), we find that $\Delta p/\Delta p_0 = 2$. If the average depth of the moist layer is 8,000 feet in the ridge, it will be 16,000 feet in the trough. This proves that (9.1) describes an effect of the right order of magnitude to account for the observed variations in the depth of the moist layer.

So far we have treated an easterly current that passes through the waves from east to west. If the basic current moves slower than the waves, troughs and ridges overtake air initially situated to their west. Air columns then move southward ahead of troughs, and northward to their rear, on *anticyclonically curved paths*. Figure 9.8 illustrates the motion of air that is being overtaken by a trough; it also shows the trajectory of such air *relative to the wave*, i.e., the wave speed has been sub-

tracted from the wind speed. As the trough line approaches a column, its relative vorticity increases but at the same time its latitude decreases. Thus f and V/r_s vary inversely; their sum may remain constant and the absolute vorticity conserved. In this case frequency equations derived from (8.10) under the assumption of conservation of *absolute* vorticity may hold (6, 17). According to Haurwitz (7),

$$c = U + \frac{\beta L^2}{4\pi^2(1 + L^2/D^2)} \quad (9.2)$$

where c is the wave speed, U the basic current, β the variation of the Coriolis parameter with latitude, L the wave length, and D the width of the disturbance.¹ The second term, often called the "dynamic" term, increases with the wave length and the width of the disturbances. If D is very small, the wave will move with almost the speed of the basic current. In the easterlies $D = L$ is often a reasonable approximation, so that $c = U + \beta L^2/8\pi^2$. Assuming $\beta = 2 \times 10^{-13} \text{ cm}^{-1} \text{ sec}^{-1}$ and $L = 2,000 \text{ km}$, the value of the dynamic term is 2 knots. Steady-state waves traveling slightly faster than the average easterly current (15 knots) can be explained on the basis of conservation of absolute vorticity.

The foregoing is of more than theoretical interest. It is true that the nondivergent wave itself is unrealistic since it allows for no weather pattern. But (9.2) enables us to determine for any combination of L and D whether a wave moving at an observed rate and obeying the initial assumptions should have bad weather east or west of the trough line. For (9.2) is a limiting case. If the wave speed c is too small compared with that demanded by (9.2), we have the situation already discussed and bad weather will be situated east of trough lines. If c is too large, the bad weather will be to the west. As the air is overtaken by the trough line, the increase in V/r_s will exceed the decrease in f . The absolute vorticity increases, and Δp must also increase for the potential vorticity to be conserved. East of the trough line the decrease in V/r_s will exceed the increase in f ; here we have a decrease in Δp and divergence.

Vertical Wave Structure. A combination of the two cases discussed will provide for reversal of the low-level convergence and divergence patterns with height when troughs and ridges are vertical or slope only slightly. As stressed in Chap. 8, such a reversal is always necessary if the surface pressure is to change very little, yet appreciable bad weather occurs. We obtain a two-layer structure of the atmosphere if we permit the easterly current to decrease with height for the case when the bad

¹ For application of Haurwitz's formula in the tropics, both u and c are defined positive toward the west.

weather is situated east of the trough line. An easterly current that moves faster than the waves near the ground and slower aloft (Fig. 9.9) is the only kind of current in which waves with appreciable weather concentration to their east can travel without change of shape. In the low levels, air columns pass through troughs from east to west on cyclonically curved paths; the relative motion is of the order of 5 knots. At higher elevations columns move through troughs from west to east on anti-cyclonically curved paths. East of the trough lines air gains cyclonic

absolute vorticity near the ground and loses cyclonic vorticity aloft. The opposite holds true west of the trough lines. As long as the vertical change of relative motion is sufficiently great, it is possible to obtain convergence near the ground and divergence aloft east of trough lines and divergence near the ground and convergence aloft west of trough lines. Motion without change of shape can then take place.

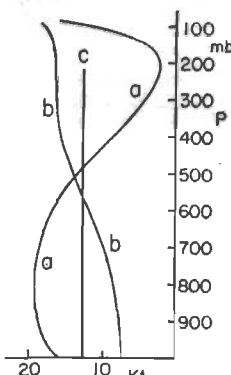
When the basic current increases with height [curve (b) of Fig. 9.9], air must move westward more slowly than the waves in the low levels and more rapidly in the higher elevations. This happens mainly when the upper air is warmer in the subtropics than in the trades. The areas of bad weather connected with a train of waves moving without change of shape will then lie to the west of the trough lines.¹ This observation may be helpful in predicting the breakdown of the steady state. In

Fig. 9.9. Variation of basic current with height relative to wave speed c if bad weather is concentrated (a) east and (b) west of trough line.

the Caribbean, for instance, waves often move quite regularly to about $80-85^{\circ}\text{W}$ and then disintegrate. The author has noted similar breakdowns in the western Pacific. In the mean, the easterlies weaken with height over the Antilles in summer, but this decrease disappears over the western Caribbean (Fig. 1.19). Around the globe wide regions with decreasing easterlies alternate with regions where the easterlies increase upward. Along the boundaries waves will change shape.

When the troughs and ridges are not vertical but slant strongly with height, the foregoing deductions must be modified. Consider a complete phase reversal with height, so that an upper trough overlies the surface ridge and an upper ridge overlies the surface trough. If the basic current is uniform at all heights and faster than the wave speed, the lower air

¹ Although no extensive statistical tests have been conducted, a study by Durham *et al.* (unpublished) has shown that in the Caribbean the bad-weather zone tends to be displaced westward relative to the troughs as the speed of the waves increases.



moving toward a trough will gain cyclonic vorticity and the air above it going toward the ridge will lose cyclonic vorticity. The requirement of a vertical reversal of the divergence is satisfied, and steady-state motion with a weather pattern and little surface pressure change can take place. This is also true for waves moving more rapidly than a uniform easterly current.

Inclusion of Shear. We consider the complete theorem

$$\frac{f + V/r_s - \partial V/\partial n}{\Delta p} = \text{const.}, \quad (9.3)$$

with use of the models shown in Fig. 8.3. These portray a sinusoidal easterly current with highest speed concentrated along single axes. Note that the wind speed is drawn so as to vary along these axes. In Fig. 8.3a speeds are highest in the trough, in Fig. 8.3b in the ridge.

Following middle-latitude models (16), we assume that the air moves through the patterns from east to west on paths parallel to the axes. Air approaching the trough in Fig. 8.3a south of the axis gains latitude, cyclonic curvature, and cyclonic shear and therefore undergoes convergence. West of the trough line the air loses latitude, cyclonic shear, and cyclonic curvature and thus undergoes divergence. North of the axis the situation is more complicated. East of the trough the air gains cyclonic curvature and latitude, but anticyclonic shear. This is equivalent to saying that it loses cyclonic shear. The three terms tend to cancel each other so that air may move at constant absolute vorticity. It could happen, however, that the shear term predominates. Then the air in this sector will lose absolute vorticity and diverge. Further, the air west of the trough line can gain absolute vorticity and converge. The weather pattern would change rapidly from south to north through the axis of strongest wind in such cases. We should observe a bad-weather area of considerable intensity east of the trough and south of the axis and another weaker one west of the trough and north of the axis.

By analogous reasoning, the air north of the axis and east of the ridge line in Fig. 8.3b will diverge; that to the west of the ridge line will converge. A definite statement cannot be made for air south of the axis, but given large variations of shear along the axis, we could have divergence west of the ridge and convergence east of it.

Although various steady-state models could be proposed by the aid of such reasoning, the subject has not been explored and so will not be pursued further. It should be added that Petterssen (11) has derived a frequency equation for nondivergent waves including shear. This solution permits steady-state waves in the easterlies that travel slower than the wind.

Forecasting

The status of forecasting tools for the tropical waves differs little from that for short waves in middle latitudes. Prediction is largely qualitative. In general, waves whose intensity remains constant travel at constant speed. Changes of shape correlate with changes of speed.

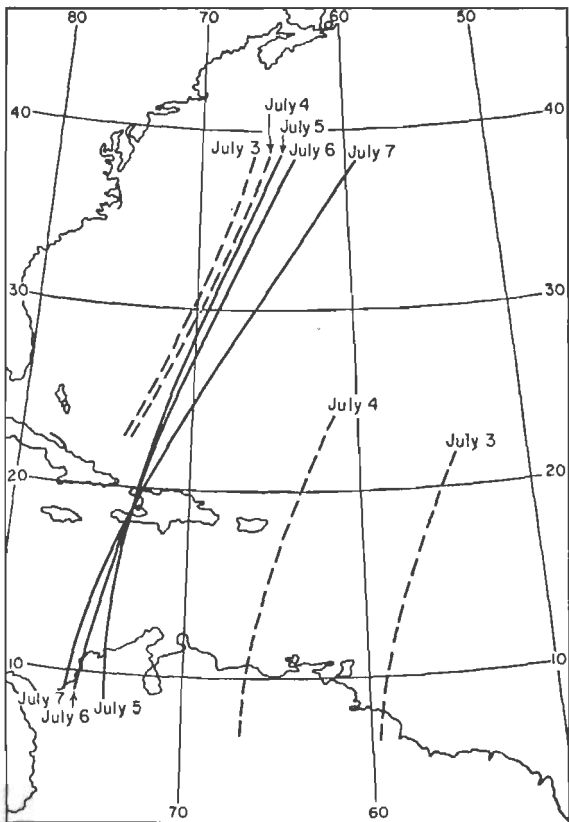


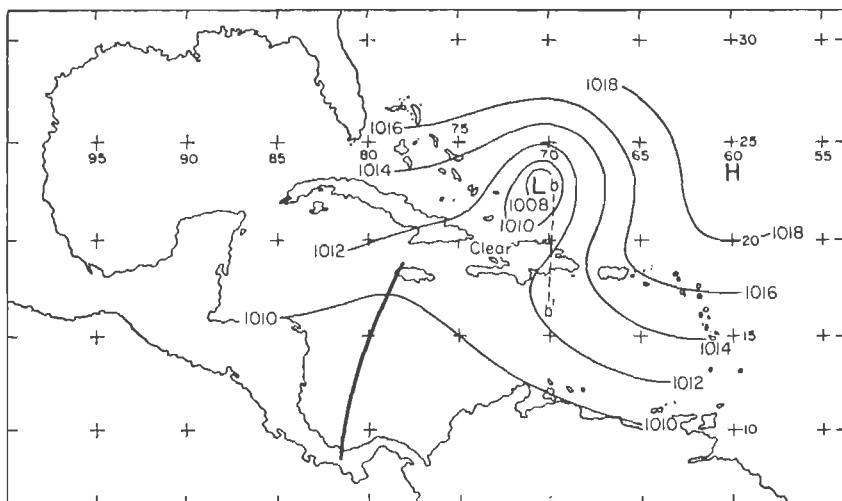
Fig. 9.10. Positions of trough lines at 10,000 feet, July 3-7, 1944 (2).

The forecaster may begin by noting structure and width of the basic current in his forecast district. This will tell him what type of steady motion is possible. During periods and in regions of broad-scale zonal flow (cf. Chap. 10) steady-state motion is probable, and extrapolation is likely to succeed. The direction of propagation is roughly normal to the trough and ridge lines and parallel to the direction of the current in which the waves are carried. In the Caribbean area, the average speed of the waves is near 15 mph. If we assume an average wave length of 15-20°

longitude, a complete wave passage over a station occupies 3–4 days. Two waves may roughly be expected to affect a station per week.

Interaction with Middle Latitudes (2). During periods of broad-scale zonal flow, both waves in the easterlies and polar westerlies slow up a little, and their amplitudes increase as they reach the same meridian in their respective latitude belts. Then, as the distance between them again increases, speed and amplitude return to their former values.

During periods of broad-scale meridional flow (Chap. 10), wave troughs in the easterlies are likely to be “captured” and become stationary or even retrograde (Fig. 9.10). After some time, fracture may occur, and



strongest. Although Cressman compiled his statistics with the aid of 10,000-foot charts, computation at other constant-level or constant-pressure surfaces should also be possible. The critical limits may change, however.

Cressman found that fracture will occur when the trough in the westerlies undergoes marked weakening and/or acceleration toward the east. Relative to the 10,000-foot level:

- Fracture will take place if the total wind shear as defined above decreases to 15 mph or less and when the trough speed increases to more than 4° latitude per day.

- Fracture will not occur if the wind shear is more than 15 mph and the trough speed less than 4° latitude per day.

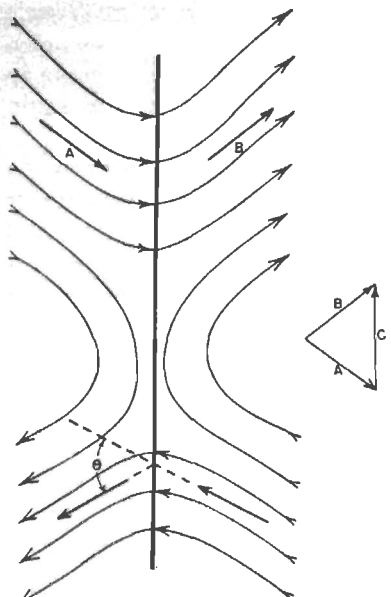
It is evident that the tropical forecaster cannot operate with maps covering the low latitudes alone. His prediction must take into account the temperate westerlies. Cressman has forcefully shown that

Fig. 9.12. Measuring intensity of waves in the westerlies during superposition on waves in the easterlies (2).

the middle-latitude forecaster should also consult tropical maps. This will enable him to predict deepening in the westerlies during superposition; he will anticipate formation of some surface low-pressure centers whose origin otherwise is not intelligible.

Formation

In most wave problems in the atmosphere, it is difficult to trace the exact beginning of a wave or train of waves. This is especially true in the tropics because of the scarcity of data. It is certain that many waves of the Atlantic can be traced back to the African coast or beyond. This is borne out by the descriptions of Regula (13) and by the fact that it has been possible to follow the movement of isallobaric centers westward along the Guinea coast of Africa. Here the easterly current, in which the waves travel, overlies a shallow layer of westerlies (Fig. 1.7). This also happens in other parts of the world, though perhaps less often. Figure 1.25 shows such a situation for the tropical Pacific east of the Philippines.



One mode of wave origin is sketched in Fig. 9.13. A large trough in the polar westerlies at times either extends well into the tropics or develops an extension equatorward. Cressman calls such troughs "extended troughs." After some time the subtropical ridge moves poleward. Then poleward and equatorward parts of the trough fracture as illustrated.

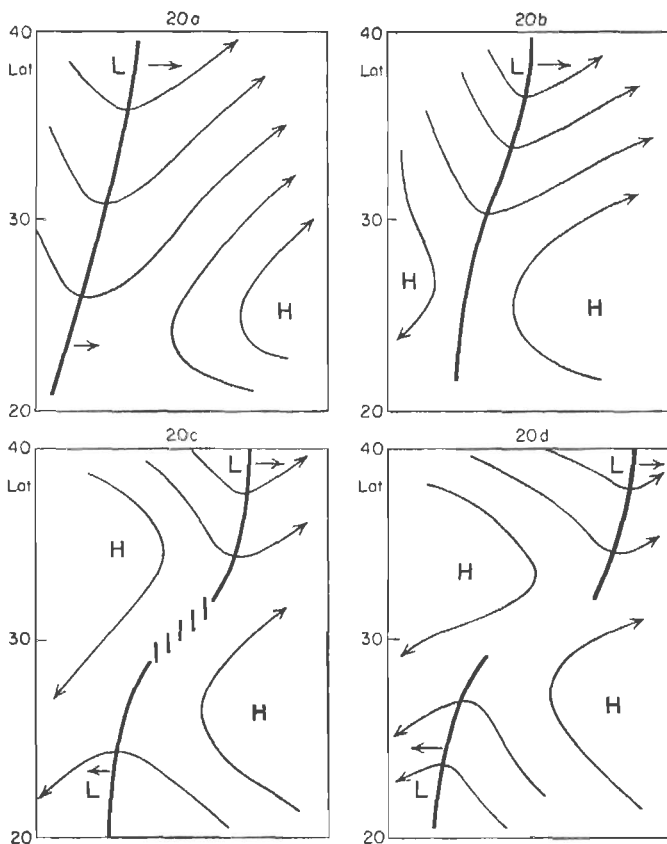


Fig. 9.13. Four stages during development of wave trough in easterlies formed by splitting of poleward and equatorward parts of extended trough (14).

The rules for fracture and, therewith, for formation of a wave trough in the easterlies are the same as those for fracture of waves in the westerlies and preexisting waves in the easterlies. Cressman notes that, of 29 waves he observed in the Atlantic in 1944, 19 moved into the field of observation and 10 originated within it as a result of fracture. Figure 9.13 thus illustrates an important mechanism for formation of waves.

Waves in the lower easterlies are also generated under large, high tropospheric cyclonic circulations often present over the trade-wind belt in summer. But a different frequency is excited in the low from that in the high levels. While the spacing of the upper vortices is 30° longitude and more, that of the lower waves averages 15° longitude.

Waves in the Dry Season

During autumn, well-developed waves in the easterlies are found progressively equatorward; this corresponds to the displacement of the belt of deep easterlies. During winter and early spring they rarely occur, at least in the Atlantic. Piersig (12) gives May 28 as the earliest date at which he found lows traveling westward from Cape Verde and Nov. 25 as the latest. Nevertheless, it is possible at times to locate westward traveling zones of convergence and divergence in the dry season during intermittent periods when the depth of the easterlies is greater than average. Intensity and rate of movement of these disturbances are proportional to the depth, strength, and persistence of the easterly current. As many as five such waves have been followed across the Caribbean in one series. Although their structure is as yet imperfectly known, the following has been observed (14).

The wind direction changes but little during passage of one of these systems, but the speed of the east current varies. At first it decreases—for instance, from 35 to 20 mph at 5,000 feet—as the system approaches and the sky clears. Then the upper winds pick up rapidly and increase to 40–50 mph with worsening weather.

As the trade-wind inversion extends more frequently over the western parts of the oceans in the dry season than in the rainy season, these disturbances may be explained by a mechanism proposed by Freeman (4). He suggests that the development of hydraulic jumps on an inversion surface may act as mechanism for generating waves in easterly currents that are marked by changes in wind speed rather than direction. Alternately one may apply the vorticity theorem again, but in this case retaining the shear term and neglecting the curvature term of the relative vorticity. Such application would presuppose a narrow easterly current, likely in the dry season.

Waves in the Equatorial Easterlies

The broad expanse of the Pacific Ocean is ideal for studying equatorial marine meteorology unhampered by the continental influences which so far have precluded a thorough investigation of the equatorial Atlantic. Regular upper-air data, though still very sparse, have been more plentiful

in this region than anywhere else on the equator. Moreover, atomic-bomb tests have provided detailed observations over a limited area around the Marshall Islands for periods ranging from weeks to months. These data have enabled Palmer (10) to make intensive analyses of weather in the central equatorial Pacific.

Seasonally, the equatorial-trough position varies less west of 170°E to 180° than it does elsewhere (Fig. 1.9). Its mean latitude approximates the global average. At the surface, the resultant wind field (Fig. 1.7) shows a strong directional convergence of northern and southern trades. The strongest speeds are found far from the trough line so that in the resultant picture intense mass convergence coincides with the trough. Nevertheless, the precipitation at any station is predominantly derived from a few days with heavy rain. It was noted at the end of Chap. 3 that this signifies that the mean resultant convergence field is produced largely by a few short-lived convergence areas attending trains of disturbances. When we glance at time sections of wind, pressure, and weather, not only in the Marshalls but also farther east at Palmyra (6°N , 162°W) and Christmas Island (2°N , 157°W), disturbances are quite apparent. The time sequence is frequently identical to that observed during wave passage over the Antilles.

Palmer has suggested that *in principle* the same type of wave motion is involved. The latitude of maximum wave intensity, however, is much lower so that the waves affect both sides of the equator. Besides, there may exist at times some tendency toward convergence of the basic current,¹ whereas in the western Atlantic all convergence is obtained from the disturbances. This would have the effect of concentrating the activity in a narrow belt and rapidly damping the waves north and south of this belt. This is, in fact, observed. Johnston Island (17°N , 168°W) often remains completely indifferent to the situation $10\text{--}15^{\circ}$ latitude farther south. In the west-central Pacific, where there are more stations, the situation is even more obvious. Strong wave passages, traced from Ponape (7°N , 158°E) across Truk (8°N , 152°E) to Yap (9°N , 138°E), may not be noticeable either at Wake (19°N , 167°E) or even at Eniwetok (11°N , 162°E).

There are other opinions as to the nature of disturbances in the equatorial trough. General discussion of this topic is left for the next chapter. Here we confine the treatment to the wave models developed by Palmer. He considers (a) wave motion in a nondivergent easterly current, (b) wave motion in a convergent easterly current. The width of the current is

¹ Note, however, that on account of the theorem of conservation of potential vorticity *steady* motion of a converging basic current moving equatorward is possible only if the relative vorticity increases more rapidly along the trajectories than the Coriolis parameter decreases (cf. also end of Chap. 12).

taken as 40° latitude, from 20°S to 20°N . This width is not compatible with what we have said about damping. Palmer's models would be more realistic if the width were taken as 20 or even 10° latitude. But the scale factor is immaterial for the following.

Nondivergent Basic Current. Palmer postulates a basic current with speed of less than 5 knots at the equator and a linear increase to 20 knots both northward and southward. The relative vorticity of the basic current is therefore cyclonic everywhere, and its value is uniform. In the undisturbed state streamlines and isobars are parallel.

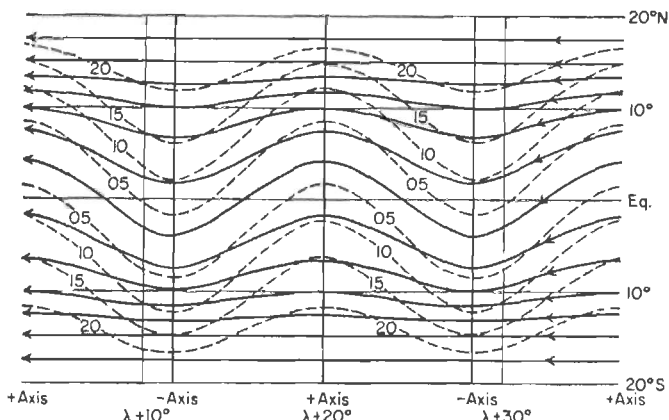


Fig. 9.14. Streamlines and isotachs when nondivergent easterly current on equator is disturbed by waves of small amplitude (10).

Figure 9.14 is a model of 1,500-foot streamlines and isotachs with wave motion superimposed on the current. The field of convergence and divergence is shown in Fig. 9.15, and the pressure field in Fig. 9.16. These diagrams indicate that Palmer is considering waves that move slower than the basic current so that the amplitude of the trajectories is greater than that of the basic current and so that trajectories and streamlines are in phase. The situation, however, is complicated by the shear in the basic current. If the waves propagate at 10 knots, the relative motion will be eastward over a large portion of Fig. 9.14. Since the lines are drawn so that the absolute vorticity is positive (cyclonic) everywhere for the respective hemispheres except in places quite close to the equator, the low speeds raise some difficulties. Palmer's observed winds, however, indicate much higher speeds; we can therefore assume westward relative motion, at least in the vicinity of the convergence and divergence centers in Fig. 9.15.

Since we worked exclusively from the northern-hemisphere viewpoint earlier in the chapter, we shall for a change analyze the situation south

of the equator. The theorem of conservation of potential vorticity, accepted by Palmer as the leading dynamical principle, is independent of any choice of coordinate system so that we can use its various forms as before except that clockwise rotation will now be cyclonic. East of the wave trough shown near $\lambda + 30^\circ$ in Fig. 9.14, the air near 10°S moves

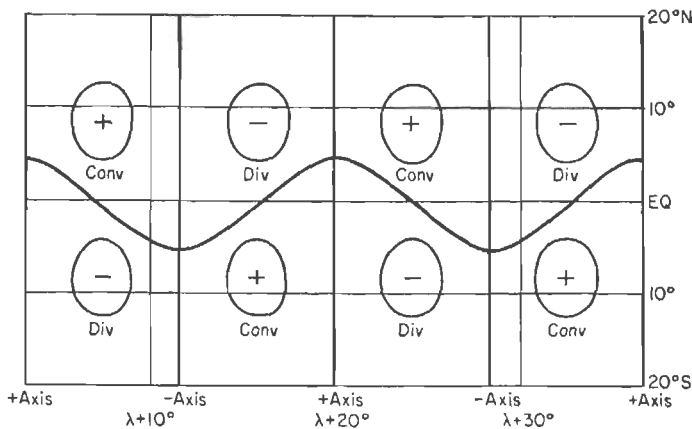


Fig. 9.15. Fields of convergence and divergence for the model of Fig. 9.14 (10).

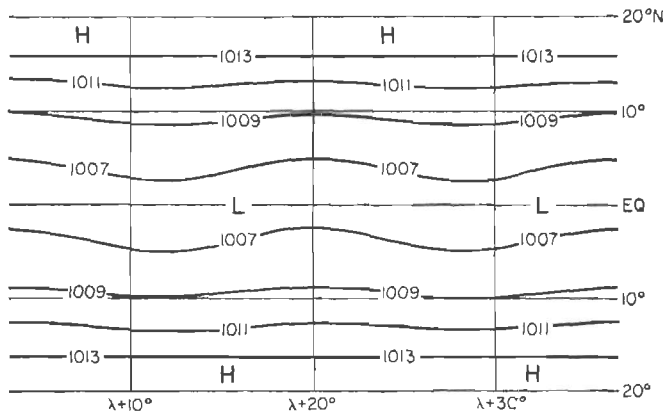


Fig. 9.16. Surface-pressure field for the model of Fig. 9.14 (10).

toward higher latitudes, increasing cyclonic curvature and increasing cyclonic shear. Therefore, according to (9.3), we shall have an increase in Δp and horizontal convergence. West of the trough line the reverse is true, and divergence is indicated here in accord with Fig. 9.15. Farther north and south the situation is less certain, suggesting that the principal bad weather east of the trough will be concentrated in a narrow zone and that, similarly, only a limited area of suppressed convection will be

encountered west of the trough line. Both the areas of above-average and suppressed convection will have a greater extent along rather than normal to the streamlines. In their center we encounter the convergence lines or asymptotes which Palmer's analyses stress.

Palmer also differentiates between the amplitude of streamlines, isotachs, and isobars. The last have the smallest amplitude, suggesting that air crosses toward higher pressure east of the trough lines and toward lower pressure west of them. Consequently, the speed of air particles decreases east of troughs, where we then have a kinetic-energy sink. The

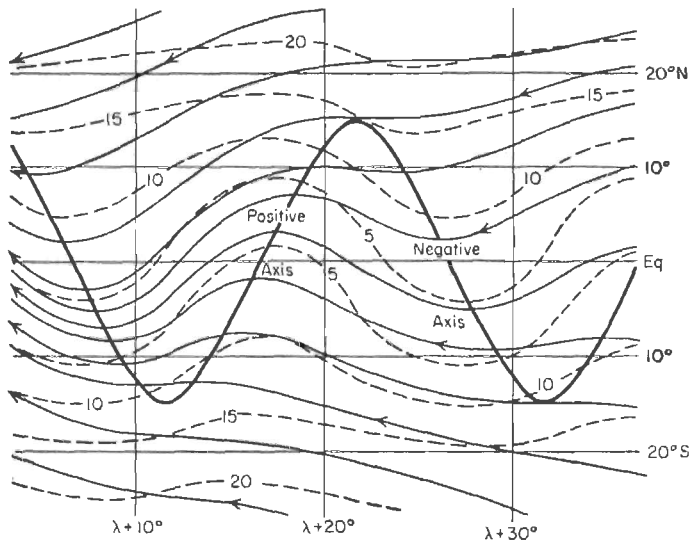


Fig. 9.17. Streamlines and isotachs when convergent easterly current on equator is disturbed by wave train (10).

air gains kinetic energy west of troughs. Such an inverse correlation between vorticity and kinetic-energy changes is frequently observed. The subject has not been further explored; we merely note that, for the indicated speed variations to take place, the trajectory amplitude must be less than that of the isotachs.

Converging Basic Current. Figure 9.17 shows qualitatively how the model of Fig. 9.14 will change when the basic current is permitted to converge. In this diagram the 90° isogon is drawn heavy. Westward amplification and lateral contraction of the wave train are apparent.

We see the corresponding divergence field in Fig. 9.18. The centers of convergence in both hemispheres approach the equator from east to west and increase in intensity; the centers of divergence are also displaced equatorward but weaken. A complete dynamic treatment of these models has not yet been carried through and cannot be attempted here.

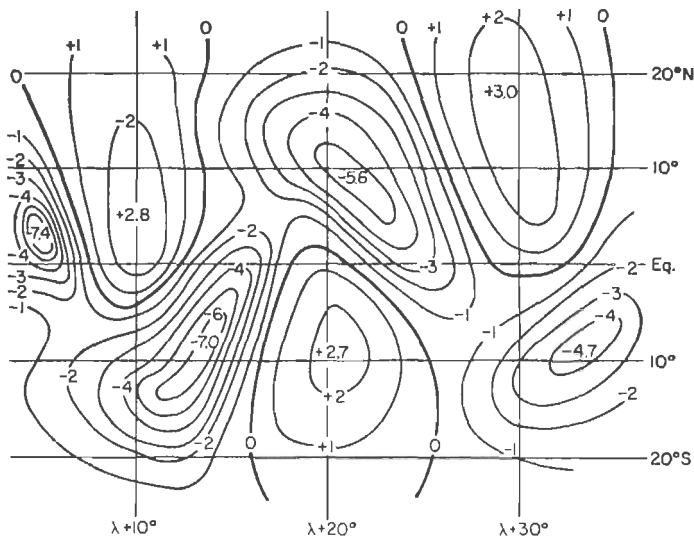


Fig. 9.18. Field of horizontal velocity divergence (10^{-6} sec^{-1}), computed from Fig. 9.17 (10).

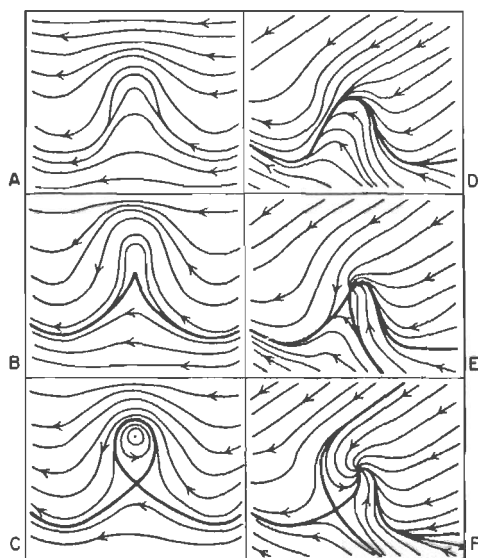


Fig. 9.19. Transformation of streamline pattern during formation of vortex in waves in equatorial easterlies: A-C in nondivergent and D-F in convergent basic current (10).

Palmer finds that at Bikati Island (3°N , 173°E), located not far from the central portion of a wave train at the end of April, 1951, the meridional wind component at 5,000 and 25,000 feet varied out of phase. Presumably, clockwise flow aloft was superimposed on counterclockwise flow below, and vice versa. If this result can be generalized through analysis of other situations, the waves of the equatorial Pacific would differ in more than detail from those of the Caribbean. In the latter we find only slight vertical tilts of troughs and ridges.

Vortex Development. Continued intensification of the convergence areas of Fig. 9.17 may lead to a breakdown of the wave pattern and to vortex formation. This is illustrated in Fig. 9.19 for both nondivergent and convergent basic currents. Palmer points out that a good reason seldom exists for the sequence of Fig. 9.19A-C. The sequence of Fig. 9.19D-F, however, is common, and he backs it on dynamic grounds.

Since the cyclonic crests in northern and southern hemispheres strengthen together, a vortex pair with centers situated on both sides of the equator may form.

REFERENCES

- (1) Bjerknes, J., *Meteor. Z.*, **54**: 462 (1937).
- (2) Cressman, G. C., *Dept. Meteor., Univ. Chicago, Misc. Rept.* 24, Part 2, 1948.
- (3) Dunn, G. E., *Bull. Am. Meteor. Soc.*, **21**: 215 (1940).
- (4) Freeman, J. C., *J. Meteor.*, **5**: 138 (1948).
- (5) Graves, M., *Bull. Am. Meteor. Soc.*, **32**: 54 (1951).
- (6) Haurwitz, B., *J. Marine Research*, **8**: 35 (1940).
- (7) Haurwitz, B., *Dynamic Meteorology*. New York: McGraw-Hill Book Company, Inc., 1941.
- (8) Haurwitz, B., *J. Meteor.*, **3**: 95 (1946).
- (9) López, M., *Bull. Am. Meteor. Soc.*, **29**: 227 (1948).
- (10) Palmer, C. E., *Quart. J. Roy. Meteor. Soc.*, **78**: 126 (1952).
- (11) Petterssen, S., *Quart. J. Roy. Meteor. Soc.*, **78**: 337 (1952).
- (12) Piersig, W., *Aus dem Archiv der deutschen Seewarte*, Vol. 54, No. 6, 1936.
- (13) Regula, H., *Ann. Hydr.*, **64**: 107 (1936).
- (14) Riehl, H., *Dept. Meteor., Univ. Chicago, Misc. Rept.* 17, 1945.
- (15) Riehl, H., *Dept. Meteor., Univ. Chicago, Misc. Rept.* 24, Part 1, 1948.
- (16) Riehl, H., et al., *Am. Meteor. Soc. Mon.* 5, 1952.
- (17) Rossby, C.-G., *J. Marine Research*, **2**: 38 (1939).
- (18) Rossby, C.-G., in *The Atmosphere of the Earth and Planets*, G. P. Kuiper, ed. Chicago: University of Chicago Press, 1949.

CHAPTER 10

SURVEY OF LOW-LATITUDE DISTURBANCES

The disturbances described rather briefly in this chapter are as important as the waves in the easterlies and deserve equal space. But the observational knowledge either is meager or conflicting. Complete models and life cycles cannot be presented. It appears best merely to describe those disturbances for which at least some fairly well established facts exist. A regional treatment cannot be attempted. The reader will realize that here is indeed a rich field for research and discovery, both empirical and theoretical.

Disturbances in and near the Equatorial Trough

At the end of the last chapter we considered what is likely to be the most promising hypothesis about equatorial-trough meteorology. But we noted that other opinions on the structure of the equatorial-trough zone have been voiced. The literature which may be classified under the heading "equatorial trough" is abundant. Most remarkable is the extreme divergence of opinions concerning nature, structure, and life cycle of the disturbances in the trough zone. As usual, when a subject is so controversial we may suspect that large regional and seasonal differences stand in the way of formulating a unified picture. In Chap. 1 we saw that the mean trough position varies regionally over 25° latitude in one season, that it migrates between seasons over a large latitude range in some regions and not at all in others, that the average sea-level pressure and the average vertical wind structure and wind variability are far from uniform along the trough line, and that on mean-wind charts the tradcs converge at a small angle along parts of the trough line, while wind shear up to 180° marks others. This structural diversity suggests that a unified picture will not be achieved until a great deal of fact finding has taken place without attempts at immediate generalization over the world.

Palmer (30, 32) has carried out the most searching investigation of the opinions uttered over the years on equatorial-trough meteorology.¹ He

¹ Since these articles carry an extensive bibliography, few references to original papers will be made.

divided these into three groups, the approach based mainly on climatological reasoning, the approach which seeks to fit extratropical-type solutions to the disturbances of the tropics, and the "perturbation" approach of which Chap. 9 is representative.

There is little need to discuss the climatological method here. Chapters 1 and 3 have shown that the variability of the surface wind reaches a secondary maximum in a narrow zone along the equatorial trough and that the rainfall is largely derived from a few disturbances rather than from uniform daily precipitation. Synoptic charts also leave no doubt as to the existence of traveling disturbances.

The Air-mass Approach. According to the Bergen school of meteorology, the atmosphere consists of several distinct and large bodies of air, called *air masses*, each relatively homogeneous in its properties when located in and near the source region. Movement to other areas, especially long tracks northward or southward, will transform the air masses so that gradients, especially of temperature and moisture, are created within them. By far the largest gradients, however, are found between two air masses of different origin. There are the fronts, which are inclined along the vertical so that the denser mass rests underneath the lighter mass. Usually, though not necessarily, the wind shear across a front is cyclonic. Little is known about the dynamics of front formation. Once they exist, however, attention focuses on them, as much bad weather occurs along their length. Wavelike deformations of frontal surfaces often grow to become cyclones. This growth can be followed reasonably well with qualitative dynamics.

To what extent can this concept account for and predict the bad weather in the tropics? Palmer emphasizes that we must distinguish clearly between the observations and theories concerning fronts. Observationally, the equatorial-trough zone or parts of it may show the wind and weather patterns found along fronts in middle latitudes. Bad weather frequently takes the form of long lines of cumulonimbus, with cirrus in the outskirts; a rapid wind shift may accompany the cloud lines. Surface-temperature falls, sometimes temperature falls aloft, accompany the arrival of the disturbed weather. According to the air-mass hypothesis, differences in temperature between the cooler trade of the winter hemisphere and the warmer trade of the summer hemisphere cause the temperature changes and the observed vertical slopes of the wind-shift lines. The two trade air masses take the place of polar and tropical air in the temperate zone.

Palmer says, "To most tropical meteorologists, after 1933, these discoveries were sufficient to identify the bad weather lines as fronts, and since they made no distinction between the empirical and the theoretical front, they adopted the entire high latitude apparatus of frontal and air-

mass analysis and forecasting. . . . Having decided that fronts and airmasses existed in the tropics, the frontal analysts of the decade 1933-1943 were concerned to describe and classify the major discontinuities of the tropics." Although several semipermanent frontal zones were found, the equatorial-trough zone stood out. Those who were concerned with the differences between northern and southern trades coined the term "intertropical front," supported by the most respected authorities (6). Others, who like Brooks and Braby (9) felt less certain about the reality of the often-elusive temperature contrast, preferred the name "equatorial front." Gradually it became apparent that the lowest surface temperatures are inside the disturbed zones, produced by evaporation from falling rain and lack of direct sunshine. On the outskirts of the zones the temperature is uniform on both sides. This has prompted a large group of meteorologists to adopt the name "equatorial" or "intertropical convergence zone" and devise new color schemes for chart representation.

Following the frontal hypothesis, intensification of the frontal zone was thought to follow cold outbreaks from the winter hemisphere. This would sharpen the temperature contrast and produce a movement of the front away from the equator. The air crossing the equator would turn toward the east, following the principle of conservation of absolute angular momentum or certain forms of the vorticity theorem (20). This would increase the wind shear, therefore also the shearing instability across the front, favoring formation of hurricanes.

The frontal viewpoint has been presented at length. It represents the only attempt to account fully for all that happens in and near the equatorial trough, and many arguments will pass before the last word on the theory has been spoken. The author believes, with Palmer, that the system of causes and explanations is open to serious doubt and that the observations must be interpreted differently. Why the hypothesis of origin of tropical storms definitely cannot be accepted will be shown in the next chapter. Concerning the body of the air-mass hypothesis Palmer states that "this theory failed to pass the test to which all theoretical work in meteorology must finally come; it was found almost useless as a guide to short period forecasting in low latitudes." The "fronts" do not behave as expected. They do not move with the speed of the wind normal to them; worse, they often appear to "jump." Their vertical slope changes rapidly, often from one observation period to the next. Detailed reports demonstrate that several areas with pronounced horizontal shear can coexist in the equatorial trough within one region such as the western Pacific but that the shear zone need not be continuous (40). These and numerous other complications have given rise to a literature anxious to save the frontal concept by introducing such modifications as

would in principle reconcile the observed weather sequences with the classical model.

Rejecting these "attempts to patch and doctor the frontal theory," Palmer recognizes that we owe the discovery of organized lines of cumulonimbus to the frontal workers. These lines do not move with the wind; nor are pressure changes useful in forecasting their displacement on many occasions. They may develop in air masses which, within the limits of observational error, are completely homogeneous in the lower troposphere. In the high troposphere the direction of the temperature gradients is variable. Palmer states, "Density contrast and cyclonic shear are conditions which are neither necessary nor sufficient for the formation of convergence lines and hence these lines are not fronts in the sense that that concept is employed in the frontal and airmass theory. . . . With these conclusions we must dismiss the whole body of theoretical explanations developed by the airmass school in the tropics, but at the same time we must incorporate their empirical findings. . . ."

One further point may be added. We have seen in Chaps. 1 and 2 that, in annual and seasonal means, trough position and movement correlate well with those of the warmest belt. Trough displacement from the equator affords air from the winter hemisphere a longer trajectory in the tropics and therefore more time for modification. *The trough is placed so that northern and southern trades reach it after complete equalization of their thermodynamic properties.* Thus the atmosphere seeks to avoid a density discontinuity at the meeting point of northern- and southern-hemisphere air.

Concerning terminology, it will be well to use only the name "equatorial trough." Like "equatorial westerlies" (Chap. 1), a causal connotation is not implied; the name merely refers to the geographic fact that a trough of low pressure exists in the equatorial zone. About this there can be no controversy. It is never advisable to put too much in a name so that the case may be overstated. We must reject the term "front"; likewise "convergence zone" is objectionable since often there is no convergence. If the shear of the horizontal wind within the equatorial trough is large, say greater than 90° , this fact may be emphasized by speaking of an "equatorial shear line"; this again is a factual term which cannot give rise to arguments.

The Perturbation Approach. Even at the peak of acceptance of the airmass theory some voices of doubt could be heard. Outstanding is Schnapauff's (45) investigation of the equatorial trough in the eastern Atlantic. Detailed analysis led him to the view that the equatorial trough in this region contains only a "front of momentum," i.e., a sharp cyclonic wind shear, rather than a density discontinuity. His work on the vertical temperature distribution in the trough (Fig. 2.27), moreover,

placed the classical simple heat-engine theory of the equatorial zone in doubt. At the surface the highest temperatures occupy the equatorial-trough zone; higher up the temperature gradient reverses and the trough contains the coolest air.

Subsequent to the work of German meteorologists in the Atlantic, active work shifted to the Pacific Ocean. Alpert (4) thoroughly covered the climatology of the eastern equatorial Pacific. He further was able to show (3) the synoptic low-level structure of the wind field with the aid of a very dense coverage of aircraft reconnaissance reports. Simpson (46) found a temperature field in the eastern Pacific similar to Schnapauff's. Figure 10.1 is a typical cross section. Fletcher (16) noted that the convergence zone often is not a simple line but has a complex character.

Palmer's main concern has been the central and western Pacific (30, 32). In treating this region he attempted to consolidate the previous work into

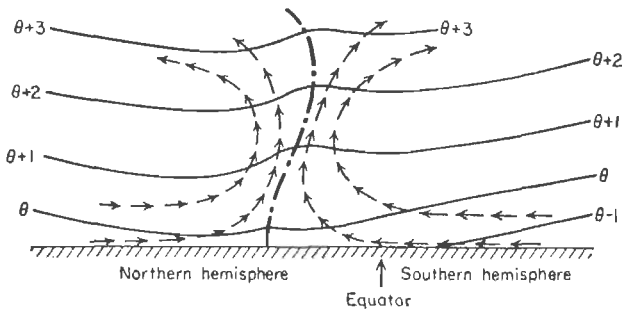


Fig. 10.1. Cross section of potential temperature through equatorial-trough zone in eastern Pacific (46).

as unified a picture as possible. It will be helpful to consult Fig. 1.7 in order to follow his ideas. Over the east-central Pacific, wind constancy is very high; in this area the equatorial-trough position oscillates but little. Small disturbances that perturb the flow along the trough either are brought into the area or develop there. They then move downstream as waves in the equatorial easterlies; we have described these waves in Chap. 9. Convergence in the basic flow tends to amplify cyclonic crests and dampen anticyclonic ones. If the axis of symmetry for the waves is on the equator, both northern and southern crests of the waves represent cyclonic circulation and will be intensified by convergence. This may lead to a distribution of wind and weather similar to that sometimes referred to as "double equatorial front."

If the axis of the wave train lies at a considerable distance from the equator during the northern-hemisphere summer, a common occurrence, the southern clockwise eddies may take on the character of anticyclonic cells in the northern hemisphere. Convergence will then prevent their

growth, and west of 160°E we mainly find intensifying cyclonic disturbances, with a train of weaker clockwise cells nearer the equator.

Palmer notes that with continued amplification closed circulations finally appear in the wave crests (Fig. 9.19). After their formation westerly winds appear for the first time near the equator. He then contends that the equatorial westerlies (of Fig. 1.7) "are merely the mean expression of the fact that the vortices form in the central parts of the Pacific and move toward the west; there the passage of so many of them (with amplification) north and south of the equator and in both the wet and dry season results in a mean west wind on the equator in the western parts of the oceans. Since this west wind is the statistical result of the vortices it is clearly fallacious to import them into a hypothetical general circulation which is then perturbed to produce the vortices."

Palmer charges the older approaches to equatorial meteorology with this error. Because an equatorial convergence zone can be found readily on mean maps, it had been assumed that it would exist on all daily charts. There is little doubt that Palmer's viewpoint is correct within certain limits. The charts he has published, however, cover too limited a longitude range to illustrate the equatorial-trough structure over larger areas. A series of charts¹ showing a greater longitude range has been published by the author (40) and his associates (22, 23). These indicate that the equatorial trough contains not a simple convergence zone along its entire length but rather a system of eddies which, at least east of $130\text{--}140^{\circ}\text{E}$, may be interpreted as equatorial waves. A first sign of instability leading to typhoon formation is sudden clockwise turning of one portion of the trade stream. Therefore we must discount one factor frequently called upon to account for deepening; the juxtaposition of two air masses with different momentum.

Figure 10.2 illustrates the typical low-level flow over the central and western Pacific during the rainy season. The lines or zones of strongest cyclonic wind shift are marked by heavy lines. Three troughs are apparent in the easterlies: at 120°E , 150°E , and 180° . The westernmost trough has already deepened and contains a typhoon; the middle one is about to start deepening. Nearer to the equator one large clockwise eddy is centered near 140°E , about halfway between the two western troughs. A weaker clockwise crest appears near 165°E , and there are indications of a third one at the eastern border of the map. No air flows northward across the equator between 170°W and 135°E , nor are there any equatorial westerlies east of $145\text{--}150^{\circ}\text{E}$. Thus the broad outline of the wave model can be seen, but the wave length, at least superficially, is double that of

¹ The lines of streamline convergence and divergence which Palmer stresses are largely missing on these charts, since routine data seldom suffice to place these lines except by way of hypothesis.

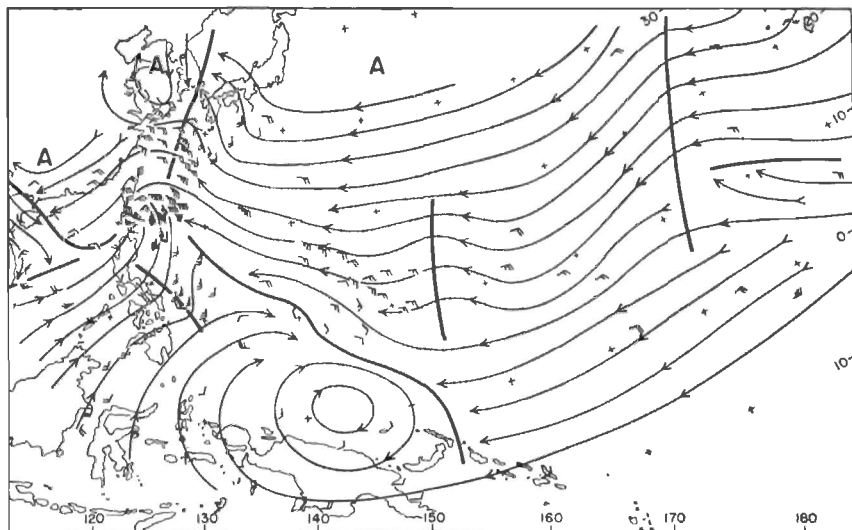


Fig. 10.2. Streamlines at 1,000 feet, Sept. 10, 1945 (40).

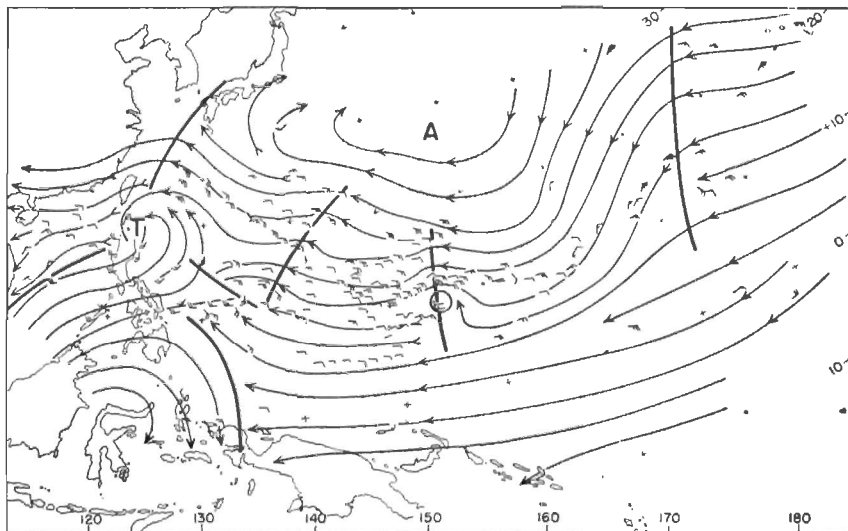


Fig. 10.3. Streamlines at 10,000 feet, Sept. 10, 1945 (40).

the average of 15° longitude. This, as happens frequently, is due to the fact that analysis of a wave train in the easterlies is least definite near the ground. At 10,000 feet (Fig. 10.3), an intermediate disturbance west of Guam is plainly evident, and also a splitting of the clockwise eddy to the south.

Figure 10.4 shows another case, in many respects similar to Fig. 10.2. Again, the counterclockwise crests are narrow and intense, the clockwise ones weaker and more spread out. As in Fig. 10.2 the equatorial westerlies are produced by the intensifying wave crests and in this case also by a disturbance in the South China Sea.

The time sections for Tarawa and Palau reproduced in Chap. 1 (Figs. 1.24 and 1.25) are for the same period as Figs. 10.2 and 10.3. The steady low-level flow at Tarawa contrasts with the agitation in the wind field farther west. At Palau, the westerly winds are confined to a

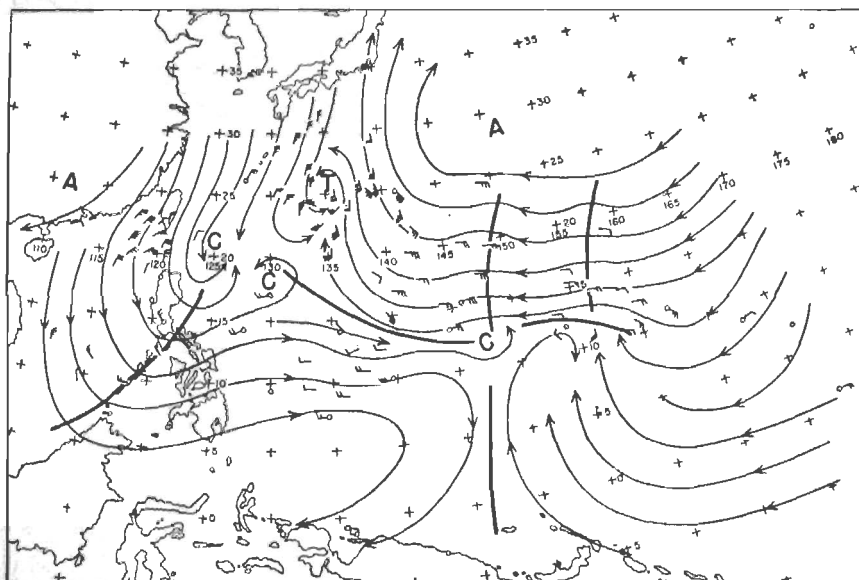


Fig. 10.4. Streamlines at 1,000 feet, Oct. 4, 1945 (23).

shallow layer, and this is often true east of the Philippines. At 10,000 feet, hardly a trace of the surface westerlies need be found. In Fig. 10.3 we find westerlies only far to the south and west of those in Fig. 10.2, and their longitudinal extent is much smaller. To the extent that thermal reasoning can be invoked, this accords quite well with the fact that trough position and surface thermal equator coincide. It disagrees superficially with the findings of Schnapauff (45) and Simpson (46), who observed a cold-core structure of the trough above the lowest levels. Recalling Fig. 1.19, this is not surprising. Since the sign of the average meridional temperature gradient aloft changes with longitude, the vertical structure of the equatorial trough must also change. The equatorial-trough zone is no more homogeneous aloft along its whole length than at the surface; we cannot compress all the data into a single model.

On account of the structural differences along the trough, doubt remains as to the extent to which Palmer's model can be generalized around the globe. He himself is careful to refrain from extensions such as others have attempted and which have been proved untenable. Over most of the western Pacific the equatorial westerlies encountered in the northern-hemisphere summer doubtless are not a basic current. But what can be said about the broad band of westerlies which blow fairly steadily between Arabia and the South China Sea? The depth of these westerlies is not always shallow; close to the equator Deppermann (15) finds an average depth of up to 15,000 feet. Bossolasco (8) has observed westerly winds throughout the troposphere for prolonged periods over equatorial East Africa. In the Belgian Congo it has been possible to demonstrate from the track of rain areas carefully analyzed with a dense network of rain gauges that disturbances often propagate eastward (10); such eastward displacement may also occur over the South China Sea and the Philippines (23). The cumulative weight of this and other evidence indicates that not all equatorial westerlies result from deepening vortices in easterly currents. Over broad areas in certain seasons these westerlies should be regarded as part of the system of basic zonal currents.

The Upper Troposphere in Summer

The exploration of the high troposphere has been handicapped even more than that of the lower layers by scarcity of observations. Its history is brief; little more than a glimpse of high-level wind patterns has been gained. This sketchy information has confirmed beyond doubt the suspicion that the leading role for many weather developments must be placed in the layer of 200-mb thickness under the tropopause.

In the western Atlantic one rarely finds a surface equatorial trough outside Panama and Central America at a considerable distance from the equator. Aloft, Bigelow (5) and Georgii and Seilkopf (18) deduced at an early date the prolonged presence of cyclonic shear zones at high levels from upper-cloud drift data. Their findings have been summarized by Stone (52). Since the beginning of high-level wind observations the existence of high-level shear lines, oriented mainly east-west, has been shown to be a frequent map feature (38, 39). The surface layer often gives no indication of these shear lines, while aloft the cyclonic turning of the winds may attain 180° . In the northern hemisphere, east winds prevail to the north and west winds to the south of the lines.

Figures 10.5 and 10.6 show a well-documented case of an Atlantic shear line. At low levels, an equatorial-trough zone overlies the western Caribbean and Central America, attended by a widespread middle- and high-cloud overcast and precipitation. The shear line slopes northward

with height over the bad-weather area, in contrast to the western Pacific in Figs. 10.2 and 10.3. It also increases in eastward extent. East of Cuba it cannot be detected in the 5,000-foot flow; at 30,000 feet it is impossible to tell where it ends. North of the shear line we find an anticyclone with nearly vertical axis centered between Bermuda and the middle Atlantic coast of the United States. To its south a second clock-

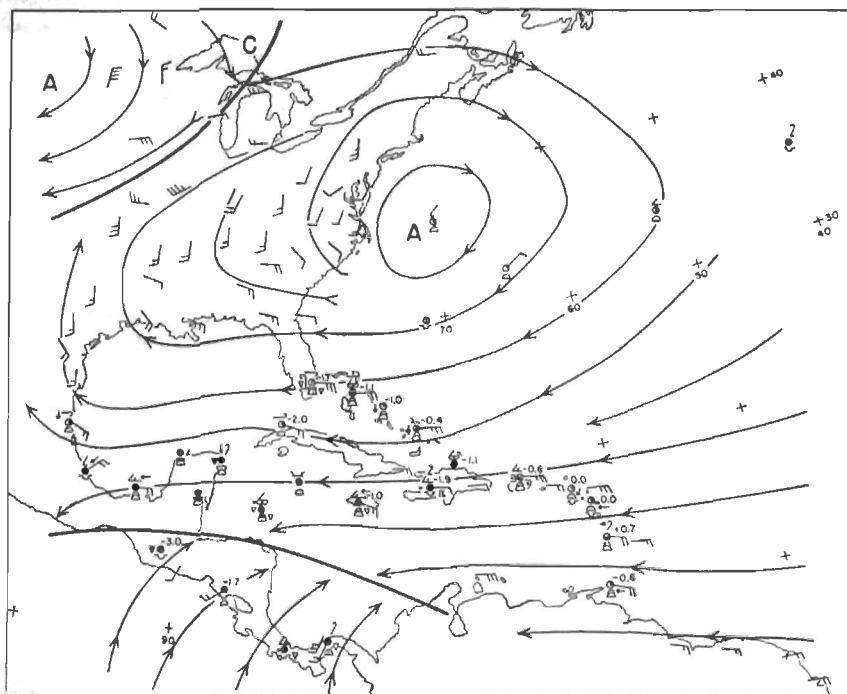


Fig. 10.5. 5,000-foot winds, surface 24-hour pressure changes, and weather, Sept. 27, 1945 (39).

wise circulation, extending at least to the equator, appears in the high troposphere.

The northern high, very large at low levels, diminishes in size with increasing altitude. Such shrinkage is typical of nearly all subtropical highs. Sometimes of huge size and covering most of an ocean at the surface, they invariably split into two or more cells aloft. Very frequently these cells are arranged as in Fig. 10.6; they are centered roughly on the same meridian and are therefore called "meridional highs." The double-band structure of the upper westerlies, with a separation of 25° latitude between the cores, is highly suggestive of what appears to be a universal general-circulation feature: *a finite latitudinal width of 20–30°*

latitude for the disturbances in the upper air. On most days three or four such belts can be distinguished between pole and equator, as given by the axes of the westerly jet streams and the centers of departure of west-wind speed from the average (cf. end of chapter).

The west Atlantic shear line of late September, 1945, persisted for an unusually long time, about a week. During this period waves in the lower easterlies could not be traced. Subsequent to Oct. 3 the whole

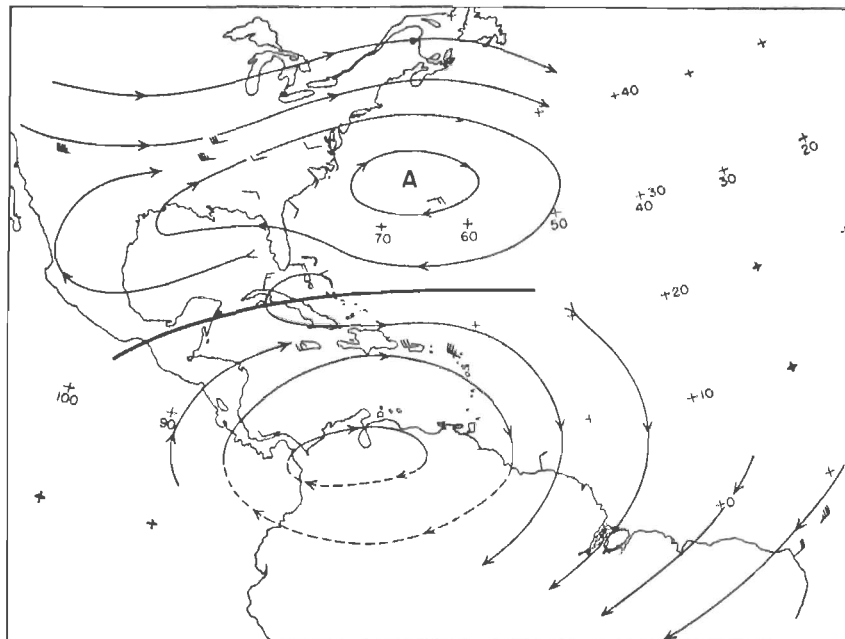


Fig. 10.6. Winds at 30,000 feet, Sept. 27, 1945 (39).

system moved northward as the long waves in the westerlies became progressive, and a trough approached the east coast of the United States. At the same time the shear line began to be observable at low levels across the whole Caribbean. We witness the rare spectacle on Oct. 6 of this shear line crossing the Antilles (Fig. 10.7). This must be regarded as an equatorial-trough type of feature. The wind shear at 5,000 feet has attained 180° . In the north we note the eastward displacement of the long wave pattern by somewhat less than one-half wave length compared with Figs. 10.5 and 10.6.

The detailed observations at San Juan, Puerto Rico, during these days (Fig. 10.8) reveal much about the structure of the disturbance. At first, as the surface pressure falls, convection is intense and the low-level winds are very high and gusty. Deep easterlies prevail on Oct. 4, with little

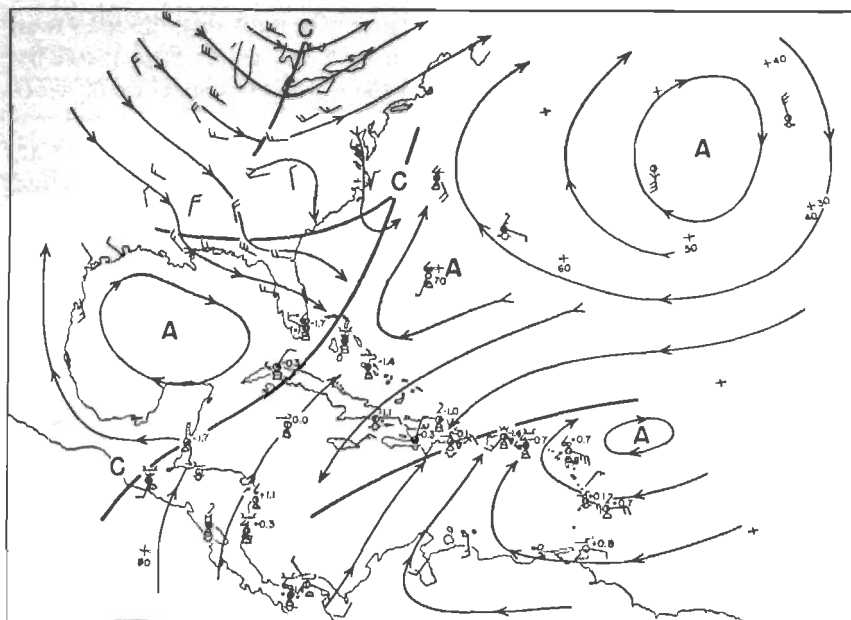


Fig. 10.7. 5,000-foot winds, surface 24-hour pressure changes, and weather, Oct. 6, 1945 (39).

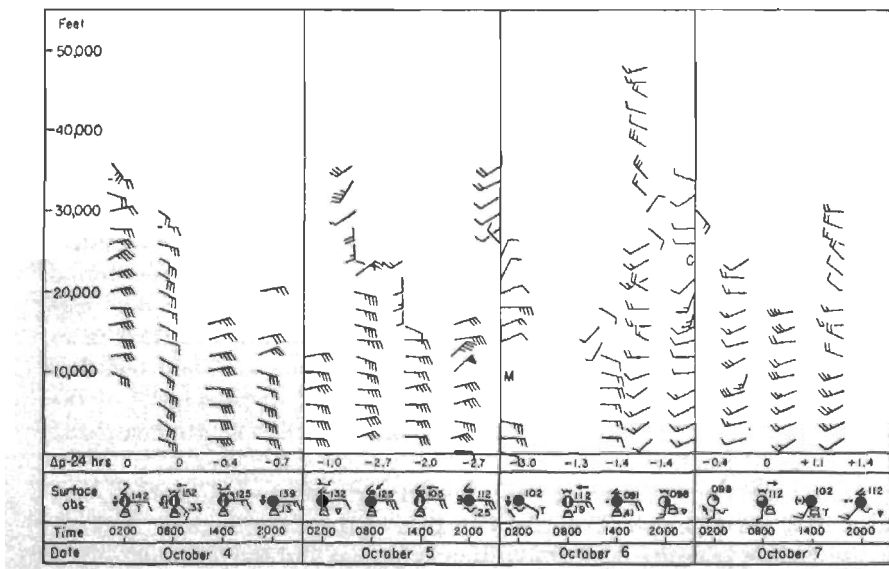


Fig. 10.8. Vertical time section at San Juan, Puerto Rico, Oct. 4-7, 1945 (39).

upward-speed variation. On Oct. 5, the base of the equatorial westerlies first appears above 30,000 feet, later at 25,000 feet. On Oct. 6, it drops to the surface as the pressure falls diminish and the sky suddenly clears for 18 hours. Deep westerlies of nearly uniform strength prevail on Oct. 7.

The two wind soundings that penetrate from easterlies to westerlies show what is quite typical, a rapid change from lower- to upper-wind system through a narrow transition layer. From the viewpoint of geostrophic advection not much temperature change would be expected. Nevertheless the changes that occurred are large for low latitudes. Pressures and temperatures aloft decreased on Oct. 4. Then the temperature began to rise at all levels, at first slowly, later more rapidly. By Oct. 6, the whole troposphere had warmed by 3 to 6°C. While the surface pressure dropped 4 mb between Oct. 4 and 6, the 300-mb height rose 400 feet. This clearly reveals the warm-core structure of the surface low-pressure trough and the cold-core structure of the upper shear line as well. Such a structure, confirmed in many later situations, could also have been inferred from the vertical slope of the system and the fact that the shear lines, unlike Figs. 10.5–10.8, often cannot be detected much below 500 mb. A narrow band of cold air extends along their axis; temperatures are higher in the outskirts both to north and south.

Middle and high cloud decks, coupled with lower cumuli, may extend across the whole system (Figs. 10.5 and 10.7), but the bad weather is most intense between surface and high-level position of the shear line. Here the upper southwesterly current is bringing in warmer air; yet the cold-core structure aloft is maintained, sometimes intensified while the air passes through the shear line. It follows that the observed thermal structure cannot be advectively produced and must have dynamic origin.

With this we have arrived at one of the principal paradoxes of tropical meteorology, the cold core frequently observed in areas of intense precipitation. The temperature lapse rate of the normal tropical atmosphere somewhat exceeds the moist-adiabatic rate, and the humidity near the ground is very high (Chap. 2). Large-scale ascent of surface air should lead to upper warming in the broad-scale convection areas. The rise of mean virtual temperature should increase the vertical distance between isobaric surfaces. Yet the air in the rain areas is denser than in the surroundings in many cases.

No complete explanation can be offered of these observations, which are a major hindrance to the understanding of tropical weather systems. Several possible solutions can be advanced, however, any one of which may give the correct answer in certain classes of situations:

1. The shear lines are cold aloft relative to their surroundings, not because of cooling inside, but because of warming outside. While this

hypothesis is appealing from the energy viewpoint, there are cases where it cannot be used; it can be shown that we are concerned with negative, not positive, temperature anomalies.

2. The mean tropical atmosphere and most individual soundings are conditionally unstable only up to about 500 mb. Higher up the lapse rate is slightly less than moist-adiabatic. Suppose now that the rain comes partly from altostratus, an occurrence far more common than once thought. We can then postulate ascent and formation of clouds and rain mainly above 500 mb, a sequence also suggested by some though not all of the data. If the ascent is moist-adiabatic and starts at 600-500 mb from columns which have the temperature structure of the mean tropical atmosphere, the equivalent potential temperature of the ascending mass will be 340.5°A , when the air is initially saturated. The difference in temperature between the rising air and the mean tropical atmosphere will be as follows: -1°A at 400 mb, -2° at 300 mb, -3° at 250 mb, and -4° at 200 mb. If the air is not saturated initially, the temperature differences will be even larger. On this basis most observed temperature gradients could be explained. The energy to raise the air and maintain the circulation has to be provided by an unknown outside source.

3. Deep air columns ascend, reaching from the ground to at least 400 mb. The level of nondivergence is high, perhaps at 500 mb. Since the air is initially unsaturated, it will begin to ascend dry-adiabatically. Column (A) of Table 10.1 gives the amount of cooling realized if the mean tropical atmosphere is lifted 55 mb, that is, if the surface air is

TABLE 10.1. TEMPERATURE CHANGES AT CONSTANT-PRESSURE SURFACES THAT RESULT (A) IF MEAN TROPICAL ATMOSPHERE IS LIFTED 55 MB; (B) IF SUFFICIENT SURFACE AIR IS TRANSPORTED ALOFT TO MIX WITH THE UPPER AIR IN EQUAL AMOUNTS

p , mb	T , $^{\circ}\text{C}$ (A)	T , $^{\circ}\text{C}$ (B)
900	-2.0	-1.5
800	-2.5	-1.0
700	-3.0	-1.5
600	-2.5	-1.0
500	-3.0	-0.5
400	-3.0	0.0

brought to condensation. During and subsequent to this ascent convective towers penetrating from below will mix with the lifted masses. This mixing will take place through entrainment, as discussed in Chap. 5. But the problem is a different one. The entrainment computations con-

sider an environment at rest. The cloud temperatures therefore cannot be lower than those of the environment except where downdrafts or evaporation of raindrops is important. Now, however, we are considering the temperature structure of a synoptic convection zone as a whole relative to its surroundings in a large-scale sense, resulting from prolonged ascent with mixing. This structure is brought about by dry-adiabatic lifting of the clear areas modified by the building and dissipation of many cumuli. While individual clouds will still be warmer than their immediate surroundings, the convection zone as a whole can become colder, in a broad-scale sense, than its environment, depending on the rate at which air from the subcloud layer is transported upward in the clouds.

Column (B) of Table 10.1 shows the cooling that will result if air from the subcloud layer moves up moist-adiabatically and then mixes in equal amounts with air having the properties given in column (A). The computation is handled as it is in Chap. 5, except that the entrainment rate has been fixed at 50 per cent and the temperature in the final state has been equalized over the whole disturbed zone. Again reasonable values of cooling are obtained, capable in many instances of accounting for the observed temperature gradients. Again it is difficult to see how the circulation can be driven through conversion of latent heat into kinetic energy.

Inspecting Figs. 10.5 and 10.6 from the dynamical viewpoint, we find that the cyclonic shear and therefore, in view of the pattern of streamlines in Fig. 10.5, the absolute vorticity increases in the trade-wind air and in the equatorial westerlies approaching the shear line in the western Caribbean at 5,000 feet. If we adopt solutions 1 or 3 above, the correct sign of the vorticity change in the upper troposphere is also readily obtained. The lower columns penetrate into the upper anticyclonic flow as they rise. They thus acquire anticyclonic relative vorticity while diverging aloft. Solution 2 also is dynamically feasible. As the clockwise cell over the Caribbean increases upward in strength, ascending sheets in this cell successively reach levels where the vorticity is more anticyclonic. Here too the proper relation between vorticity change and divergence is obtained. Reversing the argument, we could say that a current which is ascending and diverging aloft will have to build a circulation of the type seen in Fig. 10.6. It should be added that the absolute vorticity in the cell is positive from the northern-hemisphere viewpoint, at least north of 10°N .

Jet Streams. Rawin soundings of later days suggest that the meridional cell structure of Fig. 10.6 and especially the westerly clockwise curving current over the Antilles did not nearly attain the greatest intensity at 30,000 feet, that in fact the strongest increase took place above this level. This is a common feature of tropical circulations, as

brought out at the end of Chap. 1; it has been encountered in summer even in jet streams over the central United States (27). In Figs. 10.9 and 10.10 we see a Pacific situation which in some respect resembles Fig. 10.6. But the charts are for the 200-mb surface, situated in the

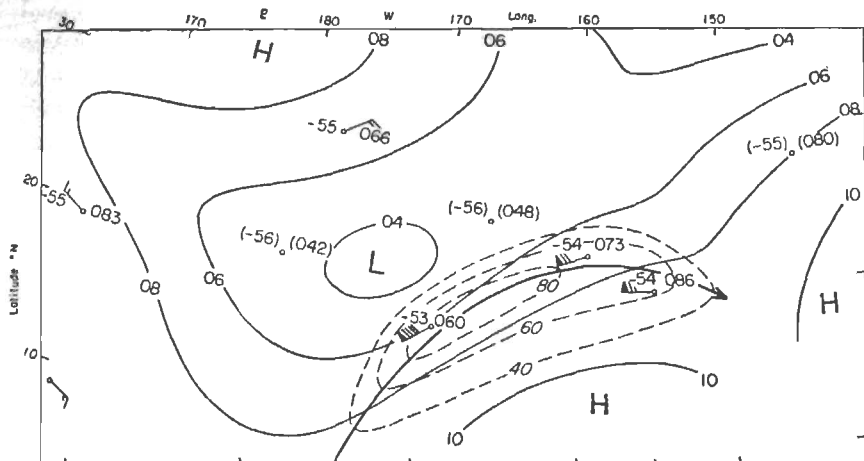


Fig. 10.9. 200-mb contours (100's feet) and isotachs (knots) (dashed) for the central tropical Pacific, July 24, 1951.

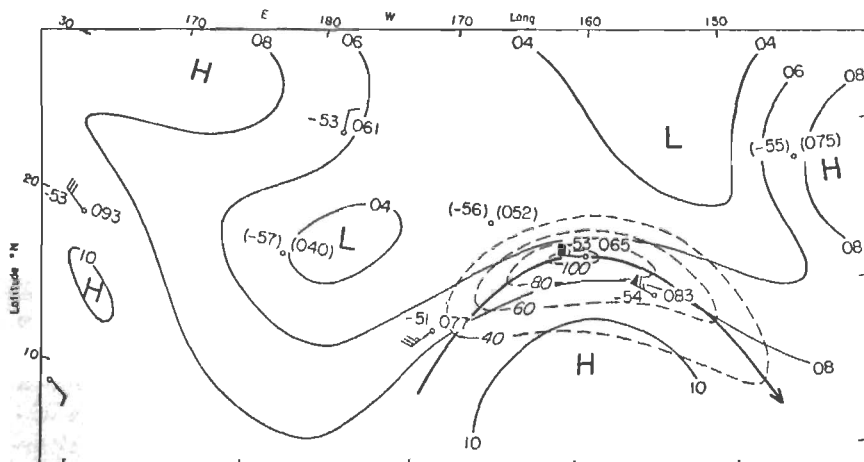


Fig. 10.10. Same as Fig. 10.9 for July 25, 1951.

layer in which the kinetic energy of the high-level perturbations attains its maximum. Previous history proves definitely that the high-velocity current does not come in as a split-off from a larger jet stream in the northwest. A check with maps and station data south of the equator also does not reveal anything that would make it possible to relate in a

definite way the jet development to an incursion of southern-hemisphere air across the equator. It would appear that the jet stream whose center passes near Johnston Island (17°N , 168°W) on July 24 and over Hawaii on July 25, 1951, originated in the equatorial central Pacific.

The existence of currents with wind speeds in excess of 100 knots at latitudes $15\text{--}20^{\circ}\text{N}$ in July had not been suspected previously. Their organization and maintenance are as difficult to understand in low as in high latitudes. It is true that owing to the lesser Coriolis force a much smaller pressure gradient can "balance" such winds in the tropics compared with the temperate zone. But the amount of energy conversion needed to produce the winds is independent of latitude. It is therefore highly significant that the temperate zone with its large temperature contrasts does not produce jet streams whose central speed averages significantly higher in July than those of the tropical Pacific. It must follow either that the mechanism of energy conversion differs in high and low latitudes, involving potential energy in the one and latent heat energy in the other case, or that if potential-energy release accounts for jet streams at all latitudes, the efficiency of the machinery in low latitudes is much higher. It is beyond doubt that progress toward the ultimate solution of the problem of wind production will be greatly accelerated by a comparison of all latitude belts.

Trains of Vortices. Interwoven with the upper disturbances just described are trains of high tropospheric vortices. In fact, we may suspect from Fig. 10.6 that a high-level cyclonic center is situated in the central Atlantic and that another may be found in the eastern Pacific. The low-latitude westerly jet streams appear only intermittently and over limited longitude bands in summer. Instead we find other circulation patterns at other times; of these Fig. 10.11 is typical. This 200-mb chart is for the same date as Figs. 10.2 and 10.3 and therefore affords an interesting comparison between high and low levels. The dashed line represents the "equatorial front" as copied from official analyses. It is clear that even if this line were correct, good forecasting would be difficult unless the 200-mb chart were consulted.

The vortices of Fig. 10.11 are centered near 20°N ; their north-south extent is roughly 20° latitude or a little more; the spacing averages 45° longitude between cyclonic centers. This spacing may be regarded as the wave length of a train of waves in air with zero basic current (Fig. 1.16) so that the perturbations appear as closed circulations. In angular measure the wave length indicates a wave number of 8 if the vortex train extends around the hemisphere. A suggestion that such a wave number is found in the monthly mean is given by Fig. 1.18. In linear measure the wave length corresponds to a wave number of 5 at latitude 50° and four at 60° . Since these values are realistic for the long waves in the

westerlies, it follows that the tropical vortex train has the same linear wave length as the long waves in the polar westerlies.

High- and low-level wave lengths differ over the tropical Pacific. The number of waves in the lower easterlies as observed at 10,000 feet (Fig. 10.3) is double that of cyclones at 200 mb. The westward displacement of the upper vortices in September, 1945, was about $6\frac{1}{2}^{\circ}$ longitude per day, an amount very nearly equal to the speed of the lower easterlies. A given station, therefore, experiences passage of one upper "wave" per week, in view of the wave length. In the lower troposphere roughly two

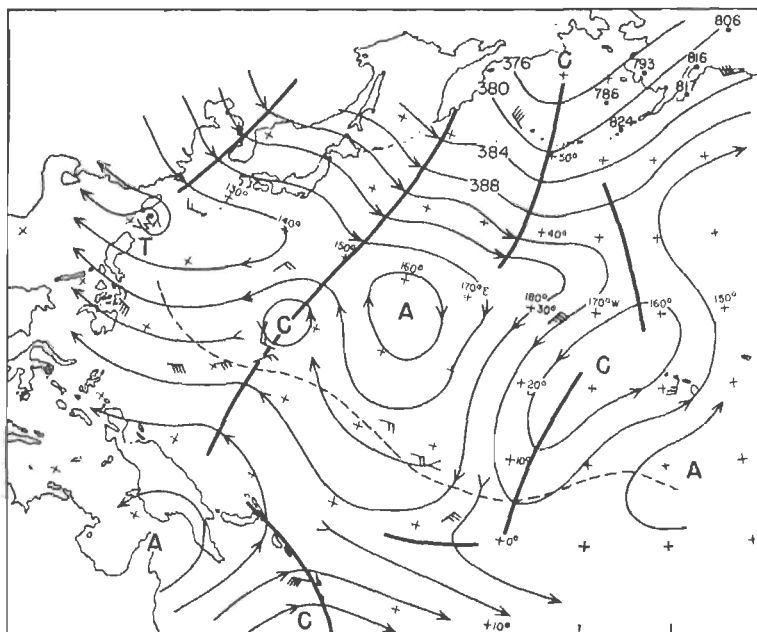


Fig. 10.11. 200-mb streamlines, Sept. 10, 1945 (40).

wave passages may be expected in this time. These observations lend support to the characterization of the low tropospheric disturbances as true waves. While initial perturbations no doubt are frequently derived from upper troughs or cyclones, the frequency of waves in the easterlies in the final state is entirely different from that at high levels. Responding to different properties of the atmosphere below 500 mb, a different type of low-level perturbation is excited. It is not without interest here that a wave length of 15° longitude can be easily recognized in Fig. 10.3 in the western but not in the central Pacific. There we observe mainly a lower reflection of the upper disturbances, but we should suspect that another wave crest, still of very small amplitude, is being developed mid-

way between the two eastern troughs. This postulated system actually reached the Marshall Islands late on Sept. 12 at the proper time, as shown by weather and wind reports.

Comparing high and low latitudes, we find long and short waves in both belts. The short waves in the lower easterlies correspond in wave length to the cyclones of higher latitudes. The high tropospheric vortices of low latitudes are comparable with the long waves in the polar westerlies. The long waves are considered as inertia oscillations arising from latitude changes of air particles as described in Chap. 8, but little is known about the dynamics of systems of vortices. Here we merely note certain observable characteristics of vortices and basic zonal currents within low latitudes, all of which differ greatly from the structure of high-latitude currents and long waves. Both in high and in low latitudes the troposphere is divided in two portions. One of these is characterized by extensive zonal currents, the other by vortices. In extratropical regions we find vortices near the ground that are overlain by a wavelike westerly current. In low latitudes, on the contrary, there is a broad zonal current with waves near the ground. Above it we meet trains of vortices.

For most of September, 1945, westward progression of the vortices continued more or less without interruption. Such steady motion is possible only if the boundary between the circulations of low and middle latitudes is well marked and maintained and if it does not suffer large displacements in latitude. When the boundary undergoes large variations, or if it is located at an appreciably lower latitude than in Fig. 10.11 (35°N), steady westward motion in the tropics cannot be expected because of interference by the westerlies. Toward the end of September, 1945, a trough of great intensity developed in the westerlies east of Japan (22). As this trough advanced toward the central Pacific (Fig. 10.12), its influence and that of the associated westerly current penetrated to latitude 20° , halting the westward march of tropical vortices at 200 mb and disrupting the train.

Figure 10.12 shows another feature of the high tropospheric circulation, sometimes referred to as "northwest break-through." Ahead of the trough advancing eastward from Asia a cyclonic shear zone oriented northwest-southeast had begun to develop on the preceding day, drawing northward a cyclonic member of the tropical vortex train. On Sept. 26, the break-through was complete and the upper cyclone nearly absorbed into the westerlies. Such a development bears a close resemblance, at least by pattern, to what has been termed "blocking" (36); it must be anticipated when the westerlies intrude into the lower latitudes while a dynamic anticyclone persists north of 30°N in the central Pacific. If the resemblance to blocking is more than superficial, the southern

branch of the blocked current will bank itself and continue eastward as a meandering wavelike current if the latitude of the block is not too low. Otherwise this current may curve clockwise to become an easterly flow, or it may even escape across the equator.

Interaction between Hemispheres. The intermittent appearance of high tropospheric westerlies on the equator, often derived on a trajectory from middle latitudes, is a foreign thought in classical views of the general circulation. Yet Fig. 10.12 and many other charts show that they do

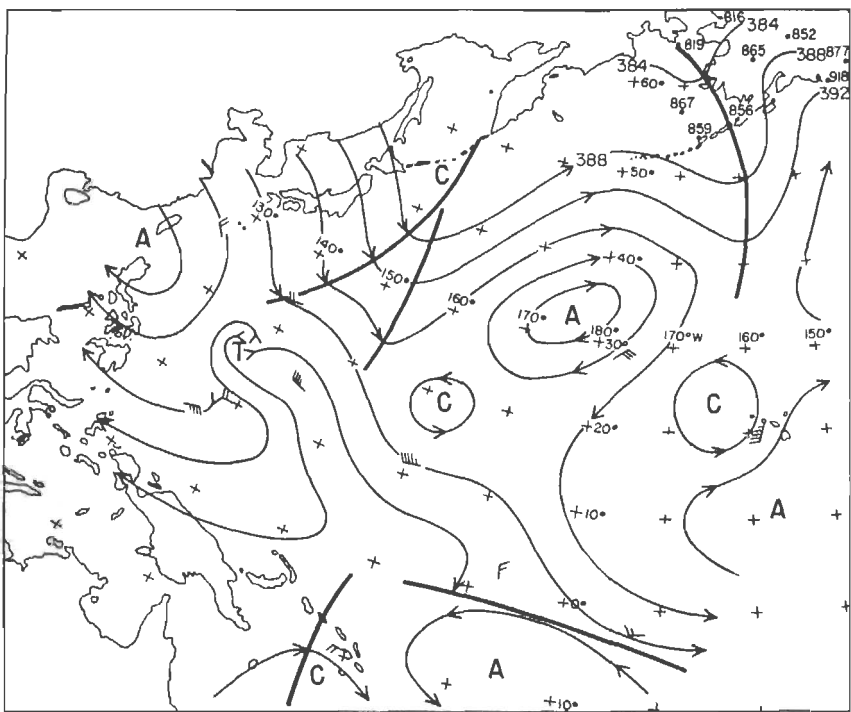


Fig. 10.12. 200-mb streamlines, Sept. 26, 1945 (22).

occur. Hubert (22), analyzing this current, suggested that it may be the mechanism by which the exchange of vorticity between the hemispheres proposed by Rossby (42) may be effected (*cf.* Chap. 12). This subject awaits further development.

Since the flow in the high levels is so unsteady, coupling at high altitudes between the circulations of northern and southern hemispheres across the equator promises to provide an important link in the understanding of some of the fluctuations of the general circulation. Because data are lacking, the subject has not received the attention it deserves. Figure 10.13 is a tentative attempt at streamline analysis at 40,000 feet

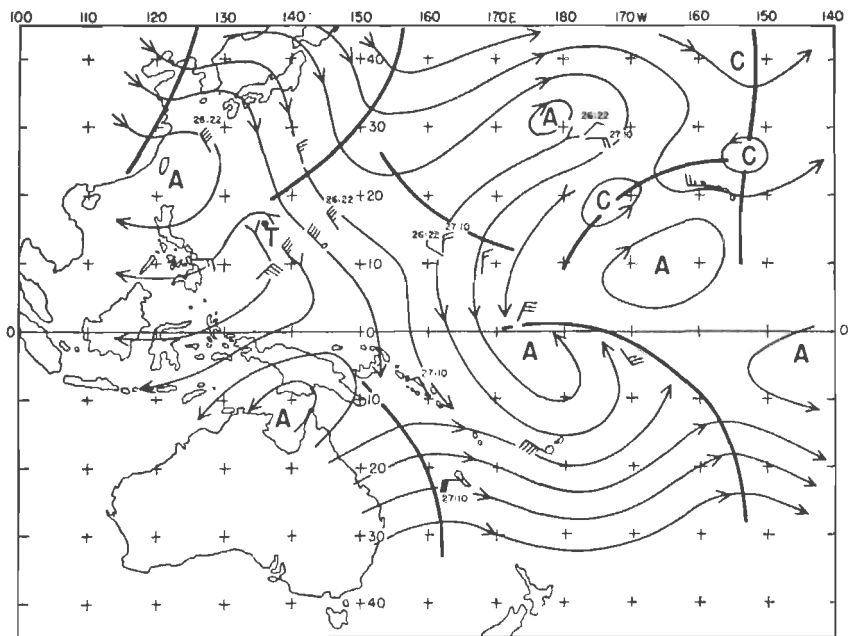


Fig. 10.13. 200-mb streamlines, Sept. 27, 1945 (23).

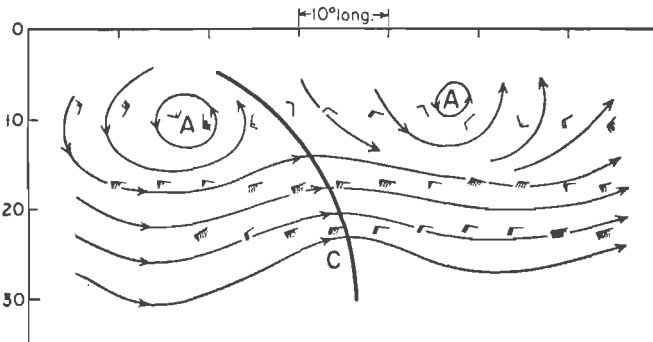


Fig. 10.14. Extrapolated 200-mb flow pattern south of equator, Sept. 25-Oct. 5, 1945 (23).

(200 mb) in the equatorial zone, prepared with the aid of continuity, time sections, and all other auxiliary devices known (23). Nevertheless, many features of the final product cannot be guaranteed. There is no guide for drawing streamlines on the equator.

Three stations were available in the southern hemisphere, situated in the Solomons, the Fijis, and New Caledonia. Time sections of these stations show that the equatorward ends of troughs in the westerly jet

stream, centered in winter between 25 and 30°S (Fig. 1.15), pass eastward quite close to the equator. The rate of motion can be determined from the sections. By considering this motion constant for the period analyzed and assuming steady state, we can convert the time-section data to a space distribution (Fig. 10.14). Here indeed is an intrusion of extratropical-type circulations into the heart of the tropics.

Figure 10.13 suggests considerable movement of air across the equator in the high troposphere. The low-level charts in this case, but not in that of Hubert (22), indicate that at least partial local mass compensation exists by means of a reverse flow at low levels. Such partial compensation has also been noted by Palmer (32), who further points out that the relative positions of the subtropical highs in both hemispheres favors broad currents across the equator in the Pacific. The centers of the southern cells lie approximately on the same longitudes as the cols between those of the northern hemisphere. This introduces meridional wind components of the same direction in certain longitude intervals of both hemispheres.

The Indian-summer Monsoon

In his reviews of tropical meteorology Palmer (30, 32) states with reference to the continents:

While the frontal explanation of tropical perturbations, and the airmass analysis based upon it, have had to be abandoned in the Pacific and in the western Atlantic, it has, according to many authors, continued to be very successful in countries bordering the Indian Ocean and in western Africa. There have been modifications of the theory and great complexity has been introduced in places into the original simple account of the equatorial front. But the fundamentals of the airmass theory as applied to the tropics have remained unchanged.

As recorded in Chap. 2, large variations in air-mass structure occur over the tropical continents. Their existence is not in doubt, but at issue is the role that should be attributed to them. When analysts concentrate exclusively on defining air masses and locating fronts, it must be presumed that they consider them as the key to all analysis and forecasting and therefore emphasize them so much. Yet it is a striking fact that the streamline configurations of synoptic charts over the continents do not differ in essentials from those over the oceans. Nor does their evolution with time take a markedly different course. One therefore wonders whether or not the emphasis has been put in the right place. Palmer, citing the work of Sawyer (44) and Solot (48), questions that the density contrast found along the fronts or shear lines over the conti-

nents is requisite for formation and growth of disturbances in the summer-monsoon regions. Serious doubts have been raised from time to time in other quarters; the author concludes that the case for the primary role of density contrasts over the continents has not been proved. Moreover, no unified description of the frontal patterns and their evolution can be discerned from the bulky literature. This renders any presentation of the air-mass viewpoint very difficult; it will not be attempted. As one example of disturbances over the continents, we shall discuss the most widely known and most spectacular of the continental circulations: the summer monsoon over India and Burma.

In April and May the rains set in generally over Burma while they are retarded over India so that temperatures rise to extremely high values in May. Then, late in May or early in June, roughly within a 3-week span, the monsoon "bursts," often accompanied by violent squalls and small but intense cyclones on its leading edge. These are anxious weeks for the population since a late monsoon may mean little rain and crop failure.

After the first burst, which carries the rain roughly to the top of the peninsula, the monsoon advances more gradually toward the Himalayas and northwestern India and Pakistan. In the Indus valley the rainy season may last only a couple of months or less; here the average variability of rainfall from one year to the next is very high (Fig. 3.15). The retreat of the monsoon, beginning in September and often lasting through November, is far less spectacular than the advance.

The Burst of the Monsoon. Many meteorologists (*cf.* 7, 21, 35, 54) have described the arrival of the summer monsoon. As early as 1686 Halley stated in the *Memoirs of the Philosophical Society of Great Britain* that the cause of the monsoon is differential heating, a theory that in principle has remained unchallenged. It is not obvious, however, why the monsoon is retarded over India as compared with Burma and with other continents of both hemispheres and why it subsequently advances in the spectacular manner that has given rise to the name "burst."

In the past, clues have been sought principally in the sea-level pressure distribution over the north and south Indian Oceans. According to Fig. 1.7 a comparable sweep of surface air across the equator does not occur elsewhere. The southerly current is shallow, however, and restricted mainly to the subcloud layer, at least north of the equator. Above 2,000 feet the winds are from the west and even north of west, indicating that the air that reaches India is derived from Africa and the Mediterranean.

One permanent feature that might help to explain the difference between the onset of the monsoon over India and elsewhere is the channelling effect produced by the height and shape of the Himalaya moun-

tains. In December (11, 35, 57) a considerable portion of the belt of westerlies circles the southern rim of the Himalayas (Fig. 10.15). In spite of the altitude of the flow shown in this figure, the streamlines follow the contours of the mountains quite well. As prescribed by these contours, a trough lies near longitudes 85°–90°E. The winter jet is narrow but intense (11), and it transports much mass. It is the dominating influence on winter weather and precipitation over southern and central China (57).

In summer (54) an entirely different picture prevails (Fig. 10.16). The westerlies have retreated to the north of the mountains, and a continuous

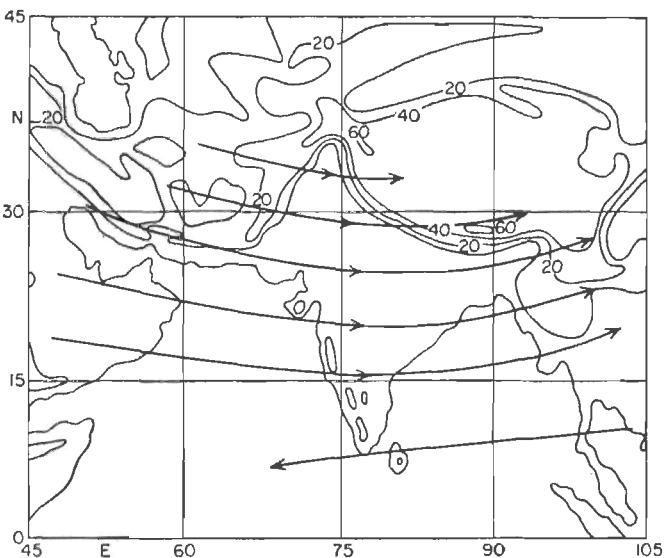


Fig. 10.15. Mean winter circulation at 8 km over India (54).

north-south trough line extends from westerlies to easterlies near 75°E, just west of the bulk of the mountains. This represents a westward displacement of 10° longitude from the wintertime position. The subtropical ridge line lies near 35°N; thus a col appears over northwestern India. North of this position the westerlies move along the northern boundary of the Himalayas with clockwise curvature.

Figures 10.15–10.16 show that Burma is always situated east of the position of the mean upper-air trough, whereas India-Pakistan lies to its west in winter and to its east in summer. Superposition of the high tropospheric flow pattern and its attendant pressure field on the low-level circulations must have the effect of accelerating the monsoon over Burma and retarding it over India as long as the trough remains in the Bay of Bengal. After it shifts to 75°E, southerly wind components pre-

vail at high levels over the entire Burma-India region and must reinforce the monsoon everywhere. It follows that the change in the upper circulation can explain the pattern of advance of the monsoon. This hypothesis permits us to relegate the heat low over northwestern India-Pakistan, often cited as a primary factor in the advance of the monsoon, to a more secondary role. The heat low arises from intense insolation under clear skies over a wide area. However, the clear skies cannot be considered as an *a priori* factor in any monsoon theory; it is just another way of saying that the monsoon is retarded. A common cause must be

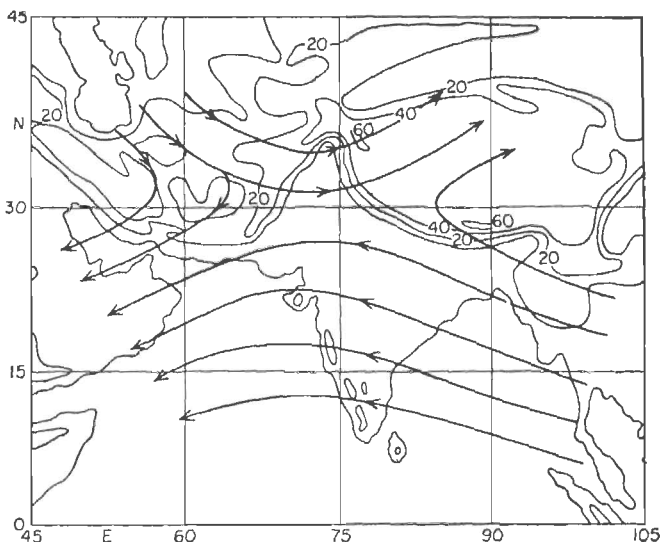


Fig. 10.16. Mean summer circulation at 8 km over India (54).

sought for the retardation and the resulting clear skies; the upper current, moving from west-northwest toward the trough near 90°E with subsidence, can provide such a cause.

To develop the hypothesis, it is necessary to show that the shift of the mean trough position occurs very rapidly and just at the right time. Further, an explanation must be provided for such a sudden displacement, an explanation which is valid in every year. Yin (60) has treated this problem in a study of the burst of 1946; the course of events in other years (17) supports his hypothesis. In order to establish at first the synoptic sequence that takes place over India-Pakistan, Yin analyzed daily wind charts for 5,000, 10,000, and 20,000 feet during May and June. The forward edge of the monsoon, the equatorial shear line, could be located with greatest accuracy at 10,000 feet. Figure 10.17 shows the flow at this level at 2-day intervals during the critical weeks;

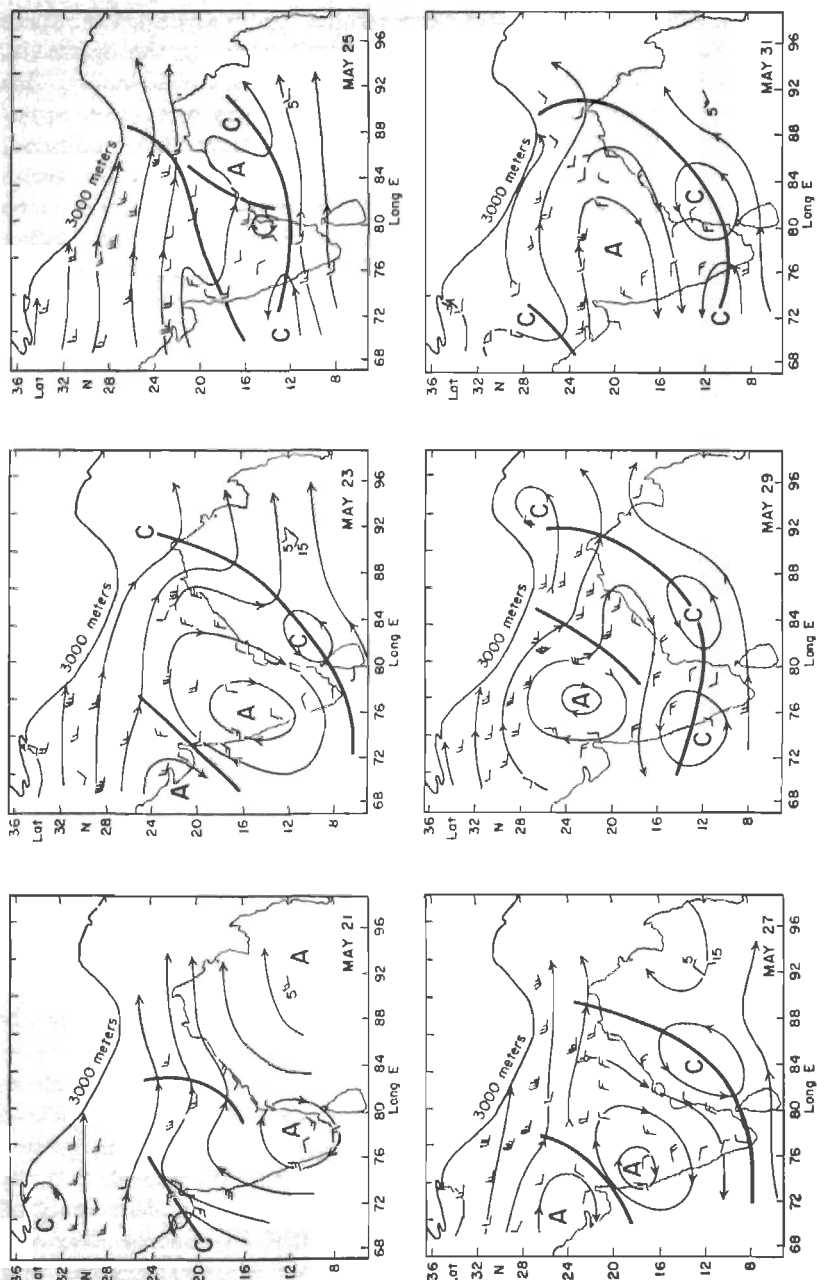


Fig. 10.17. Streamlines at 10,000 feet, May 21-June 12, 1946 (60).

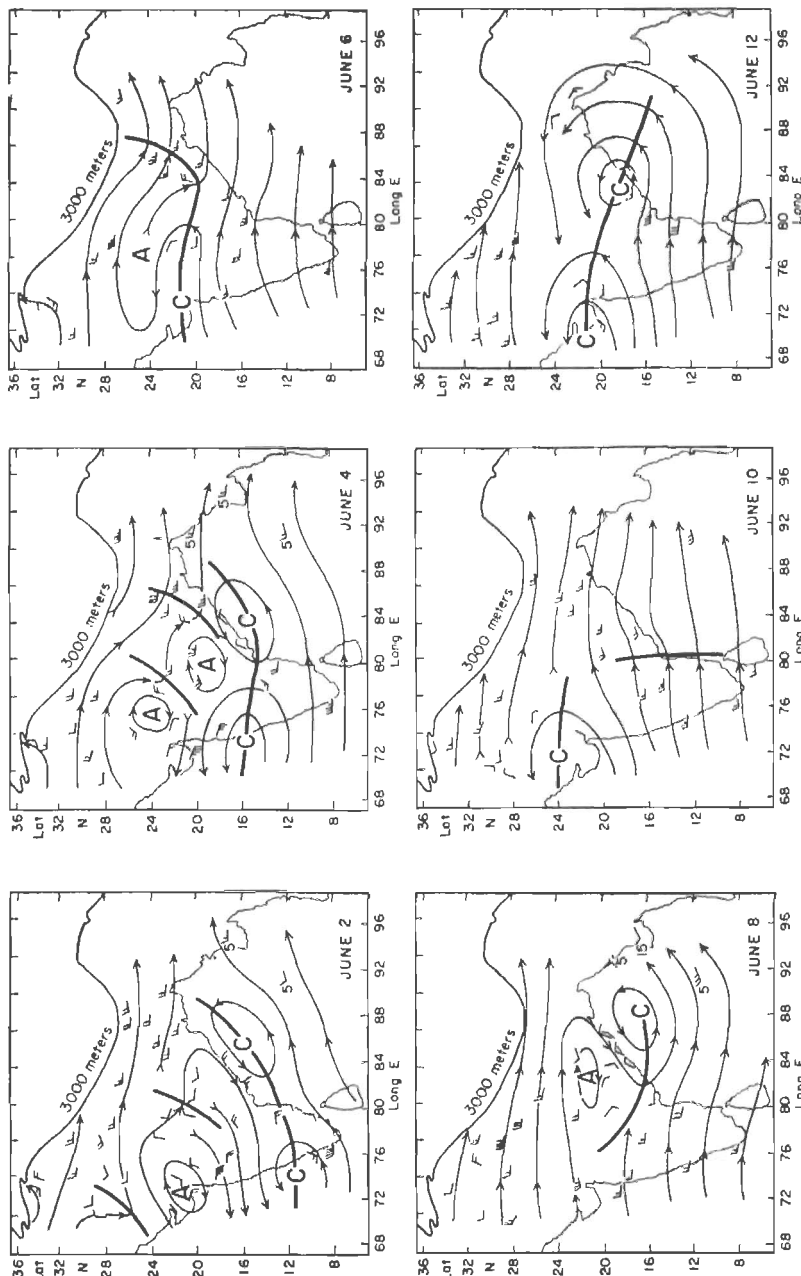


Fig. 10.17 (continued).

the heavy line of Fig. 10.18 summarizes the movement of the shear line during this period.

Initially, an anticyclonic cell overlay the central part of the subcontinent. In the north, the flow was mainly westerly, but with northerly components; the few winds over southern Burma and the Andaman Islands in the Bay of Bengal indicated southwesterly flow here. Charts of the 500-mb surface showed the trough still near its average winter location. As the flow pattern of these initial days was typical of that prevailing during most of the preceding 3 weeks, it follows from mass-continuity requirements that a portion of the air yielding copious early monsoon rains over Burma must have been the same air that had previously moved over India without producing heavy rainfall.

Subsequently, the high-pressure cells shifted northward. A shear line developed in the south and advanced into southern India, coupled with development of a westward-moving depression in the Bay of Bengal. Following an interruption from May 26 to May 31, the burst of the monsoon occurred and terminated after 6 days and an advance of 12-14° latitude. After a second retreat June 6-8, the position of the equatorial shear line became steadier near 23°N.

The 500-mb charts for the period show an initial westward displacement of the upper trough when the equatorial shear line first forms. Then the trough returned to the Bay of Bengal coincident with the first interruption of the advance of the monsoon. After the end of May the trough definitely moved to 80°W. The data therefore support Yin's hypothesis. The advance of the monsoon was linked with the westward displacement of the trough at 500 mb.

The reason for the trough movement is sought in broad-scale changes in the upper flow over at least a large portion of the northern hemisphere. Considering the zonal winds at 500 mb averaged over the whole Eurasian continent (Fig. 10.18), the strongest westerlies were located near 30°N in the first half of May. This maximum moved northward to about 40°N in the last week of the month and then disintegrated abruptly. Meanwhile a new maximum had steadily worked southward from the arctic, and there were two west wind centers in the second half of May. Then the northern current became dominant. The Bay of Bengal trough began to move westward as the low-latitude current was displaced north of the latitude of the Himalayas; the burst of the monsoon coincided with the period of its collapse.

Although analysis was uncertain because of lack of data, daily charts indicated that the changes shown in Fig. 10.18 were representative for the flow in the immediate vicinity of the mountains. The portion of the westerly stream that during the premonsoon season had circled the Himalayas along their southern border was displaced to the north of the

mountains. Because of the deformation imposed on the flow by the huge elliptical-shaped high plateau, a basic readjustment of the wave pattern aloft must occur. The orographically determined phase shift is schematically indicated in Fig. 10.19. It suggests that the rapid westward displacement of the low-latitude mean trough is enforced as the southern branch of the westerlies ceases to flow around the southern periphery of

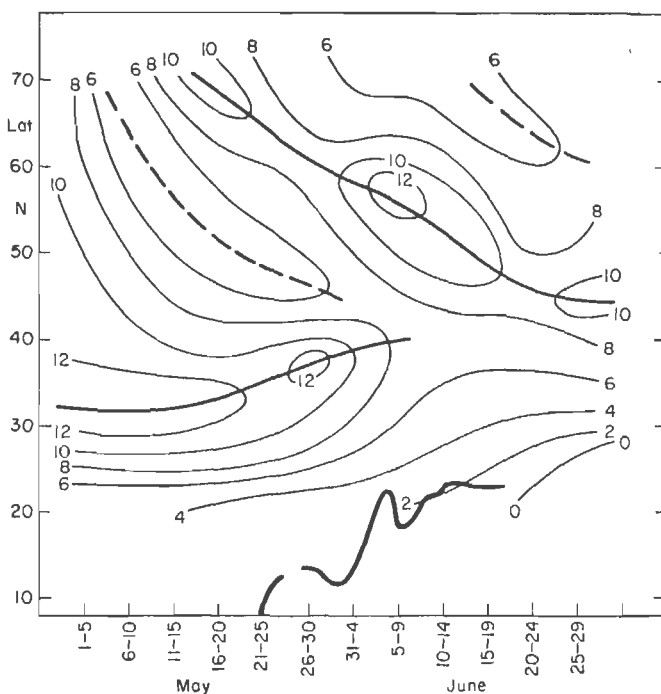


Fig. 10.18. Time section of mean zonal wind distribution (mps) between longitudes 0 and 130°E, May–June, 1946. Heavy line at bottom shows latitude of equatorial trough over India (60).

the Himalayas. The northerly component of the flow aloft over India-Pakistan is suddenly replaced by a southerly component as the subcontinent comes under the influence of the flow east of the upper trough line. This factor, together with the differential heating, brings about the violent northward advance of the monsoon.

Fluctuations in the Monsoon Season. In the early days of meteorology, the monsoon was considered to be an entity largely sealed off from outside influences by the mountains and, as such, characterized by marked steadiness. Actually, little of the air converging in northern India and Pakistan escapes across the mountains into the westerlies. In a limited sense local mass compensation takes place since the low-level air arriving

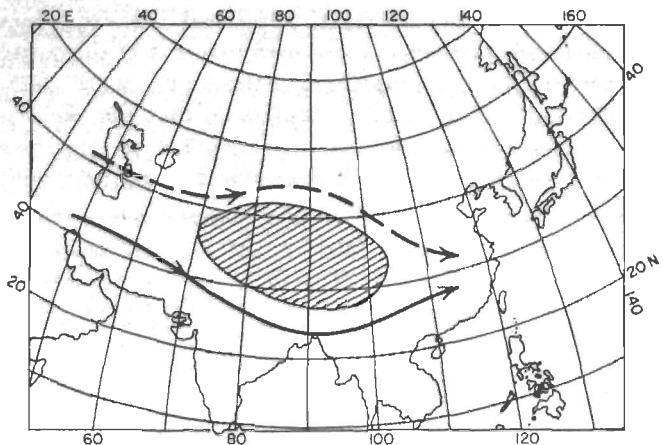


Fig. 10.19. Change in flow pattern resulting from displacement of jet stream north or south of Himalayas (60).

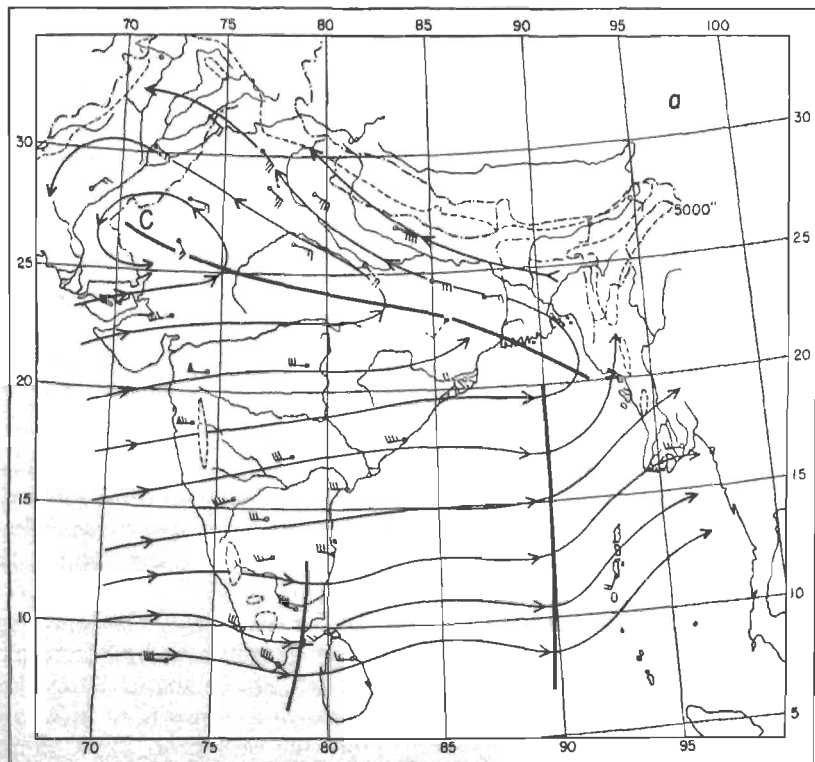


Fig. 10.20. 5,000-foot streamlines, Aug. 3, 1949 (34).

from the Arabian Sea returns toward it at high levels as an east-northeast wind. Nevertheless, both lower inflow and upper outflow are subject to marked variations, as those engaged in daily forecasting well know. They speak of "breaks" or "interruptions" of the monsoon rains, sometimes lasting 2 weeks. The rainfall analysis made at the end of Chap. 3 holds here as well as elsewhere. It should not be overlooked that,

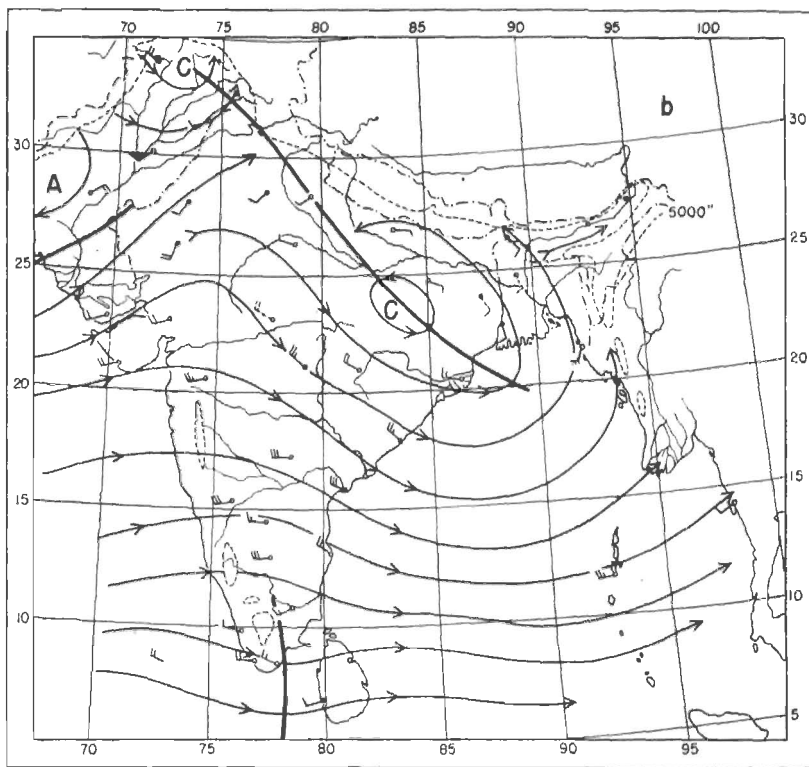


Fig. 10.21. 5,000-foot streamlines, Aug. 9, 1949 (34).

although it may rain on each of 30 days in the month at some windward stations of the west coast, even there a large fraction of the rainfall is accounted for by a very few days with rain.

Rahmatullah (34) has demonstrated the great variety of flow patterns that can occur in northern India and Pakistan in a single month at the height of the monsoon season. For August, 1949, he identified five distinct types of flow patterns. Each persisted 4–8 days and greatly influenced the rainfall pattern. Figures 10.20–10.23 are typical maps for four of the five types.

Initially (Fig. 10.20) the flow pattern conforms to that of the classical literature. The equatorial shear line, the monsoon trough, extends from east-southeast to west-northwest over the Gangetic Plains toward the central Indus Basin. Weak disturbances, not unlike those shown for the western Pacific early in this chapter, travel west-northwestward along it. Spacing and rate of motion of these disturbances are quite similar to those of the Pacific; as already stated, the whole map appearance and

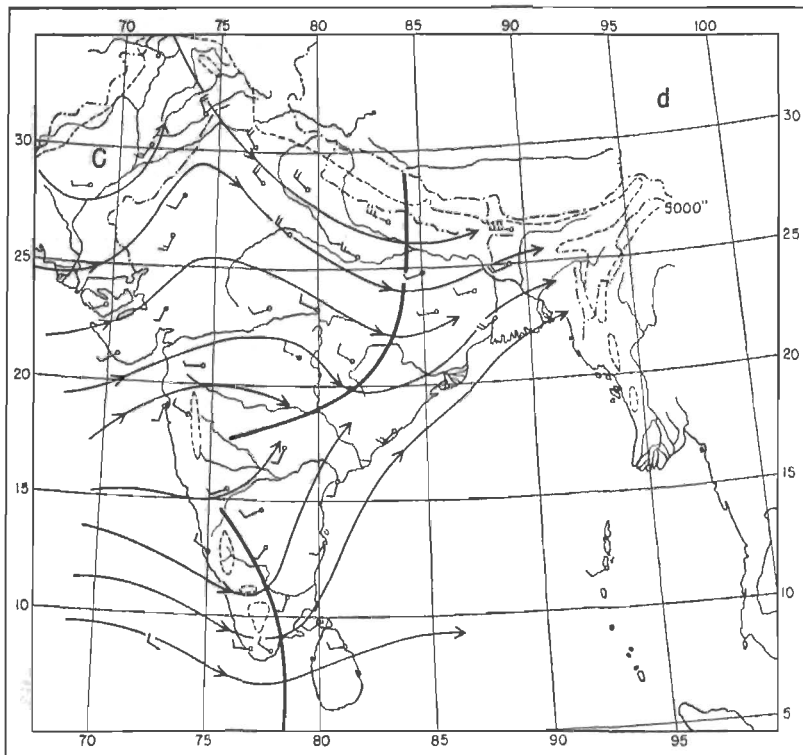


Fig. 10.22. 5,000-foot streamlines, Aug. 23, 1949 (34).

evolution do not differ greatly from those over the oceans. Rainfall is heavy in a narrow zone along the trough line. Some areas receive up to 100 per cent of the total rainfall for the month in the first week, especially in the west. By contrast, the foothills of the Himalayas and the region south of 20°N were fairly dry, receiving 20 per cent or less of their rainfall in this period.

A gradual clockwise rotation of the trough, coupled with northward displacement, follows (Fig. 10.21). Disturbances continue to be propagated northwestward as before, but the precipitation is now unevenly dis-

tributed. Some foothill areas record heavy rain, while others still are dry. Farther south drying takes place in most sections.

The equatorial trough continues its slow northward advance until the low-level easterlies disappear entirely from the subcontinent (Fig. 10.22). A cyclonic westerly circulation skirts the periphery of the mountains. The strength of the westerlies, previously 20–30 mph, now is quite weak, about 10 mph. In the south a separate disturbance is forming, indicating

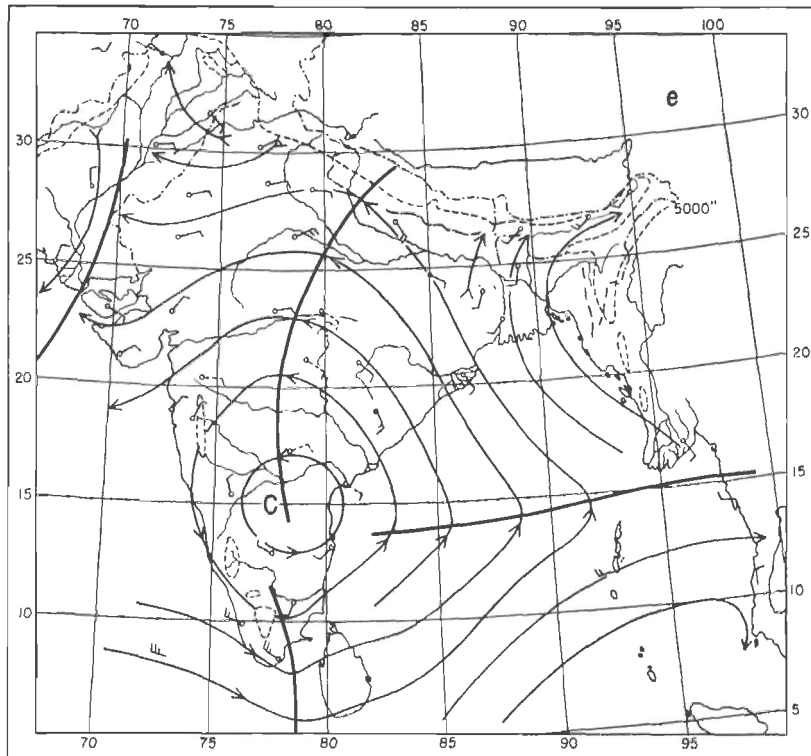


Fig. 10.23. 5,000-foot streamlines, Aug. 28, 1949 (34).

that the whole wind structure is about to break down. This is a very dry period; over a broad belt rainfall is nearly zero. Appreciable amounts are recorded only in the Punjab and the northeastern Brahmaputra Basin.

Figure 10.23 confirms a complete rearrangement of the flow. Within 2 days the westerlies vanish north of 15°N and are replaced by easterlies. A wave trough develops in the Bay of Bengal and then propagates westward across the whole peninsula. This is also a dry period in the north. A new equatorial shear line forms near 15°N.

The gradual evolution of the general circulation during the month corresponds to what has been observed over other continental areas and

over oceans. We note some resemblance to Figs. 10.5-10.8. Usually, the net displacement of equatorial shear lines is poleward. Upon reaching the latitude of the subtropical ridge they disintegrate even when there are no mountains. A new shear line develops farther equatorward, and the whole sequence is repeated. These long-period changes are not fully understood but may be related to the index cycles described at the end of this chapter.

Seasonal Forecasting. Since the rainfall of the monsoon season is the most critical variable for the food production for one-sixth or more of the world's population, meteorologists have tried for many years to predict seasonal-rainfall anomalies during the preceding spring. Most active have been G. C. T. Walker and his collaborators, especially S. K. Savur. Montgomery (24) has reviewed their work.

Statistical lag correlations of India rain with surface parameters all over the globe are the basis for the predictions. Since the nature of the general circulation and its irregular fluctuations is largely unknown, Walker feels there is no reason why he should not make use of any good lag correlation, even though the physical meaning may be obscure. Such relations, in fact, might supply clues on the general-circulation problem. Walker himself has succeeded in defining a remarkable circulation parameter for low latitudes, the southern oscillation, which he described as follows: "In general terms, when pressure is high (relative to the mean) in the Pacific Ocean it tends to be low in the Indian Ocean from Africa to Australia; these conditions are associated with low temperature in both these areas, and rainfall varies in the opposite direction to pressure. Conditions are related differently in winter and summer, and it is therefore necessary to examine separately the seasons December to February and June to August."

The statistical definition of the southern oscillation need not be discussed here. Pertinent data are pressure, temperature, and rainfall anomalies from many parts of the globe. Willett (56) has published an abbreviated formula. Little progress has been made in fitting the oscillation into schemes of variations of the general circulation in spite of the evident potentialities. For India-Pakistan, however, the oscillation and other statistical correlations provide a way to derive prognostic regression equations for the summer rain. The weakness of these equations lies in the selection of past data on the basis of best fit. There is no guarantee that any such correlations will hold in the future.

Walker's formulas have had only moderate success in spite of continuing revision, probably owing to the statistical shortcomings. With time the correlation between predicted and observed rainfall always decreases. Among the individual members of the regression equations, those based on observations outside the tropics appear to be holding best.

Outstanding is the sea-level pressure in the temperate zone of South America in April and May. It persistently correlates with subsequent monsoon rainfall with coefficients between 0.4 and 0.5. This is a remarkable fact of the general circulation; further work with the southern oscillation should eventually lead to satisfactory rainfall predictions for India-Pakistan.

Disturbances of the Cool Season

Over both continents and oceans the intrusion of high-level polar westerlies in winter gives rise to some weather sequences not unlike those of the temperate zone. Above India-Pakistan, the narrow but intense jet stream flowing around the southern rim of the mountains carries in it weak disturbances of an extratropical type, at times traced back to the Mediterranean. They are called "western disturbances." Precipitation associated with them is restricted mainly to the foothills of the Himalayas.

In the trade-wind belt, eastward-moving disturbances make their appearance as the deep easterlies of summer give way to upper westerlies. These disturbances are formed and carried in the upper current. The low-level trades change their speed and direction in response to the changes imposed from above.

Jet Streams. As in middle and high latitudes, the westerlies over the trades exhibit an undulatory wavelike motion with variable wave length, amplitude, and rate of motion. When waves of great amplitude predominate in middle latitudes, the tropical flow may be constrained to move in accord. This is also true when the center of the main belt of westerlies is displaced well toward the subtropics, which happens especially in late winter. More often, however, the low-latitude westerlies follow a course that is at least partly independent. Although the whole belt of westerlies may extend from arctic regions to latitude 10° or even less, strong winds tend to concentrate within two or three narrow zones, as we have already seen. These fast currents, the jet streams, contain most of the kinetic energy of the westerlies. Along their axes we find the areas of disturbed weather and surface-pressure rise and fall centers (1).

We have encountered such jet streams in Figs. 10.9, 10.10, 10.13, and 10.14. In the southern hemisphere the westerly current whose center lies between 25 and 30°S appears to be capable of leading an existence independent of events farther poleward for protracted periods. Under it are centered the migratory anticyclones, long known to traverse Australia and the ocean to the east with a mean periodicity of 6 days (53), equaled in regularity in no other part of the world. The upper trough lines often are accompanied at the surface by what Palmer (29) has termed "meridional fronts." This steady regime is a very dry one over the trades; it is

to be presumed that the occasional heavy winter rains over islands such as the Fijis are derived from interruptions of this regime.

In the northern hemisphere a steady jet stream does not maintain itself at a comparable latitude although the core of the westerlies in the hemispheric winter average is found between 25 and 30°N. The variability of the upper flow is very great except over southeastern Asia, where the Himalayas stabilize the circulation (57). Nevertheless there is an undeniable tendency for a jet stream to form whenever possible near latitudes 20–25°N. This has been confirmed for regions where high-level data have been taken: India, Africa, the western Atlantic, and the Pacific west of

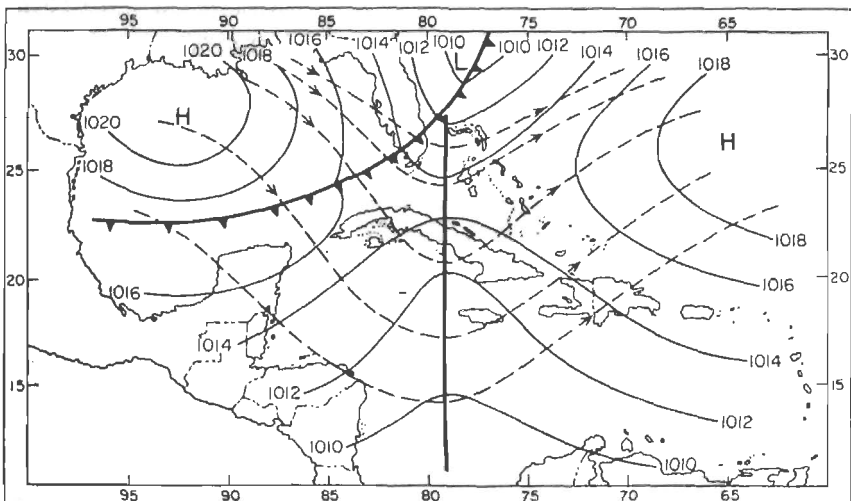


Fig. 10.24. Model of impressed trough in easterlies during winter (*upper flow dashed*) (37).

150°W.¹ Synoptic charts resemble Figs. 10.9 and 10.10, sometimes even Fig. 10.6; but closed anticyclonic cells occur only occasionally north of the southern westerlies. Commonly we have strong westerlies in high and low latitudes, with an intermediate belt of weak westerlies (39). Such a nonlinear distribution of the zonal wind shear is a semipermanent feature of greatest importance for daily weather-map analysis. The upper shear zones partly determine the dry and rainy areas.

Waves in the Westerlies. Among several models suggested by the observations, Fig. 10.24 illustrates what has been found typical of many situations at the advance of a cold outbreak into the tropics (37). On the surface chart an “inverted” trough precedes the advancing front by a long distance. The isobaric pattern is similar to that observed during

¹ In addition, jet streams with the shape of huge spirals may extend all the way from equator to arctic, encircling the whole globe.

the passage of wave troughs in the easterlies. But the winter troughs, formed as a reflection of troughs in the upper westerlies, move eastward.

Figure 10.25 is a typical vertical section across a trough. Structure and wind field are similar to those encountered aloft in the temperate zone; the trough is cold relative to its surroundings, and the tropopause is lower. As it approaches, pressure begins to fall throughout the troposphere, cooling begins at high levels, the upper winds turn to southwest and increase in strength, and the low-level trades become southeasterly as the base of the westerlies lowers. After the trough line passes, the converse obtains.

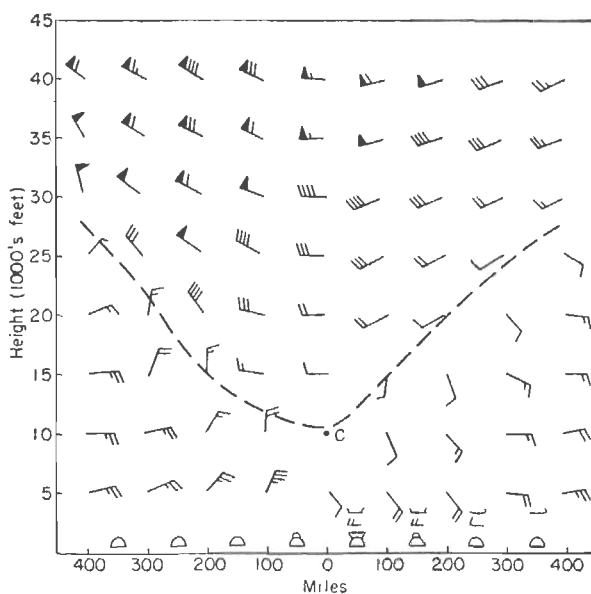


Fig. 10.25. Model of wintertime wave trough in vertical cross section (37).

During steady-state progression the dynamics of trough propagation may be handled as in Chap. 9. Since the trough advances against the easterlies, the lower-air columns always pass through it on a counter-clockwise curving path. They therefore converge to the east and diverge to the west of a trough line. At high levels the westerlies move through the trough from west to east. They acquire relative cyclonic vorticity to the west and anticyclonic vorticity to the east, when the curvature changes determine the vorticity changes. Following Eq. (8.12), we have convergence aloft west of the trough and divergence to the east if the changes of relative vorticity overbalance the latitude changes, which act in the inverse sense. With this arrangement the sign of the divergence

reverses with altitude, and the net surface-pressure changes are consequently very small. Since the troughs travel eastward, the sign of the surface-pressure changes is determined at high levels as in middle latitudes, contrary to the waves in the deep easterlies.

The described fields of vorticity change and divergence require ascending motion east of the trough and descending motion to the west. This is in accord with the observed variation in cloudiness. Cirrus, becoming altocumulus or altostratus, precedes the trough. Again we encounter the typical warm-front cloud sequence although there is no cold dome to ride over and although the coldest air is in fact situated at the western margin of the cloudy area. The rate of cumulus build-up is variable. When an inversion acts as a lid for the air moving through the trough in the lower 5,000–10,000 feet, the air above it in a layer of about 200-mb thickness is very dry. Convergence gradually weakens the lid so that the thickness of the cumuli increases toward the trough line. The lower-air columns may be too stable for convergence to remove the inversion completely. If it is broken, however, large amounts of cumulonimbi can develop quite suddenly.

Considerable complications arise when the troughs begin to stagnate or when the wave pattern is produced by an independent jet stream in low latitudes. In Figs. 10.9 and 10.10 the jet-stream center propagates eastward with anticyclonic path curvature. Downstream propagation occurs nearly always, but the trajectory may be cyclonic as well as anticyclonic. In such situations the horizontal shear and its changes cannot be neglected in determining vorticity changes. Some models with a narrow jet center in the easterlies have been discussed in Chap. 9. The reasoning for the westerlies has been outlined in several publications (*cf.* 1). A thorough discussion must await solidification of knowledge about the behavior of low-latitude jet streams and the wave patterns they set up.

Cold Fronts. Considerable research has centered around the cold outbreaks that penetrate into the trade-wind belt well to the rear of the upper-air troughs. Some writers have regarded the equatorial trough as the receptacle and eventual storage place for a never-ceasing procession of fronts marching on the equator from the temperate zone. Others have insisted, correctly, that only a few fronts reach the equator or even cross it and that it is more correct to speak of convergence lines or shear lines than of fronts over the oceans. In equatorial Africa and the Amazon Basin remnants of cold fronts do cross the equator occasionally; the lower temperatures and dew points can cause severe damage to the tropical plants.

In the great majority of situations, the temperature contrast across cold fronts becomes very small over the oceans when they reach latitude

20°N or 15°S. The air in the layer extending from the surface to 10,000 feet often executes a sharp anticyclonic turning. These columns then diverge laterally and sink as their vorticity decreases, and this sinking contributes to rapid frontolysis. Soon all weather dies out, and nothing remains on charts except a weak transition zone from lighter to stronger easterlies.

Rapid frontolysis takes place mainly just equatorward of jet-stream centers in the high troposphere. A front that breaks away from a jet stream of the temperate zone and later arrives beneath another one closer to the equator is likely to become stationary, regain intensity, give rise to bad weather, and even produce small cyclones. Before discounting an old front, it is always advisable to check its position relative to the 200-mb currents.

The strongest cold outbreaks occur during long wave progression or discontinuous retrogression in middle latitudes. These large-scale changes of the general circulation have also been referred to as *transformations* of the subtropical anticyclones. Arrival or building of a long wave ridge in the eastern Pacific or Atlantic coincides with a strong increase of the central surface pressure. This rise occurs often, though not always, upon the absorption of a large cold anticyclone into the subtropics. Equatorward from the subtropical ridge a vast body of air is suddenly moving at much too slow a rate for the new pressure gradient. Widespread equatorward acceleration and increase of wind speed set in, initiating the most spectacular weather of the cold season, termed "surge of the trades" by Deppermann (14). Over thousands of miles low-level wind speeds rise to 30–50 mph and remain high and gusty for 2 days or more. If a cold front is not initially present, one or more shear lines develop simultaneously, spreading eastward and westward in the tropical ocean along lines of enormous extent (37). Severe convection may accompany the forward edge of the surge to the heart of the tropics.

Cool-season Cyclones. Many observations confirm cyclone development over the tropical oceans in the cool season (14, 31, 32, 37, 47). A few of these are hurricanes, mainly in the western Pacific. Others have the appearance of polar-front waves and behave accordingly. The majority belong to neither of these classes. They usually are weak surface reflections of intense cold-core lows aloft; occasionally, however, the circulation is uniform throughout the troposphere. Simpson (47) has called these storms "subtropical cyclones."

The major portion of the rainstorms that account, for instance, for the winter rainfall over the eastern Pacific are not simple frontal passages. These are, in fact, likely to be quite dry. Interaction between the long waves in the westerlies and tropical perturbations initiate the rain-bearing situations which often contain the cold cyclones aloft as their most

important feature. Hence the frequency and rain productivity of these cyclones are a major factor influencing life in many parts of the subtropics.

Several aspects of the synoptic sequence during formation of the lows resemble the initial stage of hurricanes. Reports of altostratus overcast and continuous rain appear in a limited region in which 24-hour surface-pressure falls increase or develop. An area of unusually good weather develops on the equatorward side, coupled with lowering of the base of the westerlies. Simpson suggests that the cyclones may form in two ways. Superposition of a trough in the westerlies on a preexisting low-latitude cyclone aloft can activate this cyclonic circulation so that it reaches the surface. At other times occlusion of a wave cyclone in low latitudes, followed by its "cutting off" from the westerlies in the manner described by Palmén (28), is considered to be the initiating mechanism. This latter hypothesis is somewhat doubtful since dynamically the models of Simpson and Palmén differ considerably. In both types of cyclogenesis a long-wave ridge develops north of the cyclones, coupled with a northward shift of the westerlies or disintegration of a low-latitude jet stream. The map patterns at maturity are identical.

Simpson has prepared interesting statistics on wind and rainfall distribution around mature subtropical cyclones. In a rough way these two quantities are correlated: rainfall is high and winds are strong on a semi-circle whose radius varies from 7 to 3° latitude around the northern side of the storm, gradually approaching the center from east to west. Inside the core, pressure gradients and winds are weak. Rainfall, if any, is light and falls from altostratus. Rain and wind are heaviest on the east side of the semicircle. They are least on the south and southwest sides of the cyclones, as in hurricanes.

After a life cycle of variable length, the cyclones usually reestablish connection with the westerlies and move out of the tropics; at times they die out *in situ*. Rarely, and Simpson is supported by data from several regions, they develop warm-core characteristics and become small hurricanes.

Interaction between High and Low Latitudes

At various places throughout Chaps. 9 and 10 we have encountered links between the temperate and tropical zones as definite as the interaction across the equator is indefinite. The earlier discussions on the interaction between high and low latitudes will here be summarized and extended.

Short-term Interaction. Cressman (12), following previous literature, has pointed out that the observed flow patterns may be classified into

two main types. Depending on the arrangement of the subtropical cells, these types may be called *zonal* and *meridional*.

Persistent anticyclonic centers with vertical axes poleward of latitude 35°N characterize meridional flow in summer. In such situations we frequently find meridional highs separated by shear lines oriented east-west (Fig. 10.6). Between the anticyclonic cells large extended troughs may reach from arctic to equator. Conditions are favorable for poleward movement of equatorial shear lines and formation of tropical storms. Moving wave troughs in the easterlies will intensify when they intersect troughs in the westerlies.

Zonal flow predominates when the subtropical anticyclones are centered equatorward of 35°N with their major axes oriented east-west. The base of the westerlies slopes strongly toward the equator with height. Meridional highs and shear lines with east-west orientation are rare except close to the equator. Waves in westerlies and easterlies seldom combine to form extended troughs but by-pass each other with temporary deepening.

At times the whole tropical and subtropical belts of one hemisphere exhibit either one or the other of these characteristics; frequently, however, one portion has a more meridional, the other a more zonal, arrangement. Figure 10.26, which also includes the southern hemisphere, illustrates large north-south amplitudes typical of the meridional pattern.

The winter season has been studied intensively with respect to Hawaiian rainfall by Yeh (58, 59); most important is the relation between daily rainfall and latitude and intensity of the westerly jet stream in the eastern Pacific. Yeh could follow this current only at 700 mb; he therefore could not take into account separate high-level jet streams in low latitudes but only the main belt of polar westerlies of the middle latitudes. Nevertheless he obtained important results.

In order to carry out statistical correlations, Yeh devised an index suitable for representing daily rainfall in Hawaii. After determining its median value (M) for each month of the rainy season, he treated the daily rainfall in terms of departure from that median. Figure 10.27 shows a clear relation. When the jet stream is centered south of 40°N but still well to the north of the Hawaiian Islands, both median and per cent departures indicate low rainfall. Yeh relates this observation to the distribution of vertical motion relative to the jet (51). In the mean, ascent takes place in and poleward of the jet-stream center in the troposphere, descent in a limited latitude belt on its equatorward side. When the current lies south of 40°N, the islands are under the influence of the descending cell; more than half of all the days are without any rain, at least in the coastal areas. As the jet stream recedes northward, the descending cell also is displaced. Rainfall reaches very high values.

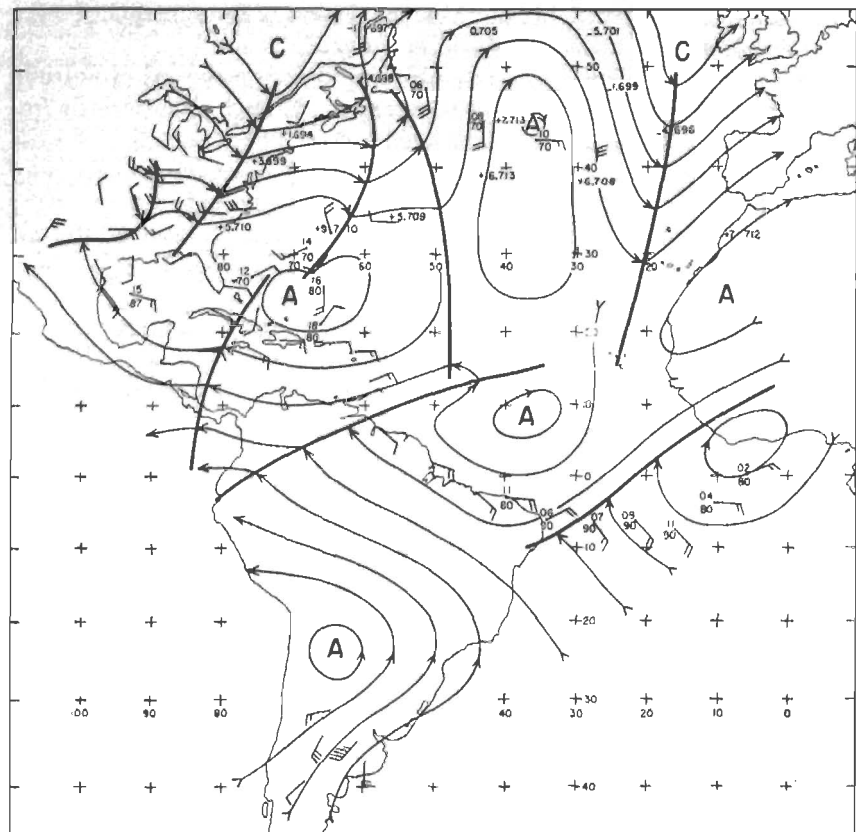


Fig. 10.26. 10,000-foot streamlines, Sept. 6, 1944 (12).

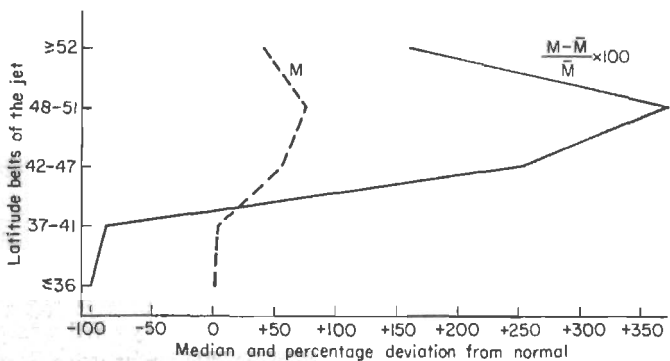


Fig. 10.27. Correlation of median rainfall index for Hawaii (dashed) and of per cent deviation of median from mean (solid), with latitude of middle-latitude jet stream in winter (59).

If we recall the streaky structure of the westerlies discussed in this chapter and the average latitude interval of about 25° that separates individual currents, it becomes plausible to suggest that a low-latitude jet stream may overlie the islands in the high troposphere when the principal belt of westerlies in middle latitudes is far north. In addition, this is just the situation that permits formation of subtropical cyclones.

Yeh's studies also indicate that zonal and meridional arrangements are as important in winter as in summer. Especially when the polar front at the surface is oriented east-west and situated near latitudes $25\text{--}30^{\circ}\text{N}$, rainfall over the islands is almost nil.

Longer-term Interaction. As shown by studies beginning before 1900, the strength of the middle-latitude westerlies goes through irregular variations, with periods ranging from 1 to several weeks. When they are stronger than average, during "high zonal index,"¹ pressure is below

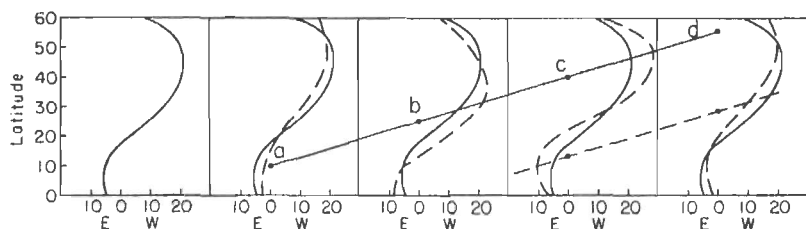


Fig. 10.28. Model of northward propagation of relative westerly maximum of mean zonal flow.

average poleward of the central westerly belt and above average in the subtropics (2). The reverse holds true during "low zonal index." It follows that the strength of westerlies and trades is correlated. Both are either above or below average when the mean is taken around at least half a hemisphere. The associated map patterns are the zonal (strong westerlies) and meridional (weak westerlies) types described.

The transition from one index type to the other often is gradual and can be traced across the latitude circles. One then speaks of an evolution of the map pattern or "index cycle" (25, 43). Various convenient summaries of index variations and attendant weather changes in middle latitudes have been prepared (1, 26). According to early views (43) the impulses giving rise to the cycles, whatever their nature, originate in the polar zones and propagate equatorward. Subsequently, studies of changes in sea-level pressure profiles (26) and of the zonal winds in middle and high troposphere (42) have proved that the origin of cycles for the northern hemisphere should frequently be sought in the equatorial zone or beyond. Consider the zonal wind profiles in Fig. 10.28. The first of

¹ Originally defined as the sea level or 10,000-foot (700-mb) pressure difference between 35° and 55°N , averaged from 0 to 180° longitude through North America.

these may represent monthly mean conditions. Suppose that during a given 3- or 5-day period the observed departure from the mean is that shown in the second diagram: in middle latitudes the strength of the westerlies is below average; in the trades the strength of the easterlies is below average or, as it may be put, the wind component from the west there is above average. Such deviation centers may travel poleward, usually at rates ranging from 2 to 4° latitude per day. As the deviation center in the trades approaches the subtropics, the subtropical ridge is depressed equatorward. Subsequently, the strength of the westerlies in middle latitudes increases and also that of the easterlies in the tropics, where a negative deviation center makes its appearance. When the positive (westerly) deviation center reaches the latitude of strongest seasonal westerlies, the high-index condition is attained. The kinetic energy in both easterlies and westerlies attains a peak at that time while energy of the north-south motion usually reaches a minimum. Finally, as the westerly deviation center passes toward the arctic, a new one emerges from the tropics.

The origin of the trends has been the subject of much speculation. Most explanations have sought initiating mechanisms near the pole, either through mechanical "relaxation" or through solar influences. Palmer (33) has been the first to suggest a mechanism for an equatorial origin based on sharp increases in the sun's ultraviolet radiation associated with flocculi. The solar influence is regarded as providing energy for the start of the trends but not their maintenance and displacement across the latitude circles.

While controversy about the validity of this and other suggested mechanisms is likely to continue for a long time, improvements in quantitative measurements of solar output should enable meteorology to settle the question of the role of nonperiodic solar influences in the coming decades. The possibility of other cosmic influences on rainfall and weather changes has been opened by Bowen (61) who, from 40-year records, has found singularities of high rainfall amount on particular calendar days (e.g., January 12) at numerous stations in both northern and southern hemispheres. In an intriguing hypothesis Bowen associates these singularities with meteoric showers which occur annually about 30 days before the days of high rainfall. The meteoric dust particles would settle slowly until they reached the supercooled water clouds of the upper troposphere where they would act as freezing nuclei and initiate the increased precipitation. While the very tentative character of the hypothesis must be stressed, it points at least to one route of exploring the influence of sudden releases of condensation heat in tropical latitudes on the general circulation.

REFERENCES

- (1) Alaka, M. A., *et al.*, *The Jet Stream*. NAVAER 50-1R-249, U.S. Navy Dept., Washington, D.C. (1952).
- (2) Allen, R. A., *et al.*, *Papers Phys. Oceanog. Meteor. Mass. Inst. Technol. and Woods Hole Oceanog. Inst.*, Vol. 8, No. 3, 1940.
- (3) Alpert, Leo, *Bull. Am. Meteor. Soc.*, **26**: 426 (1945).
- (4) Alpert, Leo, *ibid.*, **27**: 15 (1946).
- (5) Bigelow, F. H., *Monthly Weather Rev.*, **32**: 166 (1904).
- (6) Bjerknes, V., *et al.*, *Physikalische Hydrodynamik*. Berlin: Verlag Julius Springer, 1933.
- (7) Blanford, H. F., *Climates and Weather of India, Ceylon, and Burma*. New York: The Macmillan Company, 1889.
- (8) Bossolasco, M., *Tellus*, **2**: 134 (1950).
- (9) Brooks, C. E. P., and H. W. Braby, *Quart. J. Roy. Meteor. Soc.*, **47**: 1 (1921).
- (10) Bultot, F., *Inst. Nat. pour l'Étude Agronomique du Congo Belge, Bureau Climat. Communication* 6, Brussels, 1952.
- (11) Chaudhury, A. M., *Tellus*, **2**: 56 (1950).
- (12) Cressman, G. C., *Dept. Meteor., Univ. Chicago, Misc. Rept.* 24, Part II, 1948.
- (13) Defant, F., *Dept. Meteor., Univ. Chicago*, Multigraphed (1952).
- (14) Deppermann, C. E., *Outlines of Philippine Frontology*. Manila: Bureau of Printing, 1936.
- (15) Deppermann, C. E., *Upper-air Circulation (1-6 Km) over the Philippines and Adjacent Regions*. Manila: Bureau of Printing, 1940.
- (16) Fletcher, R. D., *J. Meteor.*, **2**: 167 (1945).
- (17) Flohn, H., *Ber. deut. Wetterdienstes*, U.S. Zone, No. 18, Bad Kissingen, 1950.
- (18) Georgii, W., and H. Seilkopf, *Aus dem Arch. deut. Seewarte*, Vol. 17, No. 3, 1926.
- (19) Glenn, A. H., *Bull. Am. Meteor. Soc.*, **28**: 453 (1947).
- (20) Grimes, A., *Mem. Malay. Meteor. Serv.* 2, 1938.
- (21) Harwood, W. A., *Mem. India Meteor. Dept.*, **24**: 249 (1924).
- (22) Hubert, L. F., *J. Meteor.*, **6**: 216 (1949).
- (23) La Seur, N. E., and C. L. Jordan, *A Typical Weather Situation of the Typhoon Season*. Chicago: Department of Meteorology, University of Chicago, 1952.
- (24) Montgomery, R. B., *Suppl., Monthly Weather Rev.*, No. 39, p. 1, 1940.
- (25) Namias, J., *Extended Forecasting by Mean Circulation Methods*. Washington, D.C.: U.S. Department of Commerce, Weather Bureau, 1947.
- (26) Namias, J., *J. Meteor.*, **7**: 130 (1950).
- (27) Newton, C. W., *et al.*, *Tellus*, **3**: 154 (1951).
- (28) Palmén, E., *Tellus*, **1**: 22 (1949).
- (29) Palmer, C. E., *New Zealand Meteor. Off. Prof. Notes* 1, 1942.
- (30) Palmer, C. E., in *Compendium of Meteorology*. Boston, Mass.: 1951.
- (31) Palmer, C. E., *Trans. Am. Geophys. Union*, **32**: 683 (1951).
- (32) Palmer, C. E., *Quart. J. Roy. Meteor. Soc.*, **78**: 126 (1952).
- (33) Palmer, C. E., *J. Meteor.*, **10**: 1 (1953).
- (34) Rahmatullah, M., *J. Meteor.*, **9**: 176 (1952).
- (35) Ramanathan, K. R., and K. P. Ramakrishnan, *Mem. India Meteor. Dept.*, **26**: 189 (1937).
- (36) Rex, D., *Tellus*, **2**: 196 (1950).
- (37) Riehl, H., *Dept. Meteor., Univ. Chicago, Misc. Rept.* 17, 1945.
- (38) Riehl, H., *Dept. Meteor., Univ. Chicago, Misc. Rept.* 22, 1947.

- (39) Riehl, H., *Dept. Meteor., Univ. Chicago, Misc. Rept.* 24, Part 1, 1948.
- (40) Riehl, H., *J. Meteor.*, **5**: 247 (1948).
- (41) Riehl, H., *et al.*, *J. Meteor.*, **7**: 181 (1950).
- (42) Rossby, C.-G., *Bull. Am. Meteor. Soc.*, **28**: 53 (1947).
- (43) Rossby, C.-G., and H. C. Willett, *Science*, **108**: 643 (1948).
- (44) Sawyer, J. S., *Quart. J. Roy. Meteor. Soc.*, **73**: 346 (1947).
- (45) Schnapauff, W., *Veröffentl. Meteor. Inst., Univ. Berlin*, Vol. 2, No. 4, 1937.
- (46) Simpson, R. H., *Bull. Am. Meteor. Soc.*, **28**: 335 (1947).
- (47) Simpson, R. H., *J. Meteor.*, **9**: 24 (1952).
- (48) Solot, S. B., *The Meteorology of Central Africa*. Accra: U.S. Army Air Forces, Weather Research Center, 1943.
- (49) Solot, S. B., *U.S. Weather Bur. Research Papers* 28, 1948.
- (50) Solot, S. B., *U.S. Weather Bur. Research Papers* 32, 1950.
- (51) Staff Members, Department of Meteorology, University of Chicago, *Bull. Am. Meteor. Soc.*, **28**: 255 (1947).
- (52) Stone, R. G., *Bull. Am. Meteor. Soc.*, **23**: 4 (1942).
- (53) Taylor, G., *Australian Meteorology*. New York: Oxford University Press, 1920.
- (54) Wagner, A., *Gerlands Beitr. Geophys.*, **30**: 196 (1931).
- (55) Willett, H. C., *J. Meteor.*, **6**: 34 (1949).
- (56) Willett, H. C., and F. T. Bodurtha, *Bull. Am. Meteor. Soc.*, **33**: 429 (1952).
- (57) Yeh, T. C., *Tellus*, **2**: 173 (1950).
- (58) Yeh, T. C., *et al.*, in *Am. Meteor. Soc. Mon.* 3, p. 34, 1951.
- (59) Yeh, T. C., *et al.*, *ibid.*, p. 47, 1951.
- (60) Yin, M. T., *J. Meteor.*, **6**: 393 (1949).
- (61) Bowen, E. G., *Australian J. Phys.*, 6, Dec., 1953.



CHAPTER 11

TROPICAL STORMS

Then Poseidon drove together the clouds and stirred up the sea,
In his hands the Trident; he excited violent squalls
Among all the winds. With dense scud he covered
Earth and sea; night advanced from the sky.
Together broke East Wind, South Wind and stormy West Wind,
And the North Wind from cold lands, driving huge waves.

Odyssey, V, 291-296.

A hurricane or typhoon has been an incident in the lives of many. It is not easily forgotten. A friend remembers how the home of relatives in Galveston, Texas, was picked up by the winds and deposited elsewhere. Another speaks of the great difficulty he had in keeping his family indoors during eye passage. Nothing remains more vivid in the author's memory than the hammering that went on for a whole night in Puerto Rico when a hurricane was announced and 250,000 people boarded up their homes and possessions in San Juan.

Tropical storms have caused the sinking of many ships at sea. They have inspired such stories as Joseph Conrad's "Typhoon." Through gales and inundations has grown a long history of disasters on shore. These disasters are not confined to the tropics. Honshu and New England have been exposed to some of the most violent storms on record. Typhoons have played a sizable role in warfare, as during the Pacific campaign of 1944-1945.

Since timely warning can make all the difference between enormous loss of life and none, tropical storms have been a focal point of interest and study of many Europeans setting out for distant tropical lands in the age of discovery. Outstanding among them were groups of missionaries who built up a tradition of experience in all hurricane areas. Based on local observations of wind, high cloud drift, color of sky, sea swell, and other features, they were able to perfect warning services whose accomplishments can hardly be guessed and should never be forgotten. With the advent of weather charts and rapid communications the role of the missionaries as weather forecasters has declined. The famous wind signals, once displayed in Shanghai harbor and anxiously watched by many sea captains, are in disuse. The old message "Hoist hurricane warnings"

has been displaced by the forecaster who steps before the microphone every few hours to quickly give millions of people the latest news about a storm. With an expanding horizon of data, the scientists see hurricanes as a part of broad atmospheric circulations, influenced in their behavior by the winds over distant cold lands and in turn reacting on them.

THE LIFE CYCLE

Severe tropical cyclones are known as *hurricanes* in the Atlantic and the eastern Pacific, as *typhoons* in the western Pacific, and as cyclones or hurricanes in the other areas where they occur. Their life span averages about 6 days from the time they form until they enter land or recurve into the temperate zone. Some storms last only a few hours; a few, as long as 2 weeks. The evolution of the average storm from birth to death has been divided into four stages (20, 41).

1. *Formative stage.* Tropical storms form only in the preexisting disturbances described in Chaps. 9 and 10, waves and shear lines. Deepening can be a slow process, requiring days for the organization of a large area with diffuse winds (70). It can also be explosive, producing a well-formed eye within 12 hours. Winds usually remain below hurricane force in the formative stage. Strongest winds are apt to be concentrated in one quadrant only, poleward and east of the center in deepening waves in the easterlies, more variable in the equatorial trough. Surface pressure drops to about 1,000 mb.

2. *Immature stage.* Not all incipient cyclones become hurricanes. Some have been known to die within 24 hours even though winds had attained hurricane force. Others travel long distances as shallow depressions (51). If intensification takes place, the lowest pressure rapidly drops below 1,000 mb. Winds of hurricane force form a tight band around the center. The cloud and rain pattern changes from disorganized squalls to narrow organized bands spiraling inward. Only a small area is as yet involved.

3. *Mature stage.* The surface pressure at the center is no longer falling and the maximum wind speeds no longer increasing. Instead, the circulation expands during the mature stage, which may last a full week. Whereas winds of hurricane force may blow within a 20-30 mile radius during immaturity, this radius can increase to 200 miles in mature storms. The symmetry is lost as the area of gales and bad weather extends much farther to the right of the direction of motion than to the left (looking downstream).

It is surprising how much the size of mature storms can vary. Even with central pressure less than 950 mb, the radius of some storms is only 100-200 km. If the surface pressure averages 1,000 mb over the storm

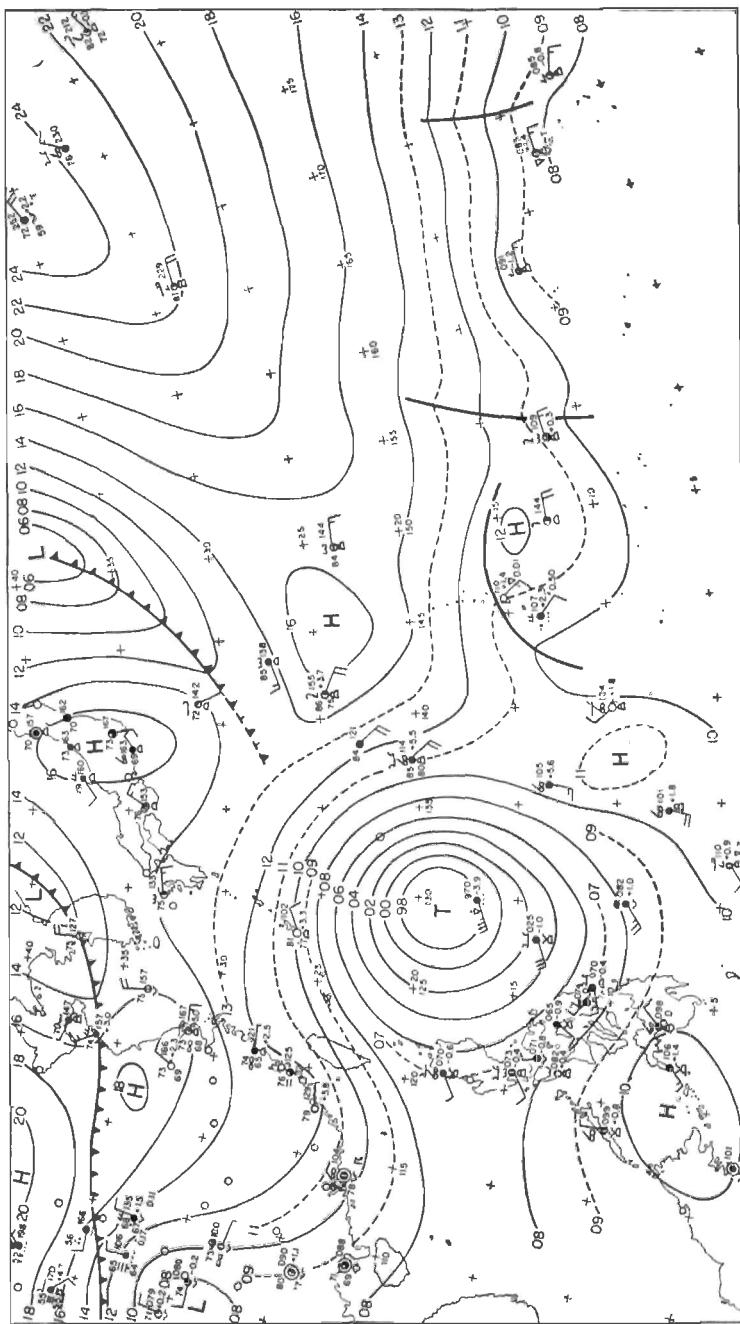


Fig. 11.1. Surface chart, Sept. 29, 1945 (38).

area, the mass will be 3×10^{11} - 10^{12} tons. In contrast, storms with similar surface pressure can attain a radius of 1,000 km (Fig. 11.1) and a mass of 3×10^{13} tons, fully two orders of magnitude greater. Only the strongest Icelandic and Aleutian lows have such a size. In the westerlies, the normal cyclone comprises about 5×10^{12} - 1×10^{13} tons.

4. *The decaying stage.* As a hurricane recycles from the tropics and enters the belt of westerlies, its size usually decreases. At times it dies; at others only the tropical characteristics decay, while the cyclone travels toward the subpolar belt, assuming a middle-latitude character, often with renewed vigor. But typical eyes have been encountered even poleward of latitude 50°.

Not all tropical storms recurve. Many dissipate after entering a continent in the tropics. A smaller number die over the tropical oceans.

SURFACE STRUCTURE OF TROPICAL STORMS

Observations taken in tropical storms over the years cover all stages of the life cycle and all storm sizes and intensities. It is no wonder, therefore, that the characteristics deduced by different investigators are not all identical. In some areas where active study has gone on, notably Japan,¹ most storms are in the decaying stage. In other areas the immature and mature stages are observed most frequently. Unless such differences are taken into account, much confusion can arise. Here, we shall be concerned mainly with the mature stage.

Surface Pressure

As we have seen in Chaps. 8-10, the surface pressure ordinarily varies little more than 0.3 per cent in the tropics. The central pressure of hurricanes may be 5 per cent, even 10 per cent, below average sea-level pressure. Sea-level isobars are therefore an excellent tool for the analysis of tropical storms. In Fig. 11.1 a large typhoon is situated east of the northern Philippines. The isobars surrounding this storm, which is moving northwestward, are not symmetrical. To the right of the direction of motion the pressure gradient between the 998- and 1,006-mb isobars is twice as strong as that to the left. Superposition of the pressure field of the storm on that of the current in which the storm is moving produces this typical asymmetry. Other deformations of the outer isobars also occur, such as the trough extending southeastward in Fig. 11.1. Analysts have often marked such a trough as a front, but since the air blows through it at a rapid rate, this interpretation cannot be defended.

¹ A list of references on the Japanese studies is contained in reference 71.

Inside the 998-mb isobar the analysis has not been completed; it would be almost impossible to draw accurate isobars. Close to the center the lines would become nearly circular as the influence of the steering current became negligible. Rather than draw all isobars it is preferable to mark the center position with a heavy dot and the letter *T*, which stands for "Tropical Storm" as distinguished from *L* for weaker tropical depressions and middle-latitude cyclones. A value for the central pressure should be noted if it is known or can be estimated fairly accurately.

Barograph traces at shore stations during hurricane passage furnish a measure of the pressure field in the core if the rate of movement is known. Traces have been published from all storm areas, especially the Philippines (15). They all show the same primary features. Figure 11.2 is

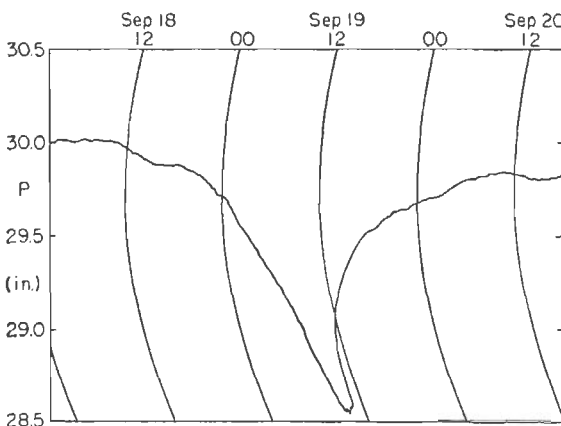


Fig. 11.2. Barograph trace at New Orleans, La., Sept. 18–20, 1947.

typical. The pressure fell with extreme rapidity in the 3 hours before arrival of the eye, then rose at an equal rate after passage. Dunn (20) cites pressure falls of as high as 40 mb in 20 minutes, observed on board ship in the Caribbean in 1943.

Pressure gradients computed from the barograph traces run from 0.5 mb/mile to 2 mb/mile and more. Total pressure drops of 50 mb in 50 miles are not uncommon. Central pressures often are phenomenal and are matched only rarely by storms over the subpolar oceans. Pressures of 950–960 mb are not unusual over the sea. Record pressures near 890 mb have been measured on at least three known occasions. Particularly reliable are the readings in the Florida Keys on Sept. 2, 1935, made in a small immature hurricane, and those obtained by Simpson (67) during a descent of reconnaissance aircraft in the eye of a large typhoon.

Lesser oscillations of variable amplitude and duration are superimposed on the general outline of hurricane barograms. Their periods, often irreg-

ular, vary from seconds to hours; their amplitude may be as much as several mb. The literature contains some heated arguments on the nature and reliability of these oscillations. The shortest periods may be attributed to the pounding of the long hurricane swells on the beaches, wind gusts, the swaying of the buildings which house the barograph under the impact of the wind (20), and nonhydrostatic pressure variations. Oscillations lasting minutes are probably related to the varying cloud structure. Except for the inner storm area the diurnal pressure variation can usually be followed quite easily.

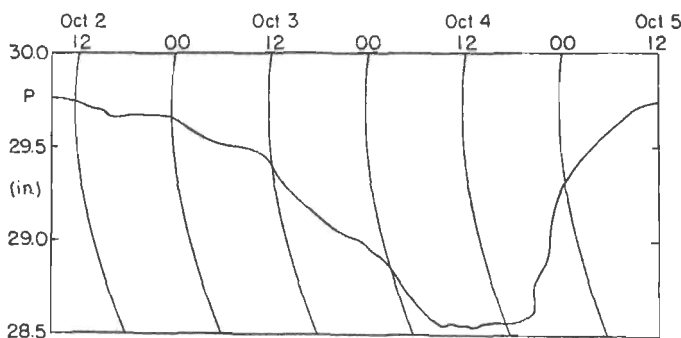


Fig. 11.3. Barograph trace at Okinawa (27°N , 128°E), Oct. 2–5, 1949. (Courtesy of C. E. Palmer.)

As one of a multitude of curiosities with which this book could be filled, Fig. 11.3 shows a barogram from Okinawa. The minimum pressure persisted for no less than 12 hours, as a typhoon became stationary over the island in an abortive attempt at recurvature.

Surface Temperature

Many published records, notably those by Deppermann (16), have proved that the surface temperature outside the eye is constant or decreases very slightly toward the center. The implications of this remarkable fact passed without notice until Byers (10) drew attention to it. The temperature of the surface air spiraling toward a center should decrease if adiabatic expansion occurred during pressure reduction. For instance, air entering the circulation with the average properties of the mean tropical atmosphere should reach the 930-mb isobar with a temperature of 20.5°C and specific humidity of 17 g/kg. Because of condensation, a dense fog should prevail at the ground inward from the 970-mb isobar. But this is never observed. It follows that *the potential temperature of the surface air increases along the inward trajectories*. We also

know that the specific humidity increases and that the cloud bases remain between a few hundred and 1,000 feet.

The surface air thus *acquires both latent and sensible heat during its travel toward lower pressure*. Figure 11.4 shows the variation of potential temperature and specific humidity during isothermal expansion, if we assume that the surface air must be lifted 20 mb in order to reach its condensation level at pressures less than 990 mb. That tropical storms contain a local heat source within their circulation will greatly facilitate the explanation of the temperature distribution aloft and of the surface barograms.

A source for the heat and moisture increment is obvious. The ocean is greatly agitated, and large amounts of water are thrown into the air in the form of spray. It is hard to say where the ocean ends and where the atmosphere begins! As the air moves toward lower pressure and begins to expand adiabatically, the temperature difference between ocean and air suddenly increases. Since the surface of contact between air and water increases to many times the horizontal area of the storm, rapid transfer of sensible and latent heat from ocean to air is made possible. In the outskirts, say beyond the 990-mb isobar, the turmoil is less and the process of heat transfer is not operative. This has been considered in Fig. 11.4 by holding potential temperature and specific humidity constant at pressures above 990 mb.

Surface Wind

By far the greatest damage is caused by the winds and wind-produced hurricane tides and waves. Among the many photographs Tannehill (70) shows of the wreckage left by hurricanes, none is more impressive than that of a royal palm with its trunk completely pierced by a long, narrow pine board. The pressure that wind exerts on buildings is roughly proportional to the kinetic energy of the wind and therefore to the square of the wind speed. With sustained winds above 120 knots the number of buildings in any community capable of withstanding the storm thus is quickly reduced. Inhabitants of tropical areas often abandon their homes for the safety of churches and public buildings, which usually have the sturdiest construction. As the area of extreme wind is always quite

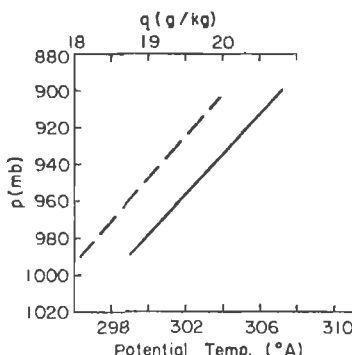


Fig. 11.4. Potential temperature and specific humidity as a function of surface pressure in hurricanes.

small, it is understandable how storms often wreak complete havoc in one community and leave nearby towns little damaged.

No one knows how high wind speeds can rise in tropical storms. At observing stations the anemometer is usually blown away at speeds which exceed 120 mph. A few anemometers, specially constructed for hurricane measurements, have recorded winds above 160 mph. Over the sea and at a distance of a few hundred feet above the ground the wind speed may attain 200 mph in a very small area.

Attempts have been made to calculate the wind speed as a function of the radius. For such purposes the storms usually are considered to be stationary, symmetrical, and frictionless. The profiles of tangential and radial wind components are deduced with some assumptions about the laws of motion valid in hurricanes. Conservation of angular momentum is one such frequent assumption. The storm is considered to be a "simple" vortex with point convergence at the center. In setting up the equations for the wind distributions it is necessary to include the effect of the earth's rotation, a factor sometimes overlooked. Given the tangential component v_θ , the radial component v_r , the distance from the center r , and the Coriolis parameter f , the equations are

$$v_\theta r + \frac{fr^2}{2} = \text{const.}, \quad (11.1)$$

$$\frac{\partial v_r}{\partial r} + \frac{v_r}{r} = 0. \quad (11.2)$$

Since (11.1) would lead to infinite speeds at the center, Deppermann (17) has proposed a Rankine vortex with velocity distribution $v_\theta/r = \text{constant}$ for the central area.

The observations do not bear out the theoretical profiles. It is true that data from storms with extreme wind maxima have been too sparse to permit complete analysis. Further, a few famous often-cited typhoons have been observed in which the relation $v_\theta r = \text{constant}$ was approximately satisfied. But the author knows of no physical law specifying conservation of relative angular momentum. If the earth's rotation is included, all observed wind profiles fall far short of that which (11.1) demands, largely owing to friction. Realizing this, some writers have been content to develop empirical formulas of the type $v_\theta r^x = \text{constant}$. In a number of cases values of x ranging from 0.4 to 0.6 have given an approximate fit. But the general problem of finding the maximum wind given data on the periphery remains unsolved.

In order to obtain an average picture of the low-level wind distribution in tropical storms, Hughes (34) has summarized a large number of reconnaissance flights of the U.S. Navy made near 1,000 feet. Once thought an impossible feat, aircraft have penetrated even large and violent

typhoons regularly since 1943 with remarkably few accidents. The reconnaissance missions either make center penetrations or circumnavigations. Figure 11.5 shows an example of the latter type of flight. It is difficult, of course, to navigate with precision and make accurate wind computations in extremely bad weather.¹ Hughes therefore selected the 84 best flights out of several hundred available. Several of these covered a single stationary storm of moderate intensity. The profiles of wind, divergence, and vorticity for this typhoon are reproduced in Figs. 11.6

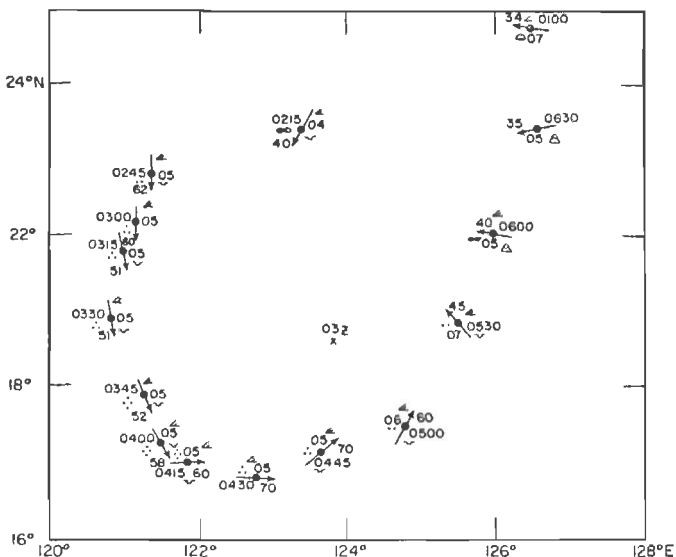


Fig. 11.5. Reconnaissance flight, Sept. 30, 1945 (38). Time of observation to right of wind arrow, altitude of aircraft (100's feet) to left, and wind speed (knots) at tip of arrow.

and 11.7. All convergence is concentrated within 100 miles from the center. It becomes extreme at a radius of 60 miles. In the outer area divergence prevails of the magnitude normally encountered in synoptic disturbances. Here descent is taking place; convective activity should therefore be below average, and this is frequently observed in the outskirts of a storm. The region where the divergence changes rapidly to intense convergence may correspond to the "bar" of the storm.

Hughes divided all moving storms into three classes, immature, small mature, and large mature. Since the wind distribution turned out to be

¹ With increasing use of radar, which can "see" the storm and its eye, circumnavigation and other types of flight not requiring penetration give excellent center fixes for operational purposes. Tracking is especially accurate when the airplane is flying in an area where its radar beam also intercepts land.

fairly similar for all three classes except in scale, only the large storms will be discussed.

Hughes averaged all flights, using a polar-coordinate system in which the direction of motion remained fixed rather than a geographical direction such as north. This procedure permits the averaging to be done

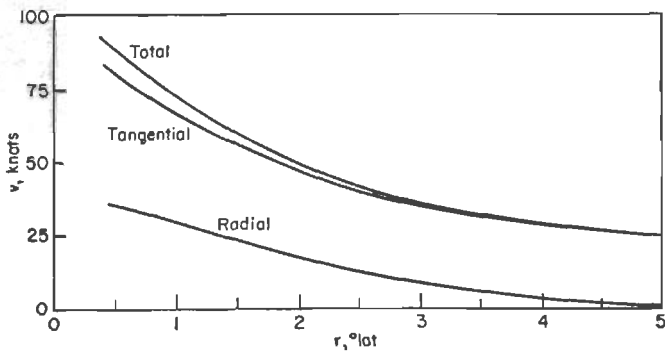


Fig. 11.6. Velocity profiles for stationary storm (34). Radius (r) is measured from center.

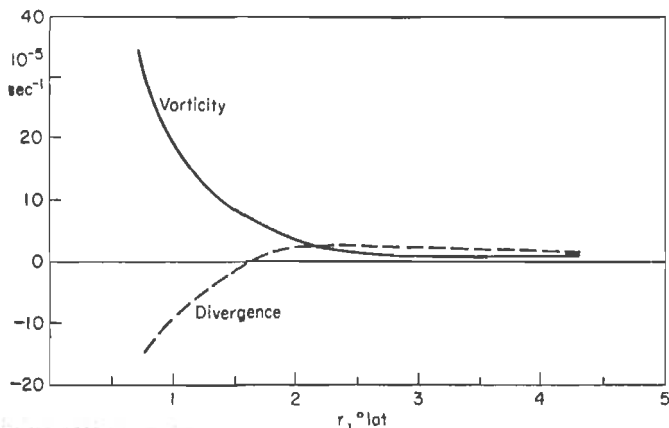


Fig. 11.7. Profiles of divergence (dashed) and vorticity (solid) computed from Fig. 11.6. Positive values: divergence or cyclonic vorticity; negative values: convergence or anticyclonic vorticity.

with respect to the direction of motion, and all asymmetry introduced by the motion is preserved. Although averaging always reduces extremes, a center of over 90 knots (100 mph) nevertheless appears in the picture of total wind speed (Fig. 11.8). Winds are higher to the right of the direction of motion than to the left. To the right, carrying current and circulation act in the same sense; to the left, they are opposed. We have already encountered this asymmetry, one of the best-known features of

tropical storms (11, 14) in the pressure field. Since Fig. 11.8 is computed from large storms, it is not surprising that winds blow at 25–30 knots far from the center. In many typhoons we find a huge outer area with radius as much as 8° latitude in which the wind speed is constant near 30 knots. This enormous peripheral circulation constitutes the main difference between large and small mature storms. Conditions in the core are quite similar.

Since the tangential by far exceeds the radial component, the field of the tangential component (Fig. 11.9) closely resembles that of total wind

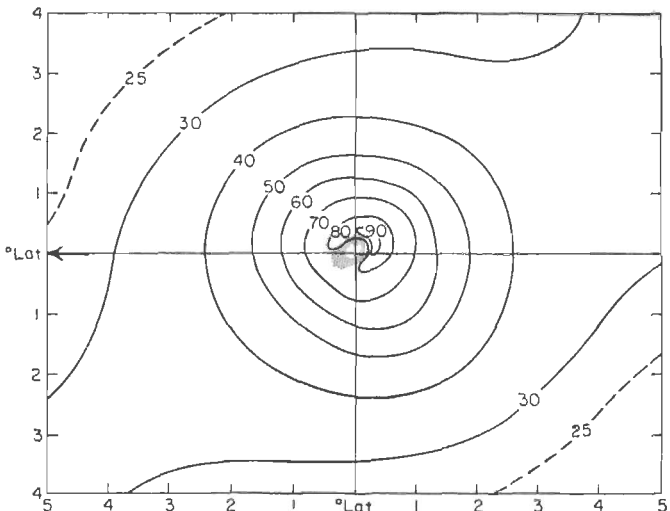


Fig. 11.8. Total wind speed (knots) near 1,000 feet for moving storms. Arrow indicates direction of storm movement (34).

speed. The radial component (Fig. 11.10) is much stronger in the rear than in the front quadrants.¹ In consequence the angle of incurvature of the flow is also greatest in these quadrants (Fig. 11.11), agreeing with earlier findings (11, 28).

From Figs. 11.10 and 11.11 it might seem that the air in the left rear quadrant was approaching the center most rapidly. Because of the storm movement, however, this is not the case. To obtain a true picture of the inflow, we must subtract the storm movement from the total velocity field and then compute the radial velocity relative to the moving center (Fig. 11.12). We now see that it is the air in the right front quadrant which is really approaching the center most rapidly. This is shown further by relative trajectories (Fig. 11.13). Air located in the right front quadrant

¹ Tropical storms are commonly divided into four quadrants oriented with respect to the direction of motion: right front, right rear, left front, left rear.

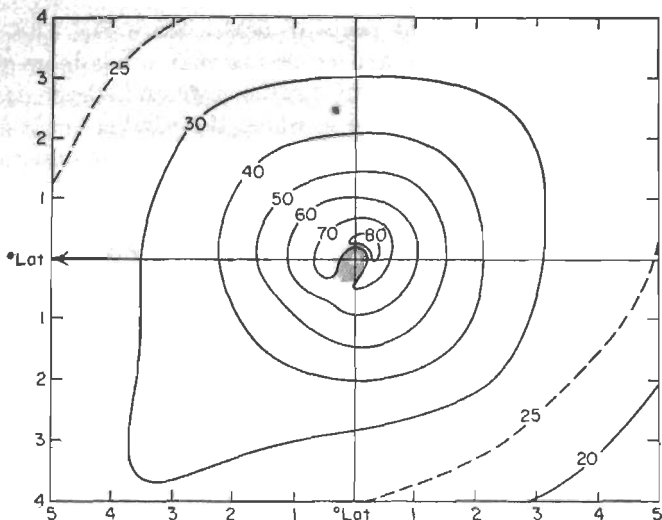


Fig. 11.9. Tangential velocity (knots) (34).

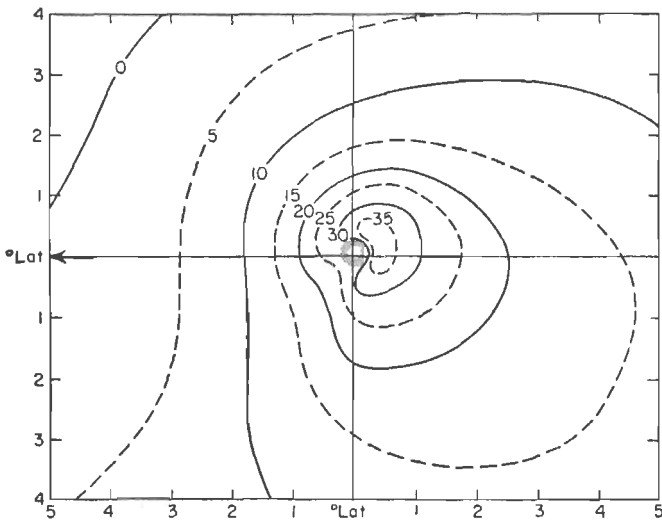


Fig. 11.10. Radial velocity (knots) (34).

will move to within 30 miles of the center in less than 4 hours. In contrast, air approaching from a radius of 4° in the left rear quadrant requires nearly a day to reach the core.

Figures 11.9 and 11.10 permit computation of the fields of divergence (Fig. 11.14) and relative vorticity (Fig. 11.15). In the central area, the values of convergence are excessive, as they also are in the case of the stationary storm (Fig. 11.7). Convergence is strongest in the left rear

quadrant. *Fully half of the storm is divergent* to a radius of about 100 miles. Accordingly, prolonged suppression of convective activity, followed by the sudden onset of heavy clouds and rain, should be experienced at the approach of a storm, and this indeed occurs in many cases.

Figure 11.15 shows that the relative vorticity and therefore certainly the absolute vorticity are positive everywhere. Recalling the definition of vorticity in natural coordinates (Chap. 8), this result is by no means obvious. The rapid inward increase of wind speed represents anticyclonic shear. Opposed is the contribution of the curvature term. According

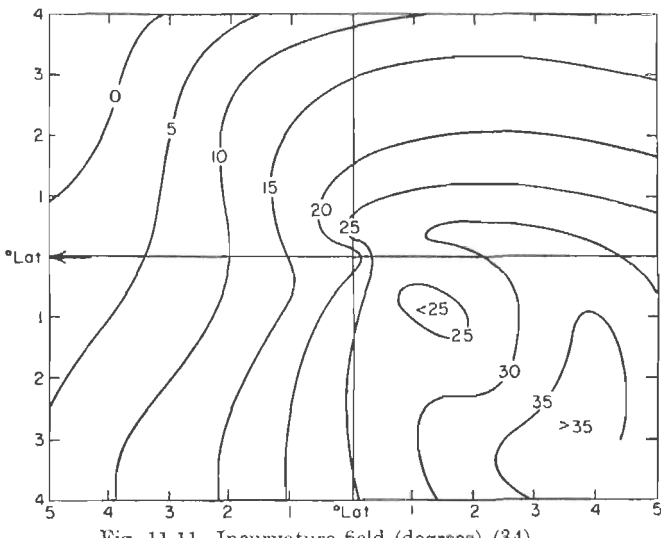


Fig. 11.11. Incurvature field (degrees) (34).

to Fig. 11.15 this term predominates as the relative vorticity increases through the core to attain values more than six times that of the Coriolis parameter at the mean latitude of tropical storms (about 20°).

Rainfall

Rain-gauge measurements give only a poor approximation of the rainfall in hurricanes. The wind drives the rain horizontally and picks up water already fallen to the ground. Even slight topographic features such as buildings, lakes, and small hills greatly influence the precipitation. Since most records stem from tropical islands, usually mountainous, reports of rainfall amount and distribution vary widely.

Recorded precipitation has been as low as a trace in October, 1941, in the Florida Keys, in spite of winds of 120 mph. It has been as extreme as 100 inches, three to four times the average annual precipitation at

most cities of the temperate zone, during one typhoon passage in the Philippines. Amounts of 20 inches are fairly common. Of course, the rain intensity of a storm, its rate of motion, and its track relative to a station bear directly on the recorded precipitation, in addition to inaccuracy of measurement and terrain influences. In order to obtain a picture as free as possible from these many effects, we can make use of Fig. 11.10 to solve a continuity problem in moisture. The rainfall (minus the evaporation) within a circle of specified radius must equal the difference between inward and outward transport of moisture across this circle.

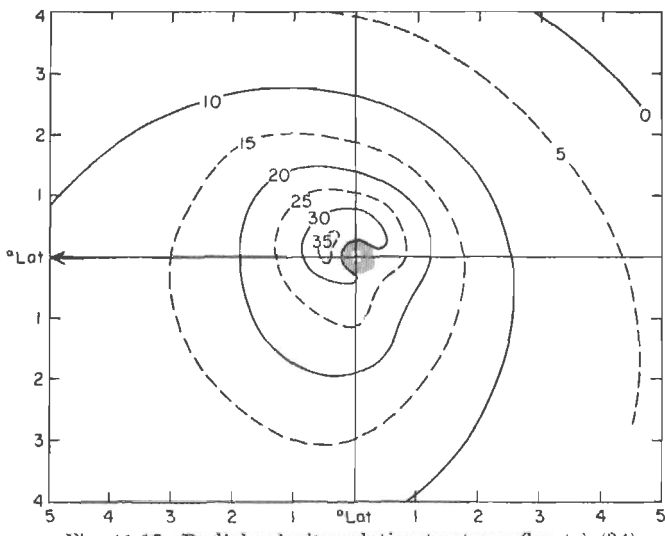


Fig. 11.12. Radial velocity relative to storm (knots) (34).

Since the outflow takes place in the high troposphere, where the moisture content of the air is less than 10 per cent that in the subcloud layer, we can neglect it for an order-of-magnitude computation. The inflow of moisture across the circle of radius r is equal to the circumference of the circle $2\pi r$ multiplied by the mean specific humidity \bar{q} of the inflow and the mass flux $v_r \Delta p/g$ across the circle. This product must be equal to πr^2 , the area within the circle, multiplied by R , the rainfall per unit area and time. Thus,

$$R = \frac{2v_r}{r} \bar{q} \frac{\Delta p}{g}. \quad (11.3)$$

Suppose \bar{q} is the specific humidity of the subcloud layer of the mean tropical atmosphere and Fig. 11.10 is taken as valid for the lowest kilometer of the atmosphere ($\Delta p = 100$ mb). Then the rainfall per unit area inside given radii and given rings is as shown in Table 11.1.

TABLE 11.1. RAINFALL IN MOVING STORMS

Radius, deg. lat.	Col. 1	Ring, deg. lat.	Col. 2
0.5	86.3	0.0-0.5	86.3
1.0	33.7	0.5-1.0	16.0
1.5	18.0	1.0-1.5	5.4
2.0	10.8	1.5-2.0	1.5
2.5	7.0		
3.0	5.0		
3.5	3.9		
4.0	3.0		

Column 1: Average rainfall inside given radius (cm/day).

Column 2: Average rainfall in given ring (cm/day).

The precipitation is concentrated in the inner core, where the slope of the barograph traces is steepest. A locality which remains for many hours near the center of a slowly moving storm may suffer a deluge, while another area, just missed by the inner core of a fast-moving storm, may

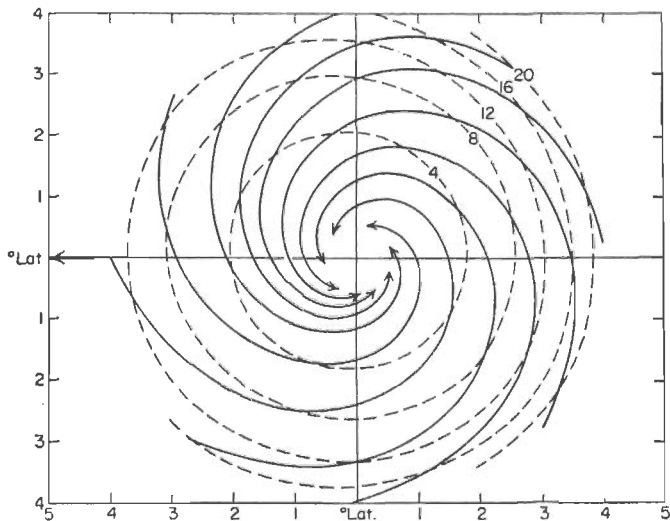


Fig. 11.13. Trajectories relative to moving center (34). Dashed lines indicate number of hours required to reach a point 0.5° latitude from center.

experience very little rain. If a storm with the rainfall distribution given by Table 11.1 moved directly across a station at an average speed of 12 knots, the storm duration would be 2 days and the total precipitation 38 cm, or 11 inches. Such an average is reasonable and compares favorably with the mean rainfall Cline (11) found for hurricanes on the Gulf coast of the United States.

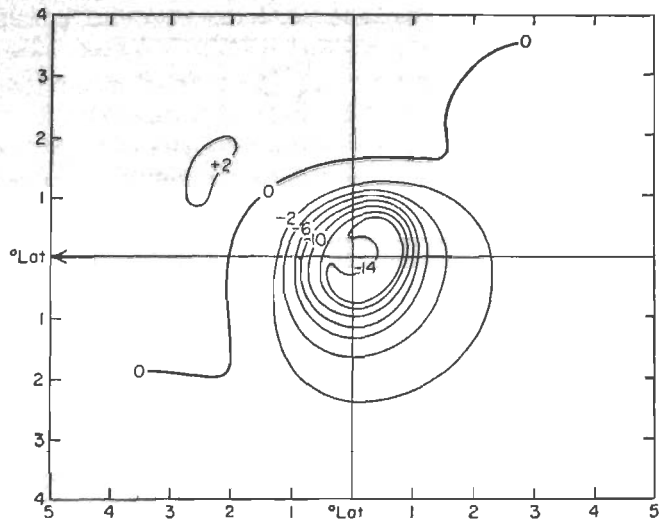


Fig. 11.14. Field of divergence (10^{-5} sec^{-1}) (34). Negative values indicate convergence.

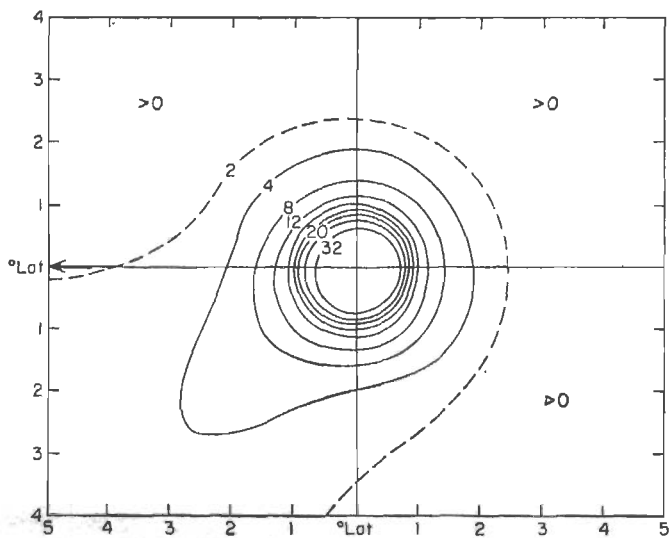


Fig. 11.15. Field of relative vorticity (10^{-5} sec^{-1}) (34).

The distribution of precipitation intensity suggested by Fig. 11.14 does not always hold (11, 14). In many Atlantic hurricanes the bad weather extends farther to the right than to the left of the direction of motion, where indeed it may end abruptly within 40 miles of the core. Usually the left front quadrant is safest for aircraft penetration if a storm is moving between west and north. Weather in the left rear quadrant may be

much more severe; there isolated bands of intense convection may extend several hundred miles from the storm center (49). These bands probably form the outer part of a system of spiraling lines of convection.

As tropical storms recurve toward higher latitudes, the precipitation pattern can change. Rainfall is concentrated in the right front quadrant of storms moving across the Gulf coast of the United States. This concentration has been ascribed to differences in friction between land and water, but another factor is the rapid weakening of the storms after they move inland. Finally, drier air, even modified polar continental air, is often drawn into the circulation by the west and northwest winds on the Gulf coast. When this happens, the sky clears quickly to the south of a northward-moving center.

Surface Characteristics of the Eye

The eye of the hurricane has held the attention of all who have written on tropical storms from the earliest times. It is one of the oddest phenomena in meteorology. Precipitation ceases abruptly at the boundary of well-developed eyes; the sky partly clears; and the wind subsides suddenly to less than 15 mph, at times to a dead calm. The sun or the stars become visible. Observers have described conditions in the eye as "oppressive," "sultry," and "suffocating," but as Dunn (20) notes, this reaction is psychological and due to the rapid transition from hurricane winds and torrential rain to relatively calm conditions.

In mature storms, the diameter of the eye averages 15 miles, less in immature storms. It may attain 40 miles in large typhoons. Although it is usually described as circular (Figs. 11.23 and 11.24), the eye sometimes becomes elongated; sometimes it is diffuse with a double-structured appearance. Modern observations, especially those made by radar, have proved that an eye does not remain in steady state but is constantly undergoing transformation. In view of the extreme conditions at the edge of the eye this is hardly surprising.

Inside the eye, the surface temperature of the air does not differ from that on the outside; with sunshine it may become slightly warmer. A few famous cases on record show a rapid temperature rise and humidity drop in the eye. These observations were once thought to indicate a breakthrough of the subsiding air to the surface, but they have since been satisfactorily explained as the result of downdrafts from mountain ranges.

On the barograph trace (Figs. 11.2 and 11.3) the eye appears as a generally flat area but often with considerable pumping. These fluctuations are probably related to mixing of the air in the eye with that of the surroundings. Sometimes the barometer drops a little from the edges

to the center of the eye; sometimes it is lowest at the edges. Such pressure gradients have not yet been explained but probably cannot be regarded as anything but transient features.

State of the Sea

The extreme wind stress exerted on the ocean surface in tropical storms produces huge waves with extreme heights, reported to be as much as 45 feet. Detailed discussion of wave generation and propagation, also

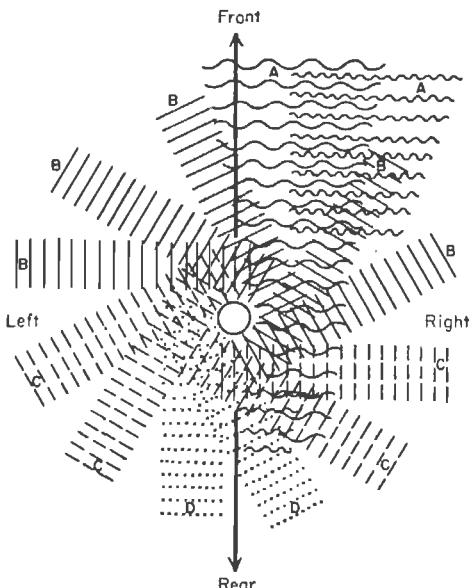


Fig. 11.16. Sketch of swell propagation in tropical cyclones (20, after 70). (Courtesy of American Meteorological Society and U.S. Air Force, Cambridge Research Center.)

of tides, may be found in textbooks on oceanography and in summary articles in the *Compendium of Meteorology* (2). Figure 11.16 shows schematically that these waves travel outward in all directions from the storm center. They are spotted, as long sea swell, 1,000 miles distant and more. The speed of propagation of the long waves may approach 1,000 miles/day. Since the average storm displacement is only one-third of this rate, the ocean waves provide early warning of an impending hurricane.

Waves generated in the right rear quadrant travel in the direction of the storm. They propagate under the influence of winds with relatively little change in direction for a longer time than waves in the other quadrants and consequently have a comparatively long fetch. Thus the

strongest swells are produced in this part of the storm. When they arrive at a distant coast line, the normal wave frequency, which may be 10-15 per minute, decreases to 2-4 per minute. The direction of the swell indicates the position of the center at the time the swell was generated. If this direction remains constant, the storm will approach the area directly. If it changes counterclockwise, the storm center will pass from right to left across the area, as seen by an observer facing the storm. A clockwise turning indicates the opposite movement.

In spite of the great ocean depths, the tremendous surface waves in hurricanes initiate vibrations at the bottom of the ocean; these may be recorded by seismographs at distant places. Such vibrations are known as *microseisms*. Because of their longer period (2-6 seconds) microseisms due to tropical storms can be distinguished from other vibrations produced, for instance, by local pounding of the surf.

The large and controversial literature on microseism has been summarized by Gutenberg (27). Although no fully satisfactory theory of transmission of wave energy has yet been evolved, the phenomenon itself is not in doubt. Many attempts have been made to determine position and intensity of tropical storms from seismic records. Since the composition of the earth at the ocean bottom and geological faults influence wave propagation and decay of wave energy, a general technique for using seismic measurements in hurricane tracking has not yet been evolved, in spite of some success at several stations. Techniques that take into account the geological peculiarities of each hurricane area may gradually be perfected.

Among the most severe effects of a hurricane is the damage done along coasts by the ocean waves. Such damage is suffered mainly where land partially surrounds water bodies such as the Bay of Bengal and the Gulf of Mexico. Sustained wind in the right-hand quadrants (in the northern hemisphere) piles up water along the shore line so that the gravitational high tide rises as much as 10 feet above normal. Such "storm tides" are of course not peculiar to the tropics; they are a constant source of danger in all constricted seas. High tides permit the long swell to penetrate the shore line and break with full force over coastal settlements.

An even greater threat is the so-called "hurricane wave," a sudden rising of the water by 10-20 feet and more. Because the wave propagates so rapidly, there is no escape. The greatest hurricane disasters, including the complete destruction of large towns, have been attributed to the sudden inundation.

In spite of the many written accounts, no clear picture emerges of the hurricane wave. Of course, the whole setting is not the best for scientific observation! Storm waves seem to be best developed in and near the eye, but at times they have reached the shore well before center passage.

Most descriptions speak of a "wall of water" breaking in from the sea, suggestive of a solitary wave. Others mention several waves or a series of waves. It has been suggested that the rise of the water may be due to the decrease of atmospheric pressure. Since this reduction is only 10 per cent at most, a rise of no more than 3 feet could be explained on this basis directly. We have seen, however, how rapidly the barometer falls within a hurricane core; a slope of 1-2 feet of the water surface in 20-30 miles can be produced by the pressure field. Here, certain types of unstable waves may be initiated.

UPPER-AIR STRUCTURE OF TROPICAL STORMS

Upper-wind Structure

One of the earliest controversies in regard to tropical storms concerned their vertical extent. Some writers claimed that they disappeared at heights as low as 3 km, that people standing on mountain tops could look down on the violent cyclonic whirls beneath them. They believed that the cirrus motion remained undisturbed and indicated the direction in which the cyclone was moving. Others insisted that hurricanes reach to great heights, 10 km or more. They thought that cirrus radiated in all directions from the storm and used the change of direction of cirrus movement to track centers.

The answer to this controversy is now well known. Haurwitz (30) has shown theoretically, and high-level observations empirically, that mature storms extend through the troposphere. Quite unexpected until the era of rawinsondes, however, was the fact that the high-level flow is anti-cyclonic, that a clockwise circulation (in the northern hemisphere) overlies the low-level counterclockwise wind field above 300 mb.

Because of the great difficulties of releasing balloons in hurricane weather, we must piece together isolated bits of information to deduce the upper-wind structure. Synoptic streamline charts are no more available for the upper levels than for the surface. No balloon ascents have been made in the belt of extreme wind, but many soundings reach to within 100 miles of storm centers. They all show the same general features if reports from the decaying stage are excluded. We also have a fair number of ascents from the formative stage. Figure 11.17 shows the passage of an incipient typhoon at Guam which within 2 days became a storm of huge proportions. The wind direction reverses completely between the surface and 40,000 feet. Ahead of the center, winds turn clockwise with height; to its rear, counterclockwise. Scattered data above 55,000 feet indicate that the stratospheric easterlies continue to blow undisturbed in spite of the upheaval underneath. This is the prime

reason why we can state with confidence that the *top of mature storms is situated very close to the 100-mb level, the average tropopause height.*

E. S. Jordan (36) has computed a mean picture of the circulation pattern at different heights, based on about 130 wind reports reaching at least 30,000 feet. As data within 2° latitude from the storm centers were very scarce, only the area outside the 2° radius could be analyzed. The zone of strongest surface-pressure fall, wind, and precipitation remains unexplored aloft.

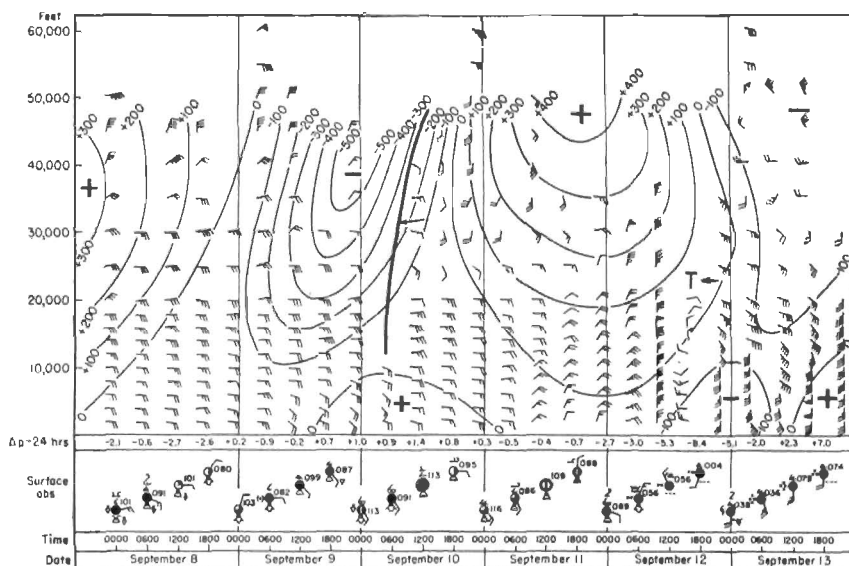


Fig. 11.17. Vertical time section at Guam (14°N , 145°E) Sept. 8-13, 1945 (51). Solid lines are 24-hour height changes of constant-pressure surfaces (feet).

At 7,000 feet, the field of the tangential wind component (Fig. 11.18) resembles that of Fig. 11.9. At 18,000 feet the pattern is unchanged except for some decrease of speed. A marked change, however, is noticeable at 30,000 feet. Speeds have decreased considerably. A zero line separating counterclockwise- and clockwise-rotating winds appears in the outer portion of the circulation. Still higher, this zero line is contracting toward the center. Inside, the strength of the cyclonic circulation continues to weaken upward steadily. Outside, speeds in the ring of air rotating anticyclonically have risen above 20 knots. Figure 11.19a is an average picture of the distribution of lateral and vertical shear. Both shears are strongest at the highest levels close to the core. The change from cyclonic to anticyclonic circulation takes place only slowly in the low levels but proceeds quickly above 30,000 feet in the layers of outflow.

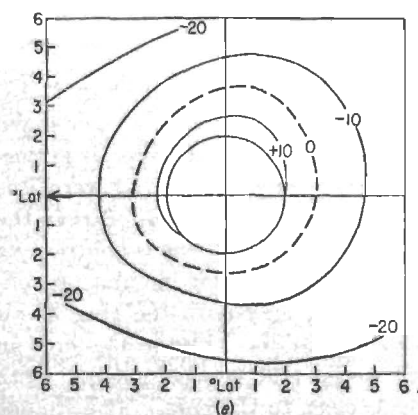
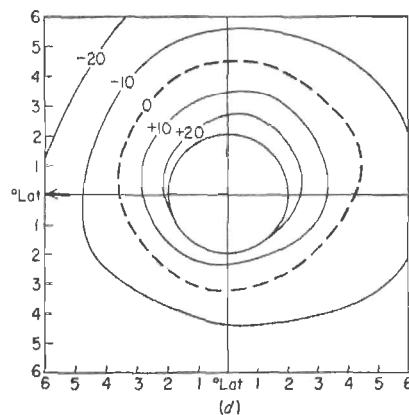
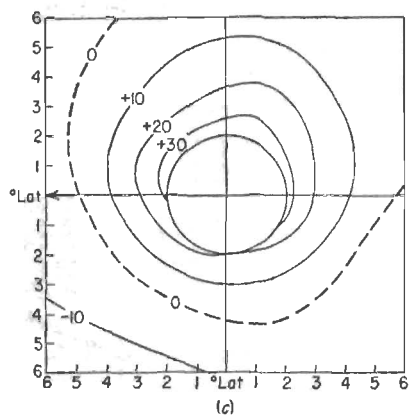
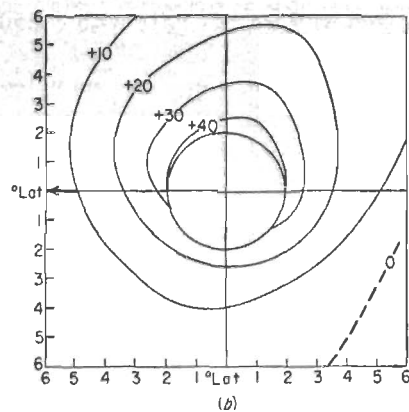
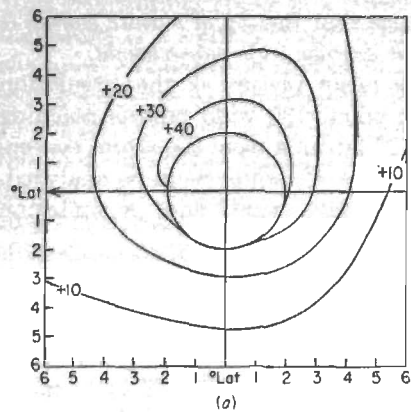


Fig. 11.18. Tangential velocity (knots) at (a) 7,000 feet, (b) 18,000 feet, (c) 30,000 feet, (d) 40,000 feet, and (e) 45,000 feet.

Figure 11.19b shows the average distribution of relative vorticity. Values are positive in the lowest levels, but the area occupied by cyclonic vorticity contracts upward and vanishes above 400 mb. The horizontal shear is anticyclonic everywhere. At low levels cyclonic curvature makes a greater contribution to the relative vorticity than the shear. But the anticyclonic shear increases with height while the curvature term decreases. Above 30,000 feet both shear and curvature terms are anticyclonic over a widening area.

Since we are discussing an averaged wind field, all gradients shown are smaller than would be observed in many instantaneous wind fields. Even so, the relative vorticity attains $-4.5 \times 10^{-6} \text{ sec}^{-1}$ at 200 mb. The

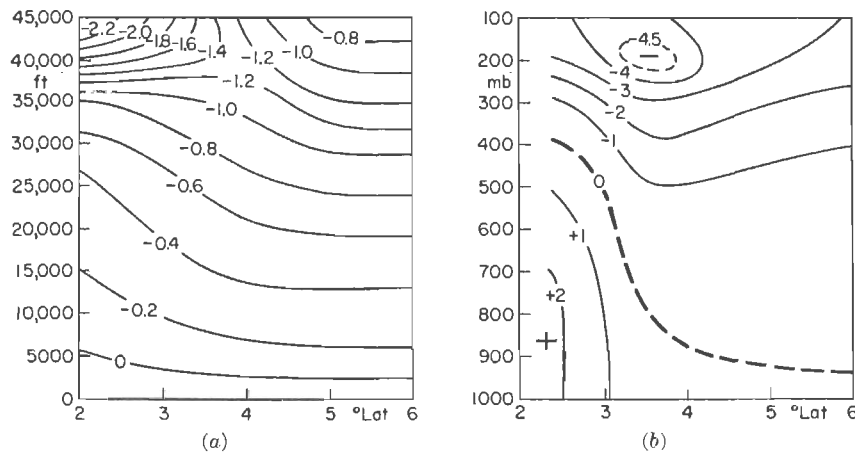


Fig. 11.19. (a) Cross section of vertical shear of tangential velocity (knots per 1,000 feet) and (b) relative vorticity (10^{-6} sec^{-1}) (36).

Coriolis parameter within the latitude range of the majority of the storms is $5-6 \times 10^{-6} \text{ sec}^{-1}$; the mean absolute vorticity therefore approaches zero.

The field of the radial component could be ascertained with some certainty only at the lowest and highest levels. Through the deep layer from 10,000 to 30,000 feet radial speeds are small and vacillate between inflow and outflow. It is best to say that radial motion is zero in this layer. *All major inflow is confined to the low troposphere; all outflow, to the high troposphere.*

At 7,000 feet (Fig. 11.20) the net inflow across the 2° ring is only one-third that in Fig. 11.10. Even this smaller inflow should cease nearer the center. We shall see in connection with the temperature field that all inflow in the zone of high wind and heavy rain is probably restricted to the lowest 3,000 feet. At 45,000 feet pronounced outflow is centered along the direction of motion. As additional evidence Fig. 11.21 indi-

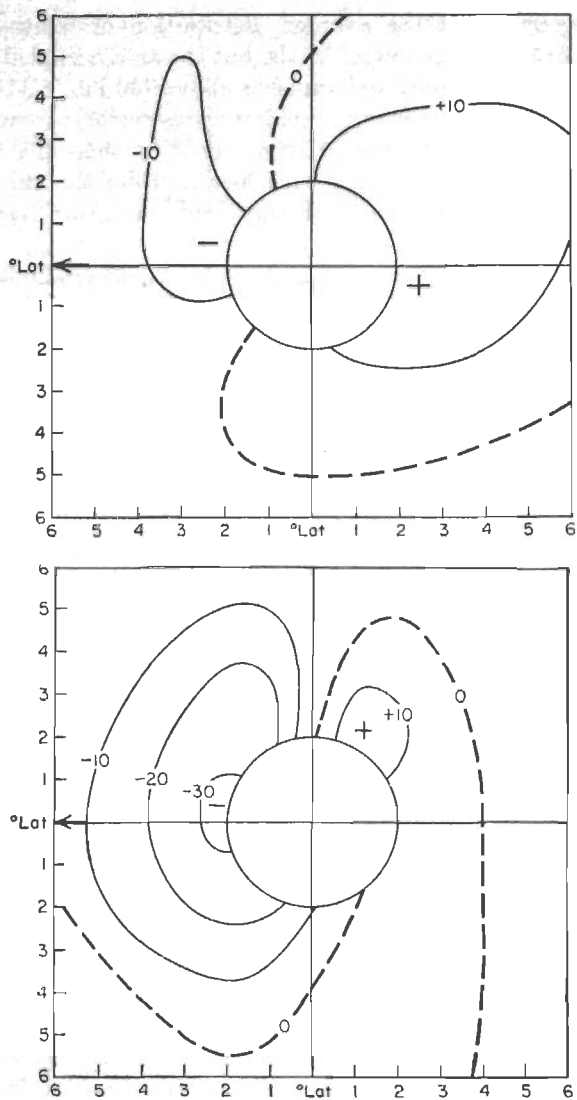


Fig. 11.20. Radial velocity (knots) at 7,000 feet (top) and 45,000 feet (bottom) (36).

cates concentration of the outflow in the high troposphere. This figure shows the vertical variation in pressure difference between the mean tropical atmosphere and a mean hurricane sounding (Fig. 11.27) computed by Schacht (62). Some uncertainty exists in the highest levels because of scarcity of data. Therefore Fig. 11.21 shows both the computed percentage in the tropopause region and the percentages which

should be observed if the easterlies remained undisturbed above 100 mb. The percentage changes little from the ground to 700 mb, then decreases upward. Near 11 km, pressure inside and outside are equalized; this is just in the layer in which anticyclonic flow becomes marked. Still higher, pressures inside the storm exceed those outside, greatly facilitating the outflow.

The total velocity field at 45,000 feet (Fig. 11.22) is spectacular. Near the center the circulation is cyclonic but becomes anticyclonic within a radius of 3-4°. The clockwise cell to the right of the direction of motion does not appear to be a fictitious feature introduced by the averaging, since in particular situations winds turn clockwise rapidly to the right of the storm path (38).

At 45,000 feet the field of relative motion differs from the total wind field in that the inflow still apparent in the right rear quadrant disappears. Air particles diverge from the storm area in all directions. In the shear zone between the cyclonically and anticyclonically rotating air we observe smaller clockwise-rotating eddies. Whether or not the exact location of these eddies holds in all individual cases is open to question, but an anticyclonic shear zone with eddy structure is usually observed.

Dynamic Aspects of the Outflow. It is not yet possible to construct a complete three-dimensional wind and pressure field in tropical storms; so the exact form of the equations of motion governing the outflow cannot be stated. Considering frictional effects to be of secondary importance, Durst and Sutcliffe (21) suggest that conservation of angular momentum [Eq. (11.1)] may be a valid law for the rising air. Most of the ascent starts in the narrow ring of the inner core. For instance, 75 per cent of the air shown in Fig. 11.10 as entering the outer circulation begins to move upward only after penetrating to within 60 miles or less of the center. We shall restrict our consideration to this narrow current. In spite of the extreme increase of the pressure-gradient force near the center, the radial velocity decreases in the inflow as the combined increase of centrifugal and surface frictional forces becomes even larger. At some distance above the surface, probably at 2,000-3,000 feet, the inward motion of the rising air ceases. If friction can be left out of account here, the balance of forces is given by the pressure-gradient and centrifugal forces, *i.e.*, we have cyclostrophic balance.

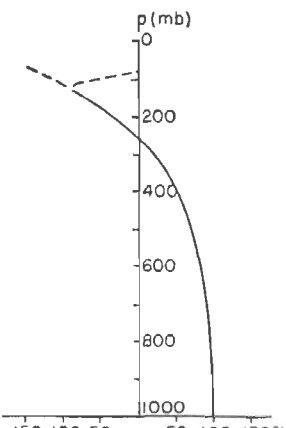


Fig. 11.21. Vertical profile of mean pressure difference between inside and outside of hurricanes, expressed in per cent of the surface difference (50).

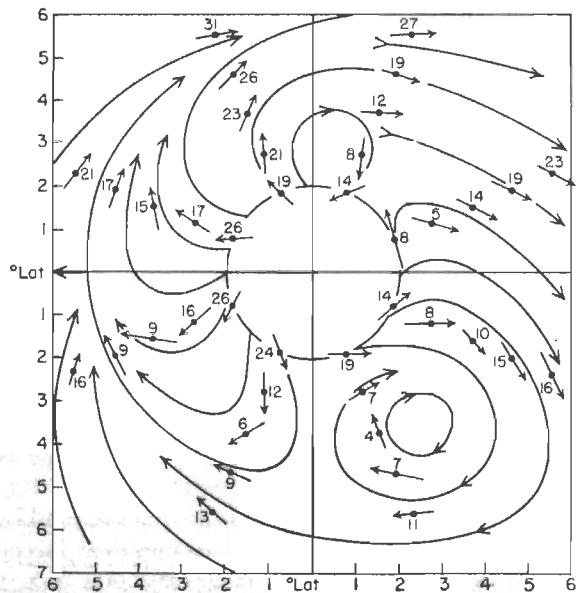
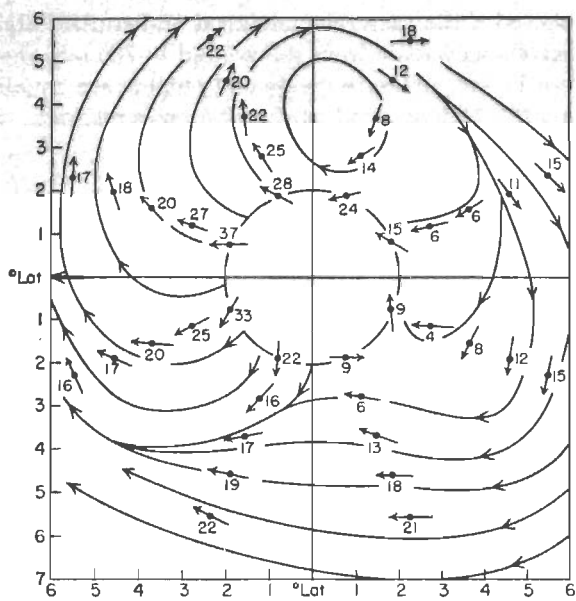


Fig. 11.22. Total velocity at 45,000 feet (top) and flow relative to moving center at 45,000 feet (bottom) (36).

Since the pressure gradient does not change much up to 700 mb, the ascent may be nearly vertical to this level and the vertical gradient of wind speed small. In the middle troposphere the pressure-gradient force decreases so that the centrifugal force begins to exceed the pressure-gradient force. The air is accelerated outward from the center toward higher pressure so that its speed begins to decrease. Above 250 mb, pressure-gradient and centrifugal forces combine and the outward acceleration becomes extreme.

If Eq. (11.1) holds we can compute the radius at which the tangential speed becomes zero along the rising trajectories. Evaluating the constant in (11.1),

$$(v_{\theta}r)_0 + \frac{r_0^2 f}{2} = v_{\theta}r + \frac{r^2 f}{2}, \quad (11.4)$$

where the subscript zero denotes conditions at the place where the air leaves the surface. The second term on the left-hand side of (11.4) is very small and may be omitted. Thus, for $v_{\theta} = 0$,

$$r = \sqrt{2v_{\theta_0}r_0/f}. \quad (11.5)$$

Let us say that a storm is located at latitude 20° ($f = 5 \times 10^{-5}$ sec $^{-1}$). Given $r_0 = 60$ miles and $v_{\theta_0} = 100$ knots, $r = 245$ miles. If $v_{\theta_0} = 60$ knots, $r = 190$ miles. Given $r_0 = 30$ miles and $v_{\theta_0} = 100$ knots, $r = 175$ miles.

In Fig. 11.18d, e the lines of zero tangential speed lie approximately at these radii. The surface-wind distribution (Fig. 11.9) is such that (11.5) verifies within the limits of accuracy of the charts. It is impossible to be more specific. But the probability is high that the zero lines of Fig. 11.18d, e actually represent the intersection of the main body of rising air with the respective surfaces and, further, that (11.1) is true in the first approximation.

Our analysis not only gives a correct picture of the wind field following the trajectories of the rising core current, but the correct wind distribution in space is also obtained. Near the surface (11.1) is not applicable; owing to friction the winds increase inward more slowly than the principle of conservation of absolute angular momentum demands. If now the wind decreases in the outflow in accord with (11.1), the air will reach a given radius with less cyclonic tangential speed than it possessed during inward passage near the surface. This means that the tangential speed will decrease everywhere along the vertical and eventually change to anti-cyclonic tangential speed as observed. It also follows that if the storm is not growing, tangential momentum will be lost to the sea surface for continuity. Such transfer of course takes place; the production of ocean currents leading to high tides on shore has already been discussed.

Cloud Systems of Tropical Storms

Although the cloud sequence varies considerably from one storm to the next, accounts of many eyewitnesses of the precursory signs are remarkably uniform. On the day before the storm the weather is often unusually good and the barometer above normal. Arrival of a long sea swell is the first warning. Then the barometer slowly begins to drop, and the wind may start blowing from an unusual direction. In the low levels normal convective activity is suppressed, and the amount and depth of the cumuli are below average. Simpson (67) speaks of an "ominous absence of isolated or random convective cloudiness." At the highest levels a cloud sequence begins which is closely akin to that observed during warm-front approach in middle latitudes. Cirrus makes its appearance, followed by cirrostratus, altostratus, and altocumulus. Then several brief periods of cumulus congestus with showers may be experienced as the outer ends of the convection spirals approach and pass. The barometer falls more rapidly, and the wind increases; finally a dark wall of clouds approaches, the "bar" of the storm. With its arrival the full force of the hurricane is unleashed.

We have already noted that there is good agreement between the low-level cloud sequence and the field of divergence and vertical motion computed in Figs. 11.7, 14. Now we may add that the description of the upper clouds accords with the observations and deductions about the winds aloft. A narrow current, at first ascending almost vertically, then flowing rapidly outward in the upper troposphere, will produce exactly the reported cloud sequence.

Radar Bands. Observers' accounts have long indicated that the fury of a hurricane does not persist constantly, not even in the very core. Extreme violence alternates with periods of comparative lull. Little analysis of these oscillations was possible until the advent of radar led to a remarkable discovery (40, 75). The central storm area is not filled with cloud uniformly throughout the troposphere. Rather we find narrow, elongated bands of heavy rain echo on radar screens, interspersed with areas where the echo is feeble or absent (Fig. 11.23). Some of the bands have their roots hundreds of miles from the center. From there they spiral inward.

Figure 11.24 shows short-period variations in band structure producing a narrow, solid ring of extreme rain about a small hurricane approaching Cuba from the south in October, 1952. Some caution is required in drawing conclusions from radar photographs (75). Owing to attenuation of the energy a single photograph may reveal only those rain bands closest to the screen. And the radar beam will intersect raindrops at higher and higher levels with increasing distance from the screen since the beam travels

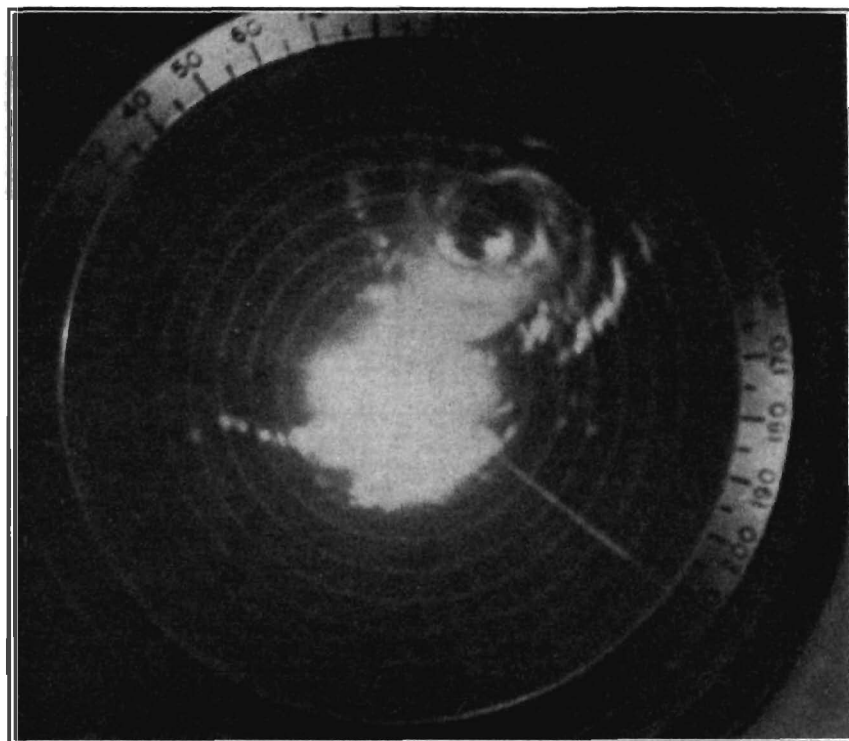


Fig. 11.23. Photograph of hurricane radarscope. Scale: 20 miles between circles. (*Official U.S. Navy photograph.*)

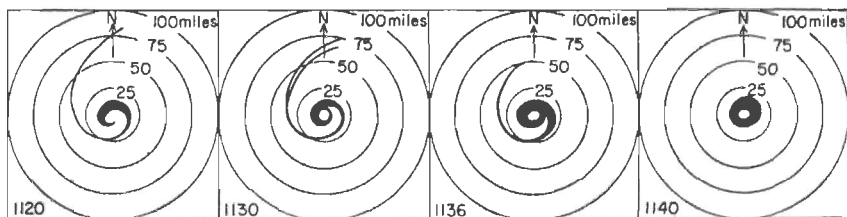


Fig. 11.24. Traces of radar photographs taken by naval reconnaissance south of Cuba, Oct. 23, 1952. (*Official U.S. Navy photograph.*)

on a straight path, whereas the earth curves. Successive photographs taken by reconnaissance aircraft during circumnavigation and penetration are the best method to obtain a complete picture. Because the aircraft covering the storm shown in Fig. 11.24 always remained in the same quadrant, there is little doubt that only part of the rain bands were observed. Indications of other bands appear in some photographs, but these are weak and discontinuous. Nevertheless, Fig. 11.24 is highly

interesting for the fractional information it offers. The hurricane was in the immature stage at the time of the flight; it had organized in the Caribbean only on the preceding day. Its center was small, tight, and extremely violent, a perfect immature cyclone. The central pressure was near 930 mb; gusts of 180 mph were recorded on the shore. Cuba's central coast sustained great damage when the storm struck.

The diameter of the eye is about 8 miles. Around it lies a band, also approximately 8 miles wide, which appears as a very bright circle with sharp inner and outer edges. This band represents the zone in which the radial velocity is rapidly decreasing inward, where convergence may be as much as 10^{-3} sec $^{-1}$ and vorticity 10^{-2} sec $^{-1}$, fully two orders of magnitude more than the highest values of Fig. 11.15.

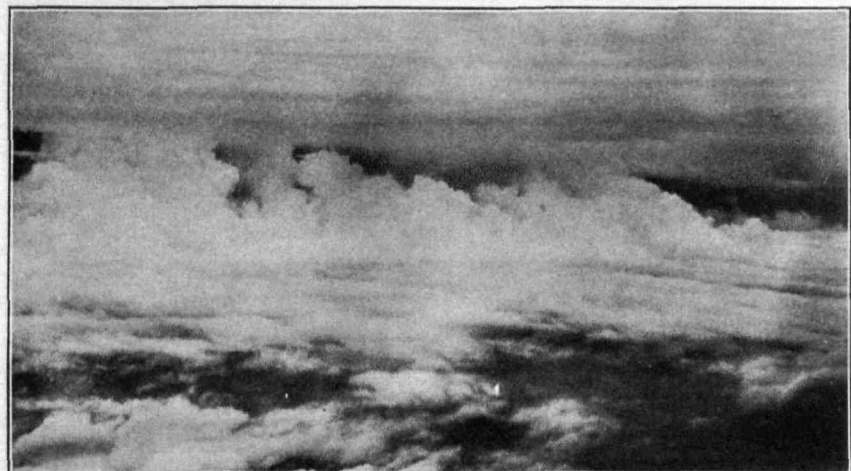


Fig. 11.25. Photograph of cloud line forming radar band in a typhoon. (Courtesy of R. H. Simpson.)

The bright ring is an unmistakable feature of all photographs. Short-period changes shown in Fig. 11.24 are far less certain, since the radar-beam reflection is always strongest on the side nearest the airplane. Initially, the central ring as recorded is not closed, and a single principal convergence line, hardly more than 2 miles wide, spirals inward. A few minutes later the band is beginning to forge a closed circle. Then the spiral dies away, a development hardly in doubt since it takes place on the side nearest the aircraft. Finally we see a closed ring of extreme rain. It is remarkable how much this figure (regarded as a picture) suggests the name "eye," which has been a standard term for centuries. We cannot be sure that spiral bands do not reach the solid ring of rain at the time of Fig. 11.24 (*far right*); but the process of eye formation shown by the series is quite typical of what has been reported from other storms.

The rain structure as seen by radar proves that the low-level convergence is concentrated along the bands. Such a structure of the convergence zone of course cannot appear in an average field of convergence as Fig. 11.14 shows. In the instantaneous picture, the streamlines crowd along several convergence lines which closely parallel the direction of the

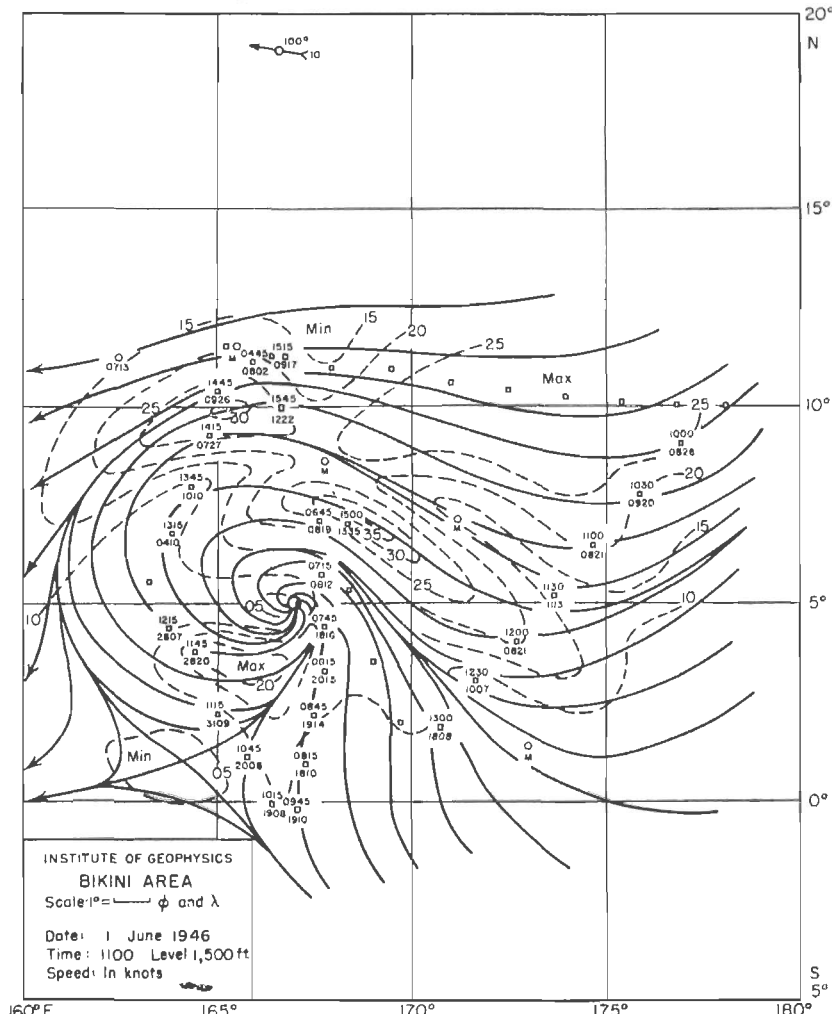


Fig. 11.26. Wind field at 1,500 feet, June 1, 1946 (47).

surface wind. Simpson (67) encountered six such lines during his reconnaissance flight in the Pacific in 1951. Figure 11.25 is a spectacular photograph of one of these in the outskirts of that typhoon. The convergence lines are a principal feature of Palmer's (47) analysis of a forming tropical storm in the Marshall Islands area of the Pacific (Fig. 11.26).

Wexler (75) quantitatively analyzed the bands of one Atlantic and two Pacific storms. The structure of the rain area, of course, varies with size and age of storms, during recurvature and other changes of track. Wexler's statistics can therefore serve only as a general guide on the band structure in large mature storms, as he intended. The length of the bands ranged from 35 to 200 miles, the number of bands from one to seven. Their average width was several miles, but sometimes close to the center only 1-2 miles, similar to Fig. 11.24. The band width appeared to increase with increasing distance from the center. The average width of the spacing between bands was of the same magnitude. Close to the center some bands were only 1-2 miles apart; in the outskirts, often more than 10 miles.

Wexler discusses possible explanations of the bands, emphasizing the speculative nature of the subject. Cumulus clouds over the sea frequently occur in rows, extending along the vertical wind shear (Chap. 5). Wexler states:

If, now, a circular vortex is introduced into a region of the cloud streets originally oriented along the wind, these streets will become circular. If the vortex is accompanied by convergence (*i.e.* if the vortex is a "sink") then these streets or bands will spiral inward toward the center. Their width and spacing will change, depending on the vertical wind and density gradients and the distribution and magnitude of the horizontal convergence associated with the vortex.

It is believed that this process is essentially that which occurs in the formation of the hurricane bands. The prevailing cloud bands are drawn into the hurricane circulation, which thereupon accentuates those bands of the proper wave length and dissipates the remaining ones. This "resonance" effect causes the clouds comprising the "chosen" bands to grow into the cumulonimbus type. The resulting pattern, as viewed from above, is very similar to spiral nebulae.

Slope and Walls of Eye. Wexler also mentions discrepancies between positions of the storm center as determined by radar and isobaric analysis. Since ground radar intercepts the raindrops of the middle troposphere when the eye is about 100 miles distant, an assumption of vertical tilt of the hurricane axis might explain the discrepancies. The tilt hypothesis is correctly rejected, because a horizontal gradient of mean virtual temperature of more than 35°C in the lowest 11,000 feet would be needed to accomplish the lateral displacement of the pressure center in Wexler's case. Another possible solution is separation of pressure and wind centers as suggested by Shaw (64) for high-latitude cyclones and by Deppermann (14, 15) for typhoons.

Postflight summaries from reconnaissance missions do not reveal appreciable and consistent slopes of hurricane cores with height. But the inner edge of the cloud wall frequently slants outward with height, especially above 30,000 feet. Wood and Wexler (76) and Wexler (74) have

described a reconnaissance flight off the Atlantic coast of the United States in which they encountered such a slope. These findings support the previous deductions about ascent and outward displacement of the air in the rain area.

Conditions, of course, will not always be uniform. Simpson (67) gives the following vivid description of his eye penetration:

Here was one of Nature's most spectacular displays. The eye was a vast coliseum of clouds, 40 miles in diameter, whose walls rose like galleries in a great opera house to a height of approximately 35,000 feet where the upper rim of the clouds was smoothly rounded off against a background of deep blue sky. The sea surface was obscured by a stratocumulus undercast except for two circular openings on the east and west sides of the eye, respectively. Clouds in the undercast layer were grouped in bands which spiralled cyclonically about each of these openings or clear spots, both of which were approximately five miles wide. This horizontal alignment of clouds suggested the possibility that two separate small eddy circulations were present within the eye envelope.

In the geometric center of the eye the stratocumulus undercast bulged upward in a domelike fashion to a height of 8,000 feet. Light turbulence in the tops of this dome was comparable to that in ordinary ocean cumulus.

The walls of the eye on the west side were steep, either vertical or overhanging, and had a soft stratiform appearance. On the east side however clouds were more of a cumuliform type with a hard cauliflower appearance. In this sector the walls of the eye rose with a gradual concave slope to the upper rim. The overall appearance indicated that the axis of symmetry in the vertical plane was tilted to the east or northeast.

This description, in conjunction with all other evidence, suggests that the eye boundary is not rigid, that in the low levels air from the eye is mixed outward, and that air from the rain area penetrates inward (35). If the boundary were rigid and impenetrable, we should have to find, for reasons of mass continuity, a wind inside the eye blowing in the direction and with the speed of the storm propagation. Such a wind is not observed. In all probability the air situated in the major radar bands makes incursions from time to time into the eye in the low levels; these can account for the irregular cloud cover observed at all altitudes in eyes. In this way the center of a hurricane can change appearance constantly. For a short while the eye may be symmetrical. Then, as a spiral begins to intrude, the symmetry is lost; for some time the eye may be oblong, or there may be two eyes.

Thermal Structure of the Rain Area

Observations taken since the development of radiosonde instruments have confirmed the classical idea that air in the interior of tropical storms

is less dense than that in the surroundings. The principal conclusion of studies based on these observations (45, 50, 53, 62) is that inside the rain area *the vertical temperature distribution is the same as that obtained by raising an air particle dry-adiabatically from the surface to the condensation level and from there moist-adiabatically to about 300 mb* (Fig. 11.27). Byers (10) likens the hurricane to a huge parcel of air. Temperatures observed in the rain area are the highest possible in ascending air.

This situation is quite different from the zones of organized convection described in Chaps. 9 and 10. In those disturbances some ascent of surface air takes place; but convergence extends to relatively high levels. Air initially situated anywhere between sea level and 500 mb is entrained

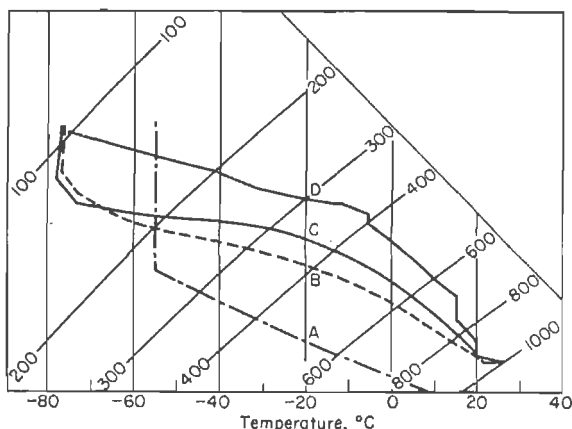


Fig. 11.27. Tephigram (54) showing (A) U.S. Standard Atmosphere, (B) mean tropical atmosphere (62), (C) sounding in rain area of hurricanes, and (D) eye sounding (52). (Courtesy of American Meteorological Society.)

and moves upward. In consequence the convection zones are often denser aloft than their surroundings. Comparison of these disturbances with tropical storms forces us to the conclusion that *entrainment does not take place in the inner core of hurricanes and that convergence is restricted to the subcloud layer*.

Figure 11.27 illustrates only the *gross difference* of the thermal structure of tropical storms relative to their surroundings. If the air ascended everywhere with the surface properties of the mean tropical atmosphere, temperature gradients within the rain area would not be observed. Even in the middle troposphere, however, the temperature increases, slowly at first, then rapidly toward a hurricane center (Fig. 11.28). To account for this internal temperature gradient, we revert to the earlier observation that the heat and moisture content of the air flowing toward a center near the ground increases. Figure 11.29 shows the consequences of this

heat gain. Curve *A* is the same as curve *C* of Fig. 11.27; curve *B* represents the ascent of air after isothermal expansion to 960 mb and a moisture increase of 1.5 g/kg (Fig. 11.4). The area enclosed between these curves is as large as that between curves *B* and *C* in Fig. 11.27. Even so our

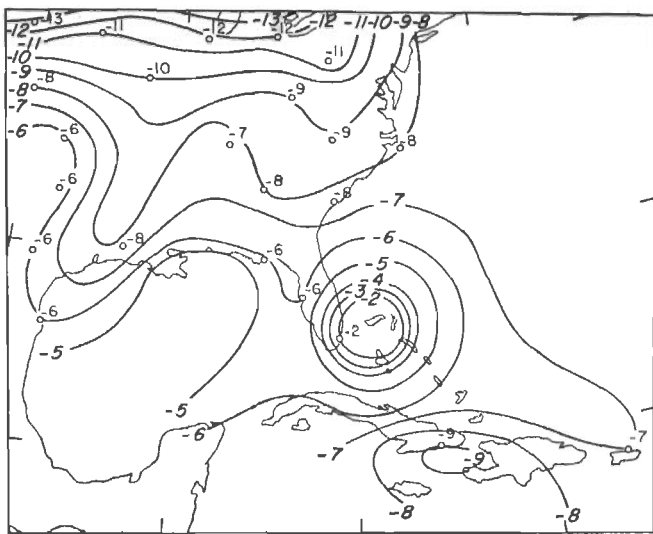


Fig. 11.28. 500-mb temperatures, Sept. 17, 1947, 0300Z (45).

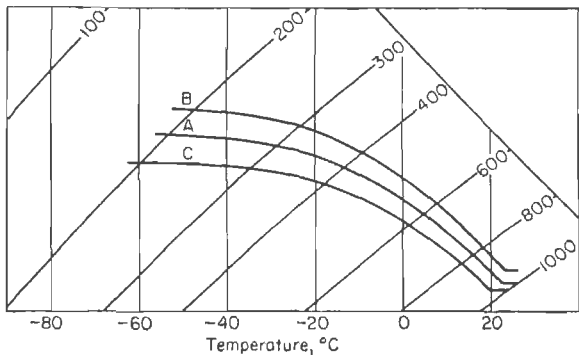


Fig. 11.29. Tephigram showing (A) ascent curve of air with surface properties $T = 26^{\circ}\text{C}$, $g = 18 \text{ g/kg}$ [repetition of curve (C) of Fig. 11.27]; (B) ascent of the same air after isothermal expansion to 960 mb and moisture increase of 1.5 g/kg; (C) ascent of surface air with $T = 24^{\circ}\text{C}$, specific humidity = 16 g/kg (53).

example is by no means extreme. Ascent from a surface pressure of 900 mb would intersect the 400-mb surface near the 0°C isotherm. Through the local heat source large temperature gradients are introduced into the rain area. These gradients are smallest near the ground, then grow to maximum values near 200 mb, in the layer of strongest outflow.

Figures 11.27 and 11.29 give temperature as a function of pressure following the ascending air. They therefore show the *vertical temperature distribution* that would be obtained from radiosonde flight if the air rose on a path without a marked outflow component. This should be true to about 300 mb. Individual ascents confirm it by following the moist-adiabatic lapse rate. In the layer of strong outflow and high clouds we should expect more stable conditions, perhaps even an isothermal stratum. Consider curve *B* of Fig. 11.29, which crosses the 200-mb surface at a temperature of -47°C . If the air reaching this level has moved outward from the core to a distance of 200–250 miles, in view of our momentum considerations, it will be superimposed on air rising along curve *A* in the lower atmosphere. It may even arrive on top of columns with the properties of the mean tropical atmosphere. Somewhere, therefore, a radiosonde flight should encounter a transition from a lower moist-adiabatic layer to curve *B* of Fig. 11.29. This transition zone is a stable layer whose altitude increases outward, quite analogous to warm-front surfaces. Individual soundings begin to depart from the moist-adiabatic lapse rate usually between 300 and 200 mb. Such a departure even appears in the mean hurricane sounding (curve *C* of Fig. 11.27) above 220 mb.

We can utilize these observations to explain the barograph traces and surface-pressure gradients in the core. If the atmosphere remains undisturbed above 100 mb, temperature gradients in the troposphere must account for the fall of the barometer from the hydrostatic viewpoint. The boundary of tropical storms in the horizontal is located where the temperature difference between the high-level outflow and the surroundings vanishes. From there the surface pressure decreases slowly inward as the outflow layer thickens. The lower and middle troposphere begin to contribute substantially only within 100–200 miles from the center, where active surface convergence and ascent start, leading to a warming of the whole troposphere. From this point inward the pressure fall accelerates.

Assuming undisturbed conditions at 100 mb, we can compute whether or not curve *B* of Fig. 11.29 or any other core sounding can account for the observed surface pressure. We find that they cannot, that even the very warm soundings are not warm enough. Since the hurricane ascents give the warmest possible temperature obtainable through ascent, we must invoke a descending mechanism to obtain still higher temperatures.

Thermal Structure of the Eye

The speculations of the early literature regarding descending motion in the eye have been more than fully verified by measurements. Since the time of the first penetrations by aircraft, pilots have reported large and

sudden temperature rises. Aircraft descents and "dropsondes" have provided good information on the temperature structure of the eye in the lowest 2-3 km. Jordan (35) has summarized the data of 35 soundings taken in typhoons in 1951 (Table 11.2).

The range of potential temperature at all levels is very great and considerably exceeds that of temperature near the surface; this again indicates that the ocean surface controls the air temperature near sea level. The variability higher up is due in part to the fact that the storms included in the table were of widely varying intensity. In part it results from lack of homogeneity in individual eyes. Simpson (67), for instance, found temperature differences of 4-7°C above 5,000 feet on two soundings taken in the same eye only a few hours apart. Below 5,000 feet temperatures did not change. Figure 11.30 shows the extreme sounding taken by Simpson. Surface pressure is very low, only 900 mb; the temperature, over 26°C; and the specific humidity, 22 g/kg. These data confirm the process of isothermal expansion with absorption of moisture. The subcloud layer ends at 840 mb and is overlain by a deep isothermal stratum with rapid upward decrease of moisture. At 700 mb, the temperature is 26°C; at 500 mb, 16°C, the highest 500-mb temperature on record. Upon leaving the eye on the return trip, Simpson recorded a temperature fall of 18°C in 60 miles.

Complete ascents through the troposphere in eyes of mature storms are few. The best evidence comes from two radiosonde flights taken at Tampa, Florida (52, 66). Because it is very difficult to send balloons up into an eye, there is no certainty that the balloons were still in the eye when they reached the high troposphere. In both cases, however, the eye was large, and chances are good that the balloons did not drift outside and that the temperature structure is representative.

The sounding of October, 1945 (curve D of Fig. 11.27) shows great stability in the lower troposphere, similar to Fig. 11.30 though not nearly so extreme. Higher up the lapse rate is very steep. Departures from the normal tropical atmosphere are greatest from 800 to 400 mb, indicating subsidence amounting to several kilometers. Neither of the two soundings reached the tropopause; there was no evidence of a "sucking

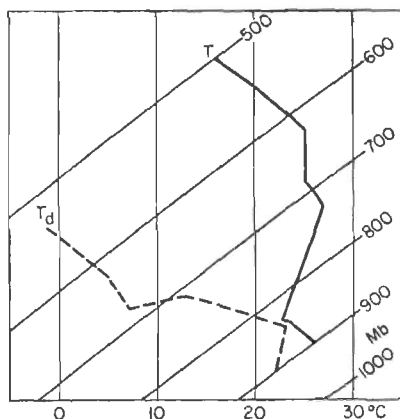


Fig. 11.30. Tephigram of dropsonde observation in eye near 20°N, 136°E, Aug. 15, 1951 (35, 67).

TABLE 11.2. MEAN, RANGE, AND MEAN DEVIATION OF TEMPERATURE AND POTENTIAL TEMPERATURE IN THE TYPHOON EYE

Elevation	Mean temperature, °C	Max. and min. °C	Mean deviation, °C	Potential temperature, °A	Range, °C	Mean deviation, °C
Surface	25.7	24-29	1.0	302.7	12	2.6
0.5	23.9	22-28	0.8	305.7	11	2.7
1.0	22.4	18-29	1.7	309.2	14	3.5
1.5	21.1	18-28	1.9	312.8	18	3.6
2.0	19.8	16-26	2.1	316.8	20	3.6
2.5	18.3	14-25	2.1	319.6	20	3.8

down" of the primary tropopause. On the contrary, it is probable that the tropopause is highest above the eye, analogous to the situation in dynamic anticyclones. As the ascent curves intersect the mean tropical atmosphere at 100 mb, it is probable that the tropopause was situated only a short distance above the top of the soundings.

Introduction of the eye soundings and a sloping eye boundary makes it possible to explain fully the very low surface pressures observed, first demonstrated by Haurwitz (30). The steepest slope of the barograph curve

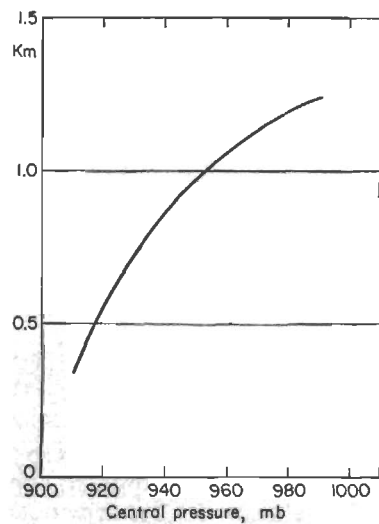


Fig. 11.31. Mean height of base of stable layer in eye vs. central storm pressure (35).

eyes with the central pressure. The lower the pressure, the lower should be this base, because a deeper layer of warm air is needed to account for the surface pressure. Jordan's correlation (Fig. 11.31) fulfills these requirements, lending further weight to the contention that temperature

Jordan (35) also correlated the height of the base of the stable layer in

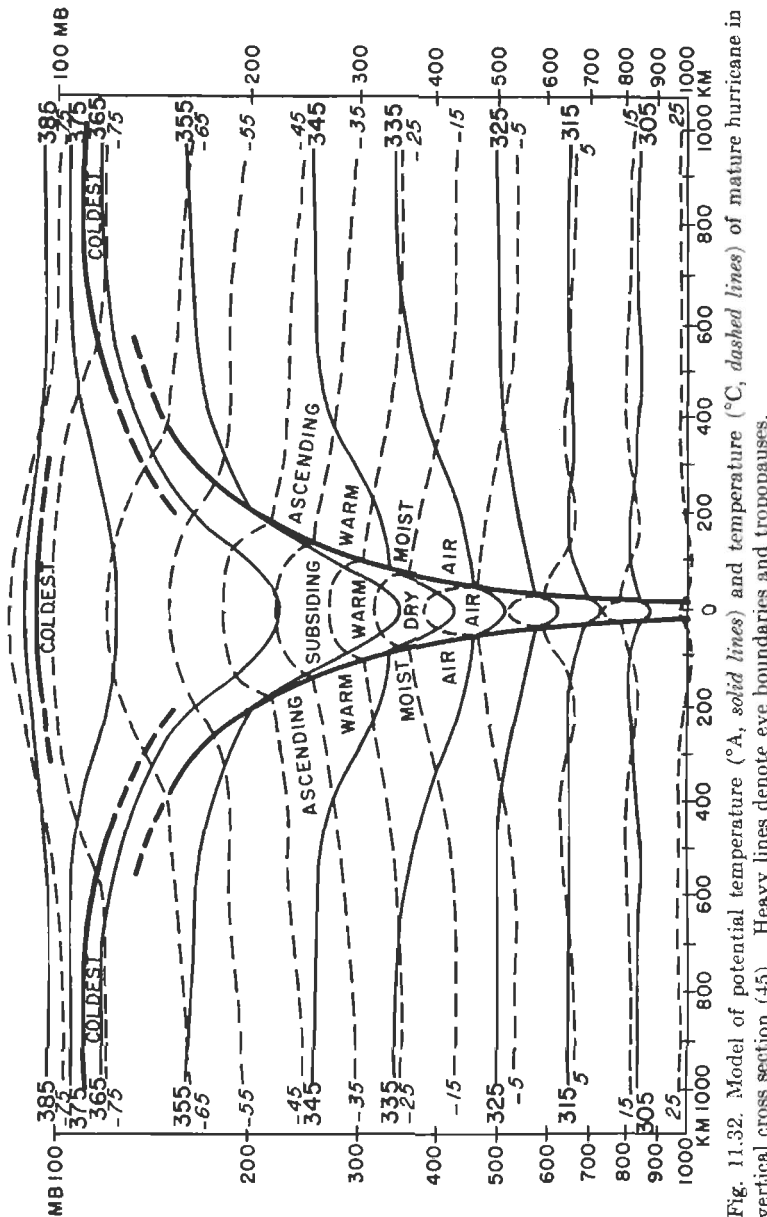


Fig. 11.32. Model of potential temperature ($^{\circ}A$, solid lines) and temperature ($^{\circ}C$, dashed lines) of mature hurricane in vertical cross section (45). Heavy lines denote eye boundaries and tropauses.

variations above 100 mb need not be invoked to furnish a reasonable explanation of the hurricane pressure field.

Palmén (45) has summarized in a model the knowledge of the thermal structure of tropical storms. This model (Fig. 11.32), based mainly on special observations taken as a severe hurricane approached Miami, Florida, in September, 1947, reveals the features established: (a) horizontal isotherms in the lower atmosphere and gently sloping isotherms in the upper troposphere in the outskirts; (b) a marked though irregular temperature rise in the low levels in the rain area; (c) a larger temperature rise aloft; (d) a sloping eye boundary with very high temperature inside; (e) a slight tropopause bulge above the eye and general disappearance of the vortex at 100 mb.

Energy Aspects

If we add the pressure field and streamlines in the vertical plane to Fig. 11.32, we obtain the model for the rain area sketched in Fig. 11.33. This model shows a simple heat engine, with circulation about the sole-

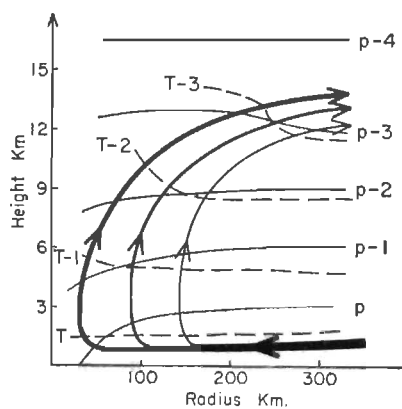


Fig. 11.33. Outline of vertical circulation, temperature T , and pressure P in rain area of tropical storm.

noids in the kinetic-energy-producing sense. Near the surface, air moves from high toward low pressure, converges, and increases its heat content. As it ascends, latent heat of condensation is liberated. Consequently, the air near the center is warmer than its surroundings through a deep layer, and the vertical distance between surfaces of constant pressure is larger. The pressure-gradient force, directed toward the center at the surface, decreases upward and eventually reverses its direction (Fig. 11.21). Air particles moving upward near the center will be accelerated out-

ward. Since their displacement in the horizontal plane is toward higher pressure, they lose kinetic energy below the level where the pressure gradient reverses. Still higher, the tangential kinetic energy again increases (Fig. 11.18d, e); the outflow there is directed toward lower pressure in the horizontal plane.

In the course of a hurricane's life a vast quantity of air is drawn into the circulation and funneled upward. Given a storm with average inflow and duration of 1 week, the air in the subcloud layer contained in a square

whose sides are $12\text{--}13^{\circ}$ latitude long will be raised to 200 mb or higher. The potential temperature of this air is increased by no less than $60\text{--}70^{\circ}\text{C}$ during this ascent. Only a fraction of the sensible heat gained is available to drive the storm.

The question arises how the circulation and the observed temperature field are maintained at all. Although tropical storms never remain in precisely steady state, the essential features of the wind and temperature distribution persist. Therefore the question of steady-state maintenance is legitimate. Thus far we have followed two stages of the energy transformations: (a) isothermal expansion with addition of moisture near the surface; (b) dry-adiabatic expansion to the condensation level, followed by moist adiabatic expansion. If we suppose that the streamline nearest the center in Fig. 11.33 follows curve *B* of Fig. 11.29 and that the outer streamline follows curve *A*, the observed horizontal and vertical temperature gradients inside the storm will be maintained.

If, now, the outflowing air descends in the surroundings to provide mass continuity in a closed system, this descent would follow the dry-adiabatic lapse rate after reevaporation of the small amount of water carried outward in the form of raindrops. Soon, warm air should be found in the outskirts, with temperatures comparable with those inside the eye. Such descent would quickly bring the whole hurricane circulation to a halt. It is therefore necessary to assume that a cold source is applied at some distance from the storm center (53). The situation is comparable with that encountered in man-made engines. Every engineer knows that he must provide a mechanism for draining off heat that cannot be converted to mechanical or potential energy. For the automobile the fan and the water-cooling system perform this function.

Since there is no mechanical cold source in the atmosphere, we must drop the notion of a closed thermodynamic system and admit that free exchange of air in tropical storms and in their surroundings in a large-scale sense must take place. Air flowing out at high levels from the storm mixes with the surrounding air masses that have not passed through the circulation, transferring heat to them. At the same time the mixture is carried away from the storm by the upper currents and replaced by cooler air from other portions of the globe. In this way the entire temperature field relative to the storm is maintained.

The mixing process may be considered to take place at nearly constant pressure. It is illustrated in Fig. 11.34, which shows the whole energy cycle. Curve *B* of Fig. 11.29 provides the ascent path and the normal tropical atmosphere the outside air. For the construction of the figure a sample of air has been chosen that mixes with the surroundings after ascent to 200 mb. The indicated temperature reduction from -47 to -52°C at 200 mb is possible if we consider that the surroundings normally

have a temperature of -55°C , which is observed to rise to -52°C near tropical storms. The assumed ratio of mixing is 3 parts of inside air to 5 parts of outside air. It is apparent from Fig. 11.34 that only a small percentage of the heat released during expansion of the air ascending from 1,000 to 200 mb is available for conversion to kinetic energy. Maximum conversion would be realized if the mixture descended dry-adiabatically, following the dashed horizontal line to the 340-mb level, where the temperature would become equal to that in the interior of the storm. The area enclosed by the path of the air between 200 and 340 mb (*a*) is only 12 per cent of the total area *a* + *b* enclosed by the hurricane sounding and the normal surroundings. Since temperatures comparable with those inside are not observed outside, only a fraction of the energy represented

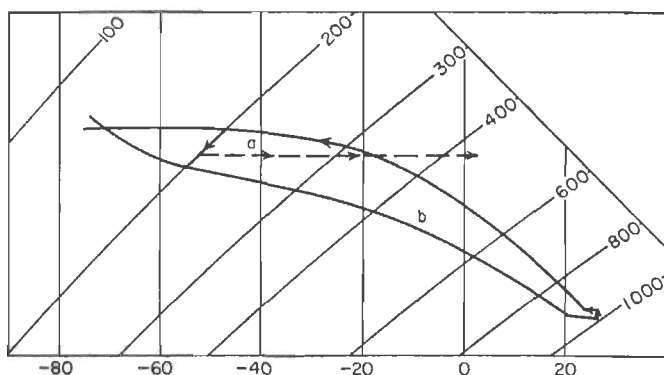


Fig. 11.34. Tephigram showing energy cycle in mature hurricane (53).

by area (*a*) must be used to drive the storm. The vast bulk of the heat released is spread over the globe.

According to several order-of-magnitude calculations (34, 39) the latent-heat release in tropical storms is $2\text{--}4 \times 10^{26}$ ergs/day. The dissipation of kinetic energy due to surface friction is estimated at only 2 per cent of this amount (32, 34). If internal friction and lateral mixing do not also drain considerable amounts of kinetic energy, realization of 15–20 per cent of area (*a*) will suffice to maintain hurricanes. The temperatures produced during such slight descent are entirely within the range of observed values.

Figure 11.34 shows clearly that a tropical storm and its surroundings are an open system. It requires weeks for the air that has risen in the storm to return to the surface under the influence of radiation. New air constantly enters the cyclone in the subcloud layer. Aloft, the surroundings provide the cooling needed to maintain the temperature field.

FORMATION OF TROPICAL STORMS

Tropical cyclones principally develop in the following areas and seasons (20):

1. Tropical north Atlantic Ocean
 - a. East of the Lesser Antilles and the Caribbean east of 70°W, July to early October
 - b. North of the West Indies, June to October
 - c. Western Caribbean, June and late September to early November
 - d. Gulf of Mexico, June to November
2. North Pacific Ocean off the west coast of Central America, June to October
3. Western North Pacific Ocean, May to November, some storms in all months
4. Bay of Bengal and Arabian Sea, May to June and October to November
5. South Pacific Ocean west of 140°W, December to April
6. South Indian Ocean
 - a. Northwestern coast of Australia, November to April
 - b. West of 90°E, November to May

No record of a fully developed tropical storm exists for the south Atlantic Ocean, the south Pacific east of 140°W, and the central north Pacific. Storms are also very rare within 5° latitude of the equator. Palmer (47) located a cyclone less than 100 miles from the equator in the Marshall Island area in April, 1951, the lowest latitude at which such a vortex has been detected.

Seasonally, the mean latitude of storm formation moves poleward in the first half of the season and then retreats equatorward. Early- and late-season cyclones form mostly in the belt from 5 to 15° in the northern hemisphere, at the height of the season between 10 and 25°. In the Atlantic, cyclogenesis between 25 and 30°N is fairly common. The poleward limit for true hurricane formation there is 35°N.

Average Frequencies

Because of open observing networks many tropical storms passed over the oceans without detection during the early years of meteorology. This is deduced from the fact that in several regions the "frequency" has risen with increasing density of observation stations. There are no reliable statistics except for the Atlantic, where ship traffic has been heavy and island stations numerous for many years. Dunn (20) nevertheless attempted a rough comparison of the productivity of the hurricane regions, although not all storms counted have reached full hurricane strength and cyclones of lesser intensity are included (Table 11.3). Most

TABLE 11.3. FREQUENCIES OF TROPICAL CYCLONES PER 10 YEARS

North Atlantic Ocean.....	73
North Pacific—off west coast of Mexico.....	57
North Pacific Ocean, west of 170°E.....	211
North Indian Ocean, Bay of Bengal.....	60
North Indian Ocean, Arabian Sea.....	15
South Indian Ocean, west of 90°E.....	61
South Indian Ocean, northwestern Australia.....	9

uncertain are the frequencies in the south Pacific Ocean: according to some estimates tropical cyclones are as numerous there as in the north Pacific; according to others the frequency is lower than in the Atlantic.

Storm Frequencies in the Atlantic. Colón (12), following Mitchell (43), has made a detailed study of Atlantic hurricane frequencies from 1887 to 1950. During these 64 years 433 storms were charted. Individual years contributed highly varying amounts, from 2 each in 1929 and 1930 to 21 in 1933.¹ When the record is arranged by successive 5-year totals, the frequency drops more than 50 per cent from 1890 to 1910; it then remains steady at a low level until 1930, followed by a sharp increase to the end of the record. The correlation coefficient between successive 5-year periods is 0.46. Although the coefficient between successive individual years is only 0.19, the 5-year trend is produced not by erratic frequencies in a few years, such as 21 in 1933, but by general variations of the level of activity.

TABLE 11.4. AVERAGE MONTHLY FREQUENCY OF TROPICAL CYCLONES IN THE ATLANTIC
PER 10 YEARS (12)

	May	June	July	Aug.	Sept.	Oct.	Nov.	Total
Frequency.....	1	4	5	16	24	19	4	73
Per cent frequency.....	1	6	7	22	32	26	6	100

TABLE 11.5. FREQUENCY OF STORMS IN THE EASTERN ATLANTIC, WESTERN CARIBBEAN, AND GULF PER 10 YEARS (12)

	May	June	July	Aug.	Sept.	Oct.	Nov.	Total
Formation east of 70°W longitude.....	0	0	2	12	14	7	2	37
Formation west of 70°W longitude.....	1	4	3	4	10	12	2	36

On a 10-year basis (Table 11.4), about 80 per cent of all storms occur between August and October, with a maximum of 32 per cent in Sep-

¹ Tannehill's book (70) contains a year-to-year description of all Atlantic hurricanes beginning with the earliest records.

tember. Formations east of longitude 70°W largely concentrate in these months. Farther west early- and late-season storms contribute a much greater percentage (Table 11.5).

Table 11.6 shows the probability of storm occurrence in each month. It is practically certain that at least one hurricane will occur in September; in August and October the chance is also very high. Colón

TABLE 11.6. PROBABILITIES OF STORM OCCURRENCES PER MONTH IN THE ATLANTIC (12)

	May	June	July	Aug.	Sept.	Oct.	Nov.
At least one storm.....	0.09	0.34	0.39	0.75	0.92	0.83	0.36
Two or more storms.....	0.02	0.06	0.11	0.52	0.72	0.59	0.03
Three or more storms.....	0	0.02	0.03	0.10	0.42	0.34	0.03

TABLE 11.7. AVERAGE NUMBER OF HURRICANE DAYS PER MONTH IN THE ATLANTIC (12)

June	July	Aug.	Sept.	Oct.	Nov.	Season
2	3	10	16	12	3	46

noted that formation of two or more storms in one month is often produced by storm clusters—successions of storms developing roughly in the same locality 2–4 days apart.

Table 11.7 shows the average number of hurricane days per month.

Detection of Tropical Storms

Since observing stations frequently do not exist in areas of forming storms, the first warning often comes from unusual weather some distance away. A summary of the most useful indicators (18, 20) follows:

Pressure. The sea-level pressure falls more than 3–3.5 mb/day or reaches values of 5 mb or more below normal for the area and season.

Winds. In the trades, easterly winds with speeds 25 per cent and more above normal in a limited area should be suspected, especially if the flow curves cyclonically. Any wind whose direction ranges from south through west to north when it should normally be easterly is a danger signal.

Weather. Steady rain at several adjoining stations—in contrast to shower-type precipitation—or unusually heavy precipitation with cirrostratus and altostratus overcast are frequent precursors of storms.

Sea swell, tides, and microseisms have already been mentioned.

Basic Aspects of Cyclogenesis

Atmospheric machines do not differ in principle from the machines known in physics and engineering. For purposes of comparison let us note the elements necessary for the operation of a machine deriving its energy from a latent-heat supply such as oil, coal, or electric batteries:

1. Latent (stored) heat energy
2. An initiating mechanism (starter) with an independent energy source, to
3. Convert the latent heat of the energy input into sensible heat and start the engine
4. A mechanical coupling to generate motion in arbitrary planes
5. A cooling system to remove the excess heat

We can establish the following analogous sequence during generation of tropical storms:

1. The main energy input is water vapor, a form of latent heat.
2. A suitable wind arrangement acts as the starting mechanism. The kinetic energy of these winds furnishes the initial independent energy.
3. Condensation during ascent is the means by which latent heat is transformed into sensible heat. The starter therefore must be able to produce such ascent. High-level outflow and compensating lower inflow develop, *i.e.*, kinetic energy of the radial motion is generated. This circulation in the vertical plane must be arranged to survive influences that tend to destroy it.
4. Coriolis and centrifugal forces convert radial to tangential kinetic energy; after some time the tangential energy predominates.
5. High tropospheric currents provide the cooling system which carries the excess heat to other regions of the globe.

A tropical storm of full hurricane intensity will develop only if these functional elements operate flawlessly. If the machinery is faulty, a hurricane will no more form than a man-made machine will run.

The meteorological literature has not attacked cyclogenesis in the systematic manner outlined above. Small wonder, then, that none of the fragmentary qualitative hypotheses put forward have solved the problem and provided means for predicting storm formation. We shall now review these hypotheses briefly.

Theories of Hurricane Formation

Convectional Hypothesis. This is the oldest hypothesis; essentially it states the following: An unusually large number of heavy rain squalls and thunderstorms develop for some reason over a tropical ocean. These rain clouds grow together, and a cyclonic circulation develops at the

ground because of convergence, if the whole sequence takes place sufficiently far from the equator.

This model is demonstrably deficient. No starting mechanism is specified. It is not demonstrated how the circulation in the vertical plane develops; no cooling system is mentioned. We know today that many of the heaviest tropical rainfalls occur without a closed cyclonic circulation. Even closed depressions with torrential precipitation often fail to deepen, traveling in relatively steady state for 1,000-1,500 miles and more (51).

The hypothesis does not explain the pressure fall. Convergence—if developed initially—should lead to pressure rise and not fall at the surface. It is true that any upper warming produced by convection currents will produce radial outward acceleration aloft. Yet it is not clear, and has not been shown, why this outflow should become greater than the inflow. Even worse, there is no guarantee that the cloudy area will be warmer than its surroundings; we have seen that often this is not the case.

Since we lack a mechanism for organized mass removal aloft, the area of heavy showers and its surroundings will act almost as a closed system. Even if the convection currents initially are less dense than their surroundings, the latter soon will become warmer as descent develops; any incipient circulation must dissipate.

Frontal Hypothesis. About 1920, Norwegian meteorologists first suggested that shearing waves generated along inclined density discontinuities (fronts) may grow in amplitude, given the proper initial conditions. Subsequent to Brooks and Braby's paper on "The Clash of the Trades in the Pacific" (8), the zone of convergence, where the trades from southern and northern hemispheres meet, was also regarded as a boundary along which shearing instability could develop (*cf.* also the beginning of Chap. 10).

This theory represents a much more serious effort to explain cyclogenesis than the convective hypothesis. It offers a starting mechanism with an energy source; only the cooling system is omitted entirely. We cannot, however, accept the frontal hypothesis as an explanation.

Several objections can be raised:

1. Even though shearing instability may well be part of the starting mechanism in some situations, this is not true in all. Many storms form within the trade-wind current without an equatorial shear line.

2. The geometry is wrong for formation in the equatorial trough. Advocates of the theory visualize the trough as a front with inverted temperature gradient. The peaks of warm sectors should be found where this front bulges equatorward (Fig. 11.38); forming centers are actually situated near poleward bulges. Some writers (*cf.* 59) have tried to take account of the geometry by introducing "air-mass triple points," defined

as a meeting place of no less than three distinct air masses. The search for these three air masses in the areas of cyclogenesis has proved to be a vain one, however.

3. Most formidable of all objections is the fact that point 3 of our list cannot be satisfied. If a portion of an "equatorial front" occludes, when there is a real density difference, the whole surface layer of the nascent cyclone will soon consist of the denser air. Curve C of Fig. 11.29 illustrates the difficulties which arise if air that is only slightly denser and drier than the normal tropical atmosphere enters the core. This curve is the ascent path of air with surface temperature of 24°C and specific humidity of 16 g/kg. Temperatures aloft are much lower than those of the other ascents. They are the same as or a little lower than those of the normal tropical atmosphere (curve B of Fig. 11.27); no positive area is left on the thermodynamic chart. In fact we find a slight negative area. For comparison, the data of Figs. 11.27 and 11.29 are presented in tabular form (Table 11.8). Temperatures at selected surfaces are given for (a) the average tropical atmosphere in the Caribbean; (b) the ascent of surface air of average properties (26°C, 18 g/kg); (c) the ascent of the same air after isothermal expansion to 960 mb, with pickup of 1.5 g/kg of moisture; and (d) the ascent of air with very slight polar characteristics (24°C, 16 g/kg).

The table shows clearly in what measure a slight moisture and temperature drop acts as a deterrent to hurricane development. We must conclude that sensible heat gained from precipitation cannot be converted to kinetic energy if the colder air mass reaches the core, as the theory postulates. *It is a fundamental difference between deepening cyclones in high and low latitudes that all air entering the orbit of the latter ascends in the*

TABLE 11.8. TEMPERATURES (°C) ALOFT FOR THE CONDITIONS (a)-(d) DESCRIBED IN THE TEXT

Pressure, mb	(a)	(b)	(c)	(d)
Surface	26.0	26.0	26.0	24.0
900	20.0	22.5	22.5	18.0
700	8.0	11.0	13.5	8.0
500	-6.0	-3.0	0.5	-6.5
300	-33.0	-28.5	-23.5	-34.0
200	-55.0	-53.0	-47.0	-59.0

core, while outside the tropics polar air sinks in disturbances and only tropical air rises. A polar-front cyclone becomes filled with cold air only in the late stage, and then it is filling. Similarly, even large hurricanes weaken and sometimes disappear when a current with relatively polar character-

istics enters the core. A forecast of filling will generally be successful in such cases.

Waves in a Baroclinic Easterly Current. Without trying to develop a complete theory, Bjerknes and Holmboe (5) have suggested a starting mechanism. They consider a basic easterly current that increases with height, so that the temperature of the troposphere is warmer on the poleward than on the equatorward side of the current. Given a series of waves in this current, with an eastward tilt of trough and ridge lines with height, the amplitude of the waves can grow. Divergence may develop in a deep column above the trough line and intensify it.

The extensive reasoning behind these conclusions cannot be presented, and the reader is referred to the original paper. Palmer (47) believes that this mechanism can explain sudden cyclogenesis in some wave troughs in the easterlies moving across the western Caribbean Sea. But a variety of alternate models could be constructed. On the basis of the reasoning in Chap. 9, for instance, we could argue that a wave trough must deepen if air moves through the system from east to west at all heights when the axes of troughs and ridges are nearly vertical. Given any such model, it is necessary to demonstrate (a) that it will satisfy all other requirements for hurricane growth and (b) that it actually occurs. Neither proof as yet has been given for the baroclinic easterly wave. It is certain, however, that hurricanes can form when the easterlies do not increase upward; the mechanism therefore is not applicable to all cases.

Dynamic Instability. Still another model for a starting mechanism has been proposed by Sawyer (61), based on earlier work by Solberg (68). Suppose a particle is accelerated to the left of an initial easterly motion which may have been geostrophic. The particle then moves toward lower pressure and gains speed. If the pressure gradient along the path is fairly uniform, the wind speed will soon have increased beyond the speed which the pressure gradient can support in geostrophic equilibrium; the particle will then be forced to turn to the right and curve back toward higher pressure. This situation is called "dynamically stable." If the pressure gradient increases rapidly along the path of the particle, the latter may have subgeostrophic speed wherever it arrives and may continue to move across the isobars toward lower pressure. Since it will never return to its starting latitude, the situation is called "dynamically unstable."

Similar reasoning holds for acceleration to the right of the initial motion. It can further be applied to a vortex rather than to an easterly (or westerly) current. Solberg (68) has shown that, given a symmetrical ring of air, the particles will travel at a constant rate across the isobars, if the absolute vorticity is zero. If it is positive, the motion will be dynamically stable; if negative, unstable.

This is the mechanism for tropical cyclogenesis which Sawyer (61) has proposed. Given an initial vortex with negative absolute vorticity aloft, introduction of any outward component will produce a tendency for the outflow to increase and for the surface pressure to fall. This hypothesis is interesting, because high-level events are considered to be leading, in contrast to the frontal and convection hypotheses. Low-level convergence develops in reaction to pressure changes imposed from aloft. Since there is a time lag, the initial surface-pressure fall is plausible.

Sawyer's criterion is more easily realized in low than in high latitudes, because the value of the Coriolis parameter is much smaller, *i.e.*, smaller anticyclonic relative vorticities suffice to obtain absolute anticyclonic vorticity. Proof of the existence of such negative absolute vorticities *prior* to cyclogenesis, however, has not been given. In fact, a vortex with a layer of zero vorticity is the finished product (Fig. 11.19) rather than the starting point. We also do not find a zone of strong anticyclonic shear, comparable with that on the south side of the polar westerlies, in the region where tropical storms form. Finally, the models of Solberg and Sawyer assume that the wind speed is constant at any radius around the ring investigated. All indications are that variations of speed around a ring or along a current play as great a role in the generation of tropical cyclones as for middle-latitude storms (*cf.* 57).

The survey of hypotheses could be continued at length. Numerous descriptions of flow patterns and synoptic sequences have been advanced to explain cyclogenesis. Although such models often give the right answer, they sometimes break down because atmospheric processes are not uniquely tied to the configuration of upper or lower flow patterns.

Although none of the hypotheses discussed has been acceptable, this does not imply that their authors have not brought out important facts, theoretical or empirical. In trying to coordinate these ideas and to incorporate the evidence accumulated through experience with high-level charts, the ensuing discussion will follow the five-point listing presented initially. All emphasis will be placed on the operative processes, not on any particular circumstances used to illustrate these processes.

The Energy Input

Tropical storms form in those ocean areas and in those seasons in which the sea surface temperature is highest (Fig. 11.35). Here the accumulation of latent and sensible heat in the atmosphere should reach its maximum. We find, in fact, that temperatures and dew points of the surface air correlate well with the sea temperature (Chap. 2). Moreover, the water usually is warmest in the western parts of the oceans; both the sea and the air have had an opportunity to store heat continually on their

long trek westward across the tropics. The moist layer reaches its greatest depth here.

Palmén (45) notes that tropical storms form only in those oceanic regions away from the equator where the surface water has a temperature above 26–27°C. This seems to be a critical limit. There are no reports of fully developed hurricanes from the south Atlantic, the south Pacific east of 140°W, and the east-central north Pacific—the low-latitude regions of relatively cold water, and short sea and air trajectories in tropical regions. Alternately, Fig. 1.9 shows that the equatorial trough does not penetrate into the south Atlantic and eastern south Pacific; its latitude varies little in the storm-free part of the Pacific Ocean. These facts need by no means be unrelated.

Of special interest are the small hurricane regions just west of Central America and Australia. Ocean temperatures exceed the critical value,

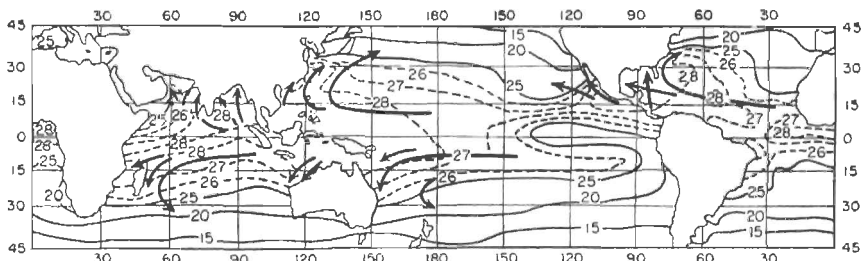


Fig. 11.35. Principal hurricane paths and surface water temperatures during warmest season (15).

and storm formations are observed. Some of these storms move westward; soon they arrive over colder water and die out.

This discussion fits well with our earlier finding that tropical storms are sensitive to slight temperature and moisture variations. In a region where storms normally form, cyclogenesis should therefore be impeded if (1) dew point and temperature of the surface air are below average or if (2) the sea surface temperature is colder than normal.

Although the literature has from time to time suggested a correlation between storm frequency and sea-surface-temperature anomalies, little systematic work has been done. Evidence gathered, however, by one of the author's collaborators, E. S. Jordan, has shown that monthly anomalies with magnitude of 1°C are frequent in the west Atlantic hurricane region. Continuity within the area and from month to month is much better than one might expect from low-quality ship observations. The temperature anomalies, especially when negative, correlate well with seasonal hurricane frequencies. It is certain that reliable synoptic charts of

sea-surface-temperature deviations from the mean on a monthly or shorter time basis could provide a valuable aid for longer-term prognoses.

The Starting Mechanism

We observe universally that tropical storms form only within preexisting disturbances. Chapter 9 contains models of initial deepening in wave troughs in the easterlies; we encounter various other anomalies of low-level flow during impending cyclogenesis, such as sharp clockwise veering of the trades (Figs. 10.2, 10.4, and 10.26).

An initial disturbance therefore forms part of the starting mechanism. A weak cyclonic circulation, low pressure, and a deep moist layer are present at the beginning. The forecaster need not look into areas which contain no such circulations. Hurricanes will not grow from small waves formed spontaneously along an initially undisturbed interface. Nor does their development depend on internal "stability" characteristics of the unperturbed easterlies.

The second part of the starter is the arrival of some outside influence that acts to intensify the initial disturbance. Such intensification may take place along a large portion of a wave trough in the easterlies. Several vortices then form at once (33, 50); with time one of these becomes dominant.

It must be the function of the starter to increase the rate of organized ascent inside the disturbance and also to intensify the surface-pressure gradient. This may be accomplished by lowering the pressure inside or by strengthening the adjoining anticyclone. Both solutions may happen; we shall consider only the first. In accord with Sawyer (61) we place the initiating event in the high tropospheric layer between 300 mb and the tropopause.

From a variety of map sequences encountered during cyclogenesis, Fig. 11.36 is a representative model from the viewpoint of the physical processes which take place. A northerly current in the layer 300–100 mb acts on an initial low-level disturbance. This current may be weakened or intensified through superposition of members of the vortex train that overlies the trade-wind belt in summer (Chap. 10) and the long waves in the polar westerlies. Out-of-phase superposition will weaken the meridional and strengthen the zonal flow; in-phase superposition will strengthen the meridional and weaken the zonal circulation. These changes in the kinetic energy of the high tropospheric flow are produced by a corresponding superposition of pressure-rise and -fall centers. For instance, as a rise center moving westward at 200 mb in the tropics and a rise center moving eastward in middle latitudes reach the same longitude they become superimposed and the rises are increased. If two fall centers

farther east meet in the same way, the east-west pressure gradient is increased and the intermediate northerly flow becomes subgradient.

This description can lead to further problems such as the dynamics and maintenance of the traveling pressure-change centers at high levels. However, these are not part of the present inquiry, which concerns the

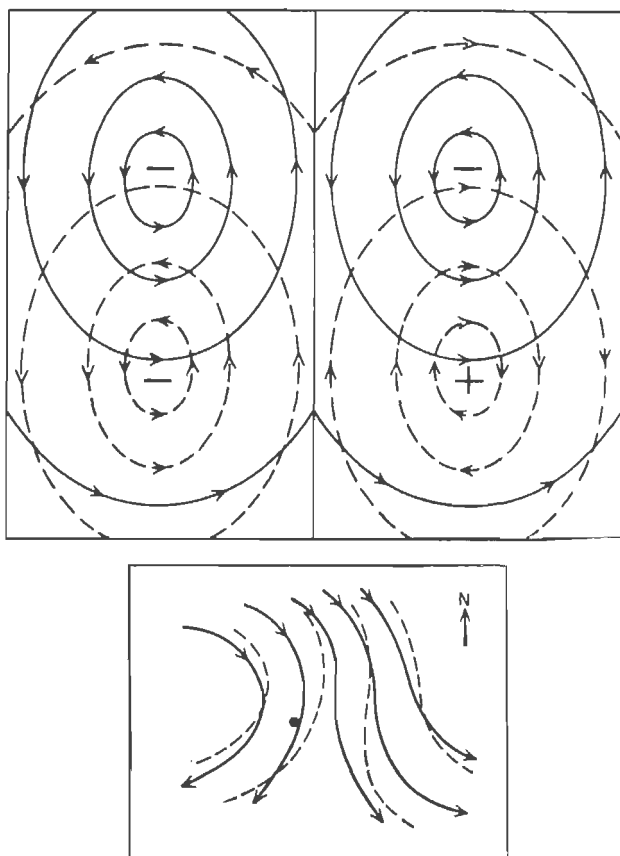


Fig. 11.36. Streamlines of perturbation centers during in-phase and out-of-phase superposition (top); northerly high-level current acting on low-level disturbance (bottom) (53).

immediate processes leading to cyclogenesis. After strengthening of the pressure gradient the northerly current at 200 mb accelerates by turning toward lower pressure. Divergence develops on its right margin, looking downstream, and convergence on the left. The vorticity theorem will be satisfied if the central portion accelerates most strongly, for this will lead to development of anticyclonic shear on the right and cyclonic

shear on the left side. The movement toward lower latitudes also helps to meet the requirement of vorticity decrease on the right.

We may deduce from the foregoing that the initial disturbance in Fig. 11.36 has been placed in the only suitable position for cyclogenesis. In contrast, a location to the left of the upper current would lead to filling. This does not imply that the lower disturbance can never underlie cyclonically curving flow aloft. But the arrangement must be such that the cyclonic vorticity of the upper columns moving over it decreases with time.

Divergence on the right side of the current produces a pressure fall at all levels beneath. The lower air then is accelerated toward the area of reduced pressure, where it converges, acquires cyclonic vorticity, and begins to ascend.

Herewith the role of the starter is completed. The situation described so far is very frequent; perhaps it occurs somewhere every day over the warm parts of the tropical oceans. Yet the number of storms is small; usually we observe only the temporary strengthening of wave troughs described in Chaps. 9 and 10. This suggests that the starting mechanism often misfires because other factors necessary for hurricane formation are not all present.

Release of Latent Heat and Circulation in the Vertical Plane

The circulation that has been set in motion must meet one principal requirement. The ascent must transport enough mass upward through any level (for instance, the 40,000-foot level) to compensate for the lateral divergence above that level. Unless this happens, the pressure at high levels will fall and the pressure gradient that provides for outflow will be destroyed. Then the lower inflow will soon exceed the outflow, and the circulation dies. Once a storm has attained the immature stage, the requirement changes somewhat; the air then carries excess centrifugal momentum upward from below owing to the decrease of circulation with height, and this helps to perpetuate the outflow. At the beginning we cannot utilize this mechanism and therefore must sustain and accelerate the circulation by means of the thermal field.

Figure 11.37 shows the circulation C initiated by the starter. We may deduce the rate of acceleration of this circulation, dC/dt , from Bjerknes's theorem, used here in the slightly approximate form

$$\frac{dC}{dt} = -R \oint T d \ln p - f \frac{dA}{dt} - A \frac{df}{dt}, \quad (11.6)$$

where R is the gas constant of air, T is the temperature, p is the pressure, f is the Coriolis parameter, and A is the horizontal area

around which the circulation is measured. The integration sign \oint denotes integration around a closed curve. Initially, the circulation is in the vertical plane, and the last two terms play no part. These terms of mechanical transformation can act only upon an existing circulation; they form part of the mechanical linkage to be considered as the fourth step. Only the first term, called the *solenoid term*, provides means to exchange heat and potential into kinetic energy. It follows from (11.6), with some approximation, that the circulation of Fig. 11.37 will be accelerated if the temperature of the ascending columns exceeds that of the descending columns. As a subsidiary condition, the pressure must decrease along the surface from the region of descent to the region of ascent. The vertical distance between isobaric surfaces is greatest in the area of upward motion; the pressure gradient, directed toward this area near the ground, will decrease upward and reverse at higher altitudes.

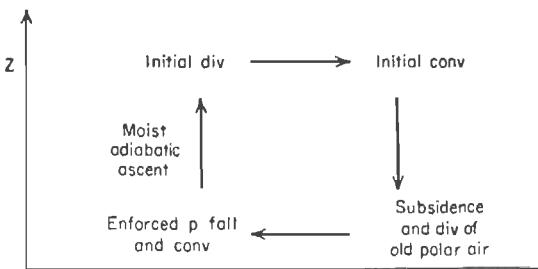


Fig. 11.37. Model of vertical cross-stream circulation (53).

According to all hurricane models, condensation is responsible for the temperature gradient. There is no reason to question this hypothesis, but later we shall also include outside cooling. The initial temperature and moisture distribution must be such that it will permit the rain area to become less dense than its surroundings. As we found in Chaps. 9 and 10, this is by no means always the case; condensation frequently takes place in a framework that requires work done by the surroundings for its maintenance. The requirements for a warm rain area are twofold: (a) moist-adiabatic ascent of the air rising from the subcloud layer must yield on the thermodynamic diagram a positive area with respect to the surroundings; (b) entrainment of cooler and drier air must not hinder this ascent, and ascent of any nonsaturated air in the middle and upper troposphere must be avoided.

Condition (a) is met if the atmosphere has a structure that approximates the mean tropical atmosphere. Ascent can then produce curve C of Fig. 11.27, which will yield a positive area. Any atmosphere that is too cool near the ground or too warm in the middle troposphere is thus

ruled out; this eliminates all regions and synoptic situations with a dry inversion. It favors all regions with high surface temperature and dew point and high ocean temperature.

This reinforces the argument presented under The Energy Input. The transfer of sensible heat from ocean to atmosphere, though small in magnitude compared with the latent-heat transfer, is a vital link here just as it was in maintaining evaporation (Chap. 5). Palmén (45) strikingly points out that even over the western Caribbean—the region with warmest sea surface temperature in the Atlantic—air ascending from the sub-cloud layer will be warmer than the surroundings only in summer but not in winter (Fig. 2.13). This goes a long way toward explaining the lack of winter hurricanes in that region, especially when it is considered together with the upper dryness at that time of year.

During the rainy season, stabilization and drying occur through descent during intermittent intrusion into the tropics of the polar westerlies. When the anticyclonic shear zone of the westerlies overlies the trades, situations that are potentially cyclogenetic do not even develop in the lower troposphere (50). Conversely, the subtropical ridge line aloft and the drying effect of descent along the southern edge of the westerlies are often limited to the region north of 15°N in the western Pacific during the dry season. This permits the occasional appearance of rainy-season-type situations closer to the equator, and some typhoons form in all months of the year.

Condition (b) poses considerable difficulties, and we may surmise that many incipient circulations fail to deepen because they are unable to meet this requirement. A satisfactory discussion would depend on very detailed and frequent observations during the hours of cyclogenesis. These never exist, and so any discussion must remain tentative. The fact that storms form only in preexisting disturbances with deep moist layers suggests that in a limited area a high moisture content of the atmosphere to great heights is necessary; this would reduce to a minimum the resistive effects of entrainment and ascent of air initially located at upper levels.

We may postulate in addition a small vertical wind shear, at least up to 500–400 mb, and this is often obtained. Vertical columns will then remain a unit, and the moisture aloft will not be blown away. A strong wind shear resists building and maintenance of trade cumuli and thunderstorms, as we saw in Chap. 5; cyclogenesis is probably affected in the same way. The only alternative would be a deep moist layer over an area so large that the vertical shear did not matter. This situation is rare. It follows that a basic current with strong vertical shear in the lower layers would be an obstacle; as yet this point has not received the attention it deserves.

In summary, condensation heat can produce temperature increases aloft and a circulation acceleration only if the prevailing lapse rate is such that moist-adiabatic ascent of the subcloud layer results in warming. An initial deep moist layer over a limited area, at least 10^4 km^2 , will ensure minimum resistance against ascent of the lower air columns; a small vertical shear will permit the moist layer to remain a unit.

The Mechanical Linkage

Let us now apply (11.6) to a ring of particles near the surface. These particles converge as they are drawn toward lower pressure, at least in a central area. When the theorem is applied to such a ring, the solenoid term approaches zero because the temperature is almost uniform near the surface and initial surface-pressure gradients are small. Only the mechanical transformation terms are operative. Equation (11.6) then becomes identical with the vorticity equation (8.10). The latter is a special form of the circulation theorem; the more complete form (11.6) permits us to relate vertical and horizontal circulations in the energy cycle. In the present problem the horizontal circulation develops by means of acceleration of the vertical cell. The initial field of cyclonic isobars and winds assures that the vertical acceleration will not be disorganized and break down into numerous convection cells which nullify each other but that the surface air will be driven toward a central zone. Only at this point does Eq. (8.10) or (11.6) for horizontal rings become of interest. The whole framework may be likened to a machine which through a system of gears provides for generation of various kinds of motion in several planes. In the present case the motion is rotatory about the vertical and horizontal axes.

During the initial stages of cyclogenesis the term $f dA/dt$ in (11.6) provides the mechanical linkage exclusively. Even in the later stages $A df/dt$, an all-important term for the long waves in the westerlies, does not assume much importance in the hurricane problem. We may therefore work with the transmission mechanism $f dA/dt$ alone. It follows immediately that vertical cannot be converted into horizontal circulation at the equator where the Coriolis parameter is zero; this is the reason why hurricanes do not form on the equator. At some distance from the equator, however, the circulation increases with a decrease in the area enclosed by the ring of particles. The air particles begin to rotate cyclonically about the core as they approach it at low levels; the opposite will take place at high levels.

We have now pursued the mechanical linkage about as far as practicable. In the formative stage strong winds often are generated and maintained in one quadrant only; it is not obvious why these winds may

need as much as 2-3 days to spread around a center. We also do not know why some storms in their later stages acquire maximum winds of only 60-70 knots and why others attain 150-175 knots. There is a connection with the heat-conversion efficiency of the vertical cell and the resistive effect of ground friction, but the details remain to be worked out. The linkage mechanism may also be approached from the viewpoint of rings with arbitrary orientation in space, *i.e.*, neither vertical nor horizontal (50). In this formulation conversion of circulation about a horizontal into circulation about the vertical axis becomes part of the problem.

The Cooling System

High-level cold advection on the periphery of a storm is the mechanism that removes the excess heat generated. While many models are possible, that of Figs. 11.36 and 11.37 has proved realistic in numerous instances. The northerly current in the high troposphere carries colder air equatorward along its left-hand margin in a long sweep from middle latitudes; the origin of this air is in the cold layer found on the equatorward side of westerly jet streams in middle latitudes above the level of strongest winds. The cooler current converges with the outflow from the storm area; the mixture acquires cyclonic vorticity and sinks. Frequently the gain of cyclonic vorticity is so large that we see formation or intensification of a high-level cyclone several hundred miles east of a tropical storm moving toward west or northwest (51, 56).

The condition for maintenance of the temperature field is that the cold advection balance the heating due to outflow from the storm area and sinking. Although data are seldom sufficient for a computation, thickness patterns and vertical wind shear well to the rear of forming and mature hurricanes give qualitative support. Frequently, but by no means always, cold advection takes place also in the lower troposphere when a polar air mass is accelerated equatorward in consequence of the superposition aloft (56). This air spreads laterally and subsides, and the sinking reinforces the descending branch of the circulation cell in Fig. 11.37, acting to accelerate the whole cell. Of course, there will be no storm if the polar air invades the area of the tropical depression itself. When for some reason the polar outbreak takes place too far west, the whole development ceases.

It is interesting that this model does find a role for old polar air, so prominently mentioned in the literature. Figure 11.38 illustrates the change in viewpoint about the relative position of polar air and tropical disturbance. According to the lower model the sinking of the accelerated northeast trade provides a second suitable means for removing air aloft

from the tropical depression and allowing it to settle at a considerable distance.

With this we complete the inquiry into the origin of tropical storms. Though several suggestions for forecasting have been made, a complete routine for prediction in terms of flow-pattern geometry will not be offered. Because, as stated earlier, atmospheric patterns and processes are not uniquely correlated, prediction in terms of patterns must fail at least occasionally. It must be left to the forecaster to judge whether or

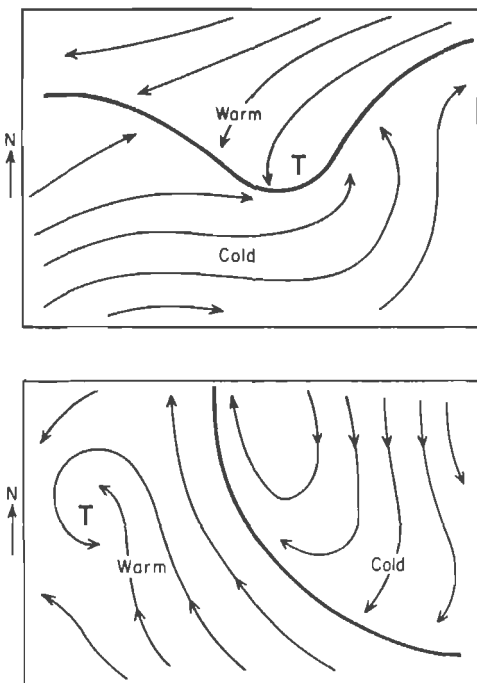


Fig. 11.38. Classical model of typhoon formation at "equatorial front" (top), and model with cyclonic vortex situated entirely in the warm air (bottom) (53).

not a given arrangement of low- and high-level winds, pressures, and temperatures is capable of fulfilling the roles necessary for cyclogenesis. Qualitatively, the energy cycle of the tropical cyclone appears to be more simple than that of any other atmospheric system. It is quite possible that an understanding of the atmospheric machinery will first be perfected for these storms.

Dissipation of Tropical Storms

Reversal of the foregoing arguments furnishes criteria for dissipation. Entrance of colder and drier air at low levels destroys the upward slope

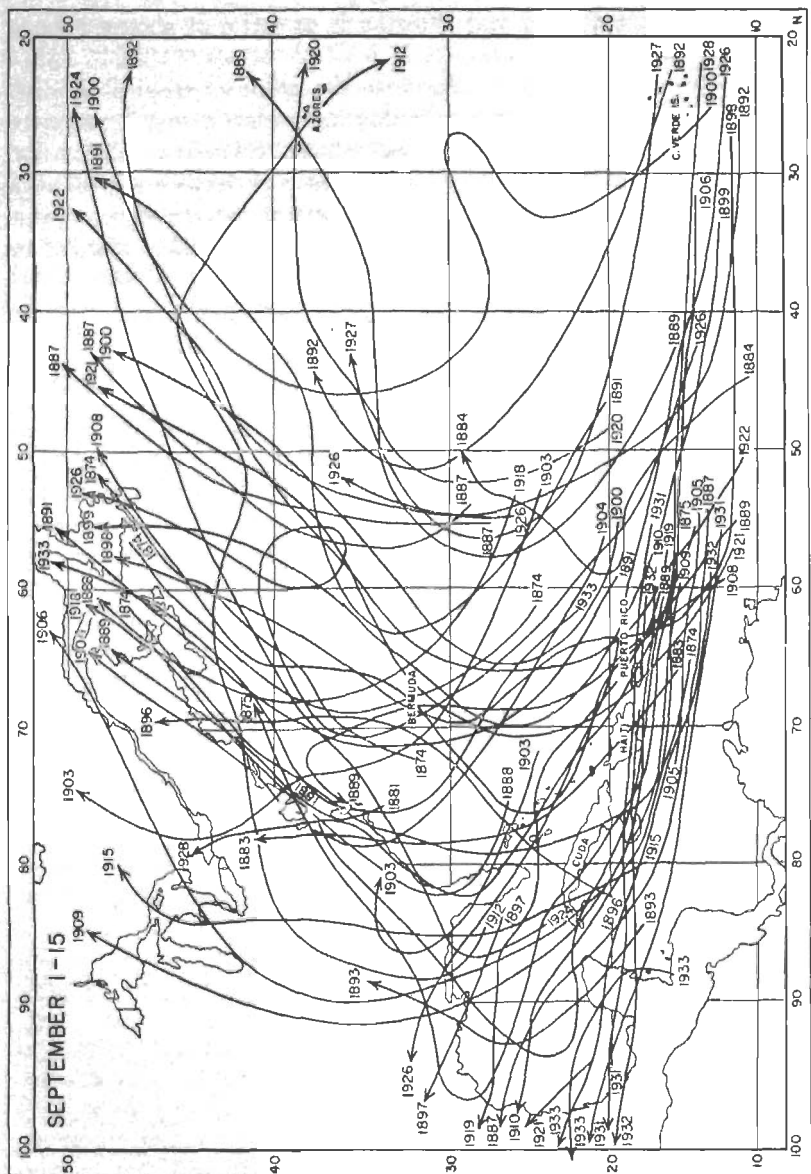


Fig. 11.39. Tracks of tropical cyclones, Sept. 1-15, 1874-1933 (70). (From Tannehill, "Hurricanes," Princeton University Press.)

of the isotherms from outside to inside the circulation. This happens if a storm moves over colder water or if a cold front impinges on the cyclone center in the tropics. After it has passed the subtropical ridge, the arrival of cold air is more likely to transform the storm into a vigorous extratropical cyclone.

Arrival of the equatorward margin of a westerly jet stream at high levels will destroy a circulation rapidly since it favors upper convergence, entrance of cold air aloft, subsidence, and drying.

Movement of a hurricane over land cuts off the surface-energy source and increases the surface friction, especially when the land is mountainous.

MOTION OF TROPICAL STORMS

Since the days when monthly surface isobars could first be drawn and tropical storm tracks charted with some accuracy, meteorologists have known that these tracks roughly paralleled the mean isobars. This led

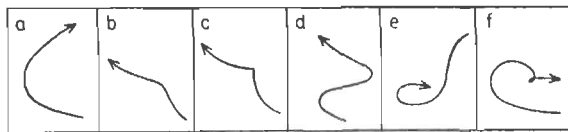


Fig. 11.40. Models of hurricane tracks.

to the concept of steering (25, 29). Considering the general shape of some recurring tracks, some writers have gone so far as to predict hurricane displacements by assuming parabolic or hyperbolic path shapes. Today we know that such simple solutions rarely give the answer. "Abnormal" tracks occur far too often. In Fig. 11.39 all tracks observed for the first half of September from 1874 to 1933 in the Atlantic (70) have been superimposed. Although an undertone suggestive of parabola or hyperbola is undeniable, all kinds of "aberrations" appear: humps, southwestward and southeastward displacements, and even loops. Figure 11.40 shows typical paths in model form. Tracks (a)-(c) are the types most frequently encountered; (d)-(f) are examples of unusual displacements. Paths that lead out of the tropics into the temperate zone are called "recurring" paths; the passage of a storm across the subtropical ridge is termed "recurvature," a somewhat inaccurate but well established name.

Tropical storms move under the influence of external and internal forces. External forces are applied by the currents that surround a storm on all sides and carry it along. Internal forces arise within the circulations themselves.

Internal Forces

In spite of all the irregularities of Fig. 11.39 most storms have one thing in common: a tendency to move poleward. This tendency, shared by cyclones at all latitudes, suggests propulsion by an "internal" force. As Rossby (60) suggests, poleward acceleration of cyclones and equatorward acceleration of anticyclones can arise from the variation of the Coriolis parameter across the width of a storm. It is difficult to measure this acceleration because data are lacking, but Cressman (13) found

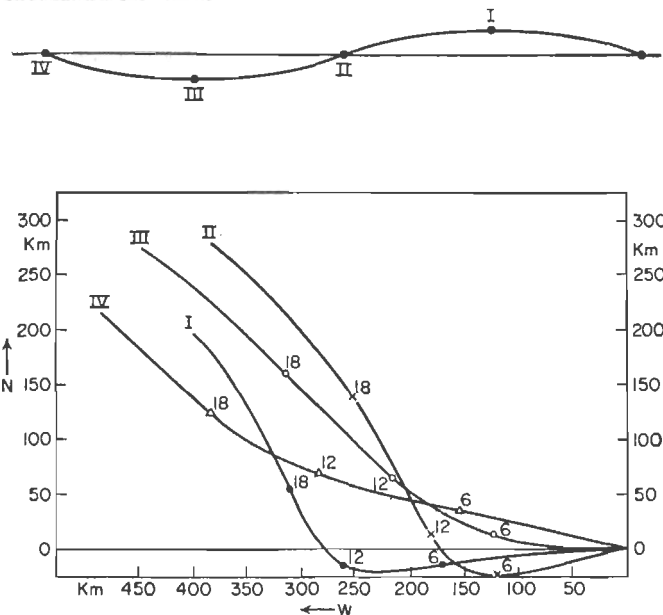


Fig. 11.41. 24-hour displacement of storm after a south component of 3.5 mps is added to easterly current of 6 mps. Roman numerals indicate at which point of internal oscillation (*upper diagram*) southerly current becomes superimposed (77).

that at times it can account for an appreciable fraction of the total displacement.

The Coriolis parameter varies much more across a storm with 1,000 km radius than one with 100 km radius. Small storms should follow the steering current more closely than large ones, and this actually happens. Large storms drift poleward at a rate of 1–2° latitude per day even when there is no carrying current. The average displacement due to the latitude effect is assessed at half this amount, often just enough to bring a storm within reach of recurvature a few days after its formation.

Yeh (77) has described a second internal mechanism, which is a result of the fact that superposition of a vortex on a steering current is non-

linear. This effect becomes manifest through smaller oscillations with amplitude of $0.5\text{--}2^\circ$ latitude and with periods of 12 hours to 2 days for the normal range of observed wind fields. During changes of steering current this oscillation partially determines how the storm will react to the new current. Figure 11.41 shows 24-hour paths of a storm computed with Yeh's model when a south component of 3.5 mps is added to an initial easterly current of 6 mps. Final positions vary, depending on the stage of the oscillation at which the southerly current becomes effective.

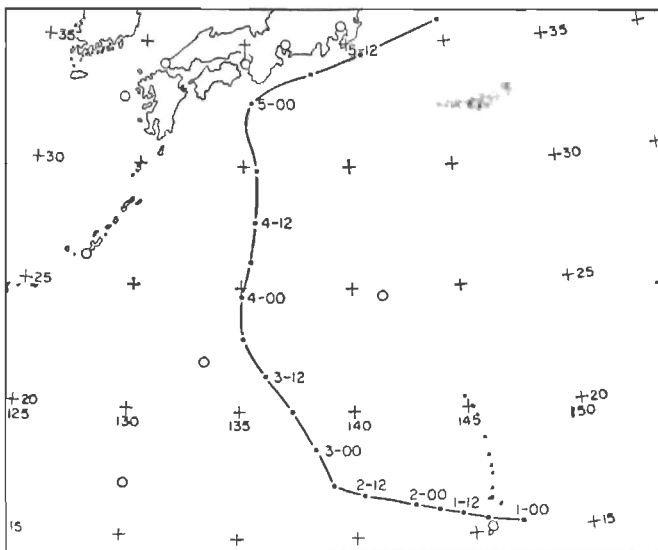


Fig. 11.42. Typhoon track, Oct. 1-5, 1945 (38).

Figure 11.42 shows a track which in general outline conforms to Yeh's model.

External Forces

Steering. In a strict sense, steering refers to the forces that guide a small disturbance in a broad, steady current. Actually these conditions are seldom fulfilled. In any situation the isobars are shaped partly by the storm itself; hence its pressure and wind field must be subtracted from the total fields to obtain a quantitative determination of the steering current. Since the precise form of the perturbation pressure field is unknown and since the superposition of storm and basic current is non-linear, the subtraction has never been carried out successfully. Instead, forecasters began to examine the upper winds (19). It was believed that since the storm circulations decrease upward, the winds aloft should afford

a better grasp of direction and also speed of the steering current. This approach proved valuable; examination of the upper winds at one level alone, however, did not provide a complete solution. Upper charts are drawn for fixed-level or constant-pressure surfaces. Wind speed and direction vary with height, sometimes more and sometimes less. Which level is best suited to yield the correct clue as to future steering?

As pointed out by Simpson (65), there has been a tendency to look to higher and higher levels to make forecasts with the steering technique, as the upper-wind observations were extended upward by the advent of rawins. After the event one can always find a level that would have given a perfect prediction. Some forecasters in responsible positions use what they call the "winds above the circulation," apparently with success, even though we have seen earlier that there is no "level above the storm" in the troposphere when a storm has attained maturity.

In an effort to improve forecasts of hurricane motion, many schemes have been advanced. For instance, Simpson suggested that storms will move along "tongues of warm air" in the layer 700-500 mb that often extend 1,000 miles ahead of a cyclone. The warm tongue is located by computing the relative topography of the 500-mb above the 700-mb surface. Mintz (42) and Moore (44) have applied ideas expressed by Bjerknes and Holmboe (5) to make quantitative forecasts of displacements. Their method is based on the asymmetry of the wind field around a storm and therefore again aims essentially to calculate the steering current. These techniques and many others have proved to be successful in some instances, but data are usually far too sparse for an accurate calculation.

Marked departures from steering, as sometimes reported, are probably due largely to inadequate knowledge of the horizontal and vertical wind structure in individual cases. But the concept of a "steering level" is an oversimplification and must be replaced by that of a "steering layer," including the troposphere up to at least 300 mb (56). We can support this contention with Fig. 11.18, at least for the average hurricane circulation.

If the observed circulation is a combination of fields of rotation and translation, we can compute the field of translation by taking half the difference of the tangential components along the axis normal to the direction of motion on both sides of a storm center. For instance, if the tangential component is E, 50 knots, at a point 3° latitude north of a westward-moving storm, and W, 30 knots, at a point 3° to its south, the steering current is E, 10 knots. This computation was carried out by E. S. Jordan (36) for the average hurricane wind field in the band $2-4^{\circ}$ from the center at all levels up to 30,000 feet. The steering current, defined as the pressure-weighted mean of the computations in this ring,

was 9.7 knots. The speed of motion of the storms included in Fig. 11.18 was 11 knots. This difference is fully within the limitations of the data. If we are to be certain that the directions of the storm motion and steering current do not differ materially, we must repeat the above calculation for the axis parallel to the direction of motion. The computation gives the normal component of the steering current at less than 1 knot. It follows that, in the mean, *tropical storms move in the direction and with the speed of the steering current*, which is defined as the pressure-weighted mean flow from the surface to 300 mb over a band 8° latitude in width and centered on the storm. This affirms the validity of the old concept of steering. In addition, the internal forces cannot produce displacements averaging more than 1-2 knots, as suggested before; otherwise a significant departure of the mean storm path from the steering current should have been found.

Interaction of Vortices. In hydrodynamics, the interaction between vortex pairs has been a subject of analysis for many years. Vortices either attract or repel each other; they rotate about a center of gravity located on the straight line or great circle connecting them. The position of this center depends on the relative mass of the vortices. If they are of equal strength, they rotate about a point situated midway between them. If not, the ratio of the two masses determines the location of the point. In addition to mass, the relative intensity of the circulation within each vortex influences the position of the center of rotation.

Interaction between vortices has been studied especially by Fujiwhara (22, 23); it has also been investigated by Haurwitz (31). Figure 11.36 illustrates the principle. In the left-hand diagram the northern cyclone experiences a force acting westward from the southern vortex. In turn, the southern center is subjected to an eastward-directed force. Thus the axis which may be drawn between the two centers will rotate counterclockwise with time. The most spectacular example of such interaction is the rotation of hurricane pairs. Among many examples Figs. 11.43 and 11.44 illustrate a famous pair which, late in August, 1945, delayed urgent diplomatic negotiations. The vortices were of equal intensity (Fig. 11.43); their tracks and that of the mid-point are plotted in Fig. 11.44. Since the mid-point itself moves, outside systems influence the hurricane pair. If we subtract the displacement of the mid-point from the tracks, we obtain the relative motion of the vortices. Now the interaction is quite clear. The storms rotate about each other and are mutually attracted. As they come closer together, their influence on each other grows and the relative rotation increases.

It is not easy to find many cases so clear-cut. Outside systems with much more mass usually dominate, and their influence must be included.

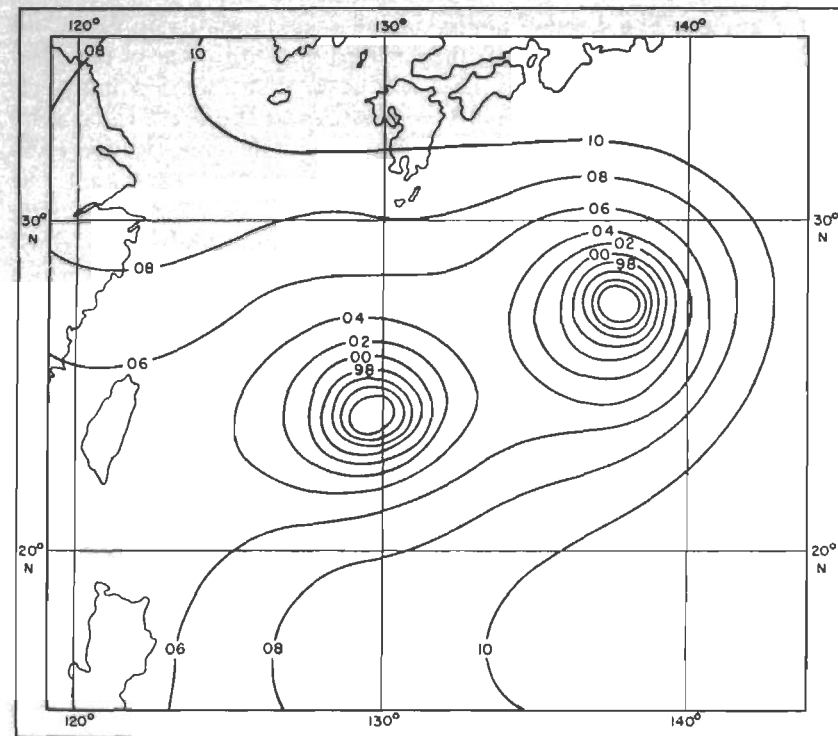


Fig. 11.43. Surface chart, Aug. 25, 1945, for the western Pacific (31).

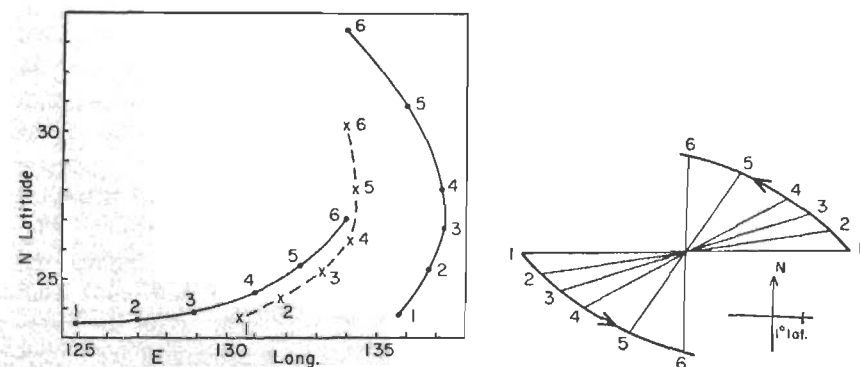


Fig. 11.44. Left: Track of typhoons of Fig. 11.43 (solid) and center of rotation (dashed) for six 12-hour intervals beginning Aug. 24, 1945. Right: relative motion of typhoons.

This introduces complications from the viewpoint of formal dynamical solutions. A stepwise prediction with numerical methods, however, may well be expected.

Although the interaction principle mainly has been applied to hurricane pairs, this may not be its most important use. Consider a pair consisting of a cyclone and an anticyclone. If the mass of the anticyclone is very great compared with that of the cyclone, we observe a quasi-stationary high and a storm that travels on a clockwise path around its periphery; this is another way to look at the steering current. The situation is not unlike that of the system moon-earth. Both bodies rotate about a common center of gravity, but the mass of the earth is so much greater than that of the moon that the center of rotation lies in the interior of the earth.

Frequently in the Pacific, more rarely in the Atlantic, storms grow to such proportions that their mass is not negligible compared with that of the anticyclone. They then influence the anticyclone; if the latter is situated north of the cyclone, it is propelled westward. Since the high, in turn, drives the storm westward, we may see the pair advancing to the west over long distances as a couplet. In the end either the high is broken down by other systems or the storm touches land. This shows that changes in the steering high are the most important factor in producing a sharp turning of the cyclone path. Such changes are usually initiated by the arrival of a mid-latitude trough from the west. This forces the high eastward or southward, often coupled with weakening. The storm is then influenced by both high and trough, and the question of recurvature arises.

Recurvature

Recurvature is the central problem in hurricane-track prediction. A storm often begins to move out of the tropics; the attempt may be successful, or it may fail. Prediction, dealing with a complete parting of the ways, is most critical. United States Weather Bureau forecasters have been aware for many years that middle-latitude influences determine recurvature. Bowie (6) and Mitchell (43) were the first to describe these influences systematically. Their work, which necessarily dealt mainly with the surface chart, has had many applications (*cf.* 73). According to Mitchell (43), "all tropical storms apparently seek to move northward (in the northern hemisphere) at the first favorable opportunity. Any tropical storm will recurve into a trough of relatively low pressure that may exist in the same region where the tropical storm arrives. No storm will break through and recurve until it reaches a region where south or southwest winds prevail aloft and relatively low pressure to the northward is shown on the weather map." Mitchell goes

on to say that recurvature is most likely to succeed when the northern trough is deep and slow-moving, while rapidly moving systems of small amplitude may produce only minor effects.

Although Mitchell's general statement stands unchallenged, many tropical storms do not recurve into a trough of low pressure even when conditions on the surface chart seem very favorable. Some cyclones even force their way poleward through high-pressure areas. Situations that look almost identical on the surface map in some instances lead to recurvature, while in others the disturbances by-pass the trough and continue westward under the influence of the succeeding high.

What enables a storm to cross a trough? Again we must look to the upper winds. These have a variable structure in recurvature situations. Sometimes forecasting is easy, in particular when the wind direction is nearly uniform through a deep layer and gradually turns from east through south to southwest around the western edge of a subtropical high-pressure cell. Here methods such as Yeh (77) developed should be fully applicable. Important difficulties arise whenever the winds aloft are weak and/or when the vertical shear is large. In such situations we can no longer speak of steering, as the behavior of the storms reflects. They slow down and for hours, sometimes days, seem to travel aimlessly except for a slow poleward drift. Qualitative reasoning, in a majority of situations, can provide a prediction of the outcome.

Recurvature Completed. The subtropical ridge aloft, initially situated poleward of a westward-moving storm, must move eastward or be displaced to a latitude lower than that of a storm for recurvature to take place. Such displacement occurs most frequently when an active trough of considerable longitudinal extent, together with an intrusion of colder air aloft, approaches the subtropics west of the center (Fig. 11.45). The base of the polar westerlies *lowers to 15,000–20,000 feet at the latitude and on the western side of the storm*. These westerlies must be maintained, as is frequently indicated by the approach of a second trough in the westerlies a short distance to the rear of the first. The storm will begin to recurve when the forward edge of the westerlies is found 500–700 miles to its west. As the trough advances eastward, the path of the cyclone curves from westward to northward.

Recurvature not Completed. Difficult situations frequently arise in prediction when storms meet strong troughs and intrusion of the polar westerlies equatorward but when the westerlies die away quickly to the rear of a trough. In such situations a warm high builds farther west (Fig. 11.46), or the trough advances from the west against a stationary warm high in the east and weakens. The meridional temperature gradient necessary for maintaining the upper westerlies disappears quickly in the southern portion of the trough, and easterly winds replace the west

winds there. This trough portion is retarded and quickly loses connection with the main body, which continues to move eastward in the higher latitudes.

Whenever the easterlies reestablish themselves quickly in this way at a latitude higher than that of the storm, the latter is carried westward by the new easterlies past the eastward-moving portion of the trough in the north. As the western high becomes the most influential vortex, the

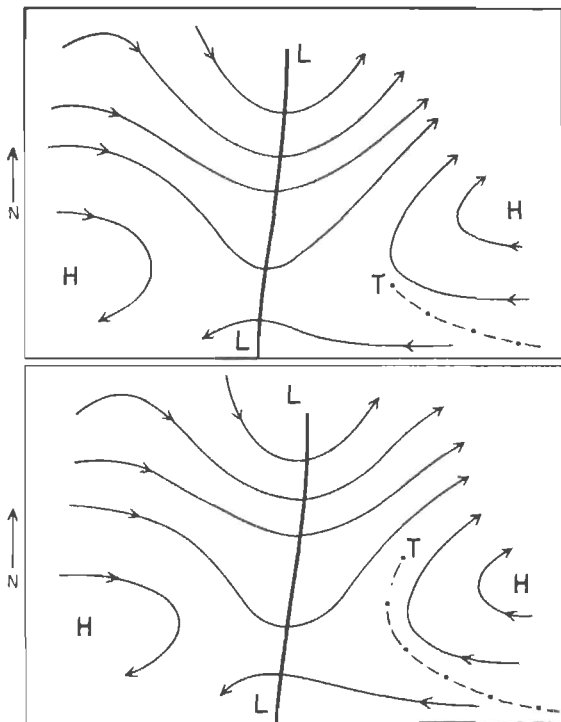


Fig. 11.45. Model of flow pattern during simple recurvature (7, 55).

storm does not complete the curve it has begun but remains nearly stationary for a short period. It then resumes motion toward northwest, west-northwest, or even west, depending on the shape and intensity of the new high. Its resulting track has the shape of a hump or cusp (Fig. 11.40b, c).

Multiple Recurvature. We can extend this type of reasoning to explain a wide variety of "abnormal" movements. Track (d) of Fig. 11.40 shows a situation in which at first the base of the westerlies lowers west of a storm and stays low. As a result the center curves toward northeast. Before it can reach high enough latitudes, however, a dynamic high either

forms north of it or overtakes it going east. The center then decelerates and turns northwestward for a second time.

This second turning is very gradual and may not be completed at all. The trough which brings about the first recurvature toward northeast may slowly become oriented northeast-southwest, at times even east-west. Its southern end remains connected with the tropical storm for a considerable time after the new upper high has reached a position north

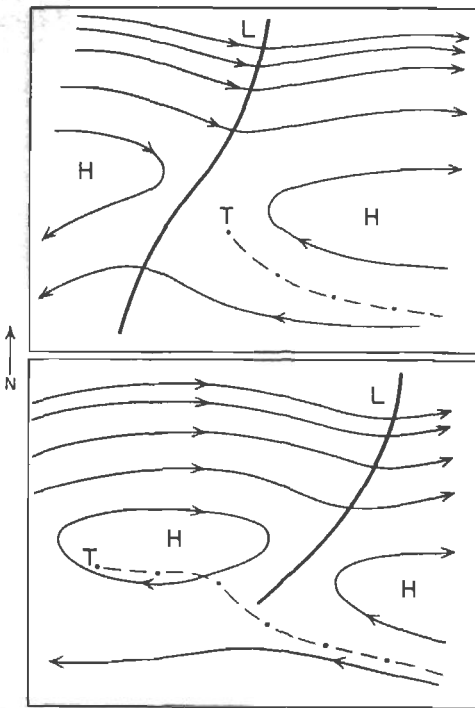


Fig. 11.46. Model of flow pattern as hurricane by-passes extratropical trough (7, 55).

of the center. A narrow band of west-southwest winds, often not apparent below 300 mb but of considerable strength at 200 mb, remains between the two easterly belts farther north and south. This band dies away very slowly, and the storm's fate may hang in the balance for 2 days—a difficult period for the forecaster.

At times, especially late in the season, a storm may enter such a narrow northeastward-slanting trough soon after its formation. The track then will be due north to north-northeast from the start. Tannehill's (70) survey of late-season tracks (Fig. 11.47) shows nearly all storms formed after Oct. 15 in the Atlantic moving on such a path, a fact which indicates the dominant influence of the southwest current east of the troughs.

Curve (e) of Fig. 11.40 is the track of a famous hurricane in November, 1935, described by Byers (9). This hurricane formed north of Bermuda as a subtropical cyclone, moved southwestward in spite of the late season under the influence of a deep northeasterly current over the Atlantic coast of the United States, and deepened to become a hurricane. It crossed Florida south of the upper high and recurved in the eastern Gulf of Mexico in a more orthodox manner. The last portion of the track, directed east-southeastward back to Florida, is again abnormal. Gentry (26) has discussed a case of similar complexity.

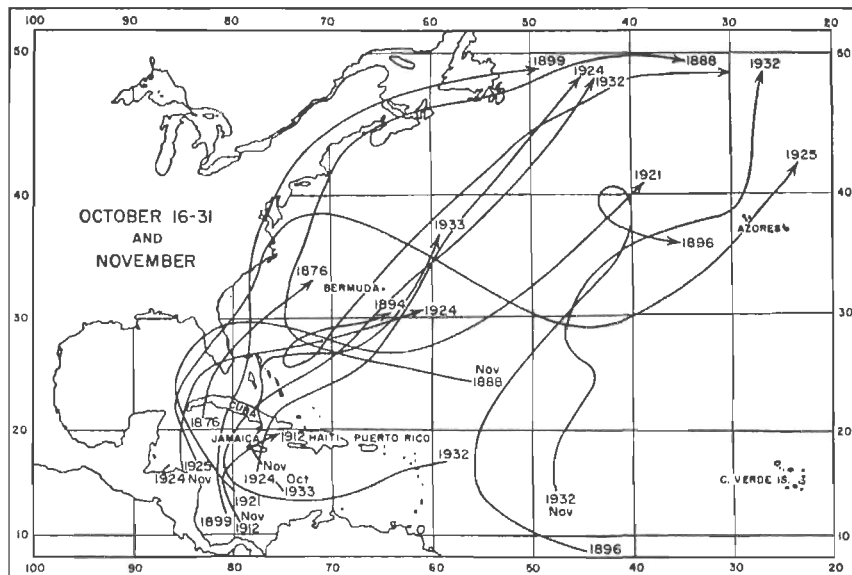


Fig. 11.47. Tracks of tropical cyclones, Oct. 15–Nov. 30, 1874–1933 (70). (From Tannehill, "Hurricanes," Princeton University Press.)

Motion toward the southwest occurs under a deep northeasterly flow. Preferred regions are the western parts of the Gulf of Mexico and the China Sea, where such upper currents are common, especially in August. Rarest of all directions of motion is southeast, illustrated in curve (f) of Fig. 11.40. This happens when a cyclone moving up a trough is overtaken by this trough, which deepens farther east. As the northwesterly flow aloft intensifies, the storm is dragged southeastward.

Forecasting Methods

Because progress has been so rapid in the field of meteorology, especially in the application of high-speed computing equipment, any rigid forecast procedure set down at the time of this writing would soon become

obsolete. A few comments may be helpful, however. There are some very practical considerations which will not become obsolete as long as surface data remain scarce and upper-air data practically nonexistent for the tropical oceans. In such a predicament statistics furnish the most logical approach.

Statistical Aspects. We have already mentioned hurricane frequencies and areas of formation. Mitchell (43) has published monthly resultant storm tracks for the Atlantic Ocean. Tannehill's book (70) contains all individual tracks for many years. Colón (12) has extended the statistical knowledge by computing for each 5° latitude-longitude square the per cent frequency with which storms have moved along each of the 16 principal directions. He also calculated the probability of a displacement along the modal direction and the average speed of motion. In the absence of

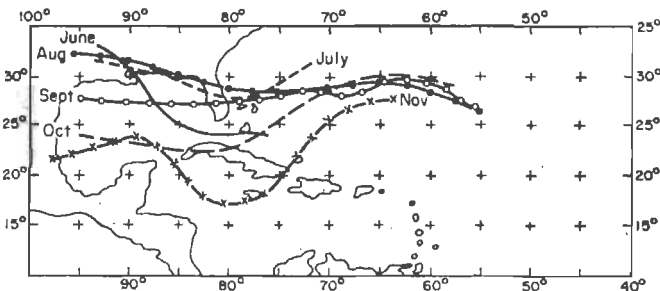


Fig. 11.48. Lines showing average latitude of recurvature (12).

data a prediction of modal direction and speed is the best guess for a new center. Colón notes that in the Atlantic the probability of a modal track is fortunately highest just in those regions where data are most scarce. A similar situation appears to exist in several other hurricane regions.

Once a track has been established, the "path method" may become a better tool than the modal direction. The past displacement indicates what the steering current has been, and this is at least some guide in estimating the future track. Colón computed the probability that the track in the next 24 hours would not deviate more than 10° from that of the previous 24 hours. He finds that straight-line extrapolation has a chance of at least 80 per cent over most of the territory south of 20°N , especially in the middle of the season when the influence of the polar westerlies usually does not reach to this latitude. Extrapolation is least accurate near the mean position of the subtropical ridge line and in the early and late parts of the season. The low persistence near the subtropical ridge results in part from slow motion as storms vacillate between the influence of easterlies and westerlies. Here we should find a maximum of recurvatures. This is confirmed in Fig. 11.48, which shows axes connecting points of highest recurvature frequency for each month of

the season. We see a fairly regular shift of these axes with the general circulation, northward from June to July–August, then southward to November.

Extrapolation need not proceed along a straight path. Instead, one can determine the chance that the path curvature will remain constant. Since storm tracks of the past seldom were charted with sufficient accuracy, such a computation involving higher-order derivatives is not feasible. However, Colón determined the modal turning of path for the nonpersistent storms. As might be expected, this turning is generally to the right, $30\text{--}40^\circ$ near the axes of recurvature, $20\text{--}30^\circ$ or even less in most other areas.

Kinematic Prediction. Petterssen's formulas for forecasting displacement and acceleration of various features of the pressure field (48) are usually difficult to apply in the tropics because reliable 3-hour pressure-tendency data do not exist. But the essential benefits of the kinematic approach can be secured through the graphical techniques developed by Defant (*cf.* 58) and Wasco (72); these in a sense are extensions of Petterssen's earlier work. Graphical kinematic techniques give excellent result in middle latitudes for 24-hour forecasts and verify far better than strictly qualitative reasoning for 48 hours; but they require good isobaric or constant-pressure analyses. In the areas and on the occasions when a kinematic prediction can be made, the probability of good verification is fair.

Recurvature Forecasting. It is fair to say that the prediction of recurvature will be as good as that of the upper flow pattern in middle latitudes. Although this topic is outside the scope of this book, we shall mention a few basic points.

In Chap. 10 we have discussed meridional and zonal arrangements of the broad-scale flow patterns. The transition from one type to the other often follows a regular course, which we have called the "index cycle." Two parameters are essential for applying the index cycle to storm prediction. They are (1) the departure from the average of the zonal wind speed at different latitudes and (2) the position, spacing, and amplitude of the long waves in the westerlies.

If the westerlies are above average in the latitude belt where, in the climatic mean, they are strongest during the hurricane season ($45\text{--}50^\circ\text{N}$ at 700–500 mb), the amplitude of the long waves is likely to be small and the interlocking between temperate and tropical zones at a minimum (Chap. 10). These circumstances do not favor recurvature; long storm tracks toward the west or northwest are probable.

If the strength of the westerlies is below average in the lower middle latitudes, the tropical easterlies will be below average. The meridional extent of troughs and ridges aloft is likely to be great; chances for recur-

vature then are good. This is true especially when the westerlies are increasing with time. Long-wave troughs and ridges most probably propagate eastward; we may look for the sequence sketched in Fig. 11.45, while Fig. 11.46 represents the more zonal type.

Troughs of smaller wave length and amplitude constantly pass through long-wave troughs. These intensify as they approach the long-wave-trough position and weaken after they leave it (24). A storm moving on a track toward west-northwest may meet several smaller troughs before it encounters the main trough. Figure 11.49 shows a sample sequence. Long- and short-wave troughs are superimposed at first, and the amplitude of the composite flow pattern is large. Then the short-wave trough moves forward, and in middle latitudes the amplitude of the westerlies decreases. The storm at first is intercepted and starts to recurve. Then, as the short-wave trough weakens and the ridge in the east recovers, it executes a hump or cusp and once again propagates westward. Meanwhile a new trough from northwest has reached the long-wave-trough position, assumed to be stationary for this illustration. The amplitude of the upper flow is again large, and a second attempt at recurvature soon begins. Since the relative distance between storm and long-wave trough has decreased, this attempt may well succeed unless a fundamental rearrangement of the middle-latitude flow pattern occurs.

Such a rearrangement is shown in Fig. 11.50, which portrays long-wave retrogression. It occurs most frequently when the speed of the zonal winds decreases with time. The second trough intensifies much farther west than in Fig. 11.49, while the eastern ridge builds rapidly and advances westward after the first trough passes. Events occasionally take a spectacular course. In September, 1947, a severe hurricane (Fig. 11.28) approaching Florida was intercepted by a trough advancing eastward through the United States. Within 24 hours the low latitude portion of this trough collapsed and was replaced by an anticyclone aloft that deepened rapidly while extending itself northward and eastward. This restored deep easterlies north of the storm, which hesitated and then turned west to strike Miami and New Orleans. Klein and Winston (37) have analyzed this case, and they point out that, among other things, the rapid transformation of the upper flow pattern could not be understood without consideration of the Pacific Ocean. Thus, in hurricane work, as in all other forecasting, maps covering only a small portion of a hemisphere will often not yield all essential clues. If prediction for 48 hours or longer is wanted, more than half a hemisphere may have to be considered in critical situations.

For 24-hour forecasting, the influences controlling storm movement appear to be situated much closer to a center, usually within the region extending from 10° to the north to 5° to the south, and from 10° to the

west to 10° to the east of the center. In a limited sample of storms, not including cyclonic binaries and storms executing cusp points, good verification has been obtained with forecast calculations based only on the 500-mb chart prepared at the time of forecasting (79).

The computing method utilizes our earlier observation that, in the mean, storms are carried by the tropospheric current; the 500-mb surface may roughly approximate the average condition of the steering layer.

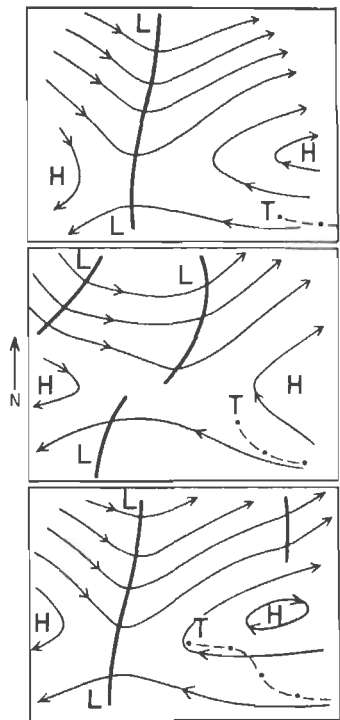


Fig. 11.49. Attempted recurvature as short-wave trough in westerlies passes through long-wave trough (7).

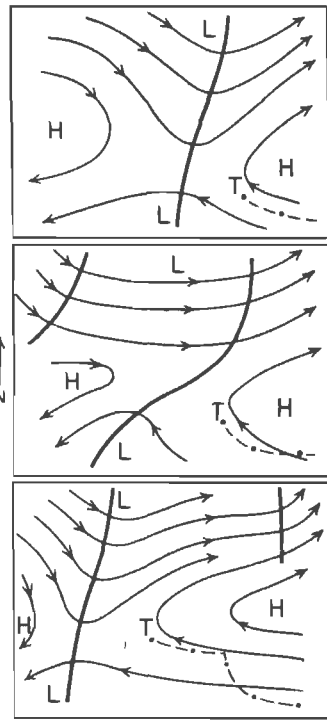


Fig. 11.50. Attempted recurvature during long-wave retrogression (7).

We compute the 500-mb height gradient from north to south and from east to west across an area of the size as stated above and centered on the storm. If the steering current is quasi-geostrophic and if influences outside the area do not materially affect conditions inside in 24 hours, the computation may yield an approximation to the storm path. After allowing for several factors, such as the meridional drift due to internal forces, the result was that about 85 per cent of the computed positions verified within 60 miles of the observed positions, and most of the remaining departures were not much larger.

It is evident that any quantitative technique, such as the one outlined, can succeed only if reliable charts are available for the calculations.

REFERENCES

- (1) Alaka, M. A., *et al.*, *The Jet Stream*. NAVAER 50-1R-249, Navy Dept., Washington, D.C. (1953).
- (2) American Meteorological Society, *Compendium of Meteorology*. Boston, Mass.: 1951.
- (3) Bjerknes, V., *et al.*, *Physikalische Hydrodynamik*. Berlin: Verlag Julius Springer, 1933.
- (4) Bjerknes, J., *Meteor. Z.*, **54**: 462 (1937).
- (5) Bjerknes, J., and J. Holmboe, *J. Meteor.*, **1**: 1 (1944).
- (6) Bowie, E. H., *Monthly Weather Rev.*, **50**: 173 (1922).
- (7) Boyce, R. C., *et al.*, *Tropical Cyclone Forecasting*. Chicago: Department of Meteorology, University of Chicago, 1950.
- (8) Brooks, C. E. P., and H. W. Braby, *Quart. J. Roy. Meteor. Soc.*, **47**: 1 (1921).
- (9) Byers, H. R., *Monthly Weather Rev.*, **63**: 318 (1935).
- (10) Byers, H. R., *General Meteorology*. New York: McGraw-Hill Book Company, Inc., 1944.
- (11) Cline, I. M., *Tropical Cyclones*. New York: McGraw-Hill Book Company, Inc., 1926.
- (12) Colón, J., *Monthly Weather Rev.*, **81**: 53 (1953).
- (13) Cressman, G. C., *Bull. Am. Meteor. Soc.*, **32**: 326 (1951).
- (14) Deppermann, C. E., *Wind and Rainfall Distribution in Selected Philippine Typhoons*. Manila: Bureau of Printing, 1937.
- (15) Deppermann, C. E., *Some Characteristics of Philippine Typhoons*. Manila: Bureau of Printing, 1939.
- (16) Deppermann, C. E., *Bull. Am. Meteor. Soc.*, **27**: 6 (1946).
- (17) Deppermann, C. E., *ibid.*, **28**: 399 (1947).
- (18) Dunn, G. E., *Bull. Am. Meteor. Soc.*, **21**: 215 (1940).
- (19) Dunn, G. E., *Monthly Weather Rev.*, **68**: 303 (1940).
- (20) Dunn, G. E., in *Compendium of Meteorology*. Boston, Mass.: 1951.
- (21) Durst, C. S., and R. C. Sutcliffe, *Quart. J. Roy. Meteor. Soc.*, **64**: 75 (1938).
- (22) Fujiwhara, S., *Quart. J. Roy. Meteor. Soc.*, **47**: 287 (1921).
- (23) Fujiwhara, S., *ibid.*, **49**: 75 (1923).
- (24) Fultz, D., *Dept. Meteor., Univ. Chicago, Misc. Rept.* 19, 1945.
- (25) Garriott, E. B., *Monthly Weather Rev.*, **23**: 167 (1895).
- (26) Gentry, R. C., *Monthly Weather Rev.*, **79**: 107 (1951).
- (27) Gutenberg, B., in *Compendium of Meteorology*, p. 1303. Boston, Mass.: 1951.
- (28) Hall, M., *Monthly Weather Rev.*, **45**: 78 (1917).
- (29) Hann, J., *Z. Öst. Ges. Meteor.*, **10**: 81, 97 (1875).
- (30) Haurwitz, B., *Monthly Weather Rev.*, **63**: 45 (1935).
- (31) Haurwitz, B., *B. Archiv Meteor., Geophys. Bioklim.*, **4**: 73 (1951).
- (32) Horiguti, Y., *Mem. Imp. Obs. Kobe*, **3**: 23 (1928).
- (33) Hubert, L., *J. Meteor.*, **6**: 216 (1949).
- (34) Hughes, L. A., *J. Meteor.*, **9**: 422 (1952).
- (35) Jordan, C. L., *J. Meteor.*, **9**: 285 (1952).
- (36) Jordan, E. S., *J. Meteor.*, **9**: 340 (1952).
- (37) Klein, W. H., and J. S. Winston, *Bull. Am. Meteor. Soc.*, **28**: 447 (1947).
- (38) La Seur, N. E., and C. L. Jordan, *A Typical Weather Situation of the Typhoon Season*. Chicago: Department of Meteorology, University of Chicago, 1952.

- (39) Longley, R. W., *Bull. Am. Meteor. Soc.*, **30**: 194 (1949).
- (40) Maynard, R. H., *J. Meteor.*, **2**: 214 (1945).
- (41) McDonald, W. F., *Monthly Weather Rev.*, **70**: 1 (1942).
- (42) Mintz, Y., *Bull. Am. Meteor. Soc.*, **28**: 121 (1947).
- (43) Mitchell, C. L., *Suppl., Monthly Weather Rev.*, No. 24, 1924.
- (44) Moore, R. L., *Bull. Am. Meteor. Soc.*, **27**: 410 (1946).
- (45) Palmén, E., *Geophysica (Helsinki)*, **3**: 26 (1948).
- (46) Palmer, C. E., in *Compendium of Meteorology*, p. 859. Boston, Mass.: 1951.
- (47) Palmer, C. E., *Quart. J. Roy. Meteor. Soc.*, **78**: 126 (1952).
- (48) Petterssen, S., *Weather Analysis and Forecasting*. New York: McGraw-Hill Book Company, Inc., 1940.
- (49) Riehl, H., *Dept. Meteor., Univ. Chicago, Misc. Rept.* 17, 1945.
- (50) Riehl, H., *Dept. Meteor., Univ. Chicago, Misc. Rept.* 24, Part I, 1948.
- (51) Riehl, H., *J. Meteor.*, **5**: 247 (1948).
- (52) Riehl, H., *Quart. J. Roy. Meteor. Soc.*, **74**: 194 (1948).
- (53) Riehl, H., *J. Appl. Phys.*, **21**: 917 (1950).
- (54) Riehl, H., in *Compendium of Meteorology*, p. 902. Boston, Mass.: 1951.
- (55) Riehl, H., and R. J. Schafer, *J. Meteor.*, **1**: 42 (1944).
- (56) Riehl, H., and N. M. Burgner, *Bull. Am. Meteor. Soc.*, **31**: 244 (1950).
- (57) Riehl, H., and S. Teweles, *Tellus*, **5**: 66 (1953).
- (58) Riehl, H., et al., *Am. Meteor. Soc. Mon.* 5, 1952.
- (59) Rodewald, M., *Meteor. Z.*, **53**: 197 (1936).
- (60) Rossby, C.-G., *J. Meteor.*, **6**: 163 (1949).
- (61) Sawyer, J. S., *Quart. J. Roy. Meteor. Soc.*, **73**: 101 (1947).
- (62) Schacht, E. J., *Bull. Am. Meteor. Soc.*, **27**: 324 (1946).
- (63) Scherhag, R., *Wetteranalyse und Wetterprognose*. Berlin: Verlag Julius Springer, 1948.
- (64) Shaw, Sir Napier, *Manual of Meteorology*, Vol. II. London: Cambridge University Press, 1936.
- (65) Simpson, R. H., *Trans. Am. Geophys. Union*, **27**: 641 (1946).
- (66) Simpson, R. H., *Monthly Weather Rev.*, **75**: 53 (1947).
- (67) Simpson, R. H., *Bull. Am. Meteor. Soc.*, **33**: 286 (1952).
- (68) Solberg, H., *Procès-Verbaux, Météor., Union géod. géophys. intern.*, Edimbourg, **2**: 66 (1939).
- (69) Sverdrup, H. U., et al., *The Oceans*. New York: Prentice-Hall, Inc., 1942.
- (70) Tannehill, I. R., *Hurricanes*. Princeton, N.J.: Princeton University Press, 1942.
- (71) Union Géodésique et Géophysique Internationale, Association de Météorologie, *Réunion de Bruxelles Rapport nationaux*. 1952.
- (72) Wasco, P. E., *Bull. Am. Meteor. Soc.*, **33**: 233 (1952).
- (73) Weightman, R. H., *Monthly Weather Rev.*, **47**: 717 (1919).
- (74) Wexler, H., *Bull. Am. Meteor. Soc.*, **26**: 156 (1945).
- (75) Wexler, H., *Ann. N.Y. Acad. Sci.*, **48**: 821 (1947).
- (76) Wood, F. B., and H. Wexler, *Bull. Am. Meteor. Soc.*, **26**: 153 (1945).
- (77) Yeh, T. C., *J. Meteor.*, **7**: 108 (1950).
- (78) Yeh, T. C., *Tellus*, **2**: 173 (1950).
- (79) Riehl, H., and Wm. H. Haggard, U.S. Navy Bureau of Aeronautics, Project AROWA, Technical Report (1954), Norfolk, Va.

CHAPTER 12

THE GENERAL CIRCULATION

This book opened with a general view of mean conditions in the tropical regions: the principal wind currents near the ground and aloft, the temperature climates, and the distribution of precipitation. Next came the treatment of the moist layer and of the cumulus clouds. A survey of the types of weather disturbance followed. These three components form the low-latitude situation which we see on any day or, after summation, in any month or year; the time-integrated picture usually is called the "general circulation." Finally, we may ask how everything hangs together. How do the many interesting details we have investigated, pieces of a jigsaw puzzle, fit into each other?

The Classical General-circulation Model

All atmospheric motion starts from inequalities in heating or cooling, especially the net radiation differences between polar and tropical belts. Since, averaged over the years, the temperature is nearly constant at all places, these differences must be balanced by heat exchange between high and low latitudes. Air currents set in motion poleward and equatorward largely effect the exchange.

Any general-circulation machine must function so as to permit conversion of heat into mechanical energy, *i.e.*, winds. The resulting wind system must satisfy the fundamental laws of motion. By specifying that the cold air in the polar zone sinks and that the warm air in the equatorial zone rises, the classical theory attempts to satisfy the first requirement [Eq. (11.6)]. Conservation of absolute angular momentum by air currents as the leading dynamical principle is the means for satisfying the second.

If air ascends in the equatorial zone and moves poleward, it acquires an eastward component of motion under conservation of momentum. This component increases rapidly as the air penetrates into higher latitudes. Sinking near the poles brings westerly winds down to the surface. Finally, as the air returns to the tropics at low levels, the westerlies diminish and eventually change to easterlies. This meridional circuit

provides for the heat exchange and for creation and maintenance of the winds. It further explains the existence of the principal wind systems, the belts of westerlies and easterlies.

This, in essence, is the classical model, first propounded by Hadley (13) in 1735. In his time the dryness of the subtropics was well known; he allowed for it by introducing a partial descent of the upper poleward current in the horse latitudes. Subsequent modifications concerned the differences between continents and oceans, monsoons and slow seasonal changes. The introduction of friction was important. Air traveling equatorward at the surface is restrained through contact with the ground from acquiring the high speeds which the momentum principle demands. Both surface westerlies and easterlies are much weaker than would be predicted by the theory. Upon leaving the surface in the equatorial zone, however, the poleward-traveling air is no longer subjected to skin friction. The upper winds therefore should reverse rapidly from easterlies to westerlies with increasing latitude, giving rise to antitrades above the low-level trades and to upper westerlies in middle latitudes that are much faster than those at the surface. This latter feature is observed.

Apart from such alterations, the model was regarded as a complete explanation until the early 1920's. Two basic premises were not questioned: (a) Latitudinal gradients so far outweigh the longitudinal ones that the general circulation may be regarded as axially symmetric. (b) The general circulation can be derived from steady-motion considerations: huge meridional cells provide for the heat exchange and determine the principal wind systems. The disturbances that bring the changing daily weather at best are ornaments but are usually nuisances.

Collapse of the Classical Model

It required courage to raise doubts about a theory so well established. Although there were earlier critics, the first major break occurred in 1921, when A. Defant (6; cf. also 9, 10) showed on the basis of classical turbulence theory that eddies in the horizontal wind field with a diameter of about 1,000 km could accomplish the meridional heat transport. Since this is the dimension of the synoptic disturbances, the question arose as to whether these circulations perhaps perform a functional role.

Shortly afterward, V. Bjerknes *et al.* (3), following Exner (7), questioned the concept of zonally symmetric rings of air moving long distances across the latitude circles. The left-hand curve in Fig. 12.1 shows the change in west-wind speed which air experiences as it moves poleward from the equator under conservation of absolute angular momentum. Already at latitude 25° its speed will be 175 knots. In middle latitudes it will be quite phenomenal, far higher than any wind ever observed.

The enormous pressure gradients necessary for air to continue poleward against the centrifugal force at such speeds do not exist.

Bjerknes (3) suggests that mass exchange over large latitude intervals can be achieved only if the hypothesis of zonal symmetry is abandoned and a cellular structure is introduced for the subtropical belt. Consider Fig. 12.2. As an air current of limited longitudinal width begins to move poleward, it will curve to the right. If, at the same time, another current tries to move equatorward farther east, the currents will converge and build a high-pressure area between them. This eliminates the need

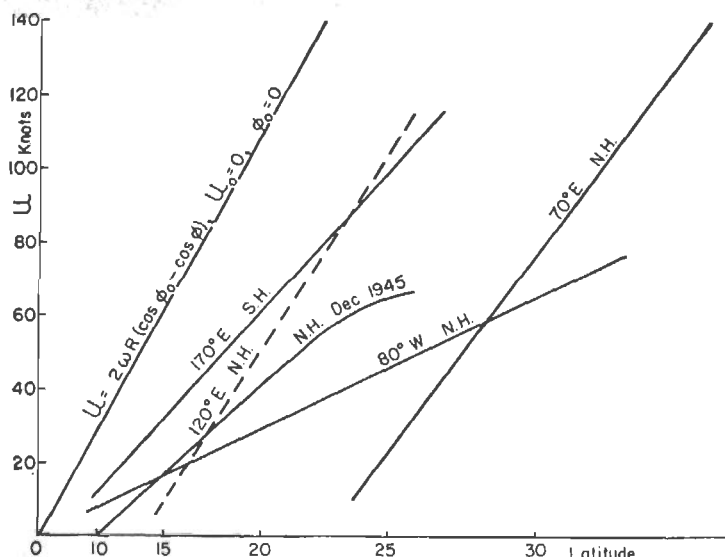


Fig. 12.1. Illustrating the departure of zonal wind distribution in high troposphere from constant absolute angular momentum in winter. Notation as in eq. 12.1. Left-hand curve slightly approximated for low latitudes.

for extreme zonal wind speeds. Currents can travel long distances poleward or equatorward without much change in wind speed in the isobaric channels around the periphery of the high; their absolute angular momentum then is no longer conserved. Daily- and mean-pressure maps at the surface and aloft (Fig. 1.18) have proved the actual existence of the cellular structure.

The rise of the polar-front theory led to further difficulties with the classical general-circulation model. If a mean convergence zone is situated at the surface around the globe in middle latitudes, with a poleward flow of air south of the mean frontal position, a corresponding zone of divergence must exist higher up on grounds of mass continuity (2, 31). This implies an equatorward drift of air at high levels, the famous

"indirect middle-latitude cell," whose existence has long been debated but which is increasingly supported by observations. If conservation of absolute angular momentum were the law of motion applicable to individual air parcels or columns, the west-wind speed should decrease upward in a reverse meridional cell. Actually, the west winds increase upward. *Application of the conservation principle to individual masses must therefore be abandoned* (33). Assuming that the westerlies are created by means of an unspecified process which concentrates the meridional temperature gradient in middle latitudes, Rossby (30) believes they will tend to have supergradient speed and brake themselves by flow toward higher pressure with an equatorward component. Through this "banking" large anticyclonic eddies are thrown off on the equatorward side.

After an attempt to forge together the old and the new (31), Rossby abandoned the classical model (32, 33, 36). By analogy with his work in oceanography (29), he introduced large-scale lateral shearing stresses as an important mechanism in shaping the general circulation. He proposed that the atmosphere tends to equalize the absolute vorticity of the upper troposphere in middle and high latitudes and that constant vorticity exchange between the subtropical ridges across the equator determines the mean wind structure of the tropics. Upper wind and pressure distributions support the hypothesis outside the tropics. For low latitudes the meteorologist, as usual, has no data to offer, but the astronomer is able to assist with observations of the displacement of sunspots relative to the sun in the solar tropics. A profile of these displacements coincides with one of Rossby's vorticity-exchange curves. The fact that the sunspots move from the west along the solar equator is very strong evidence of lateral mixing since it is the only mechanism capable of producing average eastward motion around the equator.

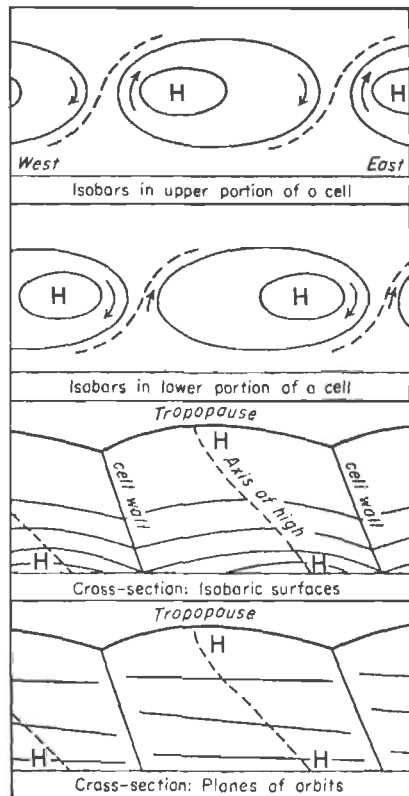


Fig. 12.2. Structure of subtropical high-pressure cell (21, after 3).

Rossby's proposals are meant only as a first step in a reorientation of the general-circulation theory. Even so, since his writings, the classical hypothesis in its entirety has no longer found any serious defenders. Rossby's viewpoint received enlarged observational backing when it became apparent that the meridional circulations fall far short of effecting the heat and momentum transports (16, 39, 40) needed to maintain the observed balance. With this, the collapse of the classical general-circulation model was complete.

Present Status of the General-circulation Theory

When it was recognized that the atmosphere must be regarded as turbulent, the complexity of the general-circulation problem increased. For a while at least all research seemed to lead away from the goal of a final solution, rather than toward it. No unified circulation theory now exists. It is not unlikely, however, that the eventual solution will have to retain some elements of the classical model. At present one speaks of the mean distribution of pressure, wind, and temperature as the climatological or statistical general circulation, considered merely as the sum of a succession of eddies. It must then be explained how these eddies operate to produce the climatic picture, the equatorial trough and the subtropical highs, the wet belts and the deserts.

Experiments carried out in the hydrodynamics laboratory of the University of Chicago have yielded some hints as to how the problem of steady meridional circulations vs. turbulent eddies might be resolved. The meteorologist investigating any problem is always handicapped by the fact that he has to deal with numerous variables and that he cannot experiment with them. In this respect the routes open for research in other branches of physics are quite superior. Quite naturally, many research workers have attempted to construct model analogues of the atmosphere. Fultz (11) has prepared a history and critique of such experiments. Although complete dynamic similarity with the atmosphere cannot be achieved, experiments can contribute far more toward an understanding of meteorology than many early investigators supposed.

Working with rotating dishpans heated at the rim and cooled in the center, Fultz (12) found that he could produce not just a general circulation but a *hierarchy* of general circulations. Discontinuities mark the transition from one type to another. Four regimes have been generated:

1. Steady meridional circulation with trades at the bottom of the pan and antitrades at the top.
2. Steady open long waves with westerly jet streams.
3. Irregular long-wave patterns with unsteady jet streams and formation and dissipation of cyclonic and anticyclonic vortices.
4. Bénard-type convection cells.

Two parameters produce transitions from one regime to another: *the rate of rotation of the dishpan and the rate of heating.* Of these the first appears to be more effective. At low rotation rates, when the relative motion of the water inside the pan is an appreciable fraction of the pan movement, model 1 is obtained. Here the vorticity is small; the case most closely resembling it on the curved earth is in tropical latitudes, where the Coriolis parameter is small or zero. Empirically, we have noted the steady trades but have not found the steady antitrades.

With increasing rotation rates, at first the steady, then the unsteady wave pattern is realized. In the third type of experiment the water movement relative to the pan is about 10 per cent of the speed of the equatorial rim of the pan; this corresponds to winds of 100 mph in the atmosphere, the closest approach to conditions in middle latitudes. At extreme rates of rotation the vortices of the third experiment contract to form patterns resembling Bénard convection cells.

We can draw the conclusion that in a certain sense the observed general circulation of the atmosphere is accidental. If the rotation of the earth were faster or slower, or if the distance from the sun were shorter or greater, our weather might bear little or no resemblance to that we know.

It is probable that a better understanding of the observed general circulation will result from extensions of the laboratory work.

The Heat Balance

Irrespective of the rise and fall of general-circulation theories, some workers have pursued the less spectacular and more laborious route of trying to compute what the general circulation must accomplish in order to preserve the essentially steady state from year to year. This road is also filled with disappointments and pitfalls. It enjoys, however, the advantage of all quantitative efforts, that a definite body of knowledge has accumulated.

Earliest among such efforts has been the calculation of the heat balance. In broadest terms, the system earth plus atmosphere absorbs more solar heat in the tropics than it emits to space by long-wave radiation. In the polar zones the opposite is true. Heat consequently must be transported from low to high latitudes for balance. In addition, the troposphere as a whole is a cold source at all latitudes so that a heat flow from the earth to the atmosphere must take place. Although radiation computations are relatively uncertain, the following heat balance, adapted from Baur and Phillips (1; cf. also 4), will roughly illustrate conditions: An average daily value of 700 cal/cm^2 reaches the outer boundary of the atmosphere from the sun. Of this amount 15 per cent is absorbed within the atmosphere, mainly by water vapor and carbon dioxide. If we omit the air above 100 mb for purposes of this calculation, this corresponds to

a temperature increase of $0.5^{\circ}\text{C}/\text{day}$. The net outgoing long-wave radiation is 34 per cent of 700 cal/cm^2 , or $1.1^{\circ}\text{C}/\text{day}$. Therefore the atmosphere as a whole cools at a mean daily rate of $0.6^{\circ}\text{C}/\text{day}$, well over $200^{\circ}\text{C}/\text{year}$. This enormous heat loss is balanced exclusively by transfer of latent heat from the ground to the atmosphere; this latent heat is made available to the atmosphere through condensation and rainfall. The radiation deficit would be covered by a mean annual rainfall of 70 cm, or 29 inches. According to some calculations, the net cooling is $0.7^{\circ}\text{C}/\text{day}$, which requires 100 cm, or 40 inches, of precipitation. Both values certainly have the order of magnitude of the estimated rainfall (Chap. 3); they are as close to reality as one can expect at the present time. It follows, and this has not been brought out clearly enough in the literature, that the condensation process is of the greatest consequence for the general circulation. Since the tropics play the leading role in the water-vapor cycle, we can expect them to have far more influence on the general circulation and its irregular variations than is usually accorded to them.

The Heat Balance as a Function of Latitude

The radiation differences to be equalized by the general circulation are not independent of it. Cloud cover and thickness affect both incoming and outgoing radiation, but the circulation determines the cloudiness. The complicated interplay will not be easily resolved. From a purely computational standpoint the heat budget can vary considerably, depending on what is assumed about the cloudiness and the radiation properties of the clouds. If the numerous additional uncertainties of radiation calculations are included, it is not surprising that different writers have derived different heat balances. Figures 12.3-12.5 are taken from Baur and Phillips (1), not because their numerical values are considered to be exact, but in order to present a set of numbers that is internally consistent. Other writers (3, 35) disagree considerably as to details, but their general results are the same.

The system earth-atmosphere on the average gains heat equatorward of about latitude 35° in the northern hemisphere and loses heat farther poleward (Fig. 12.3). Since heat gains and losses must balance, the areas enclosed by the curve and the zero line of Fig. 12.3 are equal.

The total heat accumulation of the tropics must be transported across latitude 35° , where the meridional heat flow attains its maximum (Fig. 12.4). Interestingly enough, this happens to be exactly the mean latitude of the subtropical ridge at the surface and of the strongest westerlies in the high troposphere.

The ocean currents accomplish some of the heat transfer, but their

contribution is estimated to be small (38). The flow of heat in the atmosphere is composed of both latent and sensible heat. We can separate these two components through calculation of a water budget. Given the precipitation P and the evaporation E in any latitude belt, the difference $E - P$ indicates whether moisture must be imported into or exported from this belt. We have discussed the problem of evaporation and rainfall estimates in Chaps. 3 and 5. Both quantities are known in the first approximation; the difference between them will therefore vary greatly depending on which rainfall and evaporation calculations are used.

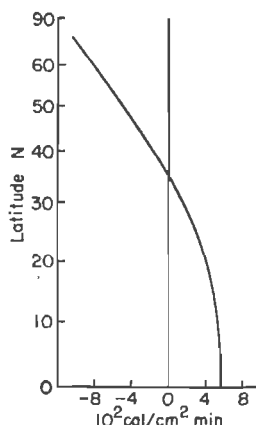


Fig. 12.3

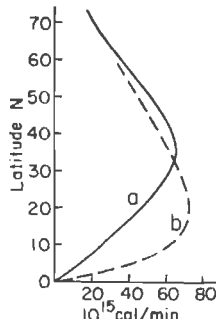


Fig. 12.4

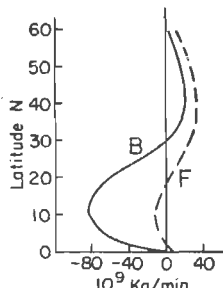


Fig. 12.5

Fig. 12.3. Mean heating or cooling of system earth-atmosphere in northern hemisphere (1).

Fig. 12.4. Net heat flux across latitude circles required for balance (1). *Solid line:* Total flux. *Dashed line:* Sensible heat.

Fig. 12.5. Water-vapor transport across latitude circles required for balance. [B: After Baur and Phillips, (1). F: After Flohn (10).]

Figure 12.5 contains the water-vapor transport as given by Baur and Phillips (1) and by Flohn (10). The two curves are similar in shape but differ greatly in amount. The difference arises because Baur and Phillips assume more rainfall in the equatorial belt than do the sources used by Flohn. This question of equatorial precipitation was raised in Chap. 3. For present purposes Fig. 12.5 shows the range of error of the available data and the limit beyond which conclusions should not be drawn. We cannot say whether either of these extremes or an intermediate curve is correct, but we can make use of the similarities.

Between latitudes 10 and 40° the vapor flux diverges; here evaporation exceeds precipitation. A part of the excess water vapor is transported equatorward in the trade-wind belt; it condenses in the equatorial zone,

where rainfall exceeds evaporation. The trade regions furnish a substantial part of the water vapor¹ which, through condensation, balances the radiation deficit. Partly because of the trade inversion, the water vapor is prevented from being precipitated locally in the trades; instead it is accumulated and carried in latent storage form to other parts of the world.

Since the total heat flow is poleward but the flow of water vapor in the trades equatorward, the sensible-heat transport must exceed the total-heat transport in the trades. This is indicated by curve (b) of Fig. 12.4, which is based on the water-vapor budget of Baur and Phillips. The latitude of maximum sensible-heat transport is lower than that for curve (a); north of 20°N the local precipitation is not sufficient to cover the radiation deficit. A part of the latent heat gained in the trades at the ocean surface is brought back to these regions in the form of sensible heat after condensation in disturbances of the equatorial-trough zone.

Heat and Moisture Transport Mechanisms

We know three principal ways by which sensible heat is transported across the latitude circles.

1. The mean meridional circulation (25; cf. Fig. 1.5) acts to move horizontally the isotherms found in average vertical cross sections (Figs. 1.14 and 1.15). This mechanism contributes at best 10 per cent to the heat balance even though it displaces colder air equatorward near the ground and warmer air poleward aloft. In low latitudes where the meridional circulation is strong, the temperature gradients are weak. In higher latitudes the opposite is true.

2. The horizontal eddies, highs, lows, troughs, ridges may possess an asymmetry between temperature and wind field such that the southerly winds are warmer than those from the north. This is an important mechanism in middle latitudes (cold outbreaks, warm fronts), but it is unlikely that it can account for the entire heat flow equatorward of latitude 35°, again mainly because of weak horizontal temperature gradients. With tropical wind data so scarce, computational work has been confined to the subtropical and middle latitudes (39). These computations suggest that at best 50 per cent of the heat flow in the subtropics can be accounted for by the eddies.

3. The mean meridional circulation (Fig. 1.5) must have ascending and descending branches (Fig. 12.8)² to provide mass continuity in the belts

¹ The belts 5–25°N and S furnish 50 per cent of the global evaporation; the belt 25°S–25°N, 60 per cent, and the belt 35°S–35°N, 80 per cent.

² It should be emphasized that this figure does not imply a *steady* circulation. On account of the unsteady wind field aloft we must assume that the southerly currents

of convergence and divergence (Fig. 3.4). In the past it has not been possible to compute the strength of these mean vertical currents with precision, since the wind data necessary to compute the meridional circulation have not been available at all altitudes. The next 10 years may bring a change, but at present we can merely make some reasonable assumptions. Agreement is general that the level at which the direction of the meridional circulation reverses is located not below 900 mb and probably not above 700–600 mb (20). Even assuming a weak circulation which reverses at 900 mb, vertical motions of 1 mm/sec, or 100 m/day, occur (Fig. 12.6). If the level of reversal is situated at 800 or 700 mb, vertical speeds well over 100 m/day will be found through fairly deep layers. This is especially true if the return current is not distributed uniformly through the upper troposphere but is concentrated in the shallow layer of active disturbances under the tropopause, as often suspected.

Consider now the temperature change $\partial T/\partial t$ at any level as influenced only by descent. Then $\partial T/\partial t = (\gamma - \gamma_d)w$, where γ and γ_d are the observed and dry-adiabatic lapse rates and w is the vertical velocity. If we wish to obtain a local temperature change of $0.6^{\circ}\text{C}/\text{day}$ and the observed lapse rates vary between 0.5 and 0.7°C per 100 m, the vertical motion needed to bring about the desired temperature change is 100–200 m/day. This proves that sinking of the magnitude produced by the meridional circulation in the trade-wind belt is likely to be a large factor in the heat balance. A part of the large heat flow shown for the tropics in Fig. 12.4 can be attributed to the fact that the poleward branch of the meridional circulation moves at much higher potential temperatures than the equatorward branch (Fig. 12.7).

The meridional circulation also plays a role in the water-vapor transport. Its flow is directed equatorward in the low levels, where the atmospheric moisture content is high (14–18 g/kg) and poleward at high levels,

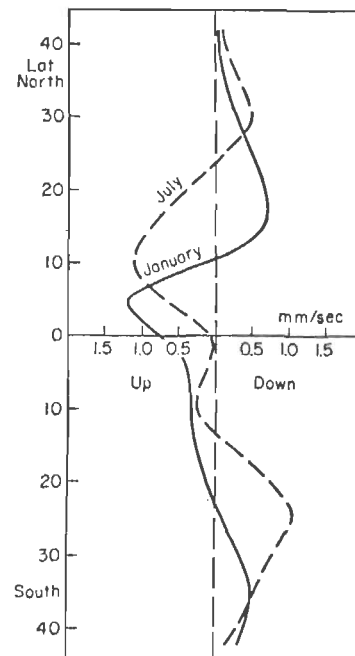


Fig. 12.6. Mean vertical motion at 900 mb (25).

east of high-level troughs carry a little more mass poleward than is transported toward the equator by the northerly winds west of the troughs.

where it is low (less than 5 g/kg, perhaps less than 1 g/kg) (Fig. 12.7). In addition the moisture transport diverges in the low levels, where the

meridional circulation diverges. It can be shown that the divergence of moisture produced by the meridional circulation has the order of magnitude of the observed divergence.

Thus the meridional circulation, which in the upper troposphere is the resultant of highly variable winds, makes an important contribution to the observed heat fluxes. It is perhaps of greatest interest that the circulation effects a sensible-heat transport poleward and a latent-heat transport equatorward in the trades. This is due to the inverse vertical gradients of potential temperature and specific

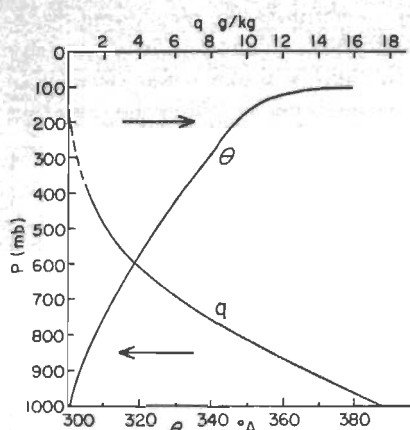


Fig. 12.7. Vertical distribution of potential temperature (θ) and specific humidity (q) of mean tropical atmosphere, and arrows indicating meridional circulation.

humidity with altitude, illustrated in Fig. 12.7. Beyond the subtropical ridge, where the meridional circulation is likely to be reversed, this scheme is not applicable.

Momentum Balance

The breakdown of the classical general-circulation theory was precipitated by the realization that the absolute angular momentum of individual particles or columns is not conserved. Nevertheless the fundamental law remains that the total angular momentum of the system earth-atmosphere must remain constant. Variations in the rate of rotation of the earth have been treated by Munk (17), but they are such that we can omit them and state that the absolute angular momentum Ω of the atmosphere alone remains constant in the mean, say, from one year to the next. By definition,

$$\Omega = \rho(u + \omega R \cos \varphi)R \cos \varphi, \quad (12.1)$$

where u is the zonal wind speed, positive toward east, R the radius of the earth, ρ the density, and ω the rate of rotation of the earth in angular measure. At the equator $\Omega = \rho(uR + \omega R^2)$, the well-known formula applicable on a rotating disk.

As air particles come in contact with the surface in the trades, their easterly speed is reduced. Conversely, we can say that the stress at the

ground acts to increase the angular momentum of the air in the trades. It follows that for balance the momentum acquired must return to the earth. This happens when eastward-moving particles come in contact with the ground.

We know that the atmosphere does not accomplish the momentum balance within limited regions or even latitude belts. Such balance would require alternating west and east winds at the surface in the trades, which are not observed. Instead we find broad belts of easterlies and westerlies, implying that in general momentum flows from earth to atmosphere in the trades and in the reverse direction in middle latitudes. Therefore angular momentum is transported from the tropics to the temperate zone; the largest flow takes place near the latitude of the subtropical ridge just as in case of the heat transfer.

It should be emphasized that, irrespective of the transfer mechanisms employed to move the momentum, it is not obvious why the transfer should occur at all, why we do not observe local momentum balance if the meridional circulation is discounted as a factor in the general circulation. The heat exchange between ocean and atmosphere in the tropics could be accomplished by alternating west and east winds just as readily as by steady easterlies.

The Observed Momentum Distribution. Before the discussion of transfer mechanisms, it will be of interest to determine the extent of deviation of the mean zonal wind distribution near the level of strongest winds (300–200 mb) from constant Ω . Figure 12.1 shows some observed wind profiles together with the theoretical one mentioned earlier. The observed profiles give wind distributions in winter at 80°W (14; cf. Fig. 1.14), 120°E (41), and 70°E (5) in the northern hemisphere, at 170°E (15; cf. Fig. 1.15) in the southern hemisphere, and an average for the northern hemisphere for December, 1945 (27). Curiously, constant Ω is attained in a limited latitude belt over eastern Asia and India, since the lines for this part of the world are parallel to the theoretical curve. Elsewhere the departures are large, especially at 80°W . At least geographically, the slope of the lines is tied to the steadiness of the upper-wind field. Over East Asia, the Himalayas control the flow around their equatorward margin, where the wind direction is nearly invariant from day to day (41). In other parts of the globe such marked orographic control is absent, and winds are variable, but more so in the northern than in the southern hemisphere.

It is very curious that in all published mean cross sections for winter along individual meridians (Chap. 1), and even for the northern hemisphere as a whole (22), the strongest west winds aloft are situated almost precisely above the surface subtropical ridge, where the large meridional circulation cell of winter ends. In summer, when this cell is weak, this

is not the case. The latitude of the subtropical wind maxima is such that they cannot be considered identical with the jet streams which are coupled with the principal cyclone trains of middle and high latitudes. This has led Palmén (19) to suggest that the subtropical jet has quite another mode of origin from the jet streams of higher latitudes. He sees the subtropical wind maxima as the result of a tendency of the meridional circulation to accumulate westerly momentum along its poleward margin (Fig. 12.8).¹ Because of the steadiness of the meridional circulation at low levels, the latitude of the subtropical jet fluctuates less than that of the polar westerlies. The higher-latitude jet streams, therefore, are lost as an entity in monthly charts, at least in the northern hemisphere, through the averaging process. The observed mean wind maximum is considered to be produced by the more stable subtropical jets. Palmén's

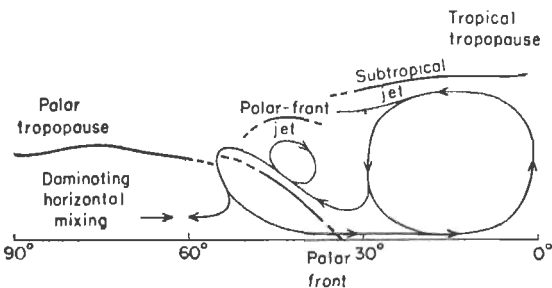


Fig. 12.8. Palmén's model of general-circulation cells (19).

viewpoint receives increasing support as high-level data from the tropics are accumulated.

Momentum-transfer Mechanisms. For a balanced momentum budget, the total momentum exchange between earth and atmosphere must be inverse and equal in amount in high and low latitudes, and the momentum picked up by the atmosphere in the tropics must be transferred across the subtropical ridge. We lack direct reliable knowledge about the momentum exchange between air and ground. Surface friction is very difficult to estimate with sufficient accuracy; especially hard to evaluate is the retardation of the air during flow over and around mountain barriers. Widger (40) has attempted to compute the transfer of momentum from ground to atmosphere in the trades; his results are probably good in the belt 20–30°N, but not farther south. He assumed that the winds at the top of the friction layer may be obtained through geostrophic computations from the surface isobars. As shown in Chap. 7, this assumption becomes increasingly poor south of 20°N. Various other

¹ Figures 10.9 and 10.10, although a summer case, illustrate the individual events that, in summation over space and time, produce the mean maxima.

estimates of the surface friction have been made (23), but all present data are uncertain.

The mechanisms available for transfer of momentum across the latitude circles are the same as those for heat. Although the meridional circulation operates in the right sense, it accounts for little more than 10 per cent of the net momentum flow across the subtropical ridge (16, 40). Horizontal eddies execute the bulk of the transfer. This inability of the meridional circulation to effect much net flow of momentum across the subtropics has little obvious connection with the question of whether the circulation is or is not responsible for transfer needs.

Palmén (19, 20) and others (25) have stressed that for purposes of momentum balances the term $\omega R^2 \cos^2 \varphi$ in (12.1) cannot be discounted. This contribution to Ω is made by the speed of revolution of the earth at any latitude. Since the earth rotates at about 1,000 mph in the tropics, this term far exceeds in magnitude that arising from the relative zonal wind u . Nevertheless it has often been dropped from momentum budgets because it does not contribute to the net flow across latitude circles. At any latitude $\omega R^2 \cos^2 \varphi$ is practically invariant throughout the depth of the atmosphere. Therefore the equatorward branch of the meridional cell in low levels carries as much of this so-called " ω momentum" equatorward as the poleward branch aloft carries poleward.

While this reasoning is correct, it is also somewhat formalistic. If we wish to consider the balance in a given layer of the atmosphere and the connection between all mechanisms in the momentum exchange, we must include the large flows of ω momentum. This has been done by Palmén and Alaka (20) for latitude belt 20–30°N in January. For their computation, shown in Fig. 12.9, they used the surface eddy stresses of Widger (40), the horizontal transport by eddies given by Mintz (16).

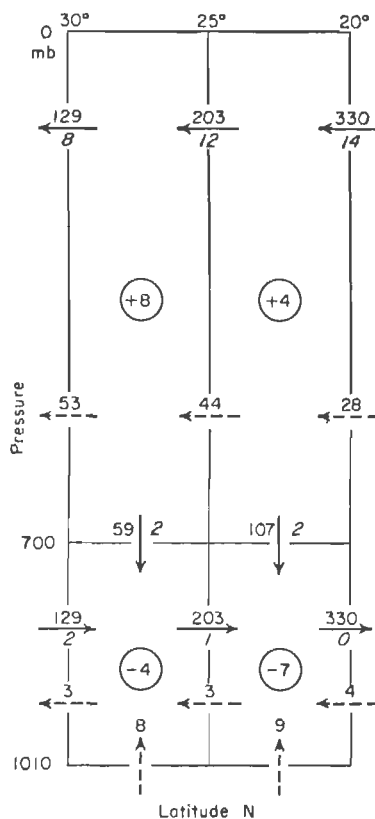


Fig. 12.9. Angular-momentum budget (20). Units: $10^{26} \text{ g cm}^2 \text{ sec}^{-2}$.

and the meridional circulation of Fig. 1.5 with level of reversal at 700 mb. In this figure the solid arrows give the momentum transport due to the circulation, the broken arrows that due to eddies. The large amounts next to the solid arrows represent the flow of ω momentum; the small amounts, the momentum transfer arising from the tendency of the meridional circulation to move north or south the whole isotach pattern seen in mean cross sections.

Between the surface and 700 mb the horizontal eddy transport plays only a minor role. There is a large horizontal divergence of ω momentum, amounting to 201 units (10^{26} g cm 2 sec $^{-2}$); this is compensated mainly by the inflow of ω momentum from above and pickup of momentum from the ocean. A small residual of 11 units (in circles) remains unaccounted for and is assumed to be transported from the upper troposphere by turbulence.

In the upper layer the convergence of ω momentum exactly equals the lower divergence as required. This momentum is partly removed downward across the level of circulation reversal, partly exported by horizontal eddy stresses to higher latitudes. The importance of the transport by eddies relative to that transported by the circulation increases with increasing latitude. At 20° it is only 10 per cent of the ω -momentum flow; at 30° it has risen to 40 per cent. Nearly 90 per cent of the net exchange across latitude 30° is accomplished by eddies.

For a balanced budget a residual accumulation, available for downward exchange by turbulence, must exist in the upper layer. Actually, 12 units are left, whereas 11 are needed, as close as one can wish to come. Physically, Fig. 12.9 implies that the two transfer mechanisms operate conjointly and that it would be unrealistic to consider one of them without the other.

Further accumulation of observations concerning meridional circulation and eddy transports (cf. 37) should, with time, permit extension of the computations to the equator. For such extensions a reliable method will have to be developed for estimating the surface stress equatorward of latitude 20°.

STRUCTURE OF THE TRADES

A complete set of balance computations for a limited area may illustrate the detailed computations of the general circulation that we may ultimately have on a world-wide basis. The area will be the trade region of the northeastern Pacific Ocean,¹ described in Chap. 2; all data used are given in Figs. 2.29 to 2.40.

¹ Really a volume; its length, from 32°N, 136°W to Honolulu (Fig. 2.29) is 2,550 km, its width is taken as 1 cm, and its depth is 3 km.

Moisture and Heat Balance in the Northeast Pacific (28)

Moisture. The calculation covers the 4-month period from July to October, 1945. Conditions in the area remained almost the same at the end compared with the beginning of the period; therefore only the following factors enter into the moisture balance: (a) horizontal and vertical import and export by the mean motion; (b) vertical transport by turbulent eddies, especially cumulus clouds; (c) sources and sinks, i.e., evaporation and precipitation.

The inflow upstream (Fig. 12.10) is 5.4 units (10^{10} cal/day); the outflow downstream, 8.2 units; the inflow through the top, 0.2 unit; and the net export by the mean motion, therefore, 2.6 units. The total evaporation is 4.9 units; so more than 50 per cent of the evaporated water is

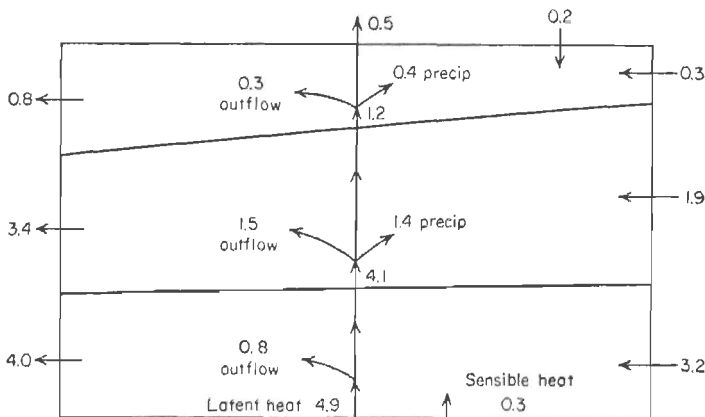


Fig. 12.10. Moisture budget for northeast trade of Pacific (units: 10^{10} cal/day) (28).

exported. The trades act to acquire moisture from the ocean which is exported in latent form to other parts of the world.

Of the evaporation 2.3 units remain in the volume and are available for rainfall and transport to the layers above 3 km. The rainfall is estimated at 1.8 units (see below); the upward transport through the 3-km level is therefore 0.5 unit. All upward flow of the moisture picked up from the ocean surface (center line of Fig. 12.10) is accomplished by turbulence, since the mean motion is downward (Fig. 2.33). In the subcloud layer the transport mechanism is diffusion; in the cloud layer, convection. As we saw at the end of Chap. 5, the cumuli are a very efficient means to transport the 4.1 units of moisture, which, according to Fig. 12.10, must be moved upward from the subcloud layer.

Sensible Heat. Because of large values of horizontal inflow and outflow, a complete sensible-heat balance cannot be computed. Changes in wind speed of only 0.2–0.3 mps—certainly within the range of error of

the measurements—produce changes in the horizontal flow equivalent to the total moisture flow, the evaporation, and the radiation. However, if we assume with Ficker (8) that the trade acts mainly as an accumulator of latent heat, the transport terms will cancel, or nearly so. The equation of continuity for sensible heat then becomes $R + LP + Q_s = 0$, where R is the radiation, LP the heat released through condensation and precipitation P , and Q_s the sensible heat picked up from the ocean surface. $Q_s = 0.3$ unit, and $R = 2.1$ units; the distribution of net cooling is shown in Fig. 12.11. It follows that $LP = 1.8$ units, corresponding to an average rain-gauge measurement of 0.13 cm/day, or 3.9 cm/month. This

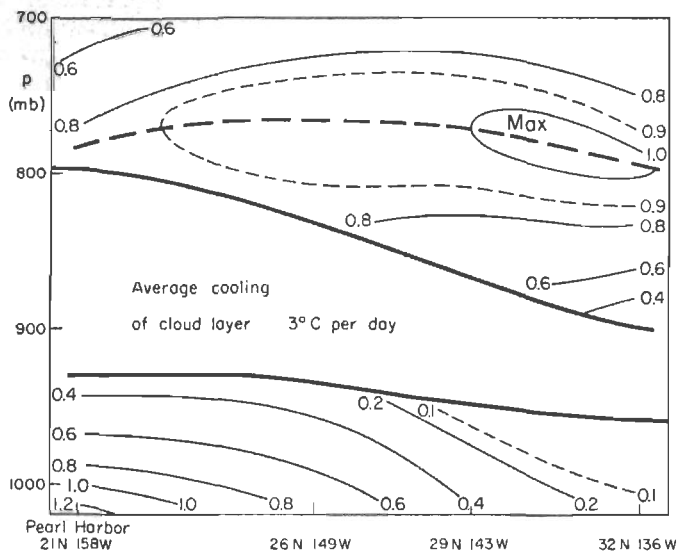


Fig. 12.11. Vertical cross section of net temperature loss ($^{\circ}\text{C}/\text{day}$) in northeastern Pacific produced by radiation (28).

value cannot be checked directly since rainfall was not measured by the weather ships. It corresponds closely, however, to the average for the area in summer; further it is somewhat less than the evaporated water available for precipitation (2.3 units) and may therefore be accepted as correct within the limitations of the data and the calculations.

It is of interest that Q_s is only 0.3 unit, 14 per cent of the radiation, or 6 per cent of the evaporation. The sensible heat absorbed by the atmosphere from the ocean plays a negligible part in the heat balance, which is adjusted almost completely through the water-vapor cycle. A small role in the balance sheet, however, does not imply a small role in the mechanism which produces the balance. For as we have seen in Chap. 5, turbulence and therefore evaporation from the sea surface are determined in large measure by the sea-air temperature difference.

Whenever the sea is colder than the air, the turbulence stops. Only when the sea is warmer do we observe eddying motion which allows many new air particles, capable of absorbing much moisture, to approach the ocean surface. This eddying is sustained by the buoyancy that the air particles acquire. The main role of Q_s is therefore to facilitate evaporation.

Momentum Balance in the Northeast Pacific

Since the area with which we are concerned is not a closed ring like the latitude belts treated earlier, the problem is somewhat different. Momentum is generated by pressure gradients along the streamlines. When, however, a closed ring is considered, we return to the same pressure after making the entire circuit and so no net momentum is produced along the ring by the pressure forces. In contrast, the pressure differs at the two ends of the east Pacific section. It is lower at Honolulu than at 32°N , 136°W ; momentum is created by this pressure difference, and it must either be carried away or be dissipated by friction.

Because integration around whole latitude circles may obscure, by means of canceling terms, some of the most important physical aspects, the limited area approach is in a sense more realistic. This seems to be true with respect to the momentum balance, since the pressure term is a full order of magnitude larger than all transport terms in the northeastern Pacific. Considering the momentum ρV , where V is oriented along the mean trajectory taken positive toward east-northeast, the total inflow at the northeastern end of the section is -1.5 units ($10^8 \text{ g cm sec}^{-2}$); the outflow in the southwest, -1.3 units; and the inflow through the top, -0.1 unit. Together the transport terms—mean plus eddying motion—produce a momentum loss toward east-northeast of 0.3 unit.

In contrast the pressure force generates momentum amounting to -6.5 units. The advective terms thus are of no importance, and essentially we have a balance involving only pressure and frictional forces. The pressure gradient along the trajectory accelerates the air toward west-southwest, and this acceleration is counteracted by friction. It is of interest that the pressure-gradient acceleration becomes zero near 700 mb at the top of the section; here the air flows along the isobars. In Chap. 2 we had noted that the divergence, prevalent in the northeast trade, also disappears near the top of the section. Therefore, the flow appears to be quasi-geostrophic at the level of nondivergence.

The retardation of wind speed at the ocean surface—the frictional gain of momentum toward east-northeast—amounts to 4.4 units, only two-thirds of the 6.8 units lost by pressure force and transport terms. Ground friction provides a balance only up to the 910-mb level, where the easter-

lies are strongest (Fig. 2.31). The need for retardation above 910 mb implies that we must import additional momentum of 2.2 units, or 55 per cent of the ground friction, by eddy turbulence from above. This is an appreciable transfer, and it is directed from high to low momentum. Where the easterlies increase with height, the transfer is upward, and where they decrease with height, it is downward. The motion may be geostrophic near the level of nondivergence, but above it eddy friction must retard the westerlies to provide for the momentum transport through the level of nondivergence. It follows that the currents of the tropical atmosphere cannot be considered laminar, as Sheppard (34) also demonstrated for the lower troposphere.

Formation and Dissolution of the Trade Inversion

Formation. The isolines of the base of the Atlantic trade inversions, which Ficker drew from the *Meteor* ascents (Fig. 2.23), have no poleward termini. The fog and inversion regimes of the American west coasts also penetrate far into the temperate zone. Thus the "roots" of the trade inversion are bound up with middle-latitude circulations; the connecting mechanism, however, has not been established. Similarly, various suggestions involving land-sea temperature differences have not been solidified into definite models. The causes of the trade-wind inversion are obscure.

Figure 12.12 shows mean surface streamlines and isotachs for the eastern Pacific in July, taken from Fig. 1.7. Superimposed are the 300-mb contours for July, 1945; these appear to be representative of longer-term means. Two troughs are evident, at 150–160°W and at 130°W. Except near the Hawaiian Islands they are situated above the regions of principal surface divergence and outflow from the anticyclonic singular point.

Although Fig. 12.12 is a mean chart, the vertical structure is typical of what one finds in daily situations and indicates the principle of the vertical coupling. The lower air acquires anticyclonic vorticity, diverges, and sinks. To compensate, the upper air acquires cyclonic vorticity and converges, and it also sinks because of the mass-continuity requirement. The convergence steepens the lapse rate in the high troposphere; the divergence stabilizes it in the low levels except for the turbulent layer near the ground. In this way the very steep lapse rates aloft and the inversion layer below are created. The altitude of the boundary is determined by the relative strength of the descending current vs. the low-level turbulent action produced by wind and by heat exchange between ocean and air (Chap. 2). It should be noted that the inversion is lowest where the sea surface temperature shows the largest negative anomalies and where the surface air is moving toward lower ocean temperatures.

Dissolution. The observations in the northeast Pacific have shown that the trade inversion rises 1 km from inflow to outflow terminus of the region despite continuous divergence and sinking of the air columns. In consequence, previous hypotheses about the breakdown of the inversion must be revised. According to these hypotheses no mixing takes place between the masses below and above the inversion until the inversion is destroyed. Figures 2.26 and 2.37 show that the potential temperature rises downstream along the inversion top, while the classical concept requires a potential-temperature decrease at a rate prescribed by the net radiation cooling.

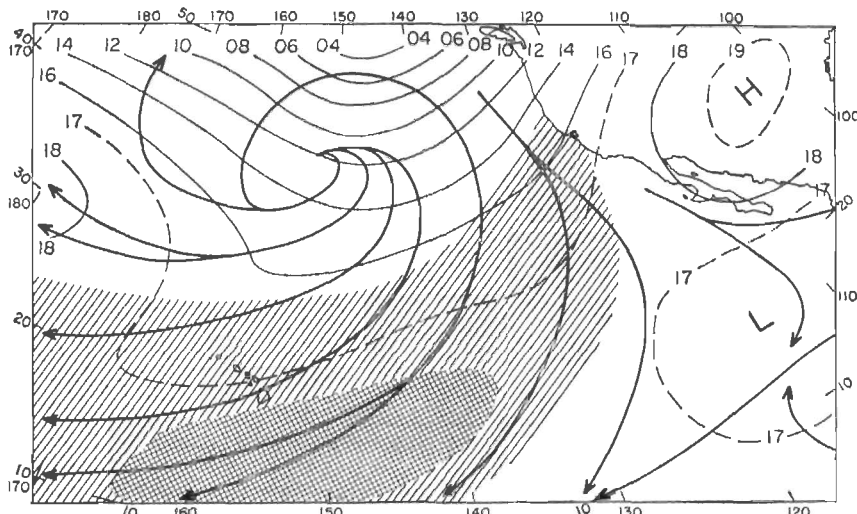


Fig. 12.12. Mean surface streamlines and isotachs (speeds above 8 knots shaded) for July, and 300-mb contours (100's feet, first digit omitted) for July, 1945.

Actually, mass transfer takes place across the inversion (Figs. 2.34 and 2.35). The outflow of mass between sea level and the base of the inversion at Honolulu is double the inflow at 32°N, 136°W. As the air travels the distance in 6 days, an average of 22 g of each air column of unit cross section is incorporated into the cloud layer each day.

It has been suggested¹ that the rise of the inversion is accomplished through the pickup of latent heat by the trade in the course of its passage over the tropical ocean. The inversion is "lifted" by the process indicated in Fig. 12.13. It is well known that the bases of the cumuli have a nearly uniform height (Chap. 5) but that the tops are irregular. Some are found within the cloud layer, some near the inversion base, and some

¹ J. Wyman and A. H. Woodcock, Woods Hole Oceanographic Institution. Mimeo-graphed. 1946

within the inversion¹ as active clouds penetrate the base. Visual observation and many photographs show that the tops of these clouds break off and evaporate quickly. In this way moisture is introduced into the lower portions of the inversion layer, where the air gradually takes on the characteristics of the cloud layer. Throughout each day a very large number of cumuli push a lesser or greater distance into the inversion in

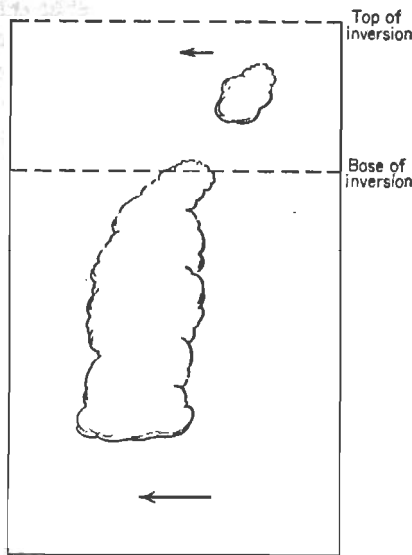


Fig. 12.13. The mechanism for raising the trade inversion (28).

this manner. Bit by bit, the whole inversion is raised. Temporary convergence in occasional synoptic disturbances may also play a part.

Further Comments on the Structure of Low and High Troposphere

The broad-scale sinking of the trade had no part in studies of the structure of the trade-wind belt until the observations revealed its existence. It could have been anticipated on theoretical grounds, however. At low levels air moves for long distances toward lower latitudes without much change of relative vorticity. Since the latter, in addition, is small, we may drop it from the theorem of conservation of potential vorticity [Eq. (8.12)]; then

$$\Delta p = \frac{f}{f_0} \Delta p_0, \quad (12.2)$$

where the subscript denotes initial values. The vertical depth of a

¹ V. J. Schaefer, *Final Report Project Cirrus*. Schenectady, N.Y.: General Electric Co. Research Laboratory, 1953.

column moving from latitude 30 to 20° should accordingly decrease by 20 per cent. In the northeastern Pacific, the calculated sinking is somewhat less, but as pointed out in Chap. 2, the divergence is likely to be underestimated, and therefore also the sinking motion.

We can extend the preceding consideration to the trade-wind belts as a whole (26). For steady state, Eq. (8.10) may be written $\partial/\partial x(u\xi_a) + \partial/\partial y(v\xi_a) = 0$. Upon integration around a latitude circle the first term vanishes. Integration with latitude yields $v\xi_a = \text{constant}$. Since the relative vorticity contributes very little,

$$f\bar{v} = \text{const}, \quad (12.3)$$

where \bar{v} now is the mean meridional circulation. Evaluation of this formula for the northern-hemisphere winter gives a satisfactory result when

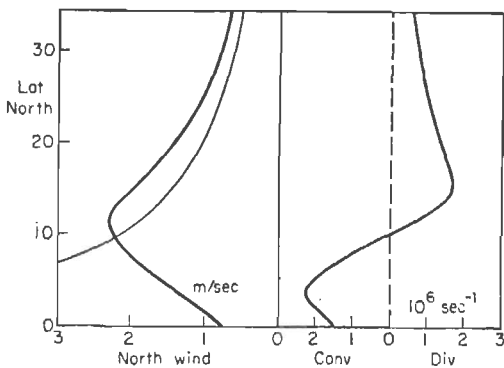


Fig. 12.14. Left: Meridional circulation for the northern-hemisphere winter (25) (heavy) and circulation computed from Eq. (12.3) (thin) (26). Right: Profile of observed divergence.

compared with the observed meridional circulation in the trade belt (Fig. 12.14). It follows that (12.13) approximates the dynamic mechanism operating in the low levels of the trades. South of the latitude, where the meridional circulation changes from divergent to convergent flow, the relation breaks down. Since the flow is still directed equatorward, the steady-state assumption can no longer hold. This is borne out by Figs. 1.4 and 1.11, which reveal an unsteady eddying motion near the surface in the equatorial-trough zone.

The Woods Hole observations described in Chap. 5 point to an explanation of the steady wind field in the moist layer of the trades (24). Rossby has emphasized that the development of large lateral turbulence eddies depends on the thermal stratification of the atmosphere. The field of motion always tends to adjust the pressure field. Pressure gra-

dients that permit at least a partially coasting motion must develop if the motion, once generated, is not to die away quickly. Hydrostatic considerations make this possible only in the presence of horizontal temperature gradients that can be intensified or decreased. In the moist layer of the trades vertical circulations predominate and preclude the formation of horizontal temperature gradients in excess of the sea surface-temperature gradient. The lateral eddies therefore recede in importance. Because of the absence of thermal stability over millions of square miles, the smallness of oceanic temperature gradients, and the effectiveness of vertical turbulence, horizontal disturbances will be held to a minimum. Flow in the low levels should be quasi-uniform, especially under the trade-wind inversions; they shield the low troposphere from disturbing influences from the high levels.¹

In the lateral eddies, the synoptic disturbances, the field of vertical motion is controlled by the horizontal. In the convective eddies the vertical thermal stratification gives rise to the motion. Since the tropical atmosphere is unstable with respect to moist-adiabatic ascent, apart from trade-wind inversions, the classical descriptions pictured a random distribution of cumulonimbi all over the tropics, surrounded by clear areas of descending air. If this were observed generally, uniform motion might prevail at high levels as it does near the ground. It would then be difficult to obtain a poleward eddy transport of absolute angular momentum! Actually the trade cumuli have their tops between 6,000 and 10,000 feet, in the mean. Above this level clouds occur rather strictly in organized convection zones. It is remarkable that the steadiness of the trades begins to decrease upward rapidly just above the tops of the trade cumuli (Fig. 2.30).

The entrainment responsible for limiting the vertical growth of cumuli (see Chap. 5) thus may have far-reaching consequences for the general circulation. The average height of the cumulus tops outside the areas with strong inversion must be indicative of the rate of conversion of heat and kinetic energy into potential energy by entrainment. Because of this conversion heat transfer upward in vertical convection cells does not carry to the upper troposphere. This compels the development of an entirely different class of disturbances, large-scale horizontal eddies in the form of wave or vortex trains, or high-level shear lines; these funnel heat aloft through organized convection. The vertical stability necessary to permit lateral concentration of isotherms aloft to support the wind field is produced by the small-scale lateral turbulence in the low levels that finds its expression in the form of entrainment.

¹The importance of these considerations decreases toward the equator; in the regime of small Coriolis forces very weak pressure gradients can produce synoptic changes of the wind field.

REFERENCES

- (1) Baur, F., and H. Phillips, *Gerlands Beitr. Geophys.*, **45**: 82 (1935).
- (2) Bergeron, T., *Geog. Publ.*, Vol. 5, No. 6, 1928.
- (3) Bjerknes, V., et al., *Physikalische Hydrodynamik*. Berlin: Verlag Julius Springer, 1933.
- (4) Byers, H. R., *General Meteorology*. New York: McGraw-Hill Book Company, Inc., 1944.
- (5) Chaudhury, A. M., *Tellus*, **2**: 56 (1950).
- (6) Defant, A., *Geogr. Ann.*, **3**: 209 (1921).
- (7) Exner, F. M., *Dynamische Meteorologie*. Vienna: Verlag Julius Springer, 1925.
- (8) Ficker, H., *Veröffentl. Preuss. Akad. Wiss. Phys. Math. Kl. Berlin*, No. 11, 1936.
- (9) Flohn, H., *Erdkunde*, **4**: 141 (1950).
- (10) Flohn, H., *Ber. deut. Wetterdienstes*, U.S. Zone, No. 18, Bad Kissingen, 1950.
- (11) Fultz, D., in *Compendium of Meteorology*, p. 1235. Boston, Mass.: 1951.
- (12) Fultz, D., Department of Meteorology, University of Chicago, multigraphed (1952, 1953).
- (13) Hadley, G., *Phil. Trans.*, **39**: 58 (1735).
- (14) Hess, S. L., *J. Meteor.*, **5**: 293 (1948).
- (15) Hutchings, J. W., *J. W.*, **7**: 94 (1950).
- (16) Mintz, Y., *Tellus*, **3**: 195 (1951).
- (17) Munk, W. H., and R. L. Miller, *Tellus*, **2**: 93 (1950).
- (18) Namias, J., *Monthly Weather Rev.*, **67**: 294 (1939).
- (19) Palmén, E., *Quart. J. Roy. Meteor. Soc.*, **77**: 337 (1951).
- (20) Palmén, E., and M. A. Alaka, *Tellus*, **4**: 324 (1952).
- (21) Petterssen, S., *Weather Analysis and Forecasting*. New York: McGraw-Hill Book Company, Inc., 1940.
- (22) Petterssen, S., *Quart. J. Roy. Meteor. Soc., Cent. Proc.*, p. 120, 1950.
- (23) Priestley, C. H. B., *Quart. J. Roy. Meteor. Soc.*, **77**: 200 (1951).
- (24) Riehl, H., *Tellus*, **2**: 1 (1950).
- (25) Riehl, H., and T. C. Yeh, *Quart. J. Roy. Meteor. Soc.*, **76**: 182 (1950).
- (26) Riehl, H., and T. C. Yeh, *ibid.*, **76**: 340 (1950).
- (27) Riehl, H., T. C. Yeh, and N. E. La Seur, *J. Meteor.*, **7**: 181 (1950).
- (28) Riehl, H., et al., *Quart. J. Roy. Meteor. Soc.*, **77**: 598 (1951).
- (29) Rossby, C.-G., *Papers Phys. Oceanog. Meteor. Mass. Inst. Technol. and Woods Hole Oceanog. Inst.*, Vol. 5, No. 1, 1938.
- (30) Rossby, C.-G., *ibid.*, Vol. 7, No. 1, 1938.
- (31) Rossby, C.-G., in *Climate and Man*. Washington, D.C.: U.S. Department of Agriculture, 1941.
- (32) Rossby, C.-G., *Bull. Am. Meteor. Soc.*, **28**: 53 (1947).
- (33) Rossby, C.-G., in *The Atmospheres of the Earth and Planets*, G. P. Kuiper, ed. Chicago: University of Chicago Press, 1949.
- (34) Sheppard, P. A., and M. H. Omar, *Quart. J. Roy. Meteor. Soc.*, **78**: 583 (1952).
- (35) Simpson, G. C., *Mem. Roy. Meteor. Soc.*, Vol. 3, No. 23, 1929.
- (36) Staff Members, Department of Meteorology, University of Chicago, *Bull. Am. Meteor. Soc.*, **28**: 255 (1947).
- (37) Starr, V. P., and R. M. White, *Tellus*, **4**: 118 (1952).
- (38) Sverdrup, H. U., *Oceanography for Meteorologists*. New York: Prentice-Hall, Inc., 1942.
- (39) White, R. M., *Tellus*, **3**: 82 (1951).
- (40) Widger, W. K., *J. Meteor.*, **5**: 291 (1949).
- (41) Yeh, T. C., *Tellus*, **2**: 173 (1950).

NAME INDEX

A

- Alaka, M. A., 371
 Alpert, I., 239
 Austin, J., 143-146

B

- Baum, W., 126
 Baur, F., 363-366
 Bellamy, J. C., 185, 186
 Bemmelen, W. v., 108
 Bénard, H., 126
 Biel, E. R., 90, 93
 Bigelow, F. H., 243
 Birstein, S. J., 175
 Bjerknes, J., 136, 137, 150, 216, 217, 329,
 344
 Bjerknes, V., 8, 189, 334, 359, 360
 Bossolasco, M., 31, 243
 Bowen, E. G., 160, 278
 Bowie, E. H., 347
 Boylan, R. K., 156
 Braby, H. W., 237, 327
 Braham, R. R., 138, 143, 146
 Brooks, C. E. P., 26, 237, 327
 Brunt, D., 127
 Bunker, A. F., 150
 Byers, H. R., 139, 143, 146, 286, 314, 351

C

- Cline, I. M., 295
 Colón, J., 25, 45, 324, 325, 352, 353
 Cramer, H. E., 144, 145, 146
 Cressman, G. C., 136, 137, 207, 225-227,
 274, 342

D

- Dean, G., 15, 26
 Defant, A., 359
 Deppermann, C. E., 243, 273, 286, 288
 Dunn, G. E., 179, 211, 297, 323
 Durst, C. S., 127, 305

E

- Exner, F. M., 359

F

- Ficker, H. v., 56, 59, 374, 376
 Fleisher, A., 143
 Fletcher, R. D., 239
 Flohn, H., 365
 Freeman, J. C., 8, 228
 Fujiwhara, S., 345
 Fultz, D., 207, 362

G

- Gentry, R. C., 351
 Georgii, W., 243
 Gutenberg, B., 299

H

- Hadley, G., 8, 359
 Harbeck, A. E., 123
 Haurwitz, B., 118, 221, 300, 318, 345
 Hess, S. L., 207
 Holmboe, J., 329, 344
 Houghton, H. G., 144-146
 Hovmoeller, E., 27
 Hubert, L. F., 254, 256
 Hughes, L., 288-290
 Hull, E. C., 139

I

- Inn, E. C. Y., 175

J

- Jacobs, W. C., 74, 76
 Jordan, C. L., 192, 317, 318
 Jordan, E. S., 301, 331, 344
 Junge, C., 156

K

Klein, W. H., 354

L

Landsberg, H., 89, 90

Langmuir, I., 160, 161

Langwell, P. A., 125

Leopold, L. B., 105, 106, 112

López, M., 218, 219

Ludlam, F. H., 161, 171

M

Mal, S., 127

Malkus, J. S., 125, 139, 144, 145, 147, 148

Marciano, J. J., 123

Mason, B. J., 162

Meinardus, W., 73, 74

Mintz, Y., 15, 26, 344, 371

Mitchell, C. L., 324, 347, 348, 352

Moore, R. L., 344

Mordy, W., 85

Munk, W. H., 368

N

Namias, J., 85

Neiburger, M., 63

O

Olascoaga, M. J., 96

P

Palmén, E., 274, 320, 331, 370, 371

Palmer, C. E., 8, 25, 52, 96, 189, 217, 229-
240, 250, 269, 278, 311, 323, 329

Petterssen, S., 137, 223, 353

Phillips, H., 363-366

Piazzi-Smyth, C., 53, 54

Piersig, W., 228

R

Rahmatullah, M., 265

Rayleigh, J. W. S., 126

Regula, H., 217, 226

Reynolds, S. E., 175

Rossby, C.-G., 205, 206, 219, 250, 342,
361, 362, 379

S

Sandstroem, J. W., 189

Sawyer, J. S., 256, 329, 330, 332

Schacht, E., 44, 304

Schaefer, V. J., 172, 378

Schnapauff, W., 59, 242

Schove, D. J., 193

Seilkopf, H., 243

Shaw, N., 312

Sheppard, P. A., 376

Simpson, G. C., 156

Simpson, R. H., 239, 242, 273, 274, 285,
308, 311, 313, 317, 344

Solberg, H., 329

Solot, S. B., 95, 256

Stidd, C. K., 112

Stommel, H., 139, 140, 143-145

Stone, R. G., 26, 64, 110, 243

Supan, A., 72, 73

Sutcliffe, R. C., 305

Sutton, O. G., 123

Sverdrup, H. U., 56, 123

Swinbank, W. C., 122

T

Tannehill, I. R., 287, 324, 340, 350-352

Thornthwaite, C. W., 88

V

Vonnegut, B., 175

W

Walker, G. C. T., 126, 268

Wasco, P. E., 353

Wexler, H., 24, 312

Wexler, R., 107

Widger, W. K., 370, 371

Williams, N. R., 126

Winston, J. S., 354

Wood, F. B., 312

Woodecock, A. H., 121, 123, 127, 128, 156,
160, 172, 377

Wright, H. L., 156

Wuest, B., 73

Wyman, J., 121, 123, 128, 377

Y

Yeh, T. C., 275, 342, 343, 348

Yin, T., 259, 262

SUBJECT INDEX

A

- Air masses, 30–32
of continents, 50–51
in equatorial trough, 236–238
of oceans, 51–53
in tropical storms, 327
Airplane observations, 183, 289, 316
Aitken counter, 156
Altimeter corrections, 185
Andes, 41
Anticyclones, subtropical, blocking, 253
cellular structure, 23
general circulation role in, 360
hurricane motion role in, 347–351
positions, mean aloft, 18
mean surface, 2
slope with height, 15–18
subsidence in, 55, 376
transformation of, 273
Antitrade, 23
Asymptotes, 191
Atmosphere, mean tropical, 44–45

B

- Bar of tropical storms, 289
Barbados, 13, 41
Barograph traces in tropical storms, 285
Basic currents, 30–32
Belem, 41, 82
Belet Uen, 42
Belgian Congo, 243
Bénard cells, 126, 362
Bikati Island, 234
Blocking, 253
Bulawayo, 41, 81
Buoyancy forces, 126, 134
Burma monsoon, 257, 262

C

- Canary Islands, 53
Cape Guardafui, 43

- Cells, subtropical, 23
(*See also* Convection cells)
Ceylon, 86
Circulation, meridional (*see* Meridional circulation)
Circulation theorem, 334
Clouds, 131–134
cumulus (*see* Cumulus clouds)
drift, upper, 14–15
drop size, 158
in equatorial shear lines, 247
formation of, 155–159
ice in, 163–166
liquid water content, 159
orographic, 105–107, 109–111
seeding in, 172–175
in subtropical cyclones, 274
supercooled water in, 163–165
synoptic analysis, 180
temperature affected by, 140–142, 248
temperatures in, 138
in tropical storms, 308–313
in waves in easterlies, 217–218
Col, 191
Condensation, 155
Condensation level, 120, 134
Continental polar air, 50
in tropical storms, 327–328
Continental tropical air, 50, 78
Continuity equation, 202
and pressure changes, 203
and vorticity theorem, 205
Convection, 119
heat transfer role in, 150–153
hypothesis of hurricane formation, 326
onset criteria, 126, 134
parcel method, 135
resistive forces against, 135, 144
slice method, 136
Convection cells, 126
laboratory, 126
orographic, 110–111
soaring, deduced from, 127
in subcloud layer, 128–131

Convection cells, in waves in easterlies, 217
 Convection points, 110, 120
 Cooling system of tropical storms, 321–322
 in formative stage, 338
 Coriolis parameter, and balance of forces, 192–194
 near equator, 209
 sea breeze as factor in, 103
 in tropical storms, 288, 330, 334
 in vorticity theorem, 205–208
 Cosmic weather influences, 278
 Cross sections, vertical, mean, at 80°W,
 18
 at 170°E, 18
 of tropical storms, 319
 Cumulus clouds, 119
 dynamics, 149–150
 entrainment, 139–150
 first formation, 134
 heat transfer by, 150–154
 life cycle, 119, 137
 parcel method, 134
 precipitation from, 163, 167
 slice method, 136
 temperatures in, 138
 and trade inversion, 54, 378
 types in tropics, 131–134
 vertical slope, 146–150
 Currents, basic, 30–32
 ocean, 39, 364
 steering, 343–345
 Cyclones, subtropical, 273–274
 (*See also* Tropical storms)
 Cyclostrophic wind, 194

D

Dakar, 80
 Detection of tropical storms, 325
 Dew-point temperature, 178, 330
 Dishpan experiments, 362–363
 equatorial westerlies in, 8
 Disturbances, secondary, 210–211, 379–380
 as cause of mean rainfall, 83, 97
 in general circulation, 359
 heat transport role in, 366–368
 over India, 1, 266
 momentum transport role in, 370–372
 Divergence and convergence, and average
 rainfall, 79
 fields of, 198
 latitudinal profiles, 78
 and pressure changes, 202–203

Divergence and convergence, relative to
 equatorial trough, 78
 and sea breeze, 103
 in thunderstorms, 139
 of trade current, 65, 379
 in tropical storms, 289, 292–293, 305–306
 Djakarta, 21, 85
 Doldrums, 1
 Drainage of air, 100
 Dropsondes, 317
 Drought, 89
 Dry ice, 172–173
 Dynamic instability, 329–330, 332

E

Easter Island, 41
 Electronic computer, 207–208
 Energy, for convection, 134, 138
 of general circulation, 358
 of jet streams, 251
 of shear lines, equatorial, 248
 of tropical storms, 320–322
 Entebbe, 42, 81
 Entrainment, 139–150
 calculation of, 141–142
 dynamic, 143
 in equatorial shear lines, 248
 evidence of, 139
 general circulation role in, 380
 of momentum, 146
 rates of, 146
 in tropical storms, 336
 Equator, meteorological, 1, 4, 39
 Equatorial convergence zone, 238
 Equatorial dry zone, 76
 Equatorial front, 236–238
 cyclogenesis in, 327–328
 Equatorial shear lines, 10, 242–249
 dynamic aspects, 249
 over India, 262–268
 solenoid field of, 247–249
 thermal structure of, 247
 Equatorial trough, 1
 divergence in, 78
 heat conversion role in, 366
 positions, mean, 1–2
 rainfall, 78
 and sea-surface temperature, 331
 seasonal changes, 12–14
 temperatures in, 59–61, 239
 and tropical-storm formation, 331
 Equatorial-trough disturbances, 235–243
 eddies, 240
 frontal approach, 236–238
 multiple structure, 239
 waves, 239

Equatorial westerlies, 31, 238, 240
over India, 262–268
in upper troposphere, 243–245

Evaporation, 88, 121
and global moisture balance, 365
and hydrologic cycle, 73
latitudinal distribution, 366
measurement of, 73, 122
from sea surface, 73, 121–123, 287
in tropical storms, 287
and wind speed, 123

Extended forecasting, 277–278

Extended troughs, 225–227

Eye of tropical storms, 309–310
clouds in, 313
lapse rate in, 317
pressure in, 297
subsidence in, 316–318
surface characteristics, 297–298
thermal structure, 316–320
upper-air temperature in, 316–320
vertical slope, 312–313

F

Fiji Islands, 84

Florida, 1, 83
summer rains, 116

Flow across equator, 6, 8
aloft, 254–256
and CAV trajectories, 207

Fog, 43, 100

Forecasting, 177
extended, 277–278
numerical, 206–208
seasonal, for India, 268–269
of tropical storms, 351–356
of waves in easterlies, 224–228

Freetown, 80

Friction, and general circulation, 359
momentum balance role in, 370
in trades, 375
in tropical storms, 288, 322, 341
wind balance as factor in, 194

Friction layer, 194

Frontal hypothesis of tropical-storm formation, 327–329

Fronts, cold, 272–273
over continents, 256–257
equatorial, 237, 239, 251
intertropical, 237

G

General circulation, classical model, 358–362
heat balance, 363–366

General circulation, hierarchy of models
in dishpan experiments, 362
high and low latitudes compared, 252–253
long waves in, 251
momentum balance, 368–372

Georgetown, 83

Geostrophic wind, 192–194
in hurricane prediction, 355
meridional profiles, 7–8
and pressure field, 22

Gradient wind, 194

Guam, 46, 84
typhoon observations, 300–301
warm rain, 159

H

Hail, 167, 170–171

Havana, 41, 83

Hawaii, 99
climatic gradients, 99, 111–114
jet stream over, 251
rainfall, and jet stream, 275
mean, 84
rainstorm frequency, 95
sea-breeze regimes, 105–107
trade inversion over, 63

Heat balance, 73
of general circulation, 363–368
of trades, 373–374

Heat transfer, through cumuli, 150–154
during entrainment, 140
at ocean surface, 121
in tropical storms, 287, 315

Himalayas, flow around, 263
role in monsoon burst, 262

Hongkong, 97

Honolulu, 41, 63, 99
(*See also Hawaii*)

Horse latitudes, 1

Humidity, continental air masses, 50
fluctuations over sea, 122
gradient in trade inversion, 55, 59, 68
maritime air masses, 53
mean tropical atmosphere, 45
tropical storms, 287

Hurricane (*see Tropical storms*)

Hurricane wave, 299

Hydraulic jump, 10, 228

I

Ice in clouds, 163–166

Index cycle, 277, 353
and monsoon fluctuations, 268
solar origin, 278

- India-Pakistan, cool-season disturbances, 269
 mean circulation, 258
 monsoon burst, 257-263
 monsoon fluctuations, 263-268
 seasonal forecasting, 268-269
 streamline analysis over, 190-191
 summer disturbances, 266
 temperatures, 41, 49
- Interaction, between hemispheres, 254-256
 of high and low latitudes, 274-278
 capture of waves in easterlies, 225
 flow-pattern types, 274-275
 formation of waves in easterlies, 226
 role of jet streams, 275
 and tropical-storm formation, 332-333
- Intertropical convergence zone, 237
- Isobars, flow across, 12, 194
 mean, at sea level, 8-12
- Isogons, 189-190
- Isotachs, 192
- Isothermal expansion, 287, 315, 321
- Isotherms, mean, layer 700-300 mb, 23
 of ocean surface, 37
 at sea level, 36
- Isovels, 192
- J**
- Jet stream, 22
 in cool season, 269-270
 in easterly current, 201
 and Hawaiian rainfall, 275
 in rotating dishpans, 362
 in warm season, 249-251
- Johnston Island, 251
- K**
- Khartoum, 41, 49, 81
 air masses over, 50-51
- Kite soundings, 55
- Krakatao winds, 24
- L**
- Land breeze, 103-108
 over Puerto Rico, 100
- Lapse rate, 43
 autoconvective, 126
 in hurricane eye, 317
 of mean tropical atmosphere, 44-45
 near ocean surface, 60
 in subcloud layer, 123
 superadiabatic, 128
- Lapse rate, superadiabatic, in trades, 60, 68-69
 near surface, 126
 in trade inversion, 55, 58, 69
 in tropical storms, 314
- Latent-heat release in tropical storms, 334-336
- Lateral mixing, 361
- Layers, moist and dry, 43
- Libreville, 80
- Life cycle, of cumulus clouds, 119, 137
 of long-term weather trends, 277
 of tropical storms, 282
- Loanda, 81
- Long waves, 221
 compared to tropical vortex train, 251
 in dishpan experiments, 362
 interaction with equatorial shear lines, 245
 mean, in August, 22-23
 and tropical-storm recurvature, 353
- M**
- Maritime tropical air, 50-53, 78
- Mars, circulation of, 8
- Marshall Islands, 323
- Mauritius, 15, 86
- Mean hurricane sounding, 314
- Mean tropical atmosphere, 44-45
- Meridional circulation, in classical general-circulation theory, 358-360
 divergence of, 78, 379
 dynamic control, 378-379
 heat transport by, 366-368
 momentum transport by, 370-372
 and potential temperature, 367-368
 relative to equatorial trough, 14
 at surface, 6
 vertical motion of, 367
- Meridional highs, 244
- Meteor* expedition, 18, 55
- Meteor showers, 278
- Meteorological equator, 1, 4, 39
- Mexico, 24
- Microanalysis, 195-197
- Microseisms, 299
- Midway Island, 41
- Moist and dry layers, 43
- Moisture, entrainment of, 140
 in subcloud layer, 123
- Moisture balance, of general circulation, 363-368
 of trades, 373
- Momentum, angular, balance of, 371
 in trades, 375-376
 conservation of, 358-360
 distribution of, 369-370

Momentum, angular, transfer mechanisms, 370
 in tropical storms, 288, 305-307
 exchange of, at surface, 121
 horizontal entrained, 146
 vertical entrained, 144-145
 Monsoon, Burma, 257, 262
 burst of, 257-263
 effect of mountains on, 262-264
 fluctuations of, 263-268
 forecasting of, 268-269
 mean streamlines, 8-10
 southwest, 31
 summer, Indian, 256-269
 winter sounding, 46, 48
 Mountain effect, on broad-scale conditions, 257-259
 on local climate, 105-107, 111-116
 in monsoon burst, 262-264

N

Nuclei, condensation of, 155-157
 freezing of, 157, 171
 sea-salt, 156, 163
 sublimation of, 164
 Numerical forecasting, 206-208

O

Ocean currents, role in heat balance, 364
 upwelling, 39
 Ocean temperatures and hurricane formation, 330-331

P

Pakistan (*see India-Pakistan*)
 Palau, 24, 27, 242
 Parcel method, 134-135
 Path method, 352
 Penang, 86
 Philippines, 10, 24, 242, 243
 rainfall skewness, 97
 seasonal rainfall, 114-116
 Pilot-balloon observations, 182
 Pilot reports, 183
 Polar air in tropical storms, 327-328, 338
 Port-au-Prince, 177
 Potential temperature, as air-mass characteristic, 50, 53
 cross section of Pacific trade, 68-69
 equivalent, 248
 and meridional circulation, 367-368
 and sea breeze, 104-105
 at top of trade inversion, 60
 in tropical storms, 287
 wet-bulb, 45, 53

Precipitation, annual, of globe, 74, 364
 artificial, 171-175
 from cumulus clouds, 163, 167
 diurnal variation, 109
 effective, 87
 growth of, from ice, 166-168
 in warm clouds, 159-163
 mean distribution, 74-76
 measurement over oceans, 72
 orographic, 111-114
 rain storms, 95
 relative to equatorial trough, 78
 from roll clouds, 110
 seasonal march, 79-87
 skewness of frequencies, 89
 from sloping cumuli, 147
 from stratiform clouds, 163, 166
 in tropical storms, 293-297, 327
 variability, 90
 (*See also Rain*)

Pressure, changes and divergence in, 202
 203

diurnal variation of, 117-118, 179
 in eye of tropical storms, 297
 hydraulic jump, 10
 mean sea-level, 1-2
 oscillations of, in tropical storms, 286,
 297
 and sea breeze, 103, 105
 surface, in tropical storms, 283-286,
 316
 synoptic analysis of, 179
 in waves in easterlies, 213-214, 231
 wind relations, 22, 192-195
 world distribution of, 8-12

Pressure gradient in tropical storms, 285,
 305

Pressure-gradient force, role in momentum balance, 375-376

Puerto Rico, diurnal rainfall variation,
 109-110
 diurnal temperature variation, 99-102
 drought season, 93
 equatorial shear lines at, 245-247
 mean upper winds, 21, 26
 rainfall, 83, 89
 stratospheric winds, 25
 waves in easterlies at, 211-212

Q

Quito, 41

R

Radar bands, 308-312
 Radiation balance, global, 363-364
 in trades, 374

Radiosonde observations, 182–183
 analysis of, 184–186
 Rain, growth of, in warm clouds, 159–163
 from melting of snow, 167
 physics of, 155–175
 (*See also Precipitation*)
 Rawin observations, 182
 analysis of, 184–186
 Recife, 41, 82
 Reconnaissance flights, 288–289
 Recurvature of tropical storms, 347–351
 average latitude of, 352
 and long waves, 353
 and zonal westerlies, 353
 Rio de Janeiro, 41, 81
 River discharge, 73
 Rotation of earth, variations, 368
 Runoff, 87

S

St. Thomas, 72
 Sea breeze, 102–108, 177
 energy of, 107
 of Hawaii, 105–106
 of Puerto Rico, 100
 solenoid field of, 103–104
 vertical structure of, 108
 Sea surface, evaporation from, 73, 121–123, 287
 rough and smooth, 123
 state of, in tropical storms, 298–300
 swell of, in tropical storms, 298
 temperatures of, 37–38, 330–332
 upwelling, 39

Seasonal forecasting for India, 268–269
 Seasons in tropics, 34–35
 Seychelles Islands, 43, 86
 Shearing stress, 194–195
 Sierra Leone, 80
 Silver iodide, 174–175
 Singapore, 85
 Slice method, 136–137
 Soaring, 127–128
 Solar weather influences, 278
 Solenoid field, of equatorial shear lines, 247–249
 of sea breeze, 103–104
 of tropical storms, 319–322, 334–336
 South China Sea, 10, 242, 243
 Southern oscillation, 268
 Specific temperature anomaly, 186
 Stability analysis, 181
 Steering current, 343–345
 Stratosphere temperatures, 46, 49
 Stratosphere winds, 24–25, 300–301

Streamlines, analysis methods, 188–192
 asymptotes, 191
 and divergence, 198
 mean, at surface, 8–14
 saddle points, 191
 singular points, 8, 191
 and vorticity, 199
 Subcloud layer, 123–131
 convection cells in, 126–131
 structure of, 123–125
 turbulence in, 124–125
 Subsidence, and convection, 136–137
 and divergence, 204
 in eye of hurricanes, 316–318
 and hurricane formation, 335, 338–339
 in subtropical highs, 376
 in waves in easterlies, 217–218
 Sun, annual march, 34
 circulation of, 361
 Sunspots, 361
 Superadiabatic lapse rate (*see Lapse rate*)
 Surge of trades, 273
 Swan Island, 46
 Swell, sea, in tropical storms, 298
 Synoptic analysis, microanalysis, 195–197
 surface charts, 186–187
 time sections, 184–186
 upper-air charts, 187–192

T

Tahiti, 41
 Tarawa, 27, 242
 Temperature, in cumulus clouds, 138
 diurnal variation, 99–102
 effect of clouds on, 140–142, 248
 influence of sea breeze on, 103–108
 ocean, and hurricane formation, 330–331
 potential, and meridional circulation, 367
 representative values, 178, 183, 236–238
 in subcloud layer, 122, 124
 surface, 34–44
 as air-mass characteristic, 50–51
 annual range, 35
 difference from sea temperature, 38, 121–122
 in equatorial Atlantic, 61
 of oceans, 38
 potential, in tropical storms, 287
 seasonal march, 38–43
 in tropical storms, 286–287
 at west coasts, 39, 53
 and thermal wind, 22–24

- Temperature, upper-air, 19–20, 43–50
in equatorial shear lines, 238, 247–
249
equivalent potential, 248
in eye of tropical storms, 316–320
layer 700–300 mb, 24
potential, at trade inversion, 60, 68
wet-bulb, 45
seasonal changes, 47
in stratosphere, 49
in tropical storms, 313–316
in waves in easterlies, 213–215
- Tendency equation, 201–202
- Teneriffe, 53
- Thermal wind, 22, 193–194
- Thermals, 120, 127–128
- Thunderstorm Project, 138, 170–171
- Thunderstorms, divergence in, 139
entrainment rates in, 146
precipitation growth in, 168–171
- Tides in tropical storms, 299
- Time-section analysis, 184–186
- Topographic influences, on diurnal rain-
fall, 110–111
on mean rainfall, 111–116
on sea breeze, 104–107
on trade inversion, 106–107
- Tornadoes, African, 217
- Tracks of tropical storms, 341
- Trade-wind inversion, 43, 53–70
discovery of, 53
dissolution of, 377–378
flow of mass through, 67, 377–378
formation of, 376
structure of, in Atlantic, 54–62
layer, 63, 151
in Pacific, 63–70
topographic influence on, 106–107
turbulence in, 378
upper-air temperature, potential, 60,
68
- Trade winds, basic current structure,
31–32
conservation of vorticity in, 378–379
deflected, 8
heat and moisture balance, 373–375
influence on sea breeze, 103–104
inversion (see Trade-wind inversion)
mean surface, 3–8
momentum balance, 375–376
steadiness of, 26–30, 379–380
vertical structure, 18–21
- Trajectories, CAV (constant absolute
vorticity), 206–207
- Trinidad, 13, 83
- Triple point, 327
- Tropical storms, bar of, 289
barograph traces in, 285
on both sides of equator, 234
cloud systems, 308–313
cooling system, 321–322, 338
Coriolis parameter in, 288, 330, 334
detection of, 325
dissipation of, 339–341
divergence and convergence in, 289,
292–293, 305–306
energy of, 320–322
entrainment in, 336
evaporation in, 287
eye of (see Eye of tropical storms)
formation of, equatorial trough and,
331
frequencies, 323–325
frontal hypothesis of, 327–329
regions of, 323, 330–331
theories of, 326–330
in waves in easterlies, 225
friction in, 288, 322, 341
humidity, 287
lapse rate in, 314
life cycle, 282
movement of, forecasting, 351–356
by internal forces, 342–343
and recurvature, 347–351
steering, 343–345
tracks, 340, 341, 351
and vortex interaction, 345–347
polar air in, 327–328, 338
pressure oscillations in, 286, 297
rainfall, 293–297, 327
recurvature of (*see Recurvature of
tropical storms*)
release of latent heat in, 334–336
solenoid field of, 319–322, 334–336
state of sea surface in, 298–300
surface pressure, 283–286, 316
temperatures in, surface, 286–287
upper-air, 313–316
tides in, 299
tropopause in, 301, 318
vertical cross sections of, 319
vertical extent of, 300–301, 312
wind in, 287–293, 300–307
- Tropopause, seasonal changes, 48
in tropical storms, 301, 318
in waves in easterlies, 215
- Turbulence, in cumuli, 147–148
and heat transfer, 150–153
near sea surface, 121–122, 287
in subcloud layer, 124–125
in trade inversion, 378
and wind balance, 194–195
- Typhoon (*see Tropical storms*)

V

- Vertical motion, and acceleration, 134, 144
 in cumuli, 151–152
 and divergence, 203–204
 of mean trade current, 65–67
 measurement of, 122
 of meridional circulation, 367
 Vortex interaction, 345–347
 Vortices, upper train of, 251–254
 Vorticity, aloft, in tropical storms, 303
 CAV trajectories, 206–207
 of cumuli, 148–150
 in equatorial shear lines, 249
 fields of, 199–201
 and flow across equator, 209
 lateral mixing of, 254, 361
 potential, 204–208
 relation of, to dynamic instability, 329–330
 to formation of trade inversion, 376
 at surface, in tropical storms, 290, 292–293
 used in numerical forecasting, 206–208
 variation, mean, in trades, 378–379
 in waves, in easterlies, 219–223, 230–232
 in westerlies, 271
 Vorticity theorem, 205

W

- Water balance, 73
 Waves, in easterlies, clouds in, 217–218
 deepening of, 225, 234
 dynamics, 219–223, 230
 forecasting, 224–228
 island effect on, 218
 models, 211–219, 228–234
 pressure in, 213–214, 231
 subsidence in, 217–218
 temperature in, 213–215
 tropopause in, 215
 vorticity in, 219–223, 230–232
 winds in, upper, 215–217, 234
 long (*see* Long waves)
 ocean, in tropical storms, 298–300
 in westerlies, 270–272

- Water, in westerlies, interaction with waves in easterlies, 225–227
 and tropical-storm motion, 347–351, 353–354
 vorticity in, 271
 Wind, as air-mass characteristic, 30–32
 cyclostrophic, 194
 diurnal variation of, 102–108, 177–178
 geostrophic (*see* Geostrophic wind)
 gradient, 194
 synoptic analysis of, 188–192
 thermal, 22, 193–194
 Wind computations, 192–195
 Wind motion near equator, 194
 Wind observations, 179–180, 182–184
 Wind shear, effect on cumuli, 146–150
 vertical, and temperature field, 193
 Winds, surface, angle with isobars, 12
 components of, 6–8
 constancy of, 5
 fluctuations of, 121–123, 128–131
 mean resultant, 2–8
 regional, 8–12
 steadiness of, 5
 in tropical storms, 287–293
 upper, constancy of, 26
 cross sections of, 19–20
 energy of, 27–28
 mean streamlines, 15–18
 standard vector deviation, 26
 steadiness of, 26–30, 64
 in stratosphere, 24–25, 300–301
 at 300 mb, 21–25
 in tropical storms, 300–307
 variation through trade inversion, 54
 in waves in easterlies, 215–217, 234
 zonal symmetry of, 23

Z

- Zanzibar, 43
 Zonal and meridional weather types, 275
 Zonal westerlies as related to tropical storm motion, 353
 Zonal wind profile, and burst of monsoon, 262–263
 and changes during monsoon season, 268
 Zonal symmetry of winds, 23

LIBRARY

National Bureau of Soil Survey &
Land Use Planning (ICAR) Bangalore

AUTHOR Riehl H. **CL NO** 551.5 (213)

TITLE Tropical meteorology

ACCN. NO. 170